Metabolic and ecological strategies of specialist bacteria mediating macroalgae breakdown

Maéva Brunet

Sorbonne Université

Ecole Doctorale 515 – Complexité du Vivant

Laboratoire de Biologie Intégrative des Modèles Marins UMR8227

Equipe de Glycobiologie Marine

Metabolic and ecological strategies of specialist bacteria mediating macroalgae breakdown

Par Maéva Brunet

Thèse de doctorat en Microbiologie Marine

Dirigée par Tristan Barbeyron et François Thomas

Présentée et soutenue publiquement le 30 novembre 2021

Devant un jury composé de :

Pr. Carol Arnosti	UNC-Chapel Hill, USA	Rapportrice
Pr. Soizic Prado	MNHN, Paris	Rapportrice
Pr. Bernhard Fuchs	MPI-Bremen, Allemagne	Examinateur
Dr. Ingrid Obernosterer	SU-CNRS, Banyuls	Examinatrice
Dr. Aurore Labourel	INRAE, Toulouse	Examinatrice
Dr. Tristan Barbeyron	SU-CNRS, Roscoff	Directeur de thèse
Dr. François Thomas	SU-CNRS, Roscoff	Directeur de thèse

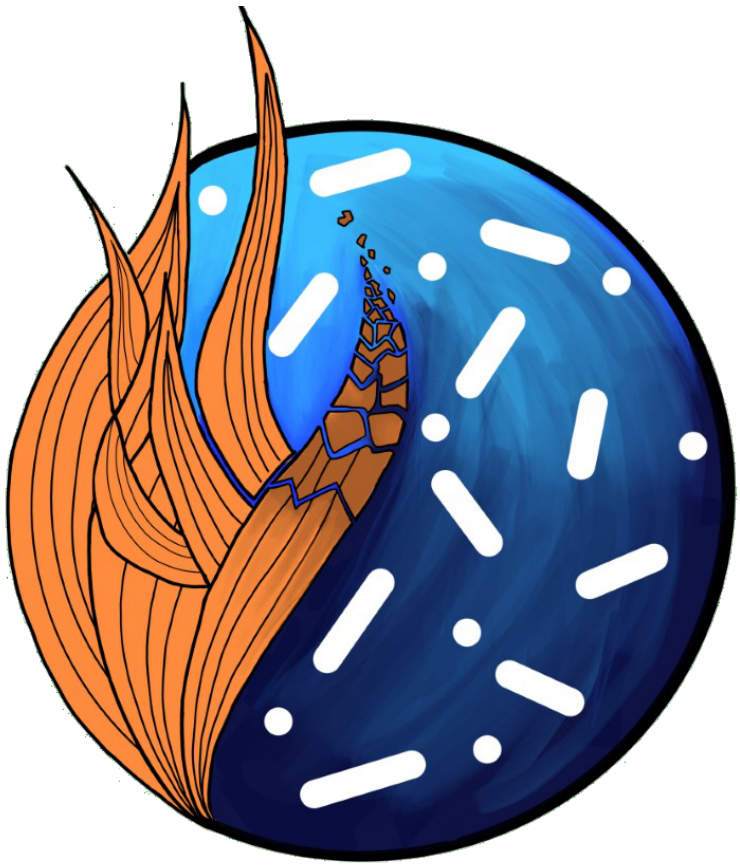

ALGAVOR

Dessiné par Nolwen Le Duff

Remerciements

First, I would like to thank the members of my defense committee, Pr. Carol Arnosti, Pr. Soizic Prado, Pr. Bernhard Fuchs, Dr. Ingrid Obernosterer and Dr. Aurore Labourel. I really appreciate that you agreed to read my manuscript.

François, Tristan, je me sens vraiment chanceuse de vous avoir eu tous les deux comme encadrants. François, merci de m'avoir fait confiance à la suite de mon stage pour faire partie de la team ALGAVOR. Merci de m'avoir accompagnée tout au long de ces 3 ans. Merci d'avoir toujours les mots justes, de ta bienveillance, de ta sérénité et de ton exigence qui m'ont beaucoup apporté. Tristan, merci d'avoir partagé avec passion tes connaissances en microbio et ta précieuse expérience, de ton enthousiasme et de tes encouragements. Merci de m'avoir transmis votre amour pour *Zobellia*, d'avoir toujours pris le temps pour moi (en particulier ces derniers mois), de votre enthousiasme à chaque fois que je vous présentais mes résultats et pour toutes vos bonnes idées et conseils pour faire avancer ce projet. J'ai vraiment toujours été dans les meilleures conditions pour réaliser cette thèse et je vous en remercie énormément.

Je remercie Nolwen, ma partner in crime dès le premier jour. Partager le labo avec toi était un vrai plaisir. Merci entre autres de ton soutien et de ton aide précieuse dans les manips, tes talents d'artiste, de m'avoir accompagné des dizaines de fois récolter des algues (même si on a pris l'eau plusieurs fois) et pour toutes les crêpes/frites/churros partagés.

Merci à tous les membres de l'équipe GM pour votre bonne humeur, les retraites enrichissantes, les pique-niques, vos encouragements, j'ai beaucoup apprécié travailler parmi vous tous ! Merci Mirjam de m'avoir accueillie dans l'équipe. Mumu, merci pour ta gentillesse, ta disponibilité, tes astuces (comment ça ils sont moches mes C-PAGE ?) et pour tout ce que tu fais pour le fonctionnement du labo. Merci Sabine pour tes petites attentions, Lionel (plus personne à embêter dans le labo depuis 3 mois ça doit te manquer !), Liz pour ton énergie communicative, et à tous les autres. Merci aussi à Manon que j'ai co-encadré pour son stage de M2 et qui m'a aidé pour les manips de biochimie.

Je remercie toutes les personnes qui m'ont formée, Gwenn à la préparation des librairies (et plus généralement Erwan L. et Gwenn qui font tourner la plateforme Genomer), Erwan C. et Gildas pour la formation RNA-seq et pour avoir répondu à tous mes soucis d'analyses de données, ainsi que Sébastien C. et Sophie pour l'utilisation du microscope confocal.
Mes sincères remerciements également à Angélique pour sa co-supervision durant mon stage de fin d'étude et sa gentillesse.
Thank you, Rudi and Bernhard, for your warm welcome in your lab, for initiating me to the wonderful world of FISH and for your advices and guidance. I really enjoyed

my stay in Bremen in the Molecol team. Special thanks also to Jörg for teaching me the different protocols and to Andreas for confocal images.
Je voudrais également remercier Florian et Dominique pour cette belle collaboration sur le projet HYPERBACT.
Merci à Yan Jaszczyszyn de l'I2BC et au personnel de BIBS pour nos échanges.

Merci aux membres de mon comité de thèse, Tatiana Rochat, Christian Jeanthon et Ali Ladram pour leurs commentaires et suggestions et un merci particulier à Tatiana pour ses conseils dans l'analyses des données transcriptomiques.

Merci à toutes les personnes qui m'ont apporté leur aide précieuse au cours de ma thèse. Je pense notamment à Jasna, la reine des FCSP, qui m'a gentiment fourni en enzymes et substrats, merci aussi à Cécile, Philippe et Jonas pour votre expertise sur les algues, à Diane pour ton aide et nos discussions dans l'analyse des sucres, à Thomas et Mirjam dans ma tentative de cristallo, à Gurvan pour les discussions sur les CAZymes, à Cécile encore, d'avoir pris le temps de me montrer l'inclusion de coupes d'algues. Merci également à tous ceux qui ont bien voulu braver le vent et la pluie pour gambader dans le champ de laminaires avec moi. Merci Martin pour les fameux systèmes de co-cultures, et Sébastien H. qui fait tourner l'imprimante 3D plus vite que son ombre. Merci aussi à Simon et Ludo.

Merci à tous les doctorants, post-doc, stagiaires que j'ai rencontré au cours de ma thèse. Thank you Elham for your friendship, our laughs and talks and your cucumber seed that turned into a pumpkin. Merci pour ton soutien Lisa (quand tu veux le surf maintenant !), merci Guillaume (organisateur attitré de soirées jeux), Eugénie, Bertille (tes tartes aux citrons sont vraiment les meilleures !), Mathilde, à tous ceux avec qui j'ai passé des bons moments en dehors du boulot, au bar, à la plage ou ailleurs. Merci Sandrine pour ta compagnie lors des trajets en covoit.

En un mot, merci à tout le personnel de la Station que j'ai pu côtoyer et qui font qu'on se sent si bien ici à Roscoff !

Merci aussi aux membres d'Abysse, en particulier à DD (fournisseur officiel de Banyuls et roi de la feijoada), Michel et Tristan pour les combos plongée / Tour du Monde le week-end qui m'ont fait le plus grand bien.

Je veux également remercier mes amis et toute ma famille. Mes parents en particulier pour leur soutien sans faille depuis toujours et malgré l'éloignement, merci pour avoir traversé la France tous les ans pour venir me voir.

Marion, tout ça aurait été beaucoup plus dur sans toi à mes côtés, alors simplement un immense merci pour tout ton amour et ton soutien au quotidien.

Table des matières

Table des figures

Table des tableaux

Table des abréviations

AA : enzyme avec une Activité Auxiliaire (*Auxiliary Activity*)
ADN : Acide DésoxyriboNucléique
AFSW: *Autoclaved* 0.2 µm *Filtered SeaWater*
AIR: *alcohol-insoluble residue*
AMAC: *2-aminoacridonein*
ANOVA: *ANalysis Of Variance*
APS: *Ammonium persulfate*
ARN : Acide RiboNucléique
BMH : Bactéries Marines Hétérotrophes
CARD-FISH: *CAtalized Reporter Deposition FISH*
CAZyme: *Carbohydrate Active enZyme*
CBM: *Carbohydrate Binding Module*
cDNA: *complementary DNA*
CE : Carbohydrate Estérases
COVH : Composés Organiques Volatiles Halogénés
CTD : domaine C-terminal (*C-Terminal Domain*)
C-PAGE: *carbohydrate-polyacrylamide gel electrophoresis*
DAPI : 4',6-diamidino-2-phenylindole
DEH : acide 4-deoxy-5-keto uronique (*4-deoxy-L-erythro-5-hexoseulose uronic acid*)
DMSO : Dimethyl sulfoxide
DNA: *DeoxyriboNucleic Acid*
DNAse: *Deoxyribonuclease*
DTT : Dithiothreitol
EDTA : Ethylenediaminetetraacetic
ECM: *ExtraCellular Matrix*
eLSA: *extended Local Similarity Analysis*
EPS: *ExoPolySaccharide*
ESI-MS: *Electrospray Ionization Mass Spectrometry*
FACE: *Fluorophore-Assisted Carbohydrate Electrophoresis*
FCSP : polysaccharide sulfaté contenant des résidus fucoses (*Fucose-Containing Sulfated Polysaccharide*)
FISH: *Fluorescence* In Situ *Hybridization*
G : acide α-1,4-L-Guluronique
GH : Glycoside Hydrolase
GLM: *Generalized Linear Model*
GT : Glycosyl Transférases
HAD : halo-acide dehalogénase (*haloacid dehalogenase*)
HMW: *High-Molecular-Weight*
HPSEC: *High Pressure Size Exclusion Chromatography*
HRP: *Horseradish peroxidase*
IPBA : N-isopropylbenzylamine
LMW: *Low-Molecular-Weight*
LPS: *LipoPolySaccharide*
M : acide β-1,4-D-Mannuronique
MALDI-MS: *Matrix Assisted Laser Desorption Ionisation Mass Spectrometry*
ME: *Electroendosmosis*
MEC : Matrice ExtraCellulaire
MMM: *Marine Minimum Medium*

MO : Matière Organique
MOD : Matière Organique Dissoute
MOP : Matière Organique Particulaire
MOPS: *3-(N-morpholino)propanesulfonic acid*
MS: *Mass Spectrometry*
NGS : Séquençage de nouvelle génération (*Next-Generation Sequencing*)
NMDS: *Non-metric Multidimensional Scaling*
NMR: *Nuclear Magnetic Resonance*
NTC: *Non-Template Control*
NTD: *N-Terminal Domain*
OD: *Optical Density*
OTU: *Operational Taxonomic Unit*
PBS: *Phosphate Buffer Saline*
PCR : réaction de polymérisation en chaine (*Polymerase Chain Reaction*)
PERMANOVA: *PERMutational ANalysis Of Variance*
PFA: *ParaFormAldehyde*
PL : Polysaccharide Lyases
PLnc: *non-classified PL*
PUL: *Polysaccharide Utilization Locus*
qPCR : PCR quantitative (*quantitative PCR*)
QS : Quorum Sensing
RNA: *RiboNucleic Acid*
rRNA: *ribosomal RNA*
RNA-seq: *RNA sequencing*
ROS : espèce réactive de l'oxygène (*Reactive Oxygen Species*)
RT: *Reverse Transcription*
RT-qPCR: *Quantitative reverse transcription PCR*
SDS: *Sodium dodecyl sulfate*
SDS-PAGE: *SDS-PolyAcrylamide Gel Electrophoresis*
SOMLIT : Service d'Observation en Milieu Littoral
SUS: *Starch Utilization System*
TBDT : transporteurs TonB-dépendant (*TonB-Dependent transporter*)
TEMED: *N,N,N',N'-tetramethylethylenediamine*
TLC: *Thin Layer Chromatography*
T6SS : Système de Sécrétion de Type-VI (*Type-VI Secretion System*)
T9SS : Système de Sécrétion de Type-IX (*Type-IX Secretion System*)
UV: Ultra-Violet
vHPO : haloperoxidases vanadium-dépendantes (*vanadium-dependant haloperoxidases*)
vIPO : *vanadium-iodoperoxidases*

Chapitre I :

Introduction Générale

I. Les microorganismes dans l'océan

Les microorganismes sont des organismes vivants unicellulaires dont la taille est inférieure à 100 µm, et qui ne sont donc visibles qu'à l'aide d'un microscope (Kirchman, 2008). Ils englobent à la fois les bactéries et les archées, qui sont des organismes procaryotes, ainsi que les protistes, des organismes eucaryotes unicellulaires. Les microorganismes dominent tous les écosystèmes de la planète dont les océans, qui représentent 71 % de la surface de la Terre. On estime que les océans contiendraient 10^{29} cellules bactériennes (Whitman *et al.*, 1998). En particulier, de nombreuses études ont démontré qu'un millilitre d'eau de mer contient approximativement 10^6 cellules bactérienne (Cole, 1982). Seuls les virus, des agents infectieux 10 à 100 fois plus petit que des bactéries nécessitant un hôte pour se répliquer, sont plus abondants que les microorganismes, il y aurait $10^9 – 10^{11}$ particules virales dans un litre d'eau de mer (Hara *et al.*, 1991). Cependant, les microorganismes sont largement majoritaires en termes de biomasse : les procaryotes représentent à eux seuls environ 90 % de la biomasse totale des océans (Suttle, 2007).

Les microorganismes ont un rôle majeur dans les cycles biogéochimiques. On appelle cycle biogéochimique l'ensemble des processus de transformations et de transports subits par les éléments chimiques présents dans l'environnement. Le carbone est l'un des principaux éléments de la matière organique (MO) constituant les êtres vivants (45–55 % de sa masse). Tout organisme vivant a besoin d'énergie et de carbone pour vivre, croître et se multiplier, mais tous n'utilisent pas les mêmes stratégies métaboliques. On distingue deux types d'organismes en fonction de la source de carbone qu'ils utilisent : les autotrophes utilisent du carbone minéral comme le CO_2, tandis que les hétérotrophes utilisent du carbone organique. Par exemple, certains organismes autotrophes fixent ainsi le CO_2 atmosphérique pour produire de la matière organique en utilisant l'eau comme pouvoir réducteur et l'énergie lumineuse via la photosynthèse : ce sont des organismes photolithoautotrophes responsables de la production primaire. On estime que la productivité primaire nette dans l'océan est de 45–55 Giga-tonnes de carbone par an (Gt C.an^{-1}) (Longhurst *et al.*, 1995; Field *et al.*, 1998; Falkowski *et al.*, 2000) soit la moitié de la production primaire de la planète (Ducklow *et al.*, 1993; Falkowski *et al.*, 1998). Plus de 90% de la production primaire marine est réalisée par le phytoplancton, c'est-à-dire les microorganismes eucaryotes photosynthétiques flottant dans la colonne d'eau et les cyanobactéries (Nagata, 2000). La matière organique ainsi produite est caractérisée par sa taille, de façon opérationnelle on parle généralement de matière organique dissoute (MOD) pour les composés qui passent à travers un filtre de 0,1-0,8 µm (Benner and Amon, 2015) et de matière organique particulaire (MOP) pour ceux qui sont retenus. Des continuums de tailles plus précis et restreints peuvent également être utilisés. La MOD est la forme majoritaire de matière organique dans les océans (662 Gt C.an^{-1}) (Hansell *et al.*, 2009).

La MO produite lors de la production primaire est composée principalement de polysaccharides (15-50 % de la MOD, 3-18 % de la MOP, Arnosti *et al.*, 2020), de lipides, d'acides aminés et organiques. La MOD représente le réservoir majeur de carbone dans l'océan et est presque exclusivement assimilée par les bactéries marines hétérotrophes (BMH) (Pomeroy, 1974), qui l'utilisent comme source de carbone et d'énergie pour leur croissance en produisant de la biomasse : c'est la production secondaire. Cette biomasse bactérienne est ensuite consommée par d'autres organismes tels que des protozoaires (protistes hétérotrophes) qui vont à leur tour être consommés par des organismes plus gros (zooplancton) et ainsi de suite, supportant l'ensemble de l'écosystème marin (**Figure I.1**). Les BMH jouent donc un rôle essentiel puisqu'elles permettent de recycler l'immense stock de carbone organique produits par les autotrophes en le réinjectant dans les réseaux trophiques supérieurs. De plus, en consommant la MO, les BMH participent à sa reminéralisation, c'est-à-dire qu'ils relarguent des nutriments essentiels (azote, phosphore, CO_2, etc.) qui stimulent la croissance du phytoplancton. Ce concept décrit par Azam *et al.*, 1983 et Ducklow, 1983 est nommé « boucle microbienne ». Cette boucle s'est par la suite complexifiée et continue d'évoluer avec la découverte de nouvelles interactions entre les microorganismes, avec notamment l'impact largement sous-estimé des virus dans ces cycles biogéochimiques (Wilhelm and Suttle, 1999). La MOP est également consommée par les BMH. De par sa structure et sa composition plus complexe, son assimilation (ainsi que celle des composés de haut poids moléculaire de la MOD - plus de 600 Da) nécessite la production d'un arsenal d'enzymes hydrolytiques extracellulaires afin de réduire la matière en composés de petite taille pouvant être importés dans les cellules puis assimilés (Arnosti, 2011).

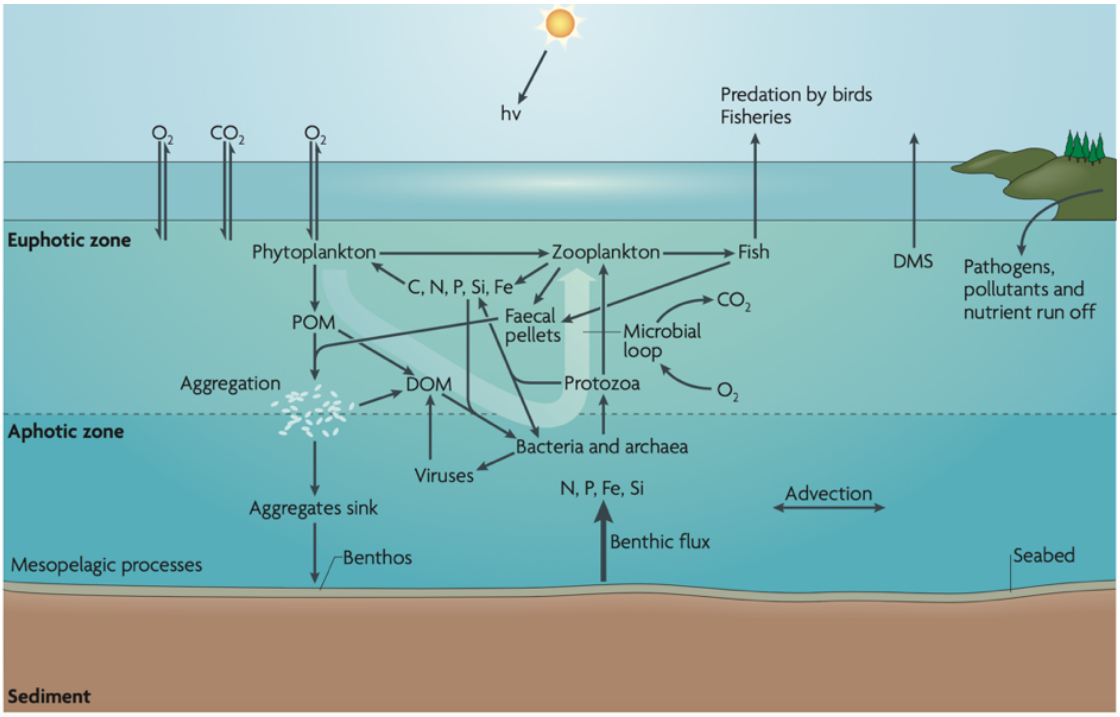

Figure I.1 : Schéma de la boucle microbienne selon Azam and Malfatti, 2007.

Par le recyclage de la matière organique, les BMH sont à la base des chaines alimentaires. Cependant, une partie de cette matière organique est réfractaire à tout processus de reminéralisation, s'agrège pour former des particules, puis sédimente dans la colonne d'eau pour finalement être lentement enfouie dans les sédiments marins. Il s'agit de la pompe biologique. Suite à l'assimilation de MO les BMH peuvent également libérer de la MOD réfractaire qui ne peut plus être recyclée par des processus biologiques et qui va rester dans la colonne d'eau, c'est la pompe microbienne. Ces deux pompes participent au stockage du carbone dans l'océan depuis des milliers d'années ; sa transformation est alors régie par des processus physicochimiques lents.

Les écosystèmes côtiers sont des zones particulières bien distinctes des zones océaniques de pleine mer. Ils sont l'interface entre la terre et l'océan et, soumis à des afflux de matière organique de part et d'autre, ils abritent ainsi un biotope et des flux de matière spécifiques. Ils contribuent à près de 20 % de la productivité primaire sur Terre et leurs rôles dans les cycles biogéochimiques sont donc considérables. Dominant les écosystèmes côtiers, les macroalgues représentent les principaux producteurs primaires, pouvant devancer le phytoplancton en termes de productivité (Mann, 1973). L'étude du recyclage de cette biomasse algale par les bactéries marines hétérotrophes est donc d'une importance écologique cruciale pour mieux appréhender les processus contrôlant les cycles biogéochimiques.

II. Les macroalgues

1. Origine et classification

Les macroalgues sont des organismes photosynthétiques pluricellulaires thallophytes eucaryotes dont le cycle de vie se déroule en milieu aquatique et qui sont caractérisés par une absence de tissus spécialisés (Graham and Wilcox, 2000). Le terme macroalgue n'a pas de valeur taxonomique car elles ne forment pas un groupe phylogénétique unique. Elles sont réparties en trois grandes lignées indépendantes (**Figure I.2**) basées principalement sur la composition des pigments impliqués dans la photosynthèse. En plus de la chlorophylle a et du carotène, les macroalgues vertes (Chlorophyta) produisent majoritairement de la chlorophylle b, les macroalgues rouges (Rhodophyta) de la phycobiline et les brunes (Phaeophyceae) de la chlorophylle c et de la fucoxanthin (MŁodzinska, 2009). Plus de 9000 espèces de macroalgues sont recensées sur la base de données internationale sur les algues AlgaeBase (http://www.algaebase.org), dont 1200, 6200 et 1800 espèces d'algues vertes, rouges et brunes, respectivement (Guiry, 2012).

Ces trois grandes lignées de macroalgues sont le résultat d'une histoire évolutive très complexe. Avec les glaucophytes, les algues vertes et rouges appartiennent au groupe des Archaeplastida qui a émergé il y a environ 1,5 milliard d'années suite à un évènement d'endosymbiose primaire au cours duquel une cyanobactérie a été phagocytée par un protiste hétérotrophe, représentant la première cellule eucaryote

photosynthétique. Les plantes terrestres quant à elles ont émergé il y a 500 millions d'années suite à la différenciation avec la lignée des algues verte (Sørensen *et al.*, 2010) et partagent ainsi de nombreuses similarités avec ces dernières. Les algues brunes dérivent d'un ancêtre photosynthétique qui a effectué une endosymbiose secondaire avec une algue rouge il y a environ 200 millions d'années et font partie du groupe des Stramenopiles (Niklas, 2004; Palmer *et al.*, 2004; Keeling, 2010). Les macroalgues brunes ont ainsi évolué indépendamment des macroalgues rouges et vertes, conduisant à des différences de composition majeures.

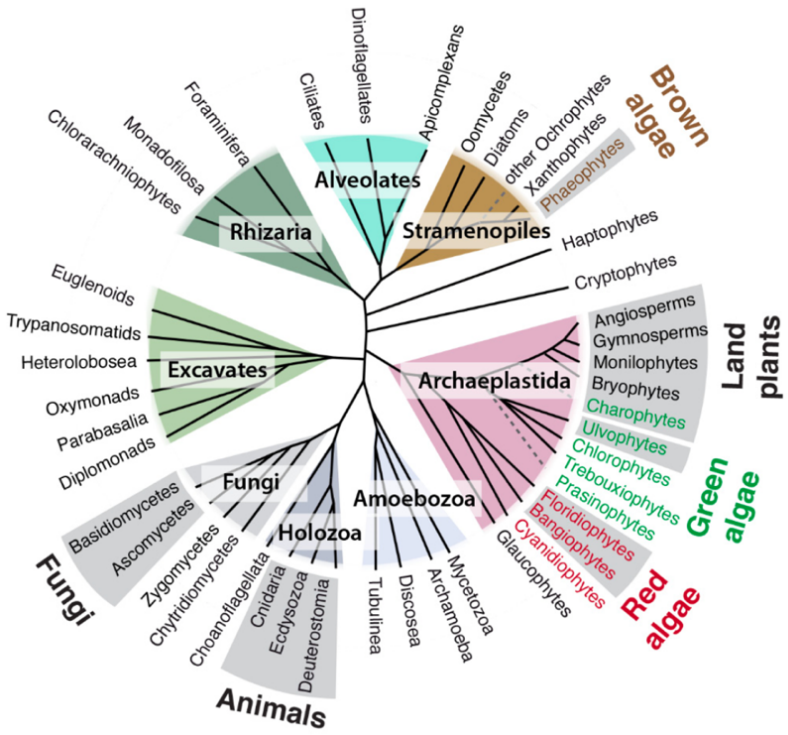

Figure I.2 : Arbre phylogénétique des espèces eucaryotes. De Kloareg et al., 2021, adapté de Coelho and Cock, 2020.

2. Un rôle capital dans les écosystèmes côtiers

Riches d'une très grande diversité génétique et pouvant occuper des milieux très diversifiés, les macroalgues sont des composants fondamentaux des écosystèmes côtiers. Elles se développent sur des fonds sableux ou rocheux selon les espèces, s'étalent sur 3,5 millions de km^2 à travers le monde et, au niveau mondial, la biomasse totale des macroalgues est estimée à 280 millions de tonnes (Carpenter and Liss, 2000). Comme les plantes terrestres, ce sont des producteurs primaires, capables de convertir le carbone inorganique (CO_2) en biomolécules organiques en utilisant l'énergie lumineuse via la photosynthèse. Leur production primaire nette globale peut atteindre 1500 téragrammes de carbone par an (Krause-Jensen and Duarte, 2016). Il est estimé que les habitats marins végétalisés des écosystèmes côtiers, tels que les forêts de macroalgues, les prés-salés ou les herbiers, participent de 1 à 10 % de la production primaire océanique nette, le reste étant dû au phytoplancton. Considérées comme les

producteurs primaires majoritaires des écosystèmes côtiers, elles représentent ainsi de véritables puits de carbone. Cependant, cette contribution des macroalgues est habituellement négligée dans l'étude du cycle du carbone (Duarte, 2017).

Les macroalgues sont reconnues pour jouer un rôle fondamental dans la structuration des écosystèmes côtiers et sont ainsi qualifiées d'espèces « ingénieures » (Jones *et al.*, 1994). Elles servent d'habitats, d'abris et de source de nutriments à de nombreux micro et macroorganismes. Les laminaires (algues brunes de l'ordre des Laminariales, **Figure I.3A**) en sont l'exemple le plus parlant. De par leur taille et leur densité, elles forment dans les zones infralittorales de véritables structures tridimensionnelles appelées « forêts » de laminaires, hébergeant une multitude d'organismes tels que des mammifères marins, des poissons, des oursins, d'autres espèces d'algues ou des microorganismes (Steneck *et al.*, 2002). Les habitats dominés par les macroalgues forment ainsi des zones soutenant une importante biodiversité (Schiel and Foster, 2006).

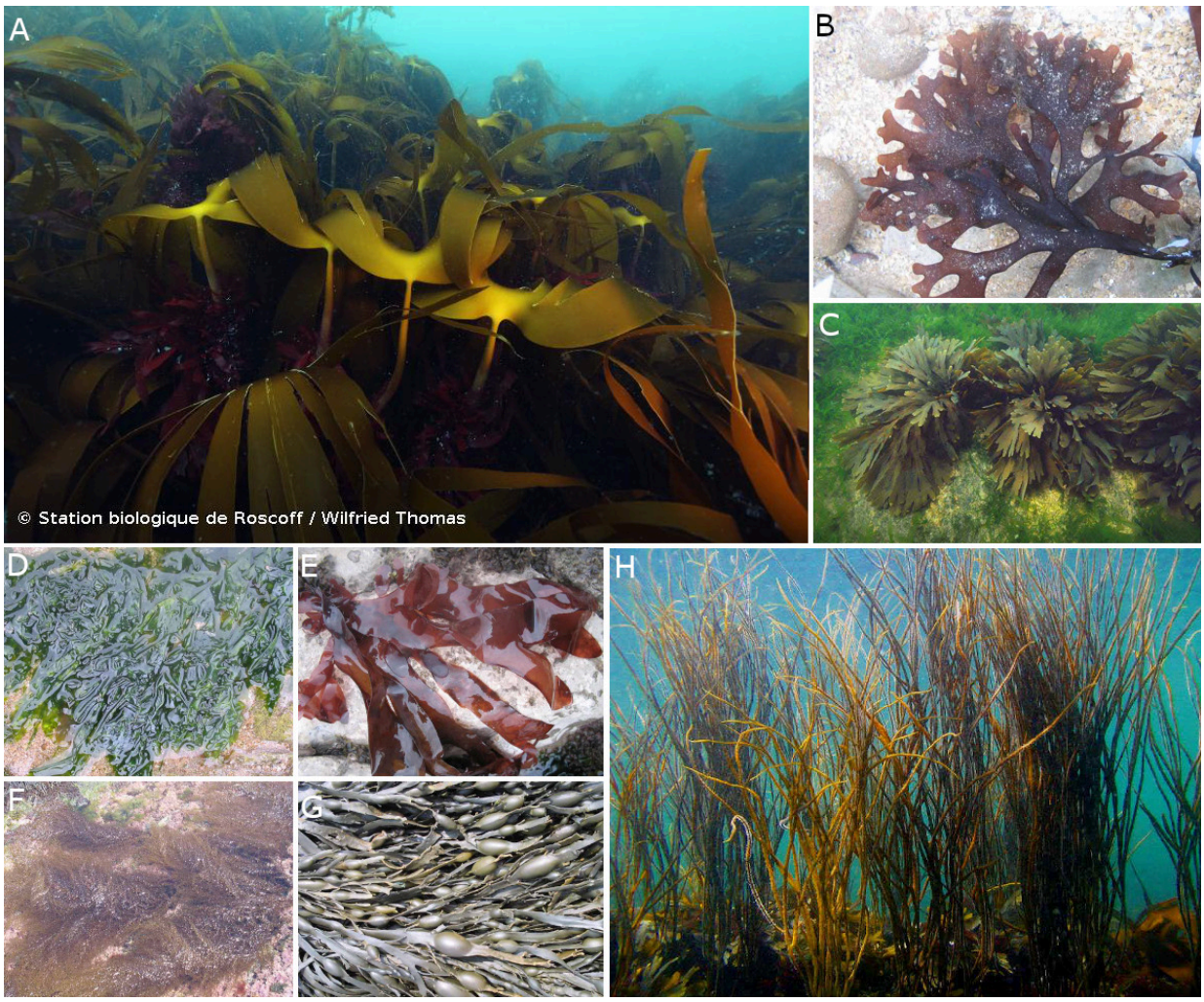

Figure I.3: Photographies de quelques espèces d'algues retrouvées sur l'estran de Roscoff. Issues du site MarLIN https://www.marlin.ac.uk/species, excepté pour A. (A) *Laminaria digitata* (B) *Chondrus crispus* (C) *Fucus serratus* (D) *Ulva lactuca* (E) *Palmaria palmata* (F) *Sargassum muticum* (G) *Ascophyllum nodosum* (H) *Himanthalia elongata*. Droit d'auteur : Wilfried Thomas (A), Judith Oakley (B, D-G), Keith Hiscock (C) et Paul Newland (H).

3. Architecture et composition de la paroi algale

a. Caractéristiques communes aux trois phyla

Beaucoup de macroalgues vivent dans la région intertidale (zone de balancement des marées) et sont soumises à d'importantes variations des paramètres environnementaux tels que la température, l'intensité lumineuse, la salinité ou l'impact mécanique des vagues. A l'instar des plantes terrestres, les cellules des macroalgues sont entourées d'une paroi riche en polysaccharides qui contribue au bon développement des tissus et à garantir leur intégrité. Elle sert d'interface avec l'environnement et c'est donc via cette paroi que l'algue va interagir avec les organismes environnants. Elle participe notamment aux échanges ioniques avec le milieu (régulation osmotique) et aux mécanismes de défense contre les facteurs biotiques (pathogènes, herbivores) et abiotiques (dessiccation ou radiation ultraviolet par exemple). La paroi cellulaire des algues est un réseau tridimensionnel (**Figure I.4**) possédant une architecture semblable à celle des végétaux terrestres. Différents modèles ont été proposés afin de comprendre leur architecture (Lahaye and Robic, 2007; Deniaud-Bouët *et al.*, 2014; Kloareg *et al.*, 2021). Cependant, la structure et la composition chimique de cette paroi varie considérablement selon les espèces, les saisons, la localisation géographique, le cycle de croissance de l'algue, la partie du thalle ou les paramètres environnementaux. Néanmoins, ces études ont permis l'identification de certaines caractéristiques communes. De par la souplesse dont fait preuve la paroi des macroalgues, contrastant avec la rigidité de celle des végétaux terrestres, le terme de matrice extracellulaire (MEC) remplace parfois celui de paroi lorsque l'on se réfère aux algues. La MEC est constituée majoritairement d'un assemblage complexe de polysaccharides (appelés polysaccharides pariétaux ou structuraux) entremêlés avec d'autres composés tels que des lipides, des protéines, des minéraux (iode, calcium, fer, cuivre et magnésium notamment), des vitamines, des acides aminées et des polyphénols (Kloareg and Quatrano, 1988; Michel *et al.*, 2010; Popper *et al.*, 2011; Deniaud-Bouët *et al.*, 2014). Comme chez les végétaux terrestres, la MEC des macroalgues est organisée en une phase squelettique (ou cristalline) entourée d'une phase matricielle (ou amorphe), qui, à l'inverse des végétaux terrestres est majoritaire (**Tableau I.1**). La phase squelettique contient des polysaccharides insolubles également présents chez les plantes terrestres, telle que la cellulose (D-glucose liés en β-1,4), qui représentent entre 1 et 8 % du poids sec de l'algue contre 40-50 % chez les plantes terrestres (Duchesne and Larson, 1989; Zeng *et al.*, 2017). La phase matricielle est composée de différentes structures d'hémicellulose (également retrouvées chez les plantes), et surtout de polysaccharides spécifiques aux algues, qui sont carboxyliques et/ou sulfatés et qui peuvent représenter jusqu'à 50% de la masse sèche des algues (Mabeau and Kloareg, 1987). Ces polysaccharides sont des analogues fonctionnels de la pectine retrouvée chez les plantes. Contrairement aux plantes où la phase squelettique est prédominante, l'importance de la phase amorphe chez les algues résulte en une plus grande flexibilité, leur permettant de résister à l'action des courant et des vagues. Les polysaccharides de la phase matricielle diffèrent selon les lignées de macroalgues (**Tableau I.1**, **Figure I.4**).

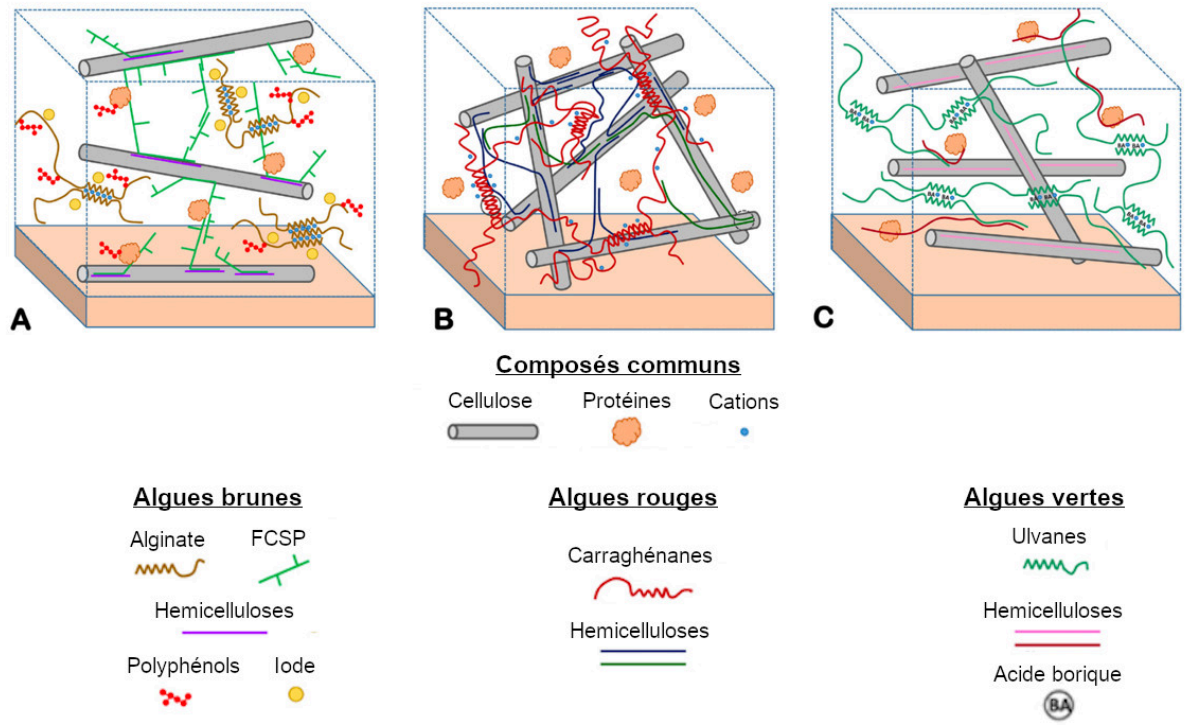

Figure I.4 : Modèle de la matrice extracellulaire des macroalgues brunes (A), rouges carraghénophytes (B) et vertes (C). FCSP : Fucose-Containing Sulfated Polysaccharides. Adapté de Kloareg et al., 2021.

Tableau I.1 : Polysaccharides majoritairement retrouvés dans les parois des plantes terrestres et d'algues. * : polysaccharides carboxyliques. # : polysaccharides sulfatés. FCSP : Fucose-Containing Sulfated Polysaccharides. Adapté de Popper *et al.*, 2011.

	Plantes terrestres	**Algues vertes**	**Algues rouges**	**Algues brunes**
Phase cristalline	Cellulose			
Phase matricielle	Hémicelluloses			
	Pectines*	Ulvanes*#	Carraghénanes# Agars# Porphyranes#	Alginates* FCSP#

Les algues rouges produisent essentiellement des galactanes sulfatés, soit des agars soit des carraghénanes (**Figure I.5**). Ce sont des polymères formés de résidus galactose liés alternativement par des liaisons glycosidiques β-1,4 et α-1,3. Ils se caractérisent par la présence (non-systématique) d'un pont 3,6-anhydro-galactose sur les unités α-L-galactose pour les agars et sur les unités α-D-galactose pour les carraghénanes. Les résidus L-galactose des agars peuvent être sulfatés en O6, on parle alors de porphyrane. Selon le degré de sulfatation du disaccharide répétitif constituant le polymère, différentes sous-familles de carraghénanes existent, les trois principales étant les κ- (un ion sulfate par disaccharide), ι- (deux ions sulfate par disaccharide) et λ-carraghénanes (trois ions sulfate par

disaccharide). Les algues vertes synthétisent principalement de l'ulvane, qui peut représenter 30 % de la masse sèche de l'algue (Lahaye and Robic, 2007), composé de L-rhamnose-3-sulfate, d'acide D-glucuronique, d'acide L-iduronique et de D-xylose. Chez les algues brunes, l'acide alginique (alginate) et des polysaccharides sulfatés contenant des résidus fucoses (FCSP) sont majoritaires. La paroi des algues brunes est discutée plus en détails dans le paragraphe suivant.

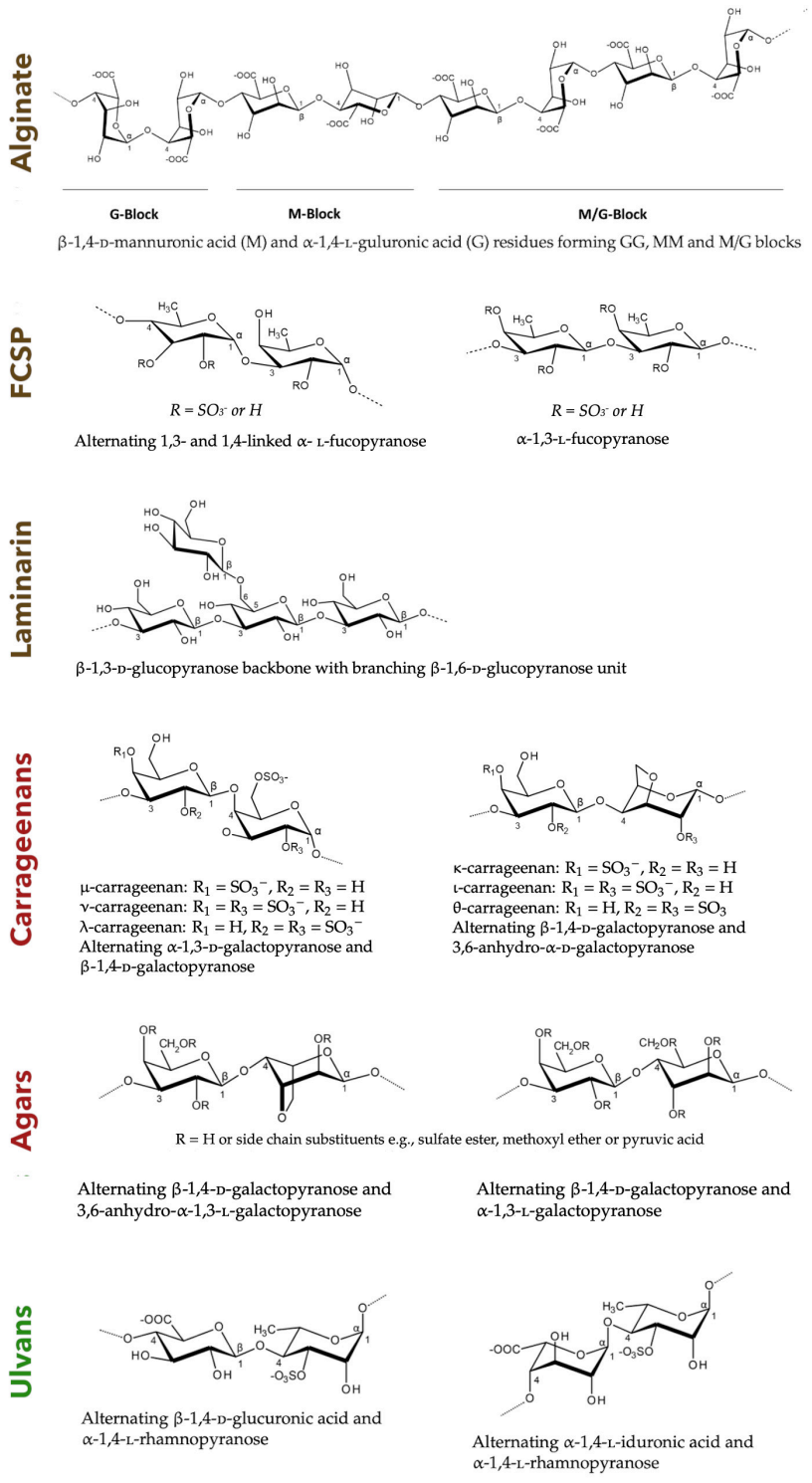

Figure I.5: Différentes structures retrouvées au sein des polysaccharides d'algues brunes (alginate, FCSP, laminarine), rouges (carraghénanes, agars) et vertes (ulvanes). Adapté de Jönsson et al., 2020.

b. Composition des macroalgues brunes

On estime qu'environ 2000 espèces de macroalgues brunes ont été décrites à ce jour. Les ordres les plus fournis sont les Ectocarpales, les Fucales, les Dictyotales et les Laminariales (> 100 espèces) (Bringloe *et al.*, 2020). Les espèces d'algues brunes prépondérantes sur la côte nord bretonne sont les espèces appartenant aux genres *Laminaria*, *Saccharina* (Laminariales), *Fucus*, *Ascophyllum, Himanthalia* et *Pelvetia* (Fucales).

Au sein de la phase matricielle, l'alginate représente entre 10 et 45 % du poids sec de l'algue (Kloareg and Quatrano, 1988). C'est un polymère linéaire formés de deux types d'acides uroniques, l'acide β-1,4-D-mannuronique (M) et l'acide α-1,4-L-guluronique (G). Ces deux oses sont soit disposés en bloc homopolymériques le long du polymère formant des blocs MM ou GG, soit dispersés le long du polymère formant des blocs hétéropolymériques MG. La proportion des motifs M et G et leur agencement confèrent des propriétés rhéologiques différentes à l'algue. L'alginate gélifie en présence de cations divalents, généralement le calcium. Les blocs GG ont une plus forte affinité pour ces cations divalents et vont former des gels plus cassant que les blocs MM ou MG (Haug *et al.*, 1974). Le ratio M/G varie entre les espèces mais aussi au sein d'une même espèce et entre les différentes parties de l'algue au sein d'un même individu (Kloareg and Quatrano, 1988; Skriptsova *et al.*, 2004).

Les FCSP quant à eux, représentent 4-45 % du poids sec de l'algue (Fletcher *et al.*, 2017) et présentent une structure bien plus complexe. Le terme FCSP a récemment été proposé pour désigner l'ensemble des polysaccharides sulfatés des algues brunes qui contiennent au moins un résidu fucose (Ale and Meyer, 2013; Deniaud-Bouët *et al.*, 2017). Il englobe donc à la fois les fucanes et les fucoïdanes (**Figure I.6**). Les fucanes sulfatés sont des polymères pouvant être ramifiés constitués uniquement de résidus L-fucose sulfatés dans la chaîne principale. Les branchements peuvent contenir ou non des résidus fucose. Le terme fucoïdanes se réfère à des hétéropolymères sulfatés ramifiés plus complexes où les résidus fucose ne sont présents que dans les ramifications mais jamais dans la chaine principale. La chaîne principale est composée de divers oses neutres (galactose, mannose, xylose, rhamnose, etc.) et éventuellement d'acides uroniques (acide glucuronique et galacturonique notamment) (Ponce and Stortz, 2020; Sichert *et al.*, 2021). Les FCSP présentent de nombreuses substitutions, notamment des groupement sulfates, mais aussi des groupements acétyles ou méthyles. Il n'y a donc pas de structure ni de composition type de FCSP, d'autant plus que celles-ci sont extrêmement variables entre les espèces et au sein d'un individu en fonction des paramètres environnementaux (Haug *et al.*, 1974; Bruhn *et al.*, 2017; Deniaud-Bouët *et al.*, 2017; Fletcher *et al.*, 2017; Ponce and Stortz, 2020).

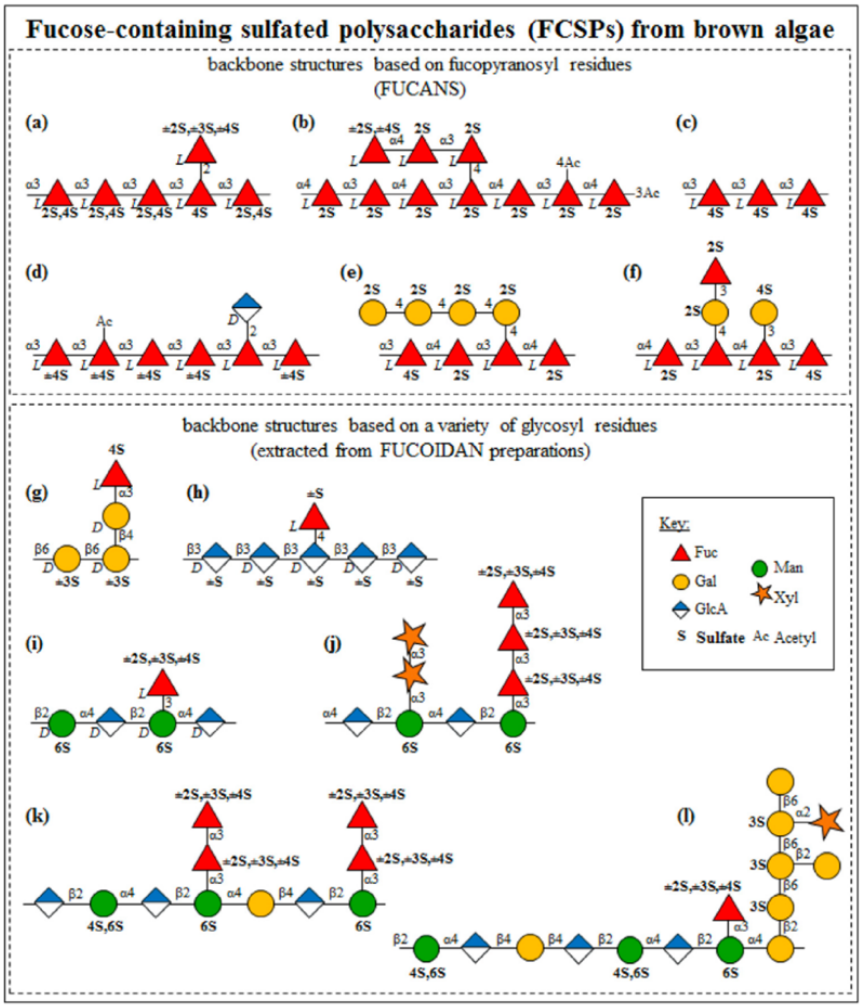

Figure I.6 : Représentation non-exhaustive de différentes structures de fucanes et fucoïdanes retrouvées chez diverses algues brunes. De Deniaud-Bouët et al., 2017.

Il avait été suggéré que la teneur en fucose et en sulfate variait en fonction de la localisation de l'algue sur l'estran. Plus le temps d'immersion des algues est faible, plus la teneur en fucose et sulfate est élevée, suggérant le rôle des fucanes sulfatés dans les mécanismes de régulation de l'hydratation et du stress osmotique (Mabeau and Kloareg, 1987; Skriptsova *et al.*, 2012). Ainsi il était suggéré que les espèces appartenant à l'ordre des *Fucales*, généralement situés dans la partie supérieure de l'estran, soient plus riches en fucose et sulfate que les *Laminariales* vivant plus bas. Cependant, ces travaux prenaient en compte un nombre limité d'espèces. Une étude récente répertoriant les analyses de composition des FCSP effectuées sur plus de 100 espèces d'algues brunes ne confirme pas cette hypothèse et met plutôt en évidence une multitude de facteurs qui peuvent influencer la composition des FCSP, masquant toute différence basée sur la taxonomie ou sur le lieu de vie (Ponce and Stortz, 2020). La comparaison de résultats issus de différentes études reste toutefois approximative étant donné les importantes variations de composition que l'on peut trouver en utilisant des protocoles d'extraction différents. Les fucanes sulfatés des Fucales sont la plupart de temps constitués de résidus L-fucose liés alternativement en α-1,3 et α-1,4 qui présentent respectivement un ou deux groupements sulfates en C2 et C4 (Chevolot *et*

al., 2001). Au contraire, les Laminariales et Ectocarpales présentent uniquement des résidus L-fucose liés en α-1,3 avec un groupement sulfate en C4 (Nagaoka *et al.*, 1999; Kopplin *et al.*, 2018). La complexité et la variabilité des FCSP les rendent difficiles à caractériser et requièrent des combinaisons de méthodes analytiques poussées. Ainsi, jusqu'à présent, peu d'informations sont connues sur leur structure au niveau moléculaire (Sichert *et al.*, 2021).

Des structures d'hémicelluloses sont également présentes dans la phase matricielle de l'ECM des algues brunes (β-1,3-glucanes et β-1,3-1,4-glucans, Raimundo *et al.*, 2017; Salmeán *et al.*, 2017).

Des teneurs significatives en protéines (3-15 %, proportion toutefois bien inférieure au 40 % approximatifs détectés chez les algues rouges, Mišurcová, 2011), minéraux (7-36 %), phénols (1-13 %), vitamines, acides aminées et lipides (1-5 %) ont été estimées au sein de la MEC des algues brunes (Fleurence, 1999; Galland-Irmouli *et al.*, 1999; Verhaeghe *et al.*, 2008; Deniaud-Bouët *et al.*, 2014; Schiener *et al.*, 2015). Celle-ci est ainsi composée d'un large éventail de composés distincts qui s'enchevêtrent et interagissent ensemble pour former une matrice tridimensionnelle dont l'alginate et les FCSP sont les composés majoritaires. Peu d'informations sont disponibles sur l'agencement des composés et la nature exacte des interactions. D'après une étude réalisée sur des Fucales, il semblerait que les FCSP s'emboitent avec les chaines de β-glucanes, dont la cellulose, et que ce réseau FCSP-cellulose soit englué dans la matrice d'alginate, avec peu de liaisons covalentes entre les deux réseaux (Deniaud-Bouët *et al.*, 2014). De plus, il a été montré que les polymères d'alginate et les phénols sont étroitement interconnectés et qu'ils jouent un rôle majeur dans la rigidité de la paroi (Schoenwaelder and Wiencke, 2000; Deniaud-Bouët *et al.*, 2014). Enfin, il est suggéré que l'alginate serait étroitement associé avec les structures d'hémicellulose β-1,3-1,4-glucanes (Salmeán *et al.*, 2017).

En plus des polysaccharides pariétaux, les macroalgues possèdent également des sucres de réserve à l'intérieur des cellules. Chez les algues brunes, le carbone de réserve est stocké principalement sous forme de laminarine, (β-1,3-glucane avec des branchements β-1,6 occasionnels) qui peut représenter jusqu'à 35 % du poids sec (Michel *et al.*, 2010; O'Sullivan *et al.*, 2010; Schiener *et al.*, 2015) ou de mannitol (polyol du mannose), un exsudat soluble dans le milieu pouvant passer à travers la membrane cellulaire (Groisillier *et al.*, 2014). La proportion de ce dernier varie grandement selon l'espèces d'algue étudiée et peut représenter jusqu'à 20-30 % du poids sec de l'algue pour certaines espèces de laminaires (Kornprobst, 2005; Zubia *et al.*, 2008).

c. Mécanismes de défense

Afin de survivre dans les écosystèmes riches en biodiversité, les macroalgues doivent faire face à de nombreux prédateurs. La première étape pour se protéger d'une attaque est de reconnaître les agresseurs. L'algue peut reconnaitre des molécules spécifiques aux bactéries pathogènes, on parle alors d'éliciteurs exogènes (Nürnberger *et al.*, 2004). Il a également été montré que les algues pouvaient reconnaitre des

oligosaccharides libérés suite à la dégradation de leur propre paroi (Küpper *et al.*, 2001, 2002; Cosse *et al.*, 2007). Ces oligosaccharides sont appelés éliciteurs endogènes.

i. Les espèces réactives de l'oxygène

En réponse aux stress, les macroalgues produisent massivement des espèces réactives de l'oxygène (ROS), telles que les ions superoxyde (O_2^-), le peroxyde d'hydrogène (H_2O_2) ou des radicaux hydroxyles ($HO^\cdot$) (Weinberger and Friedlander, 2000; Küpper *et al.*, 2001; Cosse *et al.*, 2007). C'est ce que l'on appelle communément l'explosion oxydative (*oxidative burst* en anglais), un mécanisme de défense conservés au sein des eucaryotes. Cette réponse s'opère rapidement et est de nature transitoire. Elle a été détectée seulement 2-3 minutes après l'ajout d'oligosaccharides d'alginate (bloc GG) chez *L. digitata*, et pendant 30 min (Küpper *et al.*, 2001). L'explosion oxydative n'est pas déclenchée uniformément chez les différentes espèces, par exemple, si les Laminariales réagissent à l'ajout de bloc d'alginate GG, ce n'est pas le cas des Fucales et Ectocarpales (Küpper *et al.*, 2002). De plus, il a été montré que les produits de dégradation libérés suite à une attaque des tissus algaux induisaient la libération de ROS, mais aussi l'expression de gènes de défense et l'activation du métabolisme de composés halogénés (Cosse *et al.*, 2009).

ii. Les composés halogénés

La libération de composés organiques volatiles halogénés (COVH) est un autre type de mécanisme de défense chez les macroalgues. Ces dernières ont la faculté de concentrer les ions halogénures (iodure, bromure, chlorure) présents dans le milieu environnant. Les algues brunes accumulent en particulier les composés iodés alors que les algues rouges accumulent les composés bromés (Leblanc *et al.*, 2006). Dans le thalle de *L. digitata* par exemple, l'iode peut représenter jusqu'à 5 % du poids sec de l'algue en fonction de la saison et de l'âge des tissus (Küpper *et al.*, 1998; Ar Gall *et al.*, 2004). D'importantes variations sont également observées selon les saisons ou la localisation géographique (Nitschke *et al.*, 2018). Les haloperoxidases vanadium-dépendantes (vHPO) sont des enzymes cruciales dans le métabolisme halogéné des algues puisqu'en présence de H_2O_2 elles catalysent l'oxydation des ions halogénures en intermédiaires halogénés qui peuvent alors réagir avec des composés organiques. Chez les algues rouges, les COVH agissent comme substances biocides, répulsives ou anti-adhésion contre des microorganismes épiphytes, des pathogènes ou des herbivores (Paul *et al.*, 2006). La libération de COVH a été reportée chez *L. digitata* lors d'une attaque simulée de pathogène (Küpper *et al.*, 2008). De plus, il a été montré que les composés halogénés des algues brunes et rouges présentaient pouvaient inhiber la communication cellulaire (*quorum sensing,* QS) (Cosse *et al.*, 2007).

iii. Les composés phénoliques

Les macroalgues brunes produisent des composés phénoliques, tels que les phlorotannins et les phloroglucinols, notamment pour se protéger du rayonnement solaire (Pavia *et al.*, 1997). Les

phlorotannins sont des oligomères de phloroglucinols et sont des analogues structuraux des tannins rencontrés chez les plantes terrestres. La teneur en phlorotannins peut représenter entre 10 et 20 % du poids sec (Amsler and Fairhead, 2005) et est plus importante chez les Fucales que les Laminariales (Holdt and Kraan, 2011). Leur production est induite suite au contact avec des herbivores, rendant l'algue impropre à la consommation pour les brouteurs (Toth and Pavia, 2000; Amsler and Fairhead, 2005). Ces composés présentent de nombreuses activités biologiques, ils sont notamment connus pour leurs propriétés antimicrobiennes, antioxidantes, antitumorales ou antivirales (Zubia *et al.*, 2008). Des études suggèrent que les composés phénoliques interagissent avec la membrane bactérienne et induisent l'inactivation de certaines fonctions. Leur activité serait dépendante de leur degré de polymérisation, avec des composés de faible poids moléculaire potentiellement plus toxiques (Hierholtzer *et al.*, 2013; Shannon and Abu-Ghannam, 2016).

Les algues brunes sont ainsi capables de réguler le développement des bactéries qui colonisent leur surface et de se défendre face aux agressions de bactéries pathogènes. Malgré ces mécanismes de défense, les algues sont colonisées par des communautés microbiennes abondante formant des biofilms.

III. Dégradation bactérienne des polysaccharides algaux

1. Les interactions macroalgues-bactéries

La compétition pour les nutriments et les espaces où se multiplier est féroce au sein des communautés bactériennes. Les algues offrent des sources de nutriments et d'oxygène très prisées ainsi que de larges surfaces à coloniser. Elles sont de ce fait recouvertes d'épais biofilms bactériens d'environ 10-70 µm (Nasrolahi *et al.*, 2012; Han *et al.*, 2018), avec des densités comprises entre 10^3 et 10^9 cellules par cm^{-2} (Martin *et al.*, 2014; Lage and Graça, 2016). Avec les autres microorganismes également présents à la surface des algues, tels que les virus, les archées, les protistes, les champignons et les microalgues, ces bactéries forment le microbiote associé aux algues, on parle alors de microbiote épiphyte. Les communautés bactériennes épiphytes diffèrent largement de celles retrouvées dans l'eau de mer environnante (Lachnit *et al.*, 2009). Les phyla bactériens *Proteobacteria* (principalement les classes *Alphaproteobacteria* et *Gammaproteobacteria*), *Bacteroidetes*, *Verrucomicrobia*, *Actinobacteria* et *Planctomycetes* sont les plus représentés à la surface des trois grandes lignées d'algues (Bengtsson *et al.*, 2010; Hollants *et al.*, 2013; Florez *et al.*, 2017; Lemay *et al.*, 2018). Cependant la présence de taxons communs à l'ensemble des macroalgues n'a pas pu être mise en évidence à des niveaux taxonomiques inférieurs au phylum (Egan *et al.*, 2013; Hollants *et al.*, 2013). La diversité, l'abondance et la composition des communautés épiphytes sont en effet dépendantes de nombreux facteurs biologiques, physiques et chimiques, allant de la composition et de l'âge des tissus algaux, des variations saisonnières à la localisation géographique (Lachnit *et al.*, 2011; Egan *et al.*, 2013; Lage and Graça, 2016; Lemay *et al.*, 2018; Weigel and Pfister, 2019; Ramirez-Puebla *et al.*, 2020; Paix *et al.*, 2021). Chaque niche

écologique résultant de ces différents paramètres abrite ainsi un microbiote unique. La comparaison de différents échantillons provenant de la surface de l'algue verte *Ulva australis* a montré une faible similarité phylogénétique des communautés bactériennes associées mais une importante similarité fonctionnelle, avec un ensemble de gènes impliqués dans la survie à la surface de macroalgues retrouvées chez tous les taxons. Il a été ainsi suggéré que la composition et la structure du microbiote associé aux macroalgues sont gouvernées par des caractéristiques fonctionnelles plutôt que phylogénétiques (Burke *et al.*, 2011).

Les bactéries épiphytes sont à l'origine de multiples interactions avec les macroalgues, qui peuvent être de nature bénéfique, néfaste ou neutre pour l'algue. Un exemple bien connu d'interaction bénéfique est l'association entre les algues vertes du genre *Ulva* avec ses épibiontes (Provasoli L., 1958). Ces derniers secrètent des métabolites, en particulier de la thallusine, permettant à l'algue de réguler sa croissance et la formation du thalle, lui permettant ainsi de se développer normalement en forme de « feuille de laitue » et non en filaments (Matuso *et al.*, 2005; Singh *et al.*, 2011). De plus les bactéries épiphytes apportent des nutriments tels que du CO_2 et de l'azote fixé, nécessaires pour la photoautotrophie des macroalgues. La colonisation bactérienne de l'algue empêche également à des organismes prédateurs de venir se fixer et peut dissuader certains herbivores (Holmström *et al.*, 2002). En particulier, l'espèce *Pseudoalteromonas tunicata* (*Gammaproteobacteria*), isolée de l'algue verte *Ulva lactuca*, a été étudiée pour son importante capacité à sécréter des composés anti-adhésion ciblant de nombreux micro et macroorganismes (Egan *et al.*, 2008; Ballestriero *et al.*, 2010). Les bactéries épiphytes jouent ainsi un rôle crucial dans l'intégrité des macroalgues, leur bon fonctionnement et leur développement.
D'un autre côté, la présence d'autres taxons peut nuire aux macroalgues (différents exemples de telles interactions sont rapportés dans (Egan *et al.*, 2014). Les pathogènes *Nautella italica* R11 et *Pseudovibrio galleciensis* LSS9 par exemple colonisent et infectent l'algue rouge *Delisea pulchra* dont le thalle se décolorent en leur présence (Case *et al.*, 2010; Fernandes *et al.*, 2011; Kumar *et al.*, 2016). Les mécanismes de virulence de ces bactéries sont activés suite à la production de déterminants génétiques du QS. Afin de se défendre l'algue va libérer des composés (furanones) bloquant les molécules induisant le QS. L'action de certains taxons, tels que des membres des genres *Vibrio* et *Pseudoalteromonas*, peut également conduire à l'apparition de moisissures sur l'algue (Gachon *et al.*, 2010). Comme expliqué plus haut, les algues possèdent également des mécanismes de défense généraux leur permettant de lutter contre ces pathogènes, tels que la libération de ROS ou d'antibiotiques.

La mise en évidence de ces diverses interactions entre macroalgues et bactéries épiphytes, et plus généralement entre un hôte et l'ensemble des organismes qui y sont associés, a conduit à l'émergence du concept d'holobionte. Ce concept est basé sur le fait que l'algue et ses organismes associés forment une unité écologique fonctionnelle (Zilber-Rosenberg and Rosenberg, 2008; van der Loos *et al.*, 2019)

et qu'ils devraient être considérés comme tels au cours d'études visant à identifier l'impact de différents paramètres sur les macroalgues.

2. Le rôle crucial des bactéries marines hétérotrophes dans la dégradation algale

Différents mécanismes ont été identifiés concernant le devenir de la biomasse algale. Elle peut être consommée par des herbivores et détritivores, reminéralisée par des microorganismes, enfouie dans les sédiments ou exportée au large de la source d'origine (Duarte and Cebrian, 1996). Il a été démontré que les tissus d'algues sont difficilement assimilables par la plupart des herbivores marins. En effet, la rigidité des tissus, leur contenu pauvre en azote et l'accumulation de métabolites secondaires (composés phénoliques notamment) au sein de la paroi algale repousseraient de nombreux herbivores (Padilla, 1985; Duggins and Eckman, 1997; Granado and Caballero, 2001; Taylor *et al.*, 2002; Norderhaug *et al.*, 2003). Le recyclage de cette source importante de matière organique que représente les macroalgues repose par conséquent majoritairement sur l'action des bactéries marines hétérotrophes (Newell *et al.*, 1982; Seiderer and Newell, 1985; Duggins *et al.*, 1989). Il est estimé que 90 % de la matière organique algale est réinjectée dans les réseaux trophiques supérieurs grâce à l'action des microorganismes (Mann, 1982). Norderhaug *et al.*, 2003 ont en particulier démontré que des thalles de laminaires étaient plus facilement assimilables par la macrofaune après avoir été partiellement dégradés par des communautés bactériennes naturelles. Ainsi, par leur capacité à utiliser et à recycler la matière organique océanique, les bactéries marines hétérotrophes jouent un rôle crucial dans les cycles biogéochimiques du carbone.

Parmi les bactéries marines hétérotrophes, plusieurs taxons impliqués dans le recyclage de biomasse algale ont été identifiés à travers des études de biodiversité, de génomique et de metagénomique. Les membres des phyla *Bacteroidetes*, *Planctomycetes* et *Verrucomicrobia* et de la classe *Gammaproteobacteria* sont notamment largement étudiés dans le contexte de la compréhension des processus de dégradation des polysaccharides algaux (Teeling *et al.*, 2012; Reintjes *et al.*, 2017; Sichert *et al.*, 2020). En particulier, les membres de l'ordre des *Flavobacteriales*, qui, dans une étude répertoriant des bactéries isolées à partir de 159 espèces d'algues (Hollants *et al.*, 2013), a été identifié comme le plus abondant à la surface des algues, sont reconnus pour leur très forte spécialisation dans la dégradation de la matière organique de haut poids moléculaire provenant notamment de la biomasse algale (Kirchman, 2002; Teeling *et al.*, 2012; Fernández-Gómez *et al.*, 2013; Arnosti *et al.*, 2020).

S'il est vrai que la dégradation et l'utilisation des polysaccharides des plantes terrestres ont été massivement étudiées, ces études ne concernent que des polysaccharides dont la composition diffère largement de celle des polysaccharides algaux. Notamment, je l'ai déjà évoqué, les macroalgues produisent, contrairement aux plantes terrestres, de nombreux polysaccharides sulfatés. La diversité et la complexité de la biomasse algale impliquent que des populations bactériennes spécialistes aient

développé des voies cataboliques spécifiques pour sa dégradation. Depuis une vingtaine d'années les études visant à comprendre ces mécanismes se sont multipliés.

3. Mécanismes de dégradation

a. Les CAZymes et sulfatases

Le séquençage et l'annotation complète du premier génome de flavobactérie marine a été réalisé pour *Gramella forsetii* KT0803^T (Bauer *et al.*, 2006) et a révélé la présence de nombreuses enzymes prédites pour agir sur les carbohydrates : les CAZymes (pour *carbohydrate active enzymes*) et les sulfatases (enzymes catalysant le retrait de radicaux sulfate). Depuis, de nombreux génomes de bactéries associées aux algues ont également été annotés, révélant un nombre encore plus conséquent de CAZymes et sulfatases et soulignant leur probable implication dans la dégradation des carbohydrates. En particulier, un fort enrichissement en CAZymes a été observé chez des bactéries pathogènes et saprophytes attaquant la paroi des algues et plantes terrestres (Kaoutari *et al.*, 2013; Brouwer *et al.*, 2014; Barbeyron, Thomas, *et al.*, 2016), représentant jusqu'à 6 % des gènes totaux. La classification des CAZymes a été initiée par le docteur Bernard Henrissat et a posé les bases pour les futures études fonctionnelles, biochimiques, structurales et génomiques des enzymes impliquées dans la dégradation des polysaccharides complexes. Les CAZymes sont ainsi regroupées dans la base de données CAZy (http://www.cazy.org, Lombard *et al.*, 2014) qui comprend 5 grandes classes d'enzymes, les glycoside hydrolases (GH), les polysaccharide lyases (PL), les glycosyl transférases (GT), les carbohydrate estérases (CE) et les enzymes avec une activité auxiliaire (AA). Certaines CAZymes contiennent des modules de fixation aux sucres permettant leur adhésion aux polysaccharides, ces modules sont répertoriés sous l'appellation CBM (*carbohydrate binding module*). A l'intérieur de chaque classe, les CAZymes sont réparties en clans, en familles et sous-familles sur la base de leur similitude de séquence d'acides aminés. L'appartenance à une famille concerne des enzymes avec un repliement et un mécanisme catalytique identique. Cependant, des spécificités de substrat variées sont retrouvées au sein d'une même famille. La base de données contient à ce jour (septembre 2021) 171 familles de GH, 42 familles de PL, 114 familles de GT, 19 familles de CE, 17 familles d'AA et 88 familles de CBM. Les GH sont des enzymes catalysant le clivage des liaisons glycosidiques dans les oligo- et polysaccharides à partir d'une molécule d'eau. Les PL quant à elles n'impliquent pas de molécules d'eau et clivent les chaines d'acides uroniques au sein des polysaccharides par un mécanisme de β-élimination conduisant à la libération d'oligosaccharides insaturés. Les GT ne sont pas impliquées dans le catabolisme des sucres mais dans leur synthèse. Les CE catalysent l'enlèvement des groupements acyle ou alkyle liés aux sucres par une liaison ester. Les AA englobent des enzymes avec une activité d'oxydo-réduction et qui agissent de façon conjuguée avec d'autres CAZymes. Enfin, l'étendue des polysaccharides algaux sulfatés impliquent que les bactéries marines hétérotrophes disposent de sulfatases pour enlever les groupements sulfates. L'ensemble des sulfatases est classifié dans la base de données de SulfAtlas

(http://abims.sb-roscoff.fr/sulfatlas/?execution=e1s1, Barbeyron, Brillet-Guéguen, *et al.*, 2016) et, sur la base de leur similitude de séquence d'acides aminés, sont réparties dans 4 familles distinctes. La grande majorité des sulfatases (90 %) appartient à la familles S1 (sulfatases formyl-glycine dépendantes) qui comprend 83 sous-familles.

Les gènes codant pour ces CAZymes peuvent être isolés au sein des génomes ou bien regroupés dans des structures génomiques dédiées à la dégradation de polysaccharides particuliers, appelées loci d'utilisation de polysaccharides ou PUL (pour *Polysaccharide Utilization Loci*).

b. Les PUL

De tel PUL ont été identifiées au sein des génomes de *Bacteroidetes* (Grondin *et al.*, 2017; McKee *et al.*, 2021) et renvoient à des clusters de gènes colocalisés et corégulés représentant un ou plusieurs opérons qui codent pour des protéines œuvrant à la détection, la séquestration, la dégradation, le transport et l'assimilation de carbohydrates complexes (Bjursell *et al.*, 2006). Le regroupement et la co-expression des enzymes cruciales à l'assimilation des polysaccharides minimise la perte de substrat et favorise ainsi l'efficacité du processus (Martens *et al.*, 2009). Le premier PUL à avoir été identifié est un PUL dédié à l'utilisation de l'amidon chez *Bacteroides thetaiotaomicron* VPI-5482, une bactérie couramment retrouvée dans le microbiote intestinal humain (Anderson and Salyers, 1989; Tancula *et al.*, 1992; Shipman *et al.*, 2000). Depuis, le système de l'utilisation de l'amidon (*starch utilization system* [Sus] en anglais) est un modèle (**Figure I.7**) qui sert de base pour l'identification de nouveaux PUL.

Les PUL de *Bacteroidetes* se caractérisent par la présence d'au moins une paire de gènes homologues aux gènes *susC* et *susD*, communément appelés *susC*-like et *susD*-like et codant pour des protéines ancrées dans la membrane externe. Ces gènes sont toujours l'un à côté de l'autre. Les gènes *susD*-like encodent des protéines se fixant à des fragments du polysaccharide ciblé par le PUL et vont ainsi faciliter leur importation dans le périplasme via des transporteurs TonB-dépendants (TBDT) encodés par les gènes *susC*-like. Le fonctionnement de ce système est analogue à celui de l'ouverture d'une poubelle à pédale. SusC forme un canal pour le passage des oligosaccharides du milieu extracellulaire vers le périplasme, et SusD peut être assimilé au couvercle de ce canal qui s'ouvre afin de se fixer à un oligosaccharide et se referme une fois que l'oligosaccharide est présent dans le canal. Une fois dans le périplasme les oligosaccharides vont subir des étapes de dépolymérisation jusqu'à l'obtention de monosaccharides qui vont pouvoir être transformés et entrer dans les voies centrales du métabolisme du carbone. A noter que dans les tous les génomes bactériens, y compris celui des *Bacteroidetes*, des gènes codant pour des TBDT, sans gène *susD*-like associés, sont présents. Ces TBDT « orphelins » sont alors appelé *fhuA*-like (et non *susC*-like) et ne sont pas impliqués dans l'assimilation des polysaccharides, mais plutôt dans celle de molécules de petites tailles (Ferguson *et al.*, 1998). Les TBDT pour carbohydrates sont également présents dans d'autres phyla bactériens (Gobet *et al.*, 2018; Koch, Freese,

et al., 2019) mais sans leur protéines SusD-like associées. Celles-ci sont à ce jour exclusivement retrouvées qu'au sein du phylum *Bacteroidetes*.

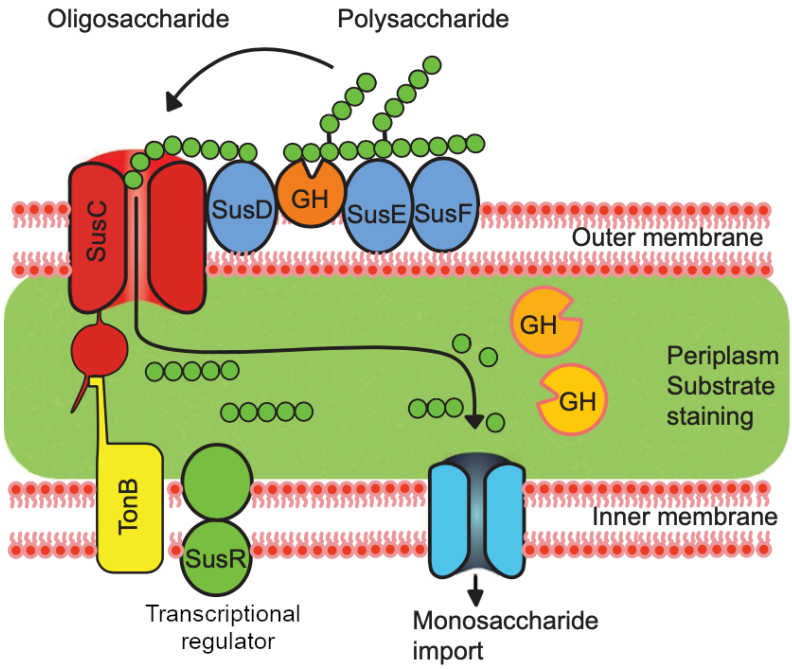

Figure I.7 : Schéma du système d'utilisation de l'amidon, un modèle de PUL. Adapté de Koropatkin et al., 2012 et Reintjes et al., 2017.

Les PUL contiennent également des gènes codant pour des CAZymes spécifiques des différentes liaisons glycosidiques présentes dans le polymère. Elles peuvent agir soit sur des polymères complexes soit sur des oligosaccharides libérés suite à la dégradation de ces polymères complexes. Les CAZymes ciblant les polysaccharides sont en général sécrétées dans le milieu extracellulaire ou ancrées dans la membrane externe, tandis que celles clivant les oligosaccharides issus des polysaccharides sont périplasmiques ou ancrées à la membrane cytoplasmique. En plus de la paire *susCD*-like et des CAZymes, les PUL peuvent également contenir des régulateurs transcriptionnels et d'autres protéines telles que des oxydoréductases, des protéases, des perméases ainsi que des enzymes impliquées dans la modification des monosaccharides. Les PUL ciblant des polysaccharides sulfatés vont également contenir une ou plusieurs sulfatases (Ficko-Blean *et al.*, 2017; Reisky *et al.*, 2019; Sichert *et al.*, 2020). Ainsi les PUL sont des structures génétiques à la base de voies cataboliques complètes (ou presque), permettant la reconnaissance rapide du polymère, sa dégradation en oligomères, leur importation dans la cellule, suivi de leur dégradation en monomère.

De nombreux PUL impliqués dans la dégradation des polysaccharides marins ont été identifiés et caractérisés chez les *Bacteroidetes*. Par exemple, concernant les polysaccharides algaux, des PUL ciblant l'alginate ont été caractérisés chez *Zobellia galactanivorans* Dsij^T (Thomas *et al.*, 2012) et *Gramella forsetii* KT0803^T (Kabisch *et al.*, 2014, ainsi qu'un PUL ciblant la laminarine), tout comme des PUL carraghénanes chez *Z. galactanivorans* Dsij^T (Ficko-Blean *et al.*, 2017) ou un PUL dédié à la

dégradation de l'ulvane chez *Formosa agariphila* KMM 3901^T (Reisky *et al.*, 2019), pour ne citer qu'eux. L'essor des techniques de séquençage de nouvelle génération (NGS) a permis le séquençage massif de génome de bactéries marines hétérotrophes, rendant possible des études de génomique comparative avec des séquences d'enzymes déjà caractérisées et permettant ainsi la prédiction de nouvelles CAZymes et sulfatases et de nouveaux PUL.

L'ensemble des PUL caractérisés expérimentalement et prédits *in silico* est répertorié dans la base donnée PULDB associée à CAZy (http://www.cazy.org/PULDB/index.php, Terrapon *et al.*, 2018). Ils constituent les principaux moyens d'acquisition de nutriments complexes chez les *Bacteroidetes*. La définition originelle d'un PUL, basée sur la présence du couple de gène *susCD*-like, est remise en question (Grondin *et al.*, 2017). Par exemple, un PUL ciblant les carraghénanes chez *Z. galactanivorans* Dsij^T a récemment été caractérisé. Ce dernier, bien que comportant les enzymes nécessaires à la dégradation des carraghénanes, ne possède pas la paire *susCD*-like qui est localisée ailleurs dans le génome, suggérant que l'identification de nouveaux PUL ne devrait pas être restreinte à la seule présence de cette paire de gènes (Ficko-Blean *et al.*, 2017). Ceci suggère également que ces machineries de type PUL ne seraient pas exclusivement réservées au phylum des *Bacteroidetes*. Ainsi, des membres des phyla *Proteobacteria* et *Verrucomicrobia* impliqués dans la dégradation des polysaccharides possèdent des clusters de gènes codant pour des CAZymes (Neumann *et al.*, 2015; Hettle *et al.*, 2019; Koch, Dürwald, *et al.*, 2019; Christiansen *et al.*, 2020; Sichert *et al.*, 2020) mais sont dépourvus du couple *susCD*-like (*susD* étant exclusivement présent chez les *Bacteroidetes*). L'utilisation des carbohydrates peut également reposer, au moins en partie, sur l'action d'enzymes codées par des gènes isolés au sein du génome, qui peuvent agir seules ou de concert, dans le cas de régulons, avec d'autres opérons contenus dans les PUL (Hehemann *et al.*, 2012; Thomas *et al.*, 2012; Ficko-Blean *et al.*, 2017). Des analyses de transcriptomiques ont montré que l'induction des PUL était étroitement contrôlée par la présence du polysaccharide ciblé ou de ses oligosaccharides (Thomas *et al.*, 2012, 2017; Ficko-Blean *et al.*, 2017; Koch, Dürwald, *et al.*, 2019) et qu'en présence de plusieurs polysaccharides, les bactéries pouvaient établir un ordre de priorité pour leur utilisation (Zhu *et al.*, 2016; Koch, Dürwald, *et al.*, 2019).

4. Des bactéries inégalement équipées

Les communautés bactériennes sont composées d'une multitude d'espèces interagissant entre elles via des mécanismes physiques, chimiques et biologiques. Parmi les bactéries utilisant la biomasse algale pour leur croissance, toutes ne possèdent pas les mêmes capacités enzymatiques pour l'assimilation des polysaccharides algaux complexes (Ivanova *et al.*, 2002; Enke *et al.*, 2019). La croissance des différents taxons au sein des communautés bactériennes repose ainsi sur des stratégies écologiques variées et des mécanismes d'interactions spécifiques. Les bactéries capables d'initier la dégradation de polymères complexes via la production d'enzymes extracellulaires sont des consommateurs primaires de la biomasse et sont appelées bactéries pionnières dans la suite du manuscrit. Au cours de la dégradation

des polymères, ces bactéries pionnières vont libérer dans le milieu des produits de dégradation et ainsi exposer de nouveaux substrats. Ceux-ci vont pouvoir être assimilés par d'autres bactéries dépourvues des outils enzymatiques nécessaires au clivage des polymères intacts. Ces bactéries, moins bien équipées, bénéficient ainsi de l'action des bactéries pionnières pour se nourrir et se multiplier, ce sont des consommateurs secondaires, désignées comme des bactéries opportunistes (Hehemann *et al.*, 2016; Jiménez *et al.*, 2017; Enke *et al.*, 2019; Arnosti *et al.*, 2020; Gralka *et al.*, 2020; Pollak *et al.*, 2021; Pontrelli *et al.*, 2021). De telles interactions coopératives au sein de consortium microbiens sont également documentées dans la dégradation de la biomasse des plantes terrestres (Jiménez *et al.*, 2017). Deux types non-exclusifs d'interactions coopératives ont été reportés au cours de l'utilisation de la biomasse (Cavaliere *et al.*, 2017) (**Figure I.8**).

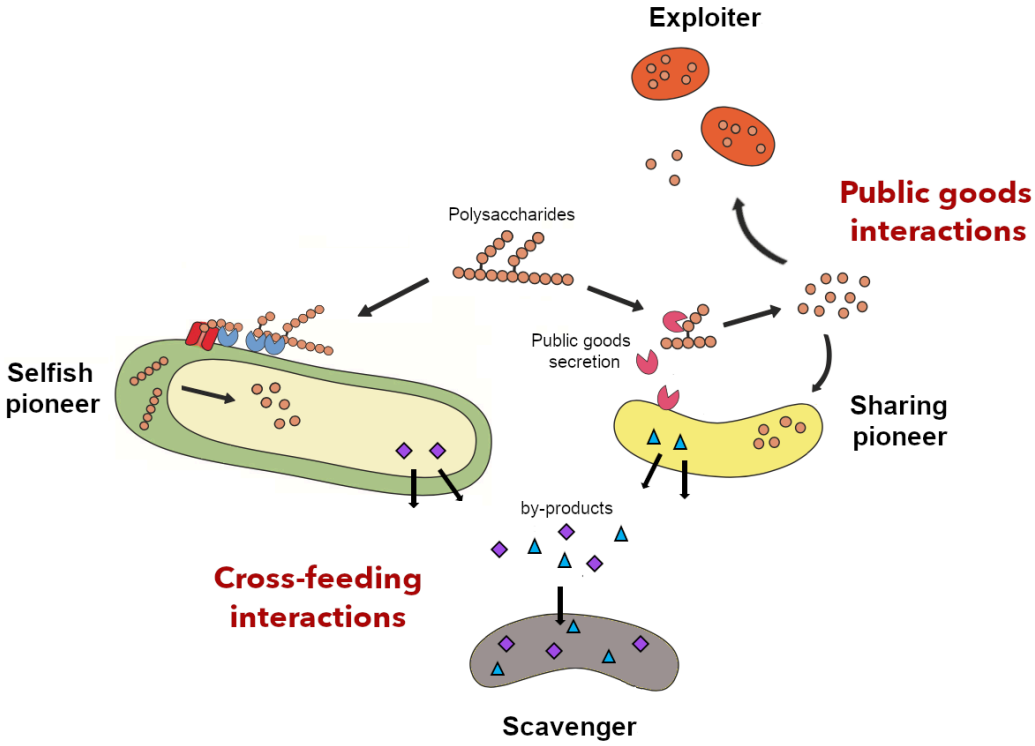

Figure I.8 : Schéma des mécanismes d'interactions coopératives entre bactéries pionnières et opportunistes (*exploiter* ou *scavenger*) Adapté et simplifié de Reintjes *et al.*, 2019.

Premièrement, les interactions peuvent être basées sur la sécrétion dans le milieu de composés dont l'action va être bénéfique au reste de la communauté, de tels composés sont par la suite appelés *public goods* (West *et al.*, 2006; Pontrelli *et al.*, 2021). Les CAZymes sécrétées par les bactéries pionnières sont par exemple considérées comme des *public goods*. Les oligosaccharides résultant de l'action de ces enzymes vont alors pouvoir être utilisés par des bactéries opportunistes spécifiques que l'on qualifiera d'exploiteurs du fait de leur capacité à exploiter les ressources produites par les *public goods* pour leur croissance, sans contribuer à la production des enzymes. La sécrétion de sidérophores, de molécules du QS ou de toxines sont d'autres types de *public goods* identifiés lors d'interactions coopératives (West

et al., 2006). Un second type d'interaction est basé sur la sécrétion de métabolites secondaires par les pionnières au cours du processus de dégradation. Ces sous-produits ou « déchets » peuvent être des acides aminés, des co-facteurs, des acides organiques, des vitamines, etc., et pourraient être directement consommés par des bactéries opportunistes alors qualifiées de charognards (*scavengers* en anglais), on parle alors de *cross-feeding*. De telles interactions ont été notamment mises en évidence au cours de la dégradation d'alginate (Enke *et al.*, 2019) et de chitine (Datta *et al.*, 2016; Pontrelli *et al.*, 2021). Des études suggèrent que les différentes stratégies adoptées par les bactéries pourraient être prédites par l'étude de leur génome (Pollak *et al.*, 2021). Les bactéries pionnières possèderaient un vaste arsenal enzymatique et des voies cataboliques complètes pour la dégradation des polysaccharides complexes. Les exploiteurs auraient des gènes permettant le transport et l'assimilation dans la cellule des oligosaccharides libérés mais seraient dépourvus de certaines enzymes clés permettant la dépolymérisation initiale du substrat. Les *scavengers* quant à eux ne possèderaient pas ou très peu d'enzymes impliquées dans l'utilisation des sucres complexes.

La production d'enzymes extracellulaires par les bactéries pionnières représente un coût énergétique important pour les cellules, qui ne serait rentabilisé que s'il était compensé par l'assimilation des produits hydrolysés. La sécrétion des enzymes dans le milieu favorise la diffusion de l'hydrolysat et augmente ainsi les pertes en substrat au profit des exploiteurs, qui eux se nourrissent sans dépenser d'importante quantité d'énergie. De telles interactions ne seraient donc viables pour les bactéries pionnières qu'en présence d'une forte concentration en substrat. La formation d'agrégats permettrait de minimiser la diffusion des oligosaccharides produits (Ebrahimi *et al.*, 2019). Certaines bactéries pionnières parviennent à privatiser l'hydrolysat en produisant des enzymes extracellulaires ancrées dans la membrane externe et non sécrétées dans le milieu. Elles sont donc en contact direct avec le substrat, ce qui leur permet d'assimiler rapidement les produits de dégradation, limitant ainsi leur disponibilité pour les bactéries opportunistes « exploiteurs » (Traving *et al.*, 2015). De telles bactéries pionnières sont qualifiées de bactéries « égoïstes » (*selfish pioneer*), en opposition aux bactéries pionnières qui partagent (*sharing pioneer*) les produits de dégradation en sécrétant les enzymes dans le milieu (Cuskin *et al.*, 2015; Reintjes *et al.*, 2017, 2019). Ce mode "égoïste" d'assimilation des polysaccharides serait assez répandu puisqu'il serait utilisé par 26 % des bactéries de l'océan Atlantique, dont des membres des *Bacteroidetes*, des *Planctomycetes* et *Gammaproteobacteria* (Reintjes *et al.*, 2017). Par leur capacité à optimiser l'utilisation des substrats, ces bactéries « égoïstes » seraient donc également adaptées à des environnements moins riches en polysaccharides ou pourraient prendre l'avantage sur d'autres bactéries dans des environnements compétitifs (Arnosti *et al.*, 2020). Les enzymes ancrées à la membrane externe représenteraient cependant des outils probablement moins adaptés que des enzymes libres dans le milieu (moins volumineuses) pour la dégradation de substrats difficilement accessibles.

De ces différentes stratégies mises en œuvre pour l'acquisition des nutriments au sein des communautés bactériennes, découlent des dynamiques de succession spécifiques et des régulations complexes des communautés (Datta *et al.*, 2016; Jiménez *et al.*, 2017). Datta *et al.*, 2016 ont par exemple démontré la colonisation rapide de particules de chitine par les communautés naturelles d'eau de mer, suivi d'une sélection de communautés spécifiques produisant des chitinases extracellulaires. Ces dernières seraient ensuite rapidement surpassées par d'autres communautés incapables d'utiliser la chitine comme source de carbone, et se nourrissant probablement de composés issus de la dégradation préalable des particules de chitine.

5. Intérêt des CAZymes dans la valorisation de la biomasse algale

Les macroalgues renferment ainsi une source inestimable de biomolécules possédant diverses propriétés biologiques, structurales et biochimiques (Hentati *et al.*, 2020; Jönsson *et al.*, 2020). Les composés extraits d'algues, que ce soit les polysaccharides, l'iode, les protéines ou les phénols, sont très largement utilisés dans l'industrie.

Les macroalgues sont utilisées depuis le début du 20ème siècle pour leur forte teneur en carbohydrates. L'alginate, les agars et les carraghénanes sont des phycocolloïdes très prisés dans l'industrie cosmétique, agroalimentaire et pharmaceutique. En plus de leurs qualités nutritionnelles, ils sont utilisés comme texturants, épaississants, agents gélifiants, stabilisants ou cryo-protecteurs. On les retrouve par exemple dans les yaourts, les crèmes, les flans, les charcuteries, les dentifrices mais aussi dans la peinture ou la colle. Les FCSP ont été largement étudiés pour des applications biologiques, pharmacologiques et pharmaceutiques. Ils sont en effet reconnus pour leur propriétés anti-tumorales, anti-cancéreuses, anti-coagulantes, anti-oxidantes, anti-virales et anti-inflammatoires (Zayed and Ulber, 2020). Il a été montré que le poids moléculaire des FCSP, leur pureté, leur degré de sulfatation ou leur composition en monosaccharides avait une influence sur ces activités. En particulier, les FCSP de faible poids moléculaire auraient une plus forte valeur ajoutée que ceux de haut poids moléculaire (Zhao *et al.*, 2016; Tsai *et al.*, 2017). Il est donc nécessaire de développer des processus de dépolymérisation des FCSP afin de maximiser leur activité biologique. Ainsi, leur modification par des enzymes agissant sur les FCSP, comme les fucoïdanases et les sulfatases, permettrait l'obtention de biomolécules spécifiques de structure et de taille recherchées (Jönsson *et al.*, 2020). Un constat similaire a également été reporté pour la valorisation des carraghénanes (Zhou *et al.*, 2004). De plus, comme expliqué plus haut, la paroi algale est une matrice 3D complexe où les différents composés sont étroitement liés et donc souvent co-extraits (Sichert *et al.*, 2021). L'utilisation des CAZymes sur ces extraits d'algues seraient un bon moyen de dégrader les composés non-ciblés afin de purifier les molécules d'intérêt.

Bien qu'encore en phase de développement, l'utilisation des macroalgues tend à s'étendre vers d'autres domaines, tels que la chimie verte et les biotechnologies, notamment dans les processus de bioraffinerie

(Nazemi *et al.*, 2021). L'utilisation d'enzymes spécifiques pourrait permettre à terme de minimiser les temps de traitement de la biomasse, les coûts de valorisation ou l'utilisation de produits chimiques lors de la déstructuration de la biomasse (Jung *et al.*, 2013; Filote *et al.*, 2021).

Les bactéries marines dégradant la biomasse algale constituent ainsi un réservoir d'activité pour la production de biomolécules d'intérêt. L'enrichissement de la banque de CAZymes déjà constituée permettrait d'élargir les spécificités de substrats et les modes d'action et d'accroître ainsi le potentiel de ces stratégies enzymatiques, qui représentent, à bien des égards, de puissants outils en vue d'optimiser les processus de valorisation de la biomasse algale.

IV. *Zobellia galactanivorans* Dsij^T, spécialiste de la dégradation des macroalgues

1. Caractéristiques générales du genre *Zobellia*

Le genre *Zobellia* appartient au phylum des *Bacteroidetes* et à la classe des *Flavobacteriia.* Il a été créé par Barbeyron *et al.*, en 2001 lors de la description de *Zobellia galactanivorans* Dsij^T et de la reclassification de [*Cytophaga*] *uliginosa* en *Zobellia uliginosa*. Il regroupe des bactéries hétérotrophes, Gram-négatives, aérobies ayant la forme de bâtonnets et formant des colonies jaune-orange, qui ne possèdent pas de flagelles mais qui se déplacent par glissement. A ce jour, neuf souches valides ont été décrites représentant 7 espèces. *Z. galactanivorans*^{T} Dsij^T a été isolée à partir de l'algue rouge *Delessaria sanguinea* à Roscoff (Barbeyron *et al.*, 2001), *Z. uliginosa* 553^T (Reichenbach, 1989) a été isolée à partir de sable en Californie, 3 souches ont été isolées à Vladivostok (Russie), Z. *amurskyensis* KMM 3526^T dans l'eau de mer, *Z. laminariae* KMM 3676^T de l'algue brune *Laminaria japonica* et *Z. russellii* KMM 3677^T de l'algue verte *Acrosiphonia sonderi* (Nedashkovskaya *et al.*, 2004) et 4 souches ont été isolées à partir de l'algue brune *Ascophyllum nodosum* à Roscoff, Z. *roscoffensis* Asnod1-F08^T, Z. *roscoffensis* Asnod2-B02-B, *Z. nedashkovskayae* Asnod2-B07-B^T et *Z. nedashkovskayae* Asnod3-E08-A (Martin *et al.*, 2015; Barbeyron *et al.*, 2021).

D'autres souches affiliées au genre *Zobellia* mais non officiellement caractérisées ont été isolées à partir de dinoflagellés dans un estuaire de Tasmanie (Australie) (*Zobellia* sp. ACEM 20, Skerratt *et al.*, 2002) ou de sédiments marins sur la côte allemande (*Zobellia* sp. OII3, Harms *et al.*, 2017). Plusieurs études de metagénomiques ont également révélé la présence de membres du genre *Zobellia* dans divers écosystèmes côtiers (Alonso *et al.*, 2007; Martin *et al.*, 2015; Dogs *et al.*, 2017) et 65 souches de *Zobellia* non valides parce que non caractérisées sont référencées dans la base de données du NCBI, la plupart isolées à partir de macroalgues.

Tableau I.2 : Capacité des différentes souches du genre *Zobellia* à hydrolyser et utiliser divers polysaccharides d'origine algale et/ou végétale. Le terme « utilisation de » renvoie à la capacité d'utiliser le composé comme seule source de carbone et d'énergie en milieu minimum. ± : légèrement positif. * : positif sur fucoidane de *A. nodosum* et *L. hyperborea* mais pas de *P. canaliculata*. $: positif dans Nedashkovskaya et al., 2004 mais non confirmé ultérieurement dans Barbeyron et al., 2021. # : communication personnelle de A. Gobet. £ : la croissance de Z. uli n'a pas été testée avec des κ-, ι- et λ-carraghénanes mais une croissance a été détectée avec des μ- et ν-carraghénanes par A. Gobet. NA : données non disponibles. Z. gal : *Z. galactanivorans*^{T} Dsij^T ; Z. uli : *Z. uliginosa* 553^T ; Z. amu : *Z. amurskyensis* KMM 3526^T ; Z. lam : *Z. laminariae* KMM 3676^T ; Z. rus : *Z. russellii* KMM 3677^T ; Z. ros F08 : *Z. roscoffensis* Asnod1-F08^T ; Z. ros B02 : *Z. roscoffensis* Asnod2-B02-B ; Z. ned B07 : *Z. nedashkovskayae* Asnod2-B07-B^T ; Z. ned E08 : *Z. nedashkovskayae* Asnod3-E08-A. A partir de Barbeyron et al., 2001, 2021; Nedashkovskaya et al., 2004.

	Z. gal	**Z. uli**	**Z. amu**	**Z. lam**	**Z. rus**	**Z. ros F08**	**Z. ros B02**	**Z. ned B07**	**Z. ned E08**
Hydrolyse de :									
Amidon	+	-	+	-	+	-	-	-	-
Agar	+	+	+	-$^{\$}$	+	+	+	-	-
Alginate	+	+	+	-	+	-	-	+	+
κ-carraghénane	+	+	-	-	NA	-	-	-	-
ι-carraghénane	+	+	-	-	NA	-	-	-	-
Chitine	-	-	-	-	-	NA	NA	NA	NA
Cellulose	-	-	-	-	-	NA	NA	NA	NA
Utilisation de :									
Amylopectine	NA	+$^{\#}$	+	-	NA	-	-	-	-
Laminarine	+	NA	+	±	NA	-	-	+	+
Lichénine	NA	+$^{\#}$	±	±	NA	±	±	-	-
Arabinoxylane	NA	NA	+	-	NA	-	-	-	-
Fucoidane	+*	-$^{\#}$	+	±	NA	-	-	+	+
Xylane	+	+$^{\#}$	+	-	NA	+	+	-	-
Ulvane	-	-$^{\#}$	+	±	NA	±	±	±	+
Alginate	+	+$^{\#}$	±	±	NA	-	-	+	+
Agar	+	NA	-	-	NA	-	-	-	-
Porphyrane	+	NA	+	+	NA	+	+	+	+
κ-carraghénane	+	NA$^{£}$	-	-	NA	-	-	-	-
ι-carraghénane	+	NA$^{£}$	-	-	NA	-	-	-	-
λ-carraghénane	+	NA$^{£}$	-	-	NA	-	-	-	-
Pectine	-	-$^{\#}$	-	-	NA	-	-	-	-
Xyloglucane	-	-	-	-	NA	-	-	-	-
Arabinane	NA	NA	-	-	NA	-	-	-	-
Galactomannane	-	NA	-	-	NA	-	-	-	-
Glucomannane	NA	NA	-	-	NA	-	-	-	-

Toutes les espèces du genre *Zobellia* ont la capacité de dégrader et d'utiliser au moins un polysaccharide connu pour être contenu dans les parois algales (**Tableau I.2**). L'analyse des génomes des membres du genre *Zobellia* a révélé une forte proportion de gènes (plus de 6 %, cette proportion étant d'environ 1-5 % pour des bactéries marine hétérotrophes de la colonne d'eau) codant pour des CAZymes (Chernysheva *et al.*, 2019, 2021; **Figure I.9**), soulignant l'importante spécialisation de ce genre dans la dégradation de polysaccharides complexes.

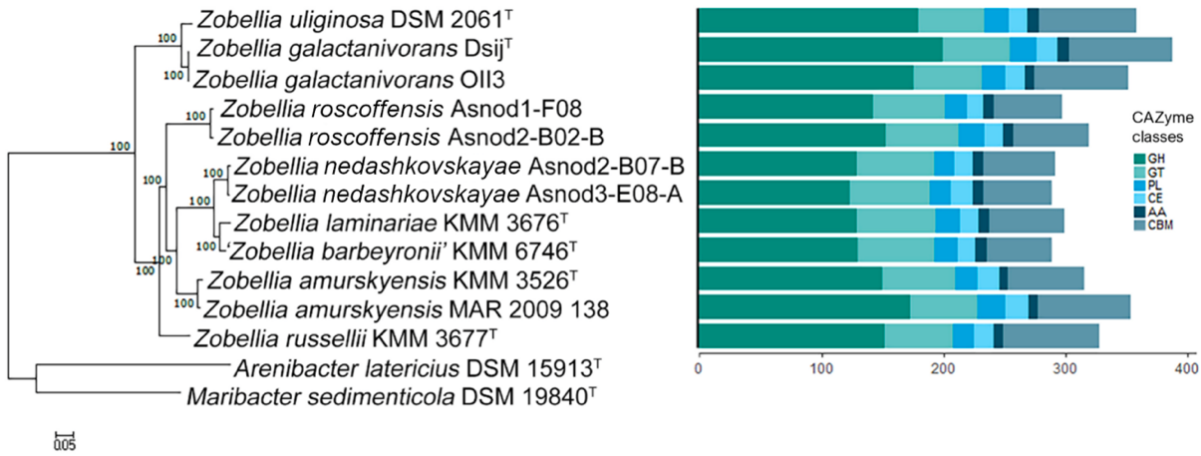

Figure I.9 : Phylogénie du genre *Zobellia* et contenu en CAZymes. Les 9 souches décrites ainsi que 3 souches isolées dont la description n'a pas encore été publiée sont représentés. Le nombre des différents types de CAZymes est indiqué pour chaque souche. Modifié de Chernysheva et al., 2021.

Cependant, les différentes espèces n'utilisent pas de la même manière les différents polysaccharides (**Tableau I.2**). En particulier, seule *Z. galactanivorans* Dsij^T est connue pour utiliser les polysaccharides d'algues rouges agar et carraghénanes pour sa croissance, bien que certaines autres espèces aient la capacité de les hydrolyser.

2. *Zobellia galactanivorans* Dsij^T

a. Généralités

Isolée de l'algue rouge *Delessaria sanguinea* en 1988 à Roscoff (Bretagne, France) pour sa capacité à dégrader les carraghénanes, la souche Dsij était initialement connue sous le nom de '*Cytophaga drobachiensis'* (Potin *et al.*, 1991). Cette souche a ensuite été caractérisée dans les travaux de Barbeyron *et al.*, en 2001 qui ont conduit à la création du genre *Zobellia* dont *Z. galactanivorans*, nommée d'après sa capacité à dégrader les galactanes, est l'espèce type. C'est une espèce aérobie stricte, chemo-organotrophe hétérotrophe qui utilise l'oxygène comme accepteur d'électron. Elle forme des colonies jaune-orange de 1 mm de diamètre sur boite d'agar après 3 jours et les cellules ont la forme de bâtonnets de 0,3-0,4 µm de large sur 3 à 8 µm de long qui se déplacent par glissement à environ 1 µm.s^{-1} (**Figure I.10**). Cette espèce peut croître en milieu de ZoBell (ZoBell and Upham, 1944) entre 13 et 45 °C avec un optimum à 35 °C, entre pH 6 et 8,5 avec un optimum à pH 7 et avec une concentration en NaCl entre 10 et 80 g.l^{-1} avec un optimum de 20-25 g.l^{-1}. Sa résistance à la streptomycine, la kanamycine, la pénicilline, l'ampicilline, la colistine et à la néomycine a été démontrée.

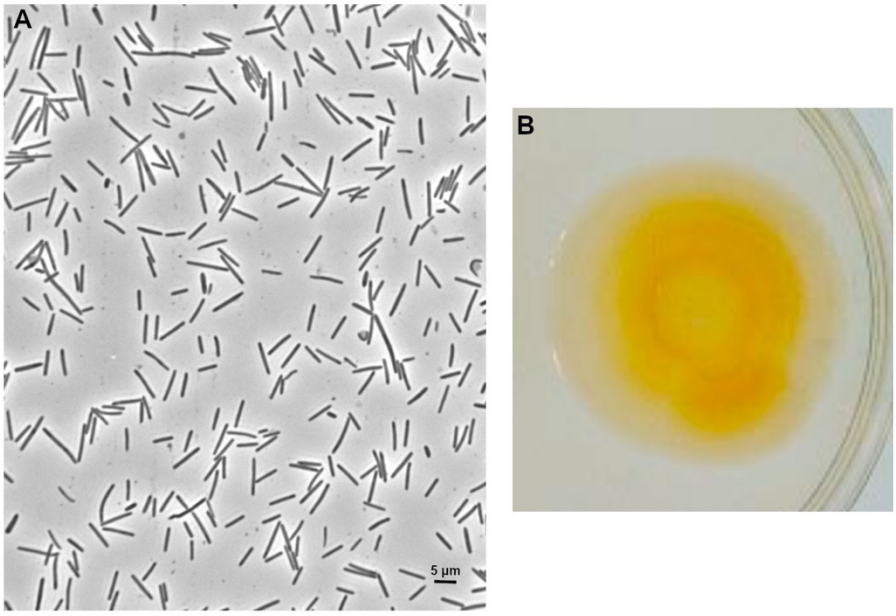

Figure I.10 : *Zobellia galactanivorans* Dsij^T. (A) Culture en milieu liquide observée avec microscope à contraste de phase. (B) Photo d'une colonie sur boite d'agar après 5 jours à 22°C, issue de Barbeyron et al., 2001.

b. Une souche spécialisée dans l'utilisation des polysaccharides algaux

i. Un potentiel génomique de dégradation hors du commun

Comme présenté dans le **Tableau I.2**, *Z. galactanivorans* Dsij^T est capable de dégrader les polysaccharides produits par les algues brunes (alginate, FCSP, laminarine) et les algues rouges (agar, carraghénanes et porphyrane) mais pas ceux des algues vertes (ulvane, xyloglucane). Comme toutes les *Flavobacteriaceae*, elle ne dégrade pas non plus la cellulose, présente dans la phase cristalline des trois phyla d'algues.

Le génome complet de *Z. galactanivorans* Dsij^T, séquencé et annoté par Barbeyron, Thomas, *et al.*, 2016, fait 5 521 712 paires de bases et son coefficient de Chargaff (GC %) est de 42,78 %. Il possède 4738 gènes codant pour des protéines dont plus d'un tiers n'ont pas de fonction connue. Au moment de l'annotation en 2016, 101 peptidases, 141 GH, 15 PL, 18 CE, 56 GT et 37 CBM ont été dénombrées, réparties dans de nombreuses familles différentes (peptidases = 37 familles, GH = 44, PL = 8, CE = 9, GT = 11, CBM = 14). Depuis, de nouvelles enzymes et de nouvelles fonctions ont été identifiées, portant le total à au moins 148 GH (48 familles), 16 PL (11 familles), 18 CE (9 familles), 56 GT (11 familles) et 39 CBM (16 familles). Au total, les CAZymes représentent 6.74 % du génome (Chernysheva *et al.*, 2019). De plus, 71 sulfatases appartenant à 17 sous-familles de la famille S1 ont été dénombrées. Ces totaux sont exceptionnellement élevés puisque qu'au moment de l'annotation de son génome, *Z. galactanivorans* Dsij^T présentait le plus grand nombre de GH, PL et CE et le second plus grand nombre de sulfatases parmi les 125 génomes de bactéries marines hétérotrophes séquencé et référencés dans la base de données CAZy. La plupart de ces CAZymes et sulfatases possèdent des peptides signaux et ont

été prédites pour être localisées dans le périplasme ou ancrées dans la membrane externe (121/141 GH, 14/15 PL and 61/71 sulfatases), suggérant leur sécrétion dans le milieu pour cibler les polysaccharides présents dans l'environnement. En outre, *Z. galactanivorans* Dsij^T possède 119 gènes codant pour des TBDT, dont 71 adjacents à un gène *susD*-like. Concernant les systèmes de sécrétion, tous les gènes essentiels impliqués dans les voies de sécrétion Sec (*general secretion*) et Tat (*twin arginine translocation*) pour la sécrétion des protéines à travers la membrane cytoplasmique sont présents. Elle possède également les gènes du système de sécrétion de Type-IX (T9SS) pour la sécrétion de protéines dans le milieu extérieur. Plusieurs études ont montré que ce système T9SS, présent exclusivement chez les *Bacteroidetes*, était impliqué dans la mobilité par glissement des cellules, la formation de biofilm et la sécrétion de polysaccharidases chez des bactéries mobiles et dans la sécrétion de facteurs de virulence chez des bactéries pathogènes non-mobiles (Sato *et al.*, 2010; Lasica *et al.*, 2017; Eckroat *et al.*, 2021). Les protéines sécrétées par le T9SS ont un domaine C-terminal (CTD) appartenant aux familles TIGRFAM TIGR04131 (protéines impliquées dans la mobilité par glissement) et TIGR04183 (protéines du système de sécrétion Por). Respectivement 13 et 30 protéines (dont plusieurs CAZymes) avec ces CTD ont été dénombrés dans le génome de *Z. galactanivorans.*

La souche *Zobellia galactanivorans* Dsij^T possède ainsi des capacités exceptionnelles pour la dégradation de polysaccharides complexes, leur transport au sein de la cellule et leur assimilation, confirmant les observations physiologiques. Elle est de ce fait considérée comme un modèle pour l'étude de la dégradation et l'assimilation des polysaccharides d'algues (Lami *et al.*, 2021). Un protocole de délétions et de complémentations génétiques a été développé pour cette souche, facilitant l'étude du rôle clé de certains gènes et la rendant encore plus pertinente pour étudier les interactions algue-bactéries (Zhu *et al.*, 2017).

ii. Utilisation de l'alginate

Le mécanisme de dégradation de l'alginate par *Z. galactanivorans* Dsij^T a été découvert par Thomas *et al.*, 2012 (**Figure I.11**). Les gènes impliqués dans la voie de dégradation de l'alginate sont répartis en deux opérons. Le premier, s'étalant du gène *zgal_2613* à *zgal_2624,* comprend notamment les gènes encodant la paire TBDT (*zgal_2621*) / SusD-like (*zgal_2620*), deux alginate lyases AlyA2 (PL7) et AlyA3 (PL17) et un régulateur de la famille GntR, AusR (*zgal_2617*). Le second opéron comprend les gènes *zgal_4130* à *zgal_4132* codant pour les alginates lyases AyA4 (PL6), AlyA5 (PL7) et AlyA6 (PL6). Deux gènes isolés ont également été identifiés, *zgal_1182* et *zgal_4327* codant pour les alginates lyases extracellulaires AlyA1 (PL7 avec CBM32) et AlyA7 (PL14, contient un CTD TIGR04183) qui sont sécrétées en continu par les cellules en absence d'alginate.

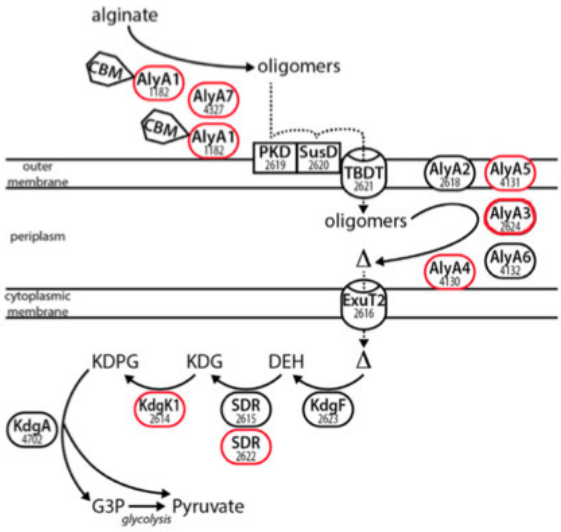

Figure I.11 : Le système de dégradation de l'alginate chez *Z. galactanivorans* Dsij^T. L'activité des enzymes représentées par un cadre rouge a été validée biochimiquement. De Dudek et al., 2020.

En présence d'alginate, les enzymes AlyA1 et AlyA7 vont initier la dépolymérisation du polymère. Leur activité est probablement complémentaire étant donné qu'AlyA1 est une endo-guluronate lyase clivant au sein de blocs GG (Thomas *et al.*, 2013) et que les lyases de la famille PL14 à laquelle appartient AlyA7 clivent des blocs MM (AlyA7 n'a pas été caractérisée biochimiquement et sa spécificité exacte n'est pas connue). Suite à leur action, des oligosaccharides avec une 4,5-insaturation à l'extrémité non réductrice sont libérés et ceux-ci vont inhiber l'action du répresseur transcriptionnel AusR exercée sur les autres gènes du système qui sont alors fortement surexprimés (Dudek *et al.*, 2020) (**Figure I.12**).

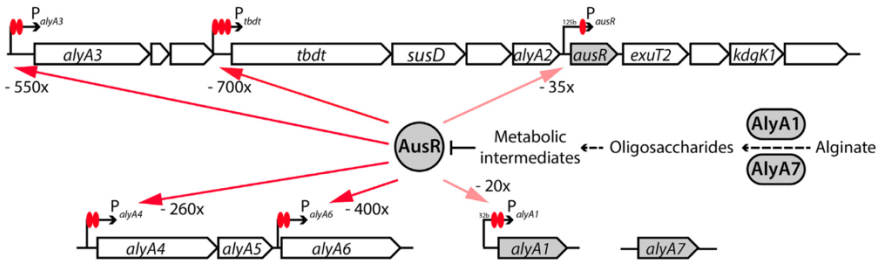

Figure I.12 : Régulation du système alginolytique chez *Z. galactanivorans* Dsij^T. De Dudek et al., 2020.

Les oligomères vont se fixer aux protéines membranaires SusD-like et être importés dans l'espace périplasmique via le TDBT avant d'être clivés en monosaccharides par les autres alginate lyases. En plus d'AlyA1, les exo-lyases AlyA3 (Jouanneau *et al.*, 2021) et AlyA5 (Thomas *et al.*, 2013) ont été caractérisées biochimiquement et clivent préférentiellement les oligo-mannuronates et guluronates respectivement. Les monosaccharides d'acides uroniques insaturés produits par ces enzymes, transformés spontanément ou via l'action de KdgF en acide 4-deoxy-5-keto uronique (DEH), puis importés dans le cytoplasme via la perméase ExuT2 et enfin, entreraient dans la voie d'Entner-Doudoroff (Preiss and Ashwell, 1962) suite à l'action successive des gluconate déshydrogenases et de

la kétodéoxygluconate kinase KdgK1. En présence d'alginate, l'expression d'AlyA7 est réprimée, ceci suggère qu'elle serait une enzyme « sentinelle » : elle aurait un rôle crucial dans les premiers instants de la dégradation en réduisant le poids moléculaire du polymère conduisant au déclenchement du système alginolytique, mais n'aurait plus d'utilité en présence d'oligo-alginates.

ii. Utilisation de la laminarine

Cinq laminarinases (β-1,3-glucanases) ont été prédites dans le génome de *Z. galactanivorans* Dsij^T appartenant aux familles GH16 (LamABCD) et GH64 (LamE). LamC et LamD possèdent un module de fixation aux carbohydrates de la famille CBM6 et CBM42 respectivement. Les 4 GH16 présentent seulement entre 29 et 37 % d'identité de séquence entre-elles et ciblent potentiellement différentes structures de laminarines (Labourel *et al.*, 2015). Les gènes codant pour LamC (*zgal_1010*), LamD (*zgal_1014*) et LamE (*zgal_1011*) sont situés dans la même région génomique. Les protéines qu'ils codent possèdent un CTD appartenant à la famille TIGR04183, suggérant que ces trois laminarinases sont potentiellement sécrétées dans le milieu extracellulaire via le T9SS. LamA et LamC ont été caractérisées biochimiquement (Labourel *et al.*, 2014, 2015) et agissent de manière endolytique préférentiellement sur des β-1,3-glucanes de laminarine d'algues (presque exclusivement pour LamA). LamA est spécialisée dans la dégradation de chaine linéaire de laminarine tandis que l'affinité de LamC pour ce type de substrat est plus faible. De plus, la conformation du site actif de LamC suggère que celle-ci pourrait cliver un polymère de laminarine présentant des ramifications (ce qui n'est pas le cas de LamA), soulignant son rôle probable dans l'initiation de la dégradation de laminarine, une hypothèse renforcée par le fait que cette enzyme soit probablement extracellulaire.

ii. Utilisation des carraghénanes

La voie catabolique complète de carraghénanes contenant des motifs κ, ι et β a été étudiée par Ficko-Blean *et al.*, en 2017 via une approche intégrative mêlant analyses bio-informatiques, biochimiques, transcriptomiques, structurales et génétiques. Elle est basée en particulier sur un PUL spécifique au 3,6-anhydro-D-galactose, allant du gène *zgal_3145* à *zgal_3159* (**Figure I.13**) et n'incluant pas de gènes *susCD*-like. Ceux-ci étant situés ailleurs dans le génome (*zgal_3580* et *zgal_3581*).

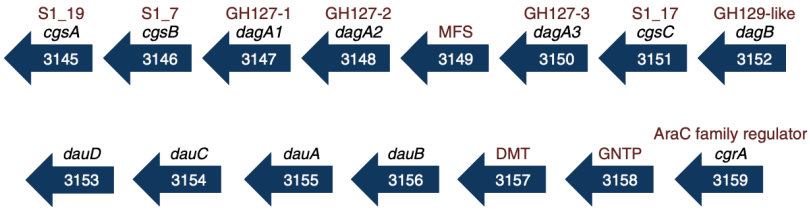

Figure I.13 : Représentation du PUL 3,6-anhydro-D-galactosidase de *Z. galactanivorans* Dsij^T. Le nom des gènes et les familles de CAZymes et sulfatases sont indiqués. De Ficko-Blean et al., 2017.

Ce PUL encode notamment quatre 3,6-anhydro-D-galactosidases (3 de la famille GH127 nommées DagA1, DagA2 et DagA3 et GH129 nommée DagB) ainsi que 3 sulfatases des sous-familles S1_19, S1_7 et S1_17. Des gènes codant pour des enzymes modifiant les monosaccharides (DauA-D), des transporteurs et un régulateur de transcription AraC sont également présents. Il a été établi que les κ- et ι-carraghénanes étaient, dans un premier temps, clivés par une κ-carraghénase de la famille GH16 (CgkA, *zgal_236*) (Barbeyron *et al.*, 1998) et trois ι-carraghénases de la famille GH82, CgiA1 (*zgal_4265*), CgiA2 (*zgal_2155*), CgiA3 (*zgal_1973*) caractérisées antérieurement (Barbeyron *et al.*, 2000; Rebuffet *et al.*, 2010) et distantes du PUL. Les différents produits de dégradation seraient désulfatés par les sulfatases du PUL (entre autres) avant l'action exolytique des 3,6-anhydro-D-galactosidases. Les monosaccharides 3,6-anhydro-D-galactose seraient ensuite modifiés par les enzymes DauA-D avant d'entrer dans la voie de la glycolyse et le cycle de Krebs. Les oligosaccharides produits seraient clivés à l'extrémité non réductrice par des β-galactosidases distantes du PUL avant d'être à nouveau hydrolysés par les 3,6-anhydro-D-galactosidases, et ce jusqu'à la dégradation complète du substrat en monosaccharides (**Figure I.14**).

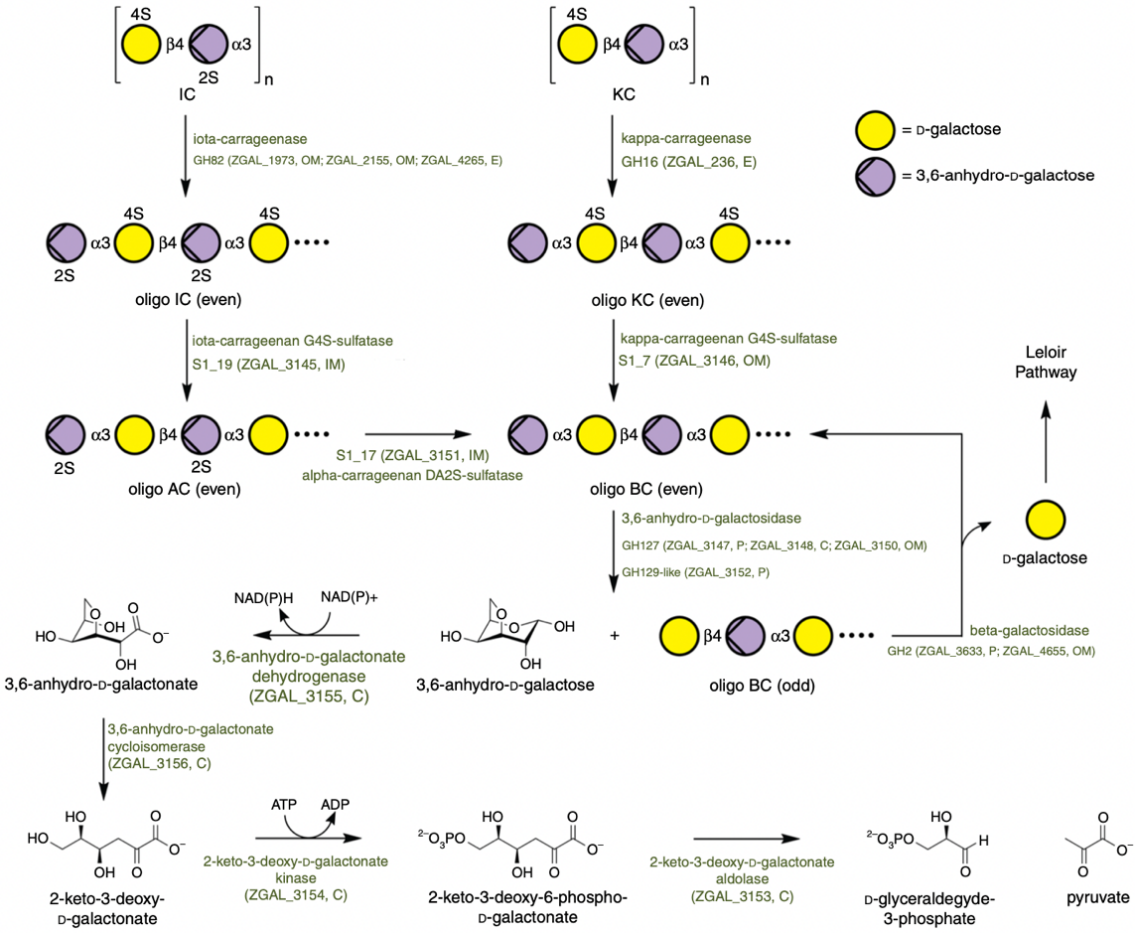

Figure I.14 : Voie métabolique complète de la dégradation des carraghénanes chez *Z. galactanivorans* Dsij^T. Simplifié de Ficko-Blean et al., 2017.

ii. Utilisation des agars

Le génome de *Z. galactanivorans* Dsij^T encode 4 potentielles β-agarases (AgaA-D) et 5 potentielles β-porphyranases (PorA-E) toutes appartenant à la famille GH16 et distantes les unes des autres. Seuls les gènes codant AgaB, PorD et PorE sont localisés au sein de PUL contenant des gènes *susCD*-like. Toutes les β-agarases ont été caractérisées biochimiquement et structurellement (Allouch *et al.*, 2003, 2004; Jam *et al.*, 2005; Hehemann *et al.*, 2010, 2012; Naretto *et al.*, 2019) ainsi que PorA et PorB (Hehemann *et al.*, 2010, 2012; Correc *et al.*, 2011). Ces enzymes présentent d'importantes différences de spécificité, en particulier, AgaC est capable d'hydrolyser des chaines d'agar beaucoup plus complexes (branchement, sulfatations, méthylations, etc.) alors que les autres ciblent préférentiellement des chaines d'agar neutres (Naretto *et al.*, 2019). De plus, AgaD et PorA ont une forte spécificité de substrat alors que AgaB et PorB ciblent des polymères hybrides agar/porphyrane (Hehemann *et al.*, 2012). Enfin, deux 3,6-anhydro-L-galactosidase de la famille GH117 nommées AhgA et AhgB, impliquées dans les dernières étapes du processus de dégradation de l'agar ont également été identifiées et caractérisées (Rebuffet *et al.*, 2011; Ficko-Blean *et al.*, 2015).

Ainsi, toutes ces études ont permis la découverte de nouvelles enzymes et de voies cataboliques complètes impliquées dans la dégradation des polysaccharides algaux purifiés. L'ensemble des CAZymes et sulfatases dont la fonction a été démontrée expérimentalement chez *Z. galactanivorans* Dsij^T est répertorié dans le **Tableau I.3**.

Tableau I.3 : Listes des CAZymes et sulfatases dont la fonction a été démontrée expérimentalement chez *Z. galactanivorans* Dsij^T. La colonne « Caractérisation » indique si les CAZymes ont été caractérisées biochimiquement (B) et structurellement (S).

Nom	Famille	Activité	Type	Gène	Polysaccharide ciblé	Caracté-risation	Références
AlyA1	PL7	alginate lyase	endo	*zgal_1182*	Alginate	B / S	(Thomas *et al.*, 2012, 2013)
AlyA3	PL17		exo	*zgal_2624*		B / S	(Jouanneau *et al.*, 2021)
AlyA4	PL6		?	*zgal_4130*		B	(Thomas *et al.*, 2012)
AlyA5	PL7		exo	*zgal_4131*		B / S	(Thomas *et al.*, 2012, 2013)
AlyA7	PL14		endo	*zgal_4327*		B	(Thomas *et al.*, 2012)
LamA	GH16	laminarinase	endo	*zgal_2431*	Laminarine	B / S	(Labourel *et al.*, 2014)
LamC	GH16		endo	*zgal_1010*		B / S	(Labourel *et al.*, 2015)
CgkA	GH16	κ-carrageenase	endo	*zgal_236*	κ-carraghénane	B / S	(Barbeyron *et al.*, 1998)
CgiA1	GH82	ι-carrageenase	endo	*zgal_4265*	ι-carraghénane	B	(Barbeyron *et al.*, 2000; Rebuffet *et al.*, 2010)
CgiA2	GH82		endo	*zgal_2155*		B	
CgiA3	GH82		endo	*zgal_1973*		B	

CgsA	S1_19	ι-carraghénane G4S-sulfatase	-	*zgal_3145*	ι-carraghénane	B	(Ficko-Blean *et al.*, 2017)
CgsB	S1_7	κ-carraghénane G4S-sulfatase	-	*zgal_3146*	κ-carraghénane	B	(Ficko-Blean *et al.*, 2017)
CgsC	S1_17	α-carraghénane DA2S-sulfatase	-	*zgal_3151*	α-carraghénane	B	(Ficko-Blean *et al.*, 2017)
DagA1	GH127	3,6-anhydro-D-galactosidase	exo	*zgal_3147*	β-carraghénane	B	(Ficko-Blean *et al.*, 2017)
DagA2	GH127		exo	*zgal_3148*		B	(Ficko-Blean *et al.*, 2017)
DagA3	GH127		exo	*zgal_3150*		B	(Ficko-Blean *et al.*, 2017)
DagB	GH129		exo	*zgal_3152*		B / S	(Ficko-Blean *et al.*, 2017)
AgaA	GH16	β-agarase	endo	*zgal_4203*	Agar	B / S	(Allouch *et al.*, 2003, 2004; Jam *et al.*, 2005)
AgaB	GH16		endo	*zgal_3573*	Agar/Porphyrane	B / S	
AgaC	GH16		endo	*zgal_4267*	Agar	B / S	(Naretto *et al.*, 2019)
AgaD	GH16		endo	*zgal_4243*	Agar	B / S	(Hehemann *et al.*, 2012)
PorA	GH16	β-porphyranase	endo	*zgal_2600*	Porphyrane	B / S	(Hehemann *et al.*, 2010)
PorB	GH16		endo	*zgal_1017*	Porphyrane/Agar	B / S	
AhgA	GH117	exo-α-1,3-(3,6-anhydro)-L-galactosidase	exo	*zgal_4663*	Agar	B / S	(Rebuffet *et al.*, 2011; Ficko-Blean *et al.*, 2015)
AhgB	GH117		exo	*zgal_3615*	Agar	B / S	(Ficko-Blean *et al.*, 2015)

Au total 50 PUL possédant la paire de gène *susCD*-like ont été identifiés (Barbeyron, Thomas, *et al.*, 2016) dont certains ont déjà été caractérisés comme décrit au-dessus. A travers l'exemple du système carraghénolytique il est bon de rappeler que la présence du couple *susCD*-like n'est pas une condition nécessaire à la prédiction d'un PUL et qu'il est fort probable que le nombre de PUL présents dans le génome de *Z. galactanivorans* Dsij^T soit sous-estimé.

Bien qu'elle ait la capacité d'utiliser des fucoidanes pour sa croissance (Barbeyron, Thomas, *et al.*, 2016), aucun PUL impliqué dans la dégradation des FCSP n'a été caractérisé fonctionnellement chez *Z. galactanivorans* Dsij^T jusqu'à présent. Cependant, plusieurs PUL putatifs contiennent de nombreuses sulfatases et fucosidases suggérant une activité fucanolytique. De plus, aucun PUL ciblant l'ulvane n'a été prédit chez *Z. galactanivorans*, en adéquation avec le fait que la bactérie n'utilise pas l'ulvane pour sa croissance.

Le transcriptome complet de *Z. galactanivorans* Dsij^T a été étudié au cours de la dégradation d'alginate par micro-arrays (Thomas, 2011) et de divers carraghénanes ou du 3,6-anhydro-D-galactose par RNAseq (Ficko-Blean *et al.*, 2017). Une étude plus générale utilisant des micro-arrays a exploré les régulations induites lors de la dégradation de différents polysaccharides d'algues brunes (alginate et laminarine) et d'algues rouges (agar, porphyrane, κ- et ι-carraghénanes) (Thomas *et al.*, 2017). Ces études ont révélé notamment d'importantes régulations communes lorsque la bactérie était cultivée sur des polysaccharides extraits d'algues d'un même phylum, bien que ces derniers ne présentent pas la même composition chimique. De nombreux gènes et clusters de gènes induits par un ou plusieurs

polysaccharides ont pu être identifiés, dont certains déjà étudiés dans les travaux décrits précédemment, supportant ainsi leur rôle essentiel dans la dégradation de la biomasse algale.

c. Un style de vie adapté pour la colonisation des macroalgues

Différents caractères fonctionnels présents chez *Z. galactanivorans* lui permettent d'établir des interactions stables avec les macroalgues. Elle possède en particulier une forte capacité d'adhérence aux surfaces, formant des biofilms denses et épais. La formation de biofilm est favorisée par la présence de mannitol, un exsudat sécrété constitutivement pas les algues brunes (Salaün *et al.*, 2012). *Z. galactanivorans* Dsij^T a la capacité d'utiliser le mannitol pour sa croissance. Un cluster de gènes a notamment été identifié pour son rôle dans l'utilisation du mannitol et une mannitol-2-dehydrogenase (ZGAL_4263) ainsi qu'une fructokinase (ZGAL_4264) ont été caractérisées biochimiquement par Groisillier *et al.*, 2015.

Comme expliqué précédemment, les macroalgues présente différents mécanismes de défense pour prévenir les attaques d'herbivores, de pathogènes ou la colonisation de micro-organismes épiphytes, tels que la libération de ROS ou de composés iodés (Küpper *et al.*, 2008; Cosse *et al.*, 2009). Le génome de *Z. galactanivorans* Dsij^T présente de nombreux gènes impliqués dans des systèmes de défense et de résistance face au stress oxydatif (Barbeyron, Thomas, *et al.*, 2016). En particulier, 2 catalases, 8 péroxidases, 2 superoxyde dismutases, 10 péroxyredoxines et 9 thiorédoxines sont présentes pour détoxifier les espèces réactives de l'oxygène. On dénombre également 1 gluthatione reductase et 3 thiorédoxine reductases qui sont impliquées dans la réponse au stress oxidatif. Les dommages causés par les ROS seraient potentiellement réparés par 5 méthionines sulfoxide réductases. *Z. galactanivorans* serait également capable de réduire l'oxyde nitrique en diazote par l'action successive d'une oxyde nitrique réductase et d'une oxyde nitreux réductase.

Trois vHPO homologues aux enzymes algales (Colin *et al.*, 2005) ainsi qu'une iodotyrosine dehalogenase et une halo-acide déhalogénase (HAD) sont également présentes. Les vHPO permettraient à la bactérie d'accumuler d'importante quantité d'iode, près de 100 fois plus que les quantités retrouvées dans l'eau de mer (Barbeyron, Thomas, *et al.*, 2016). Deux de ces vHPO ont été caractérisées fonctionnellement et structurellement par Fournier *et al.*, 2014, démontrant leur spécificité envers les iodures (ZGAL_1262 et ZGAL_2088 nommées vIPO1 et vIPO2). C'est également le cas de l'enzyme HAD dont l'implication dans le mécanisme de déshalogénation d'acides bromo et iodoacétique a été démontrée (Grigorian *et al.*, 2021). Ces différentes enzymes permettraient donc à *Z. galactanivorans* de lutter contre les ROS mais également contre les composés halogénés produits par les algues en transformant les espèces I^- et H_2O_2 en I_2, H_2O et O_2. Il a été montré que l'ajout de diiodométhane (CH_2I_2), impliqué dans la défense chimique des algues, n'inhibe pas la formation de biofilm par *Z. galactanivorans*, suggérant la capacité de cette dernière à résister aux composés halogénés libérés par les algues (Salaün *et al.*, 2012).

V. Objectifs du sujet de recherche / Research project objectives

Français

Les processus de dégradation de la biomasse algale reposent largement sur l'action des bactéries marines hétérotrophes. Cette introduction témoigne de l'étendue des progrès qui ont été réalisés ces dernières années dans la compréhension des mécanismes de dégradation des polysaccharides, en particulier de ceux extraits de la biomasse algale. Cependant, dans les écosystèmes naturels, les polysaccharides sont rarement retrouvés sous leur forme soluble et en tant que substrats uniques. Comme précédemment décrit, chez les algues, les polysaccharides font partie d'un réseau tridimensionnel complexe et sont étroitement interconnectés entre eux et à d'autres molécules aux propriétés diverses. Ils sont donc certainement beaucoup moins facilement identifiables, accessibles et biodisponibles pour les bactéries que sous leur forme purifiée. La majorité des travaux menés jusqu'à présent étaient focalisés sur l'utilisation de polysaccharides solubles purifiés, qui sont des substrats de choix pour la facilité de la mise en œuvre et la reproductibilité des expérimentations. Cependant, ces travaux ne représentent certainement pas la complexité des réponses mises en œuvre par les bactéries marines hétérotrophes pour dégrader une paroi d'algue, et passent donc potentiellement à côté d'enzymes cruciales dans le recyclage de la biomasse algale. Zhu *et al.*, en 2016 ont analysé la réponse transcriptomique de *Bacillus weihaiensis* Alg07 lors de sa croissance sur de la poudre d'algue. Bien que cette étude ait été menée sur de la biomasse totale d'algue, englobant ainsi la mixture de substrats renfermée dans les parois, elle ne reflète pas la complexité structurale et l'agencement des différents composés au sein des parois. Très récemment, la croissance d'*Alteromonas macleodii* 83-1 a été testée en présence de tissus frais de l'algue brune *Ecklonia radiata,* mais aucune croissance ou dégradation de l'algue n'a été observée en dépit de son aptitude à utiliser l'alginate purifié (Koch *et al.*, 2020). Une étude préliminaire sur *Zobellia galactanivorans* Dsij^{T} a au contraire démontré la capacité de cette dernière à utiliser des tissus frais de *Laminaria digitata* pour sa croissance et à induire une dégradation visible des tissus (Zhu *et al.*, 2017). La délétion du gène de l'alginate lyase AlyA1 a mis en lumière le rôle clé de cette enzyme dans ce processus. Ainsi, si beaucoup de bactéries peuvent utiliser les composés algaux présents sous forme soluble (polysaccharides purifiés, protéines), ces nouvelles études suggèrent que des populations bactériennes distinctes ont évolué et se sont spécialisées dans la dégradation de biomasse hautement complexe comme les tissus algaux intacts (Hehemann *et al.*, 2016). Zhu *et al.*, 2017 ont également révélé de possibles interactions coopératives entre *Z. galactanivorans* Dsij^{T} et d'autres taxons (**Figure I.15**). En particulier, des membres du genre *Tenacibaculum* (*Flavobacteriaceae*) sont capables de croître sur des tissus de *L. digitata* uniquement en présence de *Z. galactanivorans* Dsij^{T}. Après 8 jours, ces taxons représentaient ¼ des communautés bactériennes en présence de *Z. galactanivorans* contre moins de 0,1 % en son absence. Cette étude suggère donc le rôle pionnier de *Z. galactanivorans* Dsij^{T}, par sa

capacité à initier l'attaque de tissus algaux, une biomasse complexe, et à favoriser la croissance d'autres taxons, en exposant potentiellement de nouvelles niches écologiques.

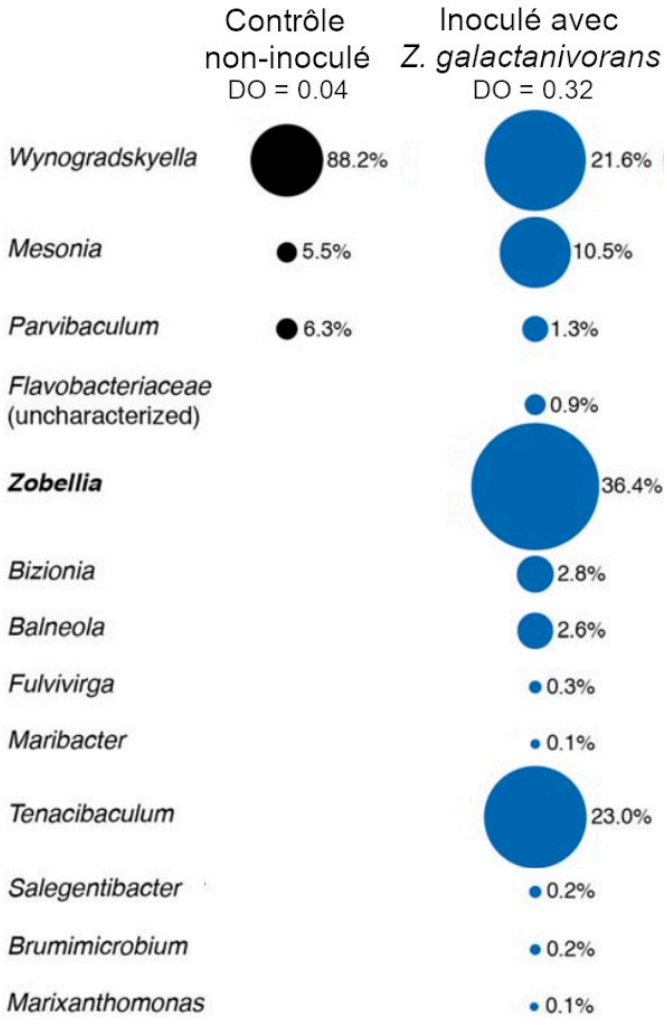

Figure I.15 : Composition des communautés bactériennes au cours de la dégradation de *L. digitata*. Composition déterminée par metabarcoding du gène de l'ARNr 16S à 8 jours au sein de microcosmes contenant des tissus de *L. digitata* comme seule source de carbone dans lesquels *Z. galactanivorans* Dsij^T a été inoculé (droite) ou non (gauche). Modifié de Zhu et al., 2017.

Cette thèse s'inscrit dans le cadre du projet ALGAVOR. Financé par l'agence nationale de la recherche (ANR-18-CE02-0001-01) et coordonné par François Thomas, ce projet cherche à élucider les mécanismes impliqués dans la dégradation des macroalgues. Les différents chapitres de cette thèse s'articulent en particulier autour de deux thèmes centraux qui sont (i) l'exploration des voies métaboliques des bactéries pionnières impliquées lors de la dégradation de macroalgues fraîches et (ii) la compréhension des processus de dégradation des tissus à l'échelle des communautés bactériennes, via la mise en évidence de différentes stratégies écologiques. Pour répondre à ces problématiques, la souche *Zobellia galactanivorans* Dsij^T a été utilisée comme modèle de bactérie pionnière pour toutes les raisons précédemment évoquées dans cette introduction.

En particulier, je me suis attachée à répondre aux questions suivantes :

- Quel est l'impact de l'accumulation et de la dégradation de macroalgues sur les communautés bactériennes épiphytes ?
- Quelle est la prévalence, l'abondance et l'activité du genre *Zobellia* dans les habitats dominés par les macroalgues ?
- Quels sont les voies métaboliques impliquées pendant la dégradation de macroalgues fraîches par les bactéries pionnières ?
- Quels sont les déterminants génétiques du comportement pionnier ?
- Quels sont les mécanismes d'interactions entre bactéries pionnières et opportunistes lors de la dégradation d'algues fraiches ?

Le **Chapitre II** présente en détail l'ensemble des méthodes de microbiologie, biologie moléculaire, biochimie, microscopie et bio-informatiques mises en œuvre dans cette thèse. Il répertorie l'ensemble des produits chimiques, substrats, souches bactériennes, amorces et sondes utilisées.

Le **Chapitre III** s'attache à investiguer les processus de recyclage de biomasse algale à travers l'étude de la dynamique des communautés bactériennes. Une collaboration avec une autre équipe de recherche de la Station Biologique de Roscoff nous a permis d'étudier *in situ* l'impact de l'accumulation et de la dégradation de laminaires sur les communautés bactériennes épiphytes et celles présentes dans le sédiment. La mesure des variations de structure et de composition des communautés a été réalisée par metabarcoding du gène de l'ARN 16S puis couplée aux métadonnées environnementales et à des analyses de prédictions fonctionnelles. Ces données ont permis d'obtenir une première vue d'ensemble de la succession des communautés bactériennes au cours de la dégradation des macroalgues et d'émettre des hypothèses quant aux différentes stratégies écologiques adoptées.

Le **Chapitre IV** s'intéresse plus particulièrement au genre *Zobellia* au sein des communautés naturelles épiphytes. Malgré son rôle majeur dans la dégradation de la matière organique complexe, ses stratégies écologiques dans l'environnement restent encore méconnues. Des approches de PCR (polymerase chain reaction) quantitative (qPCR) et de fluorescence *in situ* par hybridation ont été optimisées et validées sur des échantillons environnementaux pour la détection spécifique des membres du genre *Zobellia* dans les habitats dominés par les macroalgues (**Partie 1**). La technique de qPCR a par la suite été utilisée dans le but de réaliser un suivi saisonnier de la prévalence, l'abondance et l'activité du genre *Zobellia* à la surface de diverses macroalgues (**Partie 2**).

Dans le **Chapitre V**, le transcriptome complet de *Z. galactanivorans* Dsij^{T} lors de sa croissance sur trois macroalgues d'espèces différentes a été comparé à celui obtenu sur polysaccharides purifiés. L'objectif était de révéler les stratégies métaboliques impliquées spécifiquement lors de dégradation de tissus d'algues fraiches et de souligner ainsi l'intérêt de considérer la paroi algale dans son ensemble dans les

études de dégradation. Les aptitudes de dégradation des autres *Zobellia* spp. ont également été évaluées et couplées à des analyses de génomique comparative afin d'identifier de potentiels déterminants génétiques du caractère pionnier.

Ces analyses transcriptomiques ont permis de révéler l'induction de plusieurs PUL en présence de macroalgues fraîches. Le **Chapitre VI** se concentre sur la caractérisation préliminaire de l'un d'entre eux, prédit pour cibler des structures de FCSP. L'activité des protéines recombinantes purifiées a été testée sur différents polysaccharides afin de déterminer le substrat naturel du PUL.

Dans le **Chapitre VII**, j'ai tenté de mettre en évidence et de caractériser des mécanismes d'interactions coopératives entre bactéries pionnières et opportunistes lors de l'utilisation de tissus d'algues fraiches. En particulier, plusieurs souches du genre *Tenacibaculum* ont été testées pour leur capacité à bénéficier des produits de dégradation libérés par *Z. galactanivorans* Dsij^{T}.

Enfin, dans le **Chapitre VIII** je discute l'ensemble des résultats obtenus au cours de ce projet de thèse et aborde les perspectives qui en découlent.

English

Macroalgae are dominant primary producers in coastal ecosystems and constitute a large reservoir of organic matter worldwide. It is long known that heterotrophic bacteria, particularly *Flavobacteriia* and *Gammaproteobacteria*, are crucial for algal biomass recycling and its reinjection into higher trophic levels. Numerous works focused on the degradation and assimilation of purified algal polysaccharides, leading to the characterization of Polysaccharides Utilization Loci (PUL) and the discovery of new carbohydrates active enzymes (CAZymes). However, in natural ecosystems, polysaccharides are rarely found under their soluble form and as unique substrate. Within macroalgae, they are part of a complex tridimensional network and tightly cross-linked between each other and with others compounds. Consequently, they are likely less easily detectable, accessible and bioavailable for bacterial communities compared with their soluble form. To date, most of the studies focused on the utilization of purified soluble polysaccharides, as they are easy to work with. Nevertheless, those studies probably do not represent the complexity of the responses implemented by marine heterotrophic bacteria to degrade the algal ECM, and might then miss key enzymes involved in macroalgal biomass recycling. Zhu *et al.*, in 2016 analyzed the transcriptome of *Bacillus weihaiensis* Alg07 during the utilization of algal powder. This study considered the whole mixture of the different compounds present within the ECM, but does not reflect the structural complexity of its architecture. Very recently, the growth of *Alteromonas macleodii* 83-1 was tested with fresh tissues of the brown algae *Ecklonia radiata*, but no

tissues damage or bacterial growth was detected (Koch *et al.*, 2020) despite its abilities to use purified alginate. By contrast, a preliminary study demonstrated the capacity of *Zobellia galactanivorans* Dsij^T to use fresh *Laminaria digitata* tissues and to cause visible tissues degradation (Zhu *et al.*, 2017). Deletion of the alginate lyase gene *alyA1* shed light on its crucial role during this degradation process. Thereby, if many bacteria can use algal compounds under soluble form for their growth, these recent studies suggest that specific bacterial communities had evolved and specialized in the degradation of complex biomass such as intact algal tissues (Hehemann *et al.*, 2016). Zhu *et al.*, 2017, also revealed putative cooperative interaction between *Z. galactanivorans* Dsij^T and other taxa (**Figure I.16**). In particular, members of the genus *Tenacibaculum* (*Flavobacteriaceae*) were able to grow on *L. digitata* tissues only in the presence of *Z. galactanivorans*. After 8 days, *Tenacibaculum* spp. represented ¼ of the bacterial communities in the presence of *Z. galactanivorans* but were not detected in its absence. Hence this study reported that *Z. galactanivorans* Dsij^T, by its abilities to initiate the breakdown of macroalgae and to favor the growth of other taxa, might act as a pioneer bacteria during algal degradation.

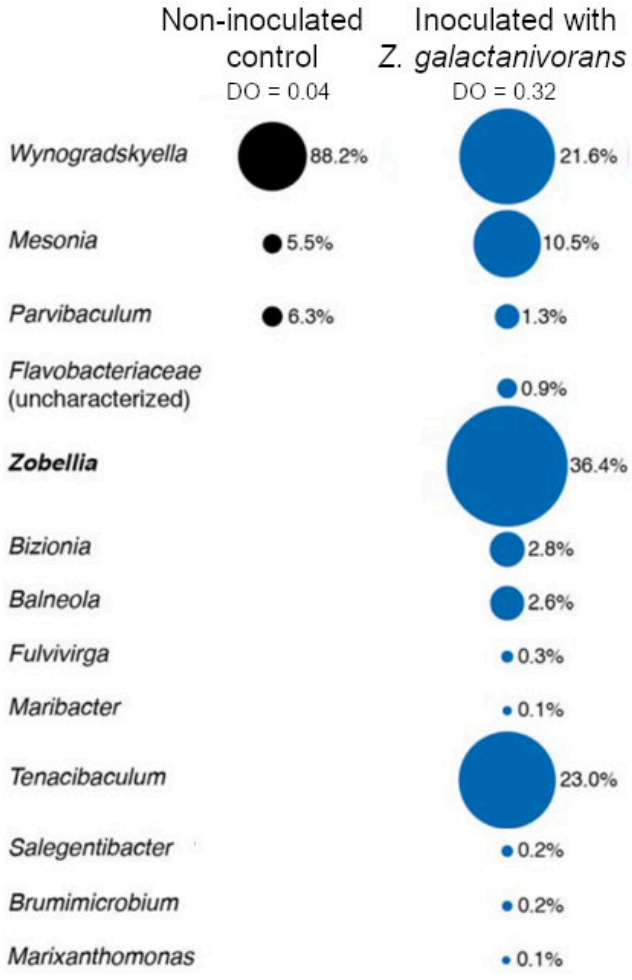

Figure I.16: Composition of the bacterial communities during the degradation of *L. digitata*. Composition was assessed by 16S rRNA gene metabarcoding after 8 days in microcosms containing *L. digitata* tissues as the sole carbon source inoculated *with Z. galactanivorans* Dsij^T (right) or non-inoculated (left). Adapted from Zhu et al., 2017.

This thesis is part of the ALGAVOR project. Financed by the national research agency (ANR-18-CE02-0001-01) and coordinated by François Thomas, this project seeks to unravel the mechanisms involved in macroalgae degradation. The different chapters of this thesis are organized around two central themes: (i) the exploration of pioneer bacteria metabolic pathways involved during the degradation of fresh macroalgae; (ii) the understanding of the processes involved in tissue degradation at the community scale, via the identification of ecological strategies. *Zobellia galactanivorans* Dsij^T strain was used as a model of pioneer bacteria to investigate these issues. In particular, I have focused on the following questions:

- What are the dynamics of macroalgae microbiota during their *in situ* accumulation and degradation?
- What is the prevalence, abundance and activity of the genus *Zobellia* in macroalgae-dominated habitats?
- Which metabolic pathways are involved during the degradation of fresh macroalgae by pioneer bacteria?
- What are the genetic determinants of the pioneer behavior?
- What are the interaction mechanisms between pioneer and opportunist bacteria during fresh macroalgae degradation?

Chapter II encompasses the different methods in microbiology, molecular biology, biochemistry, microscopy and bioinformatics applied during this thesis. It lists all the used chemical, substrates, bacterial strains, primers and probes.

Chapter III investigates the algal biomass recycling mechanisms by monitoring the dynamics of the associated bacterial communities. We studied the impact of kelp *in situ* accumulation and degradation on the epiphytic communities, as well as on the underlying sediment communities. The bacterial community composition was assessed using 16S rRNA gene metabarcoding, and the functional diversity was inferred *in silico*. These data were then linked to the associated environmental parameters, to determine the factors driving both functional and taxonomic diversity. This study allowed to glimpse into the succession of bacterial communities occurring during the macroalgal breakdown, making possible the formulation of hypotheses concerning the different ecological strategies involved.

Chapter IV examines more closely the genus *Zobellia* among natural epiphytic communities. Despite its prominent role in complex organic matter degradation, *Zobellia* ecological strategies remain poorly characterized. Quantitative polymerase chain reaction (qPCR) and catalyzed reporter deposition-Fluorescence *In Situ* Hybridization (CARD-FISH) methods were optimized and validated on natural environmental samples in order to specifically detect representatives of the *Zobellia* genus in macroalgae dominated habitats (**Part 1**). The qPCR technique was next implemented in the context of a seasonal

monitoring, quantifying the prevalence, abundance and activity of *Zobellia* at the surface of diverse macroalgae (**Part 2**).

In **Chapter V**, the full transcriptome of *Z. galactanivorans* Dsij^T obtained during its growth on three different macroalgae species was compared to one obtained on purified polysaccharides. The objectives were to unravel the metabolic strategies involved in the breakdown of complex, fresh macroalgae, and underline the necessity of studying the whole algal ECM during degradation studies. We also evaluated the degradation capacity of different *Zobellia* spp. and compared their genomic content to identify potential genetic determinants of pioneer bacteria.

The transcriptomic analyses performed during Chapter V revealed the induction of several PULs in the presence of fresh macro-algae. **Chapter VI** focuses on the preliminary characterization of one of these PULs, predicted to degrade fucose-containing sulfated polysaccharides (FCSPs). The purified recombinant proteins obtained were tested using different polysaccharides in order to determine the natural substrate of the PUL.

In **Chapter VII**, I tried to evidence and characterize cooperative interaction mechanisms between pioneer bacteria and opportunist bacteria during the use of fresh algae tissues. In particular, several strains belonging to the *Tenacibaculum* genus were tested to highlight whether they could exploit degradation products released by *Z. galactanivorans* Dsij^T.

Finally, **Chapter VIII** discusses the overall results obtained during this thesis projet and the future perspectives.

Chapter II:

Material & Methods

I. Chemical and natural compounds

Chemical products and natural compounds used in the different chapters are listed below (**Table II.1**).

Table II.1: List of the chemical products and carbohydrates used in this thesis with the respective supplier. FCSP: Fucose-containing sulfated polysaccharides.

Chemical products	Supplier
16 % Paraformaldehyde (PFA)	Electron Microscopy Science
Phosphate Buffer Saline (PBS)	Amresco
96 % ethanol (EtOH)	CARLO ERBA
96 % molecular biology grade ethanol	CARLO ERBA
X-100 Triton	Sigma-Aldrich
10 % povidone-iodine	Bought in drugstore
Sodium chloride (NaCl)	Sigma-Aldrich
Magnesium sulfate ($MgSO_4$)	Sigma-Aldrich
Hydrated magnesium chloride ($MgCl_2 \cdot H_2O$)	Sigma-Aldrich
Potassium chloride (KCl)	Sigma-Aldrich
Ammonium chloride (NH_4Cl)	Sigma-Aldrich
Calcium chloride ($CaCl_2$)	Alfa aesar
Sodium bicarbonate ($NaHCO_3$)	AnalaR
Dipotassium hydrogen phosphate (K_2HPO_4)	Sigma-Aldrich
Trizma base (Tris)	Sigma-Aldrich
37 % Hydrochloric acid (HCl)	CARLO ERBA
Ferrous sulfate ($FeSO_4$)	VWR Prolabo
Kanamycin	Sigma-Aldrich
Streptomycin	Sigma-Aldrich
Neomycin	Sigma-Aldrich
Colistin	Sigma-Aldrich
Ampicillin	Sigma-Aldrich
Sodium azide (NaN_3)	Merck
Guanidine thiocyanate	Sigma-Aldrich
Sodium acetate	Sigma-Aldrich
N-Lauroyl sarcosinate	Sigma-Aldrich
Phenol pH 4	Sigma-Aldrich
Phenol pH 7	Sigma-Aldrich
Chloroform:isoamyl alcohol	Sigma-Aldrich
RNAse-free water	Sigma-Aldrich
Turbo DNAse	Thermofisher
DNAse inactivation reagent	Thermofisher
Ethylenediaminetetraacetic (EDTA)	Sigma-Aldrich
Lysozyme	Sigma-Aldrich
Proteinase K	Sigma-Aldrich
Sodium dodecyl sulfate (SDS)	Sigma-Aldrich
3-(N-morpholino)propanesulfonic acid (MOPS)	Sigma-Aldrich
Glycerol	CARLO ERBA
Orange G	Sigma-Aldrich
Yeast extract	Fisher
Tryptone	Fisher
Glycine	Sigma-Aldrich
Ammonium persulfate (APS)	Sigma-Aldrich
N,N,N',N'-tetramethylethylenediamine (TEMED)	Fluka
Imidazole	Sigma-Aldrich
EDTA-free Protease Inhibitor Cocktail	Merck
Bromophenol blue	Bio-Rad
Coomassie blue	BDH
Dithiothreitol (DTT)	Sigma-Aldrich

Acetic acid	CARLO ERBA
Potassium hexacyanoferrate (III)	Sigma-Aldrich
2-aminoacridonein (AMAC)	Sigma-Aldrich
Dimethyl sulfoxide (DMSO)	Sigma-Aldrich
Sodium cyanoborohydride ($NaBH_3CN$)	Sigma-Aldrich
Phenol red	Sigma-Aldrich
Alcian blue	Interchim
Silver nitrate	VWR Prolabo
Sodium carbonate	Sigma-Aldrich
Ethyl acetate	Fluka
Napthoresorcinol	Sigma-Aldrich
Sulfuric acid	CARLO ERBA
Lithium nitrate ($LiNO_3$)	Fluka
Ammonium bicarbonate	Sigma-Aldrich
Hydrogen peroxide (H_2O_2)	Sigma-Aldrich
Citifluor	Euromedex
Vectashield	Eurobio
Formamide	Sigma-Aldrich
Alexa Fluor 546/488 carboxylic acid, succinimidyl ester	Life Technologies
Electroendosmosis (ME) agarose	Merck-Millipore
Methanol (MeOH)	CARLO ERBA
Blocking reagent	Roche
Dextran sulfate	Sigma-Aldrich

Carbohydrates	**Supplier**
Maltose	Sigma-Aldrich
Agarose	Eurogentech
Glucose	Sigma-Aldrich
Sucrose	Sigma-Aldrich
Alginate mainly from *Laminaria digitata*	Danisco
Alcohol Insoluble Residues from *Pelvetia canaliculata*	internal
FCSP from *Chorda filum*	Elicityl
FCSP from *Cladosiphon okamuranus*	Carbosynth
FCSP from *Durvillaea potatorum*	Carbosynth
FCSP from *Ecklonia maxima*	Carbosynth
FCSP from *Fucus serratus*	Carbosynth
FCSP from *Fucus vesiculosus*	Carbosynth
FCSP from *Laminaria digitata*	Carbosynth
FCSP from *Laminaria japonica*	Carbosynth
FCSP from *Lessonia nigrescens*	Carbosynth
FCSP from *Macrocystis pyrifera*	Carbosynth
FCSP from *Pelvetia canaliculata*	internal
FCSP from *Undaria pinnatifida*	Elicityl
Heparin from Porcine intestinal mucosa	Sigma
Pectin from apple	Sigma
Pectin from citrus	Sigma
Ulvan from *Ulva armoricana*	Elicityl
Agar	Sigma-Aldrich
Kappa-carrageenans from *Eucheuma cottonii*	Goëmar
Iota-carrageenans	Danisco

II. Sample collection in the field

To assess the succession of bacterial communities during kelp degradation (Chapter III), an *in situ* experiment was implemented from April 2017 to October 2017 in the bay of Morlaix (48°42'33.78'' N, 003°57'12.36'' W, Brittany, France) by the EDYCO team (UMR7144) during Florian de Bettignies' PhD thesis. The system set up is detailed in de Bettignies *et al.*, 2020. Briefly, cages were randomly filled with 1 kg of new blades from young healthy adult *Laminaria hyperborea* sporophytes (140–200 cm). A total of 35 cages were set at 9 m depth on a sandy floor. Three cages were randomly selected at each sampling time to collect algal surfaces, underlying and external sediments and overlying water as follows. Ten algal pieces of 1.3 cm diameter were subsampled from each cage using a sterilized stainless-steel punch. The surface sediments (0–4 cm depth) directly below each cage (underlying sediment) or 2 m away from the cages (external sediment) were sampled in sterile plastic containers. Three liters of the overlying water (1 m above the cages) were taken using Niskin bottles. Triplicates of 1 l were prefiltered at 3 µm to remove large particles and then filtered through a 0.2 µm Sterivex filter (Merck). All samples were stored at −80 °C before DNA extraction.

For specific detection of *Zobellia* spp. in the environment (Chapter IV), microbiota at the surface of algae were sampled each month during low tides with a high tidal coefficient (> 80) between February 2020 and January 2021. Due to the Covid-19 pandemic, no sampling was done in April and May 2020. Macroalgae were quickly rinsed with Autoclaved 0.2 µm Filtered SeaWater (AFSW) before microbiota were collected using sterile swabs (ZymoBiomics) on healthy specimens of *Laminaria digitata*, *Fucus serratus*, *Ascophyllum nodosum*, *Palmaria palmata* and *Ulva lactuca* at the Bloscon site (48°43'29.982'' N, 03°58'8.27'' W) in Roscoff (France). Three individuals of each species were sampled. Additionally, samples from stranded algae were retrieved: within the mixture of diverse decomposing algae, microbiota from one *L. digitata*, one *F. serratus* and one *P. palmata* specimens were collected each month. Swabbed surface was standardized to 50 cm^2 using a 5-cm square template on both sides of the algal thallus when possible (**Figure II.1A**). For *Ascophyllum nodosum*, a 1 cm-width frond was sampled over 25 cm on both sides. Three different regions of the kelp *L. digitata* were sampled: the basal meristem (young tissue, hereafter LdigB), the medium frond (ca. 20 cm away from the meristem, hereafter LdigM) and the old frond (the blade tip, hereafter LdigO). Swabs were immersed in DNA/RNA Shield reagent (ZymoBiomics), kept on ice during transport and stored at -20 °C until DNA and RNA extraction. For CARD-FISH analysis, algal pieces from the same individuals were collected using a 1.3 cm diameter ethanol-sterilized stainless-steel punch (**Figure II.1B**). Algae pieces were rinsed with autoclaved seawater and placed directly in 2 % PFA in PBS overnight at 4 °C. All fixed samples were washed twice in PBS and stored in PBS:EtOH (1:1 v/v) at -20 °C.

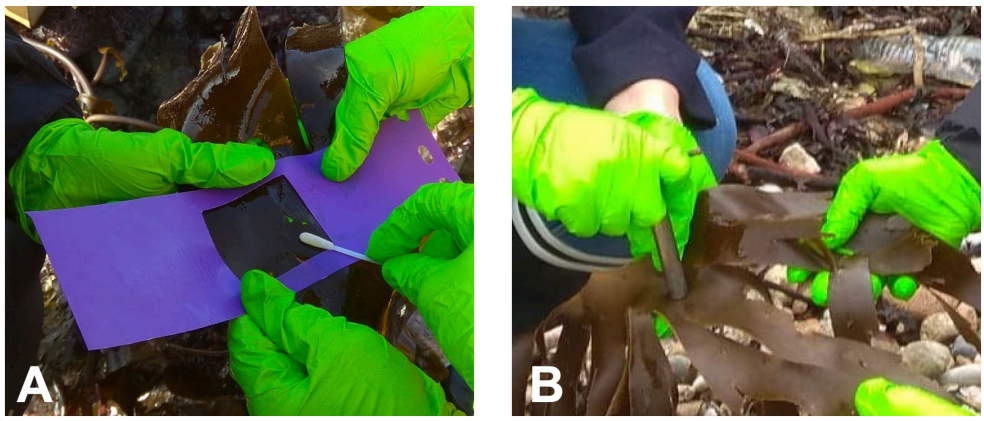

Figure II.1: Photographs taken during sample collection on the seashore. (A). A standardized algal surface was swabbed for *Zobellia* specific quantification using qPCR. (B) Algae pieces were sampled for *Zobellia*-single cell visualization using CARD-FISH.

For microcosm experiments (Chapter V and VII), whole healthy algae were collected at the same site (Bloscon, Roscoff) in plastic bag, rinsed with filtered seawater and used immediately or alternatively stored overnight in filtered seawater in 5 l bottle at 16 °C with aeration under day/night light cycle.

III. Microbiology

1. Bacterial strains

All the bacterial strains used in this thesis are listed in **Table II.2**.

Table II.2: List of the different bacterial strains used in this thesis. The context of their utilization is indicated.

Strains name	Utilization	References
Zobellia galactanivorans Dsij^T	Utilization of fresh macroalgae (Chapter V), Experimental validation of the ZOB137 FISH probe (Chapter IV), Characterization of interactions with *Tenacibaculum* sp. (Chapter VII)	(Barbeyron *et al.*, 2001)
Zobellia amurskyensis KMM 3526^T	Utilization of fresh macroalgae (Chapter V)	(Nedashkovskaya *et al.*, 2004)
Zobellia laminariae KMM 3676^T	Utilization of fresh macroalgae (Chapter V)	(Nedashkovskaya *et al.*, 2004)
Zobellia russellii KMM 3677^T	Utilization of fresh macroalgae (Chapter V), Experimental validation of the ZOB137 FISH probe (Chapter IV)	(Nedashkovskaya *et al.*, 2004)
Zobellia roscoffensis Asnod1-F08^T	Utilization of fresh macroalgae (Chapter V)	(Barbeyron *et al.*, 2021)
Zobellia roscoffensis Asnod2-B02-B	Utilization of fresh macroalgae (Chapter V)	(Barbeyron *et al.*, 2021)
Zobellia nedashkovskayae Asnod2-B07-B^T	Utilization of fresh macroalgae (Chapter V)	(Barbeyron *et al.*, 2021)
Zobellia nedashkovskayae Asnod3-E08-A	Utilization of fresh macroalgae (Chapter V)	(Barbeyron *et al.*, 2021)
Zobellia galactanivorans Dsij^T *ΔalyA1*	Characterization of interactions with *Tenacibaculum* sp. (Chapter VII)	(Zhu *et al.*, 2017)
Zobellia galactanivorans Dsij^T *ΔausR*	Characterization of interactions with *Tenacibaculum* sp. (Chapter VII)	(Dudek *et al.*, 2020)
Tenacibaculum adriaticum B390^T	Opportunist taxon candidate (Chapter VII)	(Heindl *et al.*, 2008)

Tenacibaculum aestuarii SMK-4^T	Opportunist taxon candidate (Chapter VII)	(Jung *et al.*, 2006)
Tenacibaculum aiptasiae a4^T	Opportunist taxon candidate (Chapter VII)	(Wang *et al.*, 2008)
Tenacibaculum amylolyticum C526^T	Opportunist taxon candidate (Chapter VII)	(Suzuki *et al.*, 2001)
Tenacibaculum caenipelagi HJ-26M^T	Opportunist taxon candidate (Chapter VII)	(Park and Yoon, 2013)
Tenacibaculum crassostreae JO-1^T	Opportunist taxon candidate and experimental validation of the TEN281 FISH probe (Chapter VII)	(Lee *et al.*, 2009)
Tenacibaculum dicentrarchi USC 35/09^T	Opportunist taxon candidate (Chapter VII)	(Piñeiro-Vidal *et al.*, 2012)
Tenacibaculum discolor LL04 11.1.1^T	Opportunist taxon candidate (Chapter VII)	(Piñeiro-Vidal, Riaza, *et al.*, 2008)
Tenacibaculum gallaicum A37.1^T	Opportunist taxon candidate (Chapter VII)	(Piñeiro-Vidal, Riaza, *et al.*, 2008)
Tenacibaculum geojense YCS-6^T	Opportunist taxon candidate (Chapter VII)	(Kang *et al.*, 2011)
Tenacibaculum halocynthiae P-R2A1-2^T	Opportunist taxon candidate (Chapter VII)	(Kim *et al.*, 2013)
Tenacibaculum jejuense CNURIC013^T	Opportunist taxon candidate (Chapter VII)	(Oh *et al.*, 2012)
Tenacibaculum litopenaei B-I^T	Opportunist taxon candidate (Chapter VII)	(Sheu *et al.*, 2007)
Tenacibaculum litoreum CL-TF13^T	Opportunist taxon candidate (Chapter VII)	(Choi *et al.*, 2006)
Tenacibaculum lutimaris TF-26^T	Opportunist taxon candidate and experimental validation of the TEN281 FISH probe (Chapter VII)	(Yoon *et al.*, 2005)
Tenacibaculum maritimum R2^T	Opportunist taxon candidate (Chapter VII)	(Suzuki *et al.*, 2001)
Tenacibaculum mesophilum CIP107215^T	Opportunist taxon candidate (Chapter VII)	(Suzuki *et al.*, 2001)
Tenacibaculum ovolyticum EKD 002^T	Opportunist taxon candidate (Chapter VII)	(Suzuki *et al.*, 2001)
Tenacibaculum skagerrakense D30^T	Opportunist taxon candidate and experimental validation of the TEN281 FISH probe (Chapter VII)	(Frette *et al.*, 2004)
Tenacibaculum soleae LL04 12.1.7^T	Opportunist taxon candidate and experimental validation of the TEN281 FISH probe (Chapter VII)	(Piñeiro-Vidal, Carballas, *et al.*, 2008)
Tenacibaculum xiamenense WJ-1^T	Opportunist taxon candidate (Chapter VII)	(Li *et al.*, 2013)
Maribacter forsetii KT02ds18-6^T	Negative control to assess ZOB137 specificity (Chapter IV)	(Barbeyron *et al.*, 2008)
Marinirhabdus citrea MEBiC09412^T	Negative control to assess ZOB137 specificity (Chapter IV)	(Yang *et al.*, 2018)
Lewinella marina MKG-38^T	Negative control to assess ZOB137 specificity (Chapter IV)	(Khan *et al.*, 2007)
Imperialibacter roseus P4^T	Used as negative control to assess the specificity of the TEN281 FISH probe (Chapter VII)	(Wang *et al.*, 2013)
Escherichia coli BL21 (DE3)	Expression of recombinant proteins (Chapter VI)	internal

2. Macroalgae treatment

a. Optimization

Several chemical and physical methods were tested to remove the resident epiphytic bacteria and limit bacterial contamination during the growth experiments. Under microbial hood, cut algal pieces of a red alga from the genus *Gracilaria* were rinsed in AFSW for 5 min and immersed in different solutions, either in 40 % ethanol (during 30 sec or 2 min), 50 % ethanol (20 sec or 1 min), 1 % bleach (15 and 30 sec), 0.1 % X-100 Triton (10 min) or in 0.5 or 1 % povidone-iodine (3 and 5 min). Treatment combinations were also tried: 40 % ethanol + 1 % bleach (10 sec each) or 0.1 % X-100 Triton or SDS (10 min) + 1 % povidone-iodine (5 min). Treated algal pieces were then rinsed in AFSW for 5 min, let air-dried for 15 min and rubbed on ZoBell 2216-agar (15 g.l^{-1} agar, 5 g.l^{-1} tryptone, 1 g.l^{-1} yeast extract,

100 ml milliQ water and filled with FSW to 1 l) in Petri dishes with sterile tweezers. Ethanol and bleach baths rapidly led to algae bleaching and those methods were not retained as they caused too many damages to the algae. For the other treatments, the tissues were not discolored and still in good shape. Less colonies were observed after 5 days on the Petri dishes with the treatment 0.1 % X-100 Triton (10 min) + 1 % povidone-iodine (5 min). The efficacy of this treatment was then assessed in liquid marine minimum medium as the degradation experiments will be carried out in this medium (see composition below). Bacterial growth was followed by OD_{600} measurement and **Figure II.2** shows that this treatment induced a reduction of the growth of epiphytic bacteria. Algae were also treated with UV (10 min) or sonication (15 min) prior to this chemical treatment but it did not improve the results. Then, the combination 0.1 % X-100 Triton (10 min) + 1 % povidone-iodine (5 min) appeared to remove significant amount of epiphytic bacteria without altering the algae thallus. It was then decided to apply this method for further experiments and to complement the medium with antibiotics to which *Z. galactanivorans* $Dsij^T$ is resistant to limit even more the growth of contaminants.

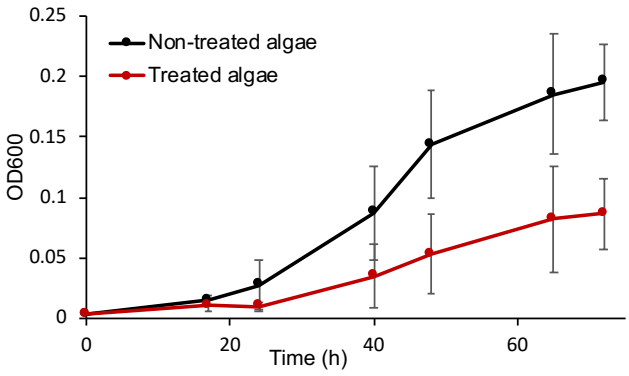

Figure II.2: Effect of the chemical treatment of algal pieces on the bacterial growth. Treated algae were immersed 10 min in X-100 Triton followed by 5 min in 1 % povidone-iodine. Values are mean of independent duplicates ± standard error.

b. Validated protocol

Before addition to microcosms (Chapters V and VII), algal tissues were cut in small pieces (2.5-3.5 cm^2 approximately) with a sterile scalpel in Ø 15 mm Petri dishes and immersed in 0.1 % X-100 Triton in milli-Q water for 10 min followed by 1 % povidone-iodine in milli-Q water for 5 min to clean them from the resident epibiotic microbiome. Algae pieces were rinsed by successive baths (at least five) in excess AFSW for 2 h to remove Triton and povidone-iodine traces as well as potential algal exudates released upon cutting.

3. Pre-cultures

For algal degradation by *Zobellia* spp. (Chapter V), bacterial strains were first grown from glycerol stock in Zobell 2216 medium (ZoBell, 1941) before being inoculated in Marine Minimum Medium referred to as MMM (24.7 $g.l^{-1}$ NaCl, 3.08 $g.l^{-1}$ anhydrous $MgSO_4$, 4.6 $g.l^{-1}$ $MgCl_2 \cdot H_2O$, 2 $g.l^{-1}$ NH_4Cl,

0.7 $g.l^{-1}$ KCl, 0.6 $g.l^{-1}$ $CaCl_2$, 0.2 $g.l^{-1}$ $NaHCO_3$, 0.6 $g.l^{-1}$ K_2HPO_4, 47.6 mM Tris-HCl pH8, 0.02 $g.l^{-1}$ $FeSO_4 \cdot 7H_2O$ and vitamins (5 $\mu g.ml^{-1}$ of pyridoxine HCl and orotic acid, 1 $\mu g.ml^{-1}$ nicotinic acid, thiamine HCl, riboflavine, D,L-pantothenic acid, D-biotin, folic acid, cyanocobalamine and ascorbic acid, 10 $\mu g.ml^{-1}$ 4-aminobenzoic acid) and complemented with 100 $\mu g.ml^{-1}$ kanamycin, 100 $\mu g.ml^{-1}$ streptomycin, 50 $\mu g.ml^{-1}$ neomycin and 14 $\mu g.ml^{-1}$ colistin, to which *Zobellia* spp. are resistant) amended with 4 $g.l^{-1}$ maltose. For co-culture experiments (Chapter VII), pre-cultures were only carried out in Zobell 2216 medium as *Tenacibaculum* spp. have limited ability to use simple sugars in MMM. Pre-cultures were grown at room temperature under agitation for 3 days. After centrifugation (3200 *g*, 10 min), pellets were washed twice in 1X saline solution (24.7 $g.l^{-1}$ NaCl, 3.08 $g.l^{-1}$ anhydrous $MgSO_4$, 4.6 $g.l^{-1}$ $MgCl_2 \cdot H_2O$, 0.7 $g.l^{-1}$ KCl) to remove any carbon trace. Cells were inoculated in microcosms at an initial optical density at 600 nm (OD_{600}) of 0.05.

4. Cultures in microcosms

Strains were grown at 20 °C at 180 rpm in MMM with 4 $g.l^{-1}$ purified sugars or macroalgae pieces as the sole carbon source (10 algal pieces for 50 ml of medium in 250 ml erlenmeyer, 3 algal pieces for 10 ml of medium in 50 ml falcon tubes). Each condition was done in triplicate or duplicate depending on the experiments. All vessels were previously autoclaved.

Co-culture systems (**Figure II.3**) consisting of two 100 ml reaction vessels with round bottom and a 65 mm flat edge opening (ref 0861050, Witeg, Germany), separated by a 0.2 µm mixed cellulose ester (MCE) filter (ref GSWP09000, Merck, Germany) were used. Thirty milliliters of MMM were poured in each compartment and 10 *L. digitata* pieces were immersed in one of them.

Bacterial growth within the microcosms was monitored by measuring OD_{600} with a spectrophotometer (Jenway) using plastic cuvettes (Sarstedt) filled with 800 µl of medium. Dilutions were performed when $OD_{600} > 0.8$. When algae fragments were present, they were allowed to settle prior OD measurement. Alternatively, OD_{600} were also measured using a microplate reader (Spark, Tecan) in 96-wells microplates (Greiner Bio-One) containing 200 µl of solution.

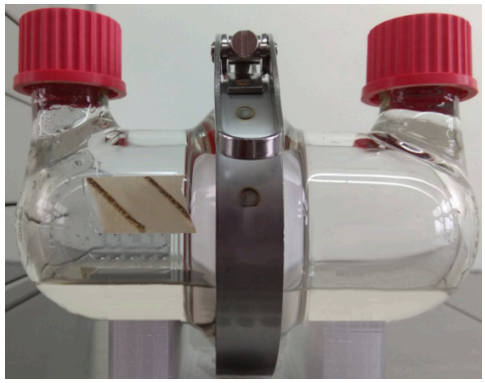

Figure II.3: Co-culture system with two compartments separated by a filter (here 0.2 µm). Bacterial cells cannot pass the filter, but it allows for metabolic exchanges. This specific vessel is sold by Witeg (ref 0861050, Germany).

5. Protein expression

Cloning of the different target genes into the expression vector pFO4 (fusion His-tag) and plasmid transformation in *Escherichia coli* BL21 (DE3) expression strain was previously done by Robert Larocque in the Marine Glycobiology group according to Groisillier *et al.*, 2010. Glycerol stocks of the recombinant strains were swabbed on LB-agar Petri dishes supplemented with ampicillin (100 $\mu g.ml^{-1}$) and resistant colonies precultured in 5 ml of LB-Ampicillin medium at 37 °C overnight. Expression of the recombinant proteins was performed in the auto-inducible ZYP-5052 medium (Studier, 2005) containing ampicillin (100 $\mu g.ml^{-1}$) for 72 h under agitation at 20 °C. For expression in small volume, 5 µl of the preculture were inoculated in 5 ml of ZYP medium in 50 ml Falcon tubes. Cells pellets were recovered after centrifugation (3200 *g*, 10 min, 4 °C). For large-scale production, 5 ml of preculture were added in 1 l of ZYP medium in 5 l Erlenmeyer flasks. The 1 l ZYP culture was divided in 4 x 250 ml volumes and centrifuged at 8000 *g* for 20 min at 4 °C. Cell pellets were stored at -20 °C until further purification.

IV. Molecular biology

1. PCR primers

The different primers used for routine PCR or qPCR/RT-qPCR are listed in **Table II.3**.

Table II.3: List of the different primers used for PCR or qPCR.

Name	Target	Sequence (5' to 3')	Reference
142F	*Zobellia*	CCTACTGTGGGATAGCCCAG	Chapter IV
285R	*Zobellia*	GCGGTCTTGGTGAGCCG	Chapter IV
289R	*Zobellia*	CATCGCGGTCTTGGTGA	Chapter IV
294R	*Zobellia*	CTACCCATCGCGGTCTT	Chapter IV
926F	Universal	AAACTCAAAKGAATTGACGG	(Bacchetti De Gregoris *et al.*, 2011)
1062R	Universal	CTCACRRCACGAGCTGAC	(Bacchetti De Gregoris *et al.*, 2011)
8F	*Bacteria*	AGAGTTTGATCCTGGCTCAG	(Edwards *et al.*, 1989)
1492R	Universal	GGTTACCTTGTTACGACTT	(Kane *et al.*, 1993)
S-D-Bact-0341-b-S-17	*Bacteria*	CCTACGGGNGGCWGCAG	(Klindworth *et al.*, 2013)
S-D-Bact-0785-a-A-21	*Bacteria*	GACTACHVGGGTATCTAATCC	(Klindworth *et al.*, 2013)
799F_rc	*Bacteria*	CMGGGTATCTAATCCKGTT	(Thomas, *et al.*, 2020)

2. RNA extraction (cells from microcosms)

During the exponential phase of the *Zobellia galactanivorans* $Dsij^T$ growth with macroalgae or purified sugars (Chapter V), 10 ml of culture medium and 2 algal pieces (when applicable) were retrieved on ice for RNA extraction of the free-living and algae-attached bacteria, respectively. On ice, 0.5 volume of cold (stored at 4 °C) killing buffer (20 mM Tris-HCl pH 7.5, 5 mM $MgCl_2$, 20 mM NaN_3) was

immediately added to the liquid samples to kill the cells, stop transcription and preserve RNA from degradation. After centrifugation (3200 *g*, 10 min, 4 °C), cell pellets were frozen in liquid nitrogen. The collected algal pieces were washed twice in 1.5 ml of killing buffer:H_2O (1:1) in 2 ml eppendorf tubes (for 1 piece) and tubes were immersed in liquid nitrogen. Samples were stored at -80 °C before further RNA extraction. For all experiments with RNA, all surfaces were cleaned with RNAse*Zap* (Invitrogen) to prevent RNA degradation.

a. RNA extraction from free-living bacteria

Free-living bacterial cells were lysed by adding 400 µl of lysis buffer I (4 M guanidine thiocyanate, 25 mM sodium acetate pH 5.2, 5 $g.l^{-1}$ N-laurylsarcosinate) and 500 µl of phenol pH 4 and incubated 5 min at 65 °C (tubes were flipped every minute). After the addition of 500 µl of chloroform:isoamyl alcohol (IAA) (24:1), tubes were vortexed and centrifuged (16000 *g*, 10 min, 4 °C). The aqueous phase was recovered carefully and extraction was repeated with 250 µl of phenol and 250 µl of chloroform:IAA. Once again, the aqueous phase was recovered and 0.25 volume of 96 % molecular biology grade ethanol was added drop by drop under agitation to precipitate potential polysaccharide traces before the addition of 250 µl of phenol and 250 µl of chloroform:IAA. The final aqueous phase was recovered after vortex and centrifugation and was mixed with 500 µl of chloroform:IAA. After vortex and centrifugation (16000 *g*, 10 min, 4 °C), the aqueous phase was mixed with sodium acetate pH 5.5 (1:10, sodium acetate:sample) and 2.5 volumes (from the recovered sample) of 96 % molecular biology grade ethanol were added. The solution was incubated at room temperature for 2 h to precipitate RNA and centrifuged (18000 *g*, 45 min, 4 °C). Pellets were washed with 500 µl of 70 % molecular biology grade ethanol, centrifuged (18000 *g*, 20 min, 4 °C) and air-dried on ice for 1 h under chemical hood before being resuspended in 30 µl of RNAse-free water. To remove DNA contamination, Turbo DNase buffer was added (1X final) and extracts were treated 1 h at 37 °C with 2 units of Turbo DNAse (Thermofisher). RNA was then purified on mini-columns NucleoSpin RNA Clean-up (Macherey-Nagel) following the manufacturer's instructions. RNA was eluted in 50 µl of nuclease-free water and stored at -20 °C.

b. RNA extraction from attached bacteria

Two algal pieces were immersed in 2 ml killing buffer:H_2O (1:1) in 15 ml Falcon tubes, vortexed 30 sec and placed 7 min in an ultrasonic bath (Ultrasonic Cleaner, 45kHz, VWR) at room temperature to detach bacteria from the algal surface. Algae were removed using sterile tweezers, buffer was centrifuged (12800 *g*, 5 min, 4 °C) and cell pellets resuspended in 400 µl lysis buffer I. RNA extraction and DNAse treatment were then performed as described above for the free-living bacteria. To avoid RNA loss on purification columns, DNAse was inactivated by adding 0.2 volume of DNAse inactivation reagent (Thermofisher). Tubes were vortexed, incubated 5 min at room temperature, centrifuged (10600 *g*, 1.5 min) and supernatant was recovered in new tubes. RNA was stored at -20 °C.

3. Simultaneous DNA/RNA extraction (from environmental samples)

Environmental DNA and RNA from swabs (collection of the algal microbiota, Chapter IV) were extracted using the DNA/RNA Miniprep kit (ZymoBiomics) following the manufacturer instructions. Briefly, samples were transferred from DNA/RNA Shield – Lysis Tube to a 2 ml eppendorf and cells lysed using a TissueLyser II (Qiagen) at maximum speed (5 repetitions of 1 min with 1 min on ice between each). Tubes were centrifuged (16000 *g*, 1 min), supernatant transferred in a new tube and one volume of lysis buffer I was added. Samples were transferred on the provided Spin-Away filter and centrifuged. DNA binds to the filter while RNA is in the flow-through. The latter was then collected, mixed with 1 volume of 96 % molecular biology grade ethanol, loaded on the provided Zymo-Spin IIICG column and centrifuged. RNA was treated with DNase I Reaction Mix for 15 min at room temperature. DNA and RNA were then purified simultaneously, the column matrix was washed twice and nucleic acids eluted in 50 µl RNase-free water. RNA and DNA were stored at -20 °C.

4. DNA extraction (from environmental samples)

Three different protocols were adapted to extract DNA from each type of sample in Chapter III (algal pieces, sediment and water). For each cage, five algal pieces (total surface of 13.3 cm^2) were incubated in 4.5 ml of lysis buffer II (750 mM sucrose, 50 mM Tris pH 8, 40 mM EDTA, 14 nM lysozyme) for 45 min at 37 °C. SDS and proteinase K were added to a final concentration of 11.6 $mg.ml^{-1}$ and 230 $\mu g.ml^{-1}$, respectively, and samples were incubated for 1 h at 55 °C. Nucleic acid extraction was performed by adding one volume of phenol:chloroform:IAA (25:24:1) to the lysate volume. After centrifugation (3200 *g*, 15 min, 19 °C) the aqueous phase was recovered, polysaccharides were precipitated with 0.3 volume of 96 % molecular biology grade ethanol followed by a new extraction with phenol:chloroform:IAA. The resulting extracted DNA was purified with the NucleoSpin Plant II kit (Macherey Nagel) following the manufacturer's instructions. DNA was eluted in 100 µl of 5 mM Tris-HCl buffer pH 8.5 and stored at -20 °C.

For water samples, DNA was extracted from Sterivex filters following a similar protocol as used for the algal samples with addition of 1.5 ml of lysis buffer II to the filter and no precipitation of polysaccharides. For sediment samples, DNA was extracted from 0.5 g of sediment using the DNeasy PowerLyzer PowerSoil Kit (Qiagen) according to the manufacturer's instructions, eluted in 100 µl of 10 mM Tris-HCl buffer pH 8.5 and stored at -20 °C.

5. Nucleic acids quantification

DNA and RNA concentrations were measured using a Qubit fluorometer with the dsDNA HS Assay Kit (or the dsDNA BR Assay Kit depending on the samples) or the RNA HS Assay Kit respectively (Invitrogen). A_{260}/A_{280} and A_{260}/A_{230} ratios were assessed with a Nanodrop.

The concentration of the DNA from the seasonal sampling (Chapter IV, Part 2) was assessed with the QuantiFluor dsDNA System (Promega) kit following the manufacturer's instructions.

6. Check for DNA contamination and RNA integrity

To assess DNA contamination within RNA extracts (from environmental samples [Chapter IV] or from the microcosms [Chapter V]), PCRs were performed. One microliter of sample was added to the PCR mixture containing 1 µl of each 5 µM primer (8F/1492R [Edwards *et al.*, 1989; Kane *et al.*, 1993] in Chapter IV and S-D-Bact-0341-b-S-17 and S-D-Bact-0785-a-A-21 [Klindworth *et al.*, 2013] in Chapter V), 10 µl of Taq 2X Master Mix (BioLabs) and 7 µl of nuclease-free water (final volume 20 µl). The amplification program consisted of an initial step for template DNA denaturation at 95 °C for 2 min followed by 30 cycles of 95 °C for 30 s, 53 °C for 30 s for primer annealing and 72 °C for 30 s for DNA polymerization and then hold at 72 °C for 5 min. PCR products were mixed with 4X loading buffer (50 % glycerol, 10 mM EDTA, 10 mM Tris-HCl pH 7.6, 1 $mg.ml^{-1}$ orange G) and analyzed by electrophoresis (30 min, 100 V) on 1-2 % agarose gel in 0.5X Tris-Acetate-EDTA buffer containing ethidium bromide (2 µl for 100 ml). Products were visualized under UV with a transilluminator (Fisher Bioblock Scientific). Smart Ladder or Small Fragments Smart Ladder (Eurogentec) were used as a standard.

RNA integrity was assessed (for RNA extracted from the microcosms [Chapter V] and for some environmental samples from the seasonal sampling [Chapter IV]) on 1 µl of sample using a Bioanalyzer 2100 system (Agilent Technology) with the Agilent RNA 6000 Pico assay kit. Integrity was considered satisfying when (i) 2 clear bands corresponding to 16S and 23S rRNA were detected and (ii) no smears, that would imply RNA degradation, were present.

7. Sequencing of nucleic acids

a. DNA Metabarcoding

Library preparation and sequencing was done for 94 samples (Chapter III) using the Genomer platform (FR2424) facilities. The concentration of DNA samples was normalized at 0.1 $ng.µl^{-1}$. Libraries were prepared according to the standard Illumina protocol "16S Metagenomic Sequencing Library Preparation" (**Figure II.4**). Briefly, a first amplification step was performed using the primers S-D-Bact-0341-b-S-17 (5'CCTACGGGNGGCWGCAG3') and 799F_rc (5'CMGGGTATCTAATCCKGTT3') targeting the V3-V4 regions of the 16S rRNA gene (Thomas *et al.*, 2020 [**Annex 1**], primers designed to avoid chloroplast amplification). PCRs were done in duplicate in a final volume of 25 µl containing 1.25 µl of each primer at 10 µM, 12.5 µl of Master Mix Q5 2X (BioLabs) and 9 µl of nuclease-free water (Ambion). PCR program was as follows: denaturation for 3 min at 95 °C followed by 25 cycles of 30 sec at 95 °C (denaturation), 30 sec at 58 °C (annealing) and

30 sec at 72 °C (elongation) and by a final elongation for 5 min at 72 °C. Both duplicates were pooled and PCR products were analyzed on 1 % agarose gel to check the amplicon size (around 550 bp) before being purified with AMPure XP beads the to remove all fragments < 100 bp. A second amplification was carried out from 5 µl of the PCR products in order to attach dual indices and Illumina sequencing adapters. Indexing PCR was performed in a final volume of 50 µl containing 5 µl of each index, 25 µl of Master Mix Q5 2X and 10 µl of water. PCR program was as described above but with 8 cycles and a hybridization temperature set to 55 °C. PCR products were purified as already described and analyzed on a Bioanalyzer 2100 system (Agilent Technology) with the Agilent DNA 1000 assay protocol for quality check (expected amplicon expected size is around 630 bp). Each sample was normalized to 1 nM in 10 mM Tris pH 8.5 according to the formula $\frac{DNA\ concentration\ in\ ng.\mu l^{-1}}{660 g.mol^{-1} \times average\ library\ size}$. Libraries were pooled (5 µl of each), denatured with 0.2M NaOH and 200 mM Tris pH 7 and diluted to 5 pM following the "NextSeq System, Denature and Dilute Libraries Guide" in the furnished buffer. The control PhiX (genomic phage DNA) was added to the library to increase the genetic diversity to a 10 % final concentration. The library was sequenced on a MiSeq paired-end sequencing run (300 cycles × 2, Illumina, San Diego, CA, USA) using the MiSeq Reagent Kit v3.

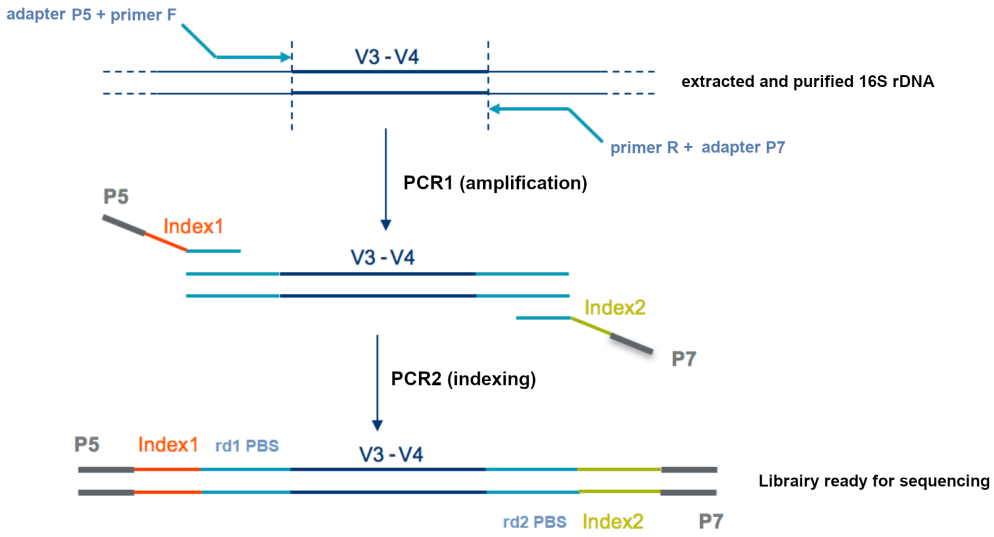

Figure II.4: Different steps of the library preparation before MiSeq sequencing. DNA fragment is first amplified with the specific primers S-D-Bact-0341-b-S-17 and 799F_rc flanked with adapters (PCR1). A second PCR is then carried out with Illumina sequencing primers (rd1/2 PBS) which are flanked with index and Illumina sequencing adapters P5/P7. It enables dual-indexed sequencing of the pooled library. The adapters will hybridize on the oligonucleotides on the flow cell.

b. RNA sequencing

Paired-end RNA sequencing (RNA-seq) (Chapter V) was performed by the Plateforme de Séquençage I2BC (UMR9198, CNRS, Gif-sur-Yvette) on a NextSeq instrument (Illumina) using the NextSeq 500/550 High Output Kit v2 (75 cycles). As Illumina did no longer supply the Illumina RiboZero rRNA Removal Kit for Bacteria at that time, rRNA depletion was carried out by mixing probes from the kit adapted for bacteria to the ones adapted for mammals.

8. Quantitative PCR (qPCR)

qPCR was carried out in 384-multiwell plates on a LightCycler 480 Instrument II (Roche). Each 5 µl reaction contained 2.5 µl of LightCycler 480 SYBR Green I Master mix 2X (Roche Applied Science), 0.5 µl of each primer (300 nM final concentration for the universal primers 926F/1062R [Bacchetti De Gregoris *et al.*, 2011] and for the *Zobellia*-specific primers described in Chapter IV, Part 1) and 1.5 µl of template DNA normalized at 0.5 ng.µl^{-1}. Each reaction was prepared in technical triplicates. The amplification program consisted of an initial step for template DNA denaturation at 95 °C for 10 min followed by 45 cycles of 95 °C for 10 s, 20 s at the chosen annealing temperature (60 °C for universal primers and 64 °C for *Zobellia*-specific primers), and 72 °C for 10 s for DNA polymerization. SYBR Green fluorescence was measured after each cycle. After the amplification step, dissociation curves were generated by measuring SYBR Green fluorescence while increasing the temperature from 65 °C to 97 °C.

Serial dilutions of purified *Zobellia galactanivorans* Dsij^{T} gDNA (prepared as in Gobet *et al.*, 2018) ranging from 10 to 10^8 16S rRNA gene copies were used as a standard curve and were amplified in triplicate in the same run as the environmental samples. Non-Template Controls (NTC) were included in the run. The LightCycler 480 Software v1.5 was used to determine the threshold cycle (Ct) for each sample. Linear standard curves were obtained by plotting Ct as a function of the logarithm of the initial number of 16S rRNA gene copies. PCR efficiency was calculated as $10^{-1/slope} - 1$. Samples with Ct outside the linear portion of the curve were considered as null.

9. Reverse transcription quantitative PCR (RT-qPCR)

Reverse transcription (RT) was conducted on 1 ng.µl^{-1} normalized RNA samples using the ImProm-II Reverse Transcription System (Promega). One microliter of provided random hexamer primers was added to 9.5 µl of sample, the mixture was incubated 5 min at 70 °C for RNA denaturation then cooled 5 min on ice. Samples were mixed with 10.5 µl of the reaction mix (4 µl of 5X Reaction Buffer, 3 µl of $MgCl_2$, 1 µl of dNTP Mix, 0.5 µl of Ribonuclease Inhibitor, 1 µl of Reverse Transcriptase). The random hexamer primers were bound to the template RNA for 5 min at 25 °C, then the first DNA strand was extended for 1 h at 42 °C and the reverse transcriptase was heat-inactivated for 15 min at 70 °C. For each sample, RT reactions were carried out with and without reverse transcriptase. qPCR was conducted as described above immediately after reverse transcription with 1 µl of 10X diluted cDNA. The number of 16S rRNA transcript copies obtained without reverse transcriptase was subtracted from the value obtained with reverse transcriptase to avoid any bias linked to DNA contamination.

V. Biochemistry

1. Small scale purification

Cell pellets from 5 ml cultures were resuspended on ice in 3 ml of lysis buffer (20 mM Tris-HCl pH 8, 500 mM NaCl, 1mM EDTA, 0,1 % Triton) supplemented with 30 µl of 500U.µl^{-1} DNAse I (Interchim) (5 U.µl^{-1} final) and transferred to a 5 ml tubes. Cell sonication was performed (6 x 10 sec with at least 1 min on ice between each repetition with an Ultrasonic Processor GE50 (setting 25, amplitude 55)) and lysis checked under the microscope. After centrifugation (20800 *g*, 30 min, 4 °C), recombinant soluble proteins contained in the supernatant were purified on His SpinTrap mini-columns (GE Healthcare) following the manufacturer instructions. Briefly, proteins were loaded and washed on the mini-columns with a binding buffer (20 mM Tris-HCl pH 8, 500 mM NaCl, 10 mM imidazole) and eluted in 200 µl of an elution buffer (20 mM Tris-HCl pH 8, 500 mM NaCl, 1 M imidazole). Before enzymatic assays, imidazole was removed from the enzyme solutions by ultrafiltration on 10 kDa cut-off membrane (regenerated cellulose membrane [Amicon Ultra, Merck-Millipore] or polyether sulfone membrane [Pall] for ZGAL_3452) in 20 mM Tris-HCl pH 8, 500 mM NaCl.

2. Large scale purification

Cell pellet(s) (corresponding to 250-750 ml of culture depending on the experiments) were each resuspended in 10 ml of lysis buffer (20 mM Tris-HCl pH 7.5, 500 mM NaCl, 20 mM imidazole, 5 U.µl^{-1} DNAse I) containing 1 tablet of cOmplete™, EDTA-free Protease Inhibitor Cocktail (Merck) and pooled. Mechanical lysis was achieved by sonication (Branson Digital Sonifier SFX 250) at 40 % of the maximal power (5 x 5 sec with 1 min on ice between each repetition, this was done several times until cell lysis was evidenced under the microscope). The lysate was centrifuged (38800 *g*, 60 min, 4 °C) and the supernatant filtered with 0.2 µm syringe filters before being loaded on a 5 ml HisTrap HP column (GE Healthcare) charged with 0.1 M $NiSO_4$ at 1 ml.min^{-1}. Unbound proteins were eluted by washing the column with 20 mM Tris-HCl pH 7.5, 500 mM NaCl, 20 mM imidazole until the UV value is stabilized at the baseline again (approximately 60 ml). Proteins were eluted using a 100 ml linear gradient of imidazole (20 mM – 1 M in 20 mM Tris-HCl pH 7.5, 500 mM NaCl) at 5 ml.min^{-1}. Fractions showing the presence of the recombinant protein at the expected molecular weight by Sodium dodecyl sulfate-polyacrylamide gel electrophoresis (SDS-PAGE) were pooled. Proteins were concentrated by ultrafiltration (3200 *g*) on 10 kDa PES membranes (Pall) and purified by size-exclusion chromatography in 25 mM Tris-HCl pH7.5, 200 mM NaCl using a column Superdex200, HiLoad 16/60 (GE Healthcare) at 1 ml.min^{-1} flow rate.

3. Sodium dodecyl sulfate-polyacrylamide gel electrophoresis (SDS-PAGE)

Protein fractions were analyzed by SDS-PAGE. Ten microliters of samples were mixed with 2 µl of 6X loading buffer (360 mM Tris-HCl pH6.8, 45 % glycerol, 9 % SDS, 9 % DTT, 0.12 % Bromophenol blue) and mixtures were incubated 5 min at 98 °C for protein denaturation. The 12 µl were loaded on 12 % (w/v) polyacrylamide gels (BioRad) and electrophoresis was conducted for 1.25 h at 160 V in 1X MOPS buffer (6.06 g of Tris, 8.38 g of MOPS and 1 g of SDS). Unstained Precision Plus Protein Standard (BioRad) was used as a ladder. Gels were stained with 0.1 % Coomassie blue for 30 min and destained overnight in a mix of 20 % ethanol and 10 % acetic acid.

4. Protein concentration

Protein concentration was measured with a Nanodrop using the extinction molar coefficient and the molecular weight of each protein (see **Table VI.1** in Chapter VI).

5. Oligosaccharide analytical methods

a. Sugar reducing-end assays

One volume of 0.2 µm filtered samples (here culture supernatant, see Chapter V) was incubated with 9 volumes of 0.2 % macroalgal polysaccharides at 28 °C overnight to assess the activity of extracellular polysaccharidases. Incubations were performed in parallel with inactive enzymes (boiled 15 min at 98 °C) as control. The amount of reducing-ends released in the incubation mixture was quantified using the ferricyanide assay (Kidby and Davidson, 1973). Twenty microliters of 5X ferricyanide (1.5 g potassium hexacyanoferrate III, 140 g dehydrated sodium carbonate, 25 mM NaOH) was added to 80 µl of the incubation mixtures in 96-wells microplate (BIOplastics). A standard curve of glucose was prepared by mixing 20 µl of 5X ferricyanide with 70 µl of milliQ-water and 10 µl of glucose at different concentrations (0.25–1.5 mM). Plate was agitated 30 s at 1000 rpm (ThermoMixer C, Eppendorf), incubated 10 min at 98 °C then cooled down 10 min at 4 °C. Each sample was assayed in technical duplicates. Eighty-five microliters of each well were transferred in a 96-wells microplate (Greiner Bio-One) and the absorbance was measured at 420 nm using microplate reader (Spark Tecan). The amount of reducing-ends was estimated in glucose equivalent using the glucose standard curve. For each sample, the value measured with the boiled enzymes was subtracted.

b. Unsaturated uronic acid assays

Polysaccharide lyases cleave uronic acid-containing polysaccharides via a β-elimination mechanism, resulting in unsaturated oligomeric products having a double bond at the non-reducing end residue, which absorb in UV. The lyase activity was then followed in real-time by measuring the increase in

absorbance at 235 nm (Spark, Tecan) every 30 sec during 20 min (unless stated otherwise). Each measurement was done in 200 µl in 96-wells microplate (Greiner Bio-One) with substrate concentration between 0.1-0.2 % and microplate was agitated 5 sec before the first measurement.

c. Fluorophore-Assisted Carbohydrate Electrophoresis (FACE)

Method was adapted from Jackson, 1996. Degradation products (approximately 50 µg of material) were dried for 2 h in a speed-vacuum centrifuge and dissolved in 2 µl of 0.1 M AMAC (2-aminoacridonein) in acetic acid:DMSO (3:17, v/v) and 2 µl of 1 M $NaBH_3CN$ in DMSO for at least 4 h at 37 °C. The AMAC-labeled saccharides were dried in vacuum for 1 h, resuspended in 20 µl of 25 % glycerol and 5 µl were loaded on a 0.75 mm polyacrylamide gel composed of a 6 % stacking gel (6 % acrylamide, 0.125 M Tris / 48 mM glycine pH 6.8, 0.17 % APS, 6.7 ng TEMED in water) and a 30 % running gel (30 % acrylamide, 0.375 M Tris / 48 mM glycine pH 8.8, 0.07 % APS, 6.8 ng TEMED in water). Electrophoresis was performed at 4 °C (cold room) in 25 mM Tris-HCl pH 8.5, 192 mM glycine for 2 h at 200 V. Oligosaccharides were visualized under UV with a transilluminator (Fisher Bioblock Scientific).

d. Carbohydrate-PolyAcrylamide Gel Electrophoresis (C-PAGE)

Method was adapted from Zablackis and Perez, 1990. Five microliters of the enzymatic reaction were added to 15 µl of 10 % sucrose with 0.01 % phenol red and 5 µl of this mix were loaded on a 0.75 mm thick polyacrylamide gel composed of a 6.5 % stacking gel (6.5 % acrylamide, 50 mM Tris / 1 mM EDTA pH 8.7, 0.16 % APS, 6.6 ng TEMED in water) and a 31 % running gel (31 % acrylamide, 50 mM Tris / 1 mM EDTA pH 8.7, 0.07 % APS, 6.9 ng TEMED in water). Electrophoresis was performed in 50 mM Tris-HCl pH 8.7, 1 mM EDTA for 1 h at 200 V. Gels were stained in 5 $mg.ml^{-1}$ of alcian blue for 10 min. After 2 h destaining in milliQ-water, the gel was soaked in 0.4 % silver nitrate (10 min) and rinsed 3 times with milliQ-water. Oligosaccharides were revealed by immersing in a solution of 70 $mg.ml^{-1}$ sodium carbonate with 1.6 $\mu l.ml^{-1}$ formaldehyde. The reaction was stopped by the addition of 17.5 M acetic acid.

e. Thin Layer Chromatography (TLC)

Two microliters of reaction mixture were spotted on silica gel-60 TLC aluminum plates (Merck). Migration was performed in acetic acid/ethyl acetate/water (25:31:22; v/v/v) for 50 min in a glass container. The oligosaccharides were visualized by immersing plates in 0.2 % napthoresorcinol/10 % sulfuric acid (1:2; v/v) in ethanol, followed by heating on a hot-plate for 10 min.

f. High Pressure Size Exclusion Chromatography (HPSEC)

HPSEC analyses were carried out by Diane Jouanneau (Station Biologique de Roscoff, UMR8227, Centre Commun de Ressources). Filtered samples (100 µl, 0.2 µm) were injected on analytical Superdex 200 Increase and Superdex 30 Increase (Cytiva) columns connected in series. The elution was conducted in 0.1 M $LiNO_3$ using an isocratic Thermo Ultimate 3000 pump working at a flow rate of 0.5 $ml.min^{-1}$. The chromatography experiments were monitored using a Wyatt Optilab Rex refractive index detector. Chromeleon software (Thermo) was used for data acquisition.

g. Mass spectrometry

Enzymatic incubations performed in 50 mM ammonium bicarbonate pH 7 were sent for Matrix Assisted Laser Desorption Ionisation Mass Spectrometry (MALDI-MS) and Electrospray Ionization Mass Spectrometry (ESI-MS) analyses at the BIBS platform (INRAE, UR 1268, Nantes).

VI. Microscopy

1. Cell fixation

Algal pieces were immersed in 2 % paraformaldehyde (PFA) in 1X PBS (137 mM NaCl, 2mM KCl and 10 mM phosphate buffer) overnight at 4 °C. Fixed samples were washed twice in PBS. Cells from liquid culture were centrifuged (12800 *g*, 10 min) and resuspended in 2 % PFA in 1X PBS overnight at 4 °C. The solution was centrifuged and fixed cell pellets rinsed twice in 1 ml of 1X PBS. All fixed samples were stored in PBS:EtOH (1:1 v/v) at -20 °C.

2. Fluorescence *in situ* hybridization (FISH)

All probes, labeled either with the fluorescent dye Atto488 (for the classical protocol, **Figure II.5A**) or with Horseradish peroxidase (HRP, for the CARD-FISH protocol, **Figure II.5B**), and helper oligonucleotides were resuspended in nuclease-free water and diluted to a working stock concentration of 8.4 $pmol.µl^{-1}$ (**Table II.4**). Probes were ordered from Biomers and helpers from Eurogentec. Active dye stock solution, HRP-labeled probes, hybridization and amplification buffers and H_2O_2 were stored at 4 °C. Alexa-labeled probes, DAPI (4',6-diamidino-2-phenylindole) and helpers were stored at -20 °C.

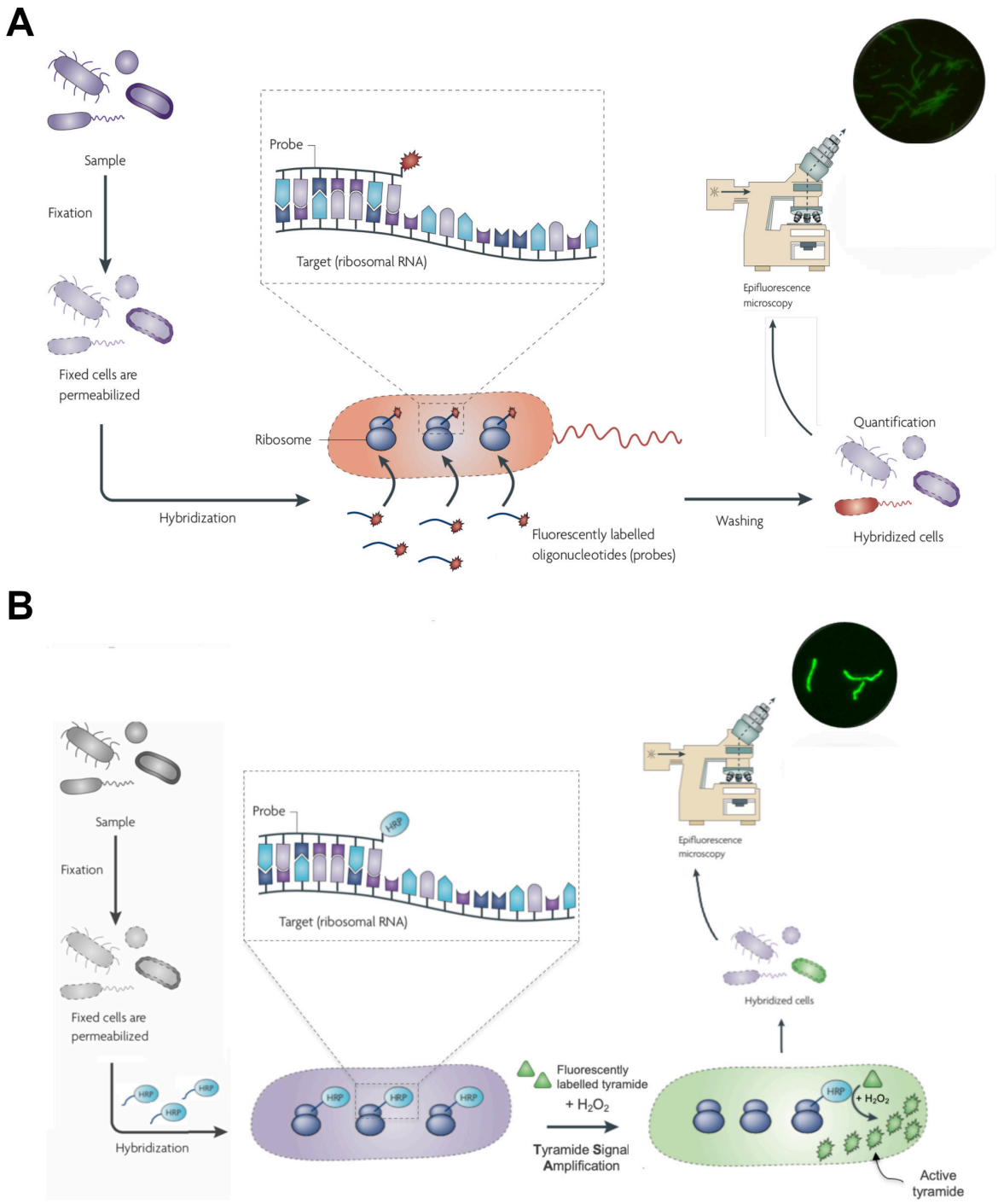

Figure II.5: FISH and CARD-FISH principles. Adapted from Amann and Fuchs, 2008. (A) Main steps for fluorescence *in situ* hybridization (FISH). FISH principle is based on the use of rRNA-targeted oligonucleotide probes labeled with fluorescent dyes which allow the detection of a defined group of microorganisms (B) Main steps for catalysed reported deposition–fluorescence *in situ* hybridization (CARD-FISH). CARD-FISH is commonly used to enhance the fluorescence signal. In this case, the probes are not directly labeled with a fluorescent dye but with the horseradish peroxidase enzyme (HRP).

Table II.4: List of the probes and helpers used during FISH or CARD-FISH protocols.

Name	Target	Sequence (5' to 3')	Reference
ZOB137	*Zobellia*	GGCTATCCCACAGTAGGG	Chapter IV
TEN281	*Tenacibaculum*	CTCAGACCCCCTACCTAT	Chapter VII
EUB338	*Bacteria*	GCTGCCTCCCGTAGGAGT	(Amann *et al.*, 1990)
EUB338-II	*Planctomycetes*	GCAGCCACCCGTAGGTGT	(Daims *et al.*, 1999)
EUB-III	*Verrucomicrobia*	GCTGCCACCCGTAGGTGT	(Daims *et al.*, 1999)
NON338	-	ACTCCTACGGGAGGCAGC	(Wallner *et al.*, 1993)
H116 (helper)	*Zobellia*	GGYAGATYGTATACGCSTTGC	Chapter IV
H155 (helper)	*Zobellia*	GTMTTAATCCAAATTTCTCTG	Chapter IV
H176 (helper)	*Zobellia*	CACATGGTACCATTTTACGGC	Chapter IV

a. Standard protocol

One microliter of fixed cells was spotted on ten-wells poly-L-lysine glass slides (ThermoScientific), air-dried and dehydrated 10 sec in successive short ethanol baths (50, 80 and 96 % ethanol). Hybridization chambers were prepared by placing a piece of paper tissue in a 50 ml Falcon tube and preheating in the hybridization oven set at 46 °C. Hybridization buffer (0.9 M NaCl, 20 mM Tris-HCl pH8, 0.01 % SDS) with the adequate formamide concentration (**Table II.5**) was mixed (9:1, final volume 2 ml) with the adequate probe labeled with the fluorochrome Atto488. Five microliters of the working solution were spotted on each well. The unused hybridization buffer was poured in the hybridization chamber, the slide was placed in the chamber (above the paper tissue) and incubated horizontally in the hybridization oven during 2 h at 46 °C. Slides were washed 15 min in preheated washing buffer (0.45 to 0 M NaCl, 1 M Tris-HCl pH8, 0 to 5 mM EDTA pH8, 0.01 % SDS) at 48 °C (see **Table II.5** for washing buffer composition). Slides were shortly washed in milli-Q water and air-dried. Counter-staining was performed by covering each well with DAPI (1 $\mu g.mg^{-1}$) during 10 min in the dark. Excess DAPI was removed with milli-Q water and the slides were air-dried. One microliter of mounting medium Citifluor:Vectashield (3:1) was spotted on each well before coverslip capping (Marienfeld). Fluorescence was observed on a Nikon 50i epifluorescence microscope (filter ET-EGFP (LP)) equipped with an AxioCam MRc camera (Carl Zeiss, Germany). When fluorescence quantification was needed, three random images per hybridization were captured and these were analyzed using the Image J software (Schneider *et al.*, 2012). The three channels (blue, red, green) were split to keep only the green one (corresponding to Atto488 emission) and the background signal was removed. For each hybridization, the maximum intensity of 50 bacteria selected by hand was measured.

Table II.5: FISH hybridization and washing (used for FISH and CARD-FISH) buffers composition according to formamide concentration.

	10%	20%	30%	35%	40%	50%	60%	70%
	FISH Hybridization Buffer							
5M NaCl (µl)	360	360	360	360	360	360	360	360
1M Tris-HCl pH 8 (µl)	40	40	40	40	40	40	40	40
Formamide (µl)	200	400	600	700	800	1000	1200	1400
MQ H_2O (µl)	1400	1200	1000	900	800	600	400	200
10% SDS (µl)	2	2	2	2	2	2	2	2
	Washing Buffer (preheated at 48°C)							
5M NaCl (µl)	4500	2150	1020	700	460	180	40	0
1M Tris-HCl pH 8 (µl)	1000	1000	1000	1000	1000	1000	1000	1000
0.5 EDTA pH 8 (µl)	0	500	500	500	500	500	500	350
MQ H_2O	Up to 50 ml	Up to 50 ml	Up to 50 ml	Up to 50 ml	Up to 50 ml	Up to 50 ml	Up to 50 ml	Up to 50 ml
10% SDS (µl)	50	50	50	50	50	50	50	50

b. Active dye stock preparation

Dried Alexa Fluor 546 carboxylic acid, succinimidyl ester (Life Technologies) was resuspended in 100 µl of dimethylformamide (DMF) and stored in the dark at room temperature. In parallel, 1 % tyramine HCl stock solution was freshly prepared in triethylamine:DMF (1:100, v/v). This stock solution was added to the resuspended dye (0.147 volume of 1 % tyramine HCl for 1 volume of dye). The mixture was incubated at room temperature in the dark between 6 and 12 h (tube was flipped every hours) and mixed with 885 µl of 96 % ethanol. The mixture was divided in 50 µl aliquots and the latter were dried overnight under vacuum. Pellets were stored at -20 °C and resuspended when needed in 50 µl of 20 $mg.ml^{-1}$ N-isopropylbenzylamine (IPBA) in water to have a 1 $mg.ml^{-1}$ active Alexa546 tyramide stock.

c. Catalyzed reporter deposition – FISH protocol (CARD-FISH)

The protocol was adapted from Pernthaler *et al.*, 2002. Fixed free-living cells stored in PBS:EtOH (1:1) solution were added in approximately 10 ml of 1X PBS and harvested using a vacuum pump onto a 0.2 µm polycarbonate membrane (Whatman) placed on a 0.45 cellulose acetate membrane (Sartorius). Polycarbonate membrane portions were cut with a sterile scalpel, embedded by dipping in 0.1 % medium electroendosmosis (ME) agarose (Merck-Millipore) and dried for at least 20 min at 37 °C on parafilm. They were then dipped briefly in ethanol with increasing concentration (50, 80 and 96 %). Cells were permeabilized by incubating the membrane portions in lysozyme (10 $mg.ml^{-1}$ in 0.05 M EDTA, 0.1 M Tris-HCl pH8 in milli-Q water, 15 min, 37 °C) in Petri dishes. After being washed twice in 50 ml of milli-Q water, membrane portions were incubated 1 min in 0.1 M HCl followed by 10 min in freshly prepared 3 % H_2O_2 to inactivate endogenous peroxidases, washed 5 min in 50 ml of 1X PBS and shortly in 50 ml of milli-Q water. Membrane portions were air-dried on Whatman paper before being dipped in the preheated hybridization mix (0.9 M NaCl, 20 mM Tris-HCl pH8, 35 % formamide, 1 % blocking

reagent, 10 % dextran sulfate, 0.02 % SDS, 28 nM probe and each helper if needed) then placed face up on a parafilm in a Petri dish and totally covered with the mix. Petri dishes were separated by spacers in a preheated humid chamber with tissue paper soaked with 2 ml of a solution containing 35 % formamide and 0.9 M NaCl in milli-Q water (see **Figure II.6**) and incubated for 2.5 h at 46 °C. Samples were first washed briefly in preheated washing buffer (70 mM NaCl, 1 M Tris-HCl pH8, 5 mM EDTA, 0.01 % SDS) to remove the excess of working solution followed by a 15 min incubation in the same buffer at 48 °C and 15 min in 1X PBS. They were air-dried and, as described for the hybridization step, dipped and covered with a detection solution (1X PBS, 2 M NaCl, 0.1 % blocking reagent, 10 % dextran sulfate, 0.0015 % H_2O_2 and 1 µg.ml^{-1} of Alexa546 or 488-labeled tyramides) 45 min in humid chamber at 46 °C for amplification. Membrane portions were washed 10 min in 1X PBS in the dark, twice briefly in 50 ml of milli-Q water and dehydrated in 50 ml of 96% ethanol for 1 min. They were covered with DAPI (1 µg.mg^{-1}) for 10-15 min in the dark on parafilm and then washed briefly twice in milli-Q water and in 96 % ethanol. Slides were mounted once samples were completely dry with Citifluor:Vectashield (3:1).

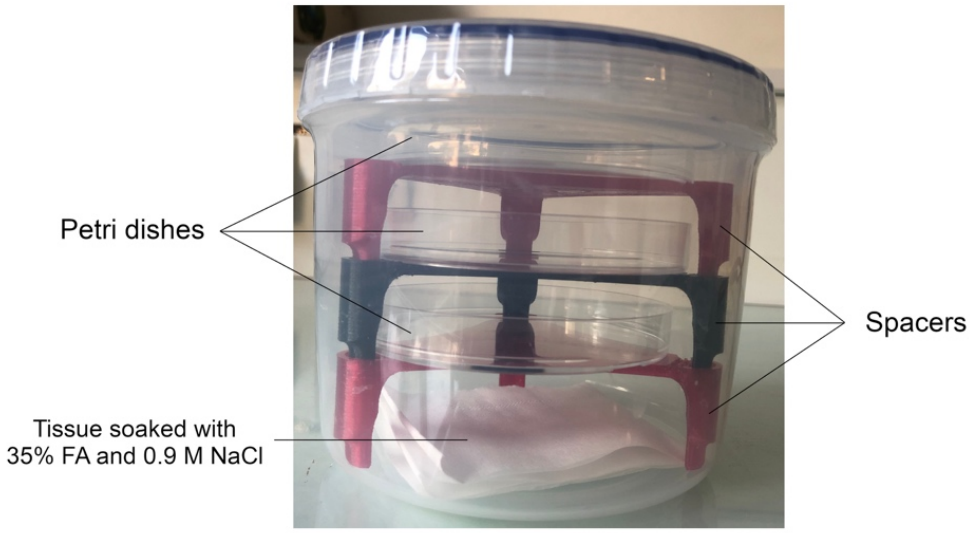

Figure II.6: Humid chamber used for CARD-FISH protocol. Algal samples on slides or alternatively filters on parafilm were placed on Petri dishes separated by spacers. Tissue was soaked with 2 ml of a solution containing the adequate formamide percentage (here 35 %) and 0.9 M NaCl in milli-Q water. Spacers were designed for 3D printing by Andreas Ellrott (MPI Bremen, Molecol team).

Sequential CARD-FISH was carried out to detect simultaneously free-living *Zobellia* and *Tenacibaculum* cells (Chapter VII). A first step of hybridization and amplification was done with the *Zobellia*-specific probe and the fluorochrome Alexa546 as described above. HRPs were inactivated just after the amplification step by dipping the membrane portions in freshly prepared 3 % H_2O_2 for 10 min followed by washings in 1X PBS, milli-Q water and 96 % ethanol and kept overnight at -20 °C. A second step of hybridization and amplification with the *Tenacibaculum*-specific probe and the fluorochrome Alexa488 was performed in the same way, followed by DAPI counter staining as described above. Slides were stored at -20 °C.

Membrane portions were visualized with a Leica DMi8 epifluorescent microscope equipped with an oil objective 63X and a Leica DFC3000 G camera (Wetzlar, Germany).

To visualize algal microbiota, algal tissues were directly attached on the slide at the beginning of the protocol: they were dipped in 0.1% ME agarose, placed on a glass slide and air-dried for > 30 min at 37 °C. Protocol was similar to what was done with filters except that samples were bleached 10 min in the successive ethanol baths and endogenous peroxidases were inactivated by incubation in 0.15 % H_2O_2 in methanol (30 min). An area was delimited on the slide with a pap pen around the algal sample to avoid buffer leakage during hybridization and amplification due to the uneven algal surface. Samples were visualized with a confocal microscope Leica TCS SP8 equipped with HC PL APO 63x/1.4 oil objective and K-Cube filters A UV, N2.1 and I3 using the 405, 552 and 488 nm lasers to detect DAPI, Alexa546 and Alexa488 signal, respectively. Z-stack images were collected (layers of 0.15-0.4 µm thickness). Cell counts were processed on maximum intensity images with the software Imaris v9.5.1.

VII. Bioinformatics

1. FISH/CARD-FISH probe design

Probes specific to the genera *Zobellia* and *Tenacibaculum* were designed (**Table II.4**) using the ARB software (Ludwig *et al.*, 2004; http://www.arb-home.de). Available 16S rRNA gene sequences from the targeted groups (45 sequences for *Zobellia*, 19 for *Tenacibaculum*) were aligned using SINA v1.6.1 and added to the Silva reference database (SILVA132_SSURef_12.12.17) in ARB to be included in the Silva tree. All sequences from the targeted genus were selected for probe search using the PROBE DESIGN tool with the following parameters: Length of probe: 18, Temperature: 30-100 °C, G+C content: 50-100 and by adjusting the parameters Max. non-group hits and Min group hits until a probe with a satisfying coverage was found.

To design a probe specific to the genus *Tenacibaculum*, all the species belonging to this genus were first selected to find a specific sequence. Nevertheless, the tool MATCH PROBE in ARB revealed that an important proportion of other bacteria, especially *Polaribacter* species, were also detected. On phylogenetic trees, the type species *T. maritimum* seems to cluster apart from the rest of the *Tenacibaculum* representatives and is phylogenetically close to *Polaribacter*. It was then decided to design two probes: one specific to *T. maritimum* (MAR835) and another targeting all the others *Tenacibaculum* species (TEN281). This solution showed better *in silico* results in terms of specificity. Probe specificity was tested *in silico* using the SILVA tool TestProbe (https://www.arb-silva.de/search/testprobe/) against the reference database SILVA 138.1 SSU Ref with 0 mismatch allowed.

Three non-labeled helper oligonucleotides (21 nt) were designed to bind adjacent to the ZOB137-target site in order to enhance the probe signal (see H116, H155 and H176 in **Table II.4**).

2. qPCR primer design

Zobellia-specific PCR primer design was done by François Thomas using DECIPHER (http://www2.decipher.codes/DesignPrimers.html) with 139 aligned 16S rRNA gene sequences from flavobacteria, including 52 *Zobellia* strains and 87 sequences representing 23 close genera (see Chapter IV, part 1). Primers were searched to amplify 75-200 bp products, with DECIPHER default parameters. The designed sets of primers were tested for specificity against the reference database SILVA 138.1 SSU Ref using SILVA TestPrime (https://www.arb-silva.de/search/testprime/) with 0 mismatch allowed.

3. Metabarcoding – pre-processing

The following steps were carried out on the computing cluster of the ABiMS platform (FR2424, Station Biologique de Roscoff), which is part of the Biogenouest core facility network. Raw sequence reads were trimmed to remove low quality bases and Illumina adapters using Trimmomatic v0.38 with the following options: ILLUMINACLIP:Adaptaters.fasta:2:30:10 SLIDINGWINDOW:4:25 LEADING:25 TRAILING:25 MINLEN:150 (Bolger *et al.*, 2014). Overlapping paired-end sequence reads were assembled using PANDAseq v2.11 and assembled sequences between 400 and 500 bp long were kept (Masella *et al.*, 2012). All the following steps for sequence processing were performed in the pipeline FROGS (Find Rapidly OTU - Operational Taxonomic Unit - with Galaxy Solution) developed for the Galaxy platform (http://galaxy3.sb-roscoff.fr, Escudié *et al.*, 2017). Sequences were clustered into OTUs using SWARM v2 (Mahé *et al.*, 2015), with local clustering threshold d=1. This method differs from the classical clusterisation method based on a sequence similarity threshold (usually 97 %). The SWARM method was built to avoid the biases linked to (i) the choice of this similarity threshold (*t*) (which would be too stringent for fast evolving lineages but too relaxed for slow evolving ones) and (ii) the random selection of a central sequence (red point in **Figure II.7A**) against which the other sequences are compared (close sequences might then belong to another OTU, represented by the green points). With SWARM, a sequence is chosen randomly as the "seed" (red point in **Figure II.7B**) of an OTU and all sequences displaying a number of nucleotide mismatches equal to or less than *d* (value set by the user) is added to the OTU and become "sub-seeds". All the remaining sequences having *d* or less mismatch with at least one sub-seed are added to the OTU and so on. When no more sequence can be added to the OTU, the latter is closed and a new one is created. With this iterative growth process, an OTU grows to its natural limits and is not dependent of the initial seed selection. Here, the local clustering threshold *d* was set to 1. PCR chimera detected with VCHIME from VSEARCH v1.1.3

(Rognes *et al.*, 2016) and singletons were filtered out and OTUs were taxonomically assigned using the RDP classifier (Wang *et al.*, 2007) on the Silva 16S rRNA (v132) database.

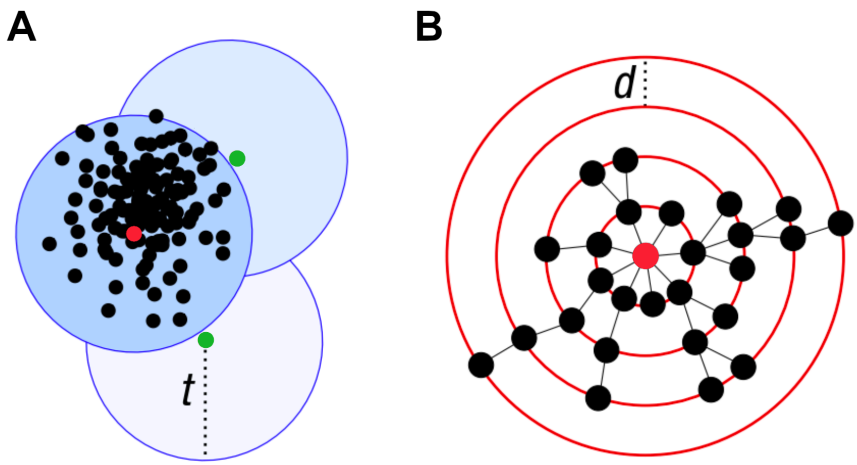

Figure II.7: Schematic view of the classical clusterisation method (A) and the SWARM method (B). Adapted from Mahé et al., 2014.

4. Metabarcoding – downstream analyses

Samples from the bacterial community dataset were rarefied (100 permutations) to 24482 sequences using the *rarefy_even_depth* function (phyloseq package) prior to alpha diversity indices calculations. ANOVA (analysis of variance, *aov* function) test was conducted to compare diversity indices over time. When significant ANOVA results were found ($p < 0.05$), a post-hoc Tukey HSD (*TukeyHSD* function) test was calculated and p-values were corrected using the Benjamini-Hochberg method. Dissimilarities in community structure were calculated using the Bray–Curtis dissimilarity index (*ordinate* function) before non-metric multidimensional scaling (NMDS). Permutational analysis of variance (PERMANOVA, 999 permutations) was used using the *adonis* function to discriminate groups of samples according to time or type of compartment (algae, sediment, seawater). Mean dispersions within the compartments were performed with the *betadisper* function (999 permutations). Contextual parameters measurements were fitted onto the NMDS using the *envfit* function. The above multivariate and statistical analyses were carried out using the packages *phyloseq*, *vegan, ggplot* and *EcolUtils* on the R software v3.5.0 (Wickham, 2009; Mcmurdie and Holmes, 2013; Oksanen *et al.*, 2013; R Core Team, 2018). Differential sequence abundance analysis through time was performed at the OTU level using the generalized linear model (GLM) test with the *ALDEx2* R package (Fernandes *et al.*, 2014).
To build association networks, extended Local Similarity Analysis (eLSA v1.0.4) (Xia *et al.*, 2011) was performed on a dataset comprising the contextual metadata and the relative sequence abundance of OTUs. A delay of one time point was allowed for temporal associations. P-values were estimated using the permutation method, with 1000 permutations. Q-values were estimated to control false positives. Default eLSA parameters were used otherwise. The network was visualized and analyzed in Cytoscape v3.3.0 (Shannon *et al.*, 2003). Only associations with $|LS| \geq 0.5$, $Q \leq 0.05$ and $P \leq 0.001$ were represented

with the "edge-weighted, spring-embedded layout" (nodes are strongly repelled or attracted as a function of their LS value; spring strength = 50, spring rest length = 100, strength of disconnected spring = 0.05, rest length of disconnected spring = 500, and strength to avoid collisions = 500). Clusters were detected using the MCODE algorithm (Bader and Hogue, 2003) with "hair" and "fluff" options and otherwise default parameters.

Ecologically relevant functions were predicted were made using the FAPROTAX v1.2.2 database and script (Louca *et al.*, 2016) against the rarefied OTUs dataset with the assigned taxonomy. In addition, the Phylogenetic Investigation of Communities by Reconstruction of Unobserved States (PICRUSt2 v2.1.4) pipeline (Douglas *et al.*, 2020) was run with the default parameters (except min_reads set to 5) to get metagenome predictions for EC numbers. Functions and enzymes with differential sequence abundance over time were assessed by calculating p-value of the GLM test with ALDEx2.

5. RNAseq – pre-processing

Demultiplexed and adapter-trimmed reads provided by the sequencing platform were processed with the Galaxy platform (https://galaxy.sb-roscoff.fr). Trimmomatic (Galaxy Version 0.38.0) was used to perform quality filtering of the reads (SLIDINGWINDOW:4:20 LEADING:3 TRAILING:3 AVGQUAL:25 MINLEN:20). Reads quality was checked using *multiqc* v1.7 (Ewels *et al.*, 2016) on the ABiMS computing cluster. Transcript quantification was done using the pseudo-mapper Salmon (Patro *et al.*, 2017, Galaxy Version 0.8.2) with the *Z. galactanivorans* Dsij^T reference genome (retrieved from the MicroScope platform [https://mage.genoscope.cns.fr/] "zobellia_gal_DsiJT_v2"; Refseq NC_015844.1) and the following parameters: Type of index: quasi, Perfect Hash: False, Suffix Array:1 and the default advanced parameters. Raw counts for individual samples were merged into a single expression matrix for downstream analysis.

rRNA content was assessed using SortMeRNA (Galaxy Version 2.1b.4) with default parameters. Cleaned reads were also mapped on the *Z. galactanivorans* Dsij^T reference genome using Bowtie2 (Langmead and Salzberg, 2012; Galaxy Version 2.3.2.2) with the following parameters: Minimum/Maximum fragment length for paired-end alignment:50/500, Mate orientation: fr, selection of the simple very sensitive end-to-end mode.

6. RNAseq – downstream analyses

All downstream analyses were conducted in R v3.6.2 (R Core Team, 2018). Principal component analysis was performed using the *DESeq2* v1.26.0 package (Love *et al.*, 2014) after rlog transformation. Differential abundance analyses were also carried out with this package and genes displaying a log2 fold change $|log2FC| > 2$ and a Bonferroni-adjusted p-value < 0.05 were considered to be significantly differentially expressed. The upset plot was done using the *ComplexUpset* package (Lex *et al.*, 2014; Krassowski, 2020). Hierarchical clustering was performed using the *hclust* function with the Ward's

minimum variance method (Murtagh and Legendre, 2014). All graphics were made with the *ggplot2* package (Wickham, 2016).

7. Comparative genomics

The number of glycoside hydrolases, polysaccharide lyases, carbohydrate esterases and sulfatases present in the genome of the different *Zobellia* spp. was searched using the dbCAN database on the MicroScope platform. Homologs were searched for genes of interest using synteny results in MicroScope with a 50 % identity and a 80 % alignment coverage cutoff.

Chapter III:

Bacterial community dynamics during kelp degradation

Résumé du chapitre

Les macroalgues sont des producteurs primaires majoritaires des écosystèmes côtiers. Parmi celles-ci, les laminaires, de grandes algues brunes formant d'importantes forêts sous-marines, peuplent abondamment les écosystèmes côtiers tempérés. Une partie de cette biomasse est régulièrement arrachée ou sectionnée lors de tempêtes ou suivant le cycle de vie des algues et peut s'échouer en grande quantité dans des zones subtidales voisines, créant ainsi de nouvelles niches écologiques par un apport considérable de matière organique. Il est alors intéressant d'un point de vue écologique, d'évaluer l'impact d'une telle accumulation de matière organique et de sa dégradation sur l'écosystème. La dégradation de cette biomasse et sa réinjection dans les réseaux trophiques supérieurs dépendent essentiellement de l'action des bactéries marines hétérotrophes. L'objectif de cette étude est donc d'évaluer l'impact de cette accumulation de matière organique sur la dynamique des communautés bactériennes afin de mettre en lumière les différentes stratégies écologiques mises en œuvre au cours de sa dégradation.

Ce travail a été mené en collaboration avec l'équipe Ecogéochimie et Fonctionnement des Ecosystèmes Benthiques de la Station Biologique de Roscoff qui a mis en place une expérimentation *in situ* ayant pour but de mimer ce phénomène d'accumulation de macroalgues observé après des tempêtes (de Bettignies *et al.*, 2020). Des cages contenant des morceaux d'algues ont été immergées à 10 mètres de profondeur et échantillonnées à intervalles réguliers pendant 6 mois afin de suivre le devenir des algues en dégradation. A chaque temps d'échantillonnage, des prélèvements d'algues, de sédiments et d'eau environnante ont été récupérés afin de caractériser les variations de diversité, de composition et de structure des communautés bactériennes dans ces différents compartiments *via* une approche de metabarcoding du gène de l'ARN 16S.

Une forte succession a été observée au sein des communautés épiphytes et se décline en deux phases. Lors des 6 premières semaines, les algues détachées ont été principalement colonisées par des bactéries connues comme spécialistes de l'utilisation de polysaccharides complexes (*Bacteroidia*). Après 11 semaines, d'autres bactéries se sont installées, notamment des *Actinobacteria*. Elles pourraient être des bactéries opportunistes, profitant des composés plus simples libérés lors de la dégradation algale par les premières bactéries spécialistes. Par ailleurs, cette accumulation de laminaires a également montré un impact sur les communautés bactériennes du sédiment sous-jacent, favorisant notamment la croissance de bactéries anaérobies (vivant sans oxygène).

Les résultats obtenus fournissent ainsi des informations sur la composition du microbiote associés aux algues en décomposition, qui reste encore peu étudié, et témoignent de l'importance des bactéries marines hétérotrophes dans le recyclage de la biomasse algale. Les différentes phases de succession observées suggèrent l'utilisation de différents types de substrats au sein des communautés et met ainsi en lumière de potentielles interactions coopératives entre les groupes fonctionnels.

Au sein de ce chapitre, j'ai réalisé les expérimentations et participé aux analyses des données et à l'écriture de l'article avec François Thomas et Angélique Gobet. Nolwen Le Duff a effectué les mesures de qPCR sur les différents échantillons. Ces résultats ont été publiés en début d'année 2021 dans le journal *Environmental Microbiology*.

environmental microbiology

Environmental Microbiology (2021) **00**(00), 00–00 doi:10.1111/1462-2920.15389

Accumulation of detached kelp biomass in a subtidal temperate coastal ecosystem induces succession of epiphytic and sediment bacterial communities

Maéva Brunet,[1] Florian de Bettignies,[2] Nolwen Le Duff,[1] Gwenn Tanguy,[3] Dominique Davoult,[2] Catherine Leblanc,[1] Angélique Gobet[1,4*] and François Thomas[1*]

[1]*Sorbonne Université, CNRS, Integrative Biology of Marine Models (LBI2M), Station Biologique de Roscoff (SBR), Roscoff, 29680, France.*

[2]*Sorbonne Université, CNRS, UMR 7144 AD2M, Station Biologique de Roscoff (SBR), Roscoff, 29680, France.*

[3]*Sorbonne Université, CNRS, FR2424, Genomer, Station Biologique de Roscoff, Roscoff, 29680, France.*

[4]*MARBEC, Univ Montpellier, CNRS, Ifremer, IRD, Sète, France.*

Summary

Kelps are dominant primary producers in temperate coastal ecosystems. Large amounts of kelp biomass can be exported to the seafloor during the algal growth cycle or following storms, creating new ecological niches for the associated microbiota. Here, we investigated the bacterial community associated with the kelp *Laminaria hyperborea* during its accumulation and degradation on the seafloor. Kelp tissue, seawater and sediment were sampled during a 6-month *in situ* experiment simulating kelp detritus accumulation. Evaluation of the epiphytic bacterial community abundance, structure, taxonomic composition and predicted functional profiles evidenced a biphasic succession. Initially, dominant genera (*Hellea*, *Litorimonas*, *Granulosicoccus*) showed a rapid and drastic decrease in sequence abundance, probably outcompeted by algal polysaccharide-degraders such as *Bacteroidia* members which responded within 4 weeks. *Acidimicrobiia*, especially members of the Sva0996 marine group, colonized the degrading kelp biomass after 11 weeks. These secondary colonizers could act as opportunistic scavenger bacteria assimilating substrates exposed by early degraders. In parallel, kelp accumulation modified bacterial communities in the underlying sediment, notably favouring anaerobic taxa potentially involved in the sulfur and nitrogen cycles. Overall, this study provides insights into the bacterial degradation of algal biomass *in situ*, an important link in coastal trophic chains.

Received 6 October, 2020; revised 14 December, 2020; accepted 2 January, 2021. *For correspondence. Tel.: 0033-256-452-148; Fax.: 0033-298-292-324. E-mail francois.thomas@sb-roscoff.fr (F.T.) and Tel.: 0033-499-573-250; Fax.: 0033-499-573-294. E-mail: angelique.gobet@ifremer.fr (A.G.) †These authors contributed equally.

Introduction

Brown macroalgae of the order *Laminariales*, collectively known as kelps, are crucial foundation species that thrive in coastal regions of temperate and Arctic seas worldwide. Kelps feature some of the highest growth rates and primary productivity on the planet (Mann, 1973). Kelp biomass thus represents an abundant standing stock of organic matter, primarily composed of polysaccharides and proteins that account for ca. 50% and 3%–15% of the dry weight, respectively (Kloareg and Quatrano, 1988; Fleurence, 1999). Up to 82% of the kelp primary production can be exported as dissolved or particulate organic matter to the shores or neighbouring intertidal, subtidal and benthic zones (Krumhansl and Scheibling, 2012). This may be due to the drift of naturally detached old blades as well as the fragmentation or dislodging of kelps caused by hydrodynamic forces such as strong storm events (Krumhansl and Scheibling, 2012; de Bettignies *et al*., 2015; Krause-Jensen and Duarte, 2016). This massive input of organic matter can strongly influence the stranding ecosystems, creating new niches for meiofauna and microorganisms (Duarte and Cebrián, 1996). This is particularly relevant in benthic subtidal habitats where sediments are otherwise devoid of kelps. The turnover of algal biomass largely depends on bacterial degradation processes (Mann, 1982; Newell *et al*., 1982) and is influenced by several physico-chemical parameters. For example, small fragments are degraded faster, and degradation is favoured when temperature and hydrodynamics increase (Krumhansl and Scheibling, 2012).

Live macroalgae host diverse and abundant bacterial communities (Burke *et al*., 2011), with about 10^6 to 10^9 bacterial cells.cm^{-2} on algal surfaces (Martin *et al*., 2014). Bacteria play an important role in algal health and physiology: they can provide vitamins to the host, defend the host against pathogens via antibiotic production, or degrade algal tissues (Egan *et al*., 2013, 2014; Minich *et al*., 2018). Epiphytic bacterial communities have been thoroughly characterized for an increasing number of kelp species and generally comprise large proportions of *Alphaproteobacteria*, *Gammaproteobacteria*, *Bacteroidetes*, *Verrucomicrobia* and *Planctomycetes* (Bengtsson and Øvreås, 2010; Lemay *et al*., 2018). Studies further revealed that kelp epiphytic communities are stable over large spatial scales (Marzinelli *et al*., 2015), can be species-specific (Lemay *et al*., 2018), depend on the age of algal tissues (Weigel and Pfister, 2019; Ramirez-Puebla *et al*., 2020) and follow reproducible seasonal successions that may be explained by water temperature (Bengtsson *et al*., 2010; Minich *et al*., 2018). In addition, physiological parameters varying at the algal surface may impact communities. Oxygen release by the alga can promote the growth of aerobic bacteria but also harm epiphytic bacteria by producing reactive oxygen species (ROS) (Goecke *et al*., 2010; Egan *et al*., 2013). Kelps may also control resident or pathogenic microorganisms by secreting secondary metabolites such as halogenated compounds (Egan *et al*., 2014). In contrast to epiphytic communities on intact macroalgae, the specific bacterial communities colonizing detached kelps and their succession are still understudied. Total microflora has been determined essentially from kelp detritus stranded on intertidal areas (Koop *et al*., 1982; Bouvy *et al*., 1986; Delille and Perret, 1991). Even less information is available on the taxonomy, function and succession of bacterial communities colonizing large submersed accumulations of kelp fragments on benthic subtidal habitats. Furthermore, kelp accumulation and degradation processes are also expected to influence sediment communities, which are known to harbour contrasted and more diverse microbial communities compared to the overlying water column (Gobet *et al*., 2012).

We previously reported an experimental approach to mimic dislodgement and accumulation of the kelp *Laminaria hyperborea* on a subtidal sandy bottom ecosystem of the north-western coast of Brittany, France (de Bettignies *et al*., 2020). We showed that algal biomass decomposition started after 2 weeks and reached a critical step after 11 weeks, with an increase in respiration rate and phlorotannin content. After 24 weeks, 85% of the algal biomass was lost. Using samples collected during the same experiment, we investigated here the changes in bacterial community abundance and composition and predicted functions associated with the *in situ* degradation of the kelp biomass over 6 months, in four compartments: *L. hyperborea*'s tissues, sediments directly underneath the experimental cages (hereafter 'underlying sediment'), control sediments 2 m away from the cages and devoid of kelp tissues (hereafter 'external sediment'), and the overlying seawater 1 m above the cages. We tested the following hypotheses: (i) the bacterial diversity and community structure are specific to a given compartment; (ii) there is a succession of different bacterial groups associated with the degradation of *L. hyperborea*'s tissues; and (iii) bacterial communities in the underlying sediment are affected by the degrading kelp tissues and different from the external sediment.

Results

Fluctuations and diversity patterns of the bacterial community during kelp degradation

The characteristics of the 92 samples analysed in this study are listed in the Supporting Information Table S1. Total bacterial abundance was estimated by quantitative PCR in each compartment using 16S rRNA gene copy number as a proxy. The average number of 16S rRNA gene copies on kelp surfaces was initially 2.27×10^8 copies.cm^{-2}. Considering an average of four copies of 16S rRNA gene per bacterial cell (Větrovský and Baldrian, 2013), it corresponds to ca. 6×10^7 cells.cm^{-2}. It decreased significantly to 5.65×10^7 copies.cm^{-2} (ca. 1.4×10^7 cells.cm^{-2}) during the first 2 weeks and remained stable afterwards [analysis of variance (ANOVA), $F_{7,16} = 7.37$, $P < 0.001$; Fig. 1A]. Over the 6 months, 16S rRNA gene copy number significantly increased in the surrounding seawater (ANOVA, $F_{7,16} = 4.02$, $P = 0.010$), the underlying sediment (ANOVA $F_{7,16} = 3.83$, $P = 0.012$) and to a lesser extent in the external sediment (ANOVA $F_{7,14} = 4.32$, $P = 0.010$) (Fig. 1B and C). Notably, the number of 16S rRNA gene copies was similar between the two sediment compartments the first 2 weeks, but the increase tended to be stronger in the underlying sediment (4.6-fold change between 0 and 24 weeks) than in the external sediment (1.7-fold change).

Alpha-diversity indices were two to three times higher in sediment samples compared to kelp-associated and water column samples (Fig. 1D and F; Supporting Information Fig. S1). The OTU richness and the Shannon index from kelp-associated samples increased significantly in the first 11 weeks (OTU richness from 351–493 to 2090–2312, Shannon index from 2.4–3.1 to 5.4–5.6; ANOVA, $F_{7,15} = 44.68$, $P < 0.001$ and $F_{7,15} = 54.78$, $P < 0.001$, respectively) before reaching a plateau. Bacterial diversity slightly increased in the water column throughout the experiment (ANOVA, $F_{7,16} = 48.73$, $P = 0.001$ for OTU richness and $F_{7,16} = 62.50$, $P = 0.001$

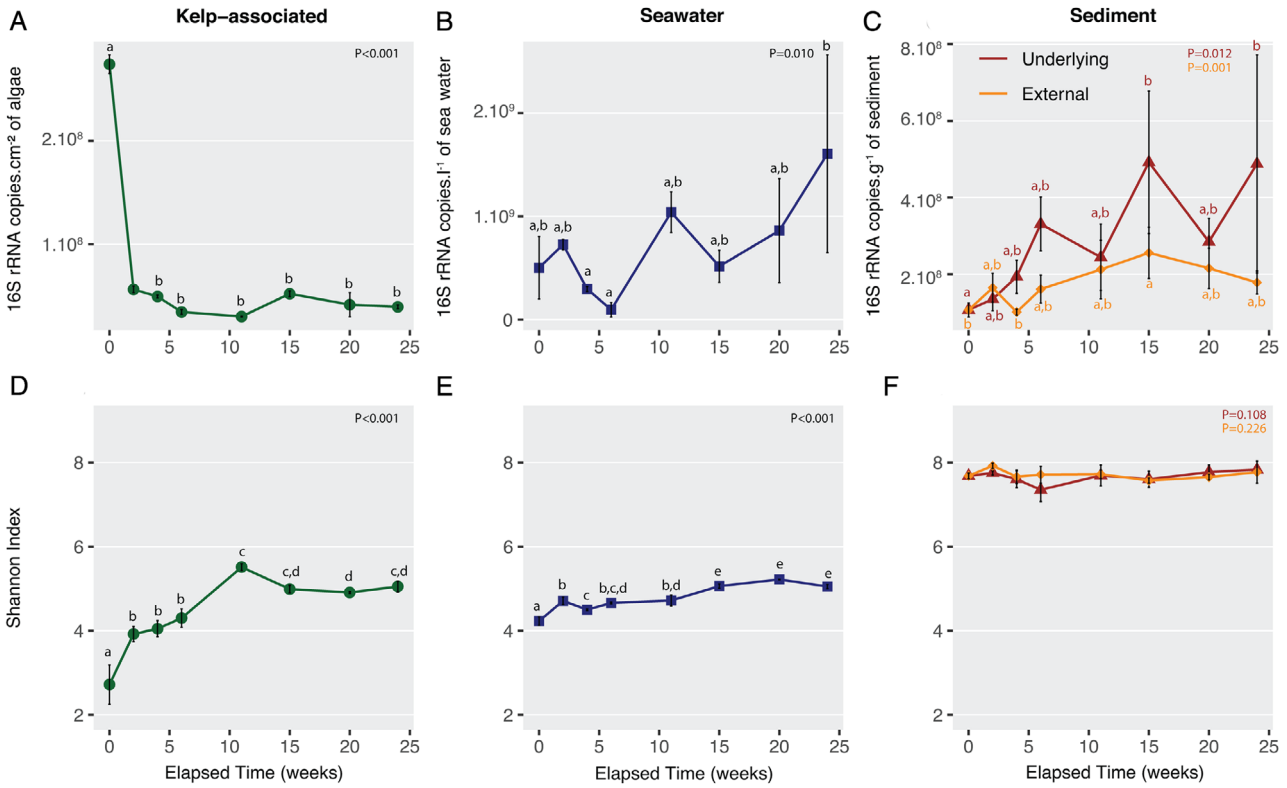

Fig 1. Abundance and diversity estimates of the bacterial community in the four compartments. Fluctuation of bacterial 16S rRNA gene copy number in the kelp-associated (A), the water column (B), and the underlying and the external sediment (C) compartments, and of the Shannon index in the kelp-associated (D), the water column (E), and the underlying and the external sediment (F) compartments during the degradation of *L. hyperborea*. ANOVA analysis was conducted to compare diversity indices over time. When significant ANOVA results were found ($P < 0.05$), a post hoc Tukey HSD test was calculated. Accordingly, different letters indicate significant differences between sampling dates. Values are mean ± standard deviation ($n = 3$, except n = 2 at 0 week in kelp-associated and 11 weeks in external sediment for Shannon index and at 2 and 11 weeks in external sediment for 16S rRNA copy number).

for Shannon index) while it stayed stable in the underlying and the external sediment samples ($P > 0.05$). Further, sample compartment showed a strong impact on the bacterial community structure (permutational analysis of variance PERMANOVA, $F_{3,84} = 35.77$, $P < 0.001$, Fig. 2A). Pairwise comparisons showed significant dissimilarities between each compartment ($P = 0.001$), although less pronounced between external and underlying sediments (Supporting Information Table S2). A higher dispersion was visible on the principal coordinates analysis (PCoA) within the algal samples (mean dispersion: 0.60) compared to the other compartments (seawater 0.55, underlying sediment 0.56, external sediment 0.53; $P < 0.001$). Only 1 946 OTUs, i.e. 2.2% of the total number of OTUs were shared between the four compartments (Fig. 2B). The sequences contained in this core set of OTUs are present in different proportions of the complete dataset in each compartment, they represented 12% of the sequence abundance in kelp-associated samples, 17% in seawater, 12% in underlying sediment and 7% in external sediment. In contrast, 58.2% (51 344 OTUs) of the total number of OTUs were specific to a given compartment, but they represented only 10% of the total number of sequences in the dataset.

Succession of epiphytic bacteria on kelp tissues

The structure of the kelp-associated bacterial community was impacted by the elapsed degradation time (PERMANOVA, $F_{7,15} = 6.33$, $P = 0.001$), showing distinct groups for freshly detached kelps (week 0) and samples collected between weeks 2–6 or 11–24 (Fig. 3A). Pairwise ANOVA comparisons confirmed that samples from weeks 2–6 significantly differed from samples from weeks 11–24 ($F_{1,19} = 13.46$, $P = 0.003$). Although visible on the ordination plot, the difference between samples from week 0 and the other groups could not be reliably tested due to one missing sample. Constrained ordination using distance-based redundancy analysis (db-RDA) showed that four environmental parameters were significant explanatory variables, namely remaining biomass

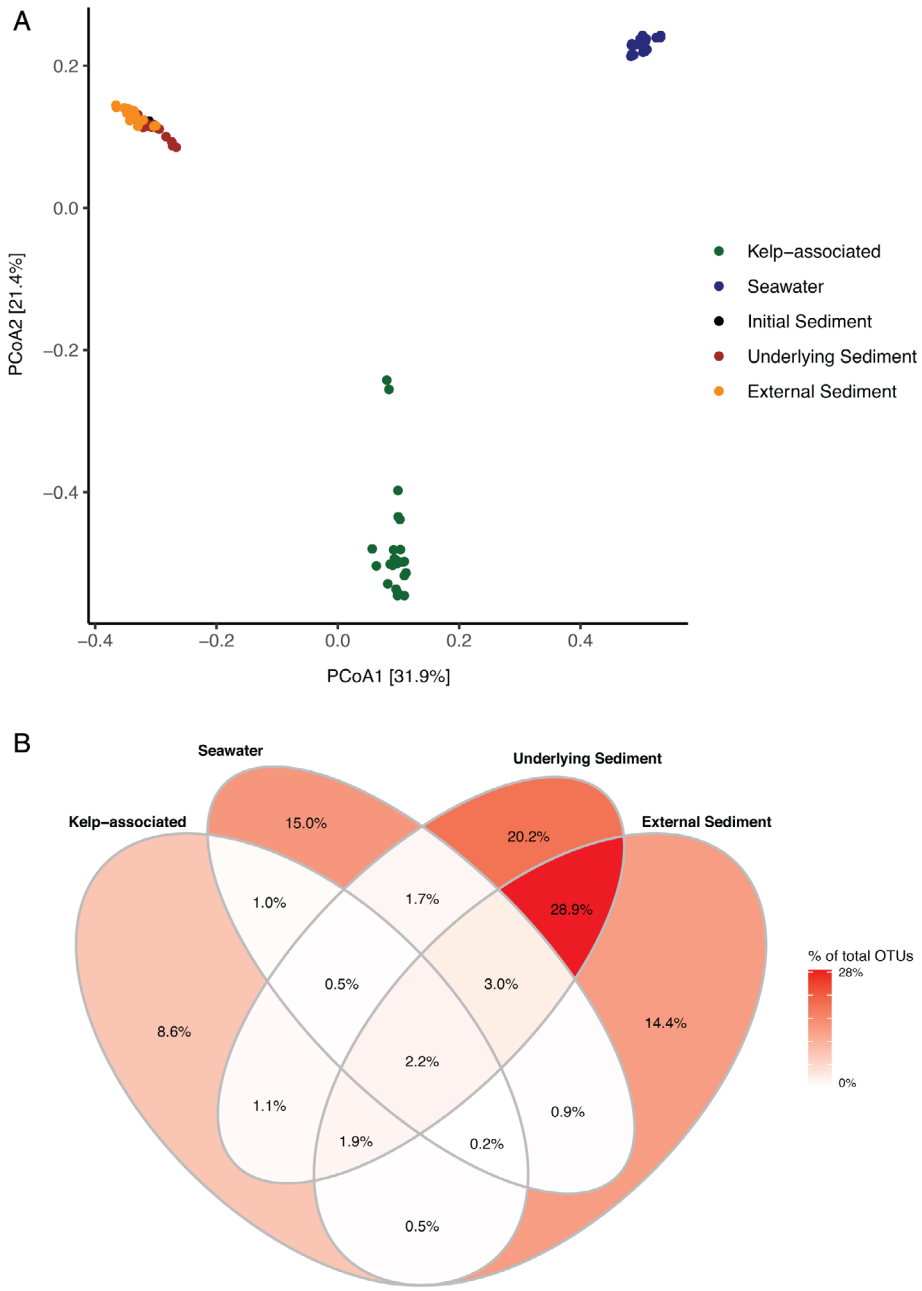

Fig 2. Bacterial community structure in the four compartments during the degradation of detached *L. hyperborea*. A. Two-dimensional representation of a PCoA calculated from the Bray–Curtis dissimilarity index. The plot represents samples from all time points. B. Proportion of OTUs unique to one compartment or shared between compartments, calculated from the total number of 88 194 OTUs in the dataset.

($F_{1,15}$ = 11.09, P = 0.001), respiration ($F_{1,15}$ = 6.35, P = 0.001), temperature ($F_{1,15}$ = 3.80, P = 0.002) and light ($F_{1,15}$ = 2.39, P = 0.025).

To further understand these patterns of the community structure, we investigated fluctuations of bacterial taxonomic groups at the kelp surface. The epiphytic community of freshly detached kelps was dominated by *Alphaproteobacteria* and *Gammaproteobacteria* (ca. 62% and 32% of all sequences at week 0, respectively), while other classes represented less than 3% (Fig. 3B). In particular, 83% of the sequences retrieved from kelp-associated samples at week 0 belonged to only 10 OTUs, with four of them assigned to *Litorimonas* and three to *Hellea* (Supporting Information Fig. S2). The *in situ* degradation of kelp biomass was associated with a succession pattern in the taxonomic composition of the epiphytic community (Fig. 3B; Supporting Information Fig. S2). *Alphaproteobacteria* remained the most abundant class throughout the experiment, although their contribution started decreasing after 4 weeks and reached 40% after 24 weeks. The proportion of *Bacteroidia* increased early on from 2.5% at week 2 to 14.6% after

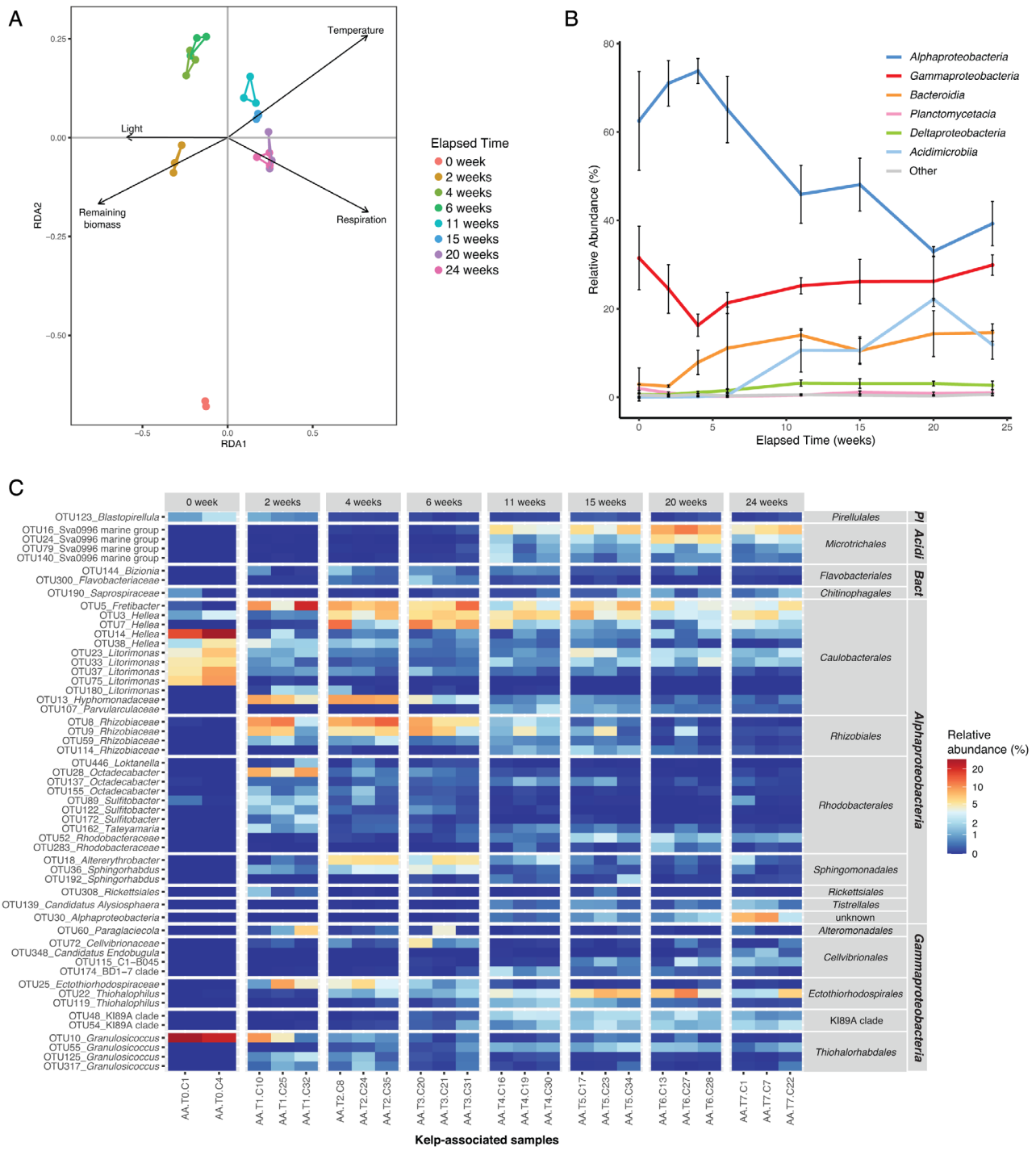

Fig 3. Fluctuations of kelp-associated bacterial communities during the degradation of detached *L. hyperborea*. A. db-RDA plot with vectors representing significant contextual predictors. Samples from the same sampling date are connected by coloured segments. B. Relative abundance of bacterial classes in kelp-associated samples during the 6 month-experiment. Sequence relative abundances of classes representing less than 0.5% of all sequences at each sampling time were summed into the 'Other' category. Values are mean ± standard deviation (n = 3, except for T0 n = 2). C. Relative abundance of differentially abundant kelp-associated OTUs during the experiment. OTUs showing significant differential abundance (P < 0.05) and representing at least 1.5% of the sequences in at least one sample are shown. OTUs were annotated at the genus level. For unclassified genera, taxa were assigned to the lowest taxonomic level identified. OTUs were grouped by class and order. Pl: *Planctomycetacia*; Acidi: *Acidimicrobiia*; Bact: *Bacteroidia*.

24 weeks. *Acidimicrobiia* were rare (<0.5%) until week 6 but increased afterwards, peaking at 22% relative sequence abundance at week 20. The contribution of *Deltaproteobacteria* increased slightly from the initial sampling date (0.6%) to week 11 (3.2%) and stayed stable afterwards. This pattern differed from the one observed in the surrounding seawater (Supporting Information Fig. S3A), where a seasonal increase of *Gammaproteobacteria* during summer (weeks 11–15) coincided with a decrease of *Alphaproteobacteria* and *Bacteroidia*.

A differential abundance test detected 249 OTUs (i.e. 1.8% of the total OTUs) for which the relative sequence abundance significantly changed with kelp degradation time ($P < 0.05$) (Supporting Information Table S3). For clarity, we only display in Fig. 3C the 54 differential OTUs that represent ≥1.5% of the total community in at least one sample. Among these, seven OTUs affiliated to *Granulosicoccus* (*Gammaproteobacteria*) and *Litorimonas* and *Hellea* (*Alphaproteobacteria*) were abundant at the beginning of the experiment and decreased over time (Tukey; $P < 0.001$ between week 0 and 2). This decrease was particularly drastic for OTU10 (*Granulosicoccus*) and OTU14 (*Hellea*), which accounted for 25.4% and 22.5% at week 0 and only 0.03% and 1.1% after 24 weeks respectively ($P < 0.001$). The sequence abundance of 18 *Alphaproteobacteria* OTUs out of the 32 represented in Fig. 3C increased during the first 4 weeks of the experiment and then decreased. The sequence abundance of 8 out of 14 *Gammaproteobacteria* OTUs, including members of *Cellvibrionales*, *Ectothiorhodospirales* and the KI89A clade, increased after 11 weeks of degradation. In particular, one OTU related to *Thiohalophilus* (OTU22) peaked at 7% mean relative sequence abundance at week 20. The sequence abundance of four OTUs related to the Sva0996 marine group (*Microtrichales*, *Acidimicrobiia*) showed an important increase between 6 and 11 weeks of experiment ($P = 0.003$). The most abundant one (OTU16) represented 0.1% of the communities after 6 weeks vs. 5.6% after 6 months. Finally, 14% (35/249) of the differential OTUs belonged to *Bacteroidia* (Supporting Information Table S3) but are not represented in Fig. 3C since they did not pass the 1.5% abundance threshold we chose for clarity.

We built a correlation network of the kelp-associated bacterial communities to search for potential associations (Fig. 4). The final network comprised 134 nodes and 572 edges. Sixty-seven percent of the associations were positive, including those with a maximum delay of one sampling date (384 and 188 positive and negative associations, respectively). Among the 10 contextual variables included in the dataset, eight showed significant associations within the network. The variables with the most associations were 'Temperature' (23 significant edges), "C/N" (22 significant edges) and 'Respiration' (19 significant edges) (Supporting Information Fig. S4). Most positive associations of OTU relative sequence abundance to respiration and C/N ratio were delayed. Community respiration was negatively correlated with algal biomass, indicating that the bulk of oxygen consumption did not come from algal respiration. Instead, respiration was positively correlated with temperature, which is expected to increase bacterial activity. Eight clusters were detected in the network (Supporting Information Table S4), which might represent strong microbial associations, i.e. nodes that are highly connected to each other but weakly connected to nodes outside of their module. In particular, the two strongest clusters 1 and 2 comprised 66% of the nodes in the network (Fig. 4, inset) and were almost mutually exclusive, suggesting they denote two different communities during the bacterial succession. Most OTUs from cluster 2 showed a major change in their relative sequence abundance during the first 6 weeks (Supporting Information Fig. S5). This suggests that cluster 2 represents associations occurring early during the bacterial succession. Seventy-five percent of these OTUs from cluster 2 belonged to *Alphaproteobacteria* (Supporting Information Table S5). None of these OTUs had significant associations to environmental parameters (Fig. 4). In contrast, OTUs from cluster 1 were more diverse (Supporting Information Table S5), significantly associated with a number of environmental parameters (Fig. 4) and showed a later response (Supporting Information Fig. S6). Only four OTUs were shared between clusters 1 and 2 (Fig. 4, inset, nodes in crimson colour), including OTU923 (*Arenicella*, *Gammaproteobacteria*), OTU190 (*Saprospiraceae*, *Bacteroidia*), OTU5587 (*Hellea*, *Alphaproteobacteria*) and OTU361 (*Litorimonas*, *Alphaproteobacteria*). These shared OTUs showed the highest closeness centrality (a measure indicating the distance of a node to all other nodes) of the entire network (CC > 0.4) and might therefore act as hubs connecting the two types of communities found in clusters 1 and 2.

Putative functional profiles were inferred from 16S rRNA data using FAPROTAX for the kelp-associated communities (Fig. 5), leading to the assignation of 3 753 OTUs to at least one functional group (31.4% of all OTUs). The predicted abundance of functional groups involved in aerobic chemoheterotrophy and the oxidation of sulfur compounds increased from 2 weeks on before a slight decrease at 11 weeks. Moreover, predicted groups involved in fermentation and nitrate reduction were virtually absent initially (< 18 and 28 estimated sequence read counts, respectively) and more represented during the degradation (55–997 and 177–899 estimated sequence read counts, respectively). Since sugars constitute a major part of algal biomass, we specifically assessed the

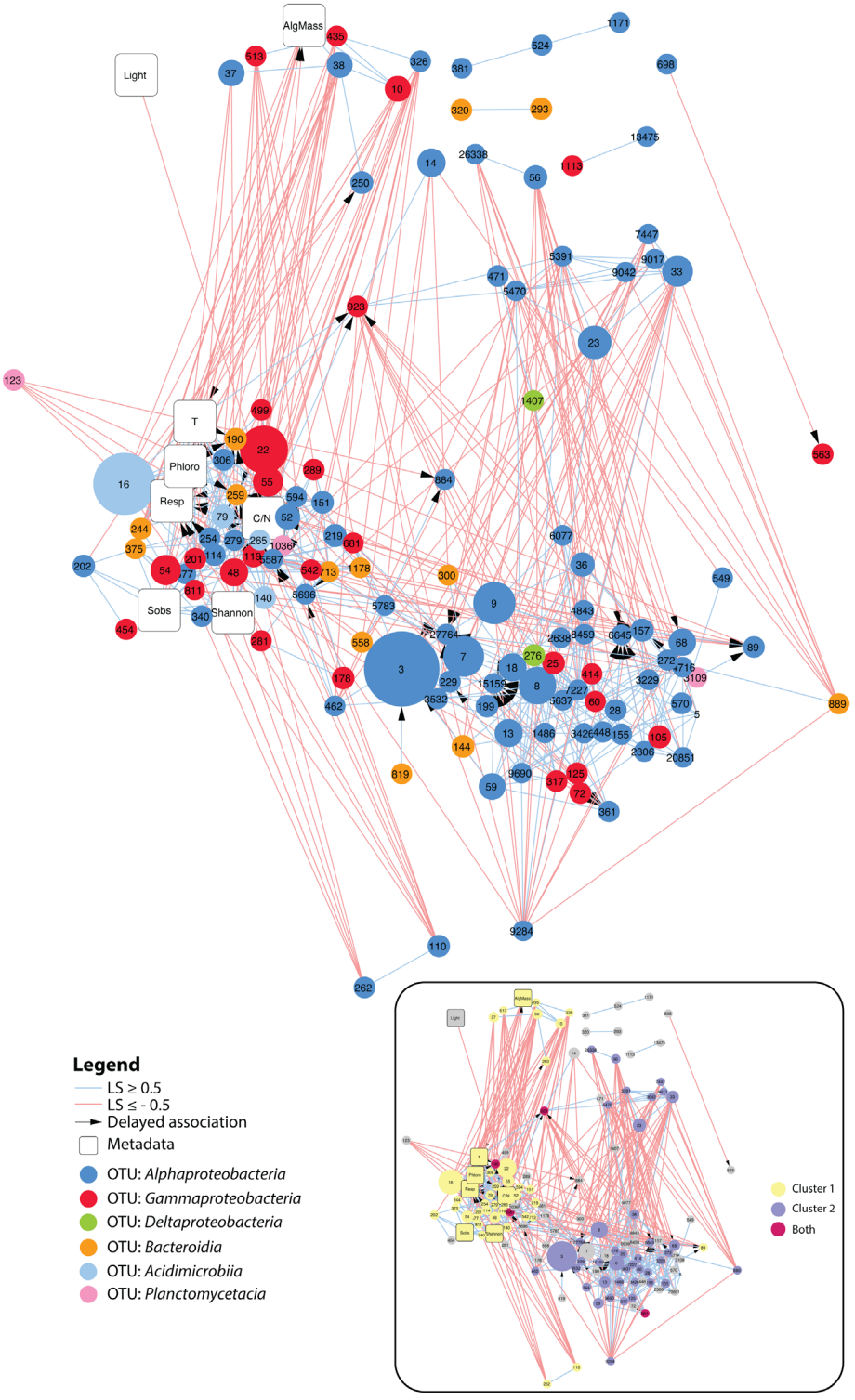

Fig 4. Extended local similarity analysis (eLSA) network obtained for kelp-associated bacterial communities throughout the eight sampling time points. OTU nodes are colour-coded based on taxonomy, and their size is proportional to the median relative abundance throughout the experiment. Positive and negative associations are depicted by light blue and light red lines, respectively. Arrows indicate delayed temporal associations (maximum delay = 1 sampling date). Network characteristics were as follows: clustering coefficient 0.358; characteristic path length 3.171; diameter 8; average number of neighbours 8.54; maximum number of neighbours 23; network density 0.064. Inset: the same network where nodes are coloured depending on their belonging to the main cluster 1 (yellow) and cluster 2 (purple) or both (crimson). AlgMass: remaining algal biomass; T: water temperature; Phloro: concentration of phlorotannins in kelp tissue; Resp: community respiration; Sobs: number of bacterial OTUs; C/N: carbon to nitrogen ratio of kelp tissue.

predicted relative sequence abundance of glycoside hydrolases (GH) and polysaccharide lyases (PL) with PICRUSt2. The mean Nearest Sequenced Taxon Index (NSTI) was 0.21 ± 0.03. NSTI estimates the extent to which microorganisms in a given sample are related to sequenced genomes used to infer metagenomes and ranges from 0 (high similarity) to 1 (no similarity). The relatively high NSTI values obtained here denote that few genomes of kelp-associated bacteria are available yet, and that predictions should be interpreted carefully. The

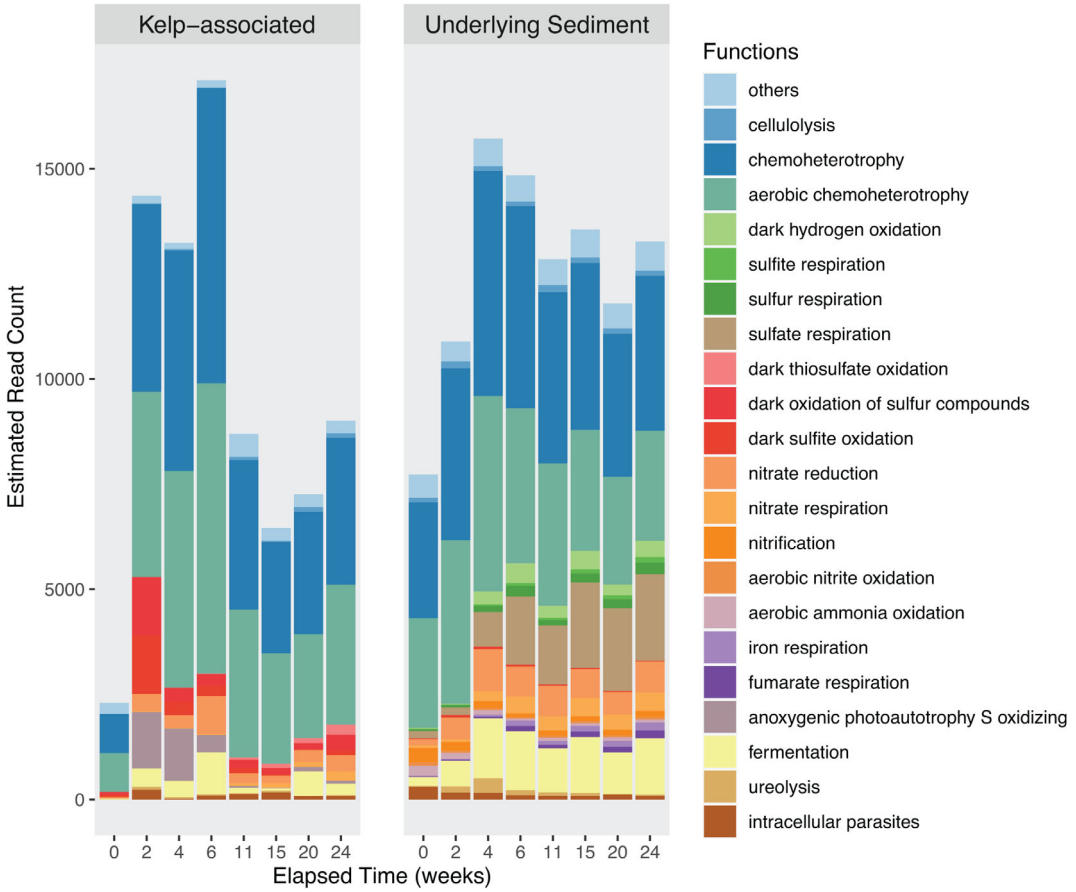

Fig 5. Putative functional groups of kelp-associated and underlying sediment communities throughout kelp degradation. The OTUs from the rarefied dataset were parsed against the FAPROTAX database to assign putative functions to taxonomically defined OTUs. Only functions varying significantly across time based on the ALDEx2 analysis were represented ($P < 0.05$).

predicted relative sequence abundance of endolytic enzymes such as cellulase and endo-1,4-β-xylanase decreased over time (Supporting Information Fig. S7). In contrast, the predicted relative sequence abundance of several exolytic GHs increased significantly with elapsed time of degradation, either at an early stage, from 2 weeks (i.e. α-glucosidase, α-galactosidase and β-mannosidase) or later, after 6 weeks (i.e. α-amylase, 4-α-D-{(1- > 4)-α-D-Glc}trehalose trehalohydrolase, α-mannosidase) .

Effect of algal degradation on sediment bacterial communities

We further focused on the effect of kelp accumulation on sediment bacterial communities of the receiving ecosystem. Beta-diversity analysis of the underlying sediment samples showed an effect of the elapsed degradation time on the bacterial community structure (Fig. 6A) (PERMANOVA, $F_{7,16} = 2.10$, $P < 0.001$). Constrained ordination using db-RDA showed that three environmental parameters were significant explanatory variables, namely remaining biomass ($F_{1,16} = 4.53$, $P = 0.001$), respiration ($F_{1,16} = 1.97$, $P = 0.009$) and temperature ($F_{1,16} = 1.95$, $P = 0.012$). Sediment communities were initially dominated by *Gammaproteobacteria* and *Bacteroidia* (about 36% and 23% of all sequences at week 0, respectively) (Fig. 6B**)**. Only ca. 9.5% of OTUs present in the underlying or external sediments were shared with the algal epiphytic microbiota (Fig. 2B). The abundance of these OTUs in the sediments and in the kelp-associated compartments represented 22.3% and 20.8% of the overall sequence abundance, respectively. Bacterial communities in external sediments were stable with a slight increase of *Bacteroidia* during kelp degradation (Supporting Information Fig. S3B), while changes were more pronounced in the underlying sediment (Fig. 6B). Furthermore, about 40% of the OTUs detected in the underlying sediments (containing 13% of the number of sequences in the underlying sediments) were not found in the external sediments (Fig. 2B). In underlying sediments, the sequence relative abundance of *Gammaproteobacteria* decreased

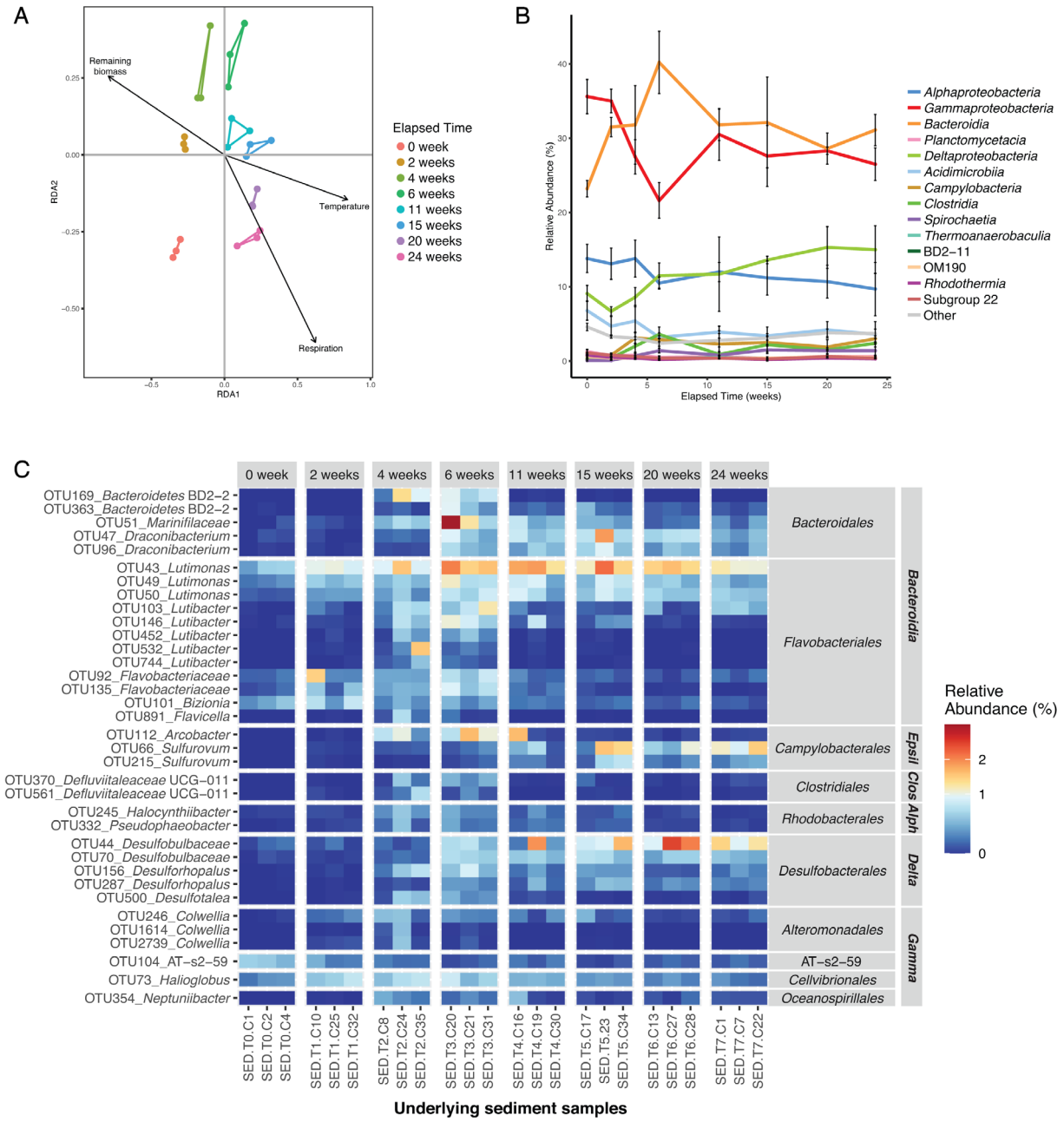

Fig 6. Fluctuations of bacterial community structure in the sediment underlying *L. hyperborea* during its degradation. A. db-RDA plot with vectors representing significant contextual predictors. Samples from the same sampling date are connected by coloured segments. B. Relative abundance of bacterial classes in underlying sediment samples during the 6 month-experiment. Sequence relative abundances of classes representing less than 0.5% of all sequences at each sampling time were summed into the 'Other' category. Values are mean ± standard deviation (n = 3). C. Relative abundance of differentially abundant OTUs in the underlying sediment during the experiment. OTUs showing significant differential abundance ($P < 0.05$) and representing at least 0.5% of the sequences in at least one sample are shown. OTUs were annotated at the genus level. For unclassified genera, taxa were assigned to the lowest taxonomic level identified. OTUs were grouped by class and order. Epsil: *Epsilonproteobacteria*; Clos: *Clostridia*; Alph: *Alphaproteobacteria*; Delta: *Deltaproteobacteria*; Gamma: *Gammaproteobacteria*.

until week 6, reaching 22% before an increase at 31% and stabilization around 27%. This was different from external sediments, where *Gammaproteobacteria* gradually decreased to 27% until week 15. The sequence relative abundance of *Bacteroidia* increased rapidly in underlying sediments, peaking at about 40% after 6 weeks before stabilization around 31%. This increase was less pronounced in external sediments. The relative sequence abundance of *Alphaproteobacteria* in underlying sediments slightly decreased from about 14% at week 0 to

10% at week 24, while it stayed stable in external sediments. *Deltaproteobacteria* were enriched along the time course, representing about 9% of the total sequence relative abundance at week 0 and reaching 15% and 11% at week 24 in underlying and external sediments, respectively. Differential abundance analysis detected 177 OTUs (i.e. 0.3% of the total number of OTUs) for which the relative sequence abundance significantly changed in the underlying sediment during kelp degradation ($P < 0.05$), while 27 were detected in external sediments (Supporting Information Table S6 and S7). Among these, only 11 OTUs affiliated with *Bacteroidia*, *Deltaproteobacteria* and *Gammaproteobacteria* were found to significantly vary with time in both underlying and external sediments (Supporting Information Fig. S8). For consistency, we applied the same filter to differential OTUs in underlying sediment than that used for kelp-associated samples (>1.5% relative abundance in at least one sample), but only seven OTUs passed this criteria. Consequently, we lowered the cut-off at 0.5% to show 35 differential OTUs (Fig. 6C). The sequence abundance of the 35 represented OTUs stayed generally stable during the first 2 weeks. The sequence abundance of 16 members of *Bacteroidales* and *Flavobacteriales* (*Bacteroidia*) as well as two *Clostridiales* (*Clostridia*) and two *Rhodobacterales* (*Alphaproteobacteria*) increased between 0 and 4 weeks (Tukey; $P = 0.015$, $P = 0.005$, $P = 0.010$, respectively) and decreased afterwards ($P = 0.001$, $P = 0.044$, $P = 0.037$ between 6 and 24 weeks, respectively). Five *Desulfobacterales* OTUs (*Deltaproteobacteria*) increased between 0 and 6 weeks ($P = 0.015$) and two *Sulfurovum* OTUs (*Campylobacteria*) increased between 0 and 15 weeks ($P = 0.011$).

Putative functional profiles were inferred for underlying sediment communities (Fig. 5). The 10 657 OTUs were assigned to at least one functional group (24.5%). The predicted abundance of functional groups involved in aerobic chemoheterotrophy, nitrogen cycle and fermentation increased during the first 4 weeks and remained stable afterwards. In contrast, sulfate-reducing functional groups increased throughout the degradation process. The predicted sequence abundance of the sulfate respiration group increased 10 times over 24 weeks.

Discussion

In temperate coastal ecosystems, large amounts of kelp tissues are exported to the seafloor naturally or following seasonal storms. To investigate the degradation dynamics and the effect of kelp tissue accumulation on receiving ecosystems, a 6-month experiment was deployed on a low subtidal sandy floor. Here, we investigated the bacterial community succession associated with the degradation of *L. hyperborea* tissue accumulated on the seafloor in four compartments: the degrading kelp, the seawater, the underlying and the external sediment.

Microbial communities are specific to a given compartment

Bacterial diversity patterns showed specific communities and succession in the four compartments. In particular, half of the kelp-associated OTUs were not detected in any other compartment. This observation was expected as each compartment features contrasting biotic and abiotic conditions. The kelp surface is an interface between the alga and its surrounding environment where specific metabolic exchanges occur (e.g. defence, biofilm control). This is an organic-rich environment, ideal for copiotrophs but with high competition between microorganisms for surface colonization, which might select for K-strategists (Andrews and Harris, 1986; Fierer *et al*., 2007). In contrast, the water column is more substrate-depleted, which may select for oligotrophs and K-strategists. Finally, sediments concentrate decaying organic matter, available for r-strategist copiotrophs, and oxygen availability as well as chemical conditions varying with depth offer multiple microniches. This likely explains the higher diversity with various microbial life strategy-types in this compartment compared to kelp-associated and seawater samples. Overall, bacterial diversity was not strongly impacted in the seawater and external sediments during the 6-month period, pointing to a local effect of kelp accumulation. Indeed, constant water renewal due to tides and currents likely dilutes the compounds liberated upon degradation (Masson, 2002). In the following paragraphs, we focus on the major changes observed in kelp-associated and underlying sediment communities.

Bacterial communities associated with healthy kelp tissue

Throughout the experiment, kelp-associated bacterial communities were dominated by *Alphaproteobacteria* and *Gammaproteobacteria*. These bacterial classes are regularly found among the most abundant on brown algal tissue (Lachnit *et al*., 2011; Stratil *et al*., 2013; Martin *et al*., 2015; Ramirez-Puebla *et al*., 2020). At the initial sampling date, in April 2017, the surface of fresh *L. hyperborea* hosted an abundant resident bacterial community, concurring with previous studies showing 10^6–10^9 cells.cm^{-2} on kelp surfaces (Corre and Prieur, 1990; Martin *et al*., 2014). The initial community had a low diversity and was dominated by a few OTUs affiliated to *Granulosicoccus* (*Gammaproteobacteria*), *Hellea* and *Litorimonas* (*Alphaproteobacteria*). These genera were always present in the epiphytic community of *L. hyperborea* and were previously detected on other brown algae such as *Macrocystis pyrifera* (Florez *et al*., 2019), *Taonia atomaria* (Paix *et al*., 2019), *Fucus vesiculosus* (Lachnit *et al*., 2011; Stratil *et al*., 2013), and

L. digitata (Gobet, personal communication). We detected < 1% *Planctomycetia* and *Verrucomicrobia* in the initial communities. This contrasts with previous studies using fluorescent *in situ* hybridization and denaturing gel gradient electrophoresis where these taxa contributed up to 50% of epiphytic bacteria on *L. hyperborea* at the Norwegian coast (Bengtsson and Øvreås, 2010; Bengtsson *et al*., 2010). This discrepancy may be due to (i) ecological differences between Norway and Brittany coasts, (ii) seasonal variations and (iii) the technique used to survey the microbial community (Zinger *et al*., 2012). The primer used for our metabarcoding approach, designed to minimize amplification of plastid sequences, may partly miss *Planctomycetia* and *Verrucomicrobia* (Thomas *et al*., 2020).

Dynamics of bacterial communities at the surface of degrading kelp tissues

The kelp-associated bacterial community shifted after 2 weeks. 16S rRNA gene copies decreased fourfold and stayed stable during the 6 months. This could reflect both a decrease in the total number of bacteria attached to the kelp surface and a shift towards taxa featuring fewer 16S rRNA gene copies per genome such as *Acidobacteria* (Větrovský and Baldrian, 2013). Analysis of kelp-associated community composition further showed a biphasic succession, with changes during the first 11 weeks followed by stabilization of the bacterial community composition until 24 weeks. This corroborates the kinetics of algal biomass degradation (de Bettignies *et al*., 2020), which showed a rapid loss of algal biomass until week 11 that slowed down until week 24. During the 6-month experiment, oxygen consumption increased in cages while algal biomass decreased. Although this could partially be due to colonization by fauna (de Bettignies *et al*., 2020), it likely indicates the important contribution of kelp-degrading bacteria to the holobiont respiration (here, the kelp host and its associated fauna and microbiota) (de Bettignies *et al*., 2020). Overall, we suggest that the observed changes in kelp-associated bacterial communities result from a succession of heterotrophic taxa with different substrate niches, as previously observed for the degradation of terrestrial plant biomass (Jiménez *et al*., 2017) and marine polysaccharide particles (Enke *et al*., 2019). During the first phase, kelp biomass was colonized by bacteria specialized in the degradation of complex algal polysaccharides and exudates. This corroborates results we previously obtained, showing an increase of mannitol- and alginate-utilizing bacteria between 0 and 2 weeks (de Bettignies *et al*., 2020). The activity of these early degraders likely opened new substrate niches and increased the accessibility for opportunistic scavenger bacteria that responded during the second phase. Some of these changes might be partly due to seasonal variations that would also occur on intact, non-detached algal tissue. This is suggested by the significant effect of temperature and light found with db-RDA and the number of associations between individual OTUs and temperature in the network. Previous studies showed that seasonal parameters influence brown algal microbiomes, notably increasing temperature that can favour the growth of *Flavobacteriales*, *Rhodobacterales* and *Rhizobiales* (Stratil *et al*., 2013; Minich *et al*., 2018). In addition, the observed increase in OTU richness is stronger than what was previously measured on kelps due to seasons (Weigel and Pfister, 2019) tissue aging (Bengtsson *et al*., 2012) or temperature elevation (Minich *et al*., 2018), suggesting a combined effect of degradation and seasonal variations. Furthermore, kelp defence reactions in early time points (e.g. emission of reactive oxygen species and halogenated compounds) that occur in stress situations such as blade detachment, cutting, displacement and degradation (Cosse *et al*., 2007) may select for a resistant fraction of the resident bacterial community. The control exerted by living kelps on biofilm formation through surface metabolites (Bengtsson *et al*., 2012; Salaün *et al*., 2012) might also be relaxed during algal decay, possibly explaining some of the observed changes.

During the first phase of the succession (0–6 weeks), the diversity of the kelp-associated community increased, due to a decrease in the abundance of initially dominant OTUs affiliated to *Litorimonas*, *Hellea* and *Granulosicoccus*. These genera were reported as primary surface colonizers (Dang and Lovell, 2016; Ramirez-Puebla *et al*., 2020) but might be outcompeted by specialist algae-degraders. In parallel, a number of OTUs that were initially absent or rare at the kelp surface showed a transient increase in abundance during the first 6 weeks of degradation, including *Alphaproteobacteria* (e.g. *Fretibacter*, *Hellea*, unclassified *Rhizobiaceae*, *Octadecabacter*, *Sulfitobacter*, *Tateyamaria*, *Altererythrobacter*) and *Gammaproteobacteria* (e.g. *Paraglaciecola*, unclassified *Ectothiorhodospiraceae*). The same changes were not detected in the surrounding seawater, suggesting that they result more from an enrichment of initially rare taxa at the kelp surface than from a colonization by free-living bacteria. The rapid and transient enrichment of these bacteria on detached blades might be due to their capacity to assimilate low-molecular weight algal compounds. For instance, a study on the *Fucus spiralis* microbiota showed that *Sulfitobacter* and *Octadecabacter* isolates were able to grow on mannitol (Dogs *et al*., 2017), a brown algal polyol whose exudation is enhanced upon stress such as blade damage. Members of the genus *Tateyamaria*, previously found on kelp (Bengtsson *et al*., 2012), can use the brown algal storage compound laminarin (Sass *et al*., 2010). The first phase of the succession was also

characterized by a global increase in the relative sequence abundance of numerous *Bacteroidia* OTUs which individually represented a low proportion of the microbiota, and stayed stable afterwards. *Bacteroidia* are commonly known as particle-associated taxa (Thiele *et al*., 2015) and positively respond to an input of marine polysaccharides (Wietz *et al*., 2015; Balmonte *et al*., 2018, 2019; Enke *et al*., 2019). In particular, members of the family *Flavobacteriaceae* are specialized in the degradation of algal biomass (Thomas *et al*., 2011; Teeling *et al*., 2012). *Flavobacteriaceae* are known to colonize algal surfaces and form biofilms (Mann *et al*., 2013) and to possess numerous polysaccharide utilization loci (PULs) (Grondin *et al*., 2017) that encode a great number and diversity of carbohydrate-active enzymes for the breakdown of algal polysaccharides, together with regulators and transporters. Genomes of marine flavobacteria frequently feature PULs predicted to be involved in the degradation of brown algal polysaccharides such as alginate, laminarin and fucoidan (Barbeyron *et al*., 2016; Kappelmann *et al*., 2019). Notably, the PUL dedicated to alginate, the most abundant polysaccharide in kelps, was biochemically characterized and shown to account for the full substrate degradation into simple sugars (Thomas *et al*., 2012; Dudek *et al*., 2020). Therefore, the *Bacteroidia* detected here on detached kelps likely contributed to the decomposition of the algal biomass.

During the second phase of the succession (11–-24 weeks), kelp-associated bacterial community was the most diverse, suggesting that new niches were available for bacterial colonization. The most striking observation is the enrichment in *Acidimicrobiia*, mainly due to OTUs related to the Sva0996 marine group. This group may be ubiquitous as it was previously detected on the brown macroalgae *Taonia atomaria* (Paix *et al*., 2019) and *L. digitata* (Gobet, personal communication), as well as sponges and ascidians (Steinert *et al*., 2015; Verhoeven *et al*., 2017; Dat *et al*., 2018), in deep marine sediments (Chen *et al*., 2016) and in the water column of oligotrophic environments (Reintjes *et al*., 2019). Little is known about the Sva0996 marine group, except its ability to use phytoplankton-derived dissolved proteins and potential importance in the dissolved organic nitrogen cycle (Orsi *et al*., 2016). Here, the enrichment in Sva0996-affiliated bacteria during the second phase of kelp degradation could suggest a liberation of soluble material from the kelp tissue. The second phase of the succession was also characterized by an enrichment in several gammaproteobacterial OTUs. The increase in *Cellvibrionaceae* might reflect their ability to use complex polysaccharides as those found in kelp biomass, a widespread trait in the family (Spring *et al*., 2015). Also increasing after 11 weeks, OTUs affiliated to the clades KI89A and BD1-7 belong to the oligotrophic marine *Gammaproteobacteria* (OMG) group (Cho and Giovannoni, 2004; Spring *et al*., 2015). Although more typical of oligotrophic environments, these clades were previously found on brown macroalgae (Dittami *et al*., 2016; Paix *et al*., 2019). Their increase in relative abundance towards the end of the 6-month period might reflect a seasonal effect, as previously observed in coastal marine bacterioplankton whereby an OTU affiliated to the KI89A clade was more abundant during the summer (Alonso-Sáez *et al*., 2015). Finally, the strong increase observed for an OTU related to *Thiohalophilus*, a sulfur-oxidizing chemolithoautotrophic gammaproteobacteria, could result from a boosted sulfur cycle in the underlying sediment (see next section).

Effect of kelp degradation on sediment communities

Bacterial diversity in sediments was higher and stable throughout the experiment compared to algal surfaces and water samples. This likely reflects the complexity of the sediment environment, that receives organic deposits all year-round and offers contrasted microscale niches (Boudreau *et al*., 2001; de Beer *et al*., 2005; Ettinger *et al*., 2017). Comparisons of underlying and external sediments indicate that algal degradation had mostly a local effect directly underneath the accumulated kelps. The low proportion of OTUs shared between kelp-associated and underlying sediment communities suggests that this change in community composition is not due to a direct transfer of OTUs from algae, but to a change of environmental conditions linked to kelp accumulation and degradation. Indeed, in the underlying sediment, there was a shift in abundance between the two most abundant bacterial classes, with the *Gammaproteobacteria* decreasing in sequence relative abundance until week 6 and the *Bacteroidia* increasing and remaining the most abundant group until 24 weeks. As stated in the section above, bacteria from the class *Bacteroidia* such as the *Flavobacteriaceae* are involved in degradation of complex molecules such as algal polysaccharides. This taxonomic group is likely enriched in the underlying sediment through the experiment as fragments of degrading algal tissue are continuously deposited onto the seafloor. Both the limited oxygen diffusion due to kelp accumulation and the activity of aerobic degrading bacteria are expected to rapidly deplete O_2 in underlying sediments. Accordingly, differential sequence abundance analyses and functional predictions indicated an increase of taxa involved in sulfur and nitrogen cycles, as well as fermentation. Although some of these changes might partially be due to seasonal variations (Gobet *et al*., 2012; Marchant *et al*., 2014), our data showed a significant effect of algal accumulation since early changes (2–4 weeks) were not seen in external sediments. Further, during tissue degradation, there was an increase in *Deltaproteobacteria*, a group regularly found in

temperate coastal sediment and known for sulfate and nitrate reduction (Mußmann *et al*., 2005). Sulfate reduction is one of the most common anaerobic degradation pathways for organic matter in marine sediments (Wasmund *et al*., 2017). Subsequently, several OTUs related to *Desulfobacterales* and *Clostridiales* were enriched during the degradation. Members of these orders are well-known sulfate reducers and are frequently detected in temperate marine sediments rich in organic matter (Muyzer and Stams, 2008; Gobet *et al*., 2012; Mahmoudi *et al*., 2015; Ettinger *et al*., 2017). *Desulfobacterales* feature metabolically versatile and larger genomes than other sulfate-reducing bacteria (SRB), which might allow a faster response to organic matter inputs (Strittmatter *et al*., 2009). OTUs related to *Arcobacter* and *Sulfurovum* were also enriched in underlying sediments during the degradation. These genera can oxidize reduced sulfur compounds produced by SRB (e.g. H_2S, thiosulfate) back to sulfate, therefore completing the sulfur cycle (Wasmund *et al*., 2017). Furthermore, FAPROTAX analysis showed a functional enrichment of nitrate reduction pathways. Nitrate reducers use either denitrification to N_2 or dissimilatory nitrate reduction to ammonium (DNRA). Here, the massive input of organic matter and probable increase in sediment sulfide concentrations due to SRB enrichment would be expected to favour DNRA (Burgin and Hamilton, 2007; Hardison *et al*., 2015). Therefore, we can speculate that kelp degradation allows retaining nitrogen inputs as bioavailable ammonium instead of loss as N_2. Similar to these results, a recent study (Aires *et al*., 2019) also showed that additions of red or green algal biomass (*Gracilaria vermiculophylla* or *Ulva rigida*, respectively) strongly favoured *Desulfobacterales*, *Bacteroidales*, *Clostridiales* and *Campylobacterales*. Therefore, at the order level changes in sediment bacterial communities due to seaweed accumulation do not appear to be specific to the type of algae.

Conclusion

In conclusion, following kelp detachment and accumulation on the seafloor, the structure and composition of the epiphytic bacterial community shifted, showing a biphasic succession of early degraders and secondary colonizers that might exploit different substrate niches. Besides this direct effect on kelp-associated bacteria, we also evidenced changes in the underlying sediments, showing that kelp accumulation likely has a global effect on the microbial communities of receiving ecosystems. This work paves the way for future studies investigating the functional determinants, mechanisms and bacterial interactions of the epiphytic microbiota during the kelp breakdown process.

Experimental procedures

In situ *experiment and sampling procedure*

The *in situ* experiment was conducted from April 2017 to October 2017 in the bay of Morlaix (48°42'33.78'' N, 003°57'12.36'' W) on the north-western coast of Brittany (France) and detailed elsewhere (de Bettignies *et al*., 2020). Briefly, cages were randomly filled with 1 kg of new blades from young healthy adult *L. hyperborea* sporophytes (140–200 cm). A total of 35 cages were set at 9 m depth on a sandy floor to simulate an accumulation of kelp fragments. Three cages were randomly selected at each of eight sampling times (0, 2, 4, 6, 11, 15, 20, 24 weeks) to sample algal surfaces, underlying and external sediments and overlying water as follows. Ten algal pieces of 1.3 cm diameter were subsampled from each cage using a sterilized stainless steel punch. The surface sediments (0–4 cm depth) directly below each cage ('underlying sediment') or 2 m away from the cages ('external sediment') were sampled in sterile plastic containers. 'Initial sediment' was collected immediately prior to the cages set-up. Three litres of the overlying water (1 m above the cages) were taken using Niskin bottles. Triplicates of 1 l were prefiltered at 3 μm to remove large particles and then filtered through a 0.2 μm Sterivex filter (Merck, Darmstadt, Germany). All samples were stored at −80°C before DNA extraction. Measurements of contextual parameters related to physico-chemical conditions (temperature, light, percent organic matter in sediment) and state of the kelp tissue (remaining biomass, oxygen consumption, photosynthetic capacity, carbon/nitrogen ratio, phlorotannin content) were detailed elsewhere (de Bettignies *et al*., 2020) and summarized in the Supporting Information text. The list of samples and contextual parameters is available in the Supporting Information Table S1.

DNA extraction. We adapted a protocol for DNA extraction from the algal surface. Algal pieces were immersed in a bacterial lysis buffer, without previous grinding of the tissues to prevent extraction of endophytic bacteria and algal plastids while efficiently lyzing epiphytic bacteria. After incubation, algal pieces were discarded and DNA was extracted only from the soluble lysate using a phenol:chloroform:isoamyl alcohol extraction combined with filtration steps of the NucleoSpin PlantII kit (Macherey Nagel, Hoerdt, France). For water samples, DNA was extracted from the 0.2 μm filters following a similar protocol as used for the algal samples. For sediment samples, DNA was extracted from 0.5 g of sediment using the DNeasy PowerLyzer PowerSoil Kit (Qiagen, Courtaboeuf, France). For further details, please see the Supporting Information text.

16S rRNA gene copies quantification. The total number of bacterial 16S rRNA gene copies in each sample was assessed by quantitative real-time PCR as described previously (Bacchetti De Gregoris *et al*., 2011), using the universal primers 926F/1062R. This primer pair has a predicted coverage of 55% for chloroplast-derived 16S rRNA genes (Silva Testprime on SSU r138.1). Therefore, we cannot exclude that a small proportion of quantified 16S rRNA gene copies originates from chloroplasts. Amplification and detection were performed in a LightCycler 480 Instrument II. For each sample, triplicate reactions were prepared as described in the Supporting Information text. Serial dilutions of purified bacterial genomic DNA ranging from 10^3 to 10^8 16S rRNA gene copies equivalent were used as a standard curve and were amplified in triplicate in the same run as the environmental samples. A non-template control was included in the run. Results were analysed using the LightCycler 480 Software v1.5. One-way ANOVA analyses followed by pairwise post-hoc Tukey HSD were conducted with time as fixed factor, individually for each compartment. Details on qPCR assays are given in the Supporting Information Table S8, following the MIQE guidelines (Bustin *et al*., 2009).

Library preparation, sequencing and sequence processing. As a positive control, we constructed a mock community based on the genomic DNA of 32 pure marine bacterial isolates as reported previously (Thomas *et al*., 2020). Libraries were prepared for the 94 samples (24 algal samples, 24 water samples, 3 initial sediment samples, 21 underlying sediment samples, 20 external sediment samples, one mock community and one negative control (PCR molecular grade water)). Libraries were prepared using the primers S-D-Bact-0341-b-S-17 (5' CCTACGGGNGGCWGCAG 3′) and 799F_rc (5' CMGGGTATCTAATCCKGTT 3′) targeting the V3-V4 region of the 16S rRNA gene and sequenced on a MiSeq paired-end sequencing run (300 cycles × 2, Illumina, San Diego, CA, USA) as described previously (Thomas *et al*., 2020). 16S rRNA gene amplicon sequences are available at NCBI under BioProject ID PRJNA667331. Raw Illumina sequence reads were trimmed to remove low-quality bases and Illumina adapters using Trimmomatic v0.38 (Bolger, Lohse and Usadel, 2014, for details see Supporting Information text). Overlapping paired-end sequence reads were assembled using PANDAseq v2.11 and assembled sequences between 400 and 500 bp long were kept (Masella *et al*., 2012). All the following steps for sequence processing were performed using the sequence processing pipeline FROGS (Find Rapidly OTU with Galaxy Solution) developed for the Galaxy platform (http://galaxy3.sb-roscoff.fr, Escudié *et al*., 2018). Sequences were clustered into OTUs using SWARM v2 (Mahé *et al*., 2014). PCR chimera and singletons were filtered out and OTUs were taxonomically assigned using the RDP classifier (Wang *et al*., 2007) on the Silva 16S rRNA (v132) database.

Multivariate and statistical analyses. Prior to further analysis, one kelp-associated sample from week 0 **(**AA-T0-C2 in the Supporting Information Table S1**)** was removed from the dataset due to its poor sequencing depth (3 302 sequences) compared to other samples (range 24 482–123 368 sequences). Samples from the bacterial community dataset were rarefied (100 permutations) to 24 482 sequences prior to OTU richness and Shannon diversity index calculation. Dissimilarities in community structure were calculated using the Bray–Curtis dissimilarity index (Bray and Curtis, 1957) before principal coordinate analysis (PCoA). Permutational analysis of variance (PERMANOVA, 999 permutations) was applied using *adonis* to discriminate groups of samples according to time or type of compartment (Anderson, 2001), followed by multivariate pairwise comparisons using *pairwise.perm.manova*. Mean dispersions within the compartments were calculated using *betadisper* (999 permutations). The effect of environmental factors on kelp-associated and underlying sediment communities were assessed using distance-based redundancy analysis (db-RDA) (Legendre and Andersson, 1999) with *capscale* function followed by ANOVA. Environmental factors were log10-transformed prior to this analysis. Only significant environmental factors were selected for db-RDA visualization (ANOVA, $P < 0.05$). The above multivariate and statistical analyses were performed in R v3.5.0 with the packages *phyloseq*, *vegan*, *ggplot* and *EcolUtils* (Wickham, 2009; Mcmurdie and Holmes, 2013; Oksanen *et al*., 2013; R Core Team, 2018). Differential sequence abundance analysis through time was performed at the OTU level for kelp-associated and underlying sediment communities using the GLM test with the *ALDEx2* R package (Fernandes *et al*., 2014). The variation of selected differential OTUs through time was further tested using ANOVA followed by Tukey HSD post hoc test.

An association network was built for kelp-associated bacterial communities. Extended Local Similarity Analysis (eLSA v1.0.4) (Xia *et al*., 2011) was performed on a dataset comprising 10 contextual parameters (eight environmental factors and two bacterial diversity measures) and the relative sequence abundance of OTUs found in at least 19 samples (135 OTUs). This prevalence filter was set according to recommendations in Röttjers and Faust (2018). A delay of one sampling date was allowed for temporal associations. P-values were estimated using the permutation method, with 1 000 permutations. Q-values were estimated to control for false positives. Default eLSA parameters were used otherwise. The

network was visualized in Cytoscape v3.3.0 (Shannon *et al*., 2003). Only associations with $|LS| \geq 0.5$, $Q \leq 0.05$ and $P \leq 0.001$ were represented with the 'edge-weighted, spring-embedded layout' (nodes are strongly repelled or attracted as a function of their LS value; spring strength = 50, spring rest length = 100, strength of disconnected spring = 0.05, rest length of disconnected spring = 500, and strength to avoid collisions = 500). Clusters were detected using the MCODE algorithm (Bader and Hogue, 2003) with 'haircut' and 'fluff' options and otherwise default parameters.

Functional profiles for kelp-associated and underlying sediment communities were inferred using the FAPROTAX v1.2.2 database and script (Louca *et al*., 2016) against the rarefied OTU dataset with the assigned taxonomy. In addition, PICRUSt2 v2.1.4 (Douglas *et al*., 2020) was run with the default parameters (except min_reads set to 5) to get metagenome predictions for EC numbers. Differences in sequence abundance of functional groups and enzymes over time were assessed using the GLM test with ALDEx2.

Acknowledgements

The authors thank the marine operation staff of Roscoff Biological Station (*Service Mer & Observation SBR*), especially Laurent Levêque, Yann Fontana, Wilfried Thomas, Matthieu Camusat, Noël Guidal and François Le Ven for their help with scuba diving fieldwork and experimental set-up. The authors thank Dr. Simon Dittami for critical reading of this manuscript, as well as Murielle Jam and Dr. Hetty Kleinjan for their help during sampling. The authors thank two anonymous reviewers for their useful comments that helped improved this manuscript. This work has benefited from the facilities of the Genomer platform and from the computational resources of the ABiMS bioinformatics platform (FR 2424, CNRS-Sorbonne Université, Roscoff), which are part of the Biogenouest core facility network. This work has benefited from the support of the UMR 8227 and from the French Government via the National Research Agency programs IDEALG (ANR-10-BTBR-04) and ALGAVOR (ANR-18-CE02-0001-01). A.G. acknowledges support by the Institut Français de Recherche pour l'Exploitation de la Mer (IFREMER).

References

Aires, T., Muyzer, G., Serrão, E.A., and Engelen, A.H. (2019) Seaweed loads cause stronger bacterial community shifts in coastal lagoon sediments than nutrient loads. *Front Microbiol*, **9**: 3283.

Alonso-Sáez, L., Díaz-Pérez, L., and Morán, X.A.G. (2015) The hidden seasonality of the rare biosphere in coastal marine bacterioplankton. *Environ Microbiol* **17**: 3766–3780.

Anderson, M.J. (2001) A new method for non-parametric multivariate analysis of variance. *Austral Ecol* **26**: 32–46.

Andrews, J.H., and Harris, R.F. (1986) R- and K-selection and microbial ecology. In *Advances in Microbial Ecology*, Marshall, K.C. (ed). Boston, MA: Springer, pp. 99–147.

Bacchetti De Gregoris, T., Aldred, N., Clare, A.S., and Burgess, J.G. (2011) Improvement of phylum- and class-specific primers for real-time PCR quantification of bacterial taxa. *J Microbiol Methods* **86**: 351–356.

Bader, G.D., and Hogue, C.W.V. (2003) An automated method for finding molecular complexes in large protein interaction networks. *BMC Bioinformatics* **4**: 1–27.

Balmonte, J.P., Buckley, A., Hoarfrost, A., Ghobrial, S., Ziervogel, K., Teske, A., and Arnosti, C. (2019) Community structural differences shape microbial responses to high molecular weight organic matter. *Environ Microbiol* **21**: 557–571.

Balmonte, J.P., Teske, A., and Arnosti, C. (2018) Structure and function of high Arctic pelagic, particle-associated and benthic bacterial communities. *Environ Microbiol* **20**: 2941–2954.

Barbeyron, T., Thomas, F., Barbe, V., Teeling, H., Schenowitz, C., Dossat, C., *et al*. (2016) Habitat and taxon as driving forces of carbohydrate catabolism in marine heterotrophic bacteria: example of the model algae-associated bacterium *Zobellia galactanivorans* Dsij^{T}. *Environ Microbiol* **18**: 4610–4627.

de Beer, D.D., Wenzhöfer, F., Ferdelman, T.G., Boehme, S. E., Huettel, M., van Beusekom, J.E.E., *et al*. (2005) Transport and mineralization rates in North Sea sandy intertidal sediments. *Limnol Ocean* **50**: 113–127.

Bengtsson, M., Sjøtun, K., and Øvreås, L. (2010) Seasonal dynamics of bacterial biofilms on the kelp *Laminaria hyperborea*. *Aquat Microb Ecol* **60**: 71–83.

Bengtsson, M.M., and Øvreås, L. (2010) *Planctomycetes* dominate biofilms on surfaces of the kelp *Laminaria hyperborea*. *BMC Microbiol* **10**: 261.

Bengtsson, M.M., Sjøtun, K., Lanzén, A., and Øvreås, L. (2012) Bacterial diversity in relation to secondary production and succession on surfaces of the kelp *Laminaria hyperborea*. *ISME J* **6**: 2188–2198.

de Bettignies, F., Dauby, P., Thomas, F., Gobet, A., Delage, L., Bohner, O., *et al*. (2020) Degradation dynamics and processes associated with the accumulation of *Laminaria hyperborea* (Phaeophyceae) kelp fragments: an in situ experimental approach. *J Phycol* **56**: 1481–1492.

de Bettignies, T., Wernberg, T., Lavery, P.S., Vanderklift, M. A., Gunson, J.R., Symonds, G., and Collier, N. (2015) Phenological decoupling of mortality from wave forcing in kelp beds. *Ecology* **96**: 850–861.

Bolger, A.M., Lohse, M., and Usadel, B. (2014). Trimmomatic: A flexible trimmer for Illumina sequence data. *Bioinformatics* **30**: 2114–2120.

Boudreau, B.P., Huettel, M., Forster, S., Jahnke, R.A., McLachlan, A., Middelburg, J.J., *et al*. (2001) Permeable marine sediments: overturning an old paradigm. *Eos (Washington DC)* **82**: 133–136.

Bouvy, M., Le Romancer, M., and Delille, D. (1986) Significance of microheterotrophs in relation to the degradation process of subantarctic kelp beds (*Macrocystis pyrifera*). *Polar Biol* **5**: 249–253.

Bray, J.R., and Curtis, J.T. (1957) An ordination of the upland forest communities of southern Wisconsin. *Ecol Monogr* **27**: 325–349.

Burgin, A.J., and Hamilton, S.K. (2007) Have we overemphasized the role of denitrification in aquatic ecosystems? A review of nitrate removal pathways. *Front Ecol Environ* **5**: 89–96.

Burke, C., Thomas, T., Lewis, M., Steinberg, P., and Kjelleberg, S. (2011) Composition, uniqueness and variability of the epiphytic bacterial community of the green alga *Ulva australis*. *ISME J* **5**: 590–600.

Bustin, S.A., Benes, V., Garson, J.A., Hellemans, J., Huggett, J., Kubista, M., *et al*. (2009) The MIQE guidelines: minimum information for publication of quantitative real-time PCR experiments. *Clin Chem* **55**: 611–622.

Chen, P., Zhang, L., Guo, X., Dai, X., Liu, L., Xi, L., *et al*. (2016) Diversity, biogeography, and biodegradation potential of actinobacteria in the deep-sea sediments along the southwest Indian ridge. *Front Microbiol* **7**: 1340

Cho, J.C., and Giovannoni, S.J. (2004) Cultivation and growth characteristics of a diverse Group of Oligotrophic Marine *Gammaproteobacteria*. *Appl Environ Microbiol* **70**: 432–440.

Corre, S., and Prieur, D. (1990) Density and morphology of epiphytic bacteria on *Laminaria digitata*. *Bot Mar* **33**: 515–523.

Cosse, A., Leblanc, C., and Potin, P. (2007) Dynamic Defense of marine macroalgae against pathogens: from early activated to gene-regulated responses. *Adv Bot Res* **46**: 221–266.

Dang, H., and Lovell, C.R. (2016) Microbial surface colonization and biofilm development in marine environments. *Microbiol Mol Biol Rev* **80**: 91–138.

Dat, T.T.H., Steinert, G., Cuc, N.T.K., Smidt, H., and Sipkema, D. (2018) Archaeal and bacterial diversity and community composition from 18 phylogenetically divergent sponge species in Vietnam. *PeerJ* **6**: e4970.

Delille, D., and Perret, E. (1991) The influence of giant kelp *Macrocystis pyrifera* on the growth of subantarctic marine bacteria. *J Exp Mar Bio Ecol* **153**: 227–239.

Dittami, S.M., Duboscq-Bidot, L., Perennou, M., Gobet, A., Corre, E., Boyen, C., and Tonon, T. (2016) Host-microbe interactions as a driver of acclimation to salinity gradients in brown algal cultures. *ISME J* **10**: 51–63.

Dogs, M., Wemheuer, B., Wolter, L., Bergen, N., Daniel, R., Simon, M., and Brinkhoff, T. (2017) *Rhodobacteraceae* on the marine brown alga *Fucus spiralis* are abundant and show physiological adaptation to an epiphytic lifestyle. *Syst Appl Microbiol* **40**: 370–382.

Douglas, G.M., Maffei, V.J., Zaneveld, J., Yurgel, S.N., Brown, J.R., Taylor, C.M., *et al*. (2020) PICRUSt2: an improved and extensible approach for metagenome inference. *bioRxiv* 672295.

Duarte, C.M., and Cebrián, J. (1996) The fate of marine autotrophic production. *Limnol Oceanogr* **41**: 1758–1766.

Dudek, M., Dieudonné, A., Jouanneau, D., Rochat, T., Michel, G., Sarels, B., and Thomas, F. (2020) Regulation of alginate catabolism involves a GntR family repressor in the marine flavobacterium *Zobellia galactanivorans* Dsij^{T}. *Nucleic Acids Res*, **48**: 7786–7800.

Egan, S., Fernandes, N.D., Kumar, V., Gardiner, M., and Thomas, T. (2014) Bacterial pathogens, virulence mechanism and host defence in marine macroalgae. *Environ Microbiol* **16**: 925–938.

Egan, S., Harder, T., Burke, C., Steinberg, P., Kjelleberg, S., and Thomas, T. (2013) The seaweed holobiont: understanding seaweed-bacteria interactions. *FEMS Microbiol Rev* **37**: 462–476.

Enke, T.N., Datta, M.S., Schwartzman, J., Cermak, N., Schmitz, D., Barrere, J., *et al*. (2019) Modular assembly of polysaccharide-degrading marine microbial communities. *Curr Biol* **29**: 1528–1535.e6.

Escudié, F., Auer, L., Bernard, M., Mariadassou, M., Cauquil, L., Vidal, K., *et al*. (2018) FROGS: find, rapidly, OTUs with galaxy solution. *Bioinformatics*, **34**: 1287–1294.

Ettinger, C.L., Voerman, S.E., Lang, J.M., Stachowicz, J.J., and Eiser, J.A. (2017) Microbial communities in sediment from *Zostera marina* patches, but not the *Z. marina* leaf or root microbiomes, vary in relation to distance from patch edge. *PeerJ* **5**.e3246

Fernandes, A.D., Reid, J.N.S., Macklaim, J.M., McMurrough, T.A., Edgell, D.R., and Gloor, G.B. (2014) Unifying the analysis of high-throughput sequencing datasets: characterizing RNA-seq, 16S rRNA gene sequencing and selective growth experiments by compositional data analysis. *Microbiome* **2**: 15.

Fierer, N., Bradford, M.A., Jackson, R.B. (2007). Toward an ecological classification of soil bacteria. *Ecology*, **88**(6), 1354–1364.

Fleurence, J. (1999) Seaweed proteins. *Trends Food Sci Technol* **10**: 25–28.

Florez, J.Z., Camus, C., Hengst, M.B., Marchant, F., and Buschmann, A.H. (2019) Structure of the epiphytic bacterial communities of *Macrocystis pyrifera* in localities with contrasting nitrogen concentrations and temperature. *Algal Res* **44**: 101706.

Gobet, A., Böer, S.I., Huse, S.M., Van Beusekom, J.E.E., Quince, C., Sogin, M.L., *et al*. (2012) Diversity and dynamics of rare and of resident bacterial populations in coastal sands. *ISME J* **6**: 542–553.

Goecke, F., Labes, A., Wiese, J., and Imhoff, J.F. (2010) Chemical interactions between marine macroalgae and bacteria. *Mar Ecol Prog Ser* **409**: 267–300.

Grondin, J.M., Tamura, K., Déjean, G., Abbott, D.W., and Brumer, H. (2017) Polysaccharide utilization loci: fuelling microbial communities. *J Bacteriol*: JB.00860-16.**199**(15), e00860-16

Hardison, A.K., Algar, C.K., Giblin, A.E., and Rich, J.J. (2015) Influence of organic carbon and nitrate loading on partitioning between dissimilatory nitrate reduction to ammonium (DNRA) and N_2 production. *Geochim Cosmochim Acta* **164**: 146–160.

Jiménez, D.J., Dini-Andreote, F., DeAngelis, K.M., Singer, S. W., Salles, J.F., and van Elsas, J.D. (2017) Ecological insights into the dynamics of plant biomass-degrading microbial consortia. *Trends Microbiol* **25**: 788–796.

Kappelmann, L., Krüger, K., Hehemann, J.H., Harder, J., Markert, S., Unfried, F., *et al*. (2019) Polysaccharide utilization loci of North Sea *Flavobacteriia* as basis for using SusC/D-protein expression for predicting major phytoplankton glycans. *ISME J* **13**: 76–91.

Kloareg, B., and Quatrano, R.S. (1988) Structure of the cell walls of marine algae and ecophysiological functions of the matrix polysaccharides. *Ocean Mar Biol Annu Rev* **26**: 259–315.

Koop, K., Newell, R., and Lucas, M. (1982) Biodegradation and carbon flow based on kelp (*Ecklonia maxima*) debris in a Sandy Beach microcosm. *Mar Ecol Prog Ser* **7**: 315–326.

Krause-Jensen, D., and Duarte, C.M. (2016) Substantial role of macroalgae in marine carbon sequestration. *Nat Geosci* **9**: 737–742.

Krumhansl, K.A., and Scheibling, R.E. (2012) Production and fate of kelp detritus. *Mar Ecol Prog Ser* **467**: 281–302.

Lachnit, T., Meske, D., Wahl, M., Harder, T., and Schmitz, R. (2011) Epibacterial community patterns on marine macroalgae are host-specific but temporally variable. *Environ Microbiol* **13**: 655–665.

Legendre, P., and Andersson, M.J. (1999) Distance-based redundancy analysis: testing multispecies responses in multifactorial ecological experiments. *Ecol Monogr* **69**: 1–24.

Lemay, M., Martone, P., Keeling, P., Burt, J., Krumhansl, K., Sanders, R., and Parfrey, L. (2018) Sympatric kelp species share a large portion of their surface bacterial communities. *Environ Microbiol* **20**: 658–670.

Louca, S., Parfrey, L.W., and Doebeli, M. (2016) Decoupling function and taxonomy in the global ocean microbiome. *Science* **353**: 1272–1277.

Mahé, F., Rognes, T., Quince, C., de Vargas, C., and Dunthorn, M. (2014) Swarm: robust and fast clustering method for amplicon-based studies. *PeerJ* **2**: e593.

Mahmoudi, N., Robeson, M.S., Castro, H.F., Fortney, J.L., Techtmann, S.M., Joyner, D.C., *et al*. (2015) Microbial community composition and diversity in Caspian Sea sediments. *FEMS Microbiol Ecol* **91**: 1–11.

Mann, A.J., Hahnke, R.L., Huang, S., Werner, J., Xing, P., Barbeyron, T., *et al*. (2013) The genome of the alga-associated marine flavobacterium *Formosa agariphila* KMM 3901^{T} reveals a broad potential for degradation of algal polysaccharides. *Appl Environ Microbiol* **79**: 6813–6822.

Mann, K.H. (1982) *Ecology of Coastal Waters : A Systems Approach*, Berkeley: University of California Press.

Mann, K.H. (1973) Seaweeds: their productivity and strategy for growth. *Science* **182**: 975–981.

Marchant, H.K., Lavik, G., Holtappels, M., and Kuypers, M. M.M. (2014) The fate of nitrate in intertidal permeable sediments. *PLoS One* **9**: e104517.

Martin, M., Barbeyron, T., Martin, R., Portetelle, D., Michel, G., and Vandenbol, M. (2015) The cultivable surface microbiota of the brown alga *Ascophyllum nodosum* is enriched in macroalgal-polysaccharide-degrading bacteria. *Front Microbiol* **6**: 1487.

Martin, M., Portetelle, D., Michel, G., and Vandenbol, M. (2014) Microorganisms living on macroalgae: diversity, interactions, and biotechnological applications. *Appl Microbiol Biotechnol* **98**: 2917–2935.

Marzinelli, E.M., Campbell, A.H., Zozaya Valdes, E., Vergés, A., Nielsen, S., Wernberg, T., *et al*. (2015) Continental-scale variation in seaweed host-associated bacterial communities is a function of host condition, not geography. *Environ Microbiol* **17**: 4078–4088.

Masella, A.P., Bartram, A.K., Truszkowski, J.M., Brown, D.G., and Neufeld, J.D. (2012) PANDAseq: paired-end assembler for Illumina sequences. *BMC Bioinformatics* **13**: 31.

Masson, D. (2002) Deep water renewal in the strait of Georgia. *Estuar Coast Shelf Sci* **54**: 115–126.

Mcmurdie, P.J., and Holmes, S. (2013) Phyloseq: an R package for reproducible interactive analysis and graphics of microbiome census data. *PLoS One* **8**: 1–11.

Minich, J.J., Morris, M.M., Brown, M., Doane, M., Edwards, M.S., Michael, T.P., and Dinsdale, E.A. (2018) Elevated temperature drives kelp microbiome dysbiosis, while elevated carbon dioxide induces water microbiome disruption. *PLoS One* **13**: 1–23.

Mußmann, M., Ishii, K., Rabus, R., and Amann, R. (2005) Diversity and vertical distribution of cultured and uncultured *Deltaproteobacteria* in an intertidal mud flat of the Wadden Sea. *Environ Microbiol* **7**: 405–418.

Muyzer, G., and Stams, A.J.M. (2008) The ecology and biotechnology of sulphate-reducing bacteria. *Nat Rev Microbiol* **6**: 441–454.

Newell, R., Field, J., and Griffiths, C. (1982) Energy balance and significance of microorganisms in a kelp bed community. *Mar Ecol Prog Ser* **8**: 103–113.

Oksanen, J., Blanchet, F.G., Kindt, R., Legendre, P., Minchin, P.R., O'Hara, R.B., et al. (2013) Vegan: community ecology package.

Orsi, W.D., Smith, J.M., Liu, S., Liu, Z., Sakamoto, C.M., Wilken, S., *et al*. (2016) Diverse, uncultivated bacteria and archaea underlying the cycling of dissolved protein in the ocean. *ISME J* **10**: 2158–2173.

Paix, B., Othmani, A., Debroas, D., Culioli, G., and Briand, J.F. (2019) Temporal covariation of epibacterial community and surface metabolome in the Mediterranean seaweed holobiont *Taonia atomaria*. *Environ Microbiol* **21**: 3346–3363.

R Core Team (2018) R: a language and environment for statistical computing.

Ramirez-Puebla, T., Weigel, B., Jack, L., Schlundta, C., Pfister, C., and Mark Welch, J. (2020) Spatial organization of the kelp microbiome at micron scales. *bioRxiv* 2020. https://doi.org/10.1101/2020.03.01.972083.

Reintjes, G., Tegetmeyer, H.E., Bürgisser, M., Orlić, S., Tews, I., Zubkov, M., *et al*. (2019) On-site analysis of bacterial communities of the Ultraoligotrophic South Pacific gyre. *Appl Environ Microbiol* **85**: 1–14.

Röttjers, L., and Faust, K. (2018) From hairballs to hypotheses–biological insights from microbial networks. *FEMS Microbiol Rev* **42**: 761–780.

Salaün, S., La Barre, S., Dos Santos-Goncalvez, M., Potin, P., Haras, D., and Bazire, A. (2012) Influence of exudates of the kelp *Laminaria digitata* on biofilm formation of associated and exogenous bacterial epiphytes. *Microb Ecol* **64**: 359–369.

Sass, H., Köpke, B., Rütters, H., Feuerlein, T., Dröge, S., Cypionka, H., and Engelen, B. (2010) *Tateyamaria pelophila* sp. nov., a facultatively anaerobic alphaproteobacterium isolated from tidal-flat sediment, and emended descriptions of the genus *Tateyamaria* and of *Tateyamaria omphalii*. *Int J Syst Evol Microbiol* **60**: 1770–1777.

Shannon, P., Markiel, A., Ozier, O., Baliga, N.S., Wang, J.T., Ramage, D., *et al*. (2003) Cytoscape: a software environment for integrated models of biomolecular interaction networks. *Genome Res* **13**: 2498–2504.

Spring, S., Scheuner, C., Göker, M., and Klenk, H.P. (2015) A taxonomic framework for emerging groups of

ecologically important marine gammaproteobacteria based on the reconstruction of evolutionary relationships using genome-scale data. *Front Microbiol* **6**: 281.

Steinert, G., Taylor, M.W., and Schupp, P.J. (2015) Diversity of *Actinobacteria* associated with the marine ascidian *Eudistoma toealensis*. *Marine Biotechnol* **17**: 377–385.

Stratil, S.B., Neulinger, S.C., Knecht, H., Friedrichs, A.K., and Wahl, M. (2013) Temperature-driven shifts in the epibiotic bacterial community composition of the brown macroalga *Fucus vesiculosus*. *Microbiology* **2**: 338–349.

Strittmatter, A.W., Liesegang, H., Rabus, R., Decker, I., Amann, J., Andres, S., *et al*. (2009) Genome sequence of *Desulfobacterium autotrophicum* HRM2, a marine sulfate reducer oxidizing organic carbon completely to carbon dioxide. *Environ Microbiol* **11**: 1038–1055.

Teeling, H., Fuchs, B.M., Becher, D., Klockow, C., Gardebrecht, A., Bennke, C.M., *et al*. (2012) Substrate-controlled succession of marine bacterioplankton populations induced by a phytoplankton bloom. *Science* **336**: 608–611.

Thiele, S., Fuchs, B.M., Amann, R., and Iversen, M.H. (2015) Colonization in the photic zone and subsequent changes during sinking determine bacterial community composition in marine snow. *Appl Environ Microbiol* **81**: 1463–1471.

Thomas, F., Barbeyron, T., Tonon, T., Génicot, S., Czjzek, M., and Michel, G. (2012) Characterization of the first alginolytic operons in a marine bacterium: from their emergence in marine *Flavobacteriia* to their independent transfers to marine *Proteobacteria* and human gut *Bacteroides*. *Environ Microbiol* **14**: 2379–2394.

Thomas, F., Dittami, S.M., Brunet, M., Le Duff, N., Tanguy, G., Leblanc, C., and Gobet, A. (2020) Evaluation of a new primer combination to minimize plastid contamination in 16S rDNA metabarcoding analyses of alga-associated bacterial communities. *Environ Microbiol Rep* **12**: 30–37.

Thomas, F., Hehemann, J.-H., Rebuffet, E., Czjzek, M., and Michel, G. (2011) Environmental and gut *Bacteroidetes*: the food connection. *Front Microbiol* **2**: 93.

Verhoeven Joost, T.P., Kavanagh, A.N., and Dufour, S.C. (2017). Microbiome analysis shows enrichment for specific bacteria in separate anatomical regions of the deep-sea carnivorous sponge *Chondrocladia grandis*. *FEMS Microbiology Ecology* **93**: fiw214.

Větrovský, T., and Baldrian, P. (2013) The variability of the 16S rRNA gene in bacterial genomes and its consequences for bacterial community analyses. *PLoS One* **8**: 1–10.

Wang, Q., Garrity, G.M., Tiedje, J.M., and Cole, J.R. (2007) Naive Bayesian classifier for rapid assignment of rRNA sequences into the new bacterial taxonomy. *Appl Environ Microbiol* **73**: 5261–5267.

Wasmund, K., Mußmann, M., and Loy, A. (2017) The life sulfuric: microbial ecology of sulfur cycling in marine sediments. *Environ Microbiol Rep* **9**: 323–344.

Weigel, B.L., and Pfister, C.A. (2019) Successional dynamics and seascape-level patterns of microbial communities on the canopy-forming kelps *Nereocystis luetkeana* and *Macrocystis pyrifera*. *Front Microbiol* **10**: 346.

Wickham, H. (2009) *ggplot2*. New York, NY: Springer-Verlag.

Wietz, M., Wemheuer, B., Simon, H., Giebel, H.A., Seibt, M. A., Daniel, R., *et al*. (2015) Bacterial community dynamics during polysaccharide degradation at contrasting sites in the southern and Atlantic oceans. *Environ Microbiol* **17**: 3822–3831.

Xia, L.C., Steele, J.A., Cram, J.A., Cardon, Z.G., Simmons, S.L., Vallino, J.J., *et al*. (2011) Extended local similarity analysis (eLSA) of microbial community and other time series data with replicates. *BMC Syst Biol* **5**: S15.

Zinger, L., Gobet, A., and Pommier, T. (2012) Two decades of describing the unseen majority of aquatic microbial diversity. *Mol Ecol* **21**: 1878–1896.

Supporting Information

Additional Supporting Information may be found in the online version of this article at the publisher's web-site:

Appendix S1: Supporting Information

Accumulation of detached kelp biomass in a subtidal temperate coastal ecosystem induces succession of epiphytic and sediment bacterial communities.

Maéva Brunet[1], Florian de Bettignies[2], Nolwen Le Duff[1], Gwenn Tanguy[3], Dominique Davoult[2], Catherine Leblanc[1], Angélique Gobet[1,4]* et François Thomas[1]*
*both authors contributed equally. Corresponding authors

SUPPLEMENTARY MATERIAL

Supplementary Methods

Measurements of contextual parameters

Detailed procedures are described in (de Bettignies, Dauby, Thomas, *et al.*, 2020). Water temperature, light intensity and water motion were measured continuously during the experiment using sensors. Community respiration was measured by measuring oxygen consumption from each cage, during *in situ* incubations in benthic chambers. Further analyses of the cage content were performed in the laboratory. The remaining kelp biomass was estimated by dividing the final wet mass by the initial wet mass measured at the beginning of the experiment. Phlorotannins were extracted in a 70% ethanol buffer (pH 2.6) and quantified using a modified Folin-Ciocalteu method. C:N mass ratio of the tissues was determined on an elemental analyser (Flash EA1112, ThermoScientific) coupled to an isotope ratio mass spectrometer (IRMS Delta plus, ThermoScientific) via a gas interface (Conflo III, ThermoScientific). *In vivo* chlorophyll *a* fluorescence of photosystem II (PSII) was measured using a fluorometer (Diving-PAM; Heinz Walz, Effeltrich, Germany) to assess the photosynthetic capacity of the tissues (expressed as quantum efficiency of PSII (Fv/Fm)). The proportion of organic matter in sediment was determined by measuring the weight loss from dry sediment samples (48h at 60°C) when ignited at 500°C for 6 h.

DNA extraction

Three different protocols were adapted to extract DNA from each type of sample (algal pieces, sediment and water). For each cage, five algal pieces (total surface of 13.3 cm^2) were incubated in 4.5 ml of lysis buffer (750 mM Sucrose, 50 mM TRIS pH 8, 40 mM EDTA, 0,014 mM lysozyme) for 45 min at 37°C. SDS and proteinase K were added to a final concentration of 11.6 $mg.ml^{-1}$ and 230 $\mu g.ml^{-1}$, respectively, and samples were incubated for 1 h at 55°C. Nucleic acid extraction was performed by adding one volume of phenol:chloroform:isoamyl alcohol (25:24:1) to the lysate volume. After centrifugation (4500 rpm, 15 min, 19°C) the aqueous phase was recovered, polysaccharides were precipitated with 0.3 volume of 96% ethanol followed by a new extraction with phenol:chloroform:isoamyl alcohol. The resulting extracted DNA was purified with the NucleoSpin Plant II kit (Macherey Nagel) following the manufacturer's instructions. DNA was eluted in 100 µl of 5 mM Tris/HCl buffer pH 8.5. For water samples, DNA was extracted from Sterivex filters following a similar protocol as used for the algal samples with addition of 1.5 ml of lysis buffer to the filter and no precipitation of polysaccharides. For sediment samples, DNA was extracted from 0.5 g of sediment using the DNeasy PowerLyzer PowerSoil Kit (Qiagen) according to the manufacturer's instructions, and eluted in 100 µl of 10 mM Tris/HCl buffer pH 8.5.

16S rRNA copies quantification

The total number of bacterial 16S rRNA copies in each sample was assessed by quantitative real-time PCR using the universal primers 926F/1062R (Bacchetti De Gregoris *et al.*, 2011). Amplification and detection were carried out in a 384-multiwell plate on a LightCycler 480 Instrument II. Each reaction was conducted in technical triplicate for each sample with 2.5 µl of the LightCycler 480 SYBR Green I Master mix 2X (Roche Applied Science), 0.5 µl of each primers (3 µM), 0.5 µl of 10X TBT-PAR additive (1.5 M Trehalose, 2 $mg.ml^{-1}$ Invitrogen BSA UltraPure, 2% Tween-20, 17 mM Tris-HCl pH8) (Samarakoon *et al.*, 2013) and 1 µl of DNA template normalized at 0.01 $ng.\mu l^{-1}$ for a final volume of 5 µl per reaction. The targeted 16S rRNA gene sequence was amplified with an initial hold of 95°C for 10 min followed by 45 cycles of 95°C

for 10 s, 60°C for 20 s, and 72°C for 10 s. After the amplification step, dissociation curves were generated by increasing the temperature from 65°C to 97°C. Serial dilutions of *Zobellia galactanivorans* Dsij^T purified genomic DNA ranging from 10^3 to 10^8 16S rRNA gene copies equivalent were used as a standard curve and were amplified in triplicate in the same run as the environmental samples. A Non-Template Control (NTC) was included in the run. The LightCycler 480 Software (version 1.5) was used to visualize the results and determine the threshold cycle of each sample. The resulting standard curves were analyzed to assess the amplification efficiency and to calculate the linear regression between the threshold cycle and the number of 16S rRNA gene copies. ANOVA analyses were conducted to assess differences between samples, followed by a post-hoc Tukey HSD test for pairwise comparisons. Details on qPCR assays are given in **Table S8**, following the MIQE guidelines (Bustin *et al.*, 2009).

Library preparation and sequencing

The concentration of DNA samples was normalized at 0.1 ng.µl^{-1}. As a positive control, we constructed a mock community based on the genomic DNA of 32 pure marine bacterial isolates as reported previously (Thomas *et al.*, 2020). Libraries were prepared in parallel for the 94 samples (24 algal samples, 24 water samples, 3 initial sediments, 21 underlying sediment, 20 external sediment, one mock community and one negative control (PCR grade water)). Library were prepared using the primers S-D-Bact-0341-b-S-17 (5' CCTACGGGNGGCWGCAG 3') and 799F_rc (5' CMGGGTATCTAATCCKGTT 3') and sequenced on a MiSeq paired-end sequencing run (300 cycles x 2) as described previously (Thomas *et al.*, 2020).

Sequence filtering and taxonomic assignation

Raw sequence reads were trimmed to remove low quality bases and Illumina adapters using Trimmomatic v0.38 with the following options: ILLUMINACLIP:Adaptaters.fasta:2:30:10 SLIDINGWINDOW:4:25 LEADING:25 TRAILING:25 MINLEN:150 (Bolger *et al.*, 2014). Overlapping paired-end sequence reads were assembled using PANDAseq v2.11 and assembled sequences between 400 and 500 bp long were kept (Masella *et al.*, 2012). All the following steps for sequence processing were performed in the pipeline FROGS (Find Rapidly OTU with Galaxy Solution) developed for the Galaxy platform (http://galaxy3.sb-roscoff.fr, Escudié *et al.*, 2017). Sequences were clustered into OTUs using SWARM v2 (Mahé *et al.*, 2015), with local clustering threshold d=1. PCR chimera detected with VCHIME from VSEARCH v1.1.3 (Rognes *et al.*, 2016) and singletons were filtered out and OTUs were taxonomically assigned using the RDP classifier (Wang *et al.*, 2007) on the Silva 16S rRNA (v132) database.

References for supplementary Methods

Bacchetti De Gregoris, T., Aldred, N., Clare, A.S., and Burgess, J.G. (2011) Improvement of phylum- and class-specific primers for real-time PCR quantification of bacterial taxa. *J Microbiol Methods* **86**: 351–356.

de Bettignies, F., Dauby, P., Thomas, F., Gobet, A., Delage, L., Bohner, O., et al. (2020) Degradation dynamics and processes associated with the accumulation of *Laminaria hyperborea* (Phaeophyceae) kelp fragments: an in situ experimental approach. *J Phycol* jpy.13041.

Bolger, A.M., Lohse, M., and Usadel, B. (2014) Trimmomatic: A flexible trimmer for Illumina sequence data. *Bioinformatics* **30**: 2114–2120.

Bustin, S.A., Benes, V., Garson, J.A., Hellemans, J., Huggett, J., Kubista, M., et al. (2009) The MIQE guidelines: Minimum information for publication of quantitative real-time PCR experiments. *Clin Chem* **55**: 611–622.

Escudié, F., Auer, L., Bernard, M., Mariadassou, M., Cauquil, L., Vidal, K., et al. (2017) FROGS: Find, Rapidly, OTUs with Galaxy Solution. *Bioinformatics* **34**: 1287-1294.

Masella, A.P., Bartram, A.K., Truszkowski, J.M., Brown, D.G., and Neufeld, J.D. (2012) PANDAseq: paired-end assembler for Illumina sequences. *BMC Bioinformatics* **13**: 31.

Rognes, T., Flouri, T., Nichols, B., Quince, C., and Mahé, F. (2016) VSEARCH: A versatile open source tool for metagenomics. *PeerJ* **4**: e2584.

Samarakoon, T., Wang, S.Y., and Alford, M.H. (2013) Enhancing PCR Amplification of DNA from Recalcitrant Plant Specimens Using a Trehalose-Based Additive. *Appl Plant Sci* **1**: 1200236.

Thomas, F., Dittami, S.M., Brunet, M., Le Duff, N., Tanguy, G., Leblanc, C., and Gobet, A. (2020) Evaluation of a new primer combination to minimize plastid contamination in 16S rDNA metabarcoding analyses of alga-associated bacterial communities. *Environ Microbiol Rep* **12**: 30–37.

Wang, Q., Garrity, G.M., Tiedje, J.M., and Cole, J.R. (2007) Naive Bayesian classifier for rapid assignment of rRNA sequences into the new bacterial taxonomy. *Appl Environ Microbiol* **73**: 5261–7.

Supplementary tables

Supplementary table 1: Characteristics of the 92 samples collected and analyzed in the study. Sample AA_T0_C2 was removed from the sequence analysis due to a low number of sequences. DNA yield after extraction, 16S rRNA gene copy number, sequence abundance and OTU numbers of the non-rarefied dataset and PICRUSt weighted NSTI are mentioned for each sample, as well as measurements of the 10 contextual parameters used in the study, including 2 alpha diversity indices (OTU numbers after rarefaction and Shannon index) and 8 environmental factors. OM: Organic Matter; WW: wet weight; DW: dry weight. C/N ratio: carbon to nitrogen ratio.

Sample ID	Type	Sampling date (Day/Month/Year)	Weeks	DNA yield (ng.l^{-1}.m^{-2} of algae or l^{-1} of seawater or g^{-1} of sediment)	16S rRNA gene copies.m^{-2} of algae or l^{-1} of seawater or g^{-1} of sediment	Reads number	OTU number before rarefaction	Alpha diversity		Environmental factors						PICRUSt weighted NSTI
								OTU number after rarefaction	Shannon	Remaining Biomass (%)	OM Sediment (%)	0_2 Consumption (mg.kgWW^{-1}.h^{-1})	Fv/Fm	Temperature (°C)	Light (Lux)	Phlorotannins (mg.gDW^{-1})	C/N ratio	
AA_T0_C1	Kelp-associated	18/4/2017	0	0.5	3.37E+08	49528	649	493	3.1	100	1.50	28.6	0.72	12.74	3936	42.4	13.41	0.19
AA_T0_C2	Kelp-associated	18/4/2017	0	1.5	1.18E+08	3302	196	NA	NA	NA	NA	NA	NA	NA	NA	NA	NA	NA
AA_T0_C4	Kelp-associated	18/4/2017	0	0.4	3.68E+08	44659	434	351	2.4	100	1.50	28.6	0.66	12.74	3936	56.6	17.09	0.16
AA_T1_C10	Kelp-associated	2/5/2017	2	0.3	4.42E+07	54640	1114	793	3.8	103.7	1.10	6.3	0.73	12.34	1449	48.1	12.22	0.20
AA_T1_C25	Kelp-associated	2/5/2017	2	0.6	7.67E+07	60163	1163	789	4.1	102	01.06	6.3	0.80	12.34	1449	71.2	13.08	0.21
AA_T1_C32	Kelp-associated	2/5/2017	2	0.4	4.84E+07	60443	1263	848	3.9	106.6	1.34	6.3	0.77	12.34	1449	57.7	12.33	0.16
AA_T2_C8	Kelp-associated	18/5/2017	4	0.2	1.38E+07	31375	1125	1008	3.9	67.6	1.42	10.5	0.75	13.39	2545	76.5	13.82	0.18
AA_T2_C24	Kelp-associated	18/5/2017	4	0.2	8.28E+07	35948	1325	1120	4.3	71.1	1.58	10.5	0.74	13.39	2545	71.7	15.45	0.19
AA_T2_C35	Kelp-associated	18/5/2017	4	0.4	5.23E+07	47410	1255	959	4.0	70.1	1.73	10.5	0.74	13.39	2545	40.7	11.96	0.18
AA_T3_C20	Kelp-associated	30/5/2017	6	0.2	1.61E+07	90253	1905	1045	4.0	66.7	1.14	12.7	0.73	14.45	5089	51.2	12.43	0.18
AA_T3_C21	Kelp-associated	30/5/2017	6	0.4	6.54E+07	65328	1901	1240	4.4	45.4	1.54	12.7	0.74	14.45	5089	64.6	17.36	0.17
AA_T3_C31	Kelp-associated	30/5/2017	6	0.3	2.24E+07	58521	1919	1308	4.4	57.2	1.37	12.7	0.68	14.45	5089	70.4	15.18	0.18
AA_T4_C16	Kelp-associated	5/7/2017	11	0.3	2.41E+07	38437	2434	2089	5.5	61.5	1.23	38.0	0.73	15.93	2024	118.1	16.04	0.23
AA_T4_C19	Kelp-associated	5/7/2017	11	0.2	2.32E+07	24482	2251	2251	5.4	44.2	1.16	38.0	0.74	15.93	2024	159.1	18.30	0.21
AA_T4_C30	Kelp-associated	5/7/2017	11	0.2	4.33E+07	49974	2998	2312	5.6	43.9	1.16	38.0	0.75	15.93	2024	139.4	14.43	0.23
AA_T5_C17	Kelp-associated	3/8/2017	15	0.5	5.16E+07	46230	1609	1249	4.9	25.1	1.43	53.1	0.72	16.45	572	55.4	19.00	0.22
AA_T5_C23	Kelp-associated	3/8/2017	15	0.5	8.01E+07	38974	2065	1704	5.1	23.2	02.04	53.1	0.70	16.45	572	139.5	23.07	0.26
AA_T5_C34	Kelp-associated	3/8/2017	15	0.3	2.52E+07	80877	2696	1626	5.0	27.3	1.90	53.1	0.74	16.45	572	123.8	18.76	0.24
AA_T6_C13	Kelp-associated	8/9/2017	20	0.3	5.50E+07	50517	2243	1633	4.9	18.6	1.55	94.4	0.74	17.23	470	166.9	17.40	0.24
AA_T6_C27	Kelp-associated	8/9/2017	20	0.1	2.65E+07	36952	2202	1838	4.9	23.9	1.23	94.4	0.75	17.23	470	144.5	17.02	0.26
AA_T6_C28	Kelp-associated	8/9/2017	20	0.3	4.36E+07	67185	2710	1689	4.9	21.8	1.23	94.4	0.72	17.23	470	114.9	16.59	0.23
AA_T7_C1	Kelp-associated	5/10/2017	24	0.3	4.88E+07	43161	1994	1544	5.0	24.3	1.63	162.4	0.72	16.11	1195	111.4	18.18	0.25
AA_T7_C7	Kelp-associated	5/10/2017	24	0.3	2.86E+07	65992	2714	1753	5.0	18.2	1.65	162.4	0.72	16.11	1195	88.6	17.14	0.26
AA_T7_C22	Kelp-associated	5/10/2017	24	0.3	4.15E+07	40068	2401	1905	5.2	7.5	1.40	162.4	0.75	16.11	1195	168.1	14.48	0.24
SW_T0_E5	Seawater	18/4/2017	0	14.2	4.88E+08	71560	2491	1432	4.3	100	1.50	28.6	0.71	12.74	3936	41.3	14.87	NA
SW_T0_E3	Seawater	18/4/2017	0	18.3	4.60E+08	28377	1273	1177	4.1	100	1.50	28.6	0.71	12.74	3936	41.3	14.87	NA
SW_T0_E2	Seawater	18/4/2017	0	15.9	5.59E+08	43412	1936	1428	4.3	100	1.50	28.6	0.71	12.74	3936	41.3	14.87	NA
SW_T1_a	Seawater	2/5/2017	2	9.4	1.07E+09	54991	3119	2002	4.8	104.1	1.17	6.3	0.77	12.34	1449	59.0	12.54	NA
SW_T1_b	Seawater	2/5/2017	2	13.6	6.13E+08	74857	3548	1961	4.7	104.1	1.17	6.3	0.77	12.34	1449	59.0	12.54	NA
SW_T1_c	Seawater	2/5/2017	2	10.7	4.98E+08	59263	2843	1797	4.6	104.1	1.17	6.3	0.77	12.34	1449	59.0	12.54	NA
SW_T2_a	Seawater	18/5/2017	4	15.5	2.71E+08	30193	1751	1568	4.5	69.6	1.58	10.5	0.74	13.39	2545	63.0	13.74	NA
SW_T2_b	Seawater	18/5/2017	4	15.5	3.19E+08	90845	3169	1610	4.5	69.6	1.58	10.5	0.74	13.39	2545	63.0	13.74	NA
SW_T2_c	Seawater	18/5/2017	4	17.3	3.02E+08	51744	2442	1626	4.5	69.6	1.58	10.5	0.74	13.39	2545	63.0	13.74	NA
SW_T3_E5	Seawater	30/5/2017	6	6.9	1.65E+08	40766	2174	1689	4.7	56.4	1.35	12.7	0.72	14.45	5089	62.1	14.99	NA
SW_T3_E4	Seawater	30/5/2017	6	10.5	2.57E+07	47720	2415	1767	4.7	56.4	1.35	12.7	0.72	14.45	5089	62.1	14.99	NA
SW_T3_E2	Seawater	30/5/2017	6	9.9	9.83E+07	56325	2479	1639	4.6	56.4	1.35	12.7	0.72	14.45	5089	62.1	14.99	NA
SW_T4_E4	Seawater	5/7/2017	11	12.9	1.11E+09	55250	2336	1507	4.7	49.9	1.18	38.0	0.74	15.93	2024	138.9	16.25	NA
SW_T4_E5	Seawater	5/7/2017	11	24	8.17E+08	79833	3254	1697	4.9	49.9	1.18	38.0	0.74	15.93	2024	138.9	16.25	NA
SW_T4_E2	Seawater	5/7/2017	11	27.3	1.19E+09	59333	2369	1472	4.6	49.9	1.18	38.0	0.74	15.93	2024	138.9	16.25	NA
SW_T5_a	Seawater	3/8/2017	15	10.1	6.96E+08	71391	3722	2093	5.1	25.2	1.79	53.1	0.72	16.45	572	106.2	20.28	NA
SW_T5_b	Seawater	3/8/2017	15	15.8	4.21E+08	53298	2930	1947	5.0	25.2	1.79	53.1	0.72	16.45	572	106.2	20.28	NA
SW_T5_c	Seawater	3/8/2017	15	13.1	4.32E+08	53051	3000	1996	5.0	25.2	1.79	53.1	0.72	16.45	572	106.2	20.28	NA
SW_T6_a	Seawater	8/9/2017	20	12.9	3.76E+08	27141	2316	2192	5.2	21.4	1.34	94.4	0.74	17.23	470	142.1	17.01	NA
SW_T6_b	Seawater	8/9/2017	20	15.8	8.30E+08	43651	3078	2259	5.2	21.4	1.34	94.4	0.74	17.23	470	142.1	17.01	NA
SW_T6_c	Seawater	8/9/2017	20	30.9	1.38E+09	39178	2879	2224	5.2	21.4	1.34	94.4	0.74	17.23	470	142.1	17.01	NA
SW_T7_a	Seawater	5/10/2017	24	19.9	7.52E+08	59410	3677	2348	5.1	16.7	1.56	162.4	0.73	16.11	1195	122.7	16.60	NA
SW_T7_b	Seawater	5/10/2017	24	19.1	1.42E+09	71598	4217	2403	5.0	16.7	1.56	162.4	0.73	16.11	1195	122.7	16.60	NA
SW_T7_c	Seawater	5/10/2017	24	22.7	2.64E+09	52753	3478	2345	5.0	16.7	1.56	162.4	0.73	16.11	1195	122.7	16.60	NA
Sed_T0_C1	Initial Sediment	18/4/2017	0	7.7	8.58E+07	41729	5619	4822	7.7	100	1.50	28.6	0.72	12.74	3936	42.4	13.41	0.29
Sed_T0_C2	Initial Sediment	18/4/2017	0	9	1.20E+08	35539	5128	4577	7.6	100	1.50	28.6	0.74	12.74	3936	25	14.1	0.27
Sed_T0_C4	Initial Sediment	18/4/2017	0	9.4	1.14E+08	44897	6025	5011	7.7	100	1.50	28.6	0.66	12.74	3936	56.6	17.09	0.27
Sed_T1_C10	Underlying Sediment	2/5/2017	2	9	1.57E+08	44258	6200	5146	7.7	103.7	1.10	6.3	0.73	12.34	1449	48.1	12.22	0.26
Sed_T1_C25	Underlying Sediment	2/5/2017	2	10.2	1.47E+08	50341	6373	5156	7.8	102	01.06	6.3	0.80	12.34	1449	71.2	13.08	0.25
Sed_T1_C32	Underlying Sediment	2/5/2017	2	8.4	1.00E+08	45809	6006	5042	7.8	106.6	1.34	6.3	0.77	12.34	1449	57.7	12.33	0.25
Sed_T2_C8	Underlying Sediment	18/5/2017	4	9.8	1.57E+08	42048	6986	5754	7.8	67.6	1.42	10.5	0.75	13.39	2545	76.5	13.82	0.25
Sed_T2_C24	Underlying Sediment	18/5/2017	4	16.5	2.41E+08	27415	5022	4809	7.4	71.1	1.58	10.5	0.74	13.39	2545	71.7	15.45	0.24
Sed_T2_C35	Underlying Sediment	18/5/2017	4	12	1.81E+08	69213	7710	5383	7.6	70.1	1.73	10.5	0.74	13.39	2545	40.7	11.96	0.25
Sed_T3_C20	Underlying Sediment	30/5/2017	6	27.8	4.01E+08	81590	7040	4491	7.0	66.7	1.14	12.7	0.73	14.45	5089	51.2	12.43	0.26
Sed_T3_C21	Underlying Sediment	30/5/2017	6	22.4	3.32E+08	40280	6053	5048	7.5	45.4	1.54	12.7	0.74	14.45	5089	64.6	17.36	0.26
Sed_T3_C31	Underlying Sediment	30/5/2017	6	14.8	2.60E+08	123368	8925	5195	7.5	57.2	1.37	12.7	0.68	14.45	5089	70.4	15.18	0.26
Sed_T4_C16	Underlying Sediment	5/7/2017	11	11.1	1.52E+08	37698	5023	4407	7.5	61.5	1.23	38.0	0.73	15.93	2024	118.1	16.04	0.25
Sed_T4_C19	Underlying Sediment	5/7/2017	11	19.3	2.59E+08	35908	6352	5486	7.6	44.2	1.16	38.0	0.74	15.93	2024	159.1	18.30	0.25
Sed_T4_C30	Underlying Sediment	5/7/2017	11	18.1	3.22E+08	54504	8114	6156	8.0	43.9	1.16	38.0	0.75	15.93	2024	139.4	14.43	0.26
Sed_T5_C17	Underlying Sediment	3/8/2017	15	25.6	5.44E+08	52190	7213	5624	7.8	25.1	1.43	53.1	0.72	16.45	572	55.4	19.00	0.27
Sed_T5_C23	Underlying Sediment	3/8/2017	15	28.4	6.46E+08	47539	6294	4973	7.4	23.2	02.04	53.1	0.70	16.45	572	139.5	23.07	0.26
Sed_T5_C34	Underlying Sediment	3/8/2017	15	17.7	2.86E+08	29895	5525	5142	7.6	27.3	1.90	53.1	0.74	16.45	572	123.8	18.76	0.25
Sed_T6_C13	Underlying Sediment	8/9/2017	20	7.6	2.14E+08	104056	10174	6398	8.0	18.6	1.55	94.4	0.74	17.23	470	166.9	17.40	0.27
Sed_T6_C27	Underlying Sediment	8/9/2017	20	16.9	3.13E+08	47341	6711	5403	7.6	23.9	1.23	94.4	0.75	17.23	470	144.5	17.02	0.28
Sed_T6_C28	Underlying Sediment	8/9/2017	20	21.4	3.26E+08	63433	7284	5393	7.7	21.8	1.23	94.4	0.72	17.23	470	114.9	16.59	0.26
Sed_T7_C7	Underlying Sediment	5/10/2017	24	27.8	2.80E+08	65096	7827	5728	7.8	24.3	1.63	162.4	0.72	16.11	1195	111.4	18.18	0.28
Sed_T7_C1	Underlying Sediment	5/10/2017	24	17.6	3.71E+08	92905	8708	5700	7.8	18.2	1.65	162.4	0.72	16.11	1195	88.6	17.14	0.26
Sed_T7_C22	Underlying Sediment	5/10/2017	24	22.5	8.12E+08	52844	7501	5814	7.9	7.5	1.40	162.4	0.75	16.11	1195	168.1	14.48	0.28
Sedex_T1_Ext1	External Sediment	2/5/2017	2	0.1	NA	32070	8236	2002	8.0	104.1	0.99	6.3	0.77	12.34	1449	59.0	12.54	NA
Sedex_T1_Ext2	External Sediment	2/5/2017	2	10.3	1.91E+08	33756	5839	5332	8.0	104.1	0.98	6.3	0.77	12.34	1449	59.0	12.54	NA
Sedex_T1_Ext3	External Sediment	2/5/2017	2	9.4	1.38E+08	43413	6606	5496	7.8	104.1	1.15	6.3	0.77	12.34	1449	59.0	12.54	NA
Sedex_T2_Ext1	External Sediment	18/5/2017	4	6.5	1.05E+08	41412	5684	4771	7.6	69.35	1.39	10.5	0.74	13.39	2545	74.1	14.64	NA
Sedex_T2_Ext2	External Sediment	18/5/2017	4	4.9	9.21E+07	43769	7612	6045	7.8	69.6	1.33	10.5	0.74	13.39	2545	63.0	13.74	NA
Sedex_T2_Ext3	External Sediment	18/5/2017	4	7.3	1.06E+08	29277	5280	4948	7.6	69.6	1.49	10.5	0.74	13.39	2545	63.0	13.74	NA
Sedex_T3_Ext1	External Sediment	30/5/2017	6	9.4	1.64E+08	58268	7060	5090	7.5	56.4	2.40	12.7	0.72	14.45	5089	62.1	14.99	NA
Sedex_T3_Ext2	External Sediment	30/5/2017	6	8.7	1.23E+08	40707	5768	4934	7.7	56.4	1.96	12.7	0.72	14.45	5089	62.1	14.99	NA
Sedex_T3_Ext3	External Sediment	30/5/2017	6	4.3	1.96E+08	40336	7781	6310	7.9	56.4	1.29	12.7	0.72	14.45	5089	62.1	14.99	NA
Sedex_T4_Ext1	External Sediment	5/7/2017	11	8.8	1.58E+08	61527	7315	5274	7.6	49.9	0.91	38.0	0.74	15.93	2024	138.9	16.25	NA
Sedex_T4_Ext2	External Sediment	5/7/2017	11	16.9	2.66E+08	53209	6990	5410	7.8	49.9	1.17	38.0	0.74	15.93	2024	138.9	16.25	NA
Sedex_T5_Ext1	External Sediment	3/8/2017	15	13.3	1.96E+08	75934	7569	5146	7.6	25.2	1.22	53.1	0.72	16.45	572	106.2	20.28	NA
Sedex_T5_Ext2	External Sediment	3/8/2017	15	9.8	2.44E+08	41227	5675	4708	7.5	25.2	1.44	53.1	0.72	16.45	572	106.2	20.28	NA
Sedex_T5_Ext3	External Sediment	3/8/2017	15	15.9	3.28E+08	31981	5684	5156	7.6	25.2	1.10	53.1	0.72	16.45	572	106.2	20.28	NA
Sedex_T6_Ext1	External Sediment	8/9/2017	20	15.1	2.02E+08	31793	5070	4664	7.6	21.4	0.85	94.4	0.74	17.23	470	142.1	17.01	NA
Sedex_T6_Ext2	External Sediment	8/9/2017	20	16.6	1.71E+08	46964	5593	4575	7.6	21.4	0.91	94.4	0.74	17.23	470	142.1	17.01	NA
Sedex_T6_Ext3	External Sediment	8/9/2017	20	13.6	2.73E+08	41616	6936	5682	7.7	21.4	1.27	94.4	0.74	17.23	470	142.1	17.01	NA
Sedex_T7_Ext1	External Sediment	5/10/2017	24	11	1.53E+08	34298	7000	6238	8.1	21.3	1.59	162.4	0.72	16.11	1195	100.0	17.66	NA
Sedex_T7_Ext2	External Sediment	5/10/2017	24	14.2	1.70E+08	27075	4920	4751	7.6	16.7	1.25	162.4	0.73	16.11	1195	122.7	16.60	NA
Sedex_T7_Ext3	External Sediment	5/10/2017	24	13.9	2.12E+08	44291	4657	4014	7.7	16.7	1.30	162.4	0.73	16.11	1195	122.7	16.60	NA

Supplementary table 2: Average Bray-Curtis dissimilarities between bacterial community from each compartment (KA: kelp-associated; SW: seawater; US: underlying sediment; ES: external sediment). All pairwise ANOVA comparisons were significant (P = 0.001, Benjamini-Hochberg correction).

	KA	SW	US
SW	7.84	-	-
US	5.94	7.85	-
ES	6.12	7.99	0.92

Supplementary table 3. Associated taxonomy and relative sequence abundance ± s.d. (n = 3, except n = 2 for kelp-associated at T0) of the 249 kelp-associated OTUs whose relative sequence abundance vary significantly during kelp degradation (GLM, P < 0.05).

		Relative abundance (%) mean ± sd							
OTU id	**Taxonomy**	**0 week**	**2 weeks**	**4 weeks**	**6 weeks**	**11 weeks**	**15 weeks**	**20 weeks**	**24 weeks**
OTU3	*Bacteria; Proteobacteria; Alphaproteobacteria; Caulobacterales; Hyphomonadaceae; Hellea*	2.05 ± 1.58	0.55 ± 0.22	5.62 ± 1.86	5.96 ± 0.53	5.71 ± 0.88	5.77 ± 2.52	2.78 ± 0.4	4.63 ± 1.43
OTU5	*Bacteria; Proteobacteria; Alphaproteobacteria; Caulobacterales; Hyphomonadaceae; Fretibacter*	0.12 ± 0.17	11.7 ± 8.59	7.87 ± 1.16	7.91 ± 4.45	3.35 ± 1.49	6.25 ± 1.82	4.35 ± 1.49	4.1 ± 1.14
OTU7	*Bacteria; Proteobacteria; Alphaproteobacteria; Caulobacterales; Hyphomonadaceae; Hellea*	0	0.07 ± 0.03	5.62 ± 6.16	8.93 ± 2.86	3.06 ± 1.92	1.58 ± 0.81	1.2 ± 1.57	2.68 ± 0.95
OTU8	*Bacteria; Proteobacteria; Alphaproteobacteria; Rhizobiales; Rhizobiaceae; unknown genus*	0.02 ± 0.03	8.11 ± 4.77	11.05 ± 2.82	6.51 ± 2.14	2.02 ± 0.69	0.52 ± 0.35	0.11 ± 0.17	0.03 ± 0.02
OTU9	*Bacteria; Proteobacteria; Alphaproteobacteria; Rhizobiales; Rhizobiaceae; unknown genus*	0	4.89 ± 3.44	5.36 ± 0.69	6.22 ± 3.2	2.6 ± 1.71	2.07 ± 2.37	1.03 ± 1.57	0.17 ± 0.03
OTU10	*Bacteria; Proteobacteria; Gammaproteobacteria; Thiohalorhabdales; Thiohalorhabdaceae; Granulosicoccus*	25.41 ± 4.55	5.07 ± 4.84	0.9 ± 0.24	0.29 ± 0.23	0.1 ± 0.09	0.44 ± 0.21	0.25 ± 0.3	0.03 ± 0.01
OTU13	*Bacteria; Proteobacteria; Alphaproteobacteria; Caulobacterales; Hyphomonadaceae; unknown genus*	0	6.82 ± 2.27	9.02 ± 0.42	3.15 ± 1.22	0.73 ± 0.38	0.76 ± 0.19	0.29 ± 0.21	0.39 ± 0.24
OTU14	*Bacteria; Proteobacteria; Alphaproteobacteria; Caulobacterales; Hyphomonadaceae; Hellea*	22.49 ± 8.27	1 ± 1.32	0.49 ± 0.21	0.55 ± 0.45	0.45 ± 0.45	0.73 ± 0.24	1.29 ± 0.94	1.13 ± 0.19
OTU16	*Bacteria; Actinobacteria; Acidimicrobiia; Microtrichales; Microtrichaceae; Sva0996 marine group*	0	0.01 ± 0	0.04 ± 0.02	0.12 ± 0.11	4.44 ± 1.05	5.44 ± 1.55	9.52 ± 2.01	5.62 ± 1.37
OTU18	*Bacteria; Proteobacteria; Alphaproteobacteria; Sphingomonadales; Sphingomonadaceae; Altererythrobacter*	0	0.25 ± 0.24	5.6 ± 0.22	4.34 ± 1.67	1.71 ± 1.23	0.57 ± 0.42	0.22 ± 0.18	1.01 ± 1.32
OTU22	*Bacteria; Proteobacteria; Gammaproteobacteria; Ectothiorhodospirales; Thioalkalispiraceae; Thiohalophilus*	0.01 ± 0.01	0.08 ± 0.06	1.72 ± 0.84	1.44 ± 0.6	3.42 ± 0.62	6.68 ± 1.42	7.18 ± 3.63	3.63 ± 2.33
OTU23	*Bacteria; Proteobacteria; Alphaproteobacteria; Caulobacterales; Hyphomonadaceae; Litorimonas*	5.61 ± 2.01	1.38 ± 0.45	0.54 ± 0.08	0.41 ± 0.11	0.67 ± 0.24	3.1 ± 1.71	2.21 ± 0.41	1.83 ± 0.99
OTU24	*Bacteria; Actinobacteria; Acidimicrobiia; Microtrichales; Microtrichaceae; Sva0996 marine group*	0	0	0	0.02 ± 0.02	1.3 ± 0.65	1.96 ± 0.75	5.33 ± 0.72	2.56 ± 1.08
OTU25	*Bacteria; Proteobacteria; Gammaproteobacteria; Ectothiorhodospirales; Ectothiorhodospiraceae; unknown genus*	0	4.81 ± 4.14	4.45 ± 1.17	1.41 ± 0.65	0.14 ± 0.1	0.02 ± 0.02	0.11 ± 0.14	0.04 ± 0.03
OTU28	*Bacteria; Proteobacteria; Alphaproteobacteria; Rhodobacterales; Rhodobacteraceae; Octadecabacter*	0	7.4 ± 2.58	0.66 ± 0.5	0.54 ± 0.26	0.16 ± 0.05	0.05 ± 0.01	0	0.07 ± 0.06
OTU30	*Bacteria; Proteobacteria; Alphaproteobacteria; unknown order; unknown family; unknown genus*	0	0	0	0.02 ± 0.03	0.36 ± 0.08	0.97 ± 0.51	1.35 ± 0.69	6.68 ± 3.67
OTU33	*Bacteria; Proteobacteria; Alphaproteobacteria; Caulobacterales; Hyphomonadaceae; Litorimonas*	5.17 ± 0.43	0.76 ± 0.51	0.28 ± 0.08	0.29 ± 0.08	1.15 ± 0.79	1.7 ± 0.69	2.45 ± 1.47	1.51 ± 0.47
OTU36	*Bacteria; Proteobacteria; Alphaproteobacteria; Sphingomonadales; Sphingomonadaceae; Sphingorhabdus*	0	0.85 ± 0.42	2.77 ± 0.95	3.27 ± 0.83	0.23 ± 0.14	0.24 ± 0.1	0.14 ± 0.15	0.24 ± 0.33
OTU37	*Bacteria; Proteobacteria; Alphaproteobacteria; Caulobacterales; Hyphomonadaceae; Litorimonas*	7.17 ± 2.99	0.76 ± 0.18	0.61 ± 0.35	0.88 ± 0.65	0.33 ± 0.16	0.55 ± 0.41	0.19 ± 0.11	0.15 ± 0.1
OTU38	*Bacteria; Proteobacteria; Alphaproteobacteria; Caulobacterales; Hyphomonadaceae; Hellea*	3.6 ± 2.03	2.48 ± 1.14	1.74 ± 0.36	0.58 ± 0.2	0.37 ± 0.1	0.45 ± 0.17	0.15 ± 0.15	0.07 ± 0.09
OTU48	*Bacteria; Proteobacteria; Gammaproteobacteria; KI89A clade; unknown family; unknown genus*	0	0	0.02 ± 0.02	0.24 ± 0.08	2.45 ± 0.55	1.93 ± 0.42	1.87 ± 0.78	0.9 ± 0.31
OTU52	*Bacteria; Proteobacteria; Alphaproteobacteria; Rhodobacterales; Rhodobacteraceae; unknown genus*	0	0.02 ± 0.03	0.08 ± 0.06	0.18 ± 0.21	0.43 ± 0.11	2.1 ± 1.02	1.88 ± 0.79	1.14 ± 0.28
OTU54	*Bacteria; Proteobacteria; Gammaproteobacteria; KI89A clade; unknown family; unknown genus*	0	0.01 ± 0.01	0.08 ± 0.05	0.56 ± 0.57	1.08 ± 0.63	1.94 ± 0.68	1.46 ± 0.41	2.06 ± 0.56
OTU55	*Bacteria; Proteobacteria; Gammaproteobacteria; Thiohalorhabdales; Thiohalorhabdaceae; Granulosicoccus*	0	0.02 ± 0.01	0.31 ± 0.19	0.38 ± 0.39	1.15 ± 0.14	1.68 ± 0.72	1.38 ± 0.29	0.86 ± 0.54
OTU59	*Bacteria; Proteobacteria; Alphaproteobacteria; Rhizobiales; Rhizobiaceae; unknown genus*	0	1.46 ± 0.88	1.56 ± 1.08	0.57 ± 0.2	0.73 ± 0.2	0.44 ± 0.12	0.13 ± 0.19	0.07 ± 0.05
OTU60	*Bacteria; Proteobacteria; Gammaproteobacteria; Alteromonadales; Alteromonadaceae; Paraglaciecola*	0	2.5 ± 3.26	0.21 ± 0.16	1.43 ± 2.32	0.02 ± 0.02	0.09 ± 0.09	0.01 ± 0.02	0.16 ± 0.24
OTU72	*Bacteria; Proteobacteria; Gammaproteobacteria; Cellvibrionales; Cellvibrionaceae; unknown genus*	0	0.16 ± 0.14	0.38 ± 0.35	2.2 ± 2.44	0.04 ± 0.02	0.05 ± 0.04	0.24 ± 0.31	0.19 ± 0.3
OTU75	*Bacteria; Proteobacteria; Alphaproteobacteria; Caulobacterales; Hyphomonadaceae; Litorimonas*	7.74 ± 2.62	0.05 ± 0.05	0.01 ± 0.01	0.01 ± 0	0	0	0	0
OTU79	*Bacteria; Actinobacteria; Acidimicrobiia; Microtrichales; Microtrichaceae; Sva0996 marine group*	0	0	0.01 ± 0.01	0.08 ± 0.11	1.23 ± 1.03	1.03 ± 0.3	1.75 ± 0.91	0.86 ± 0.51
OTU89	*Bacteria; Proteobacteria; Alphaproteobacteria; Rhodobacterales; Rhodobacteraceae; Sulfitobacter*	0.23 ± 0.31	1.91 ± 0.6	0.53 ± 0.58	0.24 ± 0.13	0.05 ± 0.05	0.02 ± 0	0	0.34 ± 0.57
OTU107	*Bacteria; Proteobacteria; Alphaproteobacteria; Caulobacterales; Parvularculaceae; unknown genus*	0	0	0	0.03 ± 0.05	1.47 ± 0.92	1 ± 0.21	0.46 ± 0.1	0.27 ± 0.05
OTU112	*Bacteria; Epsilonbacteraeota; Campylobacteria; Campylobacterales; Arcobacteraceae; Arcobacter*	0	0	0.06 ± 0.03	0.01 ± 0.02	0.01 ± 0	0	0	0
OTU114	*Bacteria; Proteobacteria; Alphaproteobacteria; Rhizobiales; Rhizobiaceae; unknown genus*	0	0	0.06 ± 0.09	0.04 ± 0.04	1.02 ± 0.37	1.43 ± 0.63	0.33 ± 0.15	0.17 ± 0.09
OTU115	*Bacteria; Proteobacteria; Gammaproteobacteria; Cellvibrionales; Porticoccaceae; C1-B045*	0	0	0	0.03 ± 0.04	0.06 ± 0.02	0.86 ± 0.6	1.34 ± 1.37	1.47 ± 0.36
OTU119	*Bacteria; Proteobacteria; Gammaproteobacteria; Ectothiorhodospirales; Thioalkalispiraceae; Thiohalophilus*	0	0	0.09 ± 0.11	0.27 ± 0.26	1.52 ± 0.34	0.98 ± 0.43	0.32 ± 0.1	0.14 ± 0.02
OTU122	*Bacteria; Proteobacteria; Alphaproteobacteria; Rhodobacterales; Rhodobacteraceae; Sulfitobacter*	0	1.5 ± 0.79	0.21 ± 0.13	0.5 ± 0.35	0.05 ± 0.06	0	0	0.01 ± 0.01
OTU123	*Bacteria; Planctomycetes; Planctomycetacia; Pirellulales; Pirellulaceae; Blastopirellula*	1.66 ± 1.01	0.8 ± 0.27	0.11 ± 0.02	0.07 ± 0.05	0.1 ± 0.02	0.21 ± 0.06	0.12 ± 0.08	0.11 ± 0.07
OTU125	*Bacteria; Proteobacteria; Gammaproteobacteria; Thiohalorhabdales; Thiohalorhabdaceae; Granulosicoccus*	0	1.58 ± 0.99	0.84 ± 0.67	0.26 ± 0.18	0.13 ± 0.08	0.05 ± 0.01	0.06 ± 0.02	0.05 ± 0.05
OTU137	*Bacteria; Proteobacteria; Alphaproteobacteria; Rhodobacterales; Rhodobacteraceae; Octadecabacter*	0.02 ± 0.02	0.36 ± 0.02	0.31 ± 0.21	0.29 ± 0.05	0.89 ± 0.56	0.64 ± 0.55	0.11 ± 0.14	0.18 ± 0.16
OTU139	*Bacteria; Proteobacteria; Alphaproteobacteria; Tistrellales; Geminicoccaceae; Candidatus Alysiosphaera*	0	0	0.01 ± 0.01	0.01 ± 0.01	0.42 ± 0.18	0.67 ± 0.38	0.36 ± 0.22	1.1 ± 0.61
OTU140	*Bacteria; Actinobacteria; Acidimicrobiia; Microtrichales; Microtrichaceae; Sva0996 marine group*	0	0.01	0.01 ± 0.01	0.06 ± 0.03	1.32 ± 1.19	0.57 ± 0.35	0.67 ± 0.28	0.48 ± 0.1
OTU144	*Bacteria; Bacteroidetes; Bacteroidia; Flavobacteriales; Flavobacteriaceae; Bizionia*	0	0.29 ± 0.45	0.8 ± 0.76	0.56 ± 0.34	0.62 ± 0.15	0.2 ± 0.01	0.23 ± 0.26	0.14 ± 0.02
OTU151	*Bacteria; Proteobacteria; Alphaproteobacteria; Rhodobacterales; Rhodobacteraceae; unknown genus*	0.02 ± 0.03	0.07 ± 0.05	0.21 ± 0.06	0.34 ± 0.43	0.8 ± 0.21	0.55 ± 0.38	0.29 ± 0.18	0.06 ± 0.03
OTU155	*Bacteria; Proteobacteria; Alphaproteobacteria; Rhodobacterales; Rhodobacteraceae; Octadecabacter*	0	0.92 ± 0.61	0.77 ± 0.8	0.2 ± 0.04	0.08 ± 0.06	0.03 ± 0.03	0.06 ± 0.07	0.05 ± 0.02
OTU159	*Bacteria; Bacteroidetes; Bacteroidia; Chitinophagales; Saprospiraceae; unknown genus*	0	0	0	0	0.14 ± 0.16	0.96 ± 0.44	0.42 ± 0.42	0.66 ± 0.54
OTU162	*Bacteria; Proteobacteria; Alphaproteobacteria; Rhodobacterales; Rhodobacteraceae; Tateyamaria*	0	1.45 ± 0.86	0.27 ± 0.13	0.24 ± 0.15	0.57 ± 0.31	0.43 ± 0.21	0.28 ± 0.27	0.11 ± 0.04
OTU172	*Bacteria; Proteobacteria; Alphaproteobacteria; Rhodobacterales; Rhodobacteraceae; Sulfitobacter*	0	1.37 ± 1.41	0.21 ± 0.12	0.1 ± 0.07	0	0.04 ± 0.05	0	0
OTU174	*Bacteria; Proteobacteria; Gammaproteobacteria; Cellvibrionales; Spongiibacteraceae; BD1-7 clade*	0	0.01	0.02 ± 0.01	0.09 ± 0.11	1.45 ± 0.9	0.35 ± 0.13	0.31 ± 0.14	0.14 ± 0.14
OTU178	*Bacteria; Proteobacteria; Gammaproteobacteria; Thiohalorhabdales; Thiohalorhabdaceae; Granulosicoccus*	0	0.01 ± 0.02	0.29 ± 0.38	0.5 ± 0.64	0.37 ± 0.17	0.3 ± 0.17	0.3 ± 0.21	0.27 ± 0.2
OTU180	*Bacteria; Proteobacteria; Alphaproteobacteria; Caulobacterales; Hyphomonadaceae; Litorimonas*	0	1.33 ± 1.1	0.51 ± 0.84	0.04 ± 0.06	0.02 ± 0.02	0	0	0
OTU186	*Bacteria; Proteobacteria; Gammaproteobacteria; Arenicellales; Arenicellaceae; Arenicella*	0	0	0.01 ± 0.02	0.33 ± 0.33	0.44 ± 0.35	0.56 ± 0.68	0.34 ± 0.15	0.32 ± 0.15
OTU190	*Bacteria; Bacteroidetes; Bacteroidia; Chitinophagales; Saprospiraceae; unknown genus*	0.41 ± 0.54	0.04 ± 0.03	0.03 ± 0.02	0.1 ± 0.06	0.23 ± 0.18	0.51 ± 0.46	0.66 ± 0.46	0.91 ± 0.73
OTU192	*Bacteria; Proteobacteria; Alphaproteobacteria; Sphingomonadales; Sphingomonadaceae; Sphingorhabdus*	0	0	0	0.1 ± 0.09	0.34 ± 0.17	0.8 ± 1.27	0.04 ± 0.03	0.11 ± 0.05
OTU201	*Bacteria; Proteobacteria; Gammaproteobacteria; Arenicellales; Arenicellaceae; Arenicella*	0	0.01 ± 0.01	0.01 ± 0.01	0.06 ± 0.03	0.33 ± 0.27	0.31 ± 0.17	0.67 ± 0.09	0.61 ± 0.4
OTU202	*Bacteria; Proteobacteria; Alphaproteobacteria; Rhodobacterales; Rhodobacteraceae; Roseobacter clade NAC11-7 lineage*	0	0.11 ± 0.05	0.05 ± 0.04	0.17 ± 0.24	0.38 ± 0.04	0.31 ± 0.12	0.34 ± 0.17	0.38 ± 0.13
OTU203	*Bacteria; Proteobacteria; Gammaproteobacteria; Ectothiorhodospirales; Thioalkalispiraceae; Thioprofundum*	0	0	0.01 ± 0.01	0.04 ± 0.06	0.15 ± 0.09	0.37 ± 0.19	0.41 ± 0.09	0.8 ± 0.59
OTU210	*Bacteria; Bacteroidetes; Bacteroidia; Chitinophagales; Saprospiraceae; Portibacter*	0	0.01	0	0.01	0.06 ± 0.02	0.69 ± 0.45	0.36 ± 0.35	0.39 ± 0.38
OTU219	*Bacteria; Proteobacteria; Alphaproteobacteria; Rhodobacterales; Rhodobacteraceae; Silicimonas*	0	0.02 ± 0.02	0.01 ± 0.01	0.08 ± 0.09	0.46 ± 0.3	0.47 ± 0.2	0.33 ± 0.17	0.34 ± 0.13
OTU220	*Bacteria; Proteobacteria; Gammaproteobacteria; Thiohalorhabdales; Thiohalorhabdaceae; Granulosicoccus*	0	0	0.03 ± 0.04	0.05 ± 0.04	0.38 ± 0.3	0.59 ± 0.54	0.26 ± 0.09	0.25 ± 0.15
OTU235	*Bacteria; Proteobacteria; Gammaproteobacteria; Arenicellales; Arenicellaceae; Arenicella*	0	0.16 ± 0.19	0	0.22 ± 0.33	0.25 ± 0.09	0.25 ± 0.04	0.34 ± 0.14	0.25 ± 0.13
OTU237	*Bacteria; Proteobacteria; Gammaproteobacteria; Cellvibrionales; Cellvibrionaceae; unknown genus*	0	0	0.1 ± 0.1	0.36 ± 0.29	0.27 ± 0.2	0.13 ± 0.08	0.25 ± 0.16	0.56 ± 0.67
OTU241	*Bacteria; Proteobacteria; Alphaproteobacteria; Caulobacterales; Parvularculaceae; Amphiplicatus*	0	0	0	0	0.36 ± 0.17	0.48 ± 0.19	0.38 ± 0.09	0.3 ± 0.15
OTU250	*Bacteria; Proteobacteria; Alphaproteobacteria; Caulobacterales; Hyphomonadaceae; Hellea*	0.13 ± 0.18	0.71 ± 0.22	0.32 ± 0.14	0.58 ± 0.14	0.13 ± 0.08	0.48 ± 0.39	0.07 ± 0.09	0.03 ± 0.01
OTU253	*Bacteria; Proteobacteria; Gammaproteobacteria; KI89A clade; unknown family; unknown genus*	0	0	0.01	0.04 ± 0.04	0.31 ± 0.17	0.38 ± 0.11	0.41 ± 0.24	0.22 ± 0.16
OTU254	*Bacteria; Proteobacteria; Alphaproteobacteria; Rhodobacterales; Rhodobacteraceae; Maribius*	0	0.04 ± 0.06	0.05 ± 0.04	0.18 ± 0.22	0.12 ± 0.04	0.85 ± 0.66	0.19 ± 0.06	0.09 ± 0.06
OTU259	*Bacteria; Bacteroidetes; Bacteroidia; Chitinophagales; Saprospiraceae; unknown genus*	0.02 ± 0.03	0.01 ± 0.01	0.02 ± 0.01	0.03 ± 0.03	0.11 ± 0.06	0.47 ± 0.37	0.25 ± 0.05	0.42 ± 0.33
OTU263	*Bacteria; Proteobacteria; Gammaproteobacteria; Thiohalorhabdales; Thiohalorhabdaceae; Granulosicoccus*	0	0.88 ± 0.15	0.16 ± 0.17	0.01 ± 0.01	0.01 ± 0.01	0.01	0	0.41 ± 0.7
OTU265	*Bacteria; Actinobacteria; Acidimicrobiia; Microtrichales; Microtrichaceae; Sva0996 marine group*	0	0.01 ± 0.01	0.02 ± 0.01	0.01 ± 0.01	0.12 ± 0.07	0.03 ± 0.04	0.28 ± 0.05	0.07 ± 0.06
OTU272	*Bacteria; Proteobacteria; Alphaproteobacteria; Rhodobacterales; Rhodobacteraceae; Pacificibacter*	0	0.24 ± 0.22	0.21 ± 0.15	0.48 ± 0.12	0.02 ± 0.01	0.01 ± 0.01	0.02 ± 0.03	0.03 ± 0.02
OTU276	*Bacteria; Proteobacteria; Deltaproteobacteria; Bdellovibrionales; Bacteriovoracaceae; Peredibacter*	0	0.2 ± 0.28	0.34 ± 0.14	0.27 ± 0.21	0.12 ± 0.07	0.14 ± 0.09	0.09 ± 0.02	0.15 ± 0.07
OTU278	*Bacteria; Epsilonbacteraeota; Campylobacteria; Campylobacterales; Arcobacteraceae; Arcobacter*	0.19 ± 0.17	0.11 ± 0.07	0.08 ± 0.03	0.13 ± 0.05	0.01 ± 0.01	0	0	0
OTU279	*Bacteria; Proteobacteria; Alphaproteobacteria; Rhodobacterales; Rhodobacteraceae; Litoreibacter*	0	0.02 ± 0.04	0.05 ± 0.04	0.04 ± 0.01	0.4 ± 0.11	0.1 ± 0.05	0.24 ± 0.34	0.39 ± 0.24
OTU281	*Bacteria; Proteobacteria; Gammaproteobacteria; Thiohalorhabdales; Thiohalorhabdaceae; Granulosicoccus*	0	0	0.07 ± 0.06	0.38 ± 0.25	0.31 ± 0.3	0.26 ± 0.16	0.13 ± 0.07	0.03 ± 0.03
OTU282	*Bacteria; Proteobacteria; Deltaproteobacteria; Myxococcales; Blrii41; unknown genus*	0	0	0	0	0.05 ± 0.09	0.22 ± 0.34	0.5 ± 0.22	0.51 ± 0.43
OTU283	*Bacteria; Proteobacteria; Alphaproteobacteria; Rhodobacterales; Rhodobacteraceae; unknown genus*	0	0	0	0.01	0.24 ± 0.29	0.09 ± 0.08	0.86 ± 0.72	0.12 ± 0.09
OTU289	*Bacteria; Proteobacteria; Gammaproteobacteria; Arenicellales; Arenicellaceae; Arenicella*	0	0.1 ± 0.1	0.01 ± 0.01	0.02 ± 0.02	0.2 ± 0.09	0.41 ± 0.39	0.19 ± 0.17	0.29 ± 0.12
OTU293	*Bacteria; Bacteroidetes; Bacteroidia; Chitinophagales; Saprospiraceae; Rubidimonas*	0	0.05 ± 0.01	0.45 ± 0.56	0.14 ± 0.08	0.42 ± 0.1	0.16 ± 0.09	0.19 ± 0.05	0.11 ± 0.06
OTU300	*Bacteria; Bacteroidetes; Bacteroidia; Flavobacteriales; Flavobacteriaceae; unknown genus*	0	0.03 ± 0	0.34 ± 0.11	0.98 ± 0.73	0.15 ± 0.03	0.05 ± 0.06	0	0.04 ± 0.03
OTU306	*Bacteria; Proteobacteria; Alphaproteobacteria; Caulobacterales; Hyphomonadaceae; Hellea*	0	0.02 ± 0.03	0.16 ± 0.05	0.21 ± 0.17	0.17 ± 0.09	0.27 ± 0.33	0.25 ± 0.18	0.16 ± 0.09
OTU308	*Bacteria; Proteobacteria; Alphaproteobacteria; Rickettsiales; SM2D12; unknown genus*	0	0.69 ± 0.78	0.01 ± 0.01	0.06 ± 0.09	0.01 ± 0.01	0.23 ± 0.26	0.04 ± 0	0.03 ± 0.03
OTU317	*Bacteria; Proteobacteria; Gammaproteobacteria; Thiohalorhabdales; Thiohalorhabdaceae; Granulosicoccus*	0	0.71 ± 0.42	0.88 ± 0.79	0.23 ± 0.23	0.09 ± 0.06	0.15 ± 0.2	0.01 ± 0.02	0.2 ± 0.28
OTU344	*Bacteria; Actinobacteria; Acidimicrobiia; Microtrichales; Microtrichaceae; unknown genus*	0	0	0	0.01 ± 0.01	0.09 ± 0.09	0.1 ± 0.1	0.83 ± 0.38	0.42 ± 0.28
OTU348	*Bacteria; Proteobacteria; Gammaproteobacteria; Cellvibrionales; Cellvibrionaceae; Candidatus Endobugula*	0	0	0	0	0.01 ± 0.02	0.01	0.07 ± 0.11	0.86 ± 0.75
OTU351	*Bacteria; Proteobacteria; Alphaproteobacteria; Rhodobacterales; Rhodobacteraceae; Sulfitobacter*	0	0.5 ± 0.39	0.33 ± 0.55	0.06 ± 0.09	0.03 ± 0.04	0.01 ± 0.02	0	0
OTU375	*Bacteria; Bacteroidetes; Bacteroidia; Flavobacteriales; Flavobacteriaceae; Lutimonas*	0	0.01 ± 0.01	0.01 ± 0.01	0.01 ± 0.02	0.13 ± 0.07	0.11 ± 0.07	0.07 ± 0.02	0.14 ± 0.13
OTU379	*Bacteria; Bacteroidetes; Bacteroidia; Flavobacteriales; Flavobacteriaceae; Maribacter*	0	0.06 ± 0.06	0.35 ± 0.55	0.3 ± 0.45	0.01 ± 0.01	0	0	0
OTU386	*Bacteria; Proteobacteria; Gammaproteobacteria; pltb-vmat-80; unknown family; unknown genus*	0	0	0	0	0.12 ± 0.1	0.04 ± 0.03	0.03 ± 0.01	0.01 ± 0.01
OTU395	*Bacteria; Proteobacteria; Gammaproteobacteria; pltb-vmat-80; unknown family; unknown genus*	0	0	0	0	0.02 ± 0.02	0.11 ± 0.07	0.6 ± 0.11	0.29 ± 0.07
OTU397	*Bacteria; Proteobacteria; Gammaproteobacteria; Tenderiales; Tenderiaceae; Candidatus Tenderia*	0	0	0	0	0.2 ± 0.17	0.39 ± 0.42	0.31 ± 0.41	0.12 ± 0.09
OTU404	*Bacteria; Proteobacteria; Alphaproteobacteria; Rhizobiales; Rhizobiaceae; Ahrensia*	0	0.6 ± 0.49	0.24 ± 0.31	0.02 ± 0	0.04 ± 0.04	0.09 ± 0.1	0.01	0.04 ± 0.04
OTU407	*Bacteria; Proteobacteria; Alphaproteobacteria; Tistrellales; Geminicoccaceae; Candidatus Alysiosphaera*	0	0	0	0	0.15 ± 0.12	0.1 ± 0.02	0.15 ± 0.01	0.06 ± 0.04
OTU414	*Bacteria; Proteobacteria; Gammaproteobacteria; Alteromonadales; Colwelliaceae; Colwellia*	0.01 ± 0.01	0.55 ± 0.58	0.27 ± 0.21	0.42 ± 0.24	0.04 ± 0.03	0.01 ± 0.01	0.05 ± 0.05	0.03 ± 0.03
OTU419	*Bacteria; Actinobacteria; Acidimicrobiia; Microtrichales; Microtrichaceae; Sva0996 marine group*	0	0	0	0.01	0.01 ± 0.01	0.02 ± 0.01	0.54 ± 0.27	0.19 ± 0.21

OTU425	*Bacteria; Proteobacteria; Gammaproteobacteria; pltb-vmat-80; unknown family; unknown genus*	0	0	0	0	0.02 ± 0.01	0.03 ± 0.04	0.5 ± 0.13	0.29 ± 0.13
OTU429	*Bacteria; Bacteroidetes; Bacteroidia; Sphingobacteriales; NS11-12 marine group; unknown genus*	0	0	0.01 ± 0.02	0.04 ± 0.04	0.34 ± 0.11	0.4 ± 0.43	0.33 ± 0.15	0.19 ± 0.14
OTU431	*Bacteria; Proteobacteria; Gammaproteobacteria; Arenicellales; Arenicellaceae; Arenicella*	0	0.01 ± 0.01	0	0.01 ± 0.01	0.01 ± 0.01	0.14 ± 0.09	0.23 ± 0.09	0.6 ± 0.46
OTU435	*Bacteria; Proteobacteria; Gammaproteobacteria; Chromatiales; Sedimenticolaceae; Candidatus Thiodiazotropha*	0.85 ± 0.1	0.2 ± 0.15	0.05 ± 0.02	0.02 ± 0.02	0.01 ± 0	0.02 ± 0.02	0.04 ± 0.02	0.01 ± 0
OTU446	*Bacteria; Proteobacteria; Alphaproteobacteria; Rhodobacterales; Rhodobacteraceae; Loktanella*	0	0.61 ± 0.89	0.21 ± 0.33	0.13 ± 0.06	0.01 ± 0.02	0.01 ± 0.01	0	0
OTU448	*Bacteria; Proteobacteria; Alphaproteobacteria; Caulobacterales; Hyphomonadaceae; unknown genus*	0	0.21 ± 0.16	0.11 ± 0.05	0.17 ± 0.17	0.03 ± 0.04	0.11 ± 0.12	0.06 ± 0.03	0.11 ± 0.11
OTU461	*Bacteria; Proteobacteria; Gammaproteobacteria; Cellvibrionales; Cellvibrionaceae; unknown genus*	0	0	0.04 ± 0.04	0.07 ± 0.07	0.06 ± 0.05	0.2 ± 0.18	0.1 ± 0.08	0.38 ± 0.15
OTU470	*Bacteria; Actinobacteria; Acidimicrobiia; Microtrichales; Microtrichaceae; unknown genus*	0	0	0	0	0.03 ± 0.02	0.07 ± 0.06	0.15 ± 0.15	0.05 ± 0.07
OTU474	*Bacteria; Bacteroidetes; Bacteroidia; Flavobacteriales; NS9 marine group; unknown genus*	0	0	0	0.08 ± 0.12	0.33 ± 0.22	0.3 ± 0.18	0.12 ± 0.07	0.04 ± 0.05
OTU492	*Bacteria; Bacteroidetes; Bacteroidia; Chitinophagales; Saprospiraceae; unknown genus*	0	0	0	0	0.01 ± 0.01	0.01 ± 0.01	0.51 ± 0.52	0.16 ± 0.16
OTU495	*Bacteria; Proteobacteria; Gammaproteobacteria; Thiohalorhabdales; Thiohalorhabdaceae; Granulosicoccus*	0	0.15 ± 0.17	0.16 ± 0.09	0.02 ± 0.02	0.13 ± 0.08	0	0	0
OTU509	*Bacteria; Bacteroidetes; Bacteroidia; Flavobacteriales; Flavobacteriaceae; Mesoflavibacter*	0	0	0	0	0	0	0.34 ± 0.54	0.39 ± 0.09
OTU516	*Bacteria; Actinobacteria; Acidimicrobiia; Microtrichales; Microtrichaceae; unknown genus*	0	0	0	0	0.04 ± 0.03	0.08 ± 0.06	0.1 ± 0.12	0
OTU524	*Bacteria; Proteobacteria; Alphaproteobacteria; Sphingomonadales; Sphingomonadaceae; Erythrobacter*	0	0.14 ± 0.13	0.03 ± 0.02	0.03 ± 0.03	0.16 ± 0.07	0.05 ± 0.01	0.05 ± 0.03	0.06 ± 0.02
OTU542	*Bacteria; Proteobacteria; Gammaproteobacteria; KI89A clade; unknown family; unknown genus*	0	0	0.03 ± 0.02	0.1 ± 0.12	0.33 ± 0.18	0.09 ± 0.04	0.1 ± 0.07	0.03 ± 0.01
OTU549	*Bacteria; Proteobacteria; Alphaproteobacteria; Rhodobacterales; Rhodobacteraceae; Sedimentitalea*	0	0.14 ± 0.07	0.07 ± 0.05	0.06 ± 0.02	0.35 ± 0.19	0.03 ± 0.04	0.01 ± 0	0.02 ± 0.02
OTU550	*Bacteria; Proteobacteria; Alphaproteobacteria; Micavibrionales; Micavibrionaceae; unknown genus*	0	0.23 ± 0.15	0.01 ± 0.01	0.13 ± 0.12	0.04 ± 0.02	0.08 ± 0.02	0.04 ± 0.01	0.04 ± 0.03
OTU558	*Bacteria; Bacteroidetes; Bacteroidia; Flavobacteriales; Flavobacteriaceae; Dokdonia*	0	0.06 ± 0.01	0.14 ± 0.1	0.21 ± 0.17	0.49 ± 0.3	0.03 ± 0.05	0.04 ± 0	0.07 ± 0.04
OTU570	*Bacteria; Proteobacteria; Alphaproteobacteria; Caulobacterales; Hyphomonadaceae; unknown genus*	0	0.25 ± 0.13	0.13 ± 0.08	0.21 ± 0.28	0.21 ± 0.07	0.11 ± 0.01	0.07 ± 0.03	0.06 ± 0.03
OTU573	*Bacteria; Proteobacteria; Gammaproteobacteria; Cellvibrionales; Spongiibacteraceae; BD1-7 clade*	0	0	0.01 ± 0.01	0	0.01 ± 0.02	0.1 ± 0.01	0.24 ± 0.18	0.26 ± 0.25
OTU577	*Bacteria; Proteobacteria; Alphaproteobacteria; Rhodobacterales; Rhodobacteraceae; Octadecabacter*	0	0	0.03 ± 0.04	0.07 ± 0.07	0.13 ± 0.12	0.28 ± 0.26	0.03 ± 0.02	0.07 ± 0.06
OTU578	*Bacteria; Proteobacteria; Alphaproteobacteria; Micavibrionales; Micavibrionaceae; unknown genus*	0	0.38 ± 0.15	0.07 ± 0.05	0.03 ± 0.01	0.01 ± 0.02	0.04 ± 0.04	0	0
OTU591	*Bacteria; Proteobacteria; Gammaproteobacteria; Oceanospirillales; Nitrincolaceae; Profundimonas*	0	0.08 ± 0.06	0.38 ± 0.51	0.27 ± 0.04	0	0	0	0.19 ± 0.33
OTU593	*Bacteria; Proteobacteria; Deltaproteobacteria; SAR324 clade(Marine group B); unknown family; unknown genus*	0	0	0.01	0.02 ± 0.04	0.14 ± 0.05	0.26 ± 0.14	0.11 ± 0.04	0.09 ± 0.02
OTU594	*Bacteria; Proteobacteria; Alphaproteobacteria; Rhizobiales; Rhizobiaceae; unknown genus*	0	0.02 ± 0.02	0.1 ± 0.09	0.08 ± 0.07	0.22 ± 0.06	0.16 ± 0.07	0.09 ± 0.03	0.06 ± 0.01
OTU602	*Bacteria; Proteobacteria; Gammaproteobacteria; Arenicellales; Arenicellaceae; Arenicella*	0	0.05 ± 0.06	0	0.02 ± 0.03	0.35 ± 0.07	0.36 ± 0.1	0.09 ± 0.04	0.26 ± 0.12
OTU650	*Bacteria; Proteobacteria; Alphaproteobacteria; Sphingomonadales; Sphingomonadaceae; Erythrobacter*	0	0.01 ± 0.01	0	0	0.08 ± 0.03	0.3 ± 0.29	0.14 ± 0.2	0.1 ± 0.07
OTU658	*Bacteria; Proteobacteria; Gammaproteobacteria; Arenicellales; Arenicellaceae; HTCC5015*	0	0.01	0.09 ± 0.07	0.13 ± 0.09	0.21 ± 0.18	0.08 ± 0.07	0.02 ± 0.02	0
OTU663	*Bacteria; Proteobacteria; Deltaproteobacteria; Bdellovibrionales; Bdellovibrionaceae; Bdellovibrio*	0	0	0	0	0.22 ± 0.15	0.18 ± 0.03	0.14 ± 0.09	0.01 ± 0.01
OTU681	*Bacteria; Proteobacteria; Gammaproteobacteria; KI89A clade; unknown family; unknown genus*	0	0	0.02 ± 0.01	0.14 ± 0.1	0.26 ± 0.23	0.08 ± 0.04	0.01 ± 0.01	0.02 ± 0.02
OTU685	*Bacteria; Bacteroidetes; Bacteroidia; Chitinophagales; Saprospiraceae; unknown genus*	0	0	0	0	0	0.01 ± 0.01	0.37 ± 0.36	0.11 ± 0.1
OTU696	*Bacteria; Bacteroidetes; Bacteroidia; Flavobacteriales; Flavobacteriaceae; Maribacter*	0	0	0.03 ± 0.02	0.03 ± 0.04	0.12 ± 0.12	0.11 ± 0.1	0.12 ± 0.02	0.13 ± 0.12
OTU702	*Bacteria; Proteobacteria; Alphaproteobacteria; Caulobacterales; Parvularculaceae; unknown genus*	0	0	0	0	0.01 ± 0.01	0.17 ± 0.14	0.13 ± 0.1	0.22 ± 0.21
OTU705	*Bacteria; Proteobacteria; Deltaproteobacteria; NB1-j; unknown family; unknown genus*	0	0	0	0.02 ± 0.03	0.07 ± 0.05	0.17 ± 0.08	0.18 ± 0.05	0.07 ± 0.04
OTU710	*Bacteria; Bacteroidetes; Bacteroidia; Flavobacteriales; Flavobacteriaceae; Aquimarina*	0	0.01 ± 0.01	0	0	0.02 ± 0.01	0.06 ± 0.05	0.17 ± 0.08	0.27 ± 0.21
OTU737	*Bacteria; Proteobacteria; Alphaproteobacteria; Rickettsiales; SM2D12; unknown genus*	0	0	0	0.13 ± 0.13	0.21 ± 0.12	0.12 ± 0.11	0.01 ± 0.01	0.01 ± 0.01
OTU748	*Bacteria; Proteobacteria; Alphaproteobacteria; Sphingomonadales; Sphingomonadaceae; Altererythrobacter*	0	0	0	0.01 ± 0.02	0.02 ± 0.02	0.05 ± 0.04	0.16 ± 0.07	0.21 ± 0.11
OTU758	*Bacteria; Proteobacteria; Alphaproteobacteria; Micavibrionales; Micavibrionaceae; unknown genus*	0	0.12 ± 0.06	0.03 ± 0.01	0.06 ± 0.05	0.03 ± 0.02	0.12 ± 0.07	0.05 ± 0.08	0.02 ± 0.01
OTU772	*Bacteria; Proteobacteria; Alphaproteobacteria; Micavibrionales; unknown family; unknown genus*	0	0.01 ± 0.01	0.08 ± 0.07	0.23 ± 0.17	0.02 ± 0.03	0	0	0
OTU808	*Bacteria; Bacteroidetes; Bacteroidia; Chitinophagales; Saprospiraceae; unknown genus*	0	0	0	0	0.07 ± 0.02	0.02 ± 0.03	0.04 ± 0.02	0.03 ± 0.01
OTU810	*Bacteria; Proteobacteria; Gammaproteobacteria; Ectothiorhodospirales; Thioalkalispiraceae; Thiohalophilus*	0	0	0.14 ± 0.13	0.22 ± 0.15	0.1 ± 0.09	0.01	0.01 ± 0.01	0
OTU811	*Bacteria; Proteobacteria; Gammaproteobacteria; Gammaproteobacteria Incertae Sedis; unknown family; Endothiovibrio*	0	0.01	0.03 ± 0.03	0.12 ± 0.17	0.1 ± 0.06	0.18 ± 0.18	0.04 ± 0.05	0.01 ± 0
OTU832	*Bacteria; Proteobacteria; Alphaproteobacteria; Rhizobiales; Rhizobiaceae; Pseudahrensia*	0	0	0	0.01 ± 0.01	0.3 ± 0.15	0.18 ± 0.19	0	0
OTU850	*Bacteria; Epsilonbacteraeota; Campylobacteria; Campylobacterales; Arcobacteraceae; Arcobacter*	0	0.02 ± 0.01	0.03 ± 0.04	0.03 ± 0.01	0	0	0	0
OTU882	*Bacteria; Proteobacteria; Gammaproteobacteria; Cellvibrionales; Cellvibrionaceae; unknown genus*	0	0	0	0	0	0	0.05 ± 0.08	0.38 ± 0.47
OTU886	*Bacteria; Bacteroidetes; Bacteroidia; Flavobacteriales; Flavobacteriaceae; Ulvibacter*	0	0	0	0.01 ± 0.01	0.12 ± 0.07	0.07 ± 0.07	0.09 ± 0.06	0.12 ± 0.03
OTU899	*Bacteria; Proteobacteria; Alphaproteobacteria; Micavibrionales; Micavibrionaceae; unknown genus*	0	0	0	0	0.21 ± 0.11	0.04 ± 0.02	0.09 ± 0.06	0.03 ± 0.02
OTU913	*Bacteria; Proteobacteria; Alphaproteobacteria; Caulobacterales; Hyphomonadaceae; Litorimonas*	0	0.19 ± 0.09	0.05 ± 0.06	0.02 ± 0.01	0.01	0	0	0.01
OTU915	*Bacteria; Proteobacteria; Gammaproteobacteria; Cellvibrionales; Cellvibrionaceae; unknown genus*	0	0	0	0.02 ± 0.02	0.26 ± 0.43	0.15 ± 0.02	0.05 ± 0.05	0.01 ± 0.01
OTU942	*Bacteria; Proteobacteria; Deltaproteobacteria; Bdellovibrionales; Bacteriovoracaceae; Peredibacter*	0.02 ± 0.03	0.15 ± 0.06	0.05 ± 0.01	0.05 ± 0.04	0	0.03 ± 0.02	0	0.02 ± 0.03
OTU953	*Bacteria; Proteobacteria; Alphaproteobacteria; Caulobacterales; Parvularculaceae; unknown genus*	0	0	0.04 ± 0.01	0.05 ± 0.02	0.02 ± 0.02	0.07 ± 0.04	0.04 ± 0.01	0.1 ± 0.09
OTU972	*Bacteria; Bacteroidetes; Bacteroidia; Chitinophagales; Saprospiraceae; unknown genus*	0	0	0.01 ± 0.01	0	0.21 ± 0.17	0.15 ± 0.2	0.06 ± 0.04	0.1 ± 0.05
OTU992	*Bacteria; Bacteroidetes; Bacteroidia; Chitinophagales; Saprospiraceae; unknown genus*	0	0	0	0	0.01 ± 0	0.05 ± 0.08	0.1 ± 0.09	0.14 ± 0.16
OTU994	*Bacteria; Proteobacteria; Deltaproteobacteria; Myxococcales; Nannocystaceae; unknown genus*	0	0	0	0.01	0.08 ± 0.08	0.01 ± 0.01	0.06 ± 0.02	0.02 ± 0.02
OTU1006	*Bacteria; Proteobacteria; Gammaproteobacteria; Alteromonadales; Colwelliaceae; Colwellia*	0	0.26 ± 0.21	0.07 ± 0.07	0	0	0	0	0
OTU1024	*Bacteria; Actinobacteria; Acidimicrobiia; Microtrichales; Microtrichaceae; Sva0996 marine group*	0	0	0	0.01 ± 0.01	0.03 ± 0.04	0.01 ± 0.01	0.17 ± 0.13	0.05 ± 0.04
OTU1038	*Bacteria; Proteobacteria; Deltaproteobacteria; NB1-j; unknown family; unknown genus*	0	0	0	0	0.03 ± 0.02	0.08 ± 0.04	0.08 ± 0.06	0.14 ± 0.07
OTU1047	*Bacteria; Actinobacteria; Acidimicrobiia; Microtrichales; Microtrichaceae; Sva0996 marine group*	0	0	0	0	0.01 ± 0	0.02 ± 0.02	0.14 ± 0.09	0.12 ± 0.06
OTU1050	*Bacteria; Bacteroidetes; Bacteroidia; Chitinophagales; Saprospiraceae; unknown genus*	0	0	0	0	0	0.01 ± 0.01	0.17 ± 0.09	0.12 ± 0.02
OTU1051	*Bacteria; Bacteroidetes; Bacteroidia; Flavobacteriales; Schleiferiaceae; Schleiferia*	0	0	0	0	0.06 ± 0.04	0.11 ± 0.07	0.13 ± 0.14	0.03 ± 0.04
OTU1094	*Bacteria; Bacteroidetes; Bacteroidia; Flavobacteriales; Flavobacteriaceae; Ulvibacter*	0	0	0	0	0.07 ± 0.02	0.01 ± 0.01	0.11 ± 0.1	0.12 ± 0.01
OTU1101	*Bacteria; Proteobacteria; Gammaproteobacteria; Alteromonadales; Alteromonadaceae; Paraglaciecola*	0	0.09 ± 0.13	0.12 ± 0.1	0.34 ± 0.37	0.05 ± 0.08	0.03 ± 0.05	0	0.01
OTU1117	*Bacteria; Proteobacteria; Alphaproteobacteria; Micavibrionales; unknown family; unknown genus*	0	0	0	0	0.14 ± 0.02	0.11 ± 0.07	0.05 ± 0.03	0.02 ± 0.02
OTU1118	*Bacteria; Bacteroidetes; Bacteroidia; Chitinophagales; Saprospiraceae; Lewinella*	0	0	0	0	0	0	0.14 ± 0.03	0.15 ± 0.15
OTU1122	*Bacteria; Bacteroidetes; Bacteroidia; Chitinophagales; Saprospiraceae; unknown genus*	0	0	0	0	0	0.04 ± 0.06	0.09 ± 0.09	0.17 ± 0.22
OTU1165	*Bacteria; Bacteroidetes; Bacteroidia; Flavobacteriales; NS9 marine group; unknown genus*	0	0	0	0.01	0.07 ± 0.04	0.06 ± 0.01	0.08 ± 0.04	0.09 ± 0.02
OTU1171	*Bacteria; Proteobacteria; Alphaproteobacteria; Sphingomonadales; Sphingomonadaceae; Erythrobacter*	0	0.06 ± 0.03	0.01 ± 0.01	0.04 ± 0.02	0.07 ± 0.05	0.05 ± 0.07	0.03 ± 0.02	0.02 ± 0.01
OTU1196	*Bacteria; Bacteroidetes; Bacteroidia; Chitinophagales; Saprospiraceae; unknown genus*	0	0	0	0	0	0	0.21 ± 0.12	0.1 ± 0.07
OTU1239	*Bacteria; Proteobacteria; Deltaproteobacteria; NB1-j; unknown family; unknown genus*	0	0	0	0	0.04 ± 0.04	0.04 ± 0.03	0.13 ± 0.05	0.04 ± 0.03
OTU1241	*Bacteria; Proteobacteria; Deltaproteobacteria; NB1-j; unknown family; unknown genus*	0	0	0	0.01 ± 0.02	0.07 ± 0.04	0.06 ± 0.05	0.12 ± 0.09	0.05 ± 0.02
OTU1319	*Bacteria; Bacteroidetes; Bacteroidia; Flavobacteriales; Flavobacteriaceae; Maribacter*	0	0	0	0.02 ± 0.04	0	0.02 ± 0.01	0.09 ± 0.09	0.11 ± 0.11
OTU1345	*Bacteria; Proteobacteria; Gammaproteobacteria; Arenicellales; Arenicellaceae; Arenicella*	0	0	0	0.01 ± 0.01	0.05 ± 0.05	0.03 ± 0.02	0.01 ± 0.01	0.15 ± 0.11
OTU1364	*Bacteria; Bacteroidetes; Bacteroidia; Chitinophagales; Saprospiraceae; unknown genus*	0	0	0	0	0	0	0.15 ± 0.22	0.09 ± 0.03
OTU1365	*Bacteria; Proteobacteria; Gammaproteobacteria; Pseudomonadales; Moraxellaceae; Psychrobacter*	0	0	0	0.04 ± 0.02	0.14 ± 0.06	0.02 ± 0.03	0.01 ± 0.01	0
OTU1381	*Bacteria; Proteobacteria; Deltaproteobacteria; Bdellovibrionales; Bacteriovoracaceae; Peredibacter*	0	0	0	0	0.14 ± 0.07	0.07 ± 0.03	0.01 ± 0.01	0.02 ± 0.01
OTU1406	*Bacteria; Proteobacteria; Gammaproteobacteria; Thiohalorhabdales; Thiohalorhabdaceae; Granulosicoccus*	0	0	0	0	0.04 ± 0.05	0.1 ± 0.07	0.06 ± 0.04	0.02 ± 0.02
OTU1411	*Bacteria; Bacteroidetes; Bacteroidia; Chitinophagales; Saprospiraceae; unknown genus*	0	0	0	0	0	0	0.13 ± 0.05	0.07 ± 0.06
OTU1434	*Bacteria; Bacteroidetes; Bacteroidia; Flavobacteriales; Flavobacteriaceae; Maribacter*	0	0.07 ± 0.04	0.06 ± 0.04	0.07 ± 0.09	0.08 ± 0.13	0	0	0
OTU1486	*Bacteria; Proteobacteria; Alphaproteobacteria; Caulobacterales; Hyphomonadaceae; unknown genus*	0	0.1 ± 0.04	0.13 ± 0.02	0.05 ± 0.03	0.01 ± 0	0.01 ± 0	0.01 ± 0.01	0.01 ± 0.01
OTU1509	*Bacteria; Proteobacteria; Alphaproteobacteria; Rhizobiales; Devosiaceae; unknown genus*	0	0	0	0	0.22 ± 0.16	0.03 ± 0.02	0.02 ± 0.04	0
OTU1547	*Bacteria; Proteobacteria; Alphaproteobacteria; unknown order; unknown family; unknown genus*	0	0	0	0	0.06 ± 0.05	0.06 ± 0.06	0.03 ± 0.03	0.08 ± 0.06
OTU1549	*Bacteria; Bacteroidetes; Bacteroidia; Chitinophagales; Saprospiraceae; unknown genus*	0	0	0	0	0.01	0.02 ± 0.03	0.13 ± 0.11	0.16 ± 0.04
OTU1747	*Bacteria; Proteobacteria; Gammaproteobacteria; Oceanospirillales; Marinomonadaceae; Marinomonas*	0	0.1 ± 0.1	0.05 ± 0.02	0.13 ± 0.18	0	0	0	0
OTU1874	*Bacteria; Proteobacteria; Alphaproteobacteria; Rickettsiales; SM2D12; unknown genus*	0	0	0	0	0	0.09 ± 0.03	0.01 ± 0	0.04 ± 0.05
OTU1904	*Bacteria; Planctomycetes; Planctomycetacia; Pirellulales; Pirellulaceae; Blastopirellula*	0.07 ± 0.03	0.06 ± 0.06	0.02 ± 0.01	0.01 ± 0.01	0	0	0	0
OTU1985	*Bacteria; Proteobacteria; Alphaproteobacteria; Micavibrionales; Micavibrionaceae; unknown genus*	0	0	0	0	0.01 ± 0.02	0.1 ± 0.09	0.01 ± 0	0.02 ± 0.02
OTU2091	*Marinicella*	0	0.01	0	0.01	0.01	0.03 ± 0.01	0.03 ± 0.02	0.11 ± 0.06
OTU2175	*Bacteria; Planctomycetes; Planctomycetacia; Pirellulales; Pirellulaceae; Blastopirellula*	0	0	0	0.01 ± 0.01	0.03 ± 0	0.1 ± 0.05	0.02 ± 0	0.04 ± 0.01
OTU2186	*Bacteria; Proteobacteria; Alphaproteobacteria; Caulobacterales; Hyphomonadaceae; Hellea*	0.01 ± 0	0	0.03 ± 0.01	0.03 ± 0.01	0.02 ± 0.01	0.03 ± 0.01	0.02 ± 0.01	0.02 ± 0.01
OTU2203	*Bacteria; Bacteroidetes; Bacteroidia; Chitinophagales; Saprospiraceae; Portibacter*	0	0	0	0	0.02 ± 0.02	0.05 ± 0.02	0.03 ± 0.01	0.01 ± 0.01
OTU2242	*Bacteria; Proteobacteria; Alphaproteobacteria; Sphingomonadales; Sphingomonadaceae; Altererythrobacter*	0	0	0.06 ± 0.01	0.05 ± 0.02	0.02 ± 0.01	0	0	0.01 ± 0.01
OTU2269	*Bacteria; Proteobacteria; Gammaproteobacteria; Cellvibrionales; Spongiibacteraceae; Oceanicoccus*	0	0	0.1 ± 0.07	0.03 ± 0.04	0	0	0	0
OTU2306	*Bacteria; Proteobacteria; Alphaproteobacteria; Caulobacterales; Hyphomonadaceae; Fretibacter*	0	0.06 ± 0.05	0.05 ± 0.01	0.05 ± 0.04	0.02 ± 0.01	0.03 ± 0.01	0.02 ± 0	0.02 ± 0.01
OTU2563	*Bacteria; Planctomycetes; Planctomycetacia; Pirellulales; Pirellulaceae; Blastopirellula*	0	0	0	0	0.01 ± 0	0.05 ± 0.03	0.02 ± 0.01	0.01 ± 0.01
OTU2638	*Bacteria; Proteobacteria; Alphaproteobacteria; Caulobacterales; Hyphomonadaceae; Hellea*	0	0.01 ± 0.01	0.01 ± 0.01	0.07 ± 0.01	0	0	0.02 ± 0.02	0.02 ± 0.01
OTU2706	*Bacteria; Planctomycetes; Planctomycetacia; Pirellulales; Pirellulaceae; Blastopirellula*	0	0	0	0	0	0.05 ± 0.02	0.03 ± 0.02	0.07 ± 0.02
OTU2716	*Bacteria; Proteobacteria; Gammaproteobacteria; Oceanospirillales; Kangiellaceae; Aliikangiella*	0	0	0	0	0.02 ± 0.04	0.04 ± 0	0.04 ± 0.01	0.02 ± 0.02
OTU2727	*Bacteria; Proteobacteria; Alphaproteobacteria; unknown order; unknown family; unknown genus*	0	0	0	0	0.01 ± 0.01	0.02 ± 0.02	0.02 ± 0.01	0.08 ± 0.05
OTU2762	*Bacteria; Proteobacteria; Alphaproteobacteria; Caulobacterales; Hyphomonadaceae; Hellea*	0	0	0.02 ± 0.01	0.04 ± 0.02	0.01 ± 0.01	0.01 ± 0	0	0.02 ± 0.01

OTU3182	*Bacteria; Bacteroidetes; Bacteroidia; Chitinophagales; Saprospiraceae; unknown genus*	0	0	0	0	0.1 ± 0.12	0.03 ± 0.03	0.01 ± 0.01	0.03 ± 0.02
OTU3229	*Bacteria; Proteobacteria; Alphaproteobacteria; Caulobacterales; Hyphomonadaceae; Fretibacter*	0	0.06 ± 0.04	0.05 ± 0.02	0.04 ± 0.01	0.02 ± 0.01	0.03 ± 0.01	0.02 ± 0.01	0.02 ± 0.01
OTU3276	*Bacteria; Planctomycetes; OM190; unknown order; unknown family; unknown genus*	0	0	0	0	0.03 ± 0.01	0.03 ± 0.01	0.02 ± 0.01	0.01 ± 0.01
OTU3305	*Bacteria; Proteobacteria; Alphaproteobacteria; Rhizobiales; Rhizobiaceae; unknown genus*	0	0.15 ± 0.09	0.2 ± 0.05	0.12 ± 0.04	0.06 ± 0.05	0.01 ± 0.01	0.01 ± 0.01	0
OTU3426	*Bacteria; Proteobacteria; Alphaproteobacteria; Caulobacterales; Hyphomonadaceae; unknown genus*	0	0.02 ± 0.01	0.04 ± 0	0.01 ± 0.01	0.01 ± 0.01	0.01 ± 0	0	0
OTU3435	*Bacteria; Proteobacteria; Gammaproteobacteria; Thiohalorhabdales; Thiohalorhabdaceae; Granulosicoccus*	0.13 ± 0.02	0.02 ± 0.02	0	0	0	0	0	0
OTU3490	*Bacteria; Actinobacteria; Acidimicrobiia; Microtrichales; Microtrichaceae; Sva0996 marine group*	0	0	0	0	0.05 ± 0.01	0.05 ± 0.01	0.09 ± 0.01	0.05 ± 0.02
OTU3532	*Bacteria; Proteobacteria; Alphaproteobacteria; Rhizobiales; Rhizobiaceae; unknown genus*	0	0.07 ± 0.04	0.08 ± 0	0.09 ± 0.06	0.05 ± 0.04	0.04 ± 0.04	0.02 ± 0.03	0
OTU3729	*Bacteria; Proteobacteria; Gammaproteobacteria; Thiohalorhabdales; Thiohalorhabdaceae; Granulosicoccus*	0.2 ± 0.03	0.04 ± 0.05	0.01 ± 0	0	0	0	0	0
OTU3801	*Bacteria; Proteobacteria; Gammaproteobacteria; Thiohalorhabdales; Thiohalorhabdaceae; Granulosicoccus*	0.28 ± 0.01	0.04 ± 0.04	0.01 ± 0	0	0	0.01 ± 0.01	0	0
OTU3839	*Bacteria; Actinobacteria; Acidimicrobiia; Microtrichales; Microtrichaceae; Sva0996 marine group*	0	0	0	0	0.01 ± 0	0.01 ± 0.01	0.04 ± 0	0.01 ± 0
OTU3849	*Bacteria; Actinobacteria; Acidimicrobiia; Microtrichales; Microtrichaceae; Sva0996 marine group*	0	0	0	0	0.04 ± 0.02	0.05 ± 0.03	0.09 ± 0.03	0.05 ± 0.02
OTU4106	*Bacteria; Proteobacteria; Gammaproteobacteria; Ectothiorhodospirales; Ectothiorhodospiraceae; unknown genus*	0	0.1 ± 0.08	0.1 ± 0.03	0.02 ± 0.01	0	0	0	0
OTU4487	*Bacteria; Actinobacteria; Acidimicrobiia; Microtrichales; Microtrichaceae; Sva0996 marine group*	0	0	0	0	0.01 ± 0	0.02 ± 0.01	0.04 ± 0.01	0.02 ± 0.01
OTU4568	*Bacteria; Proteobacteria; Deltaproteobacteria; NB1-j; unknown family; unknown genus*	0	0	0	0	0.03 ± 0.03	0.01 ± 0.01	0.02 ± 0.02	0
OTU4789	*Bacteria; Proteobacteria; Alphaproteobacteria; Rhizobiales; Rhizobiaceae; unknown genus*	0	0.02 ± 0.02	0.03 ± 0.01	0.03 ± 0.01	0.02 ± 0.01	0.01 ± 0	0.01 ± 0.01	0
OTU4921	*Bacteria; Proteobacteria; Alphaproteobacteria; unknown order; unknown family; unknown genus*	0	0	0	0	0	0	0.01 ± 0	0.04 ± 0.03
OTU5061	*Bacteria; Actinobacteria; Acidimicrobiia; Microtrichales; Microtrichaceae; Sva0996 marine group*	0	0	0	0	0.03 ± 0.02	0.04 ± 0.01	0.05 ± 0.02	0.03 ± 0.01
OTU5246	*Bacteria; Proteobacteria; Alphaproteobacteria; Rhodobacterales; Rhodobacteraceae; Octadecabacter*	0	0.13 ± 0.05	0.01 ± 0.01	0.01 ± 0.01	0	0	0	0
OTU5411	*Bacteria; Actinobacteria; Acidimicrobiia; Microtrichales; Microtrichaceae; Sva0996 marine group*	0	0	0	0	0.01	0.01 ± 0	0.02 ± 0	0.01 ± 0.01
OTU5477	*Bacteria; Proteobacteria; Gammaproteobacteria; Ectothiorhodospirales; Ectothiorhodospiraceae; unknown genus*	0	0.04 ± 0.04	0.03 ± 0.01	0.01 ± 0.01	0	0	0	0
OTU5822	*Bacteria; Proteobacteria; Gammaproteobacteria; Ectothiorhodospirales; Ectothiorhodospiraceae; unknown genus*	0	0.03 ± 0.03	0.04 ± 0.01	0.01 ± 0.01	0	0	0	0
OTU5839	*Bacteria; Proteobacteria; Gammaproteobacteria; Thiohalorhabdales; Thiohalorhabdaceae; Granulosicoccus*	0.13 ± 0.04	0.04 ± 0.04	0	0	0	0	0	0
OTU5884	*Bacteria; Actinobacteria; Acidimicrobiia; Microtrichales; Microtrichaceae; Sva0996 marine group*	0	0	0	0	0.08 ± 0.06	0.07 ± 0.02	0.08 ± 0.02	0.05 ± 0.03
OTU5945	*Bacteria; Proteobacteria; Alphaproteobacteria; Rhizobiales; Rhizobiaceae; unknown genus*	0	0.05 ± 0.03	0.06 ± 0.02	0.03 ± 0	0.01 ± 0.01	0	0	0
OTU6077	*Bacteria; Proteobacteria; Alphaproteobacteria; Caulobacterales; Hyphomonadaceae; Fretibacter*	0	0.03 ± 0.03	0.03 ± 0	0.03 ± 0.03	0.02 ± 0.02	0.03 ± 0	0.01 ± 0.01	0.01 ± 0
OTU6162	*Bacteria; Proteobacteria; Gammaproteobacteria; Ectothiorhodospirales; Ectothiorhodospiraceae; unknown genus*	0	0.03 ± 0.02	0.03 ± 0.01	0.01 ± 0.01	0	0	0	0
OTU6659	*Bacteria; Proteobacteria; Gammaproteobacteria; Ectothiorhodospirales; Ectothiorhodospiraceae; unknown genus*	0	0.05 ± 0.05	0.04 ± 0.02	0.01 ± 0.01	0	0	0	0
OTU6938	*Bacteria; Actinobacteria; Acidimicrobiia; Microtrichales; Microtrichaceae; Sva0996 marine group*	0	0	0	0	0.07 ± 0.02	0.05 ± 0.01	0.09 ± 0.03	0.06 ± 0.02
OTU7314	*Bacteria; Proteobacteria; Alphaproteobacteria; Rhizobiales; Rhizobiaceae; unknown genus*	0	0.07 ± 0.05	0.11 ± 0.04	0.08 ± 0.03	0.03 ± 0.02	0.01 ± 0.01	0	0
OTU7447	*Bacteria; Proteobacteria; Alphaproteobacteria; Caulobacterales; Hyphomonadaceae; Litorimonas*	0.04 ± 0.01	0.01 ± 0	0	0	0	0.02 ± 0.01	0.01 ± 0.01	0.01 ± 0.01
OTU7547	*Bacteria; Actinobacteria; Acidimicrobiia; Microtrichales; Microtrichaceae; Sva0996 marine group*	0	0	0	0	0.01 ± 0.01	0.02 ± 0.01	0.03 ± 0	0.01 ± 0.01
OTU7719	*Bacteria; Proteobacteria; Alphaproteobacteria; Rhizobiales; Rhizobiaceae; Ahrensia*	0	0.02 ± 0.01	0.02 ± 0.01	0.02 ± 0.01	0.01 ± 0.01	0.01 ± 0.01	0.01	0
OTU7859	*Bacteria; Actinobacteria; Acidimicrobiia; Microtrichales; Microtrichaceae; Sva0996 marine group*	0	0	0	0	0.06 ± 0.06	0.04 ± 0.02	0.03 ± 0.02	0.02 ± 0.02
OTU8100	*Bacteria; Actinobacteria; Acidimicrobiia; Microtrichales; Microtrichaceae; Sva0996 marine group*	0	0	0	0	0.01 ± 0.01	0.01 ± 0	0.02 ± 0	0.01 ± 0.01
OTU9042	*Bacteria; Proteobacteria; Alphaproteobacteria; Caulobacterales; Hyphomonadaceae; Litorimonas*	0.05 ± 0.01	0.01 ± 0	0	0	0.01 ± 0.01	0.03 ± 0.02	0.02 ± 0	0.01 ± 0
OTU9573	*Bacteria; Actinobacteria; Acidimicrobiia; Microtrichales; Microtrichaceae; Sva0996 marine group*	0	0	0	0	0.01 ± 0.01	0.01 ± 0	0.03 ± 0.01	0.01 ± 0.01
OTU9972	*Bacteria; Proteobacteria; Gammaproteobacteria; Ectothiorhodospirales; Ectothiorhodospiraceae; unknown genus*	0	0.02 ± 0.02	0.03 ± 0.02	0.01 ± 0	0	0	0	0
OTU10001	*Bacteria; Proteobacteria; Alphaproteobacteria; Rhizobiales; Rhizobiaceae; Roseitalea*	0	0.03 ± 0.02	0.06 ± 0.02	0.03 ± 0.01	0.02 ± 0	0	0	0
OTU10178	*Bacteria; Proteobacteria; Gammaproteobacteria; Ectothiorhodospirales; Thioalkalispiraceae; Thiohalophilus*	0	0	0.01 ± 0	0.01 ± 0	0.02 ± 0.01	0.06 ± 0.02	0.05 ± 0.04	0.02 ± 0.02
OTU10257	*Bacteria; Proteobacteria; Alphaproteobacteria; Caulobacterales; Hyphomonadaceae; unknown genus*	0	0.02 ± 0.01	0.04 ± 0.01	0.01 ± 0.01	0	0	0	0
OTU10320	*Bacteria; Proteobacteria; Alphaproteobacteria; Sphingomonadales; Sphingomonadaceae; Altererythrobacter*	0	0	0.04 ± 0	0.02 ± 0.01	0.01 ± 0	0	0	0.01 ± 0.01
OTU10623	*Bacteria; Proteobacteria; Gammaproteobacteria; KI89A clade; unknown family; unknown genus*	0	0	0	0	0.01 ± 0	0.01 ± 0	0.01 ± 0	0.02 ± 0.01
OTU10957	*Bacteria; Proteobacteria; Gammaproteobacteria; Ectothiorhodospirales; Ectothiorhodospiraceae; unknown genus*	0	0.02 ± 0.02	0.02 ± 0	0.01 ± 0	0	0	0	0
OTU11098	*Bacteria; Proteobacteria; Alphaproteobacteria; Caulobacterales; Hyphomonadaceae; Litorimonas*	0.04 ± 0	0.01 ± 0	0.01 ± 0.01	0.01 ± 0	0	0	0	0
OTU11570	*Bacteria; Proteobacteria; Alphaproteobacteria; Caulobacterales; Hyphomonadaceae; unknown genus*	0	0.03 ± 0.01	0.04 ± 0.01	0.01 ± 0.01	0.01 ± 0.01	0.01 ± 0	0	0
OTU11777	*Bacteria; Actinobacteria; Acidimicrobiia; Microtrichales; Microtrichaceae; Sva0996 marine group*	0	0	0	0	0.03 ± 0.01	0.05 ± 0.01	0.06 ± 0.02	0.03 ± 0
OTU11975	*Bacteria; Proteobacteria; Gammaproteobacteria; Alteromonadales; Colwelliaceae; Colwellia*	0	0.01 ± 0	0.01 ± 0.01	0.03 ± 0.02	0	0	0	0
OTU12698	*Bacteria; Actinobacteria; Acidimicrobiia; Microtrichales; Microtrichaceae; Sva0996 marine group*	0	0	0	0	0.01 ± 0.01	0.02 ± 0.01	0.03 ± 0.01	0.01 ± 0.01
OTU12868	*Bacteria; Actinobacteria; Acidimicrobiia; Microtrichales; Microtrichaceae; Sva0996 marine group*	0	0	0	0	0.03 ± 0.02	0.01 ± 0.01	0.02 ± 0.01	0.01 ± 0
OTU12957	*Bacteria; Proteobacteria; Alphaproteobacteria; Rhizobiales; Rhizobiaceae; unknown genus*	0	0.03 ± 0.02	0.03 ± 0	0.02 ± 0.01	0.01 ± 0	0	0	0
OTU13709	*Bacteria; Actinobacteria; Acidimicrobiia; Microtrichales; Microtrichaceae; Sva0996 marine group*	0	0	0	0	0.04 ± 0.04	0.05 ± 0.02	0.08 ± 0.02	0.05 ± 0.01
OTU14039	*Bacteria; Proteobacteria; Gammaproteobacteria; Ectothiorhodospirales; Ectothiorhodospiraceae; unknown genus*	0	0.01 ± 0.01	0.01 ± 0.01	0.01 ± 0.01	0	0	0	0
OTU18606	*Bacteria; Actinobacteria; Acidimicrobiia; Microtrichales; Microtrichaceae; Sva0996 marine group*	0	0	0	0	0.01 ± 0.01	0.01 ± 0.01	0.03 ± 0.01	0.02 ± 0.01
OTU20851	*Bacteria; Proteobacteria; Alphaproteobacteria; Caulobacterales; Hyphomonadaceae; Fretibacter*	0	0.02 ± 0.01	0.01 ± 0	0.01 ± 0.01	0	0.01 ± 0	0.01 ± 0	0.01 ± 0.01
OTU24220	*Bacteria; Actinobacteria; Acidimicrobiia; Microtrichales; Microtrichaceae; Sva0996 marine group*	0	0	0	0	0.01 ± 0	0.01 ± 0	0.02 ± 0.01	0.02 ± 0.01
OTU31944	*Bacteria; Proteobacteria; Alphaproteobacteria; Rhizobiales; Rhizobiaceae; unknown genus*	0	0.01 ± 0.01	0.01 ± 0.01	0.01 ± 0	0	0	0	0

Supplementary table 4. Characteristics of clusters detected in the network of kelp-associated bacterial communities (Fig. 4).

Cluster rank	Score	Nodes	Edges
1	10.09	48	237
2	9.23	45	203
3	5.69	33	91
4	5.33	16	40
5	4.71	15	33
6	4.00	15	28
7	3.50	5	7
8	3.00	3	3

Supplementary table 5. Taxonomic affiliation within clusters 1 and 2 in the kelp-associated network (shown in Fig. 4).

Class	Cluster 1	Cluster 2
Acidimicrobiia	4	0
Alphaproteobacteria	20	34
Bacteroidia	5	3
Gammaproteobacteria	12	7
Deltaproteobacteria	0	1

Supplementary table 6. Associated taxonomy and relative sequence abundance ± s.d. (n = 3) of the 177 underlying sediment-associated OTUs whose relative sequence abundance vary significantly during kelp degradation (GLM, P < 0.05).

		Relative abundance (%) mean ± sd							
OTU id	**Taxonomy**	**0 week**	**2 weeks**	**4 weeks**	**6 weeks**	**11 weeks**	**15 weeks**	**20 weeks**	**24 weeks**
OTU33	*Bacteria; Proteobacteria; Alphaproteobacteria; Caulobacterales; Hyphomonadaceae; Litorimonas*	0.004 ± 0.004	0.04 ± 0.026	0.016 ± 0.008	0.033 ± 0.022	0.007 ± 0.009	0	0	0
OTU43	*Bacteria; Bacteroidetes; Bacteroidia; Flavobacteriales; Flavobacteriaceae; Lutimonas*	0.515 ± 0.158	0.975 ± 0.073	1.135 ± 0.344	1.684 ± 0.35	1.637 ± 0.321	1.589 ± 0.578	1.454 ± 0.121	1.108 ± 0.088
OTU44	*Bacteria; Proteobacteria; Deltaproteobacteria; Desulfobacterales; Desulfobulbaceae; unknown genus*	0.124 ± 0.075	0.101 ± 0.085	0.122 ± 0.055	0.628 ± 0.16	0.822 ± 0.974	1.144 ± 0.426	1.897 ± 0.879	1.202 ± 0.223
OTU47	*Bacteria; Bacteroidetes; Bacteroidia; Bacteroidales; Prolixibacteraceae; Draconibacterium*	0.048 ± 0.043	0.02 ± 0.035	0.15 ± 0.024	0.629 ± 0.294	0.645 ± 0.168	1.099 ± 0.672	0.702 ± 0.079	0.41 ± 0.106
OTU49	*Bacteria; Bacteroidetes; Bacteroidia; Flavobacteriales; Flavobacteriaceae; Lutimonas*	0.235 ± 0.062	0.531 ± 0.079	0.503 ± 0.095	0.848 ± 0.239	0.712 ± 0.3	0.716 ± 0.236	0.513 ± 0.11	0.403 ± 0.117
OTU50	*Bacteria; Bacteroidetes; Bacteroidia; Flavobacteriales; Flavobacteriaceae; Lutimonas*	0.102 ± 0.017	0.338 ± 0.017	0.387 ± 0.172	0.744 ± 0.125	0.64 ± 0.31	0.69 ± 0.19	0.564 ± 0.073	0.547 ± 0.064
OTU51	*Bacteria; Bacteroidetes; Bacteroidia; Bacteroidales; Marinifilaceae; unknown genus*	0.033 ± 0.058	0.057 ± 0.043	0.553 ± 0.121	1.796 ± 1.52	0.548 ± 0.219	0.399 ± 0.076	0.156 ± 0.047	0.273 ± 0.143
OTU66	*Bacteria; Epsilonbacteraeota; Campylobacteria; Campylobacterales; Sulfurovaceae; Sulfurovum*	0	0.03 ± 0.016	0.102 ± 0.02	0.181 ± 0.099	0.393 ± 0.295	1.034 ± 0.725	0.683 ± 0.324	1.164 ± 0.278
OTU70	*Bacteria; Proteobacteria; Deltaproteobacteria; Desulfobacterales; Desulfobulbaceae; [Desulfobacterium] catecholicum group*	0.049 ± 0.044	0.029 ± 0.01	0.136 ± 0.035	0.633 ± 0.062	0.542 ± 0.088	0.62 ± 0.138	0.512 ± 0.139	0.457 ± 0.077
OTU73	*Bacteria; Proteobacteria; Gammaproteobacteria; Cellvibrionales; Halieaceae; Halioglobus*	0.259 ± 0.069	0.633 ± 0.135	0.653 ± 0.145	0.633 ± 0.201	0.424 ± 0.032	0.321 ± 0.028	0.263 ± 0.063	0.209 ± 0.081
OTU77	*Bacteria; Bacteroidetes; Bacteroidia; Flavobacteriales; Flavobacteriaceae; Polaribacter 2*	0.011 ± 0.013	0.055 ± 0.052	0.163 ± 0.063	0.039 ± 0.015	0.01 ± 0.01	0	0.005 ± 0.006	0
OTU92	*Bacteria; Bacteroidetes; Bacteroidia; Flavobacteriales; Flavobacteriaceae; unknown genus*	0.148 ± 0.049	0.643 ± 0.682	0.373 ± 0.009	0.682 ± 0.158	0.175 ± 0.088	0.12 ± 0.04	0.082 ± 0.05	0.148 ± 0.06
OTU96	*Bacteria; Bacteroidetes; Bacteroidia; Bacteroidales; Prolixibacteraceae; Draconibacterium*	0.011 ± 0.013	0.016 ± 0.016	0.06 ± 0.007	0.51 ± 0.147	0.46 ± 0.138	0.693 ± 0.239	0.42 ± 0.143	0.321 ± 0.137
OTU101	*Bacteria; Bacteroidetes; Bacteroidia; Flavobacteriales; Flavobacteriaceae; Bizionia*	0.392 ± 0.139	0.609 ± 0.268	0.31 ± 0.11	0.351 ± 0.116	0.191 ± 0.021	0.145 ± 0.04	0.131 ± 0.053	0.095 ± 0.034
OTU103	*Bacteria; Bacteroidetes; Bacteroidia; Flavobacteriales; Flavobacteriaceae; Lutibacter*	0.007 ± 0.012	0.119 ± 0.12	0.532 ± 0.275	0.829 ± 0.348	0.142 ± 0.114	0.103 ± 0.03	0.195 ± 0.253	0.525 ± 0.113
OTU104	*Bacteria; Proteobacteria; Gammaproteobacteria; AT-s2-59; unknown family; unknown genus*	0.532 ± 0.082	0.275 ± 0.121	0.177 ± 0.036	0.099 ± 0.049	0.166 ± 0.064	0.064 ± 0.036	0.122 ± 0.033	0.125 ± 0.042
OTU112	*Bacteria; Epsilonbacteraeota; Campylobacteria; Campylobacterales; Arcobacteraceae; Arcobacter*	0	0.007 ± 0.013	0.683 ± 0.374	1.127 ± 0.453	0.567 ± 0.894	0.042 ± 0.015	0.034 ± 0.03	0.042 ± 0.015
OTU120	*Bacteria; Bacteroidetes; Bacteroidia; Flavobacteriales; Flavobacteriaceae; Aquibacter*	0.32 ± 0.053	0.269 ± 0.032	0.157 ± 0.069	0.105 ± 0.053	0.094 ± 0.057	0.031 ± 0.014	0.085 ± 0.022	0.07 ± 0.042
OTU121	*Bacteria; Bacteroidetes; Bacteroidia; Flavobacteriales; Flavobacteriaceae; Lutimonas*	0.019 ± 0.008	0.064 ± 0.039	0.116 ± 0.044	0.295 ± 0.067	0.242 ± 0.109	0.386 ± 0.121	0.348 ± 0.14	0.394 ± 0.071
OTU135	*Bacteria; Bacteroidetes; Bacteroidia; Flavobacteriales; Flavobacteriaceae; unknown genus*	0.101 ± 0.059	0.398 ± 0.254	0.409 ± 0.043	0.73 ± 0.212	0.166 ± 0.058	0.039 ± 0.027	0.015 ± 0.008	0.003 ± 0.004
OTU146	*Bacteria; Bacteroidetes; Bacteroidia; Flavobacteriales; Flavobacteriaceae; Lutibacter*	0.015 ± 0.02	0.039 ± 0.019	0.464 ± 0.286	0.842 ± 0.243	0.339 ± 0.404	0.228 ± 0.132	0.034 ± 0.024	0.035 ± 0.014
OTU153	*Bacteria; Proteobacteria; Gammaproteobacteria; Cellvibrionales; Halieaceae; Halioglobus*	0.18 ± 0.009	0.194 ± 0.018	0.142 ± 0.022	0.234 ± 0.023	0.29 ± 0.127	0.329 ± 0.045	0.304 ± 0.04	0.247 ± 0.052
OTU156	*Bacteria; Proteobacteria; Deltaproteobacteria; Desulfobacterales; Desulfobulbaceae; Desulforhopalus*	0.003 ± 0.005	0.02 ± 0.025	0.493 ± 0.286	0.62 ± 0.247	0.221 ± 0.129	0.325 ± 0.019	0.096 ± 0.013	0.236 ± 0.1
OTU158	*Bacteria; Bacteroidetes; Bacteroidia; Flavobacteriales; Cryomorphaceae; unknown genus*	0.11 ± 0.018	0.248 ± 0.09	0.237 ± 0.085	0.281 ± 0.058	0.204 ± 0.124	0.113 ± 0.037	0.076 ± 0.041	0.04 ± 0.015
OTU167	*Bacteria; Bacteroidetes; Bacteroidia; Flavobacteriales; Flavobacteriaceae; Psychroserpens*	0.002 ± 0.004	0.151 ± 0.065	0.179 ± 0.032	0.288 ± 0.184	0.189 ± 0.046	0.139 ± 0.081	0.048 ± 0.027	0.029 ± 0.02
OTU169	*Bacteria; Bacteroidetes; Bacteroidia; Bacteroidales; Bacteroidetes BD2-2; unknown genus*	0	0	0.82 ± 0.577	0.79 ± 0.183	0.006 ± 0.007	0.003 ± 0.005	0	0
OTU187	*Bacteria; Proteobacteria; Gammaproteobacteria; Cellvibrionales; Halieaceae; Halioglobus*	0.089 ± 0.025	0.082 ± 0.058	0.104 ± 0.032	0.18 ± 0.068	0.264 ± 0.102	0.376 ± 0.052	0.268 ± 0.144	0.237 ± 0.033
OTU196	*Bacteria; Bacteroidetes; Bacteroidia; Flavobacteriales; Flavobacteriaceae; Lutimonas*	0.057 ± 0.053	0.08 ± 0.073	0.126 ± 0.04	0.314 ± 0.051	0.292 ± 0.071	0.227 ± 0.114	0.211 ± 0.054	0.191 ± 0.033
OTU200	*Bacteria; Bacteroidetes; Bacteroidia; Flavobacteriales; Flavobacteriaceae; Ulvibacter*	0.229 ± 0.121	0.189 ± 0.061	0.114 ± 0.048	0.063 ± 0.027	0.043 ± 0.008	0.045 ± 0.022	0.087 ± 0.024	0.105 ± 0.022
OTU205	*Bacteria; Proteobacteria; Gammaproteobacteria; Cellvibrionales; Halieaceae; OM60(NOR5) clade*	0.098 ± 0.018	0.254 ± 0.032	0.14 ± 0.02	0.254 ± 0.063	0.293 ± 0.151	0.281 ± 0.073	0.197 ± 0.11	0.13 ± 0.05
OTU215	*Bacteria; Epsilonbacteraeota; Campylobacteria; Campylobacterales; Sulfurovaceae; Sulfurovum*	0	0.012 ± 0.014	0.012 ± 0.008	0.09 ± 0.056	0.181 ± 0.087	0.506 ± 0.347	0.213 ± 0.076	0.317 ± 0.107
OTU216	*Bacteria; Bacteroidetes; Bacteroidia; Flavobacteriales; Flavobacteriaceae; Actibacter*	0.06 ± 0.015	0.122 ± 0.051	0.083 ± 0.026	0.203 ± 0.026	0.194 ± 0.105	0.144 ± 0.068	0.159 ± 0.031	0.084 ± 0.044
OTU218	*Bacteria; Proteobacteria; Deltaproteobacteria; Desulfobacterales; Desulfobulbaceae; unknown genus*	0	0.003 ± 0.006	0.076 ± 0.041	0.228 ± 0.066	0.195 ± 0.099	0.215 ± 0.034	0.215 ± 0.114	0.192 ± 0.069
OTU242	*Bacteria; Proteobacteria; Gammaproteobacteria; Gammaproteobacteria Incertae Sedis; unknown family; unknown genus*	0.019 ± 0.011	0.066 ± 0.022	0.096 ± 0.035	0.118 ± 0.012	0.204 ± 0.141	0.221 ± 0.047	0.21 ± 0.058	0.156 ± 0.069
OTU245	*Bacteria; Proteobacteria; Alphaproteobacteria; Rhodobacterales; Rhodobacteraceae; Halocynthiibacter*	0.034 ± 0.009	0.051 ± 0.025	0.378 ± 0.15	0.301 ± 0.09	0.177 ± 0.119	0.114 ± 0.061	0.051 ± 0.035	0.016 ± 0.01
OTU246	*Bacteria; Proteobacteria; Gammaproteobacteria; Alteromonadales; Colwelliaceae; Colwellia*	0.014 ± 0.02	0.196 ± 0.069	0.378 ± 0.228	0.262 ± 0.054	0.197 ± 0.138	0.219 ± 0.196	0.048 ± 0.013	0.1 ± 0.063
OTU267	*Bacteria; Proteobacteria; Deltaproteobacteria; Desulfobacterales; Desulfobulbaceae; unknown genus*	0.013 ± 0.011	0.013 ± 0.013	0.013 ± 0.011	0.101 ± 0.029	0.173 ± 0.219	0.25 ± 0.099	0.279 ± 0.15	0.201 ± 0.079
OTU272	*Bacteria; Proteobacteria; Alphaproteobacteria; Rhodobacterales; Rhodobacteraceae; Pacificibacter*	0	0.05 ± 0.055	0.087 ± 0.051	0.026 ± 0.014	0.006 ± 0.01	0	0	0
OTU286	*Bacteria; Proteobacteria; Deltaproteobacteria; Desulfobacterales; Desulfobulbaceae; Desulfopila*	0.012 ± 0.007	0.005 ± 0.005	0.119 ± 0.067	0.347 ± 0.114	0.137 ± 0.051	0.076 ± 0.037	0.075 ± 0.018	0.06 ± 0.01
OTU287	*Bacteria; Proteobacteria; Deltaproteobacteria; Desulfobacterales; Desulfobulbaceae; Desulforhopalus*	0.001 ± 0.003	0.003 ± 0.006	0.061 ± 0.032	0.285 ± 0.067	0.231 ± 0.206	0.411 ± 0.13	0.25 ± 0.078	0.231 ± 0.03
OTU301	*Bacteria; Bacteroidetes; Bacteroidia; Bacteroidales; Prolixibacteraceae; Draconibacterium*	0.013 ± 0.013	0.002 ± 0.004	0.017 ± 0.021	0.092 ± 0.027	0.175 ± 0.125	0.202 ± 0.14	0.187 ± 0.054	0.111 ± 0.036
OTU322	*Bacteria; Bacteroidetes; Bacteroidia; Flavobacteriales; Flavobacteriaceae; Lutimonas*	0.04 ± 0.029	0.048 ± 0.021	0.083 ± 0.049	0.159 ± 0.011	0.159 ± 0.063	0.157 ± 0.019	0.091 ± 0.023	0.078 ± 0.018
OTU324	*Bacteria; Bacteroidetes; Bacteroidia; Bacteroidales; Marinifilaceae; unknown genus*	0.019 ± 0.022	0.018 ± 0.008	0.093 ± 0.052	0.228 ± 0.025	0.171 ± 0.004	0.139 ± 0.079	0.066 ± 0.022	0.096 ± 0.029
OTU330	*Bacteria; Proteobacteria; Deltaproteobacteria; Desulfobacterales; Desulfobulbaceae; [Desulfobacterium] catecholicum group*	0.012 ± 0.01	0.003 ± 0.005	0.032 ± 0.021	0.137 ± 0.054	0.135 ± 0.067	0.155 ± 0.036	0.128 ± 0.035	0.086 ± 0.022
OTU332	*Bacteria; Proteobacteria; Alphaproteobacteria; Rhodobacterales; Rhodobacteraceae; Pseudophaeobacter*	0.003 ± 0.005	0.037 ± 0.018	0.256 ± 0.244	0.247 ± 0.12	0.17 ± 0.041	0.112 ± 0.021	0.04 ± 0.007	0.031 ± 0.021
OTU334	*Bacteria; Bacteroidetes; Bacteroidia; Bacteroidales; Prolixibacteraceae; Draconibacterium*	0.006 ± 0.01	0	0.007 ± 0.007	0.09 ± 0.033	0.131 ± 0.067	0.132 ± 0.026	0.094 ± 0.03	0.094 ± 0.046
OTU335	*Bacteria; Bacteroidetes; Bacteroidia; Bacteroidales; Marinilabiliaceae; Carboxylicivirga*	0.004 ± 0.006	0.002 ± 0.003	0.025 ± 0.022	0.145 ± 0.062	0.126 ± 0.068	0.182 ± 0.1	0.111 ± 0.042	0.141 ± 0.108
OTU346	*Bacteria; Bacteroidetes; Bacteroidia; Bacteroidales; Prolixibacteraceae; Draconibacterium*	0.001 ± 0.003	0.015 ± 0.011	0.036 ± 0.027	0.087 ± 0.024	0.151 ± 0.106	0.241 ± 0.176	0.147 ± 0.012	0.094 ± 0.022
OTU354	*Bacteria; Proteobacteria; Gammaproteobacteria; Oceanospirillales; Nitrincolaceae; Neptuniibacter*	0	0.005 ± 0.006	0.284 ± 0.106	0.191 ± 0.072	0.193 ± 0.268	0.038 ± 0.026	0.085 ± 0.072	0.085 ± 0.01
OTU357	*Bacteria; Bacteroidetes; Bacteroidia; Flavobacteriales; Flavobacteriaceae; Actibacter*	0.023 ± 0.017	0.033 ± 0.012	0.048 ± 0.013	0.086 ± 0.021	0.073 ± 0.044	0.12 ± 0.015	0.094 ± 0.035	0.106 ± 0.017
OTU360	*Bacteria; Firmicutes; Clostridia; Clostridiales; Defluviitaleaceae; Defluviitaleaceae UCG-011*	0	0.006 ± 0.01	0.117 ± 0.028	0.271 ± 0.044	0.045 ± 0.06	0.073 ± 0.058	0.054 ± 0.024	0.069 ± 0.033
OTU362	*Bacteria; Bacteroidetes; Bacteroidia; Flavobacteriales; Flavobacteriaceae; unknown genus*	0.04 ± 0.025	0.224 ± 0.198	0.132 ± 0.037	0.177 ± 0.039	0.054 ± 0.032	0.048 ± 0.037	0.025 ± 0.006	0.059 ± 0.02
OTU363	*Bacteria; Bacteroidetes; Bacteroidia; Bacteroidales; Bacteroidetes BD2-2; unknown genus*	0.005 ± 0.008	0	0.085 ± 0.055	0.587 ± 0.35	0.122 ± 0.042	0.255 ± 0.193	0.108 ± 0.026	0.095 ± 0.05
OTU365	*Bacteria; Proteobacteria; Deltaproteobacteria; Desulfobacterales; Desulfobulbaceae; Desulforhopalus*	0.001 ± 0.001	0.001 ± 0.002	0.002 ± 0.003	0.085 ± 0.008	0.095 ± 0.057	0.192 ± 0.078	0.193 ± 0.049	0.139 ± 0.044
OTU369	*Bacteria; Bacteroidetes; Bacteroidia; Bacteroidales; Prolixibacteraceae; Draconibacterium*	0	0.002 ± 0.003	0.01 ± 0.008	0.05 ± 0.02	0.166 ± 0.148	0.207 ± 0.157	0.222 ± 0.018	0.142 ± 0.068
OTU370	*Bacteria; Firmicutes; Clostridia; Clostridiales; Defluviitaleaceae; Defluviitaleaceae UCG-011*	0	0.004 ± 0.007	0.255 ± 0.278	0.366 ± 0.098	0.011 ± 0.009	0.061 ± 0.085	0.018 ± 0.015	0.058 ± 0.035
OTU377	*Bacteria; Epsilonbacteraeota; Campylobacteria; Campylobacterales; Sulfurovaceae; Sulfurovum*	0.009 ± 0.015	0.126 ± 0.015	0.056 ± 0.007	0.042 ± 0.013	0.042 ± 0.032	0.088 ± 0.068	0.073 ± 0.042	0.243 ± 0.104
OTU389	*Bacteria; Bacteroidetes; Bacteroidia; Cytophagales; Cyclobacteriaceae; unknown genus*	0.002 ± 0.004	0.008 ± 0.014	0.012 ± 0.009	0.068 ± 0.041	0.159 ± 0.02	0.203 ± 0.053	0.165 ± 0.044	0.105 ± 0.062
OTU390	*Bacteria; Bacteroidetes; Bacteroidia; Bacteroidales; Bacteroidetes BD2-2; unknown genus*	0.007 ± 0.006	0.004 ± 0.007	0.006 ± 0.011	0.05 ± 0.04	0.075 ± 0.081	0.188 ± 0.125	0.247 ± 0.071	0.244 ± 0.107
OTU408	*Bacteria; Proteobacteria; Deltaproteobacteria; Desulfobacterales; Desulfobulbaceae; Desulforhopalus*	0.005 ± 0.005	0.018 ± 0.026	0.094 ± 0.028	0.165 ± 0.095	0.092 ± 0.048	0.16 ± 0.085	0.077 ± 0.018	0.175 ± 0.119
OTU415	*Bacteria; Firmicutes; Clostridia; Clostridiales; Lachnospiraceae; Vallitalea*	0	0.018 ± 0.019	0.166 ± 0.119	0.187 ± 0.08	0.02 ± 0.019	0.047 ± 0.021	0.065 ± 0.014	0.202 ± 0.024
OTU416	*Bacteria; Bacteroidetes; Bacteroidia; Flavobacteriales; Flavobacteriaceae; Lutimonas*	0.018 ± 0.009	0.023 ± 0.025	0.022 ± 0.016	0.059 ± 0.022	0.062 ± 0.033	0.076 ± 0.031	0.143 ± 0.032	0.121 ± 0.046
OTU442	*Bacteria; Epsilonbacteraeota; Campylobacteria; Campylobacterales; Arcobacteraceae; Arcobacter*	0	0.013 ± 0.008	0.341 ± 0.129	0.27 ± 0.127	0.012 ± 0.01	0.002 ± 0.002	0.004 ± 0.006	0.014 ± 0.022
OTU449	*Bacteria; Proteobacteria; Gammaproteobacteria; Vibrionales; Vibrionaceae; Vibrio*	0.006 ± 0.01	0.042 ± 0.014	0.059 ± 0.022	0.07 ± 0.027	0.242 ± 0.157	0.151 ± 0.066	0.104 ± 0.059	0.064 ± 0.03
OTU452	*Bacteria; Bacteroidetes; Bacteroidia; Flavobacteriales; Flavobacteriaceae; Lutibacter*	0	0.02 ± 0.034	0.302 ± 0.27	0.365 ± 0.158	0.019 ± 0.032	0.012 ± 0.015	0	0
OTU455	*Bacteria; Bacteroidetes; Bacteroidia; Bacteroidales; Bacteroidetes BD2-2; unknown genus*	0.002 ± 0.004	0	0.002 ± 0.003	0.023 ± 0.019	0.052 ± 0.083	0.133 ± 0.065	0.219 ± 0.027	0.12 ± 0.044
OTU456	*Bacteria; Bacteroidetes; Bacteroidia; Bacteroidales; Marinifilaceae; unknown genus*	0	0	0.048 ± 0.022	0.175 ± 0.111	0.086 ± 0.064	0.105 ± 0.022	0.053 ± 0.037	0.073 ± 0.05
OTU467	*Bacteria; Bacteroidetes; Bacteroidia; Bacteroidales; Marinifilaceae; unknown genus*	0.003 ± 0.005	0.002 ± 0.004	0.037 ± 0.019	0.085 ± 0.037	0.107 ± 0.044	0.086 ± 0.035	0.061 ± 0.042	0.06 ± 0.051
OTU475	*Bacteria; Proteobacteria; Deltaproteobacteria; Desulfobacterales; Desulfobulbaceae; Desulforhopalus*	0.007 ± 0.011	0.004 ± 0.005	0.005 ± 0.006	0.098 ± 0.047	0.089 ± 0.065	0.116 ± 0.037	0.078 ± 0.041	0.104 ± 0.063
OTU493	*Bacteria; Proteobacteria; Gammaproteobacteria; Gammaproteobacteria Incertae Sedis; unknown family; unknown genus*	0.021 ± 0.011	0.025 ± 0.016	0.017 ± 0.004	0.044 ± 0.025	0.062 ± 0.051	0.096 ± 0.036	0.149 ± 0.032	0.094 ± 0.046
OTU500	*Bacteria; Proteobacteria; Deltaproteobacteria; Desulfobacterales; Desulfobulbaceae; Desulfotalea*	0	0.009 ± 0.009	0.387 ± 0.279	0.329 ± 0.094	0.058 ± 0.027	0.008 ± 0.007	0.01 ± 0.005	0.03 ± 0.038
OTU502	*Bacteria; Bacteroidetes; Bacteroidia; Flavobacteriales; Flavobacteriaceae; unknown genus*	0	0	0.009 ± 0.004	0.045 ± 0.049	0.092 ± 0.088	0.065 ± 0.027	0.048 ± 0.032	0.047 ± 0.029
OTU506	*Bacteria; Proteobacteria; Gammaproteobacteria; AT-s2-59; unknown family; unknown genus*	0.175 ± 0.042	0.138 ± 0.046	0.049 ± 0.027	0.037 ± 0.019	0.051 ± 0.027	0.019 ± 0.019	0.029 ± 0.009	0.082 ± 0.022
OTU532	*Bacteria; Bacteroidetes; Bacteroidia; Flavobacteriales; Flavobacteriaceae; Lutibacter*	0	0.014 ± 0.012	0.611 ± 0.783	0.157 ± 0.066	0.011 ± 0.019	0.01 ± 0.009	0.003 ± 0.005	0
OTU540	*Bacteria; Bacteroidetes; Bacteroidia; Chitinophagales; Saprospiraceae; unknown genus*	0.074 ± 0.032	0.093 ± 0.018	0.034 ± 0.014	0.027 ± 0.014	0.013 ± 0.008	0.006 ± 0.002	0.028 ± 0.008	0.017 ± 0.015
OTU560	*Bacteria; Proteobacteria; Gammaproteobacteria; Alteromonadales; Colwelliaceae; Thalassomonas*	0.057 ± 0.039	0.175 ± 0.139	0.059 ± 0.008	0.04 ± 0.016	0.05 ± 0.025	0.019 ± 0.002	0.038 ± 0.027	0.003 ± 0.003
OTU561	*Bacteria; Firmicutes; Clostridia; Clostridiales; Defluviitaleaceae; Defluviitaleaceae UCG-011*	0	0.023 ± 0.031	0.323 ± 0.327	0.139 ± 0.121	0	0.022 ± 0.011	0.003 ± 0.005	0.014 ± 0.012
OTU566	*Bacteria; Proteobacteria; Gammaproteobacteria; Vibrionales; Vibrionaceae; Vibrio*	0	0.026 ± 0.005	0.045 ± 0.015	0.049 ± 0.027	0.122 ± 0.108	0.086 ± 0.038	0.069 ± 0.057	0.04 ± 0.016
OTU585	*Bacteria; Bacteroidetes; Bacteroidia; Bacteroidales; Prolixibacteraceae; Draconibacterium*	0	0.01 ± 0.01	0.022 ± 0.018	0.063 ± 0.026	0.052 ± 0.05	0.067 ± 0.007	0.095 ± 0.017	0.13 ± 0.031
OTU587	*Bacteria; Proteobacteria; Deltaproteobacteria; Desulfobacterales; Desulfobulbaceae; Desulforhopalus*	0.02 ± 0.016	0.012 ± 0.019	0.013 ± 0.002	0.094 ± 0.029	0.098 ± 0.099	0.108 ± 0.029	0.13 ± 0.07	0.135 ± 0.025
OTU603	*Bacteria; Proteobacteria; Deltaproteobacteria; Desulfobacterales; Desulfobulbaceae; unknown genus*	0.007 ± 0.006	0	0.001 ± 0.003	0.023 ± 0.004	0.05 ± 0.03	0.138 ± 0.096	0.115 ± 0.028	0.09 ± 0.051
OTU608	*Bacteria; Bacteroidetes; Bacteroidia; Flavobacteriales; Flavobacteriaceae; Aquibacter*	0.003 ± 0.005	0.032 ± 0.021	0.065 ± 0.04	0.064 ± 0.047	0.031 ± 0.021	0.016 ± 0.009	0.027 ± 0.014	0.181 ± 0.086
OTU611	*Bacteria; Bacteroidetes; Bacteroidia; Cytophagales; Cyclobacteriaceae; unknown genus*	0	0.004 ± 0.008	0.005 ± 0.006	0.061 ± 0.032	0.071 ± 0.068	0.103 ± 0.018	0.114 ± 0.054	0.078 ± 0.036
OTU612	*Bacteria; Bacteroidetes; Bacteroidia; Bacteroidales; Bacteroidetes BD2-2; unknown genus*	0	0.008 ± 0.007	0.005 ± 0.004	0.045 ± 0.028	0.092 ± 0.114	0.189 ± 0.136	0.169 ± 0.074	0.1 ± 0.037
OTU621	*Bacteria; Bacteroidetes; Bacteroidia; Flavobacteriales; Flavobacteriaceae; Polaribacter 4*	0.01 ± 0.017	0.13 ± 0.1	0.194 ± 0.126	0.144 ± 0.118	0.002 ± 0.003	0	0	0.025 ± 0.016
OTU625	*Bacteria; Proteobacteria; Gammaproteobacteria; unknown order; unknown family; unknown genus*	0.013 ± 0.005	0.031 ± 0.018	0.022 ± 0.017	0.054 ± 0.028	0.087 ± 0.072	0.08 ± 0.036	0.14 ± 0.079	0.121 ± 0.016
OTU629	*Bacteria; Proteobacteria; Gammaproteobacteria; Cellvibrionales; Halieaceae; Halioglobus*	0.041 ± 0.021	0.036 ± 0.026	0.019 ± 0.012	0.011 ± 0.006	0.058 ± 0.018	0.077 ± 0.015	0.082 ± 0.028	0.065 ± 0.032
OTU636	*Bacteria; Bacteroidetes; Bacteroidia; Bacteroidales; Bacteroidetes BD2-2; unknown genus*	0	0	0.003 ± 0.006	0.026 ± 0.01	0.029 ± 0.026	0.11 ± 0.076	0.136 ± 0.013	0.085 ± 0.016
OTU660	*Bacteria; Proteobacteria; Gammaproteobacteria; Cellvibrionales; Halieaceae; Halioglobus*	0.002 ± 0.004	0.01 ± 0.006	0.017 ± 0.023	0.031 ± 0.012	0.049 ± 0.024	0.128 ± 0.035	0.106 ± 0.057	0.071 ± 0.026
OTU670	*Bacteria; Proteobacteria; Deltaproteobacteria; Myxococcales; MidBa8; unknown genus*	0	0	0.017 ± 0.002	0.152 ± 0.049	0.082 ± 0.033	0.054 ± 0.037	0.017 ± 0.009	0.036 ± 0.031
OTU671	*Bacteria; Bacteroidetes; Bacteroidia; Flavobacteriales; Flavobacteriaceae; Algibacter*	0.005 ± 0.004	0.072 ± 0.028	0.132 ± 0.056	0.228 ± 0.076	0.108 ± 0.019	0.049 ± 0.008	0.039 ± 0.007	0.029 ± 0.005
OTU679	*Bacteria; Bacteroidetes; Bacteroidia; Flavobacteriales; Flavobacteriaceae; Maribacter*	0	0.005 ± 0.008	0.097 ± 0.02	0.119 ± 0.07	0.027 ± 0.019	0.03 ± 0.029	0	0
OTU683	*Bacteria; Bacteroidetes; Bacteroidia; Flavobacteriales; Crocinitomicaceae; Salinirepens*	0.018 ± 0.016	0.037 ± 0.021	0.183 ± 0.149	0.152 ± 0.012	0.027 ± 0.045	0	0.002 ± 0.003	0
OTU684	*Bacteria; Bacteroidetes; Bacteroidia; Bacteroidales; Bacteroidetes BD2-2; unknown genus*	0	0	0.129 ± 0.157	0.207 ± 0.099	0.01 ± 0.008	0	0.007 ± 0.01	0.032 ± 0.024
OTU706	*Bacteria; Proteobacteria; Gammaproteobacteria; Cellvibrionales; Halieaceae; Halioglobus*	0	0.01 ± 0.009	0.02 ± 0.013	0.028 ± 0.012	0.084 ± 0.047	0.082 ± 0.018	0.063 ± 0.008	0.047 ± 0.033
OTU719	*Bacteria; Bacteroidetes; Bacteroidia; Bacteroidales; Bacteroidetes BD2-2; unknown genus*	0	0.012 ± 0.021	0.003 ± 0.005	0.029 ± 0.01	0.053 ± 0.015	0.033 ± 0.014	0.068 ± 0.006	0.126 ± 0.081
OTU725	*Bacteria; Firmicutes; Clostridia; Clostridiales; Lachnospiraceae; Vallitalea*	0	0	0.117 ± 0.107	0.194 ± 0.058	0.053 ± 0.012	0.097 ± 0.064	0.039 ± 0.02	0.031 ± 0.032
OTU744	*Bacteria; Bacteroidetes; Bacteroidia; Flavobacteriales; Flavobacteriaceae; Lutibacter*	0	0.007 ± 0.011	0.259 ± 0.226	0.125 ± 0.051	0.005 ± 0.008	0.003 ± 0.006	0	0
OTU746	*Bacteria; Proteobacteria; Gammaproteobacteria; Cellvibrionales; Halieaceae; Marimicrobium*	0.004 ± 0.006	0.005 ± 0.005	0.012 ± 0.006	0.017 ± 0.006	0.056 ± 0.015	0.07 ± 0.032	0.042 ± 0.004	0.049 ± 0.02
OTU752	*Bacteria; Firmicutes; Clostridia; Clostridiales; Lachnospiraceae; Vallitalea*	0	0.003 ± 0.006	0.081 ± 0.079	0.173 ± 0.049	0.008 ± 0.008	0.034 ± 0.014	0.005 ± 0.009	0.069 ± 0.067
OTU753	*Bacteria; Firmicutes; Clostridia; Clostridiales; Ruminococcaceae; unknown genus*	0	0	0	0.034 ± 0.032	0.032 ± 0.055	0.109 ± 0.093	0.074 ± 0.043	0.121 ± 0.063
OTU761	*Bacteria; Spirochaetes; Spirochaetia; Spirochaetales; Spirochaetaceae; Spirochaeta 2*	0.004 ± 0.006	0.002 ± 0.004	0.038 ± 0.018	0.079 ± 0.008	0.067 ± 0.052	0.069 ± 0.03	0.01 ± 0.004	0.025 ± 0.021
OTU769	*Bacteria; Proteobacteria; Gammaproteobacteria; Gammaproteobacteria Incertae Sedis; unknown family; unknown genus*	0	0.001 ± 0.002	0.015 ± 0.019	0.03 ± 0.011	0.055 ± 0.073	0.072 ± 0.083	0.114 ± 0.021	0.069 ± 0.029
OTU771	*Bacteria; Bacteroidetes; Bacteroidia; Bacteroidales; Marinifilaceae; unknown genus*	0	0.01 ± 0.011	0.006 ± 0.003	0.074 ± 0.04	0.037 ± 0.039	0.035 ± 0.008	0.017 ± 0.004	0.191 ± 0.064

OTU817	*Bacteria; Proteobacteria; Deltaproteobacteria; Desulfobacterales; Desulfobulbaceae; Desulfotalea*	0	0.002 ± 0.003	0.086 ± 0.025	0.121 ± 0.033	0.023 ± 0.01	0.024 ± 0.013	0.013 ± 0.015	0.031 ± 0.024
OTU827	*Bacteria; Bacteroidetes; Bacteroidia; Bacteroidales; Prolixibacteraceae; Roseimarinus*	0	0.005 ± 0.008	0.008 ± 0.006	0.053 ± 0.021	0.011 ± 0.008	0.016 ± 0.007	0.05 ± 0.014	0.129 ± 0.035
OTU845	*Bacteria; Bacteroidetes; Bacteroidia; Bacteroidales; Prolixibacteraceae; Roseimarinus*	0	0	0	0.002 ± 0.004	0.07 ± 0.083	0.075 ± 0.061	0.08 ± 0.02	0.026 ± 0.015
OTU850	*Bacteria; Epsilonbacteraeota; Campylobacteria; Campylobacterales; Arcobacteraceae; Arcobacter*	0.001 ± 0.003	0.059 ± 0.016	0.097 ± 0.058	0.042 ± 0.033	0	0	0.001 ± 0.001	0
OTU852	*Bacteria; Bacteroidetes; Bacteroidia; Flavobacteriales; Flavobacteriaceae; unknown genus*	0	0	0	0.056 ± 0.032	0.038 ± 0.054	0.067 ± 0.065	0.015 ± 0.003	0.069 ± 0.036
OTU853	*Bacteria; Bacteroidetes; Bacteroidia; Bacteroidales; Bacteroidetes BD2-2; unknown genus*	0	0	0.038 ± 0.014	0.107 ± 0.005	0.058 ± 0.036	0.05 ± 0.044	0.01 ± 0.009	0.038 ± 0.042
OTU859	*Bacteria; Bacteroidetes; Bacteroidia; Bacteroidales; Prolixibacteraceae; Roseimarinus*	0	0	0	0.011 ± 0.013	0.041 ± 0.045	0.086 ± 0.08	0.053 ± 0.038	0.049 ± 0.026
OTU887	*Bacteria; Proteobacteria; Alphaproteobacteria; Rhodobacterales; Rhodobacteraceae; Phaeobacter*	0	0.012 ± 0.016	0.102 ± 0.057	0.074 ± 0.034	0.03 ± 0.012	0.043 ± 0.01	0.009 ± 0.005	0.009 ± 0.011
OTU891	*Bacteria; Bacteroidetes; Bacteroidia; Flavobacteriales; Flavobacteriaceae; Flavicella*	0	0.003 ± 0.006	0.313 ± 0.335	0.079 ± 0.091	0	0.001 ± 0.001	0	0
OTU893	*Bacteria; Proteobacteria; Deltaproteobacteria; Desulfobacterales; Desulfobulbaceae; unknown genus*	0	0.002 ± 0.004	0	0.011 ± 0.008	0.035 ± 0.028	0.106 ± 0.094	0.111 ± 0.071	0.057 ± 0.055
OTU909	*Bacteria; Proteobacteria; Gammaproteobacteria; Cellvibrionales; Halieaceae; Halioglobus*	0.01 ± 0.017	0	0.017 ± 0.015	0.055 ± 0.034	0.091 ± 0.01	0.102 ± 0.034	0.054 ± 0.049	0.04 ± 0.016
OTU944	*Bacteria; Bacteroidetes; Bacteroidia; Bacteroidales; Marinifilaceae; unknown genus*	0	0	0.001 ± 0.001	0.002 ± 0.004	0.002 ± 0.004	0.035 ± 0.02	0.071 ± 0.022	0.056 ± 0.054
OTU974	*Bacteria; Proteobacteria; Deltaproteobacteria; Desulfuromonadales; Desulfuromonadaceae; Desulfuromusa*	0.007 ± 0.009	0.009 ± 0.014	0.006 ± 0.002	0.043 ± 0.012	0.008 ± 0.002	0.057 ± 0.015	0.086 ± 0.045	0.061 ± 0.048
OTU1002	*Bacteria; Bacteroidetes; Bacteroidia; Bacteroidales; Marinilabiliaceae; unknown genus*	0	0	0.002 ± 0.003	0.003 ± 0.003	0.01 ± 0.018	0.018 ± 0.01	0.063 ± 0.021	0.138 ± 0.081
OTU1029	*Bacteria; Proteobacteria; Deltaproteobacteria; Sva0485; unknown family; unknown genus*	0	0	0	0.013 ± 0.012	0.035 ± 0.054	0.112 ± 0.079	0.102 ± 0.047	0.033 ± 0.03
OTU1062	*Bacteria; Proteobacteria; Alphaproteobacteria; Rhodobacterales; Rhodobacteraceae; Loktanella*	0.001 ± 0.003	0.045 ± 0.02	0.091 ± 0.061	0.031 ± 0.025	0.043 ± 0.055	0	0.006 ± 0.007	0
OTU1072	*Bacteria; Firmicutes; Clostridia; Clostridiales; Lachnospiraceae; Vallitalea*	0	0	0.119 ± 0.153	0.141 ± 0.096	0	0	0	0.001
OTU1073	*Bacteria; Bacteroidetes; Bacteroidia; Bacteroidales; Marinilabiliaceae; Saccharicrinis*	0	0	0.003 ± 0.004	0.029 ± 0.013	0.013 ± 0.023	0.037 ± 0.004	0.042 ± 0.018	0.088 ± 0.063
OTU1076	*Bacteria; Proteobacteria; Deltaproteobacteria; Desulfobacterales; Desulfobulbaceae; [Desulfobacterium] catecholicum group*	0	0.002 ± 0.004	0.011 ± 0.007	0.052 ± 0.043	0.039 ± 0.018	0.102 ± 0.099	0.036 ± 0.02	0.087 ± 0.092
OTU1079	*Bacteria; Proteobacteria; Gammaproteobacteria; Thiomicrospirales; Thiomicrospiraceae; endosymbionts*	0	0	0.015 ± 0.01	0.035 ± 0.022	0.05 ± 0.021	0.039 ± 0.014	0.05 ± 0.031	0.046 ± 0.029
OTU1092	*Bacteria; Spirochaetes; Spirochaetia; Spirochaetales; Spirochaetaceae; Spirochaeta 2*	0	0	0.01 ± 0.016	0.039 ± 0.007	0.057 ± 0.049	0.064 ± 0.006	0.058 ± 0.024	0.042 ± 0.007
OTU1107	*Bacteria; Bacteroidetes; Bacteroidia; Flavobacteriales; Flavobacteriaceae; Lutimonas*	0.001 ± 0.001	0	0.004 ± 0.004	0.017 ± 0.02	0.049 ± 0.031	0.05 ± 0.017	0.042 ± 0.015	0.022 ± 0.005
OTU1112	*Bacteria; Proteobacteria; Gammaproteobacteria; Alteromonadales; Colwelliaceae; Thalassotalea*	0.005 ± 0.005	0.04 ± 0.02	0.004 ± 0.004	0.002 ± 0.002	0.016 ± 0.018	0.059 ± 0.017	0.171 ± 0.066	0.05 ± 0.024
OTU1167	*Bacteria; Proteobacteria; Deltaproteobacteria; Desulfobacterales; Desulfobulbaceae; SEEP-SRB4*	0	0.001 ± 0.001	0.009 ± 0.01	0.023 ± 0.021	0.033 ± 0.044	0.098 ± 0.089	0.069 ± 0.012	0.058 ± 0.019
OTU1169	*Bacteria; Proteobacteria; Gammaproteobacteria; UBA10353 marine group; unknown family; unknown genus*	0.071 ± 0.019	0.056 ± 0.021	0.027 ± 0.01	0.015 ± 0.005	0.01 ± 0.008	0.001 ± 0.001	0.005 ± 0.005	0.012 ± 0.011
OTU1188	*Bacteria; Proteobacteria; Deltaproteobacteria; Desulfobacterales; Desulfobulbaceae; Desulforhopalus*	0	0.003 ± 0.006	0.065 ± 0.047	0.069 ± 0.029	0.036 ± 0.023	0.057 ± 0.027	0.012 ± 0.003	0.012 ± 0.008
OTU1191	*Bacteria; Bacteroidetes; Bacteroidia; Flavobacteriales; Flavobacteriaceae; Winogradskyella*	0	0.003 ± 0.005	0.029 ± 0.024	0.099 ± 0.043	0.016 ± 0.015	0.124 ± 0.105	0	0.004 ± 0.007
OTU1235	*Bacteria; Proteobacteria; Deltaproteobacteria; Sva0485; unknown family; unknown genus*	0.001 ± 0.001	0	0	0.002 ± 0.001	0.014 ± 0.022	0.081 ± 0.05	0.102 ± 0.024	0.05 ± 0.026
OTU1284	*Bacteria; Bacteroidetes; Bacteroidia; Cytophagales; Cyclobacteriaceae; unknown genus*	0	0.01 ± 0.003	0.009 ± 0.009	0.021 ± 0.009	0.016 ± 0.007	0.037 ± 0.018	0.049 ± 0.036	0.034 ± 0.009
OTU1286	*Bacteria; Proteobacteria; Deltaproteobacteria; Myxococcales; BIrii41; unknown genus*	0	0.001 ± 0.001	0.036 ± 0.023	0.068 ± 0.03	0.07 ± 0.032	0.032 ± 0.025	0.007 ± 0.008	0.009 ± 0.011
OTU1335	*Bacteria; Bacteroidetes; Bacteroidia; Sphingobacteriales; Lentimicrobiaceae; unknown genus*	0	0	0.008 ± 0.007	0.023 ± 0.017	0.035 ± 0.003	0.035 ± 0.012	0.019 ± 0.013	0.025 ± 0.002
OTU1340	*Bacteria; Proteobacteria; Gammaproteobacteria; Gammaproteobacteria Incertae Sedis; unknown family; unknown genus*	0	0.005 ± 0.005	0	0.015 ± 0.006	0.016 ± 0.01	0.019 ± 0.005	0.058 ± 0.048	0.056 ± 0.045
OTU1369	*Bacteria; Proteobacteria; Deltaproteobacteria; Desulfobacterales; Desulfobulbaceae; unknown genus*	0	0.004 ± 0.007	0.004 ± 0.007	0.018 ± 0.013	0.016 ± 0.013	0.038 ± 0.023	0.044 ± 0.035	0.062 ± 0.008
OTU1372	*Bacteria; Bacteroidetes; Bacteroidia; Bacteroidetes VC2.1 Bac22; unknown family; unknown genus*	0	0	0.016 ± 0.01	0.065 ± 0.008	0.041 ± 0.049	0.058 ± 0.046	0.006 ± 0.007	0.018 ± 0.02
OTU1425	*Bacteria; Bacteroidetes; Bacteroidia; Bacteroidales; Bacteroidetes BD2-2; unknown genus*	0	0	0	0.003 ± 0.003	0.014 ± 0.017	0.143 ± 0.152	0.065 ± 0.022	0.049 ± 0.024
OTU1493	*Bacteria; Firmicutes; Clostridia; Clostridiales; Lachnospiraceae; Vallitalea*	0	0	0.08 ± 0.027	0.08 ± 0.068	0.01 ± 0.01	0	0	0
OTU1498	*Bacteria; Bacteroidetes; Bacteroidia; Bacteroidales; Prolixibacteraceae; Roseimarinus*	0	0.003 ± 0.006	0.031 ± 0.031	0.161 ± 0.023	0.032 ± 0.024	0.003 ± 0.005	0	0.003 ± 0.002
OTU1500	*Bacteria; Proteobacteria; Deltaproteobacteria; Desulfobacterales; Desulfobulbaceae; Desulforhopalus*	0	0	0.009 ± 0.005	0.013 ± 0.012	0.012 ± 0.014	0.037 ± 0.01	0.025 ± 0.008	0.056 ± 0.03
OTU1516	*Bacteria; Proteobacteria; Gammaproteobacteria; Cellvibrionales; Halieaceae; Halioglobus*	0	0	0	0	0	0.033 ± 0.016	0.068 ± 0.104	0.032 ± 0.026
OTU1553	*Bacteria; Proteobacteria; Deltaproteobacteria; Desulfuromonadales; Desulfuromonadaceae; Desulfuromusa*	0	0	0	0.007 ± 0.011	0.021 ± 0.017	0.017 ± 0.004	0.039 ± 0.034	0.071 ± 0.022
OTU1560	*Bacteria; Bacteroidetes; Bacteroidia; Bacteroidales; Prolixibacteraceae; Draconibacterium*	0	0.002 ± 0.003	0.006 ± 0.006	0.013 ± 0.007	0.022 ± 0.006	0.052 ± 0.019	0.017 ± 0.006	0.038 ± 0.006
OTU1565	*Bacteria; Bacteroidetes; Bacteroidia; Flavobacteriales; Flavobacteriaceae; Lutibacter*	0.003 ± 0.005	0.011 ± 0.008	0.018 ± 0.006	0.037 ± 0.017	0.014 ± 0.012	0	0.001 ± 0.001	0.032 ± 0.019
OTU1568	*Bacteria; Bacteroidetes; Bacteroidia; Bacteroidales; Bacteroidetes BD2-2; unknown genus*	0	0.005 ± 0.009	0	0	0.019 ± 0.01	0.059 ± 0.03	0.031 ± 0.013	0.036 ± 0.025
OTU1575	*Bacteria; Spirochaetes; Spirochaetia; Spirochaetales; Spirochaetaceae; Spirochaeta 2*	0	0	0.001 ± 0.002	0.002 ± 0.002	0.03 ± 0.029	0.017 ± 0.008	0.04 ± 0.011	0.021 ± 0.001
OTU1576	*Bacteria; Firmicutes; Clostridia; Clostridiales; Defluviitaleaceae; Defluviitaleaceae UCG-011*	0	0	0	0.004 ± 0.002	0	0.029 ± 0.005	0.023 ± 0.017	0.067 ± 0.006
OTU1581	*Bacteria; Bacteroidetes; Bacteroidia; Bacteroidales; Bacteroidetes BD2-2; unknown genus*	0	0	0	0.035 ± 0.014	0.035 ± 0.021	0.048 ± 0.037	0.031 ± 0.026	0.017 ± 0.015
OTU1607	*Bacteria; Bacteroidetes; Bacteroidia; Bacteroidales; Prolixibacteraceae; Draconibacterium*	0	0	0	0.001 ± 0.001	0.007 ± 0.013	0.015 ± 0.009	0.056 ± 0.025	0.054 ± 0.013
OTU1614	*Bacteria; Proteobacteria; Gammaproteobacteria; Alteromonadales; Colwelliaceae; Colwellia*	0	0.001 ± 0.002	0.205 ± 0.266	0.033 ± 0.032	0	0.001 ± 0.001	0	0
OTU1617	*Bacteria; Bacteroidetes; Bacteroidia; Sphingobacteriales; Lentimicrobiaceae; unknown genus*	0	0.001 ± 0.002	0	0.016 ± 0.003	0.039 ± 0.006	0.026 ± 0.019	0.02 ± 0.014	0.046 ± 0.03
OTU1632	*Bacteria; Bacteroidetes; Bacteroidia; Flavobacteriales; Flavobacteriaceae; unknown genus*	0.002 ± 0.004	0.014 ± 0.02	0.023 ± 0.012	0.101 ± 0.047	0.025 ± 0.024	0	0	0.001 ± 0.002
OTU1654	*Bacteria; Bacteroidetes; Bacteroidia; Flavobacteriales; Flavobacteriaceae; Lutibacter*	0.002 ± 0.003	0.009 ± 0.003	0.099 ± 0.13	0.124 ± 0.047	0.009 ± 0.016	0.003 ± 0.003	0	0.001 ± 0.001
OTU1663	*Bacteria; Bacteroidetes; Bacteroidia; Bacteroidales; Prolixibacteraceae; Roseimarinus*	0	0	0.035 ± 0.034	0.07 ± 0.037	0	0	0	0
OTU1672	*Bacteria; Bacteroidetes; Bacteroidia; Bacteroidales; Marinifilaceae; unknown genus*	0	0.002 ± 0.003	0.114 ± 0.09	0.073 ± 0.032	0.001 ± 0.002	0	0	0
OTU1706	*Bacteria; Proteobacteria; Deltaproteobacteria; Myxococcales; MidBa8; unknown genus*	0	0	0	0.002 ± 0.003	0.05 ± 0.049	0.067 ± 0.023	0.046 ± 0.043	0.018 ± 0.021
OTU1742	*Bacteria; Proteobacteria; Deltaproteobacteria; Desulfobacterales; Desulfobulbaceae; unknown genus*	0	0	0.002 ± 0.002	0.012 ± 0.01	0.017 ± 0.024	0.049 ± 0.011	0.087 ± 0.034	0.042 ± 0.003
OTU1760	*Bacteria; Proteobacteria; Deltaproteobacteria; Desulfuromonadales; Desulfuromonadaceae; Malonomonas*	0	0	0.001 ± 0.001	0.018 ± 0.011	0.034 ± 0.02	0.031 ± 0.011	0.044 ± 0.008	0.059 ± 0.014
OTU1773	*Bacteria; Proteobacteria; Alphaproteobacteria; Rhodobacterales; Rhodobacteraceae; Roseobacter*	0.002 ± 0.003	0.018 ± 0.003	0.034 ± 0.028	0.026 ± 0.008	0.014 ± 0.005	0.009 ± 0.007	0	0
OTU1778	*Bacteria; Proteobacteria; Deltaproteobacteria; Myxococcales; MidBa8; unknown genus*	0	0	0	0.007 ± 0.005	0.044 ± 0.006	0.039 ± 0.018	0.011 ± 0.01	0.022 ± 0.016
OTU1834	*Bacteria; Bacteroidetes; Bacteroidia; Bacteroidales; Bacteroidetes BD2-2; unknown genus*	0	0	0.035 ± 0.017	0.056 ± 0.014	0.013 ± 0.008	0.012 ± 0.01	0	0.003 ± 0.005
OTU1901	*Bacteria; Bacteroidetes; Bacteroidia; Bacteroidales; Marinifilaceae; unknown genus*	0	0	0.016 ± 0.002	0.021 ± 0.01	0.023 ± 0.026	0.052 ± 0.068	0.004 ± 0.006	0.027 ± 0.009
OTU1912	*Bacteria; Proteobacteria; Alphaproteobacteria; Rhodobacterales; Rhodobacteraceae; Leisingera*	0	0	0.044 ± 0.046	0.039 ± 0.017	0.004 ± 0.006	0.013 ± 0.01	0	0.012 ± 0.004
OTU1953	*Bacteria; Bacteroidetes; Bacteroidia; Bacteroidetes VC2.1 Bac22; unknown family; unknown genus*	0.002 ± 0.004	0.006 ± 0.005	0	0.006 ± 0.002	0.026 ± 0.013	0.042 ± 0.02	0.059 ± 0.036	0.079 ± 0.051
OTU1963	*Bacteria; Proteobacteria; Deltaproteobacteria; Desulfobacterales; Desulfobulbaceae; [Desulfobacterium] catecholicum group*	0	0.002 ± 0.003	0.006 ± 0.001	0.017 ± 0.011	0.023 ± 0.019	0.038 ± 0.019	0.018 ± 0.012	0.099 ± 0.111
OTU2104	*Bacteria; Proteobacteria; Gammaproteobacteria; Oceanospirillales; Saccharospirillaceae; Reinekea*	0	0.014 ± 0.005	0.058 ± 0.054	0.019 ± 0.008	0.014 ± 0.009	0.01 ± 0.007	0	0
OTU2200	*Bacteria; Bacteroidetes; Bacteroidia; Bacteroidales; Bacteroidetes BD2-2; unknown genus*	0	0	0	0	0.003 ± 0.004	0.059 ± 0.072	0.033 ± 0.013	0.008 ± 0.003
OTU2274	*Bacteria; Proteobacteria; Gammaproteobacteria; Alteromonadales; Colwelliaceae; Colwellia*	0	0.046 ± 0.02	0.055 ± 0.038	0.012 ± 0.013	0.008 ± 0.003	0.011 ± 0.008	0.021 ± 0.001	0.001 ± 0.002
OTU2287	*Bacteria; Proteobacteria; Gammaproteobacteria; Alteromonadales; Colwelliaceae; Colwellia*	0	0.025 ± 0.014	0.057 ± 0.055	0.018 ± 0.003	0.007 ± 0.006	0	0.001 ± 0.001	0
OTU2390	*Bacteria; Proteobacteria; Gammaproteobacteria; Chromatiales; Chromatiaceae; Candidatus Thiobios*	0.008 ± 0.007	0	0	0.015 ± 0.014	0.025 ± 0.012	0.018 ± 0.014	0.039 ± 0.011	0.071 ± 0.02
OTU2413	*Bacteria; Proteobacteria; Deltaproteobacteria; Desulfobacterales; Desulfobulbaceae; Desulforhopalus*	0	0.002 ± 0.003	0.039 ± 0.018	0.018 ± 0.011	0.025 ± 0.008	0.019 ± 0.011	0.001 ± 0.001	0.007 ± 0.005
OTU2420	*Bacteria; Firmicutes; Clostridia; Clostridiales; Christensenellaceae; unknown genus*	0	0.003 ± 0.005	0	0	0.003 ± 0.005	0.033 ± 0.023	0.024 ± 0.011	0.03 ± 0.014
OTU2739	*Bacteria; Proteobacteria; Gammaproteobacteria; Alteromonadales; Colwelliaceae; Colwellia*	0	0.063 ± 0.021	0.224 ± 0.281	0.046 ± 0.059	0	0.003 ± 0.003	0	0
OTU2833	*Bacteria; Proteobacteria; Gammaproteobacteria; Alteromonadales; Psychromonadaceae; Psychromonas*	0	0.017 ± 0.001	0.084 ± 0.086	0.017 ± 0.014	0	0.003 ± 0.003	0	0.001
OTU3867	*Bacteria; Bacteroidetes; Bacteroidia; Bacteroidales; Prolixibacteraceae; Draconibacterium*	0.002 ± 0.002	0	0.001	0.009 ± 0.002	0.018 ± 0.014	0.023 ± 0.015	0.015 ± 0.004	0.008 ± 0.003

Supplementary table 7. Associated taxonomy and relative sequence abundance ± s.d. (n = 3, except n = 2 at 11 weeks) of the 27 external sediment-associated OTUs whose relative sequence abundance vary significantly during kelp degradation (GLM, $P < 0.05$).

		Relative abundance (%) mean ± sd							
OTU id	**Taxonomy**	**0 week**	**2 weeks**	**4 week**	**6 weeks**	**11 weeks**	**15 weeks**	**20 weeks**	**24 weeks**
OTU44	*Bacteria; Proteobacteria; Deltaproteobacteria; Desulfobacterales; Desulfobulbaceae; unknown genus*	0.12 ± 0.07	0.15 ± 0.07	0.09 ± 0.06	0.17 ± 0.19	0.19 ± 0.01	1.23 ± 0.4	0.51 ± 0.36	1.14 ± 0.79
OTU70	*group*	0.05 ± 0.04	0.01 ± 0.01	0.04 ± 0.03	0.17 ± 0.09	0.13 ± 0	0.39 ± 0.03	0.27 ± 0.22	0.2 ± 0.05
OTU73	*Bacteria; Proteobacteria; Gammaproteobacteria; Cellvibrionales; Halieaceae; Halioglobus*	0.26 ± 0.07	0.39 ± 0.04	0.44 ± 0.07	0.48 ± 0.11	0.2 ± 0.01	0.24 ± 0.06	0.24 ± 0.03	0.16 ± 0.06
OTU101	*Bacteria; Bacteroidetes; Bacteroidia; Flavobacteriales; Flavobacteriaceae; Bizionia*	0.39 ± 0.14	0.29 ± 0.02	0.26 ± 0.15	0.16 ± 0.05	0.11 ± 0.01	0.09 ± 0.06	0.14 ± 0.08	0.05 ± 0.02
OTU109	*Bacteria; Proteobacteria; Alphaproteobacteria; Rhodobacterales; Rhodobacteraceae; Boseongicola*	0.46 ± 0.08	0.29 ± 0.05	0.4 ± 0.08	0.32 ± 0.03	0.36 ± 0.09	0.27 ± 0.07	0.35 ± 0.04	0.17 ± 0.05
OTU132	*Bacteria; Proteobacteria; Gammaproteobacteria; Cellvibrionales; Halieaceae; Halioglobus*	0.44 ± 0.07	0.44 ± 0.14	0.48 ± 0.05	0.46 ± 0.14	0.32 ± 0.09	0.25 ± 0.09	0.24 ± 0.06	0.15 ± 0.06
OTU135	*Bacteria; Bacteroidetes; Bacteroidia; Flavobacteriales; Flavobacteriaceae; unknown genus*	0.1 ± 0.06	0.06 ± 0.02	0.09 ± 0.06	0.1 ± 0.05	0.02 ± 0.01	0	0	0.01 ± 0.01
OTU148	*Bacteria; Proteobacteria; Gammaproteobacteria; MBAE14; unknown family; unknown genus*	0.11 ± 0.02	0.15 ± 0.08	0.52 ± 0.18	0.29 ± 0.04	0.3 ± 0.1	0.29 ± 0.06	0.27 ± 0.09	0.16 ± 0.05
OTU154	*Bacteria; Bacteroidetes; Bacteroidia; Bacteroidales; Marinilabiliaceae; Carboxylicivirga*	0.09 ± 0.06	0.02 ± 0.01	0.1 ± 0.07	0.26 ± 0.16	0.17 ± 0.11	0.22 ± 0.05	0.36 ± 0.3	0.12 ± 0.06
OTU160	*Bacteria; Proteobacteria; Gammaproteobacteria; Steroidobacterales; Woeseiaceae; Woeseia*	0.15 ± 0.06	0.11 ± 0.02	0.26 ± 0.02	0.17 ± 0.04	0.3 ± 0	0.3 ± 0.06	0.22 ± 0.05	0.14 ± 0.02
OTU167	*Bacteria; Bacteroidetes; Bacteroidia; Flavobacteriales; Flavobacteriaceae; Psychroserpens*	0	0.04 ± 0	0.2 ± 0.07	0.49 ± 0.2	0.07 ± 0.02	0.12 ± 0.08	0.06 ± 0.02	0
OTU209	*Bacteria; Bacteroidetes; Bacteroidia; Flavobacteriales; Flavobacteriaceae; Aquibacter*	0.08 ± 0.02	0.14 ± 0.06	0.28 ± 0.08	0.19 ± 0.01	0.17 ± 0.06	0.2 ± 0.07	0.2 ± 0.06	0.07 ± 0.05
OTU218	*Bacteria; Proteobacteria; Deltaproteobacteria; Desulfobacterales; Desulfobulbaceae; unknown genus*	0	0 ± 0.01	0.01 ± 0.01	0.06 ± 0.08	0.05 ± 0.01	0.16 ± 0.05	0.07 ± 0.06	0.05 ± 0.03
OTU228	*Bacteria; Proteobacteria; Gammaproteobacteria; Thiohalorhabdales; Thiohalorhabdaceae; unknown genus*	0.15 ± 0.04	0.12 ± 0.05	0.29 ± 0.02	0.24 ± 0.07	0.36 ± 0.04	0.29 ± 0.11	0.26 ± 0.08	0.14 ± 0.05
OTU255	*Bacteria; Proteobacteria; Gammaproteobacteria; Cellvibrionales; Spongiibacteraceae; BD1-7 clade*	0.06 ± 0.03	0.1 ± 0.03	0.4 ± 0.15	0.21 ± 0.01	0.25 ± 0.01	0.18 ± 0.06	0.08 ± 0.05	0.1 ± 0.05
OTU287	*Bacteria; Proteobacteria; Deltaproteobacteria; Desulfobacterales; Desulfobulbaceae; Desulforhopalus*	0	0	0.01 ± 0.01	0.04 ± 0.03	0.04 ± 0.05	0.28 ± 0.1	0.07 ± 0.04	0.08 ± 0.02
OTU328	*Bacteria; Proteobacteria; Gammaproteobacteria; Vibrionales; Vibrionaceae; Vibrio*	0.06 ± 0.04	0.12 ± 0.03	0.17 ± 0.05	0.05 ± 0.03	0.04 ± 0.02	0.01 ± 0.01	0.03 ± 0.01	0
OTU336	*Bacteria; Proteobacteria; Alphaproteobacteria; Rhodobacterales; Rhodobacteraceae; Pseudoruegeria*	0.02 ± 0	0.01 ± 0.01	0.01 ± 0.01	0.06 ± 0.02	0.04 ± 0.02	0.07 ± 0.02	0.05 ± 0.02	0.05 ± 0.02
OTU475	*Bacteria; Proteobacteria; Deltaproteobacteria; Desulfobacterales; Desulfobulbaceae; Desulforhopalus*	0.01 ± 0.01	0	0	0.03 ± 0.02	0.02 ± 0.02	0.14 ± 0.03	0.05 ± 0.04	0.05 ± 0.03
OTU502	*Bacteria; Bacteroidetes; Bacteroidia; Flavobacteriales; Flavobacteriaceae; unknown genus*	0	0	0.05 ± 0.04	0.06 ± 0.05	0.07 ± 0	0.06 ± 0.02	0.16 ± 0.11	0.02 ± 0.02
OTU668	*Bacteria; Bacteroidetes; Bacteroidia; Bacteroidales; Prolixibacteraceae; Draconibacterium*	0	0	0.01 ± 0.01	0.04 ± 0.05	0.07 ± 0.06	0.18 ± 0.06	0.06 ± 0.08	0.05 ± 0.01
OTU692	*Bacteria; Epsilonbacteraeota; Campylobacteria; Campylobacterales; Arcobacteraceae; Arcobacter*	0.05 ± 0.06	0.03 ± 0.01	0.1 ± 0.06	0.07 ± 0.03	0.04 ± 0.03	0	0.02 ± 0.02	0
OTU719	*Bacteria; Bacteroidetes; Bacteroidia; Bacteroidales; Bacteroidetes BD2-2; unknown genus*	0	0	0	0	0.02 ± 0.02	0.04 ± 0.02	0.05 ± 0.05	0.03 ± 0.02
OTU947	*Bacteria; Bacteroidetes; Bacteroidia; Flavobacteriales; Crocinitomicaceae; Salinirepens*	0.02 ± 0.01	0.01 ± 0.01	0.03 ± 0.01	0.04 ± 0.01	0.05 ± 0.01	0.02 ± 0.01	0	0
OTU1064	*Bacteria; Proteobacteria; Deltaproteobacteria; Oligoflexales; Oligoflexaceae; unknown genus*	0	0	0	0	0.01 ± 0.01	0.08 ± 0.02	0.04 ± 0.04	0.04 ± 0.01
OTU1159	*Bacteria; Bacteroidetes; Bacteroidia; Flavobacteriales; Flavobacteriaceae; Gilvibacter*	0.02 ± 0.01	0.03 ± 0.01	0.02 ± 0.02	0	0.06 ± 0.03	0.04 ± 0.02	0.06 ± 0.06	0
OTU1283	*Bacteria; Firmicutes; Clostridia; Clostridiales; Clostridiaceae 1; unknown genus*	0.02 ± 0.01	0.01 ± 0.01	0	0	0.02 ± 0	0.03 ± 0.02	0.01 ± 0.02	0.05 ± 0.04

Supplementary table 8: Details of the qPCR assay, following the Minimum Information for publication of Quantitative real-time PCR Experiments (MIQE) guidelines.

Experimental design	
Definition of experimental groups	Four experimental groups (Kelp-associated, Underlying sediment, External sediment, Seawater) at 8 sampling date (week 0, 2, 4, 6, 11, 15, 20, 24)
Number within each group	n=3, except n=2 for external sediment at week 2
Sample	
Description	Kelp-associated: epiphytic communities from kelp surface; Underlying sediment: surface sediment (0-4 cm) directly underneath cages; External sediment: surface sediment (0-4 cm) 2 m away from cages; Seawater: seawater 1 m above cages
Volume of sample processed	Kelp associated: 5 algal pieces (total surface of 13.3 cm^2); Underlying and external sediment: 0.5 g; Seawater: 1 liter
Processing procedure	Kelp associated: sampling with sterilized stainless steel punch; Underlying and external sediment: sampling in sterile plastic tube; Seawater: sampling in Niskin bottles, followed by prefiltration (3 µm) and filtration at 0.2 µm
Freezing procedure	-80°C
Sample storage conditions and duration	-80°C, less than 6 months
Nucleic acid extraction	
Procedure	Kelp associated and seawater samples: lysis buffer, phenol-chloroform extraction followed by NucleoSpin Plant II kit (Macherey Nagel)
Nucleic acid quantification instrument and method	Qubit fluorometer
Purity (A260/280)	Nanodrop
qPCR target information	
gene symbol	16S rRNA gene
amplicon length	136 bp
in silico specificity screen	94.8% coverage for bacteria with Silva TestPrime on SSUr 138.1 (September 2020; 2 mismatches allowed, no mismatch 3 bases from 3' end)
qPCR oligonucleotides	
primer sequences	926F: 5'-AAACTCAAAKGAATTGACGG-3'; 1062R: 5'-CTCACRRCACGAGCTGAC-3'
manufacturer of oligonucleotides	Eurogentec
purification method	desalting
qPCR protocol	
reaction volume	5 µl
amount of DNA	10 pg
primer, Mg2+ and dNTP concentration	600 nM of each primer; Mg^{2+} and dNTP according to kit
polymerase identity and concentration	FastStart Taq DNA polymerase
buffer/kit identity and manufacturer	LightCycle 480 SYBR Green I Master (Roche)
additives	SYBR Green, TBT-PAR
Manufacturer of plates	LightCycler 480 Multiwell Plate 384 (Roche)
Complete thermocycling parameters	10 min @ 95°C; 45 cycles of 10 s @ 95°C / 20 s @ 60°C / 10 s @ 72°C; 5 s @ 95°C. Melting curve from 65°C to 97°C
reaction setup	manual
manufacturer of qPCR instrument	Roche
qPCR validation	
specificity	melting curve
Cq of NTC	35.1
Calibration curve with slope and y intercept	slope = -3.700 ; y intercept = 42.14
PCR efficiency calculated from slope	86%
Data analysis	
qPCR analysis program	LightCycler 480 Software, LCS480 1.5.0.39
Method of Cq determination	Abs Quant / 2nd Derivative Max
Number and stage of technical replicates	3 technical replicates at the qPCR stage
Statistical method for results significance	Kruskall-Wallis test, followed by post-hoc Conover test with Benjamini-Hochberg correction of p-values

Supplementary Figures

Supplementary figure 1. Fluctuations of the number of detected OTU in the kelp-associated (**A**), the water column (**B**), and the underlying and external sediment (**C**) compartments during the 6 months-experiment. Different letters indicate significant differences between sampling dates. ANOVA analysis was conducted to compare diversity indices over time. When significant ANOVA results were found ($P < 0.05$), a post-hoc Tukey HSD test was calculated. Accordingly, different letters indicate significant differences between sampling dates. Values are mean ± standard deviation (n = 3, except n = 2 for 0 week in kelp-associated and 11 weeks in external sediment).

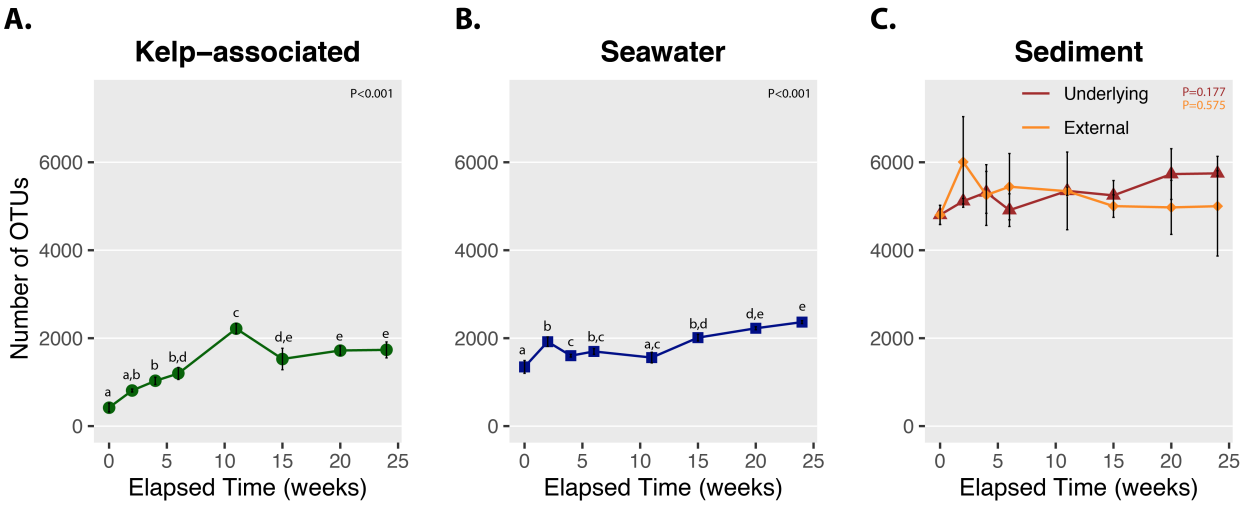

Supplementary Figure 2. Mean relative sequence abundance and taxonomic affiliation of the 10 most abundant OTUs at each sampling date in kelp-associated bacterial communities. All least abundant OTUs were omitted from the pie charts.

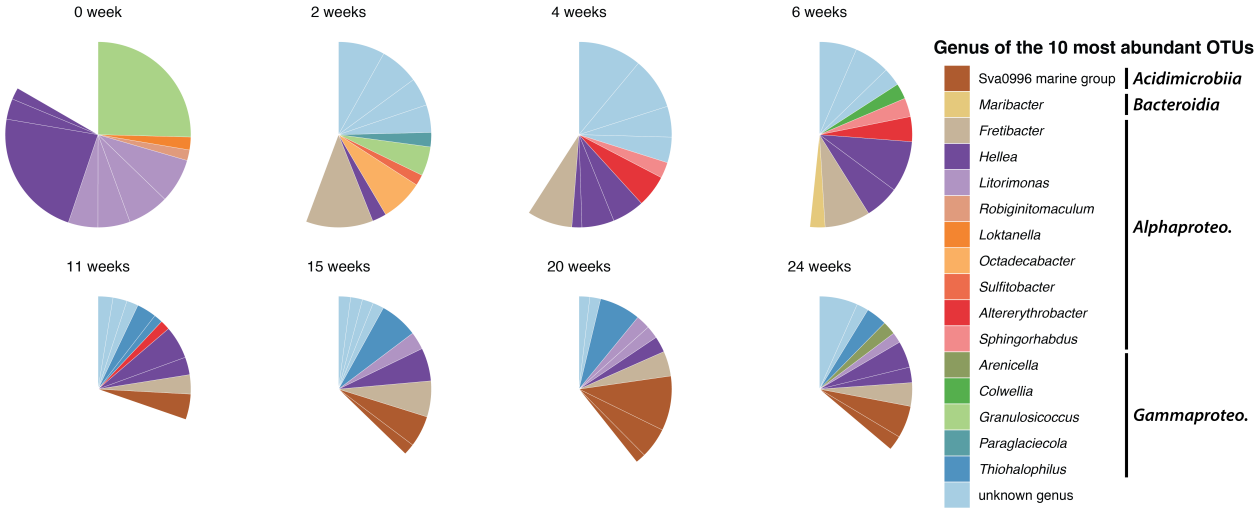

Supplementary Figure 3. Relative sequence abundance of bacterial classes in seawater (**A**) and external sediment (**B**) samples during the 6 month-experiment. Sequence relative abundances of classes representing less than 0.5% of all sequences at each sampling time were summed into the "Other" category. Values are mean ± standard deviation (n = 3, except at week 11 for external sediment n = 2).

A.

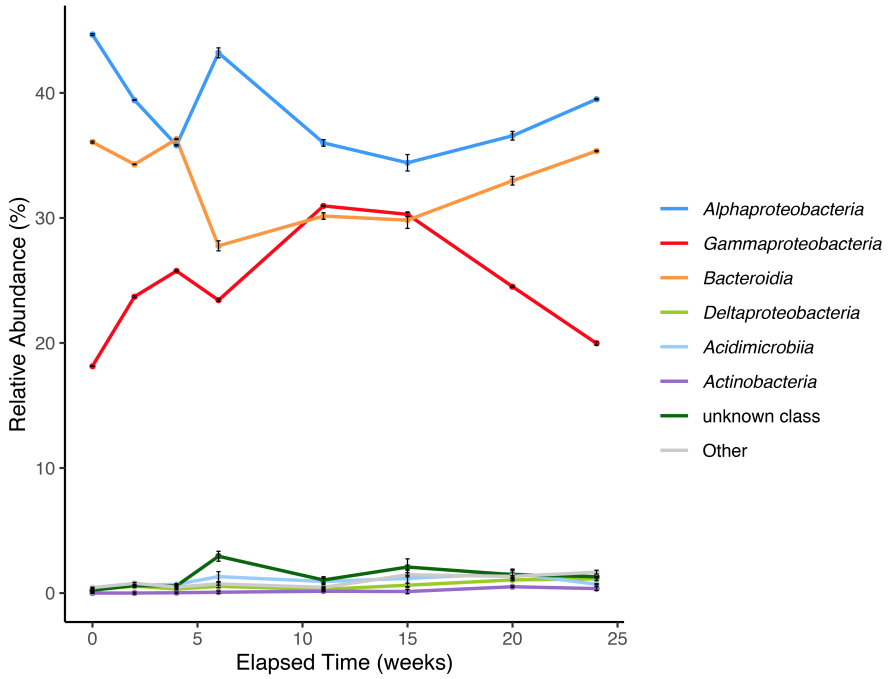

B.

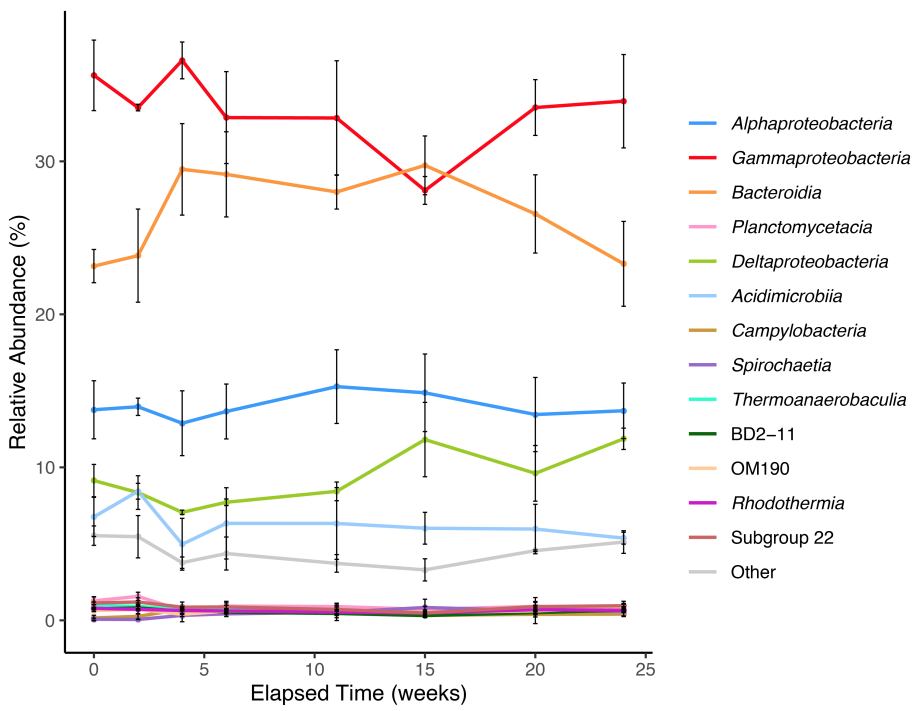

Supplementary Figure 4. Subnetworks of kelp-associated bacterial communities centered on "Temperature" (**A**) "C/N ratio" (**B**) and "Respiration" (**C**). OTU nodes are color-coded based on taxonomy, and their size is proportional to the median relative sequence abundance during the experiment. Positive and negative associations are depicted by light-blue and light-red lines, respectively. Arrows indicate delayed associations (maximum delay = 1 sampling date).

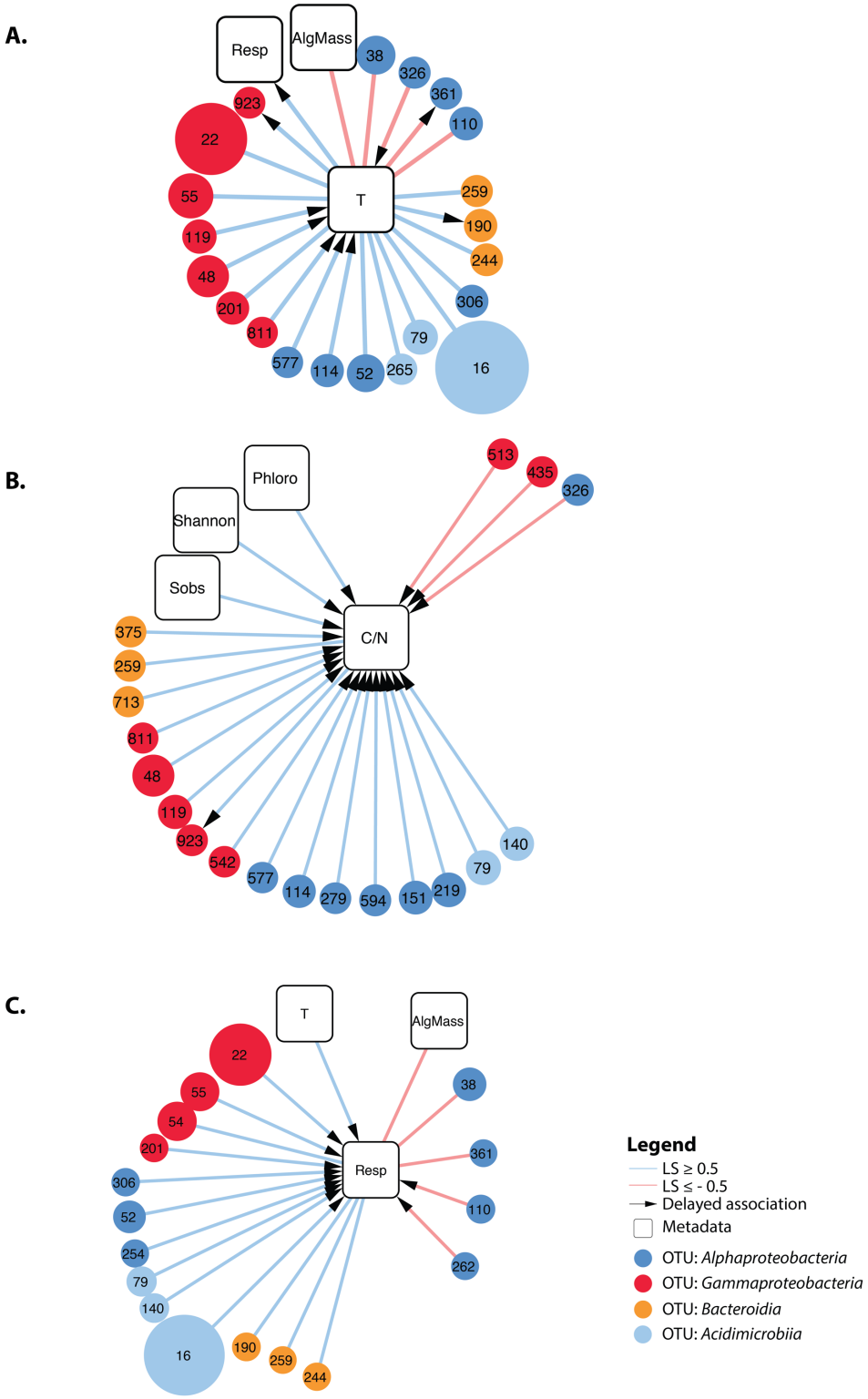

Supplementary Figure 5. Changes in relative sequence abundance over time for OTUs from cluster 2 in the kelp-associated association network. Values are means of relative sequence abundance (n = 3, except for T0 n = 2). The most detailed taxonomic affiliation is given for each OTU.

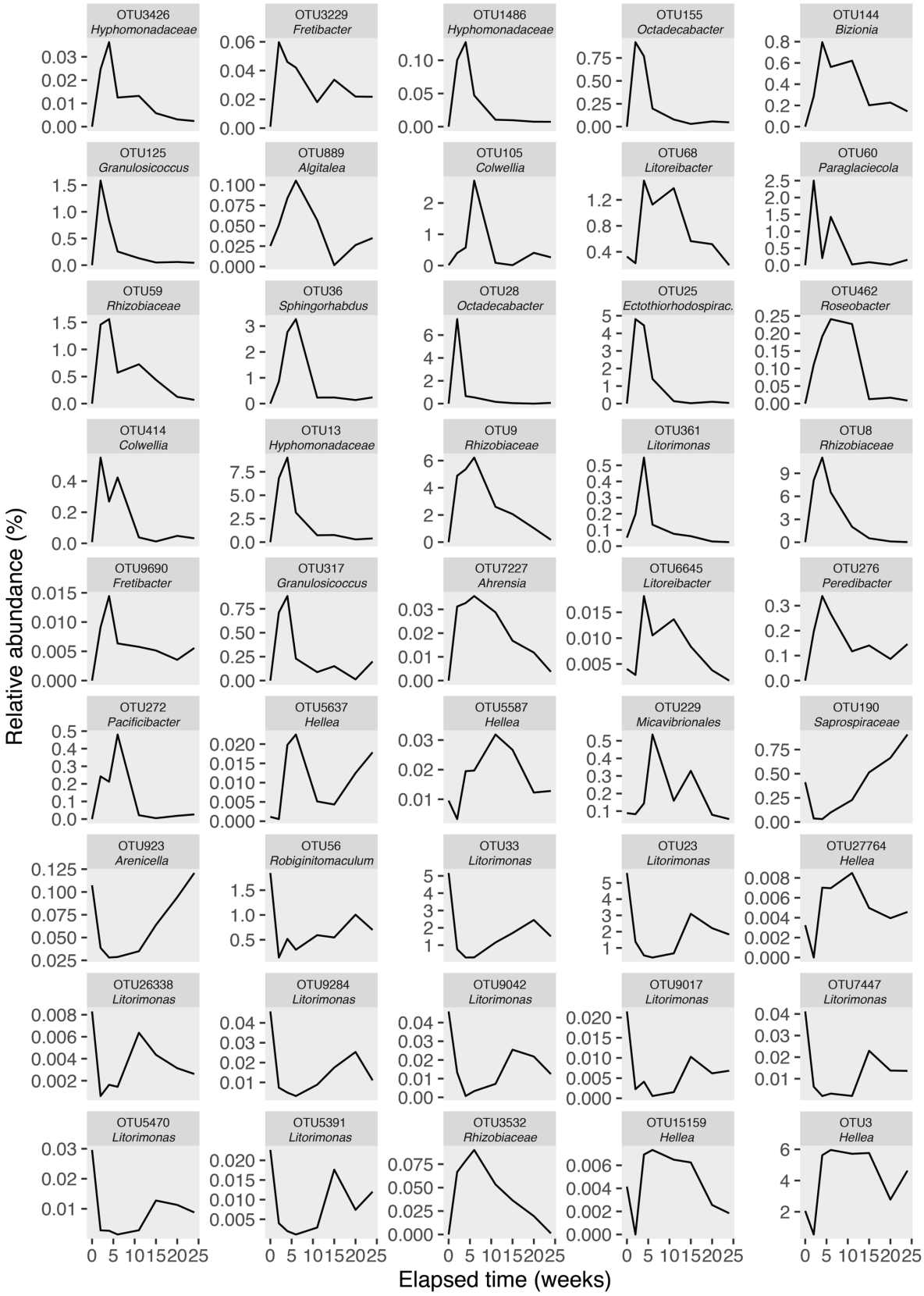

Supplementary Figure 6. Changes in relative sequence abundance over time for OTUs from cluster 1 in the kelp-associated association network. Values are means of relative sequence abundance (n = 3, except for T0 n = 2). The most detailed taxonomic affiliation is given for each OTU.

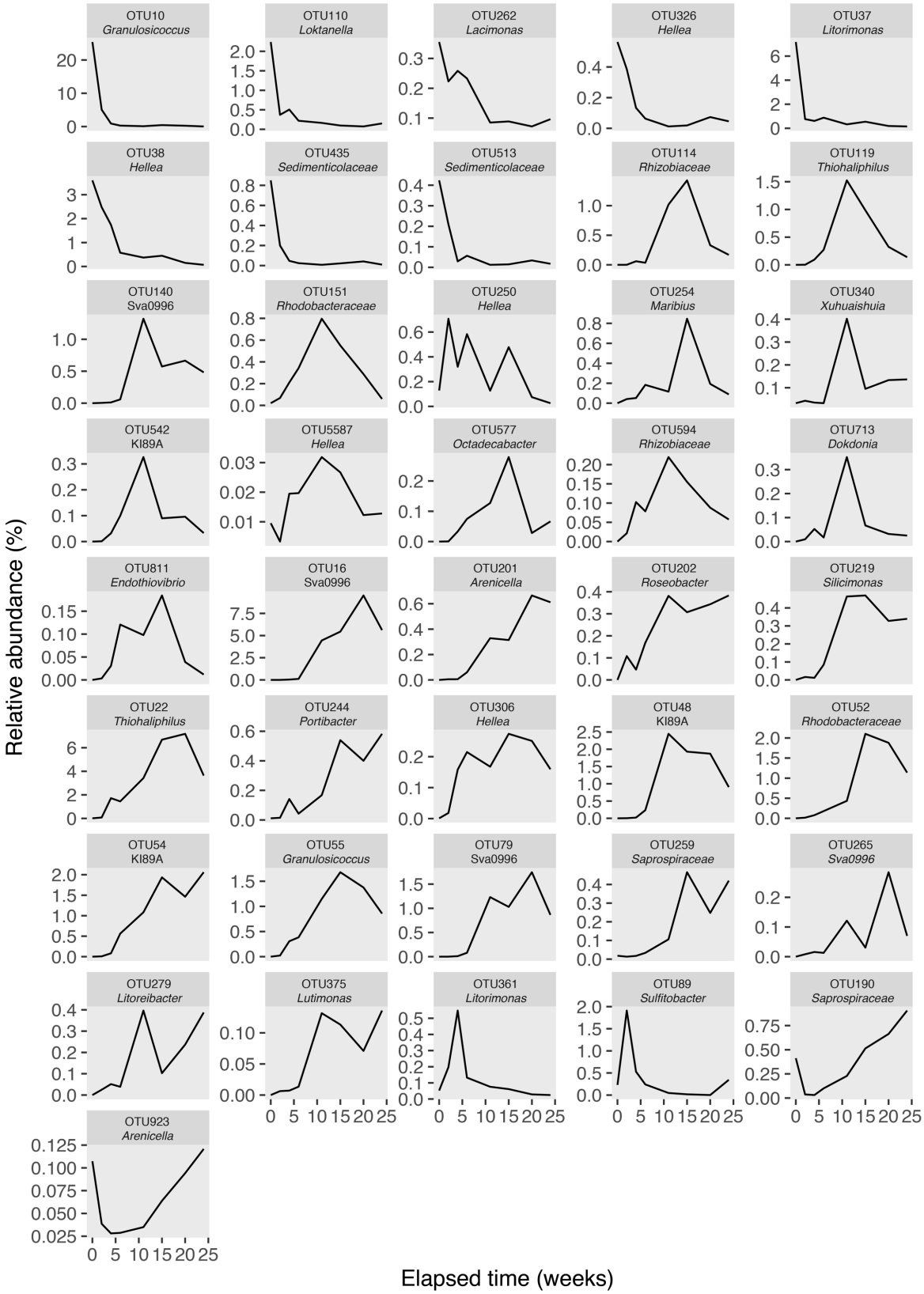

Supplementary Figure 7. Predicted relative sequence abundance over time for glycoside hydrolases obtained after running PICRUSt2 metagenome predictions on 16S rRNA data from kelp-associated bacterial communities. Only enzymes with a relative sequence abundance varying significantly with time (GLM, $P < 0.05$) and representing more than 0.01% of the predicted metagenome for at least one sampling date are shown. Values are means ± standard deviation of predicted relative sequence abundance (n = 3, except for T0 n = 2).

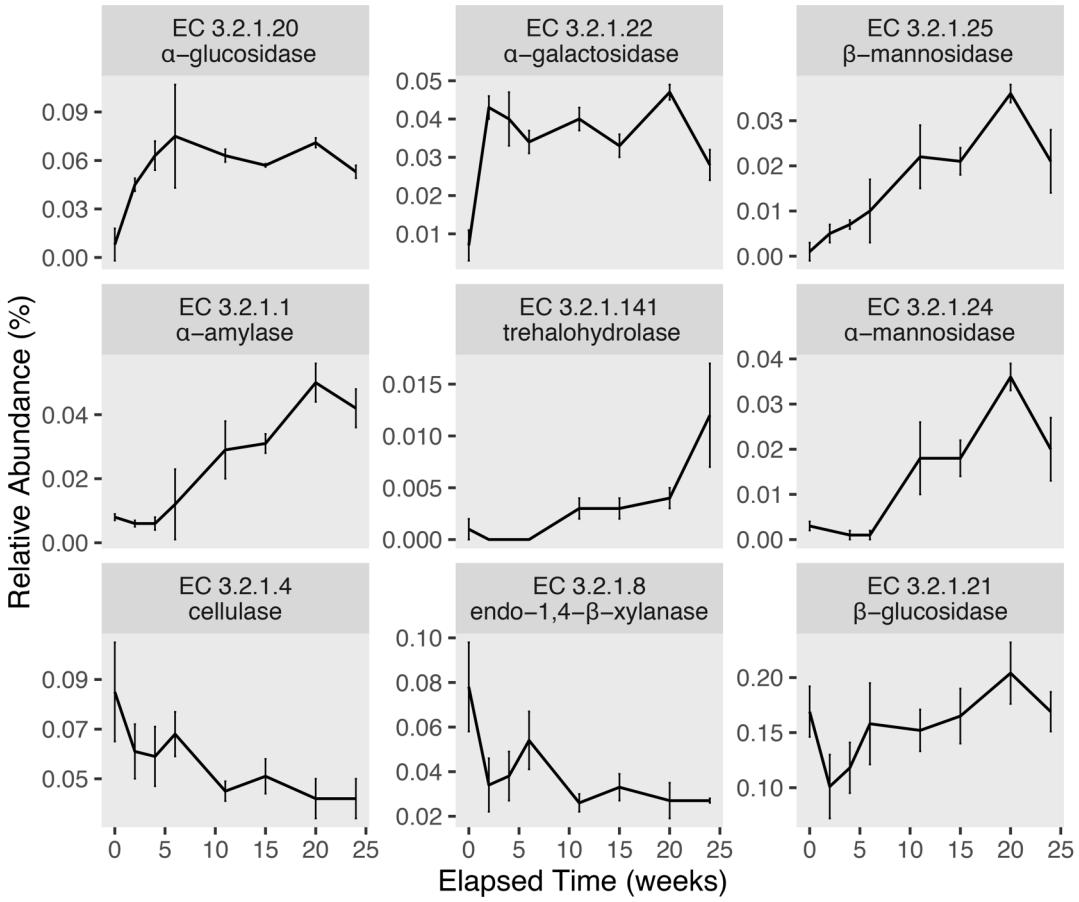

Supplementary Figure 8. Relative abundance of the 11 OTUs that vary significantly with time in both underlying (red) and external (orange) sediments. Values are mean of n = 3, except at week 11 for external sediment n = 2. The most detailed taxonomic affiliation is given for each OTU.

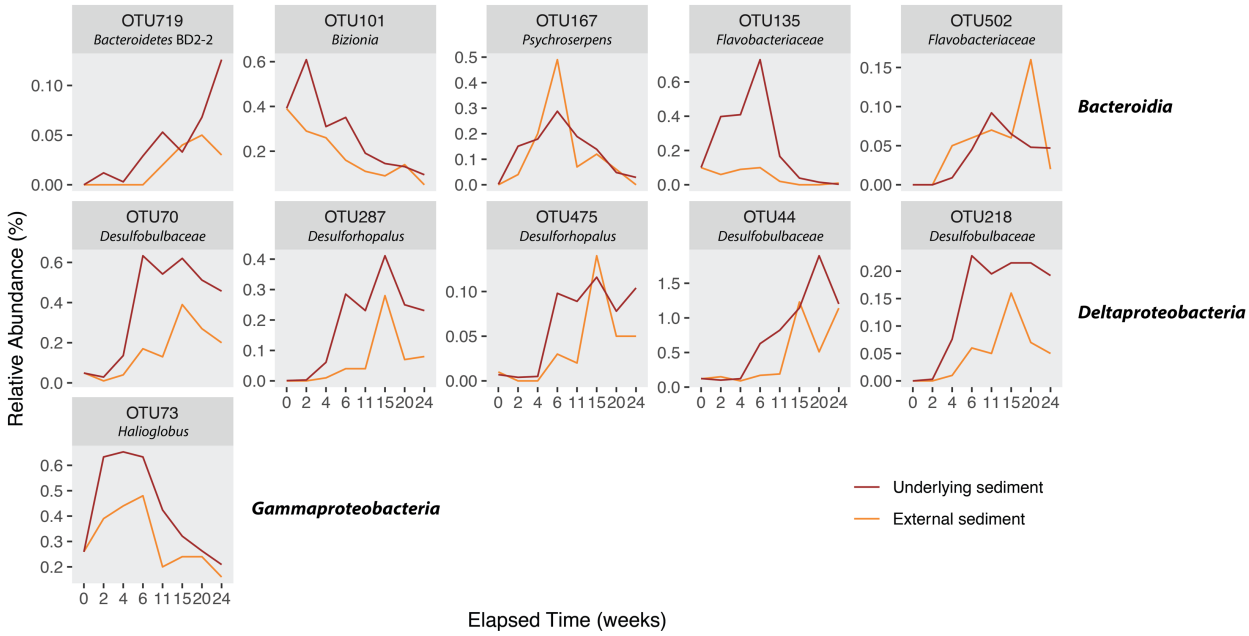

Chapter IV:

Specific detection of the genus *Zobellia* in macroalgae-dominated habitats

Résumé du chapitre

Le genre *Zobellia* est considéré comme un organisme modèle dans l'étude de la dégradation microbienne de la biomasse algale. Cependant, très peu de données sont disponibles sur la présence et l'abondance de ce genre dans les habitats dominés par les macroalgues.

Afin d'y remédier, nous avons adapté et optimisé des protocoles de PCR quantitative (qPCR) et de fluorescence *in situ* par hybridation (FISH), deux outils moléculaires largement utilisés pour la détection spécifique de taxons d'intérêt présents dans le biotope étudié. La mise en place de ces protocoles est présentée dans la **Partie 1** de ce chapitre (Brunet et al., 2021, accepté). Afin de détecter avec précision la présence de *Zobellia* spp. à la surface de macroalgues, des amorces de qPCR et une sonde FISH ciblant spécifiquement le gène de l'ARNr 16S des espèces de ce genre ont été conçues *in silico*. Leur spécificité et leur robustesse ont été confirmées sur des cultures pures. Il a été montré en particulier que même les souches présentant de fortes similarités de séquence au niveau de la région ciblée avec le genre *Zobellia,* comme des membres des genres *Maribacter*, *Lewinella* ou *Marinirhabdus*, n'étaient pas détectées. Le protocole de qPCR développé dans ce chapitre permet de déterminer avec précision entre 10 et 10^8 copies du gène de l'ARNr 16S spécifique de *Zobellia* dans un échantillon complexe. Ces deux outils complémentaires ont par la suite été appliqués sur des échantillons de macroalgues collectés sur l'estran. Le protocole de FISH a permis de visualiser des cellules de *Zobellia* au microscope confocal à la surface de l'algue rouge *Palmaria palmata* et de l'algue verte *Ulva lactuca*. Il constitue en ce sens un outil intéressant pour élucider l'organisation spatiale du genre *Zobellia* au sein du biofilm et ses potentielles interactions avec l'hôte ou les autres taxons bactériens. C'est une technique qui reste cependant à optimiser pour l'appliquer sur une plus grande diversité de macroalgues.

Dans la **Partie 2** de ce chapitre, la méthode de qPCR a été utilisée afin de quantifier l'abondance du genre *Zobellia* au sein de microbiotes épiphytes d'algues collectés tous les mois pendant 1 an sur la surface de cinq algues différentes, représentant 240 échantillons au total. La présence de *Zobellia* spp. a été détectée à la surface de macroalgues appartenant aux trois phyla et son abondance varie selon les saisons et la partie du thalle considéré. Sur des algues vivantes, le genre *Zobellia* représente moins de 0,002 % de la communauté bactérienne en été contre 0,03-0,5 % en automne-hiver. La proportion de *Zobellia* spp. sur les algues en décomposition échouées sur l'estran est environ 10 fois plus importante et s'élève à 8 % de la communauté totale dans certains échantillons. Ce résultat suggère d'un point de vue écologique le rôle crucial des espèces de *Zobellia* dans le recyclage de la biomasse algale.

Afin d'apprendre la méthode FISH/CARD-FISH et la développer pour la détection spécifique du genre *Zobellia*, j'ai effectué un séjour de 3 semaines en Avril 2019 dans l'équipe d'écologie moléculaire Molecol de l'institut Max Planck de Brême en Allemagne, aux côtés des Dr. Rudolf Amann et Bernhard Fuchs. Au sein de ce chapitre, j'ai donc participé à la mise au point de la méthode FISH/CARD-FISH

ainsi qu'à l'application des méthodes CARD-FISH et qPCR sur les échantillons environnementaux et aux analyses qui en découlent.

Part 1:

Development and optimization of qPCR and CARD-FISH protocols for the specific detection of *Zobellia* spp.

Specific detection and quantification of the marine flavobacterial genus *Zobellia* on macroalgae using novel qPCR and CARD-FISH assays

Maéva Brunet[a], Nolwen Le Duff[a], Bernhard M. Fuchs[b], Rudolf Amann[b], Tristan Barbeyron[a] and François Thomas[a#]

[a] Sorbonne Université, CNRS, Integrative Biology of Marine Models (LBI2M), Station Biologique de Roscoff (SBR), 29680, Roscoff, France.

[b] Department of Molecular Ecology, Max Planck Institute for Marine Microbiology, Bremen, Germany

Running head: *Zobellia* quantification on macroalgae

#Address correspondence to François Thomas, francois.thomas@sb-roscoff.fr

Article in press in Systematic and Applied Microbiology
https://doi.org/10.1016/j.syapm.2021.126269

Summary

Abstract

The flavobacterial genus *Zobellia* is considered as a model to study macroalgal polysaccharide degradation. The lack of data regarding its prevalence and abundance in coastal habitats constitutes a bottleneck to assess its ecological strategies. To overcome this issue, real-time quantitative PCR (qPCR) and fluorescence *in situ* hybridization (FISH) methods targeting the 16S rRNA gene were optimized to specifically detect and quantify *Zobellia* on the surface of diverse macroalgae. The newly designed qPCR primers and FISH probes targeted 98 and 100% of the *Zobellia* strains *in silico* and their specificity was confirmed using pure bacterial cultures. The dynamic range of the qPCR assay spanned 8 orders of magnitude from 10 to 10^8 16S rRNA gene copies and the detection limit was 0.01% relative abundance of *Zobellia* in environmental samples. *Zobellia*-16S rRNA gene copies were detected on all surveyed brown, green and red macroalgae, in proportion varying between 0.1 and 0.9% of the total bacterial copies. The absolute and relative abundance of *Zobellia* varied with tissue aging on the kelp *Laminaria digitata*. *Zobellia* cells were successfully visualized in *Ulva lactuca* and stranded *Palmaria palmata* surface biofilm using CARD-FISH, representing in the latter 10^5 *Zobellia* cells.cm^{-2} and 0.43% of total bacterial cells. Overall, qPCR and CARD-FISH assays enabled robust detection, quantification and localization of *Zobellia* representatives in complex samples, underlining their ecological relevance as primary biomass degraders potentially cross-feeding other microorganisms.

Keywords: *Zobellia*, qPCR, CARD-FISH, macroalgae, marine flavobacteria

Highlights

- *Flavobacteriia* are key players of carbon recycling in coastal ecosystems
- Among them, the genus *Zobellia* is considered as specialist of macroalgae degradation
- We developed qPCR and CARD-FISH assays allowing robust detection, quantification and localization of *Zobellia* on macroalgae
- These tools may help unveil the interactions between *Zobellia* spp., macroalgae and other microbial taxa

Introduction

Macroalgae are dominant primary producers in coastal ecosystems and constitute a large reservoir of organic matter worldwide. A wide range of microorganisms colonize macroalgal surfaces [20]. These biofilms contain diverse bacteria at densities ranging between 10^6 and 10^9 cells.cm^{-2} [35], which contribute to the remineralization of algal biomass [33]. Among those are the members of the genus *Zobellia* (phylum *Bacteroidetes,* class *Flavobacteriia*), first described by Barbeyron et al. [8]. To date, seven valid species compose the genus, namely *Z. amurskyensis, Z. galactanivorans, Z. laminariae, Z. nedashkovskayae, Z. russellii*, *Z. roscoffensis* and *Z. uliginosa.* They were isolated from marine environments throughout the world, notably from the surface of brown [9,37], red [40] and green macroalgae [37]. Additionally, the NCBI database references 65 unclassified *Zobellia* strains, mostly isolated from seaweeds. This genus comprises highly potent degraders of macroalgal polysaccharides. Described members of the genus *Zobellia* can grow on algal polysaccharides such as agar, porphyran and carrageenans from red algae and

62 laminarin, alginate and fucoidans from brown algae, in line with the high number of
63 carbohydrate-active enzymes (CAZyme) encoded in their genomes [10,16]. A recent survey of
64 the twelve available *Zobellia* genomes revealed that CAZyme-encoding genes accounted for
65 more than 6% of the genomic content, from 263 genes in *Z. nedashkovskayae* Asnod3-E08-A to
66 336 genes in *Z. galactanivorans* Dsij^T [15], illustrating the specialization of *Zobellia*
67 representatives in the degradation of algal polysaccharides. Accordingly, *Z. galactanivorans*
68 Dsij^T has become a model for algal polysaccharide breakdown and assimilation [32], allowing the
69 discovery of many novel polysaccharidases and Polysaccharide Utilization Loci (PULs) targeting
70 algal compounds [21,28,45]. Despite the potential of *Zobellia* strains for algal biomass recycling,
71 little is known regarding their prevalence and abundance in macroalgae-dominated habitats,
72 hindering our understanding of their role in coastal biogeochemistry. Molecular studies revealed
73 the presence of *Zobellia* members in diverse coastal ecosystems [1,19,29,34]. Searches in marine
74 metagenomes show numerous hits with high sequence identities (>90%) to *Zobellia* genes in a
75 variety of environments rich in organic carbon, including algal microbiomes, coastal sediments
76 and seawater from the Atlantic and Pacific Oceans as well as the North Sea and the English
77 Channel (**Supplementary Table 1**). Overall, this suggests a widespread distribution and
78 ecological relevance of *Zobellia* for carbon cycling in coastal ecosystems. However,
79 metagenomic sequencing does not allow a precise quantification of taxon abundance in the
80 environment and can be biased by promiscuous taxonomic sequence assignation. This prompted
81 us to develop new tools targeting the genus *Zobellia*, which would allow specific detection in
82 complex samples, cell localization and both absolute and relative quantification of its abundance.
83 Real-time quantitative polymerase chain reaction (qPCR) and fluorescence *in situ* hybridization
84 (FISH) are two well-established molecular methods for specific bacterial taxa detection. qPCR is
85 a fast, highly sensitive and specific tool allowing absolute quantification of DNA gene copies and

is suitable to detect minor amounts of target DNA [24]. qPCR assays were previously developed to quantify microbial taxa associated with macroalgae, such as endophytic eukaryotic pathogens in brown seaweeds [13,25], bacterial pathogens on *Saccharina latissima* [6] or the genus *Pseudoalteromonas* at the surface of green macroalgae [44]. FISH is a widely used method in microbial ecology for cell identification and enumeration in complex environments. Its principle is based on the use of rRNA-targeted oligonucleotide probes labeled with fluorescent dyes, which allow the detection of a defined group of microorganisms [3]. The use of horseradish peroxidase-labeled probes in combination with catalyzed reported deposition (CARD) of fluorescently labeled tyramides was then developed to enhance the fluorescence and improve the detection signal [38]. FISH combined or not with catalyzed reporter deposition (CARD-FISH) was successfully applied previously to enumerate seaweed-associated epiphytic or endophytic bacteria [12,31,46,48,49]. Here, we describe new qPCR and FISH protocols specifically targeting the genus *Zobellia*, allowing its detection, absolute quantification and localization at the surface of macroalgae. qPCR primers and FISH probes were designed and validated *in silico*. Both methods were optimized on pure bacterial cultures before being applied on environmental samples.

Material and Methods

Bacterial strains

All bacterial strains used in this study are listed in **Supplementary Table 2** and were grown in ZoBell 2216 medium [53].

106 **Environmental samples**

107 Surface microbiota were sampled in February 2020 using sterile swabs on healthy specimens of
108 *Laminaria digitata* (Ldig)*, Ascophyllum nodosum* (Anod)*, Ulva lactuca* (Ulac) and *Palmaria*
109 *palmata* (Ppal) at the Bloscon site (48°43'29.982'' N, 03°58'8.27'' W) in Roscoff (France).
110 Three individuals of each species were sampled. One additional sample was obtained from a
111 stranded specimen of *P. palmata* at the same time (PpalS). The swabbed surface was 25 cm^2 on
112 both sides of the algal thallus. Three different regions of the kelp *L. digitata* were sampled: the
113 basal meristem (young tissue, hereafter LdigB), the medium frond (ca. 20 cm away from the
114 meristem, hereafter LdigM) and the old frond (the blade tip, hereafter LdigO). Swabs were
115 immersed in DNA/RNA Shield reagent (ZymoBiomics), kept on ice during transport (< 2 h) and
116 stored at -20°C until DNA extraction. Algal pieces from the same individuals were collected with
117 sterile punchers (1.3 cm diameter), rinsed with autoclaved seawater and placed directly in 2%
118 PFA in PBS overnight at 4°C. All fixed samples were washed twice in PBS and stored in
119 PBS:EtOH (1:1 v/v) at -20°C before FISH analysis.

120 **DNA extraction**

121 Environmental DNA from swabs was extracted using the DNA/RNA Miniprep kit
122 (ZymoBiomics) within 1 month after sampling. Genomic DNA (gDNA) was extracted from *Z.*
123 *galactanivorans* Dsij^T and *Z. russellii* KMM 3677^T pure cultures as described in Gobet *et al.* [26].

124 **Primer design**

125 *Zobellia*-specific PCR primers were designed using DECIPHER
126 (http://www2.decipher.codes/DesignPrimers.html) with 139 aligned 16S rRNA gene sequences
127 from flavobacteria, including 52 *Zobellia* strains and 87 sequences representing 23 close genera

(**Supplementary File 1**). Primers were searched to amplify 75-200 bp products, with DECIPHER default parameters. The designed sets of primers were tested for specificity against the reference database SILVA 138.1 SSU Ref using SILVA TestPrime with 0 mismatch allowed (**Table 1**).

qPCR assays

qPCR was carried out in 384-multiwell plates on a LightCycler 480 Instrument II (Roche). Each 5 µl reaction contained 2.5 µl of LightCycler 480 SYBR Green I Master mix 2X (Roche Applied Science), 0.5 µl of each primer and 1.5 µl of template DNA. Each reaction was prepared in technical triplicates. The amplification program consisted of an initial hold at 95°C for 10 min followed by 45 cycles of 95°C for 10 s, 20 s at the chosen annealing temperature (T_a), and 72°C for 10 s. After the amplification step, dissociation curves were generated by increasing the temperature from 65°C to 97°C.

The qPCR protocol targeting *Zobellia* was first optimized on gDNA purified from cultured *Zobellia* strains, by testing the efficiency of three different primer pairs and varying T_a (55-65°C) and final primer concentration (100-500 nM). Strains *Cellulophaga baltica* NN015840^T, *Cellulophaga* sp. Asnod2-G02 [34] and *Maribacter forsetii* KT02ds18-6^T were used as negative controls.

The optimum parameters were then used for qPCR amplifications on environmental DNA as described below, using *Zobellia*-specific primers 142F/289R. The amplicon size was checked by 2% agarose gel electrophoresis.

Total and *Zobellia* 16S rRNA gene copies were quantified in environmental samples using the universal bacterial primers 926F/1062R [5] and the *Zobellia*-specific primers 142F/289R, respectively. Reactions were prepared with 1.5 µl of template DNA normalized at 0.5 ng.µl^{-1} with

T_a set to 60°C for universal primers and 64°C for *Zobellia*-specific primers and a primer concentration in the reaction of 300 nM for both pairs. Serial dilutions of purified *Z. galactanivorans* Dsij^T gDNA ranging from 10 to 10^8 16S rRNA gene copies were used as a standard curve and were amplified in triplicate in the same run as the environmental samples. No-Template Controls (NTC) were included in the run. The LightCycler 480 Software v1.5 was used to determine the threshold cycle (C_t) for each sample. Linear standard curves were obtained by plotting C_t as a function of the logarithm of the initial 16S rRNA gene copies. PCR efficiency was calculated as $10^{-1/slope}$ - 1 [14]. One-way ANOVA analyses followed by pairwise post-hoc Tukey HSD were conducted in R v3.6.2 [41]. Details on qPCR assays are given in **Supplementary File 2**, following the MIQE guidelines [14].

Sequencing of qPCR products

qPCR products obtained from two selected environmental samples (LdigO and PpalS) were re-amplified using a Taq DNA polymerase to add 3' A-overhangs and ligated into pCR 2.1-TOPO vector using the TOPO TA cloning kit (Invitrogen) before transformation into *Escherichia coli* NEB5α cells (New England Biolabs). Clones were grown overnight on LB-agar plates containing 50 µg.ml^{-1} kanamycin, with addition of isopropyl β-D-1-thiogalactopyranoside (IPTG) and 5-bromo-4-chloro-3-indolyl-β-D-galactopyranoside (X-Gal) following the manufacturer's instructions. For each environmental sample, 10 white or light-blue clones were randomly picked and grown separately in LB medium (50 µg.ml^{-1} kanamycin) overnight. Plasmids were purified using the Wizard Plus SV Minipreps DNA Purification System (Promega) and sequenced with the M13 Forward (-20) primer. Insert DNA sequences were analyzed by blastn against the NCBI 16S rRNA gene database.

FISH probe and helper design

The ZOB137 FISH probe specific to the genus *Zobellia* (**Table 1**) was designed using the ARB software (http://www.arb-home.de). Available *Zobellia* 16S rRNA gene sequences were aligned using SINA v1.6.1 and added to the Silva reference database (SILVA132_SSURef_12.12.17) in ARB to be included in the Silva tree. All *Zobellia* sequences were selected for probe search using the PROBE DESIGN tool with the following parameters: Max. non-group hits: 2, Min group hits (%): 100, Length of probe: 18, Temperature: 30-100, G+C content: 50-100. The newly designed ZOB137 probe, as well as the EUB338 I-III [2,18] and the NON338 [51] probes, were ordered from Biomers (www.biomers.net), labeled either with the fluorescent dye Atto488 (FISH protocol) or with the horseradish peroxidase (HRP) enzyme (CARD-FISH protocol). Three non-labeled helper oligonucleotides (21 nt) were designed to bind adjacent to the ZOB137-target site (**Fig. S1B**) in order to enhance the probe signal (see H116, H155 and H176 in **Table 1**). All probes and helpers were resuspended in nuclease-free water and diluted to a working stock concentration of 8.4 pmol.µl^{-1}.

Optimization of hybridization conditions

FISH formamide melting curves were performed with the ZOB137-Atto488 probe on pure cultures of *Z. galactanivorans* Dsij^{T} and *Z. russellii* KMM 3677^{T}. Cells were grown at room temperature in ZoBell medium for 3 days and fixed in 1% paraformaldehyde (PFA) in PBS [2]. Fixed cells were spotted on glass slides, air-dried and dehydrated in successive short EtOH-baths. Hybridization buffer (0.9 M NaCl, 20 mM Tris-HCl pH8, 0.01% SDS) with increasing formamide concentration (10 to 70%) was mixed (9:1) with the ZOB137-Atto488 probe and spotted on each well. After incubation for 2 h at 46°C, slides were washed 15 min in the corresponding preheated washing buffer (0.45 to 0 M NaCl, 1 M Tris-HCl pH8, 0 to 5 mM

EDTA pH8, 0.01% SDS) at 48°C. Counter-staining was performed with 4',6-diamidino-2-phenylindole (DAPI, 1 $\mu g.mg^{-1}$) and slides were mounted using Citifluor:Vectashield (3:1). Fluorescence was observed on a Nikon 50i epifluorescence microscope (filter ET-EGFP (LP)) equipped with an AxioCam MRc camera (Carl Zeiss, Germany). Signal intensity was quantified using ImageJ [43] on three random images per hybridization. Only the green channel was analyzed and the background signal was removed. For each hybridization, the maximum intensity of 50 randomly selected cells was measured.

CARD-FISH

CARD-FISH was performed using a method adapted from Pernthaler *et al.* [38] and optimized for the detection of alga-attached bacteria [49]. Fixed *Zobellia* cells from pure cultures were harvested onto a 0.2 µm polycarbonate membrane. Membrane portions or fixed algal samples (ca. 25-30 mm^2) were embedded in 0.1% LE agarose and bleached in ethanol with increasing concentration. Cells were permeabilized with lysozyme (10 $mg.ml^{-1}$, 15 min, 37°C). Endogenous peroxidases were inactivated by short incubation in 0.1 M HCl followed by 10 min in 3% H_2O_2 for membrane portions or by incubation in 0.15% H_2O_2 in methanol (30 min) for algal pieces. Samples were covered with the hybridization mix (0.9 M NaCl, 20 mM Tris-HCl pH8, 35% formamide, 1% blocking reagent, 10% dextran sulfate, 0.02% SDS, 28 nM probe and each helper if needed) for 2.5 h at 46°C. Samples were washed 15 min in a preheated washing buffer (70 mM NaCl, 1 M Tris-HCl pH8, 5 mM EDTA pH8, 0.01% SDS) at 48°C and 15 min in 1× PBS before being covered with a detection solution (1× PBS, 2 M NaCl, 0.1% blocking reagent, 10% dextran sulfate, 0.0015% H_2O_2 and 1 $\mu g.ml^{-1}$ of $Alexa_{546}$-labeled tyramides) for amplification (45 min, 46°C). DAPI (1 $\mu g.mg^{-1}$) counter-staining was performed and slides were mounted once samples were completely dry with Citifluor:Vectashield (3:1). Membrane portions were visualized with a

Leica DMi8 epifluorescent microscope equipped with an oil objective 100X and a Leica DFC3000 G camera (Wetzlar, Germany). Cells on algal tissues were visualized with a confocal microscope Leica TCS SP8 equipped with HC PL APO 63x/1.4 oil objective and K-Cube filters A UV and N2.1 using the 405 et 552 nm lasers to detect DAPI and $Alexa_{546}$ signal, respectively. Z-stack images were collected due to the uneven algal surface (between 21 and 75 single layers of 0.15 or 0.3 µm thickness, depending on the observed field). Total and *Zobellia* cell counts were processed on maximum intensity images with Imaris v9.5.1. A total of 21 000 cells were counted automatically from 7 different fields.

Results

Optimization of qPCR parameters for specific detection of the genus *Zobellia*

One possible forward primer (142F) and three possible reverse primers (285R, 289R and 294R) were designed to target specifically the V2 region of the 16S rRNA gene in the genus *Zobellia* (**Fig. S1A**). The target regions were identical in multiple rRNA operons found in available *Zobellia* genomes (**Supplementary Table 3**). *In silico* tests confirmed that the three primer pairs match only *Zobellia* sequences in the entire 16S rRNA database (**Table 1**). Out of the 54 *Zobellia* strains available in SILVA SSU r138.1, only the two strains *Zobellia* sp. SED8 and *Zobellia* sp. M-2 were missed by a stringent *in silico* test (no mismatch allowed), the former being rescued when relaxing the stringency (1 mismatch allowed with a 3-bp perfect match zone at 3' end of primers).

We assessed the optimal annealing temperature (T_a) and primer concentration for qPCR using 10^4 16S rRNA gene copies from two *Zobellia* strains. Since the 16S rRNA gene sequences of all valid *Zobellia* species were identical in the region targeted by primers, we focused our efforts on

242 *Z. galactanivorans* Dsij^T and *Z. russellii* KMM 3677^T, which belong to two separate subclades
243 based on core genome phylogeny [15]. Similar results were obtained with the three qPCR primer
244 pairs and only those obtained with 142F/289R are shown in **Fig. 1**. Amplification was successful
245 for the two *Zobellia* species with primer concentration ranging between 100 - 500 nM **(Fig. 1A)**
246 and T_a ranging between 55 - 65°C (**Fig. 1B**). Agarose gel electrophoresis of qPCR products
247 showed a single band at the expected amplicon size (148 nt) with *Zobellia* gDNA (**Fig. S2A**). A
248 slight increase of C_t was observed on *Zobellia* gDNA for primer concentration below 200 nM
249 (**Fig. 1B**). Therefore, primer concentration was set at 300 nM for further experiments. C_t
250 remained stable irrespective of the temperature (around 24 and 21 for *Z. galactanivorans* and *Z.*
251 *russellii* respectively).
252 Ten-fold serial dilutions of *Z. galactanivorans* Dsij^T gDNA were amplified (T_a = 60°C, [primers]
253 = 300 nM) to evaluate the qPCR dynamic range and efficiency of each primer pair. The highest
254 efficiency (88%) was observed for the pair 142F/289R, compared to 142F/285R and 142F/294R
255 (86% and 81%, respectively) (**Fig. 1C**). The linear dynamic range spanned 8 orders of
256 magnitude, from 10 to 10^8 16S rRNA gene copies. To ensure high efficiency and specificity of
257 qPCR assays on environmental samples, we further used the pair 142F/289R and a high
258 annealing temperature (T_a = 64°C). With these conditions, the strains *Cellulophaga baltica*
259 NN015840^T and *Cellulophaga* sp. Asnod2-G02 were used as negative controls to check the assay
260 specificity, since the target regions of their 16S rRNA gene sequences were the closest to that of
261 *Zobellia* based on SILVA TestPrime results (3 mismatches with 142F, 3 mismatches with 289R).
262 We also tested amplification from *Maribacter forsetii* KT02ds18-6^T (5 and 4 mismatches to 142F
263 and 289R, respectively), since *Maribacter* is the closest described genus to *Zobellia* [7]. No
264 amplification was detected with any of these negative controls (**Fig. S2A**). In addition,
265 amplification from environmental DNA yielded a single product at the expected size (**Fig. S2B**),

with melting curves showing a single dissociation peak (**Fig. S2D**) similar to that obtained on pure *Z. galactanivorans* Dsij^T gDNA (**Fig. S2C**). qPCR products obtained with two selected environmental samples (LdigO and PpalS, see below) were sequenced (**Supplementary File 3**). All retrieved sequences (20/20) had their best blastn hit against 16S rRNA gene sequences from *Zobellia* spp (**Supplementary Table 4**), confirming the specificity of the assay on natural samples. Sensitivity and specificity were further assessed using environmental DNA extracted from natural seawater devoid of *Zobellia* (no amplification detected after 45 cycles of qPCR with primers 142F/289R) mixed with 10-fold serial dilutions of *Z. galactanivorans* Dsij^T gDNA. The proportion of *Zobellia* was calculated by dividing *Zobellia* 16S rRNA gene copies (amplification with primers 142F/289R) by total 16S rRNA gene copies (amplification with primers 926F/1062R) (**Fig. 1D**). Measured and theoretical proportions were highly congruent, confirming the specificity of the method toward *Zobellia* spp. The assay shows a strong sensitivity, as it can detect minor proportions of *Zobellia* DNA (approximately 0.01%, i.e., 5 16S rRNA genes copies) when combined with environmental DNA. Detection was saturated when the proportion of *Zobellia* was close to 100% (**Fig. 1D**, top-right corner), a situation unlikely to happen in natural samples.

Characterization of the newly-designed FISH probe ZOB137

Probe design yielded one candidate, ZOB137 (**Table 1**) covering 100% of the target group. ZOB137 target site was similar to that of primer 142F (**Fig. S1B**). *In silico* analysis showed ZOB137 matches the 54 *Zobellia* sequences available in the SILVA SSU r138.1 database. Three outgroup hits were found (uncultured members of the genera *Aquibacter* and *Euzebyella*).
We optimized the hybridization stringency for FISH with ZOB137, i.e. the highest formamide (FA) concentration in the hybridization buffer that does not result in loss of fluorescence intensity

of the target cells [39]. Melting curves were obtained from hybridizations of *Z. galactanivorans* Dsij^T and *Z. russellii* KMM 3677^T with ZOB137-Atto488 at increasing FA concentrations (**Fig. 2**). For both strains, cell fluorescence intensity was stable until 35% FA, slightly decreased using 40% FA and dropped using 50-70% FA. Therefore, the optimal FA concentration for ZOB137 was set to 35% for further experiments. ZOB137 was tested using these conditions with two additional *Zobellia* strains, *Z. amurskyensis* KMM 3526^T and *Z. roscoffensis* Asnod1-F08^T, and a fluorescent signal was observed (data not shown).

The CARD-FISH signal obtained after hybridization of *Z. galactanivorans* remained weak and might not be detectable in environmental samples (**Fig. 3E**). The addition of three helper oligonucleotides in the hybridization mix (H116, H155 and H176) increased the signal intensity ca. 3-fold under the same exposure time (**Fig. 3F**). CARD-FISH specificity was tested using *Lewinella marina* MKG-38^T and *Marinirhabdus citrea* MEBiC09412^T that feature only one mismatch with the ZOB137 target sequence (respectively C and A instead of T at position 145). No CARD-FISH signal was observed after hybridization of both strains with ZOB137 and helpers (**Fig. 3G-H**), confirming the absence of hybridization to non-target organisms using 35% FA.

Application of *Zobellia*-specific qPCR and CARD-FISH assays on natural macroalgal microbiota

These newly-designed qPCR and CARD-FISH assays were tested on environmental samples, to detect and quantify the abundance of the genus *Zobellia* on the surface of macroalgae. Total and *Zobellia* 16S rRNA gene copies were quantified on the surface of two fresh brown macroalgae *Laminaria digitata* (base, medium and old part) and *Ascophyllum nodosum,* a fresh green

311 macroalga *Ulva lactuca* and a red macroalga *Palmaria palmata* (fresh and stranded individuals)
312 (**Fig. 4**).
313 No significant difference was observed in the average total copies.cm^{-2} between the basal (0.27 ×
314 10^{6} copies.cm^{-2}) and medium (1.8 × 10^{6} copies.cm^{-2}) part of *L. digitata* (Tukey HSD post-hoc
315 pairwise comparisons, $P = 0.8$). However, the total number of copies was significantly higher on
316 the old blade where 14.6 × 10^{6} copies.cm^{-2} were quantified ($P = 0.003$ and $P = 0.005$ in
317 comparison to LdigB and LdigM, respectively). The average total copy number on *A. nodosum,*
318 *U. lactuca* and *P. palmata* fresh and stranded was estimated at 7.2, 5.7, 5.1 and 14.6 × 10^{6}
319 copies.cm^{-2}, respectively.
320 16S rRNA gene copies were also detected on the four macroalgae with the *Zobellia*-specific
321 primers (**Fig. 4B**). The number of *Zobellia*-16S rRNA gene copies.cm^{-2} differed along the *L.*
322 *digitata* blade (ANOVA, $F_{2,6} = 31.8$, P = 0.001). It was higher on the old blade (10.5 × 10^{3}
323 copies.cm^{-2}) compared to the basal (1.3 x 10^{3} copies.cm^{-2}, Tukey HSD $P = 0.001$) and the
324 medium (2.5 × 10^{3} copies.cm^{-2}, $P = 0.002$) part. The proportion of *Zobellia* cells within the
325 epiphytic communities (**Fig. 4C**) was significantly higher on the basal part (0.54%) than on the
326 old blade of *L. digitata* (0.07%) ($P = 0.01$). Fresh *A. nodosum, U. lactuca* and *P. palmata*
327 displayed 9.7, 6.1 and 11.3 × 10^{3} *Zobellia* copies.cm^{-2} representing 0.14, 0.12 and 0.21% of the
328 total number of copies, respectively. On the surface of the stranded *P. palmata* sample, 1.3 × 10^{5}
329 *Zobellia* copies.cm^{-2} were estimated, ie. 0.87% relative abundance.
330 The genus *Zobellia* was successfully detected on the surface of the stranded *P. palmata*
331 individual and on a fresh individual from *U. lactuca* using CARD-FISH (**Fig. 5**). ZOB137-
332 hybridized cells were well visible among the epiphytic bacterial communities. A 2-3 µm thick
333 space without fluorescence was observable between the biofilm and the external algal cells, likely
334 due to the algal extracellular matrix. ZOB137-hybridized cells did not seem to form aggregates

on both macroalgae. *Zobellia* cells observed on algal tissues (**Fig. 5**) were shorter than those observed in pure cultures in rich medium (**Fig. 3F**), indicating different morphologies depending on environmental conditions. After image analysis on *P. palmata,* 1.0×10^5 *Zobellia* cells were counted per cm^2 of algal surface, representing ca. 0.43% of detected bacterial cells. *Zobellia* cells displayed a homogeneous distribution on stranded *P. palmata* but not on the surface of *U. lactuca* where *Zobellia*-specific signal was visible only in a few areas. Hence, *Zobellia* cell count was not performed on *U. lactuca* as it would not have been reliable.

Discussion

qPCR and CARD-FISH are widely used, complementary molecular methods to examine microbial abundance in environmental samples. qPCR is a fast, highly sensitive and specific tool allowing absolute quantification of gene copies, suitable to detect minor amounts of target DNA [24]. CARD-FISH is more time-consuming but is not subject to DNA extraction or PCR biases and enables direct visualization and localization of single bacterial cells associated with the host. qPCR using universal bacterial primers estimated around 10^6-10^7 total 16S rRNA gene copies.cm^{-2} on the different macroalgal species. Considering an average of 4 copies of 16S rRNA gene per bacterial cell [50], these results concur with previous studies showing 10^6-10^9 cells per cm^2 on algal surfaces [17,35]. qPCR assays on *L. digitata* samples showed that total bacterial abundance increased with kelp tissue age, corroborating observations made on different kelp species [36,42].

Newly designed qPCR and CARD-FISH assays specifically targeting the genus *Zobellia* were tested and optimized on pure cultures before application on macroalgal samples. qPCR assays using the novel *Zobellia*-specific primers 142F/289R were shown to be a robust, fast, high-

357 throughput and sensitive way to quantify the abundance of *Zobellia* spp. in environmental
358 samples. The detection limits were determined by pooling targeted with untargeted DNA, a
359 relevant approach as we aim to detect *Zobellia* in natural samples (as discussed in Skovhus *et al.*
360 [44]. This method allows the detection of minor proportions of *Zobellia* in environmental
361 samples (0.01%), which would be technically difficult using CARD-FISH.
362 CARD-FISH detection of non-abundant taxa directly on macroalgae is difficult due to the high
363 background autofluorescence of algal pigments. Here, algal bleaching was performed with
364 extended ethanol and methanol baths to reduce autofluorescence. Moreover, the addition of three
365 unlabeled helper oligonucleotides improved the CARD-FISH signal, facilitating cell
366 visualization. The secondary structure of the 16S rRNA target region for probe ZOB137 might
367 partly hinder hybridization [11,23]. The combined hybridization of multiple adjacent helper
368 oligonucleotides assisted to open the targeted region, facilitating probe binding. The use of
369 helpers for FISH was first described by Fuchs *et al.* [22] who recommended to test
370 experimentally their influence on the probe specificity. In our study, no hybridization signal was
371 detected using ZOB137 combined with helpers on two strains with single-mismatch, confirming
372 helpers did not impact probe specificity. A specific CARD-FISH signal was detected with
373 ZOB137 at the surface of macroalgae with a flat thin blade, such as the red seaweed *Palmaria*
374 *palmata* or the green seaweed *Ulva lactuca*. This new protocol represents a powerful tool to (i)
375 determine the spatial localization of *Zobellia* cells within macroalgal surface microbiota, (ii)
376 estimate their physical interactions with other taxa or the host and (iii) assess whether they are
377 structured into patches or evenly distributed on the surface, as it seems to be the case on *P.*
378 *palmata* thallus. Visualization was more complex with thicker algae such as *Laminaria*, since
379 multiple cell layers caused a strong autofluorescence masking the bacterial CARD-FISH signal.
380 Moreover, thick algal pieces sometimes decomposed during the CARD-FISH process as their

structure became weaker, more viscous and tissues tended to disintegrate during washing steps. Hence, specific taxa visualization on algal surfaces remains a challenge depending on algal species. A way to overcome these issues would be to embed algae in resin and cut thin thallus sections using a microtome prior to CARD-FISH, as it was successfully done in Ramirez-Puebla *et al*. [42] and Tourneroche *et al.* [46].

Altogether, our analyses revealed that the genus *Zobellia* was part of the microbiota of all tested macroalgae, including *U. lactuca*, *P. palmata*, *A. nodosum* and *L. digitata* on both young or old regions of the blade. This confirms its widespread distribution in algal microbiomes from temperate ecosystems, in line with *Zobellia* numerous adaptive traits to live on macroalgae such as the ability to degrade polysaccharides and to counteract antibacterial algal defense [10]. Previous studies already reported the presence of *Zobellia* spp. on *A. nodosum* (3% of the cultivable microbiota) [9,34] and *L. digitata* [47] in Roscoff. Since macroalgal microbiomes are diverse and can host hundreds of taxa [20], the observed frequency of 0.1-1% for *Zobellia* shows the quantitative relevance of this genus in macroalgae-dominated habitats. The highest *Zobellia* proportion was observed on the stranded decaying *P. palmata* individual, highlighting its putative important activity in macroalgal biomass recycling. Although not dominant in the bacterial communities, *Zobellia* spp. might act as primary degraders of algal polysaccharides due to their outstanding CAZyme repertoire, releasing degradation products that could fuel other taxa via cross-feeding interactions. In line with this, *Z. galactanivoran*s Dsij^{T} was recently shown to degrade intact kelp tissue, releasing soluble algal compounds that become accessible to opportunistic taxa [52]. The absolute number of *Zobellia* 16S rRNA gene copies was positively correlated with the age of the *L. digitata* tissues. Kelp decay is more pronounced at the tip of the blade, which might result in more available substrates for diverse bacterial algal degraders, including *Zobellia* spp. By contrast, the proportion of *Zobellia* 16S rRNA gene copies over total

copies was highest in the youngest region of *L. digitata* (i.e. the basal meristem). The high proportion of the genus *Zobellia* on young algal tissues might thus reflect its metabolic specialization towards complex polysaccharides found in the meristem, while it could be outcompeted by opportunistic taxa on the decaying old blade. *Zobellia* spp. might also be early colonizers of newly-produced meristematic tissues, reflecting their adaptation to attach to and live on algal surfaces. Moreover, intra-thallus variability of algal defense metabolites, such as iodine, reactive oxygen and nitrogen species and phlorotannins, might create different ecological micro-niches [4,27,30] selecting for specific taxa.

Using *P. palmata* surface microbiota as a test case, we showed that both the absolute number and proportion of ZOB137-hybridized cells concur with the qPCR-estimated *Zobellia* 16S rRNA gene copy number. However, it should be interpreted carefully as available *Zobellia* genomes feature between 1 to 4 copies of 16S rRNA genes (**Supplementary Table 3**), so qPCR results cannot be directly converted into a number of cells. Another bias might lie in the size of the sampled algal area, as bacteria were quantified from a 50-cm^2 surface with qPCR but CARD-FISH was performed only on 30-mm^2 algal pieces. Tourneroche and co-workers recently drew attention to the potential within-tissue spatial variability of kelp-associated bacterial communities [46]. Finally, CARD-FISH analyses detect metabolically active cells as the probe targets 16S rRNA, while here qPCR was applied on DNA samples and therefore could detect resting or dead cells. The close proximity of values obtained on stranded *P. palmata* with qPCR (1.3×10^5 copies.cm^{-2} for *Zobellia* 16S rRNA gene) and CARD-FISH (1.0×10^5 *Zobellia* cells.cm^{-2}) suggests that most *Zobellia* cells in this sample were active. In the future, the newly-designed primer pair 142F/289R could be used for reverse-transcription qPCR on RNA extracts to better estimate *Zobellia* transcriptional activity.

To conclude, we validated novel qPCR and CARD-FISH protocols to specifically target the marine flavobacterial genus *Zobellia*. We provide the first quantitative estimates of *Zobellia* absolute and relative abundance on different macroalgae, suggesting a widespread distribution. This work paves the way for further studies of the spatiotemporal dynamics of *Zobellia* in marine environments.

Acknowledgements

This work was supported by the French Government via the National Research Agency program ALGAVOR (ANR-18-CE02-0001-01).

We are grateful to Jörg Wulf and Andreas Ellrott for their help and advice during FISH experiments, to Dr. Sébastien Colin for guidance in confocal microscopy and to Dr. Erwan Corre and Jacky Ame for help with IMG analyses. This work has benefited from the facilities of the MERIMAGE and Genomer platforms (FR 2424, CNRS-Sorbonne Université, Roscoff). The authors have no conflict of interest to declare.

Author contributions following the CRediT taxonomy (https://casrai.org/credit/) are as follows: Conceptualization: FT; Formal analysis: MB, NLD, FT; Funding acquisition: FT; Investigation: MB, NLD, FT; Project administration: FT; Supervision: FT, TB, BF, RA; Visualization: MB, NLD, FT; Writing – original draft: MB, FT; Writing – review & editing: MB, BF, RA, TB, FT.

References

[1] Alonso, C., Warnecke, F., Amann, R., Pernthaler, J. (2007) High local and global diversity of Flavobacteria in marine plankton. Environ. Microbiol. 9(5), 1253–66, Doi:

10.1111/j.1462-2920.2007.01244.x.

[2] Amann, R.I., Binder, B.J., Olson, R.J., Chisholm, S.W., Devereux, R., Stahl, D.A. (1990) Combination of 16S rRNA-targeted oligonucleotide probes with flow cytometry for analyzing mixed microbial populations. Appl. Environ. Microbiol. 56(6), 1919–25, Doi: 10.1128/aem.56.6.1919-1925.1990.

[3] Amann, R.I., Ludwig, W., Schleifer, K. (1995) Phylogenetic identification and in situ detection of individual microbial cells without cultivation. Microbiol. Rev. 59(1), 143–69.

[4] Ank, G., Paradas, W. da C., Amado-Filho, G.M., da Gama, B.A.P., Pereira, R.C. (2014) Within-thallus variation on phlorotannin contents and physodes amount in *Stypopodium zonale* (Phaeophyceae). Panam. J. Aquat. Sci. 9(1), 1–7.

[5] Bacchetti De Gregoris, T., Aldred, N., Clare, A.S., Burgess, J.G. (2011) Improvement of phylum- and class-specific primers for real-time PCR quantification of bacterial taxa. J. Microbiol. Methods 86(3), 351–6, Doi: 10.1016/j.mimet.2011.06.010.

[6] Barberi, O.N., Byron, C.J., Burkholder, K.M., St. Gelais, A.T., Williams, A.K. (2020) Assessment of bacterial pathogens on edible macroalgae in coastal waters. J. Appl. Phycol. 32(1), 683–96, Doi: 10.1007/s10811-019-01993-5.

[7] Barbeyron, T., Carpentier, F., L'Haridon, S., Schüler, M., Michel, G., Amann, R. (2008) Description of *Maribacter forsetii* sp. nov., a marine *Flavobacteriaceae* isolated from North Sea water, and emended description of the genus *Maribacter*. Int. J. Syst. Evol. Microbiol. 58(4), 790–7, Doi: 10.1099/ijs.0.65469-0.

[8] Barbeyron, T., L'Haridon, S., Corre, E., Kloareg, B., Potin, P. (2001) *Zobellia galactanovorans* gen. nov., sp. nov., a marine species of *Flavobacteriaceae* isolated from a red alga, and classification of [*Cytophaga*] *uliginosa* (ZoBell and Upham 1944) Reichenbach 1989 as *Zobellia uliginosa* gen. nov., comb. nov. Int. J. Syst. Evol.

Microbiol. 51(Pt 3), 985–97.

[9] Barbeyron, T., Thiébaud, M., Le Duff, N., Martin, M., Corre, E., Tanguy, G., Vandebol, M., Thomas, F. (2021) *Zobellia roscoffensis* sp. nov. and *Zobellia nedashkovskayae* sp. nov., two flavobacteria from the epiphytic microbiota of the brown alga *Ascophyllum nodosum*, and emended description of the genus *Zobellia*. Int. J. Syst. Evol. Microbiol.

[10] Barbeyron, T., Thomas, F., Barbe, V., Teeling, H., Schenowitz, C., Dossat, C., Goesmann, A., Leblanc, C., Oliver Glöckner, F., Czjzek, M., Amann, R., Michel, G. (2016) Habitat and taxon as driving forces of carbohydrate catabolism in marine heterotrophic bacteria: Example of the model algae-associated bacterium *Zobellia galactanivorans* Dsij^{T}. Environ. Microbiol. 18, 4610–27, Doi: 10.1111/1462-2920.13584.

[11] Behrens, S., Fuchs, B.M., Mueller, F., Amann, R. (2003) Is the in situ accessibility of the 16S rRNA of *Escherichia coli* for Cy3-labeled oligonucleotide probes predicted by a three-dimensional structure model of the 30S ribosomal subunit? Appl. Environ. Microbiol. 69(8), 4935–41, Doi: 10.1128/AEM.69.8.4935-4941.2003.

[12] Bengtsson, M.M., Øvreås, L. (2010) *Planctomycetes* dominate biofilms on surfaces of the kelp *Laminaria hyperborea*. BMC Microbiol. 10(1), 261, Doi: 10.1186/1471-2180-10-261.

[13] Bernard, M., Rousvoal, S., Jacquemin, B., Ballenghien, M., Peters, A.F., Leblanc, C. (2018) qPCR-based relative quantification of the brown algal endophyte *Laminarionema elsbetiae* in *Saccharina latissima*: variation and dynamics of host—endophyte interactions. J. Appl. Phycol. 30(5), 2901–11, Doi: 10.1007/s10811-017-1367-0.

[14] Bustin, S.A., Benes, V., Garson, J.A., Hellemans, J., Huggett, J., Kubista, M., Mueller, R., Nolan, T., Pfaffl, M.W., Shipley, G.L., Vandesompele, J., Wittwer, C.T. (2009) The MIQE guidelines: Minimum information for publication of quantitative real-time PCR experiments. Clin. Chem. 55(4), 611–22, Doi: 10.1373/clinchem.2008.112797.

[15] Chernysheva, N., Bystritskaya, E., Likhatskaya, G., Nedashkovskaya, O., Isaeva, M. (2021) Genome-wide analysis of PL7 alginate lyases in the genus *Zobellia*. Molecules 26(2387).

[16] Chernysheva, N., Bystritskaya, E., Stenkova, A., Golovkin, I., Nedashkovskaya, O., Isaeva, M. (2019) Comparative genomics and CAZyme genome repertoires of marine *Zobellia amurskyensis* KMM 3526T and *Zobellia laminariae* KMM 3676T. Mar. Drugs 17(12), 661, Doi: 10.3390/md17120661.

[17] Corre, S., Prieur, D. (1990) Density and morphology of epiphytic bacteria on the kelp *Laminaria digitata*. Bot. Mar. 33(6), 515–24, Doi: 10.1515/botm.1990.33.6.515.

[18] Daims, H., Brühl, A., Amann, R., Schleifer, K.H., Wagner, M. (1999) The domain-specific probe EUB338 is insufficient for the detection of all bacteria: Development and evaluation of a more comprehensive probe set. Syst. Appl. Microbiol. 22(3), 434–44, Doi: 10.1016/S0723-2020(99)80053-8.

[19] Dogs, M., Wemheuer, B., Wolter, L., Bergen, N., Daniel, R., Simon, M., Brinkhoff, T. (2017) *Rhodobacteraceae* on the marine brown alga *Fucus spiralis* are abundant and show physiological adaptation to an epiphytic lifestyle. Syst. Appl. Microbiol. 40(6), 370–82, Doi: 10.1016/j.syapm.2017.05.006.

[20] Egan, S., Harder, T., Burke, C., Steinberg, P., Kjelleberg, S., Thomas, T. (2013) The seaweed holobiont: Understanding seaweed-bacteria interactions. FEMS Microbiol. Rev. 37(3), 462–76, Doi: 10.1111/1574-6976.12011.

[21] Ficko-Blean, E., Préchoux, A., Thomas, F., Rochat, T., Larocque, R., Zhu, Y., Stam, M., Génicot, S., Jam, M., Calteau, A., Viart, B., Ropartz, D., Pérez-Pascual, D., Correc, G., Matard-Mann, M., Stubbs, K.A., Rogniaux, H., Jeudy, A., Barbeyron, T., Médigue, C., Czjzek, M., Vallenet, D., McBride, M.J., Duchaud, E., Michel, G. (2017) Carrageenan

524 catabolism is encoded by a complex regulon in marine heterotrophic bacteria. Nat.
525 Commun. 8(1), Doi: 10.1038/s41467-017-01832-6.
526 [22] Fuchs, B.M., Glockner, F.O., Wulf, J., Amann, R. (2000) Unlabeled helper
527 oligonucleotides increase the in situ accessibility to 16S rRNA of fluorescently labeled
528 oligonucleotide probes. Appl. Environ. Microbiol. 66(8), 3603–7, Doi:
529 10.1128/AEM.66.8.3603-3607.2000.
530 [23] Fuchs, B.M., Wallner, G., Beisker, W., Schwippl, I., Ludwig, W., Amann, R. (1998) Flow
531 cytometric analysis of the in situ accessibility of *Escherichia coli* 16S rRNA for
532 fluorescently labeled oligonucleotide probes. Appl. Environ. Microbiol. 64(12), 4973–82,
533 Doi: 10.1128/aem.64.12.4973-4982.1998.
534 [24] Gachon, C., Mingam, A., Charrier, B. (2004) Real-time PCR: What relevance to plant
535 studies? J. Exp. Bot. 55(402), 1445–54, Doi: 10.1093/jxb/erh181.
536 [25] Gachon, C.M.M., Strittmatter, M., Müller, D.G., Kleinteich, J., Küpper, F.C. (2009)
537 Detection of differential host susceptibility to the marine oomycete pathogen *Eurychasma*
538 *dicksonii* by real-time PCR: Not all algae are equal. Appl. Environ. Microbiol. 75(2), 322–
539 8, Doi: 10.1128/AEM.01885-08.
540 [26] Gobet, A., Barbeyron, T., Matard-Mann, M., Magdelenat, G., Vallenet, D., Duchaud, E.,
541 Michel, G. (2018) Evolutionary evidence of algal polysaccharide degradation acquisition
542 by *Pseudoalteromonas carrageenovora* 9^T to adapt to macroalgal niches. Front. Microbiol.
543 9(NOV), 1–16, Doi: 10.3389/fmicb.2018.02740.
544 [27] Gómez, I., Español, S., Véliz, K., Huovinen, P. (2016) Spatial distribution of phlorotannins
545 and its relationship with photosynthetic UV tolerance and allocation of storage
546 carbohydrates in blades of the kelp *Lessonia spicata*. Mar. Biol. 163(5), Doi:
547 10.1007/s00227-016-2891-1.

[28] Hehemann, J.-H., Correc, G., Thomas, F., Bernard, T., Barbeyron, T., Jam, M., Helbert, W., Michel, G., Czjzek, M. (2012) Biochemical and structural characterization of the complex agarolytic enzyme system from the marine bacterium *Zobellia galactanivorans*. J. Biol. Chem. 287(36), 30571–84, Doi: 10.1074/jbc.M112.377184.

[29] Hollants, J., Leliaert, F., De Clerck, O., Willems, A. (2013) What we can learn from sushi: a review on seaweed-bacterial associations. FEMS Microbiol. Ecol. 83(1), 1–16, Doi: 10.1111/j.1574-6941.2012.01446.x.

[30] Küpper, F.C., Schweigert, N., Ar Gall, E., Legendre, J.M., Vilter, H., Kloareg, B. (1998) Iodine uptake in Laminariales involves extracellular, haloperoxidase-mediated oxidation of iodide. Planta 207(2), 163–71, Doi: 10.1007/s004250050469.

[31] Lage, O.M., Bondoso, J. (2011) *Planctomycetes* diversity associated with macroalgae. FEMS Microbiol. Ecol. 78(2), 366–75, Doi: 10.1111/j.1574-6941.2011.01168.x.

[32] Lami, R., Grimaud, R., Sanchez-Brosseau, S., Six, C., Thomas, F., West, N.J., Joux, F., Urios, L. (2021) Marine bacterial models for experimental biology. Established and emerging marine organisms in experimental biology.

[33] Mann, K.H. (Kenneth H. (1982) Ecology of coastal waters : a systems approach. University of California Press.

[34] Martin, M., Barbeyron, T., Martin, R., Portetelle, D., Michel, G., Vandenbol, M. (2015) The cultivable surface microbiota of the brown alga *Ascophyllum nodosum* is enriched in macroalgal-polysaccharide-degrading bacteria. Front. Microbiol. 6(December), 1–14, Doi: 10.3389/fmicb.2015.01487.

[35] Martin, M., Portetelle, D., Michel, G. (2014) Microorganisms living on macroalgae : diversity , interactions , and biotechnological applications. Appl. Microbiol. Biotechnol. 98, 2917–35, Doi: 10.1007/s00253-014-5557-2.

572 [36] Mazure, H.G.F., Field, J.G. (1980) Density and ecological importance of bacteria. J. Exp.
573 Mar. Bio. Ecol. 43(2), 173–82.
574 [37] Nedashkovskaya, O., Suzuki, M., Vancanneyt, M., Cleenwerck, I., Lysenko, A.,
575 Mikhailov, V., Swings, J. (2004) *Zobellia amurskyensis* sp nov., *Zobellia laminariae* sp
576 nov and *Zobellia russellii* sp nov., novel marine bacteria of the family *Flavobacteriaceae*.
577 International J. Syst. Evol. Microbiol. 54(5), 1643–8.
578 [38] Pernthaler, A., Pernthaler, J., Amann, R. (2002) Fluorescence in situ hybridization and
579 catalyzed reporter deposition for the identification of marine bacteria. Appl. Environ.
580 Microbiol. 68(6), 3094–101, Doi: 10.1128/AEM.68.6.3094.
581 [39] Pernthaler, J., Glöckner, F.O., Schönhuber, W., Amann, R. (2001) Fluorescence in situ
582 hybridization (FISH) with rRNA-targeted oligonucleotide probes. Methods Microbiol. 30,
583 Doi: 10.1016/s0580-9517(01)30046-6.
584 [40] Potin, P., Sanseau, A., Le Gall, Y., Rochas, C., Kloareg, B. (1991) Purification and
585 characterization of a new k-carrageenase from a marine *Cytophaga*-like bacterium. Eur. J.
586 Biochem. 201(1), 241–7, Doi: 10.1111/j.1432-1033.1991.tb16280.x.
587 [41] R Core Team. (2018) R: A Language and Environment for Statistical Computing.
588 [42] Ramirez-Puebla, S.T., Weigel, B.L., Jack, L., Schlundt, C., Pfister, C.A., Welch, Mark,
589 J.L. (2020) Spatial organization of the kelp microbiome at micron scales, Doi:
590 doi.org/10.1101/2020.03.01.972083.
591 [43] Schneider, C.A., Rasband, W.S., Eliceiri, K.W. (2012) NIH Image to ImageJ: 25 years of
592 image analysis. Nat. Methods 9(7), 671–5, Doi: 10.1038/nmeth.2089.
593 [44] Skovhus, T.L., Ramsing, N.B., Holmström, C., Kjelleberg, S., Dahllöf, I. (2004) Real-time
594 quantitative PCR for assessment of abundance of *Pseudoalteromonas* species in marine
595 samples. Appl. Environ. Microbiol. 70(4), 2373–82, Doi: 10.1128/AEM.70.4.2373-

2382.2004.

[45] Thomas, F., Barbeyron, T., Tonon, T., Génicot, S., Czjzek, M., Michel, G. (2012) Characterization of the first alginolytic operons in a marine bacterium: from their emergence in marine *Flavobacteriia* to their independent transfers to marine *Proteobacteria* and human gut *Bacteroides*. Environ. Microbiol. 14(9), 2379–94, Doi: 10.1111/j.1462-2920.2012.02751.x.

[46] Tourneroche, A., Lami, R., Burgaud, G., Domart-coulon, I., Li, W., Waite, D.W. (2020) The bacterial and fungal microbiota of *Saccharina latissima* (Laminariales, Phaeophyceae). Front. Mar. Sci. 7, 587566, Doi: 10.3389/fmars.2020.587566.

[47] Tourneroche, A., Lami, R., Hubas, C., Blanchet, E., Vallet, M., Escoubeyrou, K., Paris, A., Prado, S. (2019) Bacterial-fungal interactions in the kelp endomicrobiota drive autoinducer-2 quorum sensing. Front. Microbiol. 10(JULY), 1–14, Doi: 10.3389/fmicb.2019.01693.

[48] Tujula, N.A., Crocetti, G.R., Burke, C., Thomas, T., Holmström, C., Kjelleberg, S. (2010) Variability and abundance of the epiphytic bacterial community associated with a green marine Ulvacean alga. ISME J. 4(2), 301–11, Doi: 10.1038/ismej.2009.107.

[49] Tujula, N.A., Holmström, C., Mußmann, M., Amann, R., Kjelleberg, S., Crocetti, G.R. (2006) A CARD-FISH protocol for the identification and enumeration of epiphytic bacteria on marine algae. J. Microbiol. Methods 65(3), 604–7, Doi: 10.1016/j.mimet.2005.09.006.

[50] Větrovský, T., Baldrian, P. (2013) The variability of the 16S rRNA gene in bacterial genomes and its consequences for bacterial community analyses. PLoS One 8(2), 1–10, Doi: 10.1371/journal.pone.0057923.

[51] Wallner, G., Amann, R., Beisker, W. (1993) Optimizing fluorescent in situ hybridization

with rRNA-targeted oligonucleotide probes for flow cytometric identification of microorganisms. Cytometry 14(2), 136–43, Doi: 10.1002/cyto.990140205.

[52] Zhu, Y., Thomas, F., Larocque, R., Li, N., Duffieux, D., Cladière, L., Souchaud, F., Michel, G., McBride, M.J. (2017) Genetic analyses unravel the crucial role of a horizontally acquired alginate lyase for brown algal biomass degradation by *Zobellia galactanivorans*. Environ. Microbiol. 19(6), 2164–81, Doi: 10.1111/1462-2920.13699.

[53] ZoBell, C. (1941) Studies on marine bacteria I the cultural requirements of heterotrophic aerobes. J. Mar. Res. 4:75.

629 # Table

630 **Table 1. Oligonucleotides used in this study.** Specificity was tested *in silico* using the SILVA tools TestPrime and TestProbe for qPCR primers

631 and FISH probes, respectively. Searches were performed against the reference database SILVA 138.1 SSU Ref with 0 mismatch allowed.

	Target group	Name	Sequence (5' to 3')	Size of target group	Number of hits in target group	Group coverage (%)	Outgroup hits	Reference
qPCR primers pairs	*Zobellia*	142F / 285R	CCTACTGTGGGATAGCCCAG / GCGGTCTTGGTGAGCCG	54	52	96.3	0	This study
	Zobellia	142F / 289R	CCTACTGTGGGATAGCCCAG / CATCGCGGTCTTGGTGA	54	52	96.3	0	This study
	Zobellia	142F / 294R	CCTACTGTGGGATAGCCCAG / CTACCCATCGCGGTCTT	54	52	96.3	0	This study
	Bacteria	926F / 1062R	AAACTCAAAKGAATTGACGG / CTCACRRCACGAGCTGAC	1 916 523	1 565 274	81.7	0	De Gregoris *et al*., 2011 [5]
FISH probes	*Zobellia*	ZOB137	GGCTATCCCACAGTAGGG	54	54	100	3	This study
	Bacteria	EUB338, EUB338-II and EUB338-III	GCTGCCTCCCGTAGGAGT, GCAGCCACCCGTAGGTGT and GCTGCCACCCGTAGGTGT	1 916 512	1 794 219	93.6	0	Amann *et al*., 1990 [2] Daims *et al*., 1999 [18]
	None	NON338	ACTCCTACGGGAGGCAGC	-	-	-	-	Wallner *et al*., 1993 [51]
FISH helpers	*Zobellia*	H116	GGYAGATYGTATACGCSTTGC	-	-	-	-	This study
	Zobellia	H155	GTMTTAATCCAAATTTCTCTG	-	-	-	-	This study
	Zobellia	H176	CACATGGTACCATTTTACGGC	-	-	-	-	This study

632

633 # Figure legends

634

635 **Figure 1. Optimization of qPCR parameters.** A-B: Effect of primer concentration (A) and annealing
636 temperature (T_a) (B) on the cycle threshold (C_t) was determined using the primer pair 142F/289R and 10^4
637 16S rRNA gene copies. T_a was set to 60°C in A and primer concentration to 300 nM in B. C: Standard
638 curves obtained in qPCR with the three sets of primers using *Z. galactanivorans* Dsij^T gDNA diluted from
639 10^8 to 10^1 16S rRNA gene copies. D: Comparison of measured and theoretical proportion of *Zobellia* 16S
640 rRNA gene copies in environmental DNA with increasing load of *Zobellia* gDNA. The 1:1 line was drawn
641 in light grey as a comparison. Values are mean ± s.d (n = 3). In C and D, T_a = 64°C and [primer] = 300 nM.
642 In all panels (A-D), measurements were performed in technical triplicates.

643

644 **Figure 2. Dissociation curves of the probe ZOB137 determined using the strains *Zobellia***
645 ***galactanivorans* Dsij^T (A) and *Zobellia russellii* KMM 3677^T (B) under increasing formamide**
646 **concentration.** For each formamide concentration, the maximum fluorescence intensity was assessed for
647 cells on five different microscopic fields (between 30 and 70 counted cells in total for each concentration).
648 White diamonds represent the mean intensity.

649

650 **Figure 3. Epifluorescence microscopy images of bacterial cells hybridized with the CARD-FISH**
651 **probe ZOB137 (E-H) and counterstained with DAPI (A-D).** *Lewinella marina* MKG-38T and
652 *Marinirhabdus citrea* MEBiC09412T were used as negative controls to assess the specificity of the newly-
653 designed probe ZOB137. Addition of the three helpers in the hybridization mix increased the fluorescence
654 of the *Zobellia galactanivorans* cells (F) without affecting the probe specificity (G-H). Upper (DAPI-
655 stained cells) and lower (CARD-FISH signal) epifluorescent micrographs show identical fields. Exposure
656 time was 100 ms for CARD-FISH. FA = 35%.

657

Figure 4. Number of 16S rRNA gene copies per cm^2 of algal surface detected either with the universal bacterial primers (A) or with the *Zobellia*-specific primers 142F/289R (B). Proportion of *Zobellia* **(C)** was obtained by dividing the number of *Zobellia* 16S copies by the number of 16S copies detected with the universal primers for each sample. Measurements were performed in technical triplicates. LdigB, LdigM and LdigO are basal, median and apical parts of *Laminaria digitata*, respectively. Anod, *Ascophyllum nodosum*; Ulac, *Ulva lactuca*; Ppal, healthy *Palmaria palmata;* PpalS, stranded *P. palmata*. For *L. digitata* samples, within-blade variations were tested using one-way ANOVA analyses followed by pairwise post-hoc Tukey HSD. Different letters denote significant difference ($P < 0.05$).

Figure 5. *Zobellia* cells visualization in the stained biofilm of *Palmaria palmata* (A) and *Ulva lactuca* (B). Micrographs are overlay of the CARD–FISH signal (green cells, ZOB137-HRP probe with $Alexa_{546}$ as the reporter signal) and the DAPI signal (magenta cells) and represent the maximum intensity projection of Z-stack. Transversal view is shown at the bottom. Bars: 10 µm (A) and 15 µm (B).

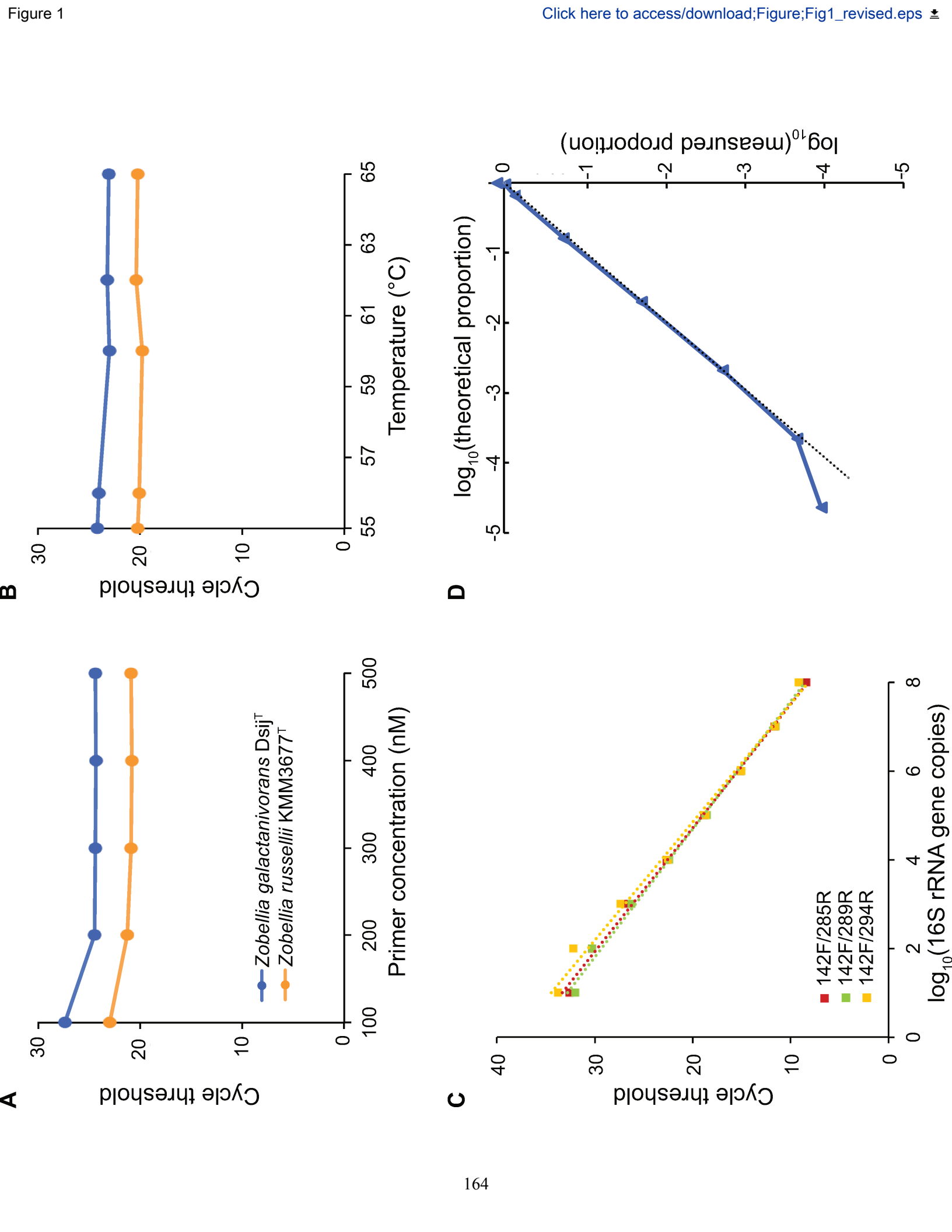

Figure 2

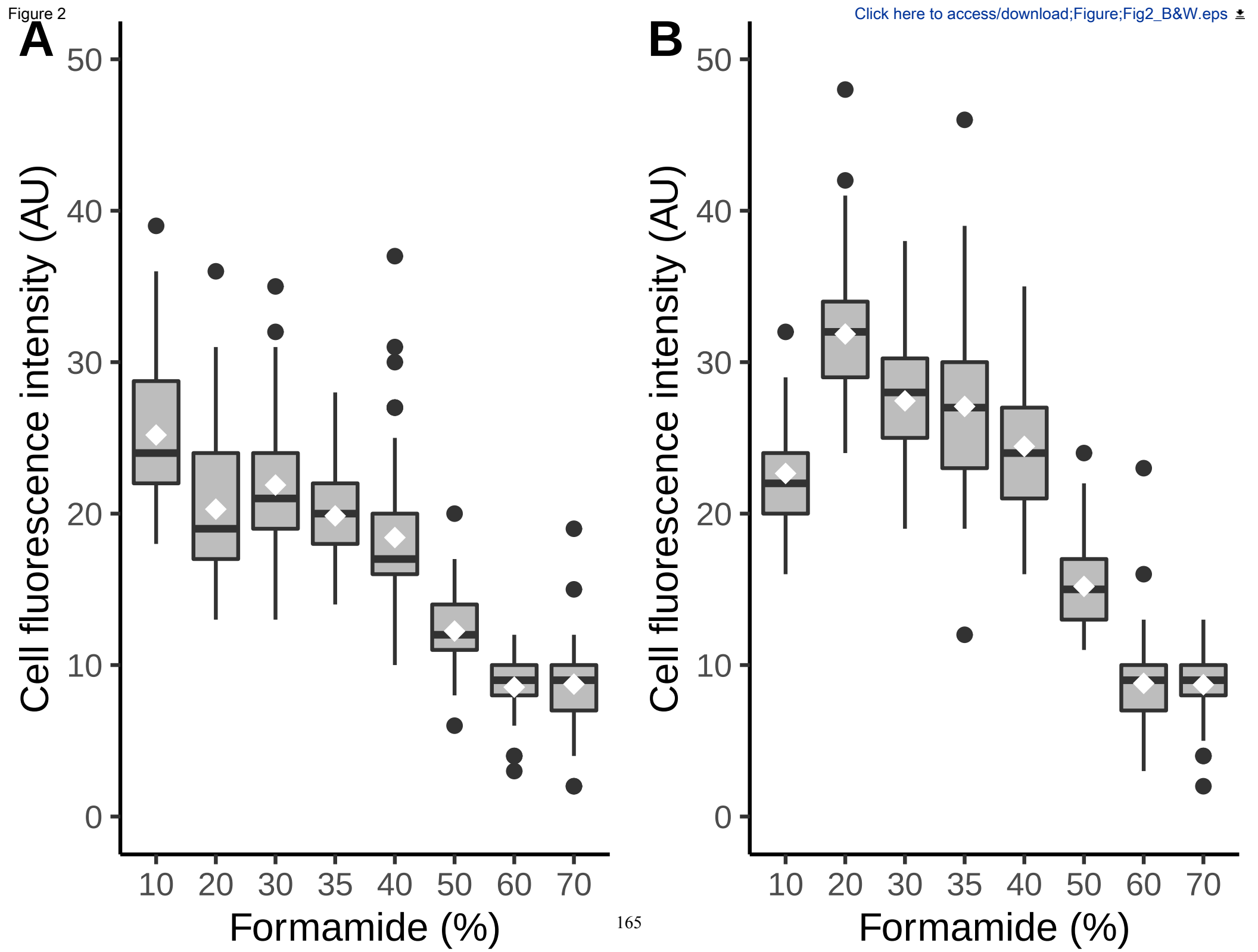

Figure 3

Figure 4

Click here to access/download;Figure;Fig4_B&W.eps

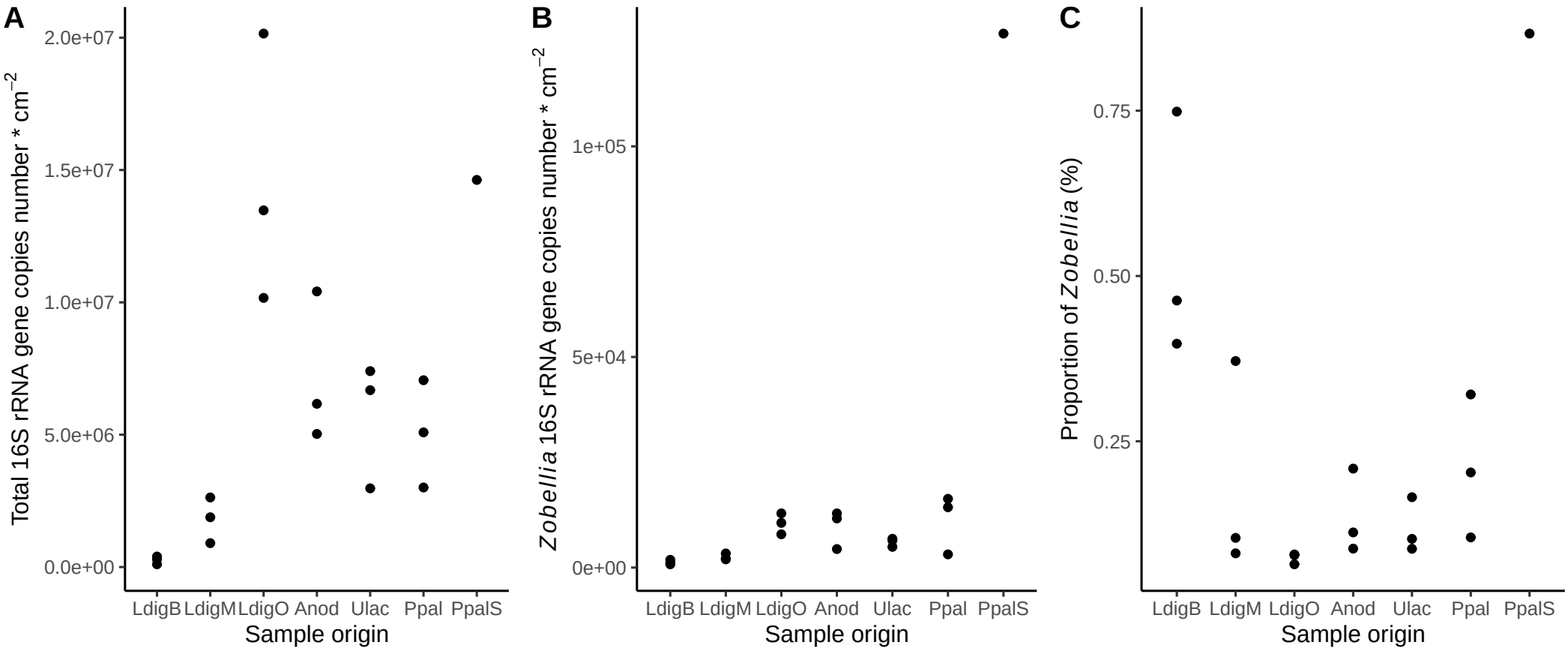

Figure 5

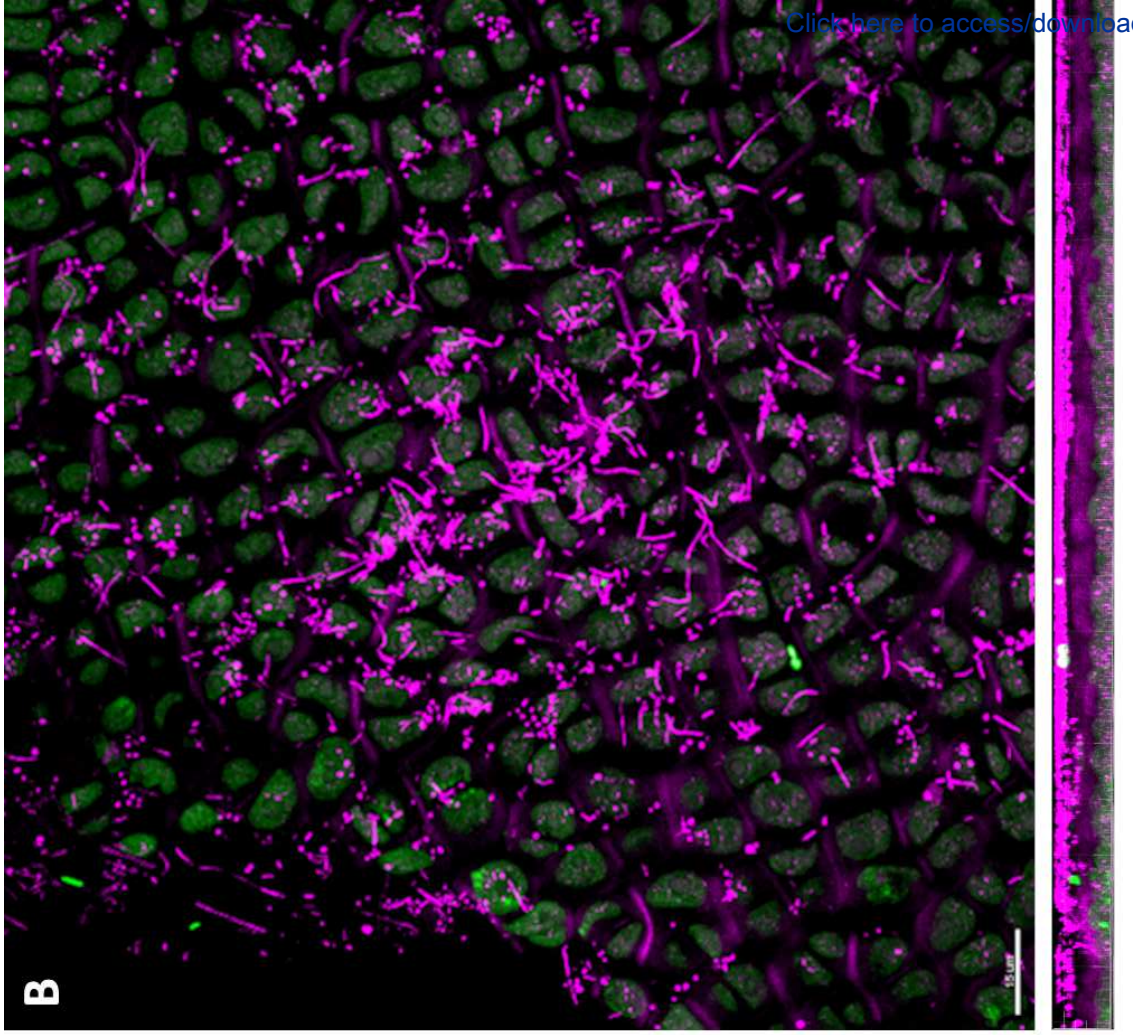

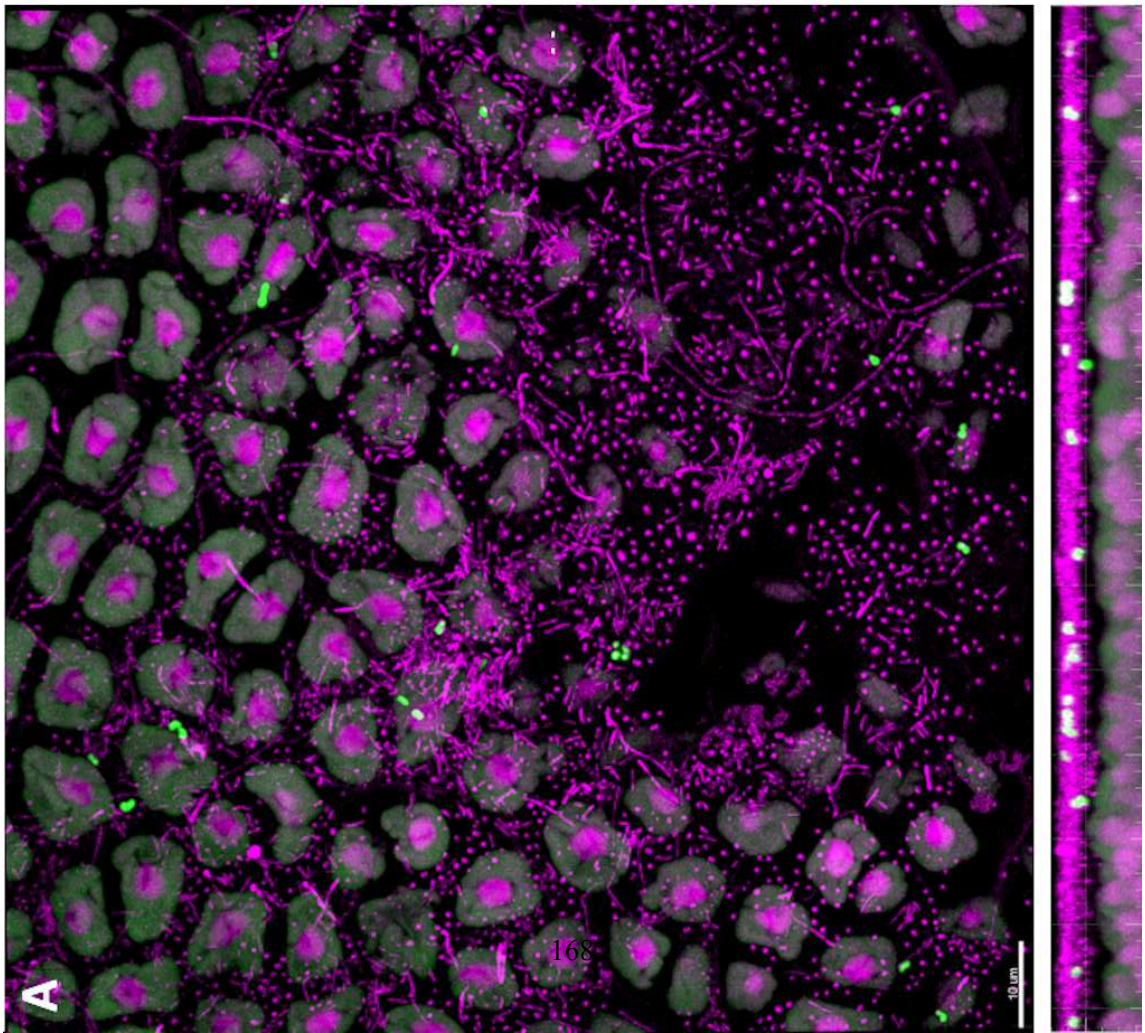

Specific detection and quantification of the marine flavobacterial genus *Zobellia* on macroalgae using novel qPCR and CARD-FISH assays

Maéva Brunet[a], Nolwen Le Duff[a], Bernhard M. Fuchs[b], Rudolf Amann[b], Tristan Barbeyron[a] and François Thomas[a#]
#Corresponding author

SUPPLEMENTARY MATERIAL

This document contains four supplementary tables, two supplementary figures and references to three separate supplementary files.

Supplementary Tables

Supplementary Table 1. Survey of genes homologous to *Z. galactanivorans* Dsij^T in marine metagenomes available on the IMG/MER platform. Only metagenome samples showing at least 50 homolog genes with >90% sequence identity to genes in *Z. galactanivorans* Dsij^T are shown.

Metagenome ID	Origin	Location	Number of 90% hits
3300009421	red alga *Porphyra*	Sidmouth (UK)	1262
3300027498	red alga *Porphyra*	Sidmouth (UK)	917
3300009410	red alga *Porphyra*	Porto (Portugal)	536
3300009192	red alga *Porphyra*	Porto (Portugal)	480
3300009415	red alga *Porphyra*	Sidmouth (UK)	393
3300032272	coastal sediment	Maine (USA)	334
3300027262	red alga *Porphyra*	Sidmouth (UK)	289
3300026840	red alga *Porphyra*	Porto (Portugal)	283
3300027028	red alga *Porphyra*	Porto (Portugal)	260
3300009508	epipelagic water	Helgoland (Germany)	231
3300009073	red alga *Porphyra*	Bantry Bay (Ireland)	162
3300032373	microbial mat	Maine (USA)	129
3300009446	red alga *Porphyra*	Maine (USA)	114
3300028600	subtidal sediment	Helgoland (Germany)	114
3300025881	epipelagic water	Helgoland (Germany)	113
3300028599	subtidal sediment	Helgoland (Germany)	105
3300027509	red alga *Porphyra*	Bantry Bay (Ireland)	93
3300032136	coastal sediment	Delaware Bay (USA)	93
2236876004	estuarine water	Columbia River (USA)	83
2236876010	estuarine water	Columbia River (USA)	83
3300010392	coastal sediment	Rhode Island (USA)	82
3300032258	coastal sediment	Maine (USA)	73
3300018420	coastal salt marsh	Skidaway Island (USA)	66
3300010430	coastal sediment	Atlantic coast	66
3300009505	epipelagic water	Helgoland (Germany)	64
3300018048	coastal salt marsh	Skidaway Island (USA)	63
3300018417	coastal salt marsh	Skidaway Island (USA)	61
3300032231	coastal sediment	Maine (USA)	61
3300018876	coastal salt marsh	Skidaway Island (USA)	60
3300027623	red alga *Porphyra*	Maine (USA)	58
3300018416	coastal salt marsh	Skidaway Island (USA)	58
3300028598	subtidal sediment	Helgoland (Germany)	57
3300025793	wetland	San Francisco Bay (USA)	57
3300009439	red alga *Porphyra*	Maine (USA)	54
3300018041	coastal salt marsh	Skidaway Island (USA)	51
3300017950	coastal salt marsh	Skidaway Island (USA)	51
3300019459	coastal salt marsh	Skidaway Island (USA)	51

Supplementary Table 2. List of bacterial strains used in this study.

Strain	Use	Reference
Zobellia galactanivorans Dsij^T	positive control for qPCR / FISH	(Barbeyron *et al.*, 2001)
Zobellia russellii KMM 3677^T	positive control for qPCR / FISH	(Nedashkovskaya *et al.*, 2004)
Zobellia amurskyensis KMM 3526^T	positive control for FISH	(Nedashkovskaya *et al.*, 2004)
Zobellia roscoffensis Asnod1-F08^T	positive control for FISH	(Barbeyron *et al.*, 2021)
Cellulophaga baltica NN015840^T	negative control for qPCR	(Johansen *et al.*, 1999)
Cellulophaga sp. strain Asnod2-G02	negative control for qPCR	(Martin *et al.*, 2015)
Maribacter forsetii KT02ds18-6^T	negative control for qPCR	(Barbeyron *et al.*, 2008)
Lewinella marina MKG-38^T	negative control for FISH	(Khan *et al.*, 2007)
Marinirhabdus citrea MEBiC09412^T	negative control for FISH	(Yang *et al.*, 2018)

Barbeyron, T., Carpentier, F., L'Haridon, S., Schüler, M., Michel, G., and Amann, R. (2008) Description of *Maribacter forsetii* sp. nov., a marine *Flavobacteriaceae* isolated from North Sea water, and emended description of the genus *Maribacter*. *Int J Syst Evol Microbiol* **58**: 790–797.

Barbeyron, T., L'Haridon, S., Corre, E., Kloareg, B., and Potin, P. (2001) *Zobellia galactanovorans* gen. nov., sp. nov., a marine species of *Flavobacteriaceae* isolated from a red alga, and classification of [*Cytophaga*] *uliginosa* (ZoBell and Upham 1944) Reichenbach 1989 as *Zobellia uliginosa* gen. nov., comb. nov. *Int J Syst Evol Microbiol* **51**: 985–97.

Barbeyron, T., Thiébaud, M., Le Duff, N., Martin, M., Corre, E., Tanguy, G., et al. (2021) *Zobellia roscoffensis* sp. nov. and *Zobellia nedashkovskayae* sp. nov., two flavobacteria from the epiphytic microbiota of the brown alga *Ascophyllum nodosum*, and emended description of the genus *Zobellia*. *Int J Syst Evol Microbiol*.

Johansen, J., Nielsen, P., and Sjøholm, C. (1999) Description of *Cellulophaga baltica* gen. nov., sp. nov. and *Cellulophaga fucicola* gen. nov., sp. nov. and reclassification of [*Cytophaga*] *lytica* to *Cellulophaga lytica* gen. nov., comb. nov. *Int J Syst Bacteriol* **49**: 1231–1240.

Khan, S.T., Fukunaga, Y., Nakagawa, Y., and Harayama, S. (2007) Emended descriptions of the genus *Lewinella* and of *Lewinella cohaerens*, *Lewinella nigricans* and *Lewinella persica*, and description of *Lewinella lutea* sp. nov. and *Lewinella marina* sp. nov. *Int J Syst Evol Microbiol* **57**: 2946–2951.

Martin, M., Barbeyron, T., Martin, R., Portetelle, D., Michel, G., and Vandenbol, M. (2015) The Cultivable Surface Microbiota of the Brown Alga *Ascophyllum nodosum* is Enriched in Macroalgal-Polysaccharide-Degrading Bacteria. *Front Microbiol* **6**: 1–14.

Nedashkovskaya, O., Suzuki, M., Vancanneyt, M., Cleenwerck, I., Lysenko, A., Mikhailov, V., and Swings, J. (2004) *Zobellia amurskyensis* sp nov., *Zobellia laminariae* sp nov and *Zobellia russellii* sp nov., novel marine bacteria of the family *Flavobacteriaceae*. *nternational J Syst Evol Microbiol* **54**: 1643–1648.

Yang, S.H., Oh, J.H., Seo, H.S., Lee, J.H., and Kwon, K.K. (2018) *Marinirhabdus citrea* sp. nov., a marine bacterium isolated from a seaweed. *Int J Syst Evol Microbiol* **68**: 547–551.

Supplementary Table 3. Number of copies of 16S rRNA genes in available genomes from the genus *Zobellia*.

Strain	Number of 16S rRNA genes
Z. amurskyensis KMM 3526^T	4
Z. amurskyensis MAR_2009_138	3
Z. russellii KMM 3677^T	2
Z. laminariae KMM 3676^T	2
Z. uliginosa DSM 2061^T	2
Z. galactanivorans DsiJ^T	2
Z. galactanivorans OII3	1
Z. roscoffensis Asnod1-F08^T	1
Z. roscoffensis Asnod2-B02-B	1
Z. nedashkovskayae Asnod2-B07-B^T	1
Z. nedashkovskayae Asnod3-E08-A	1

Supplementary Table 4. Blastn results on the NCBI 16S rRNA gene database for sequences of qPCR products

Seq. ID	Best blastn hit		First blastn hit outside *Zobellia*	
	strain	% id	strain	% id
LdigO-1	*Zobellia laminariae* KMM 3676^T	99.32	*Euzebyella marina* CY01^T	87.59
LdigO-2	*Zobellia russellii* KMM 3677^T	99.32	*Jejudonia soesokkakensis* SSK1-1^T	89.39
LdigO-3	*Zobellia laminariae* KMM 3676^T	98.65	*Euzebyella marina* CY01^T	86.86
LdigO-4	*Zobellia russellii* KMM 3677^T	97.97	*Jejudonia soesokkakensis* SSK1-1^T	87.88
LdigO-5	*Zobellia russellii* KMM 3677^T	100.00	*Jejudonia soesokkakensis* SSK1-1^T	90.15
LdigO-6	*Zobellia laminariae* KMM 3676^T	99.32	*Euzebyella marina* CY01^T	87.59
LdigO-7	*Zobellia laminariae* KMM 3676^T	99.32	*Euzebyella marina* CY01^T	87.59
LdigO-8	*Zobellia laminariae* KMM 3676^T	99.32	*Euzebyella marina* CY01^T	87.59
LdigO-9	*Zobellia laminariae* KMM 3676^T	99.32	*Euzebyella marina* CY01^T	89.05
LdigO-10	*Zobellia laminariae* KMM 3676^T	99.32	*Euzebyella marina* CY01^T	87.59
PpalS-1	*Zobellia laminariae* KMM 3676^T	99.32	*Euzebyella marina* CY01^T	87.59
PpalS-2	*Zobellia laminariae* KMM 3676^T	99.32	*Euzebyella marina* CY01^T	87.59
PpalS-3	*Zobellia laminariae* KMM 3676^T	97.97	*Euzebyella marina* CY01^T	86.13
PpalS-4	*Zobellia laminariae* KMM 3676^T	99.32	*Euzebyella marina* CY01^T	87.59
PpalS-5	*Zobellia laminariae* KMM 3676^T	98.66	*Euzebyella marina* CY01^T	85.51
PpalS-6	*Zobellia russellii* KMM 3677^T	100.00	*Jejudonia soesokkakensis* SSK1-1^T	90.15
PpalS-7	*Zobellia laminariae* KMM 3676^T	99.32	*Euzebyella marina* CY01^T	87.59
PpalS-8	*Zobellia laminariae* KMM 3676^T	99.32	*Euzebyella marina* CY01^T	87.59
PpalS-9	*Zobellia russellii* KMM 3677^T	99.32	*Euzebyella marina* CY01^T	90.51
PpalS-10	*Zobellia russellii* KMM 3677^T	98.65	*Euzebyella marina* CY01^T	89.78

Supplementary Figures

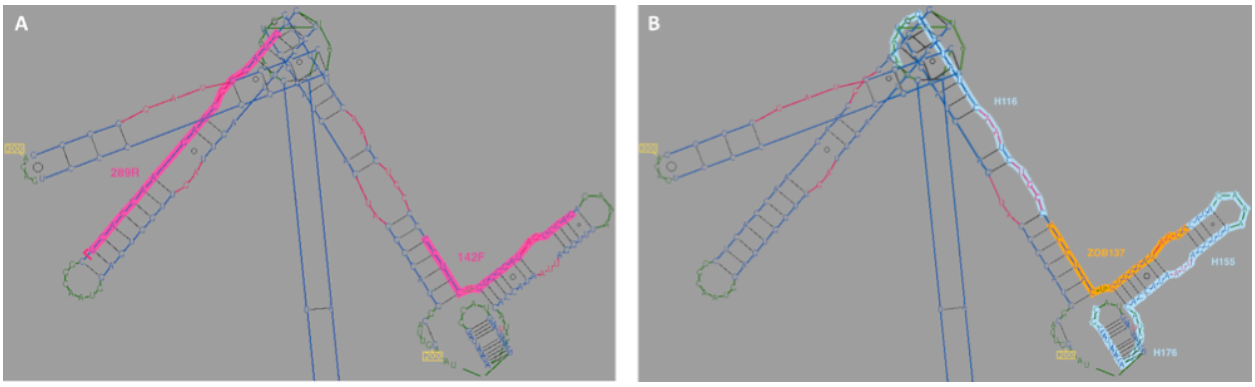

Supplementary Figure 1. Secondary structure of the *Z. galactanivorans* Dsij^T 16S rRNA V2 region. qPCR primers 142F/289R **(A)** and ZOB137 FISH probe and helpers **(B)** designed for the study are highlighted. This graphical representation was prepared using the ARB secondary structure editor.

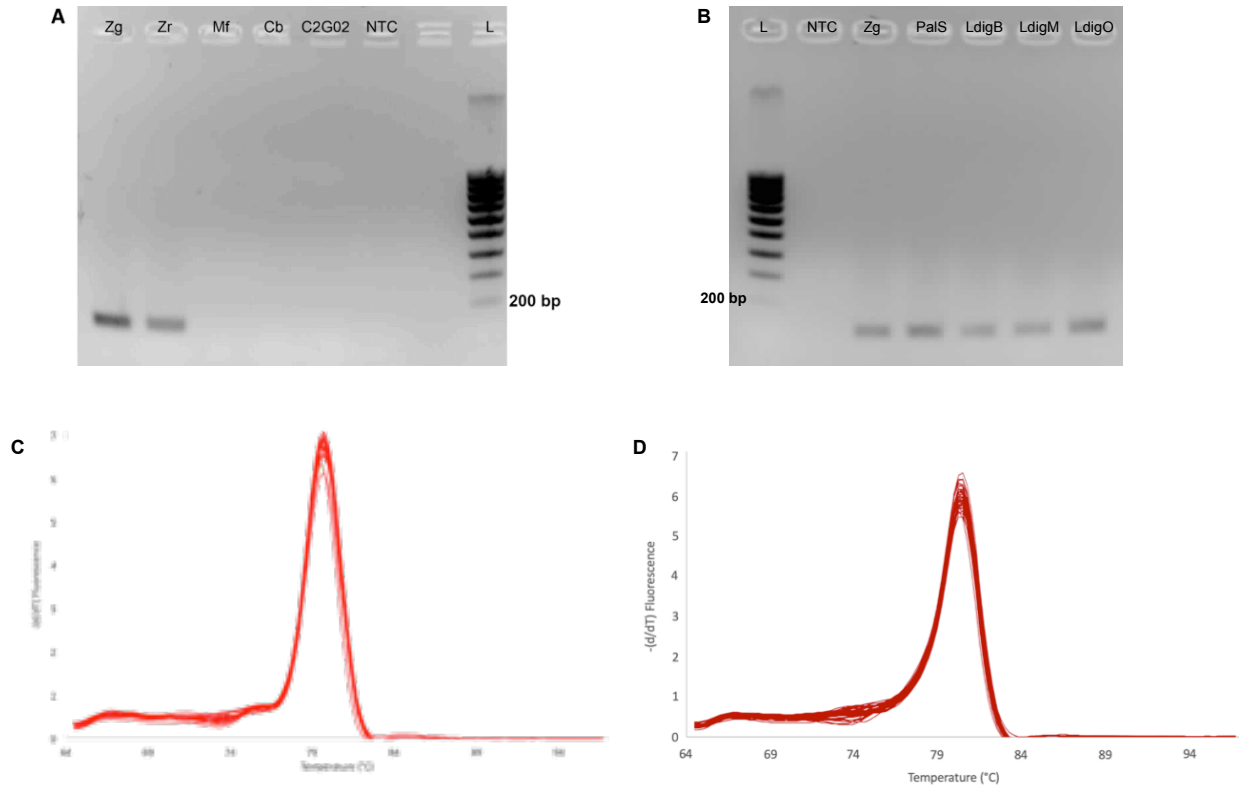

Supplementary Figure 2. (A) Agarose gel electrophoresis of PCR products obtained on *Zobellia galactanivorans* Dsij^T (Zg), *Z. russellii* KMM 3677^T (Zr), *Maribacter forsetii* KT02ds18-6^T (Mf), *Cellulophaga baltica* NN015840^T (Cb) and *Cellulophaga* sp. strain Asnod2-G02 (C2G02). NTC, no-template control; L, molecular weight ladder. **(B)** Agarose gel electrophoresis of PCR products obtained on DNA from *Zobellia galactanivorans* Dsij^T pure culture (Zg) and four algae-associated microbiota (PpalS, LdigB, LdigM and LdigO; see details in Figure 4 legend). NTC, no-template control; L, molecular weight ladder. **(C, D)** Melting curves obtained from the qPCR assays on pure *Z. galactanivorans* Dsij^T gDNA (C) and all environmental samples used in this study (D).

Supplementary Files

Supplementary File 1 (Fasta file). List of the 139 aligned 16S rRNA gene sequences from flavobacteria, including 52 *Zobellia* strains and 87 sequences representing 23 close genera, used to design *Zobellia*-specific primers with DECIPHER

See online version

Supplementary File 2 (Excel file). Details of the qPCR assay on the environmental samples, following the Minimum Information for publication of Quantitative real-time PCR Experiments (MIQE) guidelines.

Experimental design		
	Definition of experimental groups	Seven experimental groups (*L. digitata* (basal, medium and old blades), *A. nodosum*, *U. lactuca*, *P. palmata* and stranded *P. palmata*) at 1 sampling date (February 2020)
	Number within each group	n=3, except n=1 for stranded *P. palmata*
Sample		
	Description	All groups (except stranded *P. palmata)*: epiphytic communities from fresh macroalgal surface ; stranded *P. palmata:* epiphytic communities from stranded macroalgal surface
	Volume of sample processed	50 cm^2
	Processing procedure	Sampling with sterile swabs using a 5-cm square template on both sides of the algal thallus
	Freezing procedure	-20°C
	Sample storage conditions and duration	-20°C, less than 6 months
Nucleic acid extraction		
	Procedure	DNA/RNA Miniprep kit, ZymoBiomics
	Nucleic acid quantification instrument and method	Method: Quantifluor dsDNA system (Promega); Instrument: plate reader Spark Tecan
	Purity (A260/280)	Nanodrop
qPCR target information		
	gene symbol	16S rRNA gene
	amplicon length	926F/1062R: 136 bp; 142F/289R: 147 bp
	in silico specificity screen	926F/1062R: 81.7% coverage for bacteria; 142F/289R: 96.3% coverage for *Zobellia*. Coverages assessed with Silva TestPrime on SSUr 138.1 Ref database (February 2021; 0 mismatche allowed)

qPCR oligonucleotides		
	primer sequences	926F: 5'-AAACTCAAAKGAATTGACGG-3'; 1062R: 5'-CTCACRRCACGAGCTGAC-3'; 142F: 5'-CCTACTGTGGGATAGCCCAG -3'; 289R: 5'-CATCGCGGTCTTGGTGA-3'
	manufacturer of oligonucleotides	Eurogentec
	purification method	desalting
qPCR protocol		
	reaction volume	5 µl
	amount of DNA	0.75 ng
	primer, Mg2+ and dNTP concentration	300 nM of each primer; Mg^{2+} and dNTP according to kit
	polymerase identity and concentration	FastStart Taq DNA polymerase
	buffer/kit identity and manufacturer	LightCycle 480 SYBR Green I Master (Roche)
	additives	SYBR Green
	Manufacturer of plates	LightCycler 480 Multiwell Plate 384 (Roche)
	Complete thermocycling parameters	10 min at 95°C; 45 cycles of 10 s at 95°C / 20 s at 60°C (Universal primers) or 64°C (*Zobellia*-specific primers) / 10 s at 72°C; 5 s at 95°C. Melting curve from 65°C to 97°C
	reaction setup	manual
	manufacturer of qPCR instrument	Roche
qPCR validation		
	specificity	melting curve
	Cq of NTC	926F/1062R: 34.7; 142F/289R: no amplification detected
	Calibration curve with slope and y intercept	926F/1062R: slope = -3.262 ; y intercept = 37.18; 142F/289R: slope = -4.097 ; y intercept = 39.27
	PCR efficiency calculated from slope	926F/1062R: 2.026; 142F/289R: 1.754
Data analysis		
	qPCR analysis program	LightCycler 480 Software, LCS480 1.5.0.39
	Method of Cq determination	Abs Quant / 2nd Derivative Max
	Number and stage of technical replicates	3 technical replicates at the qPCR stage
	Statistical method for results significance	One-way ANOVA followed by pairwise post-hoc Tukey HSD

87
88
89

Supplementary File 3 (Fasta file). Sequences of qPCR products obtained from environmental samples LdigO and PpalS. Ten clones were randomly picked for each environmental sample.

```
>PpalS-1
CCTACTGTGGGATAGCCCAGAGAAATTTGGATTAAGACCACATAGTACTATCTTACGGCATCGTATTTATAGTTAAA
GGT TACGGTAGGGGATGAGTATGCGTCCCATTAGTTAGTTGGCGAGGTAACGGCTCACCAAGACCGCGATG
>PpalS-2
CATCGCGGTCTTGGTGAGCCGTTACCTCGCCAACTAACTAATGGGACGCATACTCATCCCCTACCGTAACCTTTAAC
TAT AAATACGATGCCGTAAGATAGTACTATGTGGTCTTAATCCAAATTTCTCTGGGCTATCCCACAGTAGG
>PpalS-3
CATCGCGGTCTTGGTGAGCCGTTACCTCGCCAACTAACTAATGGGACGCATACTCATCCCCTACCGTAACCTTTAAC
TAT AAATACGATGCCGTAGGGTAGTACTATGTGGTCTTAATCCAAATTTCTCTGGGCTATCCCACAGTAGG
>PpalS-4
CATCGCGGTCTTGGTGAGCCGTTACCTCGCCAACTAACTAATGGGACGCATACTCATCCCCTACCGTAACCTTTAAC
TAT AAATACGATGCCGTAAGATAGTACTATGTGGTCTTAATCCAAATTTCTCTGGGCTATCCCACAGTAGG
>PpalS-5
CATCGCGGTCTTGGTGAGCCGTTACCTCGCCAACTAACTAATGGGACGCATACTCATCCCCTACCGTAAC
CTTTAACTATAAATACGATGCCGTAAGATAGTACTATGTGGTCTTAATCCAAATTTCTCTGGGGCTATCC
CACAGTAGG
>PpalS-6
CATCGCGGTCTTGGTGAGCCGTTACCTCGCCAACTAACTAATGGGACGCATACTCATCCCCTACCGTAACCTTTAAC
CAT AAATACGATGCCGTAATATGGTACCATGTGGTATTAATCCAAATTTCTCTGGGCTATCCCACAGTAGG
>PpalS-7
CATCGCGGTCTTGGTGAGCCGTTACCTCGCCAACTAACTAATGGGACGCATACTCATCCCCTACCGTAACCTTTAAC
TAT AAATACGATGCCGTAAGATAGTACTATGTGGTCTTAATCCAAATTTCTCTGGGCTATCCCACAGTAGG
>PpalS-8
CATCGCGGTCTTGGTGAGCCGTTACCTCGCCAACTAACTAATGGGACGCATACTCATCCCCTACCGTAACCTTTAAC
TAT AAATACGATGCCGTAAGATAGTACTATGTGGTCTTAATCCAAATTTCTCTGGGCTATCCCACAGTAGG
>PpalS-9
CCTACTGTGGGATAGCCCAGAGAAATTTGGATTAAGACCACATGGTACCATATTACGGCATCGTATTTATGGTTAAA
GGT TACGGTAGGGGATGAGTATGCGTCCCATTAGTTAGTTGGCGAGGTAACGGCTCACCAAGACCGCGATG
>PpalS-10
CATCGCGGTCTTGGTGAGCCGTTACCTCGCCAACTAACTAATGGGACGCATACTCATCCCCTACCGTAACCTTTAAC
CAT AAATACGATGCCGTAATATGGTACTATGTGGTCTTAATCCAAATTTCTCTGGGCTATCCCACAGTAGG
>LdigO-1
CCTACTGTGGGATAGCCCAGAGAAATTTGGATTAAGACCACATAGTACTATCTTACGGCATCGTATTTATAGTTAAA
GGT TACGGTAGGGGATGAGTATGCGTCCCATTAGTTAGTTGGCGAGGTAACGGCTCACCAAGACCGCGATG
>LdigO-2
CCTACTGTGGGATAGCCCAGAGAAATTTGGATTAATACCACATGGTACCATCTTACGGCATCGTATTTATGGTTAAA
GGT TACGGTAGGGGATGAGTATGCGTCCCATTAGTTAGTTGGCGAGGTAACGGCTCACCAAGACCGCGATG
>LdigO-3
CCTACTGTGGGATAGCCCAGAGAAATTTGGATTAAGACCACATAGTACTATCTTACGGCATCGTATTCATAGTTAAA
GGT TACGGTAGGGGATGAGTATGCGTCCCATTAGTTAGTTGGCGAGGTAACGGCTCACCAAGACCGCGATG
>LdigO-4
CCTACTGTGGGATAGCCCAGAGAAATTTGGATTAATACCACATGGTACTATCTTACGGCATCGTATTTATAGTTAAA
GGT TACGGTAGGGGATGAGTATGCGTCCCATTAGTTAGTTGGCGAGGTAACGGCTCACCAAGACCGCGATG
>LdigO-5
CATCGCGGTCTTGGTGAGCCGTTACCTCGCCAACTAACTAATGGGACGCATACTCATCCCCTACCGTAACCTTTAAC
CAT AAATACGATGCCGTAATATGGTACCATGTGGTATTAATCCAAATTTCTCTGGGCTATCCCACAGTAGG
>LdigO-6
CCTACTGTGGGATAGCCCAGAGAAATTTGGATTAAGACCACATAGTACTATCTTACGGCATCGTATTTATAGTTAAA
GGT TACGGTAGGGGATGAGTATGCGTCCCATTAGTTAGTTGGCGAGGTAACGGCTCACCAAGACCGCGATG
>LdigO-7
CCTACTGTGGGATAGCCCAGAGAAATTTGGATTAAGACCACATAGTACTATCTTACGGCATCGTATTTATAGTTAAA
GGT TACGGTAGGGGATGAGTATGCGTCCCATTAGTTAGTTGGCGAGGTAACGGCTCACCAAGACCGCGATG
>LdigO-8
CATCGCGGTCTTGGTGAGCCGTTACCTCGCCAACTAACTAATGGGACGCATACTCATCCCCTACCGTAACCTTTAAC
TAT AAATACGATGCCGTAAAATAGTACTATGTGGTCTTAATCCAAATTTCTCTGGGCTATCCCACAGTAGG
>LdigO-9
CATCGCGGTCTTGGTGAGCCGTTACCTCGCCAACTAACTAATGGGACGCATACTCATCCCCTACCGTAACCTTTAAC
CAT AAATACGATGCCGTAATATAGTACTATGTGGTCTTAATCCAAATTTCTCTGGGCTATCCCACAGTAGG
>LdigO-10
```

151 CCTACTGTGGGATAGCCCAGAGAAATTTGGATTAAGACCACATAGTACTATCTTACGGCATCGTATTTATAGTTAAA
152 GGT TACGGTAGGGGATGAGTATGCGTCCCATTAGTTAGTTGGCGAGGTAACGGCTCACCAAGACCGCGATG

Part 2:

Prevalence, abundance and activity of the genus *Zobellia* at the surface of diverse macroalgae

I. Introduction

Flavobacteriia represent an important part of the epiphytic bacterial communities (Florez *et al.*, 2019). Their proportion was reported to vary seasonally in costal seawater (Gilbert *et al.*, 2012; Teeling *et al.*, 2012; Alonso-Sáez *et al.*, 2015) or at the algae surface (Kim *et al.*, 1992; Serebryakova *et al.*, 2018; Florez *et al.*, 2019), depending on algal species (Florez *et al.*, 2017) and on thallus part (Serebryakova *et al.*, 2018). Among the *Flavobacteriia*, the genus *Zobellia* is considered a specialist of algal degradation (Lami *et al.*, 2021). Seven out of the nine described strains within the genus *Zobellia* were isolated from algal surfaces and the others from beach sand and seawater (Barbeyron *et al.*, 2001, 2021; Nedashkovskaya *et al.*, 2004). In addition, *Zobellia* genes were reported in molecular studies (Alonso *et al.*, 2007; Hollants *et al.*, 2013; Dogs *et al.*, 2017) and in marine metagenomes from algal microbiomes. Hence, the genus *Zobellia* is known to be part of the bacterial communities in macroalgae-dominated habitats, but there is no data regarding its precise distribution. Here we aim to (i) assess the prevalence and abundance of the genus *Zobellia* on the surface of healthy and decaying macroalgae with different chemical compositions, (ii) determine if the abundance of the genus follows a seasonal pattern, and (iii) evaluate its metabolic activity within the biofilm.

A monthly sampling of the microbiota of five different macroalgae dominating the intertidal zone and encompassing all three algal phyla was conducted in the Roscoff area between February 2020 and January 2021. The samples were further analyzed by qPCR with the newly validated *Zobellia*-specific primers (Brunet et al., 2021, accepted, Part 1) to address the seasonal abundance and activity of *Zobellia* spp. at the surface of macroalgae. These results will likely contribute to a deeper characterization of the interactions between *Zobellia* spp. and macroalgae by unraveling the ecological strategies of the genus in the context of algal degradation.

II. Methods

1. Sampling

Surface microbiota were sampled each month during low tides with a high tidal coefficient (> 80) between February 2020 and January 2021. Due to the Covid-19 pandemic, no sampling was done in April and May 2020. Microbiota were collected using sterile swabs (Zymobiomics) on healthy specimens of the brown algae *Laminaria digitata* (Huds.) Lamouroux, 1813 (Ldig), *Fucus serratus* Linnaeus 1753 (Fser) and *Ascophyllum nodosum* (Linnaeus) Le Jolis 1863 (Anod), the red alga *Palmaria palmata* (Linnaeus) F.Weber & D.Mohr 1805 (Ppal) and the green alga *Ulva lactuca* Linnaeus 1753 (Ulac) at the Bloscon site (48°43'29.982'' N, 03°58'8.27'' W) in Roscoff (Brittany, France). Three individuals of each species were sampled. Additionally, samples from stranded algae (Std) were retrieved: within the mixture of diverse decomposing algae, microbiota from one *L. digitata*, one *F.*

serratus and one *P. palmata* specimens were collected each month. Swabbed surface was standardized to 50 cm^2 using a 5-cm square template on both sides of the algal thallus when possible. For *Ascophyllum nodosum*, a 1 cm-width frond was sampled on 25 cm on both sides. Three different regions of the kelp *L. digitata* were sampled: the basal meristem (young tissue, hereafter LdigB), the medium frond (ca. 20 cm away from the meristem, hereafter LdigM) and the old frond (the blade tip, hereafter LdigO). The different algal surfaces sampled (different species and different thallus parts) are referred to as "compartments" in the analyses. Swabs were immersed in DNA/RNA Shield reagent (ZymoBiomics), kept on ice during transport and stored at -20 °C until DNA and RNA extraction.

2. Extraction

Environmental DNA and RNA from swabs were extracted simultaneously using the DNA/RNA Miniprep kit (ZymoBiomics). All samples were processed between December 2020/January 2021 (except for February 2020 samples that were extracted two weeks after collection). DNA concentration was assessed with the QuantiFluor dsDNA System (Promega) kit and samples were normalized at 0.5 $ng.\mu l^{-1}$ before qPCR assays. RNA concentration was measured using a Qubit instrument with RNA HS Assay Kit and samples normalized at 1 $ng.\mu l^{-1}$ before reverse transcription.

3. qPCR assays

PCRs were carried out in 384-multiwell plates on a LightCycler 480 Instrument II (Roche). Each 5 µl reaction contained 2.5 µl of LightCycler 480 SYBR Green I Master mix 2X (Roche Applied Science), 0.5 µl of each primer (300 nM final) and 1.5 µl of template DNA. Each reaction was prepared in technical triplicates. The amplification program consisted of an initial denaturation at 95 °C for 10 min followed by 45 cycles of 95 °C for 10 s, 20 s at the chosen annealing temperature (Ta), and the polymerization at 72 °C for 10 s. After the amplification step, dissociation curves were generated by increasing the temperature from 65 °C to 97 °C. Total and *Zobellia* 16S rRNA gene copies were assessed by using either the universal primers 926F/1062R with Ta set to 60 °C or the *Zobellia*-specific primers 142F/289R with Ta set to 64 °C.

A dilution series of purified *Z. galactanivorans* $Dsij^T$ gDNA representing from 10 to 10^8 16S rRNA gene copies was used as a standard curve as explained in Part 1. The number of 16S rRNA gene copies from *Zobellia* was divided by that obtained with universal primers to assess the proportion of *Zobellia* copies in algal microbiota. The sample LdigB_1 in June displayed 52100 *Zobellia* 16S rRNA gene copies, which is 3.2 times more than in the sample with the second highest abundance (16300 *Zobellia* copies). After boxplot analysis of all results, it was considered an outlier and was then removed from further analyses. One-way ANOVA analyses were conducted in R v3.6.2 to assess variations depending on the type of algae (healthy vs. stranded), as well as two-way ANOVA with interaction effect between

algal compartments and sampling months. When significant ANOVA results were found ($P < 0.05$), pairwise post-hoc Tukey HSD were conducted.

4. RT-qPCR assays

RT-qPCR was successfully carried out for samples from the stranded alga. The other samples have not been analyzed yet.

Reverse transcription was conducted on the normalized RNA samples using the ImProm-II Reverse Transcription System (Promega). After addition of 1 µl of random primers to 9.5 µl of sample, RNA was denaturated by adding 10.5 µl of the reaction mix (4 µl of 5X Reaction Buffer, 3 µl of $MgCl_2$, 1 µl of dNTP Mix, 0.5 µl of Ribonuclease Inhibitor and 1 µl of Reverse Transcriptase) and incubating the mix for 5 min at 25°C, followed by 1 h at 42°C and 15 min at 70°C. For each sample, reactions were carried out with and without reverse transcriptase. qPCR was conducted immediately after reverse transcription with 1 µl of 10X diluted cDNA as described above. The number of copies obtained without reverse transcriptase was subtracted from the value obtained with reverse transcriptase to avoid any bias linked to DNA contamination.

5. Correlation with environmental data

Surface water temperature measured at 1.3 km from the collection site (Estacade sampling station) between February 2020 and December 2020 was used for correlation analyses. Data were downloaded from the SOMLIT database (Service d'Observation en Milieu Littoral; http://www.somlit.fr, Cocquempot *et al.*, 2019) on September 16th, 2021. Pearson correlation coefficients were calculated between averaged triplicates and surface water temperature using the *corrplot* package (v0.90).

III. Results

Quantitative PCR was carried out for the 240 DNA samples from algal microbiota to assess the seasonal prevalence and abundance of the genus *Zobellia* on macroalgae (**Table IV.1, Figure IV.1**). For healthy algae, we found a significant effect of both compartment type and collection month on the total ($F_{6,138} = 45.3$, $P < 0.001$; $F_{9,138} = 15.5$, $P < 0.001$, respectively) and *Zobellia* 16 rRNA gene copies number ($F_{6,138} = 15.7$, $P < 0.001$; $F_{9,138} = 47.9$, $P < 0.001$) as well as on the relative proportion of *Zobellia* copies ($F_{6,138} = 6.7$, $P < 0.001$; $F_{9,138} = 47.6$, $P < 0.001$) (**Figure IV.2A**). Interaction effects were found between compartment type and collection month for the number of total copies ($F_{54,138} = 5.1$, $P < 0.001$), the number of *Zobellia* copies ($F_{54,138} = 4.0$, $P < 0.001$) and the proportion of *Zobellia* copies ($F_{54,138} = 5.3$, $P < 0.001$), suggesting that seasonal variations depend on the type of the studied compartment and vice versa. Statistics of seasonal variations for each compartment and differences among compartment at each sampling month are represented in **Figure IV.2C**.

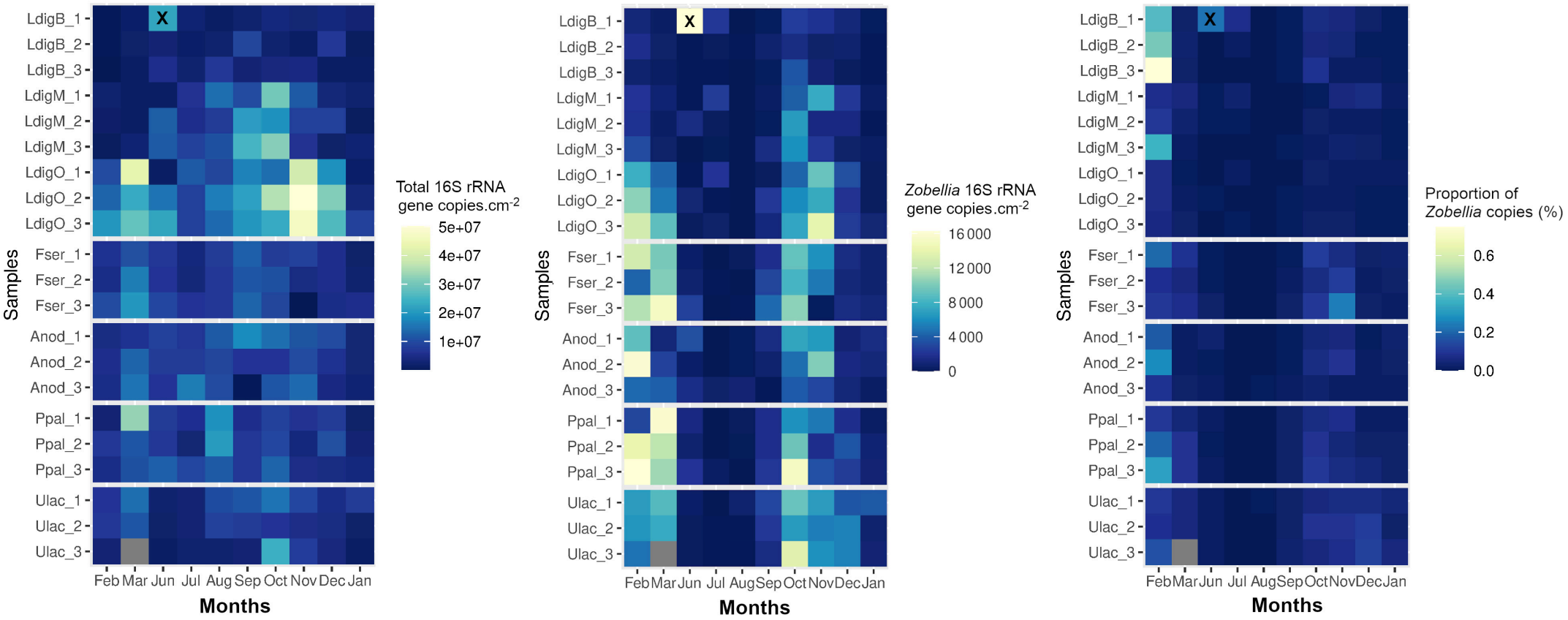

Figure IV.1: Abundance of *Zobellia* at the surface of healthy macroalgae. The number of total (left) and *Zobellia* (middle) 16S rRNA gene copies per cm^2 is shown, as well as the proportion of *Zobellia* copies (right). No data are available for Ulac_3 in march as the sample was lost. The sample LdigB_1 is considered as an outlier as 52100 *Zobellia* copies were measured. The scale maximum limit was then set at 16300, the number of copies measured in the second most abundant sample. LdigB_1 was not considered for statistical analyses.

Pairwise comparisons revealed significant compartment variations, mainly due to fluctuations along the *L. digitata* blade (**Figure IV.2A**) and not to fluctuations between algal species. The number of total copies differed according to the age of the algal tissue, the old blade of *L. digitata* displaying a higher density of 16S rRNA gene copies than the meristem or the medium frond. A similar pattern was observed for the number of *Zobellia* copies, with variations between the old blade and the meristem and the old and medium blade. The proportion of *Zobellia* copies in *L. digitata* microbiota tends to follow the opposite trend as the proportion decreased on older tissues. No significant variation was observed between the four other algae, whether we focused on the number of total or *Zobellia* copies and the *Zobellia* copy proportion. These algae were similar to *L. digitata* old blade in term of *Zobellia* copies number but similar to the meristem part when focusing on the proportion of *Zobellia* copies (except for Anod).

A seasonal pattern regarding the absolute and relative abundance of *Zobellia* copies was identified, while no clear pattern was detected for the whole bacterial community. Pairwise comparisons (**Figure IV.2B**) revealed a significantly lower amount of *Zobellia* copies during summer, from June to September. The lowest number of *Zobellia* copies was obtained in August for *L. digitata* (0-20 copies.cm^{-2} representing ca. 0-0.0005 % of the total copies) and in July for the other species (ca. 0-600 copies.cm^{-2} representing 0-0.002 % of the total copies). On the other hand, the amount of *Zobellia* copies peaked twice, in February-March and October-November, with approximately 10^3-10^4 estimated *Zobellia* 16S rRNA gene copies.cm^{-2}, representing 0.03-0.5 % of the total amount. In summer, the whole *L. digitata* blade displayed an equal distribution of the number of *Zobellia* copies (no significant differences between compartments were found, **Figure IV.2C**), while the number of total copies was ca. 3 times higher on the old blade than the meristem. By contrast, during winter-autumn (Feb, Mar, Oct, Nov), 10 times more *Zobellia* copies were detected on the old blade compared with the meristem part.

Significant negative correlations were detected between the surface seawater temperature and the absolute and relative amount of *Zobellia* copies (**Figure IV.3**), indicating that less *Zobellia* copies were found as the temperature increased. Globally, the variations in the total bacterial community cannot be explained by the seawater temperature, probably due to the broad diversity of taxa within epiphytic microbiota that likely display different temperature sensibility.

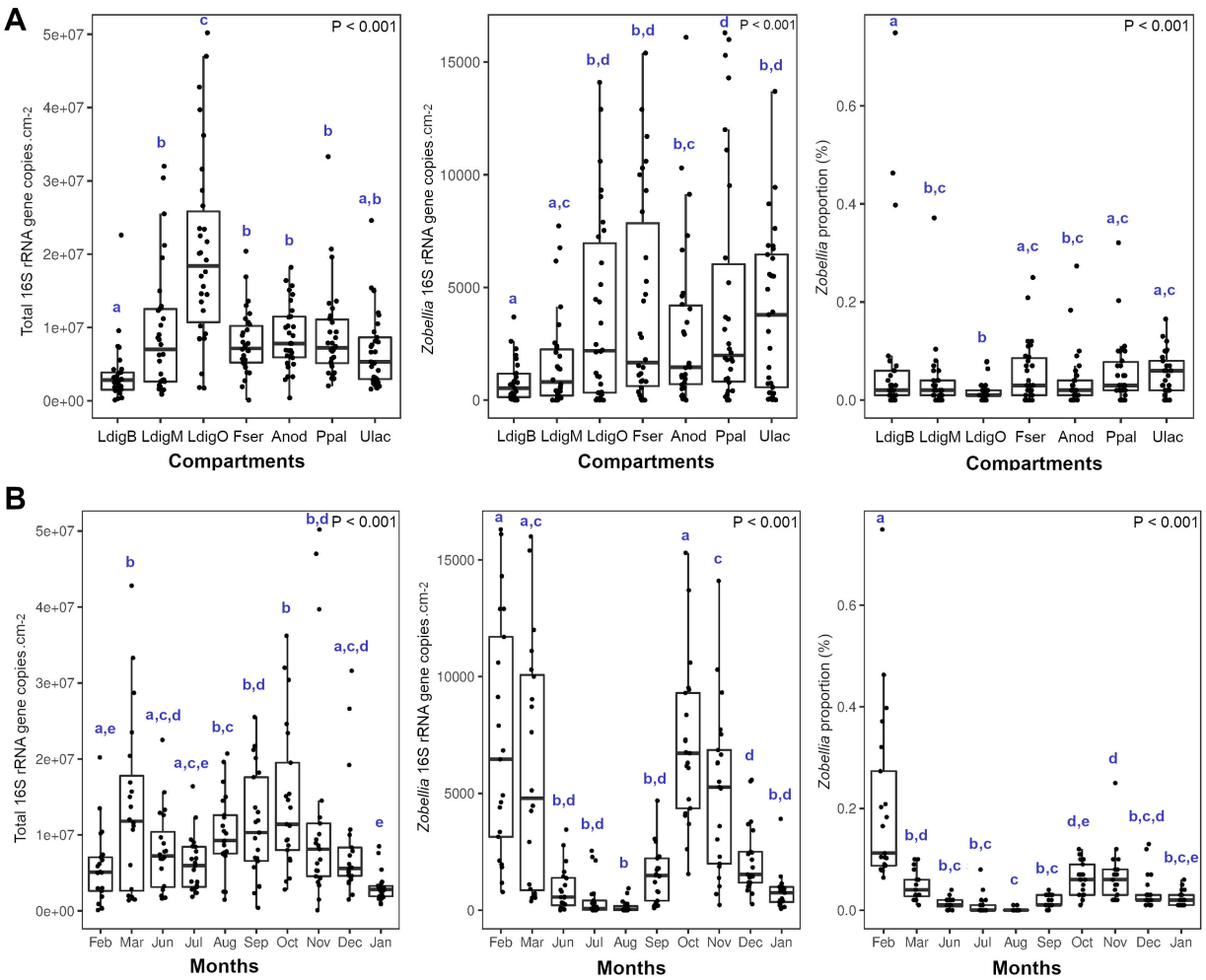

C

Compartment variations depending on the sampling month

	Total		*Zobellia*		Proportion	
	$F_{6,14}$	P-value	$F_{6,14}$	P-value	$F_{6,14}$	P-value
Feb	10	< 0.001	3.08	0.039	5.6	0.004
Mar	6.6	0.002	20.3	< 0.001	7.6	0.001
Jun	1.4	0.28	1.65	0.21	2.9	0.046
Jul	4.1	0.014	0.9	0.5	1.5	0.25
Aug	5.5	0.004	1.56	0.23	0.83	0.56
Sep	4.2	0.013	4.2	0.013	12	< 0.001
Oct	5.6	0.004	4.2	0.013	8.9	< 0.001
Nov	65.6	< 0.001	3.5	0.024	2.9	0.043
Dec	16.8	< 0.001	12.7	< 0.001	10.1	< 0.001
Jan	0.65	0.69	1.9	0.15	6.7	0.002

Seasonal variations depending on the algal compartment

	Total		*Zobellia*		Proportion	
	$F_{9,20}$	P-value	$F_{9,20}$	P-value	$F_{9,20}$	P-value
LdigB	1.5	0.23	4.5	0.003	20.2	< 0.001
LdigM	10.8	< 0.001	5.5	< 0.001	3.1	0.016
LdigO	9.4	< 0.001	17.2	< 0.001	28	< 0.001
Fser	7.3	< 0.001	12.9	< 0.001	6.6	< 0.001
Anod	1.6	0.2	5.7	< 0.001	8	< 0.001
Ppal	3.8	0.006	9.1	< 0.001	8.8	< 0.001
Ulac	3.6	0.009	17.7	< 0.001	12.7	< 0.001

Figure IV.2: Number of total (left) and *Zobellia* (middle) 16S rRNA gene copies per cm² and proportion of *Zobellia* copies (right) detected on the different compartments (A) and at different sampling months (B). Two-way ANOVA analysis was conducted (compartments x months) followed by post-hoc Tukey HSD test. Accordingly, blue letters (a, b, c, d, e) indicate those differences: if two conditions do not have at least one letter in common they are considered significantly different ($P < 0.05$). (C) As interactions between algal compartments and sampling months were found with two-way ANOVA, one-way ANOVA were conducted for each compartment and each sampling month, to assess for which months compartment variations were detected (top row) and for which compartments seasonal variations were detected (bottom row).

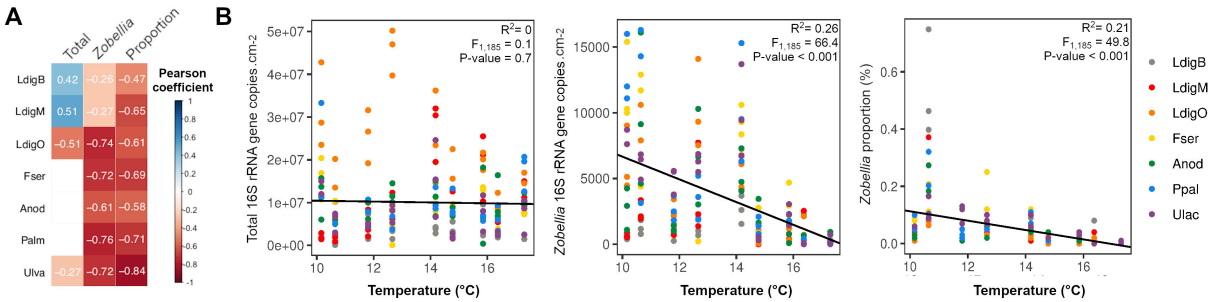

Figure IV.3: Correlation of the seasonal variations with seawater temperature. (A) Heatmap of the Pearson coefficients. Tiles are white if the correlation is not significant (P > 0.05), otherwise, Pearson coefficients are indicated. (B) Number of total (left) and *Zobellia* (middle) 16S rRNA gene copies per cm^2 and proportion of *Zobellia* copies (right) according to seawater temperature. Linear regressions were conducted: the linear trend line is represented in black and the regression coefficient R^2, the F-statistic and the p-value are indicated.

The microbiota of stranded decaying algae was also analyzed (**Figure IV.4A**). The absolute amount of *Zobellia* 16S rRNA gene copies and the *Zobellia* relative proportion were significantly higher on the stranded algae compared to the healthy ones ($F_{1,177}$ = 33.8, P < 0.001 and $F_{1,177}$ = 69.0, P < 0.001, respectively) (**Figure IV.5**). These differences were much less pronounced for the total community ($F_{1,177}$ = 5.8, P = 0.017) as the average fold-change for the comparison stranded vs. healthy was equal to 1.6 and 135 for the total and *Zobellia* community, respectively.

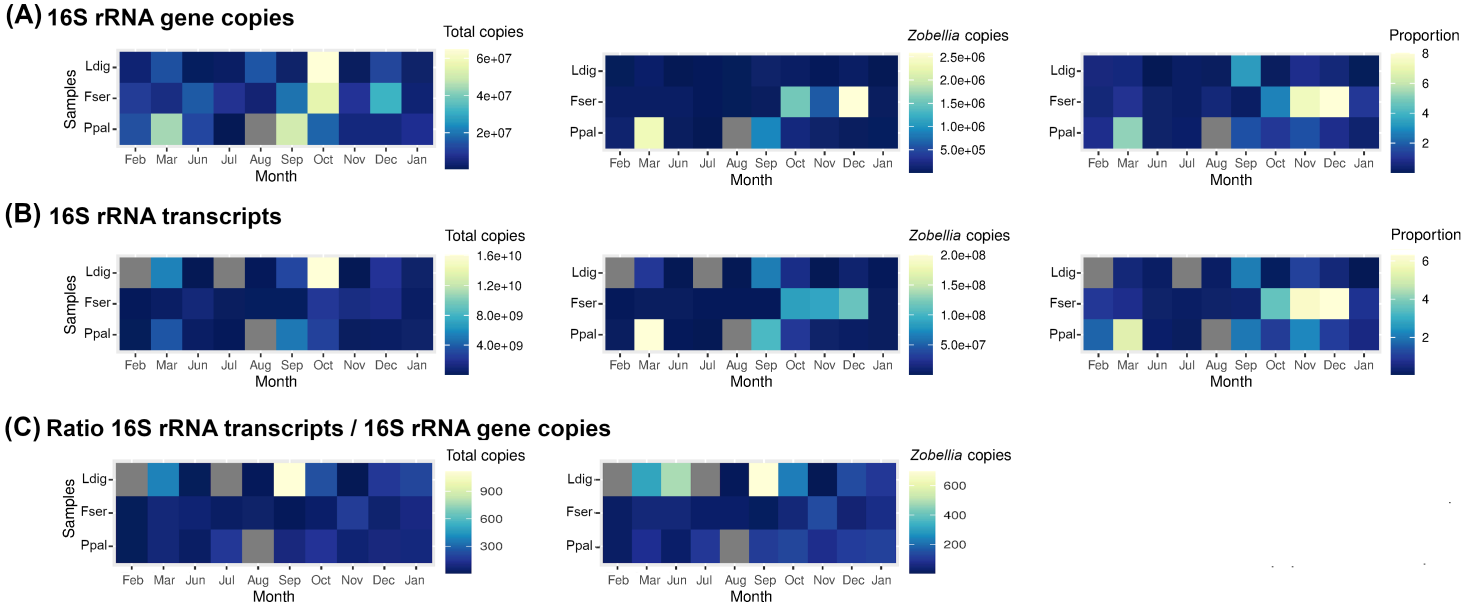

Figure IV.4: Number of total (left) and *Zobellia* (middle) 16S rRNA gene (A) and transcript (B) copies per cm^2 and proportion of *Zobellia* copies (right) at the surface of stranded algae. (C) The ratio transcript / gene copies was assessed. No data are available for replicate 3 in August as no stranded *P. palmata* was found this month. RT-qPCR was unsuccessful for replicate 1 in February and July (Ct values above the ones obtained for the Non-Template Control) with both universal and *Zobellia*-specific primers.

Zobellia represented 0.1-3.4% of the total number of 16S rRNA gene copies on stranded *L. digitata*, 0.2-8% on stranded *F. serratus* and 0.3-5.2% on stranded *P. palmata*. As observed for healthy algae, the highest absolute and relative counts were detected during the winter-autumn months.

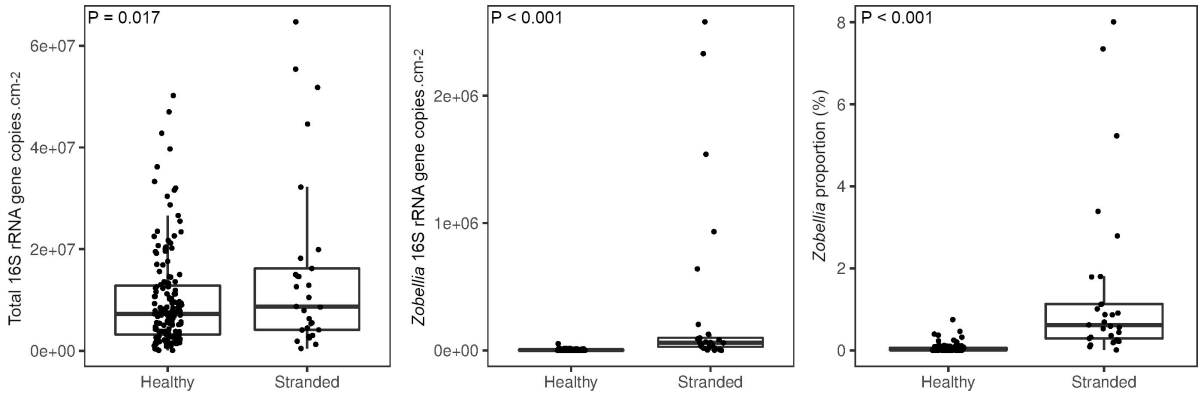

Figure IV.5: Number of total (left) and *Zobellia* (middle) 16S rRNA gene copies per cm² and proportion of *Zobellia* copies (right) at the surface of healthy and stranded algae. For healthy algae, only samples from the surface of *L. digitata*, *F. serratus* and *P. palmata* are represented as stranded specimens were collected from these three species.

For the stranded samples, RT-qPCR was also performed to determine the activity of the genus *Zobellia* on macroalgae (**Figure IV.4B**). The number of total and *Zobellia* 16S rRNA transcript copies is approximatively 100 times higher than the number of gene copies. The proportion of *Zobellia* 16S rRNA gene copies and *Zobellia* 16S rRNA transcript were very similar.

The ratio of 16S rRNA transcript copies over gene copies (cDNA/DNA) was calculated (**Figure IV.4C**) as a proxy to assess the amount of 16S rRNA molecules produced from one 16S rRNA gene and compare the transcriptional activity of the cells. No seasonal pattern could be identified, but the cDNA/DNA copies ratio seemed higher in the *L. digitata* samples. The mean cDNA/DNA ratios for *L. digitata*, *F. serratus* and *P. palmata* samples were respectively equal to 283, 63 and 97 for *Zobellia* and 307, 75 and 93 for the whole community (February, July and August months for which a value was not assessed for the three algae were excluded from the mean calculations).

IV. Discussion

1. Widespread distribution of the genus *Zobellia* on macroalgae

This study monitored for the first time the presence and abundance of the genus *Zobellia* at the surface of macroalgae over a whole year. I showed that the genus is part of the biofilm covering the five different sampled algal species, which cover all three algal phyla and whose chemical composition largely differs between one another (see Kloareg *et al.*, 2021 for review). This observation is consistent with the fact that most of the described *Zobellia* species were isolated from macroalgae (Barbeyron *et al.*, 2001, 2021; Nedashkovskaya *et al.*, 2004) and that *Zobellia* sequences were found in metagenomic studies on macroalgae (e.g. Alonso *et al.*, 2007; Dogs *et al.*, 2017). When annotating *Z. galactanivorans* Dsij^T

genome Barbeyron *et al.*, 2016, adaptive traits likely allowing stable association with macroalgal hosts were proposed (potential production of thallusin, exudates utilization, ability to cope with algal defenses, gliding motility lifestyle). Some were experimentally confirmed *in vitro*, including the ability the use mannitol and process halogenated compounds (Fournier *et al.*, 2014; Groisillier *et al.*, 2015; Grigorian *et al.*, 2021). Most of these genes related to these traits are conserved in other *Zobellia* strains, likely explaining the prevalence of the genus on macroalgal surfaces. Moreover, the described strains can assimilate several of the main polysaccharides contained in the extracellular matrix (ECM) of the three algal phyla (Barbeyron *et al.*, 2001, 2021; Nedashkovskaya *et al.*, 2004). On healthy macroalgae, the proportion of 16S rRNA gene copies from *Zobellia* reached 0.03-0.5% of the total community at some period of the year. This amount appears ecologically relevant regarding the hundreds of different taxa reported to live on macroalgae surfaces (Egan *et al.*, 2013). However, *Zobellia* is likely not one of the most abundant genera as some other taxa (such as *Granulosicoccus*, *Litorimonas* or *Hellea* spp. on kelps) can represent more than 10 % of the biofilm community on macroalgae (Paix *et al.*, 2019; Ramirez-Puebla *et al.*, 2020; Brunet *et al.*, 2021 [Chapter III]). Pioneer bacteria might not be the more abundant representatives in bacterial communities but would still play a crucial role in the ecosystem, notably compensating by their large CAZymes repertoire. A high proportion of *Zobellia* spp. would probably be harmful for the algae due to their potent hydrolytic abilities toward algal polysaccharides. However, its stable presence on the diverse algal species might suppose a neutral or beneficial interaction with the host. As reported by Egan *et al.*, 2013, bacteria might display commensal interactions with the algae and only become harmful at some point as a result of changes in the environment.

2. *Zobellia* abundance exhibits seasonal variabilities

A seasonal pattern was identified irrespective of the algal species for the number of *Zobellia* 16S rRNA gene copies and its proportion over the total number of copies. A decrease in abundance was observed between February/March and the summer months, before an increase in October/November followed by a progressive decrease in December/January. Kim *et al.*, 1992 also reported such a decrease between winter and summer for *Flavobacterium* spp. in seawater from a habitat dominated by *Porphyra* specimens. Several parameters could explain these seasonal variations, such as (i) the variation of physico-chemical parameters (ii) fluctuations related to the algae itself such as biomass composition or life cycle.

The macroalgae surface is a dynamic habitat influenced by many environmental parameters such as variations in physico-chemical parameters (temperature, oxygen, light intensity, etc.), phytoplankton bloom, storm events, etc. Fluctuations of these variables create diverse ecological niches selecting specific bacteria that possess adaptive traits reflecting the niche conditions. Here, we observed a strong negative correlation between the abundance of *Zobellia* and the temperature of surface seawater, which

ranged from 10 °C in winter to 18 °C in summer. Temperature is well-known to influence biological processes (Nedwell and Rutter, 1994) and is an important driver of bacterial community structure on macroalgae (Gilbert *et al.*, 2009; Takemura *et al.*, 2014; Paix *et al.*, 2021). The same seasonal effect was reported for all algae, suggesting that environmental parameters (seawater temperature in particular), would be the main parameters shaping *Zobellia* abundance, rather than algae-related parameters. The described *Zobellia* strains have an optimal growth temperature around 20-30 °C, but temperature likely impacts the growth differently in natural communities. Algal microbiota encompasses a large diversity of taxa interacting with each other. Higher temperature conditions might be well adapted for specific taxa whose presence might prevent the growth of *Zobellia* at the surface of macroalgae, as they might privatize the algal surface thanks to their fast growth rate or the release of antagonist metabolites to which *Zobellia* is sensitive. For example, members of the genus *Vibrio* are found on macroalgae (Takemura *et al.*, 2014; Barberi *et al.*, 2020) and are known to have a short generation time (Ulitzur, 1974). Their abundance in seawater largely depends on the temperature, with maximal counts being reported in summer (Ulitzur, 1974; Kim *et al.*, 1992; Takemura *et al.*, 2014).
To complement these quantitative data, 16S rRNA gene metabarcoding was performed on all the DNA samples and sequence analysis is still underway. It will help to link the variations in abundance of the genus *Zobellia* with the succession of other taxa and potentially reveal taxa that might hinder the presence of *Zobellia* in summer.

Changes in the chemical composition of algal tissues could also partly explain seasonal variabilities observed in the abundance of *Zobellia*. In particular, the chemicals involved in algal defense are strong selective factors for epiphytic bacterial colonizers.
Phenolic compounds are part of the algal extracellular matrix and are exuded by the algae (Abdullah and Fredriksen, 2004). Algal tissues appeared to be richer in phenolic compounds during the summer months (Parys *et al.*, 2009). They are assumed to function as thallus protectors against grazers and display bactericidal activity (Nagayama *et al.*, 2002; Hierholtzer *et al.*, 2013). Hence, they could differentially affect the abundance of some epiphytic taxa. However, nothing is known regarding the sensitivity of the genus *Zobellia* toward these phenolic compounds. The phenolic content also varies depending on the algal species and was reported to be higher in *Fucales* than *Laminariales* (Holdt and Kraan, 2011). Here, no significant difference was reported between the different algal species and no significant abundance decrease was observed for the total community in summer. It would suggest that phenol content could have only a limited effect on the composition of the bacterial community. However, it is important to consider that fluctuations within the algal tissues might not represent fluctuations within the algal exudates. Abdullah and Fredriksen, 2004 reported no significant variations in phenol concentration in *L. hyperborea* exudates through the year, but different patterns could occur with other algae and in different geographical locations. Also, previous studies reported that phenolic compounds would disrupt cell membranes, alter their permeability and that cells seems to be affected to

a different extent depending on their exact morphology (Hierholtzer *et al.*, 2013). Their mode of action indicate that they would potentially be more effective on Gram-positive rather than Gram-negative bacteria (Zubia *et al.*, 2008; Shannon and Abu-Ghannam, 2016). It would suggest a limited impact on the epiphytic communities as Gram-negative are believed to represent ¾ of the communities in marine environments (Kim *et al.*, 1992; Jensen and Fenical, 1995).

Seasonal variations of the iodine content were previously studied for the five algal species we focused on (Nitschke *et al.*, 2018). They showed that globally, iodine content was minimum during the summer month and maximum in winter. This is in accordance with Ar Gall *et al.*, 2004 which revealed that, in winter, *L. digitata* tissues were twice richer in iodine than in summer. Hence the abundance and proportion of *Zobellia* could be correlated with the iodine content in the algal tissues. *Z. galactanivorans* Dsij^T possesses genes encoding three vanadium-iodoperoxidases (vIPOs), an iodotyrosine dehalogenase and a haloacid dehalogenase (Fournier *et al.*, 2014; Barbeyron, Thomas, *et al.*, 2016; Grigorian *et al.*, 2021) and is able to accumulate high iodine concentrations (Barbeyron, Thomas, *et al.*, 2016). Homologs of these genes are also found in the eight other described strains of the genus, suggesting that the latter are well equipped to counteract the high amounts of iodinated compounds produced by macroalgae as a defense mechanism. It could be a selective advantage over other taxa for algal colonization.

Seasonal variations in sugar content and composition were reported in macroalgae (Schiener *et al.*, 2015; Fletcher *et al.*, 2017; Sfriso *et al.*, 2017) but no clear pattern could be identified, except for laminarin and mannitol that are more abundant in summer in kelp. These storage sugars display fewer complex structures than ECM polysaccharides. Their high content in summer might benefit taxa able to use these carbon sources but lacking the ability to degrade ECM polysaccharides.

The growth cycle of algae might also influence their colonization. For example, kelp blade renewal and expansion occur in spring at the meristem part (Perez, 1969). In consequence, in May, the whole blade consists of fresh tissue. Hence the low proportion of *Zobellia* in summer suggests it might not be an early colonizer. Moreover, as discussed in Bengtsson *et al.*, 2010, algal exudation is higher in summer (Abdullah and Fredriksen, 2004) and exudate consumers might dominate the biofilm. By contrast, the aging tissues in autumn-winter might select for specialist bacteria able to break down the algal extracellular matrix. Our results are consistent with previous reports of the higher abundance of *Bacteroidetes* and *Verrucomicrobia* in February and November, two phyla known to use algal complex biomass (Bengtsson *et al.*, 2010). However, I also observed a seasonal pattern in the abundance and proportion of *Zobellia* in non-kelp algal species that feature growth cycles compared to *L. digitata*. Hence, tissue renewal along the algal growth cycle might not be the main driver of *Zobellia* abundance fluctuation.

3. *Zobellia* is not equally distributed on kelp thallus

We also reported differences in *Zobellia* abundance between the different parts of the *L. digitata* thallus. As observed for the whole community, the absolute amount of *Zobellia* 16S rRNA genes seems to

gradually increase along the blade, being maximum at the distal ends. The old blade is much more damaged than the medium or the meristem part, with evident signs of decay, offering a larger pool of nutrients. Such a pattern was already reported for several kelp species (Tujula *et al.*, 2006; Staufenberger *et al.*, 2008; Weigel and Pfister, 2019; Ihua *et al.*, 2020). Interestingly, the proportion of *Zobellia* 16S rRNA gene copies over the total community tends to be higher at the meristem part. As raised in the previous part of this chapter (Brunet et al., 2021, accepted), it could result from the different ecological strategies adopted by the algal consumers. We demonstrated in chapter V that *Zobellia* spp. grew on young *L. digitata* tissues, suggesting their ability to feed on the meristem (characterized by its good integrity) in the wild. The majority of the bacterial community might not share this specific trait, likely benefiting from the larger source of accessible compounds offered by the damaged tissues at the distal part of the blade and might outcompete other taxa specialized in intact tissue degradation (Datta *et al.*, 2016; Jiménez *et al.*, 2017).

4. Search for *Zobellia* in stranded macroalgae

a. Stranded decaying macroalgae are strongly enriched in *Zobellia* copies

Detached macroalgae accumulate on the seashore forming a mixture of stranded decaying algal biomass from different species. We noticed important variations in the number of total and *Zobellia* 16S rRNA gene copies between the different stranded species. It would suggest that even if the stranded algae are forming a decomposing mixture of various macroalgae on the coast, the different species still have distinct epiphytic bacterial communities as they might offer distinct ecological niches. The proportion of *Zobellia* was approximately 10 times higher at the surface of these decaying algae compared to the healthy ones, reaching 8% in some samples from *Fucus serratus*. Those differences were less pronounced in the total community, suggesting a specific augmentation of the genus *Zobellia* in this ecological niche compared to other taxa. This very high proportion in hotspots of decaying algal biomass strengthens the ecological relevance of *Zobellia* spp. for macroalgae recycling. Decaying and healthy algae might offer distinct ecological niches and macroalgal microbiota might shift toward taxa displaying a consequent CAZyme repertoire during algal decomposition. Such shift was shown in our previous publication (Brunet *et al.*, 2021**,** Chapter III) as we reported an increase in algal polysaccharides degraders following detached kelp accumulation. Members of the genus *Zobellia* seem to be part of the resident microbial biofilm on healthy macroalgae, possibly acting as a neutral microorganism. In stranded algae-associated microbiota, its strong abilities to degrade complex algal biomass would be a selective advantage, highlighting its saprophyte behavior.

b. *Zobellia* metabolic activity on stranded macroalgae

Since rRNA content is positively correlated with growth rate (Schaechter *et al.*, 1958; Kjeldgaard and Kurland, 1963) and is degraded quickly after cell death, RT-qPCR were performed to distinguish between metabolically active cells and dead or dormant cells or free DNA fragments. The proportions of *Zobellia* 16S rRNA gene copies and *Zobellia* 16S rRNA transcripts over the total community were similar for each sample, suggesting that the *Zobellia* cells present at the surface of macroalgae are equally active compared with the other community members. The 16S rRNA transcript/gene ratio calculated for *Zobellia* copies was similar to the one calculated for the whole community. It does not seem surprising as the ecological niches resulting from the accumulation and decay of stranded algae likely select for a broad range of algal degraders actively feeding on the large amounts of substrates available. The amount of 16S rRNA transcripts was ca. 60-300-fold higher than 16S rRNA gene copies. Lankiewicz *et al.*, 2016 investigated the 16S rRNA transcript/gene ratio of copiotroph and oligotroph strains and revealed that for *Polaribacter* sp. MED152, a coastal member of the class *Flavobacteriia*, the ratio was ca. 300-500 when cultivated in the laboratory. This ratio was more than 10-fold lower in the environment (Delaware estuary), probably due to the slow growth of the strain at the sampling point. Hence, the ratio calculated in the present study are consistent with what was observed for an actively growing flavobacteria, supporting the active role of *Zobellia* in algae utilization. No relationship between the 16S rRNA transcript/gene ratio and sampling month was clearly detected, suggesting that temperature might impact differently the activity of the different taxa within the communities and they might overall compensate each other. Differences were identified between the stranded individuals. *L. digitata* was less enriched in total 16S rRNA gene copies, including *Zobellia* copies, but exhibited a transcript/gene ratio 3-fold higher than *F. serratus* or *P. palmata* specimens. This higher metabolic activity of *Zobellia* cells could be due to higher growth rates and/or higher degrading capacities. This is in accordance with our findings described in Chapter V demonstrating that *L. digitata* was the only macroalgae, over the different species I tested, displaying complete tissues breakdown in the presence of *Z. galactanivorans* Dsij^{T}.

This study provides first insights into the ecological strategies of the algae-degrader genus *Zobellia* by assessing its absolute and relative abundance in coastal ecosystems. We established its widespread distribution on all three algal phyla and identified a clear seasonal pattern. Further study with larger sampling efforts over several years and at several geographical location would be useful to confirm the results described in this study and to have a more comprehensive understanding of the distribution of *Zobellia* spp. in the wild. Combined with compositional analysis of the collected algal specimens and measurements of various environmental parameters, such data would help unravel more deeply the

ecological strategies of the model genus in macroalgae-dominated habitats.

It should be kept in mind that the number of 16S rRNA gene copies in the genome differ among the bacterial community, potentially leading to quantification biases. As raised in Part 1, qPCR could be linked with CARD-FISH approach to estimate more precisely the abundance of *Zobellia* in the wild. Overall, this study supports that, besides its well-established catabolic interest in algal polysaccharide degradation, the use of *Zobellia galactanivorans* as a model microorganism to study algae-bacteria interactions is also relevant from an ecological point of view.

Table IV.1: Characteristics of the 240 samples collected during the seasonal sampling. Prop: *Zobellia* copies proportion.

Name	Sampling date (DD/MM/YYYY)	Surface seawater temperature (°C)	Algae	[DNA] ($ng.\mu l^{-1}$)	[RNA] ($ng.\mu l^{-1}$)	DNA			cDNA		
						Total copies.cm^{-2}	*Zobellia* copies.cm^{-2}	Prop (%)	Total copies.cm^{-2}	*Zobellia* copies.cm^{-2}	Prop (%)
02_LdigB_1	10/02/2020	10.6	*Laminaria digitata* (base)	0.11	too low	2.94E+05	1.17E+03	0.40			
02_LdigB_2	10/02/2020	10.6	*Laminaria digitata* (base)	0.61	3.51	3.98E+05	1.84E+03	0.46			
02_LdigB_3	10/02/2020	10.6	*Laminaria digitata* (base)	0.40	2.62	1.04E+05	7.79E+02	0.75			
02_LdigM_1	10/02/2020	10.6	*Laminaria digitata* (medium)	2.21	3.43	2.63E+06	2.12E+03	0.08			
02_LdigM_2	10/02/2020	10.6	*Laminaria digitata* (medium)	1.63	3.4	1.88E+06	1.95E+03	0.10			
02_LdigM_3	10/02/2020	10.6	*Laminaria digitata* (medium)	0.69	too low	9.03E+05	3.35E+03	0.37			
02_LdigO_1	10/02/2020	10.6	*Laminaria digitata* (old)	10.65	4.21	1.02E+07	7.90E+03	0.08			
02_LdigO_2	10/02/2020	10.6	*Laminaria digitata* (old)	11.25	8.90	1.35E+07	1.06E+04	0.08			
02_LdigO_3	10/02/2020	10.6	*Laminaria digitata* (old)	14.78	7.87	2.02E+07	1.29E+04	0.06			
02_Fser_1	10/02/2020	10.6	*Fucus serratus*	4.98	2.95	6.17E+06	1.29E+04	0.21			
02_Fser_2	10/02/2020	10.6	*Fucus serratus*	4.44	2.98	5.03E+06	4.40E+03	0.09			
02_Fser_3	10/02/2020	10.6	*Fucus serratus*	7.78	3.07	1.04E+07	1.17E+04	0.11			
02_Anod_1	10/02/2020	10.6	*Ascophyllum nododum*	4.33	2.50	4.99E+06	9.13E+03	0.18			
02_Anod_2	10/02/2020	10.6	*Ascophyllum nododum*	6.11	2	5.88E+06	1.61E+04	0.27			
02_Anod_3	10/02/2020	10.6	*Ascophyllum nododum*	4.86	3.9	5.12E+06	4.62E+03	0.09			
02_Ppal_1	10/02/2020	10.6	*Palmaria palmata*	1.87	too low	3.01E+06	3.14E+03	0.10			
02_Ppal_2	10/02/2020	10.6	*Palmaria palmata*	6.10	5.21	7.06E+06	1.43E+04	0.20			
02_Ppal_3	10/02/2020	10.6	*Palmaria palmata*	3.68	2.2	5.09E+06	1.63E+04	0.32			
02_Ulac_1	10/02/2020	10.6	*Ulva lactuca*	9.72	19.30	6.68E+06	6.84E+03	0.10			
02_Ulac_2	10/02/2020	10.6	*Ulva lactuca*	5.94	58.00	7.40E+06	6.46E+03	0.09			
02_Ulac_3	10/02/2020	10.6	*Ulva lactuca*	4.72	11.4	2.97E+06	4.92E+03	0.17			
02_Std_1	10/02/2020	10.6	Stranded *L. digitata*	4.32	3.66	4.09E+06	2.83E+04	0.69	-	-	-
02_Std_2	10/02/2020	10.6	Stranded *F. serratus*	7.40	6.77	1.05E+07	6.16E+04	0.59	1.42E+08	1.31E+06	0.92
02_Std_3	10/02/2020	10.6	Stranded *P. palmata*	7.98	6.12	1.46E+07	1.27E+05	0.87	1.99E+08	3.45E+06	1.74
03_LdigB_1	12/03/2020	10.2	*Laminaria digitata* (base)	1.31	3.00	1.81E+06	5.34E+02	0.03			
03_LdigB_2	12/03/2020	10.2	*Laminaria digitata* (base)	1.86	4.14	1.98E+06	7.15E+02	0.04			

03_LdigB_3	12/03/2020	10.2	*Laminaria digitata* (base)	3.36	4.5	1.39E+06	3.87E+02	0.03			
03_LdigM_1	12/03/2020	10.2	*Laminaria digitata* (medium)	1.71	2.84	1.60E+06	9.02E+02	0.06			
03_LdigM_2	12/03/2020	10.2	*Laminaria digitata* (medium)	1.26	2.40	1.49E+06	5.33E+02	0.04			
03_LdigM_3	12/03/2020	10.2	*Laminaria digitata* (medium)	1.18	2.30	2.86E+06	5.93E+02	0.02			
03_LdigO_1	12/03/2020	10.2	*Laminaria digitata* (old)	41.46	10.2	4.28E+07	4.47E+03	0.01			
03_LdigO_2	12/03/2020	10.2	*Laminaria digitata* (old)	26.50	11.00	2.35E+07	5.13E+03	0.02			
03_LdigO_3	12/03/2020	10.2	*Laminaria digitata* (old)	32.63	11.8	2.87E+07	9.03E+03	0.03			
03_Fser_1	12/03/2020	10.2	*Fucus serratus*	15.22	6.64	1.07E+07	1.00E+04	0.09			
03_Fser_2	12/03/2020	10.2	*Fucus serratus*	26.32	4.77	1.69E+07	1.03E+04	0.06			
03_Fser_3	12/03/2020	10.2	*Fucus serratus*	17.41	9.57	2.04E+07	1.54E+04	0.08			
03_Anod_1	12/03/2020	10.2	*Ascophyllum nododum*	7.11	2.2	6.02E+06	1.10E+03	0.02			
03_Anod_2	12/03/2020	10.2	*Ascophyllum nododum*	14.28	4.88	1.37E+07	2.92E+03	0.02			
03_Anod_3	12/03/2020	10.2	*Ascophyllum nododum*	20.44	3.11	1.57E+07	4.25E+03	0.03			
03_Ppal_1	12/03/2020	10.2	*Palmaria palmata*	33.38	9.82	3.33E+07	1.60E+04	0.05			
03_Ppal_2	12/03/2020	10.2	*Palmaria palmata*	13.13	7.53	1.16E+07	1.20E+04	0.10			
03_Ppal_3	12/03/2020	10.2	*Palmaria palmata*	31.23	15.7	1.12E+07	1.11E+04	0.10			
03_Ulac_1	12/03/2020	10.2	*Ulva lactuca*	12.90	7.88	1.50E+07	8.71E+03	0.06			
03_Ulac_2	12/03/2020	10.2	*Ulva lactuca*	12.32	4.41	1.20E+07	7.62E+03	0.06			
03_Std_1	12/03/2020	10.2	Stranded *L. digitata*	3.59	2.40	1.47E+07	9.13E+04	0.62	5.60E+09	2.86E+07	0.51
03_Std_2	12/03/2020	10.2	Stranded *F. serratus*	6.36	38.4	6.32E+06	6.41E+04	1.01	4.89E+08	3.60E+06	0.74
03_Std_3	12/03/2020	10.2	Stranded *P. palmata*	17.88	5.23	4.46E+07	2.33E+06	5.23	3.80E+09	2.00E+08	5.28
06_LdigB_1	05/06/2020	14.8	*Laminaria digitata* (base)	9.83	22.5	2.26E+07	5.21E+04	0.23			
06_LdigB_2	05/06/2020	14.8	*Laminaria digitata* (base)	2.77	6.44	3.24E+06	2.96E+01	0.00			
06_LdigB_3	05/06/2020	14.8	*Laminaria digitata* (base)	4.62	2.30	5.55E+06	9.82E+01	0.00			
06_LdigM_1	05/06/2020	14.8	*Laminaria digitata* (medium)	0.79	3.1	1.61E+06	8.07E+01	0.01			
06_LdigM_2	05/06/2020	14.8	*Laminaria digitata* (medium)	11.51	too low	1.29E+07	1.44E+03	0.01			
06_LdigM_3	05/06/2020	14.8	*Laminaria digitata* (medium)	11.31	5.71	1.26E+07	0.00E+00	0.00			
06_LdigO_1	05/06/2020	14.8	*Laminaria digitata* (old)	1.46	5.58	1.73E+06	6.70E+01	0.00			
06_LdigO_2	05/06/2020	14.8	*Laminaria digitata* (old)	16.19	2.30	1.56E+07	1.07E+03	0.01			
06_LdigO_3	05/06/2020	14.8	*Laminaria digitata* (old)	20.77	5.37	2.25E+07	2.47E+02	0.00			
06_Fser_1	05/06/2020	14.8	*Fucus serratus*	7.67	5.46	7.03E+06	5.55E+02	0.01			
06_Fser_2	05/06/2020	14.8	*Fucus serratus*	7.53	13.8	6.85E+06	8.64E+02	0.01			

06_Fser_3	05/06/2020	14.8	*Fucus serratus*	7.67	5.33	9.67E+06	2.78E+03	0.03			
06_Anod_1	05/06/2020	14.8	*Ascophyllum nododum*	10.60	4.86	8.88E+06	3.45E+03	0.04			
06_Anod_2	05/06/2020	14.8	*Ascophyllum nododum*	9.18	4.72	7.81E+06	5.47E+02	0.01			
06_Anod_3	05/06/2020	14.8	*Ascophyllum nododum*	6.98	3.54	6.86E+06	1.64E+03	0.02			
06_Ppal_1	05/06/2020	14.8	*Palmaria palmata*	6.60	7.76	7.87E+06	1.37E+03	0.02			
06_Ppal_2	05/06/2020	14.8	*Palmaria palmata*	7.57	11.4	7.41E+06	7.91E+02	0.01			
06_Ppal_3	05/06/2020	14.8	*Palmaria palmata*	13.54	7.18	1.33E+07	2.10E+03	0.02			
06_Ulac_1	05/06/2020	14.8	*Ulva lactuca*	2.34	8.35	2.78E+06	5.73E+02	0.02			
06_Ulac_2	05/06/2020	14.8	*Ulva lactuca*	1.50	3.56	1.98E+06	3.06E+02	0.02			
06_Ulac_3	05/06/2020	14.8	*Ulva lactuca*	0.93	2.20	1.73E+06	3.26E+02	0.02			
06_Std_1	05/06/2020	14.8	Stranded *L. digitata*	0.82	too low	1.27E+06	8.02E+01	0.01	2.01E+07	3.92E+04	0.20
06_Std_2	05/06/2020	14.8	Stranded *F. serratus*	9.71	7.91	1.62E+07	5.91E+04	0.36	1.06E+09	3.17E+06	0.30
06_Std_3	05/06/2020	14.8	Stranded *P. palmata*	9.59	13.20	1.29E+07	4.11E+04	0.32	4.72E+08	1.18E+06	0.25
07_LdigB_1	06/07/2020	16.4	*Laminaria digitata* (base)	2.23	10.4	2.95E+06	2.28E+03	0.08			
07_LdigB_2	06/07/2020	16.4	*Laminaria digitata* (base)	2.42	2.68	1.85E+06	3.13E+02	0.02			
07_LdigB_3	06/07/2020	16.4	*Laminaria digitata* (base)	3.33	6.18	2.81E+06	3.25E+01	0.00			
07_LdigM_1	06/07/2020	16.4	*Laminaria digitata* (medium)	4.45	5.81	6.33E+06	2.54E+03	0.04			
07_LdigM_2	06/07/2020	16.4	*Laminaria digitata* (medium)	5.43	3.50	5.41E+06	2.96E+02	0.01			
07_LdigM_3	06/07/2020	16.4	*Laminaria digitata* (medium)	9.42	3.94	9.01E+06	1.48E+02	0.00			
07_LdigO_1	06/07/2020	16.4	*Laminaria digitata* (old)	12.16	6.09	1.23E+07	2.13E+03	0.02			
07_LdigO_2	06/07/2020	16.4	*Laminaria digitata* (old)	10.03	6.65	8.49E+06	5.82E+01	0.00			
07_LdigO_3	06/07/2020	16.4	*Laminaria digitata* (old)	7.55	5.90	8.43E+06	7.08E+02	0.01			
07_Fser_1	06/07/2020	16.4	*Fucus serratus*	3.90	4.74	3.81E+06	0.00E+00	0.00			
07_Fser_2	06/07/2020	16.4	*Fucus serratus*	4.13	3.02	3.85E+06	1.20E+02	0.00			
07_Fser_3	06/07/2020	16.4	*Fucus serratus*	9.92	3.91	6.83E+06	0.00E+00	0.00			
07_Anod_1	06/07/2020	16.4	*Ascophyllum nododum*	7.28	5.21	6.91E+06	4.84E+01	0.00			
07_Anod_2	06/07/2020	16.4	*Ascophyllum nododum*	7.66	3.27	7.82E+06	0.00E+00	0.00			
07_Anod_3	06/07/2020	16.4	*Ascophyllum nododum*	22.43	4.2	1.64E+07	6.82E+02	0.00			
07_Ppal_1	06/07/2020	16.4	*Palmaria palmata*	6.99	7	5.95E+06	0.00E+00	0.00			
07_Ppal_2	06/07/2020	16.4	*Palmaria palmata*	4.56	7.95	3.39E+06	0.00E+00	0.00			
07_Ppal_3	06/07/2020	16.4	*Palmaria palmata*	8.74	2.8	9.39E+06	4.12E+02	0.00			
07_Ulac_1	06/07/2020	16.4	*Ulva lactuca*	2.03	too low	3.09E+06	9.24E+00	0.00			

07_Ulac_2	06/07/2020	16.4	*Ulva lactuca*	3.52	5.12	3.15E+06	6.83E+01	0.00			
07_Ulac_3	06/07/2020	16.4	*Ulva lactuca*	1.79	2.84	2.37E+06	1.96E+01	0.00			
07_Std_1	06/07/2020	16.4	Stranded *L. digitata*	2.45	2.10	2.55E+06	5.51E+03	0.22	-	-	-
07_Std_2	06/07/2020	16.4	Stranded *F. serratus*	7.94	2.5	8.60E+06	1.95E+04	0.23	2.97E+08	5.63E+05	0.19
07_Std_3	06/07/2020	16.4	Stranded *P. palmata*	0.51	10.8	4.61E+05	1.36E+03	0.29	7.80E+07	1.43E+05	0.18
08_LdigB_1	05/08/2020	17.3	*Laminaria digitata* (base)	1.41	too low	1.47E+06	0.00E+00	0.00			
08_LdigB_2	05/08/2020	17.3	*Laminaria digitata* (base)	3.41	5.48	2.49E+06	3.61E+01	0.00			
08_LdigB_3	05/08/2020	17.3	*Laminaria digitata* (base)	6.45	5.63	7.43E+06	0.00E+00	0.00			
08_LdigM_1	05/08/2020	17.3	*Laminaria digitata* (medium)	13.59	5.30	1.50E+07	0.00E+00	0.00			
08_LdigM_2	05/08/2020	17.3	*Laminaria digitata* (medium)	9.22	6.33	7.67E+06	0.00E+00	0.00			
08_LdigM_3	05/08/2020	17.3	*Laminaria digitata* (medium)	12.95	6.53	1.12E+07	0.00E+00	0.00			
08_LdigO_1	05/08/2020	17.3	*Laminaria digitata* (old)	9.20	3.58	9.14E+06	0.00E+00	0.00			
08_LdigO_2	05/08/2020	17.3	*Laminaria digitata* (old)	16.85	12.6	1.70E+07	0.00E+00	0.00			
08_LdigO_3	05/08/2020	17.3	*Laminaria digitata* (old)	15.58	6.18	1.45E+07	0.00E+00	0.00			
08_Fser_1	05/08/2020	17.3	*Fucus serratus*	9.03	8.45	7.82E+06	3.70E+02	0.00			
08_Fser_2	05/08/2020	17.3	*Fucus serratus*	9.65	7.1	7.25E+06	0.00E+00	0.00			
08_Fser_3	05/08/2020	17.3	*Fucus serratus*	9.05	4.61	7.53E+06	6.92E+01	0.00			
08_Anod_1	05/08/2020	17.3	*Ascophyllum nododum*	12.09	7.71	1.23E+07	2.24E+02	0.00			
08_Anod_2	05/08/2020	17.3	*Ascophyllum nododum*	11.16	4.93	9.24E+06	1.78E+02	0.00			
08_Anod_3	05/08/2020	17.3	*Ascophyllum nododum*	11.06	4.09	1.02E+07	9.38E+02	0.01			
08_Ppal_1	05/08/2020	17.3	*Palmaria palmata*	21.28	4.35	1.96E+07	2.70E+02	0.00			
08_Ppal_2	05/08/2020	17.3	*Palmaria palmata*	25.94	9.78	2.07E+07	1.48E+02	0.00			
08_Ppal_3	05/08/2020	17.3	*Palmaria palmata*	16.44	9.68	1.26E+07	0.00E+00	0.00			
08_Ulac_1	05/08/2020	17.3	*Ulva lactuca*	7.83	11.8	1.05E+07	7.33E+02	0.01			
08_Ulac_2	05/08/2020	17.3	*Ulva lactuca*	11.32	2.3	8.64E+06	1.09E+02	0.00			
08_Ulac_3	05/08/2020	17.3	*Ulva lactuca*	4.36	8.16	2.53E+06	3.38E+01	0.00			
08_Std_1	05/08/2020	17.3	Stranded *L. digitata*	5.58	4.97	1.50E+07	2.82E+04	0.19	1.03E+08	2.03E+05	0.20
08_Std_2	05/08/2020	17.3	Stranded *F. serratus*	2.71	26.7	4.49E+06	2.49E+04	0.56	2.35E+08	7.04E+05	0.30
09_LdigB_1	17/09/2020	15.8	*Laminaria digitata* (base)	2.20	16.7	2.33E+06	1.97E+02	0.01			
09_LdigB_2	17/09/2020	15.8	*Laminaria digitata* (base)	8.27	3.5	9.56E+06	8.09E+02	0.01			
09_LdigB_3	17/09/2020	15.8	*Laminaria digitata* (base)	3.03	2	3.18E+06	2.23E+02	0.01			
09_LdigM_1	17/09/2020	15.8	*Laminaria digitata* (medium)	9.02	2.96	1.03E+07	4.03E+02	0.00			

09_LdigM_2	17/09/2020	15.8	*Laminaria digitata* (medium)	20.89	4.44	2.12E+07	1.72E+02	0.00			
09_LdigM_3	17/09/2020	15.8	*Laminaria digitata* (medium)	28.97	11.5	2.55E+07	1.49E+03	0.01			
09_LdigO_1	17/09/2020	15.8	*Laminaria digitata* (old)	20.76	10.4	1.76E+07	3.25E+02	0.00			
09_LdigO_2	17/09/2020	15.8	*Laminaria digitata* (old)	33.79	5.29	2.17E+07	2.22E+03	0.01			
09_LdigO_3	17/09/2020	15.8	*Laminaria digitata* (old)	25.67	9.52	2.01E+07	1.20E+03	0.01			
09_Fser_1	17/09/2020	15.8	*Fucus serratus*	15.78	10.9	1.30E+07	1.80E+03	0.01			
09_Fser_2	17/09/2020	15.8	*Fucus serratus*	16.66	14.40	1.19E+07	2.94E+03	0.02			
09_Fser_3	17/09/2020	15.8	*Fucus serratus*	12.95	7.36	1.36E+07	4.69E+03	0.03			
09_Anod_1	17/09/2020	15.8	*Ascophyllum nododum*	19.14	5.92	1.82E+07	1.54E+03	0.01			
09_Anod_2	17/09/2020	15.8	*Ascophyllum nododum*	7.98	7.48	6.56E+06	7.75E+02	0.01			
09_Anod_3	17/09/2020	15.8	*Ascophyllum nododum*	0.76	10.6	3.95E+05	8.96E+01	0.02			
09_Ppal_1	17/09/2020	15.8	*Palmaria palmata*	7.49	14.4	5.74E+06	1.73E+03	0.03			
09_Ppal_2	17/09/2020	15.8	*Palmaria palmata*	9.39	5.75	6.99E+06	1.79E+03	0.03			
09_Ppal_3	17/09/2020	15.8	*Palmaria palmata*	7.10	3.68	6.92E+06	2.27E+03	0.03			
09_Ulac_1	17/09/2020	15.8	*Ulva lactuca*	14.12	2.68	1.17E+07	3.05E+03	0.03			
09_Ulac_2	17/09/2020	15.8	*Ulva lactuca*	12.43	17.30	8.02E+06	2.30E+03	0.03			
09_Ulac_3	17/09/2020	15.8	*Ulva lactuca*	3.20	9.62	3.24E+06	1.45E+03	0.04			
09_Std_1	17/09/2020	15.8	Stranded *L. digitata*	1.81	4.70	2.80E+06	9.48E+04	3.39	3.13E+09	6.60E+07	2.11
09_Std_2	17/09/2020	15.8	Stranded *F. serratus*	7.33	43	1.99E+07	5.18E+04	0.26	2.13E+08	7.64E+05	0.36
09_Std_3	17/09/2020	15.8	Stranded *P. palmata*	22.29	26.3	5.18E+07	9.32E+05	1.80	5.10E+09	1.03E+08	2.02
10_LdigB_1	19/10/2020	14.2	*Laminaria digitata* (base)	3.40	26.50	3.87E+06	2.61E+03	0.07			
10_LdigB_2	19/10/2020	14.2	*Laminaria digitata* (base)	3.21	5.08	2.81E+06	1.55E+03	0.06			
10_LdigB_3	19/10/2020	14.2	*Laminaria digitata* (base)	4.04	7.41	4.27E+06	3.69E+03	0.09			
10_LdigM_1	19/10/2020	14.2	*Laminaria digitata* (medium)	27.19	6.7	3.04E+07	4.14E+03	0.01			
10_LdigM_2	19/10/2020	14.2	*Laminaria digitata* (medium)	17.47	12.3	1.95E+07	6.76E+03	0.03			
10_LdigM_3	19/10/2020	14.2	*Laminaria digitata* (medium)	34.15	9.19	3.20E+07	6.17E+03	0.02			
10_LdigO_1	19/10/2020	14.2	*Laminaria digitata* (old)	10.80	16.5	1.46E+07	4.36E+03	0.03			
10_LdigO_2	19/10/2020	14.2	*Laminaria digitata* (old)	30.56	8.92	3.62E+07	6.09E+03	0.02			
10_LdigO_3	19/10/2020	14.2	*Laminaria digitata* (old)	28.02	12.30	2.34E+07	7.25E+03	0.03			
10_Fser_1	19/10/2020	14.2	*Fucus serratus*	8.16	8.82	8.00E+06	9.30E+03	0.12			
10_Fser_2	19/10/2020	14.2	*Fucus serratus*	11.57	6.42	1.12E+07	8.36E+03	0.07			
10_Fser_3	19/10/2020	14.2	*Fucus serratus*	9.95	7.53	9.28E+06	1.06E+04	0.11			

10_Anod_1	19/10/2020	14.2	*Ascophyllum nododum*	13.48	10.4	1.51E+07	7.30E+03	0.05			
10_Anod_2	19/10/2020	14.2	*Ascophyllum nododum*	8.11	6.76	6.85E+06	4.75E+03	0.07			
10_Anod_3	19/10/2020	14.2	*Ascophyllum nododum*	11.31	2.85	1.14E+07	4.05E+03	0.04			
10_Ppal_1	19/10/2020	14.2	*Palmaria palmata*	8.01	9.43	8.61E+06	6.31E+03	0.07			
10_Ppal_2	19/10/2020	14.2	*Palmaria palmata*	11.54	6.25	9.38E+06	9.52E+03	0.10			
10_Ppal_3	19/10/2020	14.2	*Palmaria palmata*	14.34	7.87	1.36E+07	1.53E+04	0.11			
10_Ulac_1	19/10/2020	14.2	*Ulva lactuca*	10.89	5.91	1.54E+07	9.44E+03	0.06			
10_Ulac_2	19/10/2020	14.2	*Ulva lactuca*	6.62	12.4	6.64E+06	6.72E+03	0.10			
10_Ulac_3	19/10/2020	14.2	*Ulva lactuca*	16.60	8.27	2.46E+07	1.37E+04	0.06			
10_Std_1	19/10/2020	14.2	Stranded *L. digitata*	11.74	13.80	6.47E+07	8.40E+04	0.13	1.61E+10	1.98E+07	0.12
10_Std_2	19/10/2020	14.2	Stranded *F. serratus*	22.13	72.00	5.54E+07	1.54E+06	2.79	2.36E+09	8.57E+07	3.62
10_Std_3	19/10/2020	14.2	Stranded *P. palmata*	5.63	35.50	1.82E+07	2.04E+05	1.12	2.72E+09	2.72E+07	1.00
11_LdigB_1	16/11/2020	12.7	*Laminaria digitata* (base)	2.59	21.4	3.36E+06	1.99E+03	0.06			
11_LdigB_2	16/11/2020	12.7	*Laminaria digitata* (base)	1.71	2.40	1.48E+06	6.89E+02	0.05			
11_LdigB_3	16/11/2020	12.7	*Laminaria digitata* (base)	3.45	2.97	4.30E+06	1.02E+03	0.02			
11_LdigM_1	16/11/2020	12.7	*Laminaria digitata* (medium)	13.36	2.40	1.23E+07	7.73E+03	0.06			
11_LdigM_2	16/11/2020	12.7	*Laminaria digitata* (medium)	9.50	4.69	8.59E+06	1.38E+03	0.02			
11_LdigM_3	16/11/2020	12.7	*Laminaria digitata* (medium)	12.29	3.45	6.25E+06	2.29E+03	0.04			
11_LdigO_1	16/11/2020	12.7	*Laminaria digitata* (old)	27.53	3.35	3.97E+07	9.32E+03	0.02			
11_LdigO_2	16/11/2020	12.7	*Laminaria digitata* (old)	22.28	17.3	5.02E+07	7.53E+03	0.02			
11_LdigO_3	16/11/2020	12.7	*Laminaria digitata* (old)	34.54	24.1	4.70E+07	1.41E+04	0.03			
11_Fser_1	16/11/2020	12.7	*Fucus serratus*	11.78	22.30	8.92E+06	6.32E+03	0.07			
11_Fser_2	16/11/2020	12.7	*Fucus serratus*	5.39	4.19	4.55E+06	5.27E+03	0.12			
11_Fser_3	16/11/2020	12.7	*Fucus serratus*	0.21	2	8.85E+04	2.23E+02	0.25			
11_Anod_1	16/11/2020	12.7	*Ascophyllum nododum*	11.66	7.82	1.15E+07	6.66E+03	0.06			
11_Anod_2	16/11/2020	12.7	*Ascophyllum nododum*	10.02	7.50	1.01E+07	1.03E+04	0.10			
11_Anod_3	16/11/2020	12.7	*Ascophyllum nododum*	12.87	5.44	1.45E+07	3.03E+03	0.02			
11_Ppal_1	16/11/2020	12.7	*Palmaria palmata*	7.71	5.44	6.75E+06	5.21E+03	0.08			
11_Ppal_2	16/11/2020	12.7	*Palmaria palmata*	4.03	3.73	3.78E+06	1.87E+03	0.05			
11_Ppal_3	16/11/2020	12.7	*Palmaria palmata*	6.92	too low	5.28E+06	3.60E+03	0.07			
11_Ulac_1	16/11/2020	12.7	*Ulva lactuca*	7.58	too low	9.40E+06	6.86E+03	0.07			
11_Ulac_2	16/11/2020	12.7	*Ulva lactuca*	5.89	5.99	5.32E+06	5.50E+03	0.10			

11_Ulac_3	16/11/2020	12.7	*Ulva lactuca*	6.13	4.12	8.12E+06	6.29E+03	0.08			
11_Std_1	16/11/2020	12.7	Stranded *L. digitata*	1.53	2.3	1.88E+06	1.71E+04	0.91	7.27E+06	8.41E+04	1.16
11_Std_2	16/11/2020	12.7	Stranded *F. serratus*	6.25	3.75	8.71E+06	6.40E+05	7.35	1.50E+09	9.11E+07	6.07
11_Std_3	16/11/2020	12.7	Stranded *P. palmata*	4.60	16.4	5.49E+06	9.81E+04	1.79	3.64E+08	8.31E+06	2.28
12_LdigB_1	15/12/2020	11.8	*Laminaria digitata* (base)	3.54	7.29	3.80E+06	1.19E+03	0.03			
12_LdigB_2	15/12/2020	11.8	*Laminaria digitata* (base)	6.19	4.29	7.29E+06	8.44E+02	0.01			
12_LdigB_3	15/12/2020	11.8	*Laminaria digitata* (base)	1.49	5.63	1.49E+06	2.60E+02	0.02			
12_LdigM_1	15/12/2020	11.8	*Laminaria digitata* (medium)	3.25	4.32	3.65E+06	2.40E+03	0.07			
12_LdigM_2	15/12/2020	11.8	*Laminaria digitata* (medium)	6.99	3.38	8.34E+06	1.39E+03	0.02			
12_LdigM_3	15/12/2020	11.8	*Laminaria digitata* (medium)	1.77	4.26	2.12E+06	7.04E+02	0.03			
12_LdigO_1	15/12/2020	11.8	*Laminaria digitata* (old)	15.15	2.3	1.92E+07	3.42E+03	0.02			
12_LdigO_2	15/12/2020	11.8	*Laminaria digitata* (old)	32.46	15.4	3.16E+07	2.16E+03	0.01			
12_LdigO_3	15/12/2020	11.8	*Laminaria digitata* (old)	20.22	26.7	2.66E+07	2.47E+03	0.01			
12_Fser_1	15/12/2020	11.8	*Fucus serratus*	7.45	14.1	5.69E+06	1.45E+03	0.03			
12_Fser_2	15/12/2020	11.8	*Fucus serratus*	6.80	6.37	5.57E+06	1.18E+03	0.02			
12_Fser_3	15/12/2020	11.8	*Fucus serratus*	6.19	too low	5.14E+06	1.53E+03	0.03			
12_Anod_1	15/12/2020	11.8	*Ascophyllum nododum*	8.57	3.11	1.00E+07	1.01E+03	0.01			
12_Anod_2	15/12/2020	11.8	*Ascophyllum nododum*	7.02	4.16	6.16E+06	1.47E+03	0.02			
12_Anod_3	15/12/2020	11.8	*Ascophyllum nododum*	4.82	6.94	4.61E+06	1.08E+03	0.02			
12_Ppal_1	15/12/2020	11.8	*Palmaria palmata*	15.90	3.47	7.87E+06	1.83E+03	0.02			
12_Ppal_2	15/12/2020	11.8	*Palmaria palmata*	11.22	10	1.07E+07	3.68E+03	0.03			
12_Ppal_3	15/12/2020	11.8	*Palmaria palmata*	5.35	4.34	4.71E+06	2.50E+03	0.05			
12_Ulac_1	15/12/2020	11.8	*Ulva lactuca*	11.31	2.64	5.13E+06	3.79E+03	0.07			
12_Ulac_2	15/12/2020	11.8	*Ulva lactuca*	10.64	18.1	4.67E+06	5.58E+03	0.12			
12_Ulac_3	15/12/2020	11.8	*Ulva lactuca*	6.23	17.20	4.14E+06	5.52E+03	0.13			
12_Std_1	15/12/2020	11.8	Stranded *L. digitata*	2.61	9.09	1.26E+07	6.66E+04	0.53	2.11E+09	9.54E+06	0.45
12_Std_2	15/12/2020	11.8	Stranded *F. serratus*	15.18	16.1	3.22E+07	2.58E+06	8.01	1.84E+09	1.16E+08	6.31
12_Std_3	15/12/2020	11.8	Stranded *P. palmata*	1.75	16.80	5.36E+06	4.68E+04	0.87	5.12E+08	5.50E+06	1.07
01_LdigB_1	14/01/2021	NA	*Laminaria digitata* (base)	2.49	4.71	3.05E+06	2.14E+02	0.01			
01_LdigB_2	14/01/2021	NA	*Laminaria digitata* (base)	1.03	5.03	1.02E+06	5.54E+01	0.01			
01_LdigB_3	14/01/2021	NA	*Laminaria digitata* (base)	1.40	4.01	1.58E+06	1.36E+02	0.01			
01_LdigM_1	14/01/2021	NA	*Laminaria digitata* (medium)	1.98	2.71	2.62E+06	4.17E+02	0.02			

01_LdigM_2	14/01/2021	NA	*Laminaria digitata* (medium)	1.00	too low	8.74E+05	9.28E+01	0.01			
01_LdigM_3	14/01/2021	NA	*Laminaria digitata* (medium)	2.46	3.25	2.83E+06	3.89E+02	0.01			
01_LdigO_1	14/01/2021	NA	*Laminaria digitata* (old)	1.48	2.2	1.81E+06	3.50E+02	0.02			
01_LdigO_2	14/01/2021	NA	*Laminaria digitata* (old)	3.78	3.59	3.67E+06	3.30E+02	0.01			
01_LdigO_3	14/01/2021	NA	*Laminaria digitata* (old)	6.16	10.10	8.50E+06	1.04E+03	0.01			
01_Fser_1	14/01/2021	NA	*Fucus serratus*	1.58	2.30	1.92E+06	8.24E+02	0.04			
01_Fser_2	14/01/2021	NA	*Fucus serratus*	2.88	4.78	2.73E+06	8.27E+02	0.03			
01_Fser_3	14/01/2021	NA	*Fucus serratus*	4.73	4.52	5.43E+06	1.11E+03	0.02			
01_Anod_1	14/01/2021	NA	*Ascophyllum nododum*	3.69	2.30	3.28E+06	1.44E+03	0.04			
01_Anod_2	14/01/2021	NA	*Ascophyllum nododum*	2.74	2	3.28E+06	1.14E+03	0.03			
01_Anod_3	14/01/2021	NA	*Ascophyllum nododum*	2.12	2.1	2.88E+06	5.02E+02	0.02			
01_Ppal_1	14/01/2021	NA	*Palmaria palmata*	1.83	2.10	2.03E+06	4.03E+02	0.02			
01_Ppal_2	14/01/2021	NA	*Palmaria palmata*	4.04	3.76	3.06E+06	9.23E+02	0.03			
01_Ppal_3	14/01/2021	NA	*Palmaria palmata*	2.71	4.81	3.81E+06	9.63E+02	0.03			
01_Ulac_1	14/01/2021	NA	*Ulva lactuca*	4.77	8.88	7.61E+06	3.91E+03	0.05			
01_Ulac_2	14/01/2021	NA	*Ulva lactuca*	1.60	2.3	2.20E+06	7.47E+02	0.03			
01_Ulac_3	14/01/2021	NA	*Ulva lactuca*	1.52	2.79	1.60E+06	9.95E+02	0.06			
01_Std_1	14/01/2021	NA	Stranded *L. digitata*	0.63	6.31	3.03E+06	2.79E+03	0.09	6.50E+08	2.80E+05	0.04
01_Std_2	14/01/2021	NA	Stranded *F. serratus*	2.52	4.65	4.12E+06	4.65E+04	1.13	4.26E+08	3.43E+06	0.81
01_Std_3	14/01/2021	NA	Stranded *P. palmata*	3.06	14.5	7.92E+06	3.48E+04	0.44	7.13E+08	4.22E+06	0.59

Chapter V:

Degradation of fresh macroalgae by *Z. galactanivorans* Dsij^{T}

Résumé du chapitre

Jusqu'à présent de nombreuses études se sont intéressées à la dégradation des polysaccharides algaux purifiés par les bactéries. Elles ont permis la caractérisation fonctionnelle, biochimique et structurale de nombreuses CAZymes menant à la description de voies cataboliques complètes. Cependant ces études ne reflètent certainement pas la complexité des processus nécessaires à la dégradation d'une paroi d'algue. Cette dernière est en effet un réseau tridimensionnel complexe, composé d'un enchevêtrement de différents polymères interagissant entre eux ainsi qu'avec de nombreuses autres molécules.

Dans ce chapitre, je me suis donc intéressée à l'utilisation de la macroalgues fraiches, directement récoltées sur l'estran, par *Zobellia galactanivorans* Dsij^T. La **Partie 1** s'attache à caractériser la capacité de *Z. galactanivorans* à utiliser différentes macroalgues brunes dont la composition chimique diffère et les mécanismes métaboliques impliqués. Une croissance significative a été mise en évidence à partir de tissus de *Laminaria digitata*, *Fucus serratus* et *Ascophyllum nodosum,* révélant ainsi le caractère pionnier de *Z. galactanivorans* pour l'utilisation de la biomasse algale fraîche. L'importante activité alginolytique mesurée et la capacité de *Z. galactanivorans* à utiliser l'algue, même lorsqu'elle n'est pas en contact avec celle-ci, révèle que la dégradation des tissus algaux repose sur la sécrétion d'enzymes extracellulaires dans le milieu. Ces résultats suggèrent le probable rôle de *sharing pioneer* de *Z. galactanivorans*, qui, par la libération de produits de dégradation dans le milieu, pourrait favoriser la croissance d'autres taxons moins bien équipés enzymatiquement pour utiliser la biomasse algale. Le transcriptome complet de *Z. galactanivorans* au cours de la dégradation algale a révélé l'induction de l'expression de PUL spécifiquement dédiés à l'assimilation des polysaccharides d'algues brunes. Certains de ces PUL, tout comme d'autres clusters de gènes, impliqués par exemple dans la réponse au stress oxydatif ou dans le système de sécrétion de type IX, n'étaient induits que par la présence de macroalgues fraîches et non par celle de polysaccharides purifiés (alginate, FCSP). Globalement, les réponses obtenues soulignent l'intérêt de considérer l'algue dans son ensemble afin de mieux appréhender les processus de dégradation. La capacité des autres souches du genre *Zobellia* à initier l'attaque des tissues de macroalgues a également été évaluée. Toutes les souches testées peuvent utiliser la biomasse algale comme seule source de carbone mais *Z. galactanivorans* est la seule à décomposer complètement les tissues. Des analyses de génomiques comparatives ont été menées au sein du genre dans le but d'identifier de potentiels gènes à l'origine du caractère pionnier de *Z. galactanivorans.*

Je me suis également intéressée à l'utilisation de tissus frais d'algues rouges par *Z. galactanivorans* Dsij^T (**Partie 2**). Malgré sa capacité à utiliser des polysaccharides d'algues rouges (agar, carraghénanes et porphyrane), aucune croissance n'a été détectée initialement à partir de morceaux provenant de différentes espèces d'algues. Plusieurs hypothèses pouvant expliquer cette incapacité d'utiliser la biomasse d'algue rouge ont été testées, révélant un accès plus difficile aux polysaccharides de la paroi, probablement dû à la présence d'une cuticule protéique à la surface de certaines algues rouges.

J’ai réalisé l’ensemble des expérimentations et analyses de ce chapitre, avec l’assistance de Nolwen Le Duff pour la culture des différentes souches de *Zobellia* à partir d’algues fraîches. Le séquençage RNAseq a été effectué par la plateforme de séquençage à haut débit de l’I2BC (Paris-Saclay).

Part 1:

Insights into the metabolic mechanisms of a sharing pioneer bacteria during fresh brown macroalgae utilization

I. Introduction

Macroalgae are key structuring players in coastal ecosystems, providing food and shelter for diverse organisms. They cover approximately 3.5 million km^2 worldwide and their net primary productivity is estimated at 1521 $TgC.yr^{-1}$ (Krause-Jensen and Duarte, 2016). As such, they are main primary producers in coastal zones and act as a global carbon sink (Duarte *et al.*, 2005). Brown, red and green macroalgae extracellular matrices (ECM) are rich in carbohydrates which represent up to 50 % of the dry weight (Kloareg and Quatrano, 1988). Major structural polysaccharides of land plant ECM are also found in marine algae but in minor proportions, especially cellulose and hemi-cellulose and more rarely pectin. Instead, specific algal polysaccharides dominate the algal ECM and differ depending on the phylum. Alginates and fucose-containing sulfated polysaccharides (FCSPs) are produced in brown algae, agars, porphyrans and carrageenans in red algae and ulvans in green algae. Alginates are linear polymers consisting of β-D-mannuronic (M) and α-L-guluronic acids (G) arranged in homopolymeric (polyM, polyG) or heteropolymeric blocks (polyMG). They are the main components of the brown algal ECM, representing between 10 and 45 % of the algal dry weight (Kloareg and Quatrano, 1988). FCSPs, accounting for 4-13 % of the dry weight (Fletcher *et al.*, 2017), are either linear or highly branched polysaccharides containing α-linked L-fucose residues (within the backbone and/or the branches) together with a variety of other neutral monosaccharides constituents (galactose, mannose, xylose, rhamnose…) and uronic acids (Deniaud-Bouët *et al.*, 2017). They present many substituents, mainly sulfate and acetyl groups. The structure of brown algal polysaccharides is consequently highly heterogeneous and varies according to species, seasons, geographical locations, thallus part, algal growth stages and environmental factors (Haug *et al.*, 1974; Bruhn *et al.*, 2017; Deniaud-Bouët *et al.*, 2017; Fletcher *et al.*, 2017; Ponce and Stortz, 2020). Within the ECM, these carbohydrates are cross-linked and associated with proteins (3-15 %), minerals (7-36 % such as iodine, calcium, iron, copper and magnesium), phenols (1-13 %), vitamins, amino acids and small amounts of lipids (1-5 %) (Fleurence, 1999; Verhaeghe *et al.*, 2008; Deniaud-Bouët *et al.*, 2014; Schiener *et al.*, 2015) to form a complex matrix. Besides ECM polysaccharides, brown algae also produce storage carbohydrates such as laminarin (β-1,3-glucan) and mannitol (Michel *et al.*, 2010). It is long known that heterotrophic bacteria are crucial for the mineralization of algal biomass (Mann, 1982). Macroalgae surfaces are constantly colonized by diverse bacterial communities with densities varying from 10^2 to 10^9 cells cm^{-2} of macroalgal tissue (Egan *et al.*, 2013). It has been shown that a fraction of these communities, mainly *Bacteroidetes*, *Gammaproteobacteria*, *Verrucomicrobia* and *Planctomycetes,* had adapted to feed on this complex and diverse biomass, showing abilities to hydrolyze soluble high molecular weight algal compounds thanks to a considerable enzymatic arsenal (Kirchman, 2002; Thomas, Hehemann, *et al.*, 2011; Teeling *et al.*, 2012; Wietz *et al.*, 2015). Over the last 20 years, many studies focused on the algal polysaccharide-processing capabilities of marine heterotrophic bacteria (many are reviewed in Arnosti *et al.*, 2020), deciphering new catabolic pathways and unraveling the role of new carbohydrate active

enzymes (called CAZymes and classified in the CAZy database http://www.cazy.org, Lombard *et al.*, 2014), including glycoside hydrolases (GHs), polysaccharide lyases (PLs) or carbohydrate esterase (CEs), and sulfatases (classified in SulfAtlas http://abims.sb-roscoff.fr/sulfatlas/, Barbeyron *et al.*, 2016). In *Bacteroidetes*, CAZymes are usually organized within clusters of coregulated genes involved in carbohydrate binding, hydrolysis and transport, known as Polysaccharide Utilization Loci (PULs). The regulations of these PULs during purified algal substrate degradation were recently studied in a few transcriptome-wide gene expression analyses, for both cultivated marine bacteria (Zhu *et al.*, 2016; Ficko-Blean *et al.*, 2017; Tang *et al.*, 2017; Thomas *et al.*, 2017; Koch, Dürwald, *et al.*, 2019) as well as natural seawater bacterial communities using meta-transcriptomic profiling (Bunse *et al.*, 2021). However, information on the mechanisms involved in raw algal material assimilation are scarce. Previously, Zhu *et al.*, 2016 focused on the assimilation of crushed brown macroalgae (kelp powder) by "*Bacillus weihaiensis*" Alg07^T. They suggested a successive utilization of the brown algal polysaccharides by the cells, an observation in line with another study where *Alteromonas macleodii* 83-1, was grown on an alginate/laminarin/pectin mixture (Koch, Dürwald, *et al.*, 2019). Gu *et al.*, 2021 showed that a single recombinant amylase could digest different raw dried macroalgae. However, these studies did not reflect the complexity of the transcriptomic responses which might occur during the degradation of complex substrate assembly in the field, such as healthy algae, characterized by their structurally and chemically complex ECM. Indeed, ECMs are a source of a large variety of substrates interacting together, more or less accessible as some polysaccharides, known for their gelling properties, might entrap other components, such as other polymers or proteins, and hinder their accessibility (Fleurence, 1999). Considering the algae as a whole could reveal novel genes and catabolic pathways, not induced by soluble purified polysaccharides, but playing key roles in algal biomass recycling in the field.

Recently, it has been suggested that not all the bacteria able to use soluble algal compounds are equally equipped to breakdown intact macroalgae (Hehemann *et al.*, 2016). As an example, the gammaproteobacterium *A. macleodii* has strong capacities for algal polysaccharide utilization but was unable to cause visible tissue degradation when grown on intact brown algal tissues from *Ecklonia radiata* (Koch *et al.*, 2020). As suggested by the authors, this species might then feed on algal exudates or benefit from the action of specialized bacterial communities, well equipped to process the initial attack of the algal ECM. These latter could act as pioneers of the degradation by exposing new substrate niches from the macroalgal tissues for less efficient community members considered as scavengers (Hehemann *et al.*, 2016; Arnosti *et al.*, 2020; Gralka *et al.*, 2020).

The genus *Zobellia* (*Flavobacteriaceae* family), frequently found associated with macroalgae (eg. Martin *et al.*, 2015; Dogs *et al.*, 2017), is composed of 9 validly described strains classified in 7 species (Barbeyron *et al.*, 2001, 2021; Nedashkovskaya *et al.*, 2004). They appear to be potentially specialized in algal polysaccharide utilization as their genome encodes a high amount of CAZymes, between 263

and 336 genes representing from 6.4 to 7.6 % of the coding sequences (Barbeyron, Thomas, *et al.*, 2016; Chernysheva *et al.*, 2019, 2021), and sulfatases. In particular, *Zobellia galactanivorans* Dsij^T, isolated from a red macroalga (Potin *et al.*, 1991; Barbeyron *et al.*, 2001), is considered as a model strain to study macroalgal polysaccharide utilization (Lami *et al.*, 2021). It allowed the discovery of many novel CAZymes and the description of new PULs targeting alginates (Thomas *et al.*, 2012, 2013; Dudek *et al.*, 2020), carrageenans (Ficko-Blean *et al.*, 2017), agars (eg. Jam *et al.*, 2005; Hehemann *et al.*, 2012), laminarin (Labourel *et al.*, 2014, 2015) and mannitol (Groisillier *et al.*, 2015) by unravelling biochemical and regulatory mechanisms. Moreover, Thomas *et al.*, 2017 detected the induction of specific catabolic pathways in the presence of diverse algal carbohydrates and revealed common transcriptomic regulations when *Z. galactanivorans* Dsij^T was grown on polysaccharides from the same algal phylum. This strain is also well equipped to cope with algal stress defenses and can accumulate iodine (Fournier *et al.*, 2014; Barbeyron, Thomas, *et al.*, 2016; Grigorian *et al.*, 2021). A previous study suggested that *Zobellia galactanivorans* Dsij^T act as a pioneer in the breakdown of the kelp *Laminaria digitata* and demonstrated the crucial role of the alginate lyase AlyA1 in this process (Zhu *et al.*, 2017).

In this study, we aim to better understand the mechanisms controlling fresh macroalgae degradation. To tackle this issue, (i) the complete transcriptome of *Z. galactanivorans* Dsij^T was analyzed during the degradation of three brown macroalgae with distinct chemical composition and compared with purified sugars to decipher key genes and mechanisms specifically triggered on fresh tissues and (ii) the ability of *Z. galactanivorans* to degrade fresh algae tissues was compared with other *Zobellia* spp. to assess its singular behavior and hypothesize on potential genetic determinant in fresh macroalgae breakdown.

II. Experimental procedure

1. Purified substrates

Maltose (Sigma-Aldrich), alginate (Danisco, Grindsted FD176) and FCSPs extracted from *Ascophyllum nodosum* (Algues & Mer, HMWFSA15424, fraction > 100 kDa) were tested for growth. To check for alginate contamination, FCSPs were incubated with the alginate lyase AlyA1 (Thomas *et al.*, 2013) and degradation products were detected on Carbohydrate-PAGE (Zablackis and Perez, 1990). Therefore, assays to measure the uronic acid content (Blumenkrantz and Asboe-Hansen, 1973; Filisetti-Cozzi and Carpita, 1991) in the FCSPs were carried out and showed that uronic acids accounted for approximately 24 % (w/w), which is higher than the 9 % estimated by Cumashi *et al.*, 2007 on FCSPs from *A. nodosum*. This means that in the worst case, i.e. if FCSP structures do not contain uronic acids which is unlikely, ¾ of the substrate is actually FCSPs.

Alginate, agar (Sigma-Aldrich), kappa- (Goëmar, extracted from *Eucheuma cottonii*) and iota-carrageenans (Danisco, 2544-97-01) were used for enzymatic assays.

2. Strains

Eight *Zobellia* strains were used in this study, *Z. galactanivorans* Dsij^T, *Z. amurskyensis* KMM 3526^T, *Z. laminaria*e KMM 3676^T, *Z. russellii* KMM 3677^T, *Z. roscoffensis* Asnod1-F08^T, *Z. roscoffensis* Asnod2-B02-B, *Z. nedashkovskayae* Asnod2-B07-B^T and *Z. nedashkovskayae* Asnod3-E08-A. These strains were first grown from glycerol stock in Zobell 2216 medium (ZoBell, 1941) at room temperature before being inoculated in minimum marine medium (referred to as MMM, described in (Thomas, *et al.*, 2011) and complemented with 100 µg.ml^{-1} kanamycin, 100 µg.ml^{-1} streptomycin, 50 µg.ml^{-1} neomycin and 14 µg.mL^{-1} colistin, to which all the tested *Zobellia* strains are resistant) and amended with 4 g.l^{-1} maltose as the sole carbon source. After centrifugation (4200 rpm, 10 min), pellets were washed twice in 1X saline solution. Cells were inoculated in microcosms at OD_{600} 0.05. The ability of these strains to use soluble algal compounds was assessed in previous studies (Barbeyron *et al.*, 2001, 2021; Nedashkovskaya *et al.*, 2004) and is summarized in **Table V.S1**.

3. Macroalgae treatment

Healthy *Laminaria digitata*, *Fucus serratus* and *Ascophyllum nodosum* were collected in May at the Bloscon site (48°43'29.982'' N, 03°58'8.27'' W) in Roscoff (Brittany, France). Algal tissues were cut in small pieces (ca. 2.5-3.5 cm^2) with a sterile scalpel and immersed in 0.1 % Triton in milli-Q water for 10 min followed by 1 % iodine povidone in milli-Q water for 5 min to clean them from the resident epibiotic microbiome. Algae pieces were rinsed in excess sterilized autoclaved seawater for 2 hours.

4. Microcosm set up and sample collection

Zobellia strains were grown at 20 °C under agitation in MMM with macroalgae pieces as the sole carbon source. Each condition was tested in triplicate. All vessels were autoclaved.

The eight *Zobellia* strains used in this study were grown in 10 mL with three *L. digitata* pieces cut in the meristem part (up to 15 cm from the base).

Z. galactanivorans was grown in 50 ml with 10 brown macroalgal pieces, either young *L. digitata* (<20 cm), *F. serratus* or *A. nodosum*. For comparison it was also grown in the same conditions using 4 g.l^{-1} maltose, alginate or FCSPs. During the exponential phase, 10 ml of culture medium and 2 algal pieces were retrieved on ice for RNA extraction of the free-living and algae-attached bacteria, respectively. On ice, one volume of killing buffer (20 mM Tris-HCl pH 7.5, 5 mM $MgCl_2$, 20 mM NaN_3) was added to the liquid samples and the collected algal pieces were washed twice in killing buffer:H_2O (1:1). After centrifugation of liquid samples (4200 rpm, 10 min), cell pellets were placed in liquid nitrogen, as well as algae pieces. Samples were stored at -80 °C before further RNA extraction. For enzymatic assays, culture medium was sampled, filtered onto a 0.2 µm filter and stored overnight at 4 °C until incubation with the different polysaccharides.

Co-culture systems were used to test the growth of *Z. galactanivorans* when cultivated in contact or physically separated from the algal tissues. Incubations were carried out in 100 ml reaction vessels comprising two compartments with round bottom and a 65 mm flat edge opening (ref 0861050, Witeg, Germany), separated by a 0.2 µm MCE filter (ref GSWP09000, Merck, Germany). Thirty milli-liters of medium were poured in the two compartments and ten *L. digitata* pieces were immersed in one. For enzymatic assays, culture medium was sampled at different times, filtered onto a 0.2 µm filter and directly incubated with alginate.

5. RNA extraction and purification

Free-living bacteria cells were lysed by adding 400 µl of lysis buffer (4 M guanidine thiocyanate, 25 mM sodium acetate pH 5.2, 5 $g.l^{-1}$ N-laurylsarcosinate) and 500 µl of phenol and incubated 5 min at 65 °C. RNA was extracted using phenol-chloroform. Extracts were treated 1 h at 37 °C with 2 units of Turbo DNAse (Thermofisher) and purified on mini-columns NucleoSpin RNA Clean-up (Macherey-Nagel) following the manufacturer's instructions. RNA was eluted in 50 µl of nuclease-free water.

RNA from algae-attached bacteria was extracted as follows. Algal pieces were immersed in killing buffer, vortexed and placed 7 min in an ultrasonic bath to detach bacteria from the algal surface. Algae were removed, buffer was centrifuged (5 min, 11 000 rpm) and cell pellets resuspended in lysis buffer. RNA extraction and DNAse treatment were performed as described above for the free-living bacteria. To avoid RNA loss on purification columns, DNAse inactivation reagent (Thermofisher) was added to inactivate DNAse and removed after 5 min incubation by centrifugation. The absence of DNA contamination in all RNA samples was checked by PCR with universal primers S-D-Bact- 0341-b-S-17 and S-D- Bact-0785-a-A-21 targeting the 16S rRNA gene (Klindworth *et al.*, 2013). RNA was quantified on a Qubit fluorometer (Thermofisher) using the Qubit RNA HS assay kit and its integrity assessed on a Bioanalyzer 2100 system (Agilent Technology) with the Agilent RNA 6000 Pico assay kit.

Paired-end RNA sequencing (RNA-seq) was performed by the Plateforme de Séquençage I2BC (UMR9198, CNRS, Gif-sur-Yvette) on a NextSeq instrument (Illumina) using the NextSeq 500/550 High Output Kit v2 (75 cycles) which included a Ribo-Zero ribosomal RNA depletion step. A total of 25 samples were sequenced (**Table V.S2**). Sequencing failed for samples FL_Fser1 and Att_Ldig2 due to poor sample quality.

6. RNA-seq analysis

Demultiplexed and adapter-trimmed reads were processed with the Galaxy platform (https://galaxy.sb-roscoff.fr). Trimmomatic (Galaxy Version 0.38.0) was used to perform quality filtering of the reads. Filtered reads with less than 20 bp in length were discarded. Transcript quantification was done using

the pseudo-mapper Salmon (Patro *et al.*, 2017**,** Galaxy Version 0.8.2) with the *Z. galactanivorans* Dsij^T reference genome (retrieved from MicroScope "zobellia_gal_DsiJT_v2"; Refseq NC_015844.1). Raw counts for individual samples were merged into a single expression matrix for downstream analysis. Principal Component Analysis was performed using the *DESeq2* v1.26.0 package (Love *et al.*, 2014) in R v3.6.2 (R Core Team, 2018) after rlog transformation. Differential abundance analyses were also carried out with this package and genes displaying a log2 fold change |log2FC| > 2 and a Bonferroni-adjusted p-value < 0.05 were considered to be significantly differentially expressed. The upset plot was done using the *ComplexUpset* package. Hierarchical clustering was performed using the Ward's minimum variance method (Murtagh and Legendre, 2014). The *ggplot2* package was used to make graphics.

7. Enzymatic activity assays

One volume of filtered supernatant was incubated with 9 volumes of 0.2 % macroalgal polysaccharides (alginate, agar, kappa- or iota-carrageenans) at 28 °C overnight to assess extracellular polysaccharidases activity. Incubations were performed in parallel with inactive enzymes (boiled 15 min at 98 °C) as control. The amount of reducing ends released in the incubation mix was quantified using the ferricyanide assay (Kidby and Davidson, 1973). For each sample, the activity measured with the boiled enzymes was subtracted. Finally, the mean value (n=3) measured for the uninoculated microcosms was subtracted. Significant differences (P<0.05) from 0 were tested using t-tests.

8. CARD-FISH

CARD-FISH assays were performed on samples from an independent microcosm experiment with *L. digitata* tissues as the carbon source. Algae pieces were collected at different times after inoculation of *Z. galactanivorans*, rinsed twice in milli-Q water, fixed overnight at 4 °C with 2 % paraformaldehyde, washed twice in PBS and stored in PBS:EtOH (1:1 v/v) at -20 °C. CARD-FISH was performed as described in Brunet *et al*., 2021, accepted (Chapter IV, Part 1) using the *Zobellia*-specific probe ZOB137 with helpers. Cells on algal tissues were visualized with a confocal microscope Leica TCS SP8 equipped with HC PL APO 63x/1.4 oil objective using the 488 and 638 nm lasers to detect Alexa488 signal and algal autofluorescence signal, respectively. Z-stack images were collected (layers of 0.29 µm thickness) by using 1024x1024 scan format and a scan speed of 400 Hz. Z-stacks were visualized using the surface channel mode of the 3D viewer module implemented in the Leica Las X software.

9. Comparative genomics

The number of glycoside hydrolases, polysaccharide lyases, carbohydrate esterases and sulfatases present in the genome of the different *Zobellia* spp. was determined using the dbCAN database on the

MicroScope platform (https://mage.genoscope.cns.fr). Homologs were searched for genes of interest using synteny results on the same platform with a 50 % identity and an 80 % alignment coverage cutoff.

III. Results

1. *Zobellia galactanivorans* Dsij^T degrades and utilizes fresh brown macroalgae tissues as carbon source

Growth was tested with three brown macroalgae from two different orders and with distinct chemical composition, *Laminaria digitata* (order Laminariales), *Fucus serratus* and *Ascophyllum nodosum* (order Fucales), as the sole carbon and energy source. As a comparison, *Z. galactanivorans* was also cultured on brown algal polysaccharides (alginate or FCSPs). Control conditions included growth on a simple sugar (maltose), as well as non-inoculated media. Growth was detected on the three algal species **(Figure V.1A)**, with tissue bleaching and damages only visible on *L. digitata* pieces after 65 h (**Figure V.1B**). In the absence of *Z. galactanivorans* inoculation, no growth was detected in *L. digitata* and *F. serratus* microcosms (except in one replicate for the later), however a bacterial growth was observed on *A. nodosum* at 65 h (OD_{600} = 0.3). This is probably due to resident epiphytic bacterial communities that resisted the chemical and the antibiotic treatments applied, given that the *A. nodosum* cultivable epiphytic microbiota is enriched in macroalgal-polysaccharides degrading bacteria (Martin *et al.*, 2015).

The extent and kinetics of algal tissue colonization by *Z. galactanivorans* was assessed using CARD-FISH on *L. digitata* tissues. No *Zobellia* cells were detected initially on the kelp surface, whereas cell patches were visible after 22 h (**Figure V.1C**). The non-fluorescent gap between the bacterial and the algal cells suggests that at this early colonization stage *Z. galactanivorans* started to form biofilm on the mucilage coating *L. digitata* and did not penetrate into the tissues. After 46 h, *Z. galactanivorans* colonization was more pronounced but still arranged in patches and cells were not only localized on the surface but also deeper within the tissues. This process progressed at 70 h as the tissues were completely covered by cells and most of them were localized between the algal cells and disrupted their structural integrity. The absence of algal autofluorescence signal below 25-30 µm is the result of its rapid decrease in intensity as we move away from the coverslip.

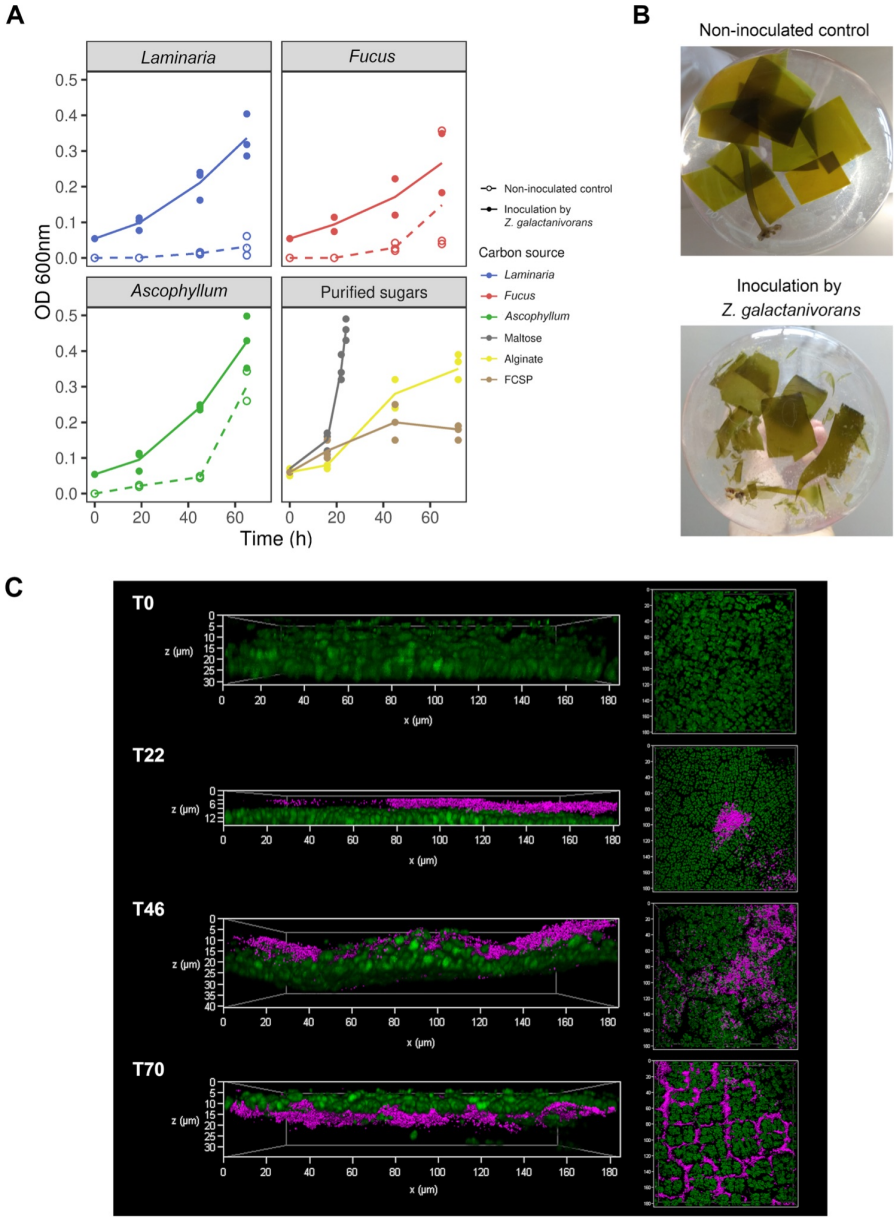

Figure V.1: Ability of *Z. galactanivorans* Dsij^T to use fresh brown macroalgae for its growth. (A) Growth of *Z. galactanivorans* on either macroalgae pieces (*Laminaria digitata*, *Fucus serratus* and *Ascophyllum nodosum*) or purified sugars (maltose, alginate and FCSPs). Individual points for replicate experiments are shown. Lines are means of independent replicates (n = 2 or n = 3). (B) Photographs showing the integrity of the *L. digitata* tissues after 65 h. (C*) L. digitata* tissues colonization by *Z. galactanivorans* during the degradation. Micrographs are overlay of the CARD–FISH signal (magenta, *Zobellia*-specific probe with Alexa488 as the reporter signal) and the algal autofluorescence (green) and were obtained with the surface channel mode of the 3D viewer. For the different times, transversal views are shown on the left and top views on the right.

2. Transcriptomic shift during macroalgae degradation

Z. galactanivorans Dsij^T transcriptome was analyzed during the degradation of the three macroalgae and compared with the responses occurring on maltose, alginate and FCSPs. Between 44 and 93 % of the sequenced reads obtained from free-living bacteria mapped on the genome of *Z. galactanivorans* Dsij^T (**Table V.S2**) for cells grown with macroalgae and between 88 and 96 % for cells grown with purified

sugars.

PCA revealed that transcriptomic profiles differed depending on the carbon source (**Figure V.2A**). Except for samples from *F. serratus* microcosms, triplicates from all conditions clustered together. However, dispersion was higher for macroalgal samples than purified sugars. Transcriptomes of cells grown with *L. digitata* were closer to that obtained with alginate or FCSPs compared to *A. nodosum* or *F. serratus*.

Differential abundance analysis revealed 1117 and 864 genes up- and down-regulated with at least one substrate, respectively, using maltose as the control condition (Bonferroni-adjusted p-value < 0.05, |log2FC| > 2) (**Table V.S3**). Among them, 56 % (628 upregulated genes) and 52 % (449 down-regulated genes) showed substrate-specific regulations (**Figure V.2B)**. In particular, half of the genes regulated with *A. nodosum* and FCSPs were not differentially expressed in any other conditions. Among the genes shared with at least two substrates, the highest intersection size was observed between alginate and FCSPs (270 genes). *L. digitata* was the algae inducing the highest number of regulations shared with at least one polysaccharide (399, 254 and 217 genes with *L. digitata*, *F. serratus* and *A. nodosum* respectively). Focusing on the genes responding to two macroalgae but not the third one, we found that more regulations were shared between *L. digitata* and *F. serratus* (116 genes) than *F. serratus* and *A. nodosum* (89 genes) or *L. digitata* and *A. nodosum* (13 genes). Finally, a core set of 70 up-regulated and 59 down-regulated genes responded to the three macroalgae. Among the core set of up-regulated genes, 13 are involved in carbohydrate metabolism and transport.

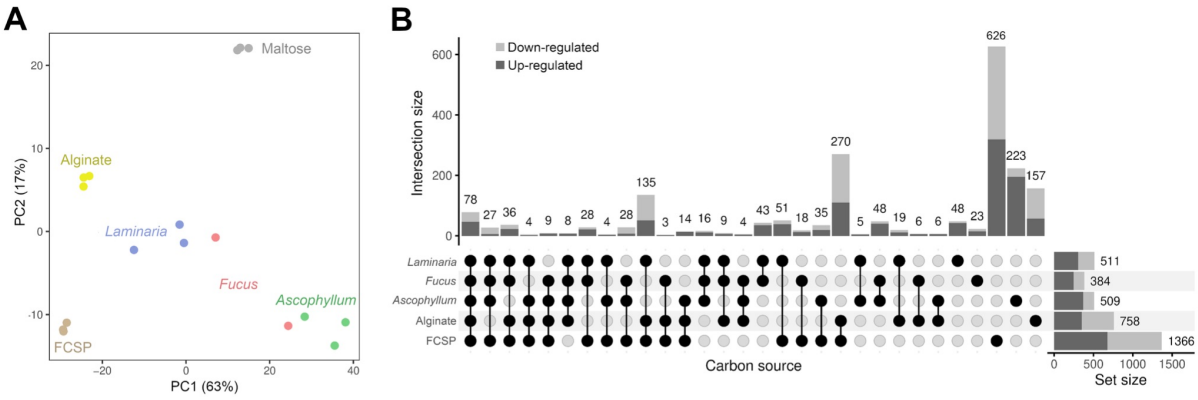

Figure V.2: General features of the transcriptomic responses occurring in free-living *Z. galactanivorans* Dsij^T during growth with macroalgae. (A) Principal Component Analysis of the gene expression. (B) Upset plot of the differentially expressed genes with maltose as the control condition (Bonferroni-adjusted p-value < 0.05 and |log2FC| > 2). Set size represents the total amount of genes regulated in each condition.

3. Growth with macroalgae induced specific carbohydrate catabolic pathways

We further focused our expression analysis on all predicted PULs from *Z. galactanivorans* Dsij^T. Fifty PULs containing the susC-like/susD-like pair were previously identified during genome annotation (Supplementary Table S3 in Barbeyron, Thomas, *et al.*, 2016). Another recently described PUL (Ficko-Blean *et al.*, 2017), targeting 3,6-anhydro-D-galactose and involved in carrageenan catabolism (but lacking the susC-like/susD-like pair), was added to the analysis as PUL51. The hierarchical clustering of expression data grouped together PULs targeting simple sugars (maltose and fructose) as well as starch and chitin (**Figure V.3A**). The starch PUL12 was strongly repressed in all conditions while the chitin PUL31 showed a significant repression only with the algal polysaccharides.

The alginate-specific PUL29 was the only one significantly overexpressed in all conditions compared with maltose (mean log2FC of 4) and the highest expression was observed with *L. digitata* samples (**Figure V.3B**, **Figure V.S1**). Moreover, PULs predicted to target other brown algal polysaccharides were triggered and clustered together. In particular, *L. digitata* significantly induced the expression of PUL3, 34 and 35 likely targeting FCSPs since they encode sulfatases and fucosidases, as well as PUL26 and 27 whose function is unclear, PUL1 (xylan) and PUL14 (sulfated polysaccharides). The PUL3 and 27 were also significantly induced during the growth on *F. serratus,* while PUL4 and 28 targeting β-glucan and laminarin responded to *A. nodosum*. Indeed, alginate induced the expression of genes contained in unclear PULs (PUL 26 and 45), in the fucose PUL7 and α-glucan PUL8. With FCSPs as the carbon source, a large diversity of 16 induced PULs was observed. PUL6, 26, 27 and 45 (unclear), like PUL8 and 10 (β- and α-glucan) and PUL38 (FCSPs) were especially strongly up-regulated. Overall, four PULs induced by macroalgae did not respond to the purified polysaccharides (PUL3, 4, 34 and 35), including three potentially targeting FCSPs.

No PUL known to be involved in red algal polysaccharides catabolism (PUL40, 42, 49 and 51) clustered with this set of overexpressed PULs. This analysis revealed that the growth on brown macroalgae induced the overexpression of specific PULs dedicated to the breakdown of brown algal polysaccharides only. These results are in line with the measured activity of extracellular polysaccharidases in the microcosm supernatants containing algal tissues (**Figure V.3C**). Enzyme mixtures were assayed against alginate, agar and carrageenans and only the alginolytic activity was significantly higher when *Z. galactanivorans* was grown on macroalgae compared with the non-inoculated control (t-test, $P<0.05$).

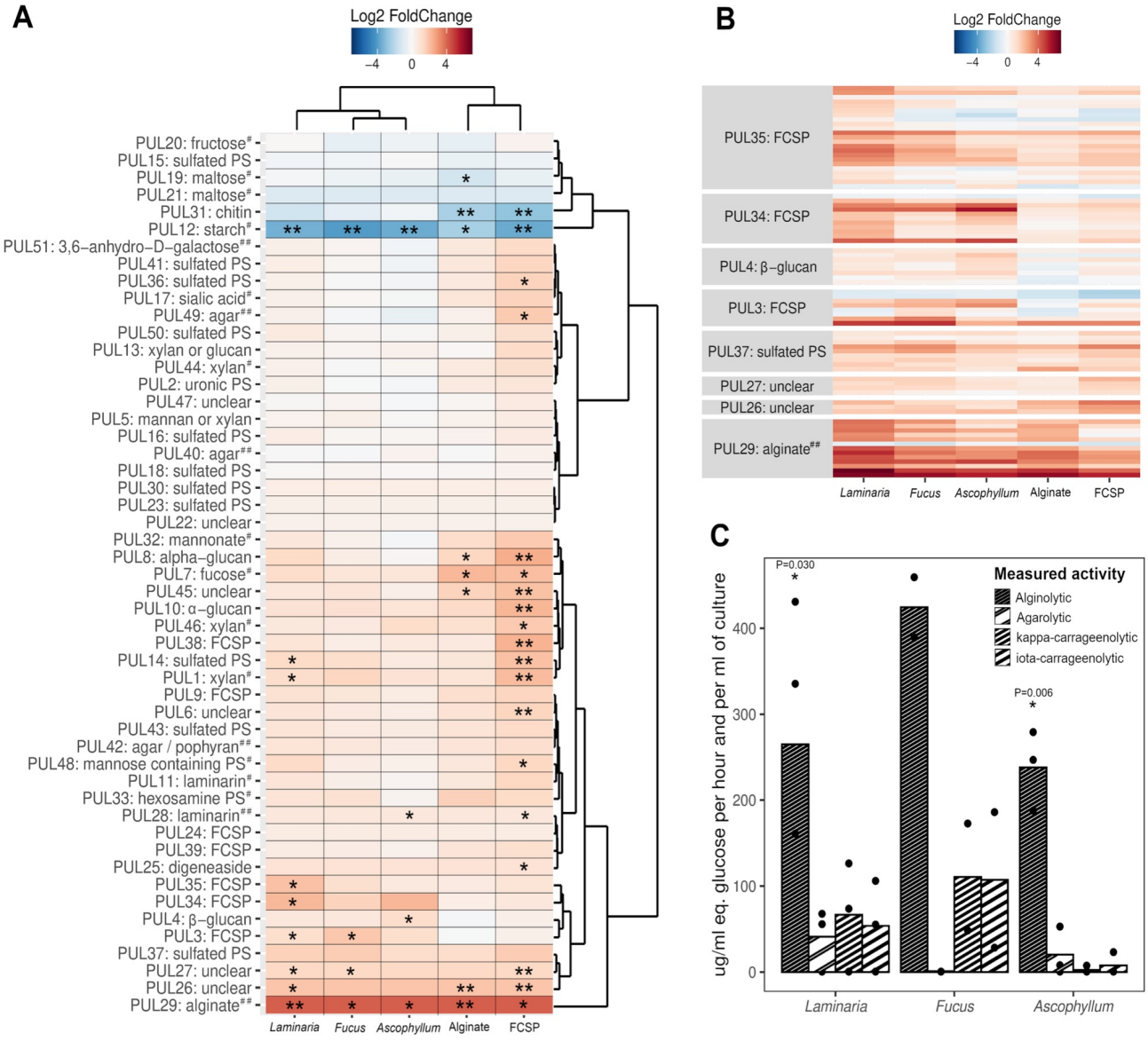

Figure V.3: Regulation of the catabolic pathways during the degradation of fresh algal tissues. (A) Heatmap of the 51 PULs identified in the genome of *Z. galactanivorans* Dsij^T. For each PUL, the mean log2FC of all genes is represented, taking maltose as a control condition. Carbon sources and PULs were arranged according to a hierarchical clustering analysis (Ward's method). A PUL was considered regulated (induced in red, repressed in blue) if more than 50 % of the genes were significantly differentially expressed (*) and strongly regulated if more than 80 % of the genes were significantly differentially expressed (**). Putative substrates targeted by the PULs are indicated. Hash signs denote PULs biochemically characterized previously in *Z. galactanivorans* (##) or in another organism (#). (B) Heatmap representing the log2FC of individual genes contained in the PULs induced with macroalgae and which clustered together in A. (C) Activity of extracellular polysaccharidases secreted in the microcosms containing macroalgae. The mean value measured in the uninoculated controls was subtracted from each value. Bars are means of independent replicates (n = 2 or 3) shown as individual points. Significant difference from zero was tested when n = 3 (t-test; *, P<0.05). FCSP: fucose containing sulfated polysaccharide; PS: Polysaccharide.

4. T9SS and oxidative stress response induction were specific to the growth on fresh algal tissues

To unravel pathways governing the degradation of complex, fresh macroalgal biomass by *Z. galactanivorans* Dsij^T, the transcriptomic profiles with macroalgae were not only compared with

maltose but also with the purified algal polysaccharides. With fresh *L. digitata*, *F. serratus* or *A. nodosum*, 41, 59 or 189 genes were specifically induced when compared both with the polysaccharides and maltose, respectively (**Table V.S4**). A large gene cluster was up-regulated with *L. digitata* and *F. serratus*, from *zgal_1071* to *zgal_1105.* It notably encodes three oxidoreductases, a DNA topoisomerase and a peroxiredoxin, suggesting that this cluster may play a role in the response against the oxidative stress. Other genes encoding antioxidant proteins were triggered, especially on *L. digitata*, such as the superoxide dismutase SodC (ZGAL_114) or a β-carotene hydroxylase (ZGAL_2972), as well as a protein belonging to the carboxymuconolactone decarboxylase family (ZGAL_1598) which includes enzyme involved in antioxidant defense (Chen *et al.*, 2015). The two catalases (ZGAL_1427 and ZGAL_3559) encoded in the *Z. galactanivorans* Dsij^T genome were also induced in the presence of *L. digitata* and *F. serratus* in comparison to maltose and alginate. Expression of genes encoding general stress response proteins was also up-regulated, in particular universal stress protein (ZGAL_3483 and ZGAL_3862) or CsbD-like protein (ZGAL_2609).

Several genes predicted to encode components of the Type 9 Secretion System (T9SS) were significantly induced during the growth on fresh algal tissues, in particular with *A. nodosum* (14 out of the 33 genes identified in the genome, against 1 and 5 with *L. digitata* and *F. serratus* respectively) (**Figure V.4**). They include particularly genes encoding SprF family proteins, as well as T9SS-associated PG1058-like protein. In addition, 7 induced genes encoded proteins of unknown function that contain conserved C-terminal domains (CTDs) belonging to the TIGRFAMs TIGR04131 (gliding motility - ZGAL_2022, 2761, 2762, 3727) and TIGR04183 (Por secretion system - ZGAL_93, 1124, 4310). These conserved CTDs are typical of proteins secreted by the T9SS. Globally, with maltose as control, the T9SS mechanism was strongly overexpressed with *A. nodosum* (mean log2FC of the T9SS-related genes induced in at least one condition = 3.0, against 0.7 and 1.9 for *L. digitata* and *F. serratus* respectively) but down-regulated with Alginate (-2.2) and FCSPs (-1.4). Also, Vgr family proteins (ZGAL_408, 3389), involved in the Type 6 Secretion System (T6SS) were induced with *A. nodosum*. Many other gene clusters were upregulated with macroalgae compared to purified substrates. The larger one was a cluster containing genes involved in glycolysis, ATP synthase and ABC transport system, from *zgal_3848* to *zgal_3883*, which was up-regulated with *F. serratus* and *A. nodosum*. Another cluster of four genes (*zgal_2988-zgal_2991*) was induced with macroalgae. It contains two GTs and a protein annotated to be likely involved in EPS/LPS biosynthesis, and then might have a role in biofilm formation at the surface of macroalgae.

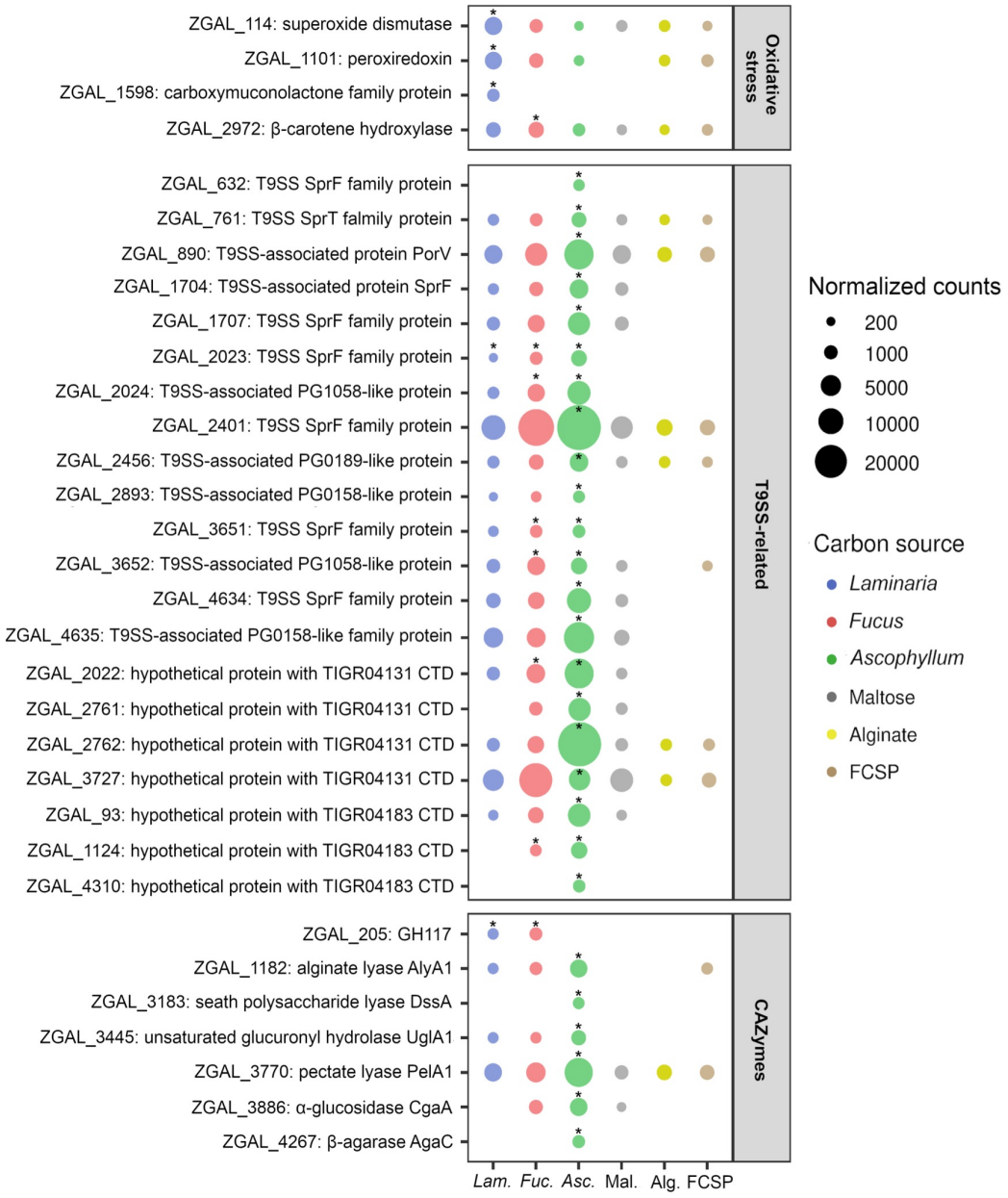

Figure V.4: Selection of genes specifically induced by fresh macroalgae. Mean expression values (n = 3, except for *F. serratus* n = 2) of selected genes significantly triggered (*) with at least one macroalgae compared to both the purified polysaccharides and maltose (see Table V.S4). No dot was represented if the mean read count was below 200.

Few genes coding for CAZymes were significantly up-regulated when *Z. galactanivorans* Dsij^T was grown with macroalgae compared to all the purified sugars (**Figure V.4**). Among them, two genes belonged to PULs likely active on FCSPs, *zgal_205*, encoding a GH117 in PUL3 and up-regulated with *L. digitata* and *F. serratus*, and *zgal_3445* (*uglA1*, GH88) within the PUL34, strongly up-regulated with *A. nodosum*. Other genes not contained in PUL structures, such as *alyA1* (*zgal_1182*, alginate lyase PL7), *cgaA* (*zgal_3886*, glucan 1,4-α-glucosidase GH15), *agaC* (*zgal_4267*, β-agarase GH16), *pelA1* (*zgal_3770*, pectate lyase PL1) and *dssA* (*zgal_3183*, sheath polysaccharide lyase PL9) were induced with *A. nodosum*.

5. Similar transcriptomic profiles between free-living and algae-attached bacteria

The transcriptome of algae-attached *Z. galactanivorans* Dsij^T was also analyzed and compared to that of free-living bacteria. A high proportion of eukaryotic rRNA (4-70 %) was detected in these samples, while it was below 1 % for the free-living samples **(Table V.S2)**. Therefore, for some samples, a large fraction of the coding regions was not covered (0 read mapped). To minimize possible bias due to poor sequencing depth, we discarded the samples from *A. nodosum* microcosms for analysis (up to 70 % of uncovered coding regions) and only considered upregulated genes (and not the down-regulated ones) in attached bacteria versus free-living bacteria. Overall, very few significant up-regulations were detected (**Figure V.5A**). With *L. digitata*, 19 genes were significantly induced (Bonferroni-adjusted p-value < 0.05) in attached bacteria vs. free-living bacteria, including in particular 2 TetR-type transcriptional regulators, 2 YceI family proteins which could be involved in oxidative stress response via the isoprenoide synthesis (Handa *et al.*, 2005; Weber *et al.*, 2006) and 5 chaperone proteins. Among the 14 genes identified on *F. serratus,* there are 2 TonB-dependent receptors which are not associated with a SusD-like protein then likely not involved in carbohydrate metabolism. Several genes from the same genomic region (*zgal_4237-4246*), involved in stress responses were also induced on both algae.

No gene encoding CAZymes was significantly induced in attached vs. free-living bacteria, suggesting that biofilm formation is not required to induce the production of hydrolytic enzymes. This hypothesis was tested in an additional experiment to assess whether or not forming biofilm at the surface of the macroalgae is essential for *Z. galactanivorans* to get access to algal substrates, using extracellular alginolytic activity as a proxy (**Figure V.5B**). Although the increase of alginolytic activity was delayed when *Z. galactanivorans* was separated from the algae by a 0.2 µm filter, the activity was similar in both conditions after 90 h. After 6 days, the algal tissues were fully degraded when *Z. galactanivorans* and *L. digitata* were in contact. The degradation was slower when *Z. galactanivorans* was separated from *L. digitata*, after 6 days algae pieces were peeling and in decomposition but still had their original shape.

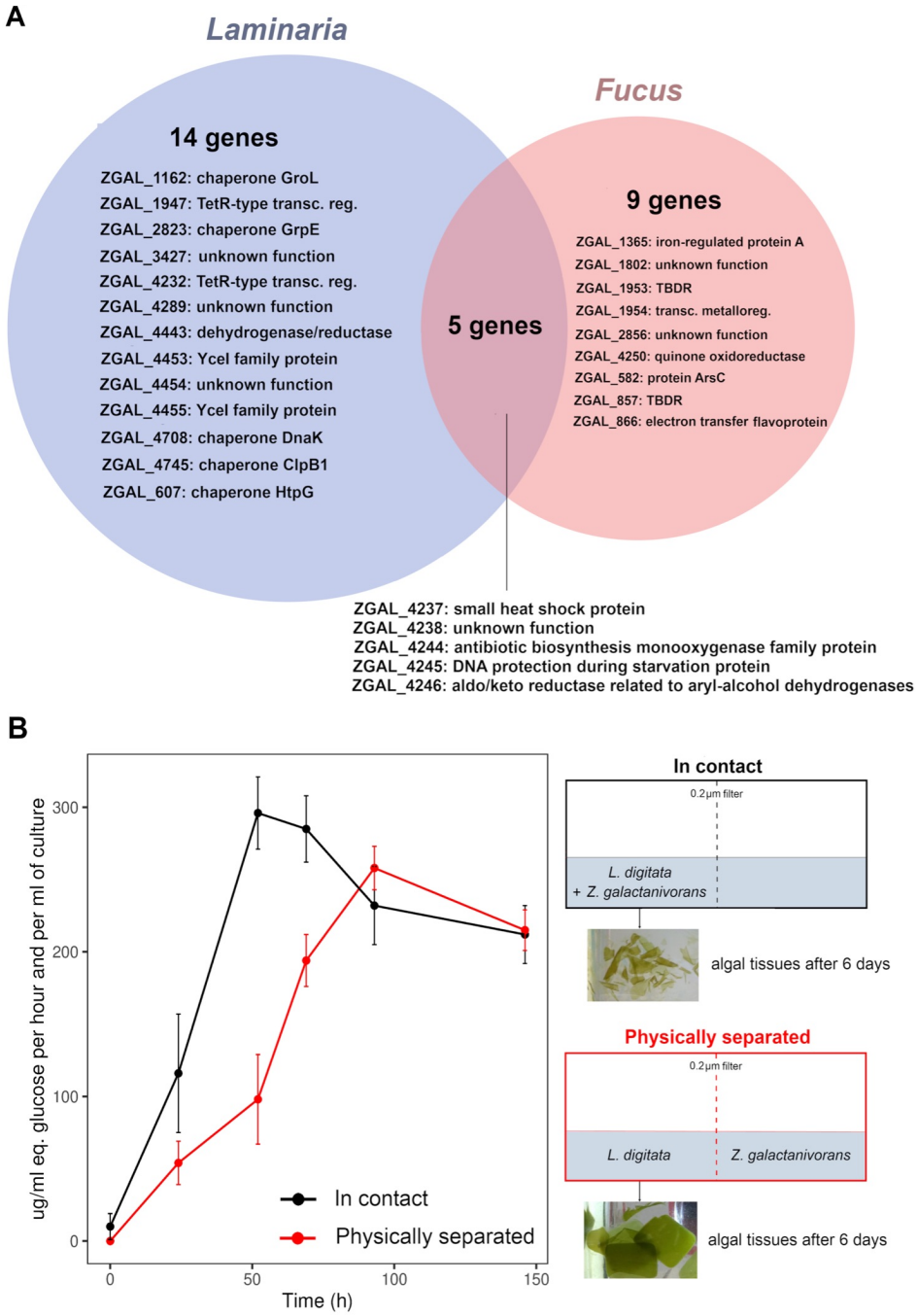

Figure V.5: Effect of the attachment to macroalgae during the degradation. (A) Number of genes (Bonferroni-adjusted p-value < 0.05) up-regulated in algae-attached bacteria compared to free-living bacteria. The annotation of each gene is provided. (B) Alginolytic activity of the enzymes secreted when *Z. galactanivorans* was grown in contact with *L. digitata* (black) or separated from *L. digitata* by a 0.2 µm filter (red). A photograph of the tissue aspect after 146 h is shown. The activity was measured in each compartment (left and right) and summed. Values are mean ± s.d. (n = 3).

6. Comparative physiology and genomics of fresh macroalga degradation in *Zobellia*

To investigate if the ability to degrade fresh algal biomass is shared within the genus *Zobellia*, eight *Zobellia* strains were grown with *Laminaria digitata* pieces (**Figure V.6**). All eight strains had the ability to use the fresh *L. digitata* tissues for their growth. *Z. galactanivorans* Dsij^T had the highest final cell density (OD_{600} = 1.5) and shortest generation time (5.09 h) of all tested strains. It is worth noting that *Z. galactanivorans* reached much higher cell density when grown with the meristem part of adult individuals compared with young plantlets displaying a much thinner thallus, and then offering lower carbon amount (as in **Figure V.1**). While the iodine metabolism in macroalgae is related to defense mechanisms, the higher iodine content measured in plantlets (Küpper *et al.*, 1998; Ar Gall *et al.*, 2004) could also explain these growth differences. *Z. nedashkovskayae* Asnod3-E08-A showed only limited growth (final OD_{600} = 0.4) and the longest generation time (t_{gen} = 16.33 h). However, this strain formed cell aggregates in the culture medium, probably leading to underestimated OD measurements. Other strains (which did not form aggregates) showed intermediate final cell density ($OD_{600} \approx 1$) and generation time (5.92 - 11.74 h). These growth differences were reflected in the final aspect of macroalgal pieces, where *Z. galactanivorans* Dsij^T was the only strain to completely breakdown algal tissues after 91 h. In microcosms containing the *Z. nedashkovskayae* strains the algal tissues started to peel and to breakdown at the corners of the pieces. For the other strains, no visible trace of degradation was detected. The number of genes predicted to encode GHs, PLs, CEs or sulfatases was estimated within the genome of each strain (**Figure V.6A**) and correlation with the generation time was assessed (**Table V.S5**). A strong negative correlation was found between the number of GHs and the generation time (Spearman, rho = -0.90; P = 0.006; *Z. nedashkovskayae* Asnod3-E08-A was removed from the analysis). Among the 305 genes up-regulated when *Z. galactanivorans* Dsij^T grew with *L. digitata* compared to maltose, 22 are specific to *Z. galactanivorans* as no homolog was found in the genome of the seven other *Zobellia* strains (**Table V.S6**). They include two GHs, *zgal_3349* (GH20) contained in PUL33 (putatively targeting an hexosamine polysaccharide) and *zgal_3470* in the FCSP PUL35, and a susC-like TBDT (*zgal_3441*) just upstream the FCSP PUL34. Other up-regulated genes within PUL34/35 are not conserved in all the *Zobellia* strains (**Figure V.6B**). Likewise, several genes of the alginolytic PUL29 (*zgal_2613* to *2624*) were not detected in other *Zobellia* strains, especially in the two *Z. roscoffensis* strains which lack 5 of them. Also, the gene *alyA1* (*zgal_1182*) encoding an extracellular endo-alginate lyase was only conserved in the *Z. nedashkovskayae* strains. Several genes located downstream the alginolytic PUL (*zgal_2628-2635*) are also specific to *Z. galactanivorans* Dsij^T or conserved in only one other strain. Two other genes encoding proteins involved in carbohydrate assimilation (*zgal_334* and *zgal_2296* encoding a GHnc and a lipoprotein with CBM22, respectively) are missing in five strains. *zgal_334* is located in a cluster of genes encoding sulfatases, fucosidases and

PLs and might be part of a PUL targeting FCSPs (not found in the 51 PULs identified as the pair *susCD*-like is absent).

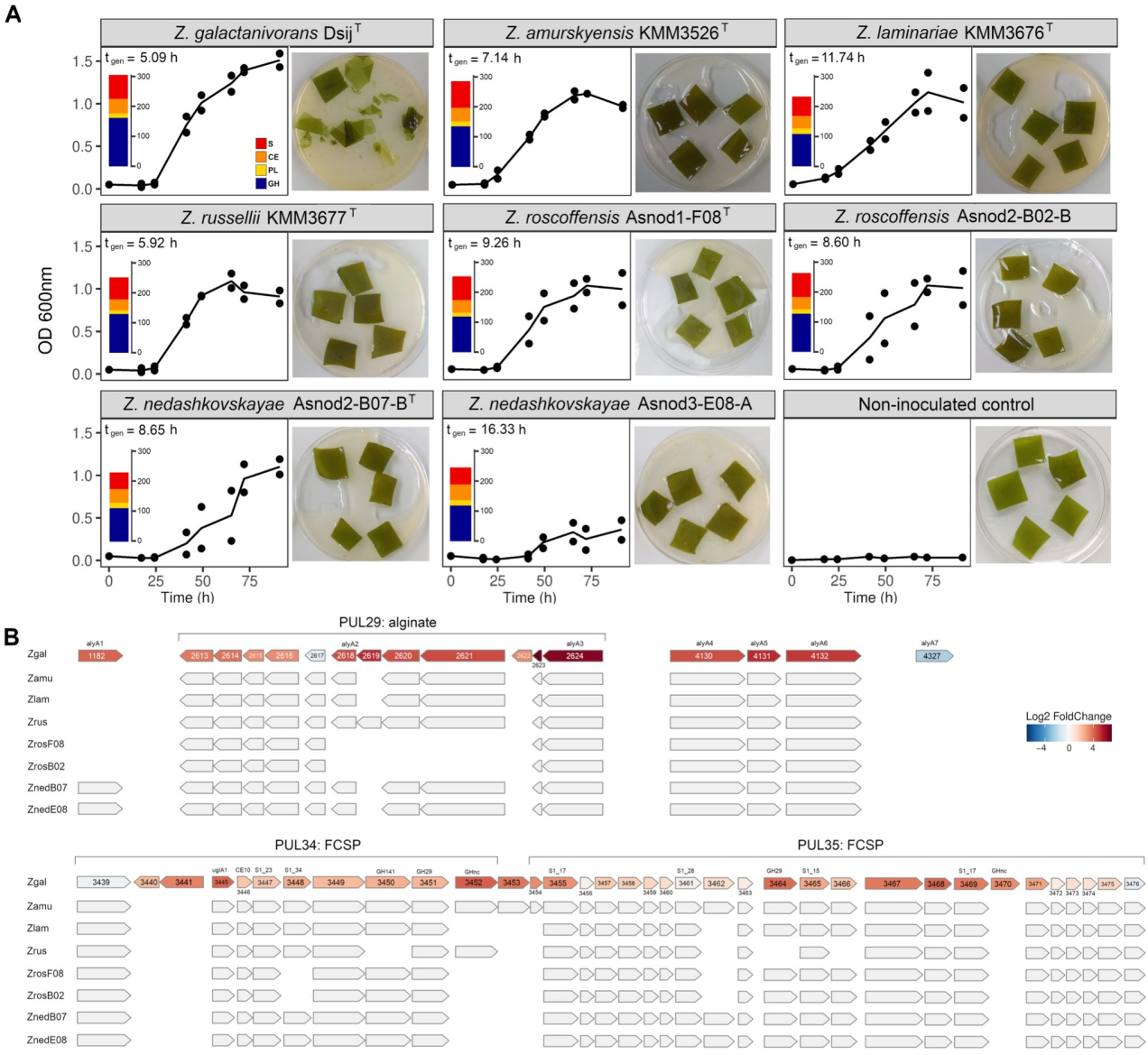

Figure V.6: Ability of *Zobellia* spp. to use fresh *L. digitata* for its growth. (A) Growth of eight *Zobellia* strains with *L. digitata* pieces. The generation time t_{gen} is indicated for each strain as well as the number of glycoside hydrolases (GH, blue), polysaccharides lyases (PL, yellow), carbohydrate esterases (CE, orange) and sulfatases (S, red) predicted in their genome (dbCAN search on the MicroScope platform). Individual points for duplicate experiments are shown. Lines are means of independent replicates (n = 2 or n = 3). (B) Comparison of genomic loci among the eight *Zobellia* strains. For *Z. galactanivorans*, genes were colored according to their expression log2FC for the comparison *L. digitata* vs. maltose. Gene ID is indicated inside arrows and CAZymes and sulfatases are specified above. Top: genes involved in the alginate-utilization system. Bottom: genes contained in putative FCSP PUL34 and 35. Zgal: *Z. galactanivoran*^{T} Dsij^{T}; Zamu: *Z. amurskyensis* KMM 3526^{T}; Zlam: *Z. laminariae* KMM 3676^{T}; Zrus: *Z. russellii* KMM 3677^{T}; ZrosF08: *Z. roscoffensis* Asnod1-F08^{T}; ZrosB02: *Z. roscoffensis* Asnod2-B02-B; ZnedB07: *Z. nedashkovskayae* Asnod2-B07-B^{T}; ZnedE08: *Z. nedashkovskayae* Asnod3-E08-A.

IV. Discussion

1. *Zobellia galactanivorans* Dsij^T acts as a sharing pioneer in brown macroalgae degradation

Marine heterotrophic bacteria from different functional guilds are not equally equipped to process algal biomass, including the polysaccharide-rich complex supramolecular ECM network. Recently, several frameworks were proposed to conceptualize these contrasted ecological strategies (Hehemann *et al.*, 2016; Arnosti *et al.*, 2020; Gralka *et al.*, 2020). First, pioneer bacteria degrade complex organic matter by the production of specific hydrolytic enzymes. The hydrolysate can then either be assimilated by the pioneers themselves and/or shared with other bacterial community members referred to as exploiters or scavengers, which lack the required enzymatic tools and cannot feed on intact substrates. Here, we showed that *Z. galactanivorans* Dsij^T has the capacity to use fresh healthy algal tissues for its growth. Similar growth rates were observed with the three algal species tested that display distinct morphologies and chemical compositions. Furthermore, *Z. galactanivorans* was able to completely break down *L. digitata* tissues. This corroborates its role as pioneer in algae recycling, as first suggested by Zhu *et al.*, 2017. The limited breakdown of Fucales tissues might be explained by their higher content in phlorotannins (Holdt and Kraan, 2011), which display antimicrobial activity and may reduce tissue digestibility (Paul *et al.*, 2001; Lopes *et al.*, 2012). By contrast, Koch *et al.*, 2020 indicated that the gammaproteobacterium *Alteromonas macleodii* uses various soluble algal polysaccharides but does not cause damages on intact *Ecklonia radiata* (Laminariales) tissues, probably lacking the relevant enzymatic tools. During the degradation, *Z. galactanivorans* secreted extracellular alginolytic enzymes and colonized the algal surface, which might be key features to access carbohydrates within the ECM and breakdown intact tissues. In addition, we showed that *Z. galactanivorans* does not require a physical contact with *L. digitata* to degrade it, suggesting that the algal breakdown strongly relies on secreted extracellular enzymes. Accordingly, the increase in alginolytic activity was similar whether the two organisms were in contact or not, even if it displays a delay in the latter case due to diffusion time. These secreted enzymes could release low molecular weight compounds acting as public goods that would fuel other bacteria. Our results therefore suggest that *Z. galactanivorans* would be a "sharing" pioneer, in opposition to "selfish" pioneers which sequester the low-molecular-weight (LMW) hydrolysis products by producing surface-associated hydrolytic enzymes binding the polysaccharides, leading to minor amounts of released products in the medium (Reintjes *et al.*, 2017; Pluvinage *et al.*, 2018). The release of LMW products was already demonstrated by Dudek *et al.*, 2020 and Zhu *et al.*, 2017 who detected an accumulation of alginate oligosaccharides when *Z. galactanivorans* was grown on purified alginate and algal tissues respectively. Moreover, Zhu *et al.*, 2017 revealed that the presence of *Z. galactanivorans* would enable the growth of other taxa with algal biomass as the sole carbon source, hence highlighting its sharing pioneer behavior. Such cross-feeding interactions were characterized

during alginate (Enke *et al.*, 2019) or chitin (Pollak *et al.*, 2021; Pontrelli *et al.*, 2021) assimilation for example. The other *Zobellia* spp. tested successfully grew with fresh *L. digitata* but did not cause important damages to the algal tissues as observed with *Z. galactanivorans*. It remains unclear whether (1) they fed on algal exudates, whose release might be favored by the preparation of algae for microcosm experiment, and/or (2) acted as pioneers by feeding on ECM polymers but less efficiently than *Z. galactanivorans*. The catabolic profiles on purified brown algal sugars conducted in previous works (**Table V.S1**) indicate different growth capacities. Indeed, if all strains are able to use mannitol, the main brown algal exudate, both *Z. roscoffensis* strains as well as *Z. laminariae* KMM 3676^T display limited or none abilities to grow with purified alginate, FCSPs and laminarin. Hence, with macroalgae, the latter likely feed on mannitol, whose release might be favored by the cut of the tissues (even if the extensive washing steps limited its accumulation), and not on the complex brown algal polysaccharides. Comparative genomics indicated that CAZymes content likely influences the strain capacity to breakdown and use fresh algal tissues. Despite high CAZymes content in their genome (Chernysheva *et al.*, 2019) some *Zobellia* strains probably lack key genes to efficiently degrade the *L. digitata* ECM as *Z. galactanivorans* Dsij^T does. Indeed, although key PULs targeting alginate or FCSPs and triggered with *L. digitata* were conserved in *Zobellia* genomes, some genes, in particular the most upregulated ones, were restricted to *Z. galactanivorans* Dsij^T or shared with only few strains. They notably encode proteins related to carbohydrate metabolism. For example, the alginate lyase gene *alyA1*, which was strongly upregulated by *Z. galactanivorans* Dsij^T in the presence of *L. digitata*, *F. serratus* and *A. nodosum* (log2FC 4 - 7), had homologs only in the two other strains that caused visible algal damage (*Z. nedashkovskayae* Asnod2-B07-B^T and Asnod3-E08-A). Accordingly, *alyA1* was previously shown to have a crucial role in initiating algae breakdown (Zhu *et al.*, 2017). Other strain-specific or variable genes strongly responsive to brown algal biomass might represent additional genetic determinants essential in the pioneer abilities of intact algae degraders, whose biological function remains to be elucidated (see Chapter VI). These distinct genomic repertoires would explain the different growth behavior on intact algal biomass and might suggest distinct polysaccharide/substrate niches. For example, *Z. roscoffensis* strains can use xylan (found in green and red algae) but not brown algal polysaccharides (alginate, FCSPs, laminarin) while this is the opposite for both *Z. nedashkovskayae* strains (Barbeyron *et al.*, 2021). Overall, our results highlight the relevance of *Z. galactanivorans* Dsij^T as an environmental model of sharing pioneer, while other *Zobellia* strains might be less efficient to use alginate and FCSPs and prioritize other substrates.

2. *Z. galactanivorans* transcriptome exhibits a transcriptomic shift in the presence of macroalgae

The previous studies focusing on algal biomass degradation were conducted on purified algal polysaccharides or crushed algae. Consequently, they do not consider the algal tissue complexity or the mixture of polysaccharide encountered in the field, potentially missing crucial genes and mechanisms. Here, we reported the first transcriptomic analysis during the bacterial degradation of fresh macroalgal biomass.

Complete transcriptome analysis during the growth with fresh macroalgae revealed that *Z. galactanivorans* Dsij^T metabolism shifted from simple sugars assimilation toward the degradation of brown algal polysaccharides. The transcriptome obtained with *L. digitata* presented the highest similarities with brown algal polysaccharides, suggesting access, hydrolyze and digest ECM polysaccharides within the *L. digitata* tissues more easily, resulting in visible tissue degradation. Although *F. serratus* and *A. nodosum* both belong to the order Fucales, transcriptomes obtained with *F. serratus* are not closer to that obtained with *A. nodosum* than *L digitata*. *A. nodosum* induced a wider cellular response with many specific regulations. This might partly be due to the growth of antibiotic-resistant *A. nodosum* epiphytic bacteria (as seen in the non-inoculated microcosms) that could have affected *Z. galactanivorans* behavior as bacterial interactions likely occurred. However, this also suggests that the global transcriptomic response is only partially driven by the taxonomy of the degraded alga. Compared with *F. serratus* or *L. digitata*, the *A. nodosum* thallus is much thicker. Furthermore, the latter is always found associated with various symbionts and especially with the endophytic fungus *Mycophycias ascophylli* (reviewed in Garbary *et al.*, 2017). This obligate and extensive symbiont secretes specific compounds potentially preventing tissue grazing and might also display antibacterial activity as other macroalgal endophytes (Flewelling *et al.*, 2013) or synthesized various compounds offering a larger substrate diversity. Fries, 1979 demonstrated the strong ability of this symbiont to use laminarin for its growth (while it is not able to degrade alginate), this could lead to structural modification of this polymer within the *A. nodosum* thallus potentially explain the specific catabolic regulations observed when *Z. galactanivorans* Dsij^T was grown with this alga (see below).

Although we showed that *Z. galactanivorans* Dsij^T colonized *L. digitata* tissues during the degradation, we did not evidence strong differences between the transcriptomes of free-living and surface-attached cells (except for oxidative stress response, see below). While difficulties to extract RNA from algae-attached bacteria resulted in poor sequencing coverage, it should still have been possible to detect strong upregulations in attached cells. Therefore, this result further supports that surface attachment is not a requirement for the utilization of algal biomass by *Z. galactanivorans* Dsij^T at the later stage of degradation when samples were collected for RNA-seq analysis. Transcriptomic responses might have been different at an earlier stage, before the breakdown of the tissues. Indeed, Ebrahimi *et al.*, 2019

recently showed that a minimal cell concentration is essential to initiate the breakdown of complex polysaccharides in solid matrices. In line with this, *Z. galactanivorans* cells rapidly formed discrete and dense patches on *L. digitata* tissues before visible degradation. Future time-resolved transcriptome analysis could inform on early vs. late regulations in alga-attached cells.

3. Deciphering the importance of specific mechanisms in fresh tissue breakdown, including new catabolic pathways

Alginate is the most abundant polysaccharide in brown algal ECM and likely the most accessible as it embeds the cellulose-FCSP network (Deniaud-Bouët *et al.*, 2014). This agrees with the stronger induction of the alginolytic system compared to all other PULs, regardless of the algal species. This system was particularly triggered with *L. digitata*, likely reflecting the higher alginate content in *L. digitata* tissues (22-36 %) compared to *F. serratus* (18-28 %) and *A. nodosum* (15-20 %) (Kloareg and Quatrano, 1988).

Furthermore, our analyses revealed several yet uncharacterized PULs that were triggered with macroalgae. Out of the seven predicted FCSP PULs identified in *Z. galactanivorans* Dsij^T genome based on the presence of sulfatase- and fucosidase-encoding genes, three were significantly upregulated with macroalgae but to various degrees depending on the algal species. This suggests different substrate specificities, consistent with the large structural diversity of FCSPs. Indeed, FCSPs from Laminariales are usually built of (1→3)-linked α-L-fucopyranose residues, whereas in Fucales FCSPs typically contain alternating (1→3)- and (1→4)-linked α-L-fucopyranose residues (Cumashi *et al.*, 2007; Ale and Meyer, 2013). In addition, the *F. serratus* and *A. nodosum* thallus are believed to be richer in fucose and sulfate than that from *L. digitata* (Mabeau and Kloareg, 1987; Skriptsova *et al.*, 2012) although it seems that algae taxonomy might not be the main driver in FCSP composition (Ponce and Stortz, 2020). It is worth noting that none of the putative FCSP PULs triggered by macroalgae were significantly induced in the presence of purified alginate or FCSPs. FCSPs from algal tissues probably largely differ from the purified FCSPs used here as the latter was extracted from *A. nodosum* at a different location and time and underwent several purification steps which might have altered the polysaccharide structure. In addition, purified FCSPs likely do not represent the whole range of structures found in the ECM. Indeed, FCSPs encompass fucoidans and fucans displaying various types of monosaccharides, linkages and sulfation motifs and then representing many heterogeneous structures (Deniaud-Bouët *et al.*, 2017) which might not be equally extracted depending on the purification method. Hence, studying fresh algal tissue degradation allows preserving polysaccharide structure, composition and interactions with other compounds as they appear in the environment. This may be a more effective way to reveal new specific gene clusters crucial for macroalgae breakdown but undetectable when using only purified polysaccharides.

Furthermore, due to this heterogeneity, the FCSPs probably represent highly recalcitrant substrates that required a large set of enzymes to be fully breakdown (Sichert *et al.*, 2020) reported around 100 enzymes (organized in PULs or isolated in the genome) involved in the FCSP degradation pathways in the verrucomicrobia '*Lentimonas'* sp. CC4). It has also been demonstrated that FCSPs are cross-linked with many compounds (proteins, phlorotannins, alginates) within the ECM and then usually extracted together with contaminants, even with the storage carbohydrate laminarin (Mabeau *et al.*, 1990; Deniaud-Bouët *et al.*, 2014, 2017; Lorbeer *et al.*, 2014; Ponce and Stortz, 2020) resulting in an even higher substrate diversity that would explain the induction of various gene clusters with macroalgae and purified FCSPs. In particular, the two PULs with unclear function (PUL26 and 27) could target additional components of the ECM that would be co-extracted with FCSPs as they are induced with both FCSPs and macroalgae.

On the other hand, the two identified laminarin PULs were poorly regulated with the three algae. Therefore, *Z. galactanivorans* Dsij^T might then use first ECM polysaccharides (such as alginate and FCSPs) leading to ECM network destruction and later access storage polysaccharides such as laminarin. Such a substrate prioritization of the multiple carbon sources of raw algal material was previously raised for [*Bacillus*] *weihaiensis* Alg07^T as the induction of its alginolytic system preceded the induction of the genes involved in laminarin and mannitol degradation when grown on algal powder (Zhu *et al.*, 2016). Koch *et al.*, 2019 showed that *Alteromonas macleodii* 83-1 prioritized laminarin over alginate and pectin when grown on a mixture of purified and soluble polysaccharides. The successive assimilation of these polysaccharides might then differ whether they are under their soluble form or associated with many compounds within macroalgae, underlining the importance to consider the ECM architecture to understand the process of macroalgae decomposition. However, the β-glucan PUL4 and ZGAL_3183 induced in the presence of *A. nodosum* were also triggered with purified laminarine (β-1,3-glucans) (Thomas *et al.*, 2017). The substrate specificity of PUL4 is unknown but it could target *A. nodosum* specific laminarin-like structure. ZGAL_3183 is homologous to the gene *dssA* which encodes a lyase degrading sheath polysaccharide surrounding other bacteria (Takeda *et al.*, 2000). *Z. galactanivorans* might have to compete with other microorganisms (in line with the growth of epiphytic bacteria with *A. nodosum*) by attacking their EPSs and it would be consistent with the specific induction of T6SS-related genes (Vgr family proteins) with *A. nodosum* only, as T6SS is known to exert antibacterial activity (Navarro-Garcia *et al.*, 2019). Nevertheless, Thomas *et al.*, 2017 pointed out that ZGAL_3183 could also be involved in the hydrolysis of alternative motifs in laminarin, such as N-acetylhexosamine-terminated. As raised above, the presence of endosymbionts from *A. nodosum* could result in specific laminarin structures that would explain the specific induction of putative laminarin-like catabolic systems with *A. nodosum*.

The fact that LamE was the only laminarinase induced with *A. nodosum* (with *F. serratus* as well), among the 5 identified in the genome of *Z. galactanivorans* Dsij^T, supports this hypothesis as LamE is the only one to belong to the family GH64 and not GH16, suggesting an activity on different motifs.

Growth with macroalgae tissues also directed cellular metabolism toward counteracting algal defense responses. One of the algal defense mechanisms is the massive production of reactive oxygen species (ROSs), which is partly induced by endogenous elicitors (i.e. oligo-alginates) derived from the degradation of their own cell wall (Küpper *et al.*, 2001). Here, we showed that ROS-scavenging enzymes (e.g. superoxide dismutases, peroxidases and catalases), were induced with algae and especially with *L. digitata*. Degradation of *L. digitata* tissues by *Z. galactanivorans* likely produced large amounts of elicitors leading to an important algal defense. ROSs could also have been released following the algae cut but the majority was probably removed during the extended washing steps. In contrast, it was shown that *A. nodosum* and *F. serratus* do not respond to the addition of endogenous elicitors (Küpper *et al.*, 2002), potentially explaining the lower induction of antioxidant pathways in *Z. galactanivorans* Dsij^T. The induction of defense mechanisms against oxidative stress was even more pronounced in bacteria attached to *L. digitata* tissues through the expression of chaperones. This likely reflects the higher ROS concentration at the algal surface than in the medium where the compounds are diluted. Surprisingly, despite the algal emission of iodine as a chemical defense, none of the enzymes involved in iodine accumulation identified in *Z. galactanivorans* Dsij^T genome (i.e. three vanadium-dependent iodoperoxidases, Fournier *et al.*, 2014) were induced with *L. digitata* and *F. serratus*. One vanadium-dependent iodoperoxidase (vIPO3) and the haloacid dehalogenase (HAD, Grigorian *et al.*, 2021) were significantly up-regulated with *A. nodosum* compared with alginate and maltose respectively. Although not significant, the HAD expression was also 3-fold higher with *Laminaria* and *Fucus* compared with maltose. Potential unknown alternative or additional mechanisms allowing the cells to cope with iodine might have been triggered in the presence of macroalgae.

T9SS-related genes were strongly induced by macroalgae and particularly by *A. nodosum*, but not with alginate or FCSPs. This indicates that T9SS might have an essential role during the degradation of fresh macroalgae. This *Bacteroidetes*-specific secretion system was formerly known as the Por secretion system PorSS (reviewed in Lasica *et al.*, 2017). T9SS is notably required by *Flavobacterium johnsoniae* in biofilm formation and to secrete chitinases as well as cell-surface gliding motility adhesins, and by the pathogen *Porphyromonas gingivalis* to deliver protease virulence factors (Sato *et al.*, 2010; Eckroat *et al.*, 2021)**.** In many *Bacteroidetes*, several PULs are coupled with the T9SS for the secretion of extracellular enzymes containing a T9SS-specific CTD domain (McKee *et al.*, 2021). Our results suggest that *Z. galactanivorans* strongly relies on T9SS to secrete ECM-targeting CAZymes and/or attach to macroalgal surfaces. Besides T9SS-related genes, clusters encoding glycosyl transferases were also specifically induced by macroalgae. They might participate in EPS production and facilitating cell attachment and biofilm formation.

V. Conclusion

This study provides the first insights in the bacterial transcriptomic response during fresh macroalgae utilization and represents a source of potential genetic determinant for further functional characterization. Altogether, our results raised the relevance to consider the whole complexity of macroalgae tissues in further degradation studies, as it would take a step forward in the understanding of the algal biomass recycling through the identification of new metabolic pathways or the characterization of bacterial cooperative interactions.

VI. Acknowledgments

The authors thank Tatiana Rochat for advice during transcriptomic analyses, Sébastien Colin for guidance in confocal manipulation, Philippe Potin and Cécile Hervé for helpful discussions and Yan Jaszczyszyn from the I2BC sequencing platform. This work has benefited from the facilities of the Genomer platform and from the computational resources of the ABiMS bioinformatics platform (FR 2424, CNRS-Sorbonne Université, Roscoff), which are part of the Biogenouest core facility network. This work was funded by the French Government via the National Research Agency programs ALGAVOR (ANR-18-CE02-0001-01) and IDEALG (ANR-10-BTBR-04).

VII. Supplementary Figure

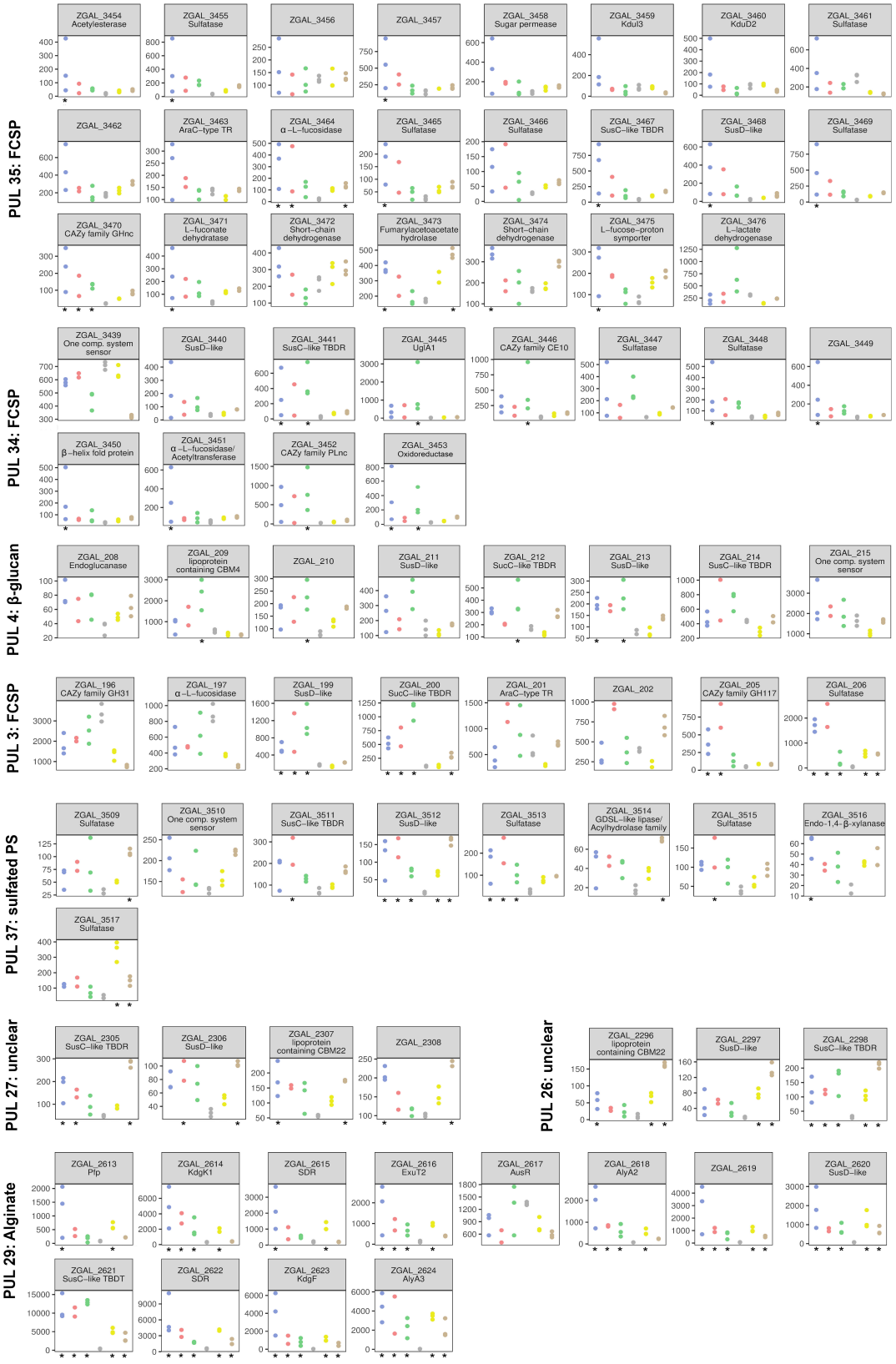

Figure V.S1: Normalized expression of the genes contained within the PULs shown in Figure V.3B. *: genes significantly overexpressed in the corresponding condition compared with maltose. Blue: *L. digitata*; Red: *F. serratus*; Green: *A. nodosum*; Grey: Maltose; Yellow: Alginate; Brown: FCSPs

VIII. Supplementary Tables

Table V.S1: Ability of the eight *Zobellia* strains tested in this study to use purified brown algal polysaccharides. From Barbeyron *et al*., 2001, 2021; Nedashkovskaya *et al*., 2004. Zgal: *Z. galactanivorans* Dsij^{T}; Zamu: *Z. amurskyensis* KMM 3526^{T}; Zlam*: Z. laminariae* KMM 3676^{T}; Zrus: *Z. russellii* KMM 3677^{T}; ZrosF08: *Z. roscoffensis* Asnod1-F08^{T}; ZrosB02: *Z. roscoffensis* Asnod2-B02-B; ZnedB07: *Z. nedashkovskayae* Asnod2-B07-B^{T}; ZnedE08*: Z. nedashkovskayae* Asnod3-E08-A. FCSP: Fucose-containing sulfated polysaccharides.

	Zgal	Zamu	Zlam	Zrus	Zros F08	Zros B02	Zned B07	Zned E08
Alginate	+	±	±	NA	-	-	+	+
FCSP	+	+	±	NA	-	-	+	+
Laminarin	+	+	±	NA	-	-	+	+
Mannitol	+	+	+	NA	+	+	+	+

Table V.S2: General characteristics of the different RNA samples.

Sample	Type	OD600 at sampling time	RNA concentration (ng/µl)	ratio A_{260}/A_{280}	ratio A_{260}/A_{230}	Genome coverage (%)	Prokaryotic rRNA (%)	Eukaryotic rRNA (%)	Number of fragments post trimming	Genes not covered (%)
FL_Ldig1	Free-living	0.3	2.8	1.7	0.7	74.7	6.1	0.7	3.09E+07	0.1
FL_Ldig2	Free-living	0.4	19.8	1.8	1.4	58.6	6.4	0.7	2.90E+07	0
FL_Ldig3	Free-living	0.3	3.9	1.7	0.7	92.9	27.0	1.0	1.09E+07	1
FL_Fser1	Free-living	0.9	18.2	1.4	1.0			not sequenced		
FL_Fser2	Free-living	0.2	33.2	2.1	0.6	80.0	2.1	0.8	2.62E+07	0
FL_Fser3	Free-living	0.3	21.3	2.1	0.9	43.5	1.5	0.7	1.78E+07	0.5
FL_Anod1	Free-living	0.4	35.8	1.6	1.1	68.7	1.2	0.1	1.25E+07	1.7
FL_Anod2	Free-living	0.4	29.0	1.5	0.9	78.6	2.7	1.0	1.24E+07	0.1
FL_Anod3	Free-living	0.5	90.0	2.1	1.6	59.1	0.8	0.1	3.22E+07	0.2
FL_Maltose1	Free-living	0.5	187.0	2.1	2.0	87.5	6.0	0.2	9.51E+06	0.5
FL_Maltose2	Free-living	0.5	185.0	2.1	1.3	90.5	12.6	0.1	1.11E+07	0.3
FL_Maltose3	Free-living	0.4	232.0	2.1	2.0	90.6	11.8	0.1	1.57E+07	0.1
FL_Alginate1	Free-living	0.4	365.0	1.7	0.9	93.6	6.9	0.2	1.21E+07	0.1
FL_Alginate2	Free-living	0.3	128.0	1.8	0.7	93.3	6.6	0.2	1.46E+07	0.1
FL_Alginate3	Free-living	0.4	1340.0	1.9	1.1	94.5	7.8	0.1	3.31E+07	0
FL_FCSP1	Free-living	0.2	117.0	1.6	0.9	95.6	4.4	0.0	3.39E+07	0
FL_FCSP2	Free-living	0.2	112.0	1.6	0.8	95.2	4.1	0.0	3.10E+07	0.1
FL_FCSP3	Free-living	0.2	91.7	1.6	0.9	95.5	6.4	0.1	3.24E+07	0
Att_Ldig1	Attached	0.3	7.2	1.6	0.1	6.2	4.6	28.8	2.62E+07	3.5
Att_Ldig2	Attached	0.4	too low	1.7	0.4			not sequenced		
Att_Ldig3	Attached	0.3	too low	1.4	0.1	24.1	8.5	56.0	2.63E+07	5
Att_Fser1	Attached	0.9	8.6	0.9	0.1	46.1	6.1	10.2	8.80E+06	0
Att_Fser2	Attached	0.2	13.0	1.0	0.1	69.1	0.5	3.9	7.96E+06	0
Att_Fser3	Attached	0.3	13.7	0.8	0.2	32.4	4.0	16.5	1.54E+07	27
Att_Anod1	Attached	0.4	2.4	0.7	0.2	15.1	2.8	70.7	1.53E+07	1
Att_Anod2	Attached	0.4	too low	0.7	0.2	35.5	4.0	54.5	2.28E+06	60
Att_Anod3	Attached	0.5	too low	0.7	0.2	19.7	3.3	62.1	7.88E+06	41

Table V.S3: Genes upregulated either with *Laminaria*, *Fucus* or *Ascophyllum* when compared either to maltose, alginate or FCSP. Log2FC is indicated and highlighted in red if P-value < 0.05.

			Log2Fold-Change								
Gene ID	**Gene name**	**Gene function**	***Lam* vs. Mal**	***Lam* vs. Algi**	***Lam* vs. FCSP**	***Fuc* vs. Mal**	***Fuc* vs. Algi**	***Fuc* vs. FCSP**	***Asco* vs. Mal**	***Asco* vs. Algi**	***Asco* vs. FCSP**
ZGAL_1007		RNA polymerase ECF-type sigma factor	-1.9	-0.3	1.6	-0.5	1.1	3.0	-1.2	0.3	2.2
ZGAL_1011	lamE	lamE Endo-1,3-beta-glucanase, family GH64	1.3	0.5	0.2	2.1	1.3	1.1	1.7	0.9	0.7
ZGAL_1018		Hypothetical protein	-0.5	0.5	-0.9	-0.4	0.6	-0.8	0.9	1.9	0.5
ZGAL_1019		Elastase	-2.9	1.8	-1.5	-0.4	4.4	1.0	1.4	6.2	2.8
ZGAL_1021		Glycoside hydrolase, family GH16	-0.8	0.6	1.2	-0.5	0.9	1.5	-0.3	1.0	1.7
ZGAL_1025		Sulfatase, family S1-20	1.5	0.6	0.1	0.7	-0.3	-0.8	0.6	-0.3	-0.8
ZGAL_1026	nahA1	nahA1 Beta-N-acetylhexosaminidase, family GH20	1.3	0.7	0.2	0.7	0.1	-0.4	0.1	-0.4	-0.9
ZGAL_1029		SusD-like lipoprotein	1.2	-0.4	-1.1	1.4	-0.1	-0.8	1.3	-0.3	-1.0
ZGAL_105		Conserved hypothetical lipoprotein	1.0	0.3	1.3	0.6	-0.1	0.8	-0.1	-0.8	0.1
ZGAL_106		SAM-dependent methyltransferase	1.9	-0.7	-0.7	0.5	-2.2	-2.1	0.6	-2.1	-2.0
ZGAL_1063		Peroxiredoxin	1.8	-0.7	-1.1	0.8	-1.7	-2.1	3.1	0.7	0.3
ZGAL_1067	des6-2	des6-2 Linoleoyl-CoA desaturase	0.6	-0.4	-2.7	1.9	0.9	-1.4	2.8	1.8	-0.5
ZGAL_1071		Ribonuclease BN family protein	3.2	2.8	2.2	3.5	3.1	2.5	1.2	0.8	0.2
ZGAL_1072		Short-chain dehydrogenase/reductase	3.0	2.1	2.0	1.8	1.0	0.9	0.1	-0.7	-0.8
ZGAL_1073		Conserved hypothetical protein	4.5	2.9	2.5	2.8	1.2	0.8	0.3	-1.2	-1.7
ZGAL_1074		Conserved hypothetical membrane protein	2.3	2.5	2.3	2.7	2.8	2.7	0.3	0.4	0.2
ZGAL_1075		Possible Sigma-54 modulation protein	3.4	2.8	1.6	2.7	2.1	0.9	0.6	0.0	-1.2
ZGAL_1076		Putative protein	4.0	3.1	1.9	3.8	2.8	1.7	1.0	0.0	-1.1
ZGAL_1077		Citrate transporter family protein	3.3	2.5	1.9	3.7	2.9	2.2	1.8	1.0	0.4
ZGAL_1078		Small-conductance mechanosensitive channel	3.6	2.8	2.9	3.1	2.3	2.4	2.2	1.4	1.5
ZGAL_1079		Conserved hypothetical membrane protein	2.7	2.3	1.1	2.2	1.9	0.7	0.2	-0.2	-1.3
ZGAL_108		Conserved hypothetical lipoprotein	0.4	0.4	2.2	-0.3	-0.3	1.5	-0.5	-0.6	1.3
ZGAL_1080		Putative membrane protein	2.8	2.7	3.2	2.7	2.6	3.1	-0.1	-0.2	0.3
ZGAL_1082	topA2	topA2 DNA topoisomerase 1B	4.1	2.9	2.1	3.4	2.1	1.4	1.0	-0.2	-1.0
ZGAL_1083		Conserved hypothetical protein	4.1	2.6	2.2	2.9	1.4	1.0	0.9	-0.6	-1.0
ZGAL_1084		Conserved hypothetical protein	4.3	2.1	0.5	3.5	1.3	-0.3	1.8	-0.4	-1.9
ZGAL_1085		Putative membrane protein	2.3	4.0	3.6	3.2	4.9	4.5	2.1	3.8	3.4
ZGAL_1086		Conserved hypothetical protein	2.3	4.2	4.0	3.2	5.1	4.9	1.8	3.8	3.5
ZGAL_1089		Two-component system - Sensor histidine kinase	3.0	2.4	2.0	2.9	2.3	1.9	1.7	1.1	0.8
ZGAL_1091		AraC-type transcriptional regulator	4.7	2.6	-1.5	4.1	2.0	-2.1	2.2	0.1	-4.0
ZGAL_1092		Conserved hypothetical protein	3.4	2.7	0.5	2.9	2.2	0.0	0.9	0.3	-2.0
ZGAL_1094	dpsA2	dpsA2 DNA protection during starvation protein	3.4	3.4	1.6	2.9	2.9	1.1	0.4	0.3	-1.4
ZGAL_1097		Bacterial surface antigen	0.4	2.2	2.1	0.8	2.7	2.5	-0.7	1.1	1.0
ZGAL_1098		Conserved hypothetical periplasmic protein	1.0	2.0	2.4	1.5	2.4	2.8	0.4	1.4	1.8
ZGAL_1099		Alpha/beta hydrolase-fold protein	3.2	3.3	3.1	3.5	3.7	3.5	1.7	1.8	1.6
ZGAL_11		Conserved hypothetical membrane protein	-0.9	0.9	1.9	-0.3	1.5	2.5	0.0	1.8	2.7
ZGAL_1100		Putative protein	2.8	2.2	1.8	2.5	1.9	1.6	0.4	-0.2	-0.6
ZGAL_1101		Peroxiredoxin	4.1	2.5	2.1	3.0	1.4	1.0	0.8	-0.7	-1.2
ZGAL_1102	gdhA	gdhA Glucose 1-dehydrogenase	3.4	2.8	2.1	3.0	2.4	1.7	0.5	0.0	-0.7
ZGAL_1103		Short-chain dehydrogenase/reductase SDR	3.6	2.6	2.5	3.8	2.8	2.6	1.2	0.2	0.0
ZGAL_1104		Hypothetical protein	3.4	2.5	2.9	1.3	0.4	0.8	-0.1	-0.9	-0.5
ZGAL_1105		Conserved hypothetical protein	2.6	2.5	2.7	2.3	2.1	2.4	0.4	0.2	0.5
ZGAL_1106		Exopolysaccharide production protein	-1.0	0.5	1.1	-0.5	1.0	1.5	0.0	1.5	2.0
ZGAL_1107		Putative protein	-0.9	0.7	1.8	-0.5	1.1	2.2	0.4	2.0	3.1
ZGAL_1108	etkA	etkA Tyrosine-protein kinase	-2.1	0.1	1.3	-2.1	0.1	1.3	-1.3	0.9	2.1
ZGAL_1109		O-antigen transporter	-2.3	0.7	0.9	-1.5	1.4	1.6	-1.9	1.1	1.2
ZGAL_1115		Coenzyme A ligase	-0.8	1.2	0.0	0.0	2.0	0.8	-1.2	0.8	-0.4
ZGAL_1118	wcaF	wcaF Colanic acid biosynthesis acetyltransferase	-0.8	-0.4	0.7	-0.2	0.2	1.3	0.0	0.4	1.5
ZGAL_1119		Glycosyltransferase, family GT4	-1.6	0.1	1.3	-1.1	0.5	1.8	-0.1	1.6	2.8
ZGAL_112		Serine peptidase, family S9	2.2	0.1	-1.3	0.9	-1.2	-2.6	-0.5	-2.6	-4.0
ZGAL_1120		Mannosyltransferase, family GT4	-1.5	0.5	1.4	-0.6	1.4	2.4	0.5	2.4	3.4
ZGAL_1122		Conserved hypothetical periplasmic protein	-0.1	-1.8	-0.9	-0.1	-1.8	-0.9	2.1	0.5	1.4
ZGAL_1123		Hypothetical protein	1.1	-2.3	-2.1	0.9	-2.5	-2.3	3.0	-0.3	-0.2
ZGAL_1124		Conserved hypothetical periplasmic protein	0.6	3.5	2.4	2.5	5.3	4.2	4.8	7.7	6.6
ZGAL_1126	mutB	mutB Methylmalonyl-CoA mutase large subunit	0.5	1.0	-0.4	0.9	1.3	0.0	1.0	1.4	0.1
ZGAL_1127		Two-component system - Sensor histidine kinase	0.1	1.9	-2.0	0.8	2.5	-1.3	1.5	3.2	-0.6
ZGAL_1128		Two-component system - Response regulator	-1.7	2.7	0.0	-0.2	4.2	1.5	0.1	4.5	1.8
ZGAL_1130		Hypothetical protein	-1.6	-0.2	1.8	-0.2	1.3	3.3	0.3	1.8	3.8
ZGAL_1132		Conserved hypothetical protein	3.0	-0.2	0.4	3.9	0.7	1.3	3.1	-0.1	0.5
ZGAL_1133		Conserved cytochrome c -containing protein	2.1	-0.6	-0.5	2.8	0.1	0.2	1.9	-0.8	-0.7
ZGAL_114	sodC	sodC Superoxide dismutase [Cu-Zn]	2.7	2.6	3.6	0.9	0.8	1.8	-1.1	-1.3	-0.2

ZGAL_1143		Membrane fusion protein	1.1	-2.0	-0.7	1.0	-2.1	-0.9	1.4	-1.7	-0.5
ZGAL_1144		Receptor-like protein kinase	0.2	2.9	0.0	1.1	3.8	0.9	2.9	5.6	2.8
ZGAL_1146		Conserved hypothetical membrane protein	-0.4	0.3	1.3	-0.5	0.2	1.3	-0.1	0.6	1.7
ZGAL_1148	gldN	gldN T9SS periplasmic channel component	-1.1	1.1	0.5	-0.5	1.6	1.0	0.4	2.6	2.0
ZGAL_1149	gldM	gldM T9SS motor protein	-1.9	0.1	1.0	-1.4	0.6	1.5	0.3	2.3	3.1
ZGAL_115		Bacterial surface antigen	4.1	2.9	2.0	4.4	3.3	2.4	2.4	1.3	0.4
ZGAL_1150	gldL	gldL T9SS motor protein	-0.9	0.2	1.0	-0.7	0.4	1.2	1.4	2.5	3.2
ZGAL_1151	gldK	gldK T9SS periplasmic channel component	-0.7	0.9	1.7	-0.1	1.5	2.3	1.6	3.1	4.0
ZGAL_1157		Sigma-54-dependent transcriptional regulator	0.7	-0.4	1.8	0.3	-0.8	1.4	0.4	-0.7	1.5
ZGAL_116		Conserved hypothetical membrane protein	1.2	0.7	-1.2	0.7	0.2	-1.7	1.6	1.1	-0.8
ZGAL_1160	secG	secG Protein-export membrane protein secG	0.2	-0.1	2.7	1.1	0.8	3.6	0.7	0.3	3.1
ZGAL_1161	groS	groS 10 kDa chaperonin	-1.5	-1.9	4.2	0.2	-0.2	5.9	1.1	0.7	6.9
ZGAL_1162	groL	groL 60 kDa chaperonin	-1.3	-2.1	2.8	-1.6	-2.4	2.5	-0.3	-1.0	3.9
ZGAL_1166	actP	actP Copper-transporting P-type ATPase	-0.3	1.4	3.1	-0.1	1.5	3.3	-0.9	0.7	2.5
ZGAL_1168		Conserved hypothetical periplasmic protein	-1.8	0.6	1.4	-0.7	1.7	2.5	-0.2	2.1	3.0
ZGAL_1169		Hypothetical lipoprotein	-0.8	1.8	2.4	-0.5	2.2	2.8	1.9	4.6	5.2
ZGAL_1171	purH	purH Bifunctional purine biosynthesis protein PurH	-0.9	-0.4	2.2	-1.1	-0.6	2.1	-0.2	0.2	2.9
ZGAL_1172	mreB	mreB Rod shape-determining protein MreB	-0.4	0.8	1.3	0.4	1.6	2.2	1.3	2.5	3.0
ZGAL_1173	mreC	mreC Rod shape-determining protein MreC	-0.5	0.7	0.9	-0.2	1.0	1.2	1.0	2.2	2.3
ZGAL_1174	mreD	mreD Possible rod shape-determining protein MreD	-2.2	0.2	0.1	-1.0	1.4	1.3	0.2	2.5	2.5
ZGAL_1175	mrdA	mrdA Penicillin-binding protein 2, Family transpeptidase	-0.5	0.8	0.5	-0.3	1.0	0.8	0.6	1.9	1.6
ZGAL_1176	mrdB	mrdB Rod shape-determining protein RodA	-0.2	0.6	-0.6	-0.1	0.7	-0.5	0.7	1.5	0.3
ZGAL_1178	msrB2	msrB2 Peptide methionine sulfoxide reductase msrB	2.8	0.6	-2.1	0.9	-1.3	-3.9	0.3	-1.8	-4.5
ZGAL_1179	msrA1	msrA1 Peptide methionine sulfoxide reductase msrA	2.3	0.0	-2.6	0.6	-1.6	-4.2	0.1	-2.1	-4.7
ZGAL_1180		Conserved hypothetical membrane protein	2.9	0.0	-1.9	5.9	3.0	1.1	3.0	0.1	-1.8
ZGAL_1181	msrA2	msrA2 Peptide methionine sulfoxide reductase msrA	2.8	0.8	-1.1	2.5	0.5	-1.5	2.9	0.9	-1.0
ZGAL_1182	alyA1	alyA1 Endo-guluronate lyase AlyA1, family PL7_3	4.1	1.9	-0.5	4.9	2.7	0.3	7.1	4.9	2.5
ZGAL_1185		Conserved hypothetical membrane protein	-1.7	0.6	0.8	-1.1	1.2	1.4	-0.8	1.5	1.8
ZGAL_1186	lpxB	lpxB Lipid-A-disaccharide synthase, family GT19	-0.3	0.4	1.6	0.5	1.2	2.4	1.3	2.0	3.2
ZGAL_1187	spr	spr Peptidase spr, family C40	0.1	1.1	0.3	0.8	1.8	1.0	0.9	1.9	1.0
ZGAL_1189	dtpT	dtpT Di-/tripeptide transporter	1.4	0.2	1.4	1.4	0.1	1.3	1.0	-0.3	0.9
ZGAL_1190	dppA1	dppA1 Dipeptidyl-peptidase IV, family S9	1.6	-0.3	1.2	0.8	-1.0	0.4	0.5	-1.4	0.1
ZGAL_1193		Peptidyl-prolyl isomerase family protein	-0.5	-0.4	0.9	-0.8	-0.7	0.6	-0.1	0.0	1.3
ZGAL_12	trmD	trmD tRNA (guanine-N1-)-methyltransferase	-2.0	0.0	0.6	-1.4	0.6	1.2	-0.5	1.5	2.1
ZGAL_120		Two-component system - Sensor histidine kinase	0.8	0.7	-1.6	0.8	0.7	-1.7	1.6	1.5	-0.9
ZGAL_1205		Conserved hypothetical lipoprotein	2.6	0.3	-3.2	0.8	-1.5	-5.0	0.8	-1.6	-5.0
ZGAL_1206		Glycosyltransferase, family GT2	1.5	-0.2	-2.2	0.8	-1.0	-2.9	0.5	-1.2	-3.2
ZGAL_1208		AraC-type transcriptional regulator	2.3	1.5	-1.3	1.2	0.4	-2.4	0.6	-0.1	-3.0
ZGAL_1213		Conserved hypothetical membrane protein	2.3	1.2	-1.7	0.7	-0.3	-3.3	0.1	-0.9	-3.9
ZGAL_1215		Conserved hypothetical periplasmic protein	1.5	0.7	-0.7	1.4	0.7	-0.7	0.9	0.2	-1.2
ZGAL_1219		Conserved hypothetical periplasmic protein	3.3	1.0	-0.4	2.6	0.3	-1.1	1.8	-0.5	-1.9
ZGAL_1220		FAD-dependent pyridine nucleotide-disulfide oxidoreductase	2.1	0.0	-1.6	0.9	-1.2	-2.8	0.3	-1.8	-3.4
ZGAL_1222		Conserved hypothetical protein	4.6	1.1	-2.7	2.8	-0.6	-4.4	1.6	-1.9	-5.7
ZGAL_1223	rhaB	rhaB Alpha-L-rhamnosidase, family GH78	2.4	0.2	-3.3	0.5	-1.6	-5.1	0.4	-1.8	-5.3
ZGAL_1224		Glycosyltransferase, family GT2	1.3	0.7	-1.6	1.7	1.1	-1.2	3.0	2.5	0.2
ZGAL_1225		Glycosyltransferase, family GT2	-0.4	0.6	-1.6	0.3	1.2	-0.9	1.6	2.5	0.4
ZGAL_1227	argA	argA Possible Amino-acid N-acetyltransferase (N-acetylglutamate synthase)	0.8	0.2	1.7	0.5	-0.1	1.4	0.9	0.3	1.8
ZGAL_1229	argC	argC N-acetyl-gamma-glutamyl-phosphate reductase	-1.7	-1.3	1.6	-1.7	-1.3	1.6	-1.8	-1.4	1.5
ZGAL_1231	argD1	argD1 Acetylornithine aminotransferase	-2.7	-0.4	2.0	-2.4	-0.1	2.3	-2.6	-0.3	2.1
ZGAL_1233	proB2	proB2 Glutamate 5-kinase (Gamma-glutamyl kinase)	-1.0	0.4	1.6	-0.8	0.6	1.8	-0.8	0.6	1.7
ZGAL_1239	rluB	rluB Ribosomal large subunit pseudouridine synthase B	-1.1	0.1	0.9	-1.1	0.2	1.0	-0.5	0.7	1.5
ZGAL_1241		Prenyltransferase family protein	0.5	0.6	-1.5	1.0	1.0	-1.1	1.4	1.4	-0.7
ZGAL_1246		Flavoprotein	0.5	2.0	1.1	0.3	1.8	1.0	-0.1	1.3	0.5
ZGAL_1247	glpQ	glpQ Glycerophosphoryl diester phosphodiesterase	1.2	2.3	1.8	0.3	1.5	1.0	-0.1	1.0	0.5
ZGAL_1248		Glycoside hydrolase, family GH13_38	0.0	1.4	1.7	-0.3	1.1	1.4	-1.2	0.2	0.5
ZGAL_1250	pgmB	pgmB Beta-phosphoglucomutase	0.5	0.9	0.7	0.2	0.6	0.4	-0.1	0.3	0.1
ZGAL_1253		SusD-like lipoprotein	-0.7	2.0	-0.6	-1.1	1.7	-1.0	-0.2	2.6	-0.1
ZGAL_1259		Similar to ASPIC and UnbV protein containing FG-GAP repeats	-0.1	0.4	0.5	0.7	1.2	1.3	1.7	2.1	2.2
ZGAL_127		Non-heme haloperoxidase	1.7	1.1	-1.3	0.8	0.3	-2.1	0.3	-0.3	-2.7
ZGAL_1282		Conserved hypothetical periplasmic protein	2.3	-0.5	-0.6	2.0	-0.8	-0.9	1.5	-1.2	-1.3
ZGAL_1286	fdxA1	fdxA1 2Fe-2S ferredoxin	-1.1	-0.1	-1.6	-1.0	0.0	-1.6	0.7	1.7	0.2
ZGAL_1287		Conserved hypothetical protein	-2.3	0.0	-1.9	-0.8	1.6	-0.4	0.7	3.0	1.1
ZGAL_1288	yumC2	yumC2 Ferredoxin-NADP reductase	-2.4	0.4	-1.8	-1.9	0.9	-1.3	-0.4	2.4	0.2
ZGAL_1289		NifU family protein	0.8	1.7	-1.1	1.0	1.9	-0.9	0.7	1.6	-1.2
ZGAL_1290	mrpA	mrpA Protein mrp	1.9	2.0	-0.5	1.6	1.7	-0.7	0.3	0.5	-2.0
ZGAL_1299		Conserved hypothetical periplasmic protein	0.8	1.6	0.1	0.5	1.3	-0.2	1.7	2.5	1.0
ZGAL_13	rplS	rplS Ribosomal protein L19	-0.2	-0.2	4.1	0.9	0.8	5.2	1.9	1.9	6.3
ZGAL_130	dpsA1	dpsA1 DNA protection during starvation protein	1.8	2.8	-0.8	1.8	2.7	-0.9	1.3	2.2	-1.4
ZGAL_1300	fkpB	fkpB FKBP-type peptidyl-prolyl cis-trans isomerase 2	-1.1	0.8	3.0	-0.4	1.4	3.6	-0.6	1.3	3.5
ZGAL_1301		Hypothetical protein	-0.9	-0.1	0.1	-0.7	0.1	0.3	0.2	1.0	1.2
ZGAL_1302		Conserved hypothetical protein	-0.5	0.1	0.0	0.1	0.7	0.6	2.1	2.7	2.6
ZGAL_1303	tyrS	tyrS Tyrosyl-tRNA synthetase	-1.7	-0.8	0.8	-1.5	-0.6	1.1	-1.0	-0.1	1.5

ZGAL_1307		Undecaprenyl-phosphate mannosyltransferas,family GT2	1.8	-0.6	0.1	0.6	-1.8	-1.1	-0.1	-2.5	-1.8
ZGAL_1308		Glycosyltransferase, family GTnc	0.2	0.1	1.3	-0.1	-0.1	1.0	1.1	1.0	2.1
ZGAL_1309		Conserved hypothetical membrane protein	-1.4	0.4	1.5	-0.5	1.2	2.4	1.1	2.9	4.1
ZGAL_131		LysR-type transcriptional regulator	0.3	-0.3	-1.5	0.7	0.1	-1.1	1.1	0.5	-0.7
ZGAL_1310	hemD	hemD Uroporphyrinogen-III synthase	-0.6	-0.5	0.1	-0.2	-0.1	0.4	0.8	0.9	1.5
ZGAL_1312		Conserved hypothetical membrane protein	2.3	0.7	-0.6	3.4	1.9	0.5	2.2	0.6	-0.8
ZGAL_1313	lys9	lys9 Saccharopine dehydrogenase	2.2	-0.5	-0.2	1.9	-0.8	-0.4	1.9	-0.8	-0.5
ZGAL_132		Conserved hypothetical protein	1.1	1.6	2.8	1.6	2.1	3.3	1.2	1.8	3.0
ZGAL_1320	ftsX	ftsX Cell division protein, permease component	-1.4	0.6	1.3	-0.7	1.3	2.0	-0.4	1.5	2.2
ZGAL_1324		Conserved hypothetical periplasmic protein	0.0	-1.1	-1.5	1.0	-0.1	-0.5	2.4	1.3	0.9
ZGAL_1330		Conserved hypothetical protein	-1.0	-0.1	1.8	-0.9	0.1	2.0	-0.5	0.5	2.4
ZGAL_1334		Hypothetical membrane protein	-0.8	0.3	-0.2	0.0	1.2	0.7	0.7	1.8	1.4
ZGAL_1338		Conserved hypothetical protein	0.5	0.9	1.2	0.5	0.9	1.2	-0.3	0.0	0.3
ZGAL_1343		Sigma-54 dependent two-component system	1.3	-0.6	-1.1	0.9	-0.9	-1.4	1.3	-0.6	-1.1
ZGAL_1344		Conserved hypothetical periplasmic protein	0.4	-3.3	2.7	-0.9	-4.6	1.4	-2.7	-6.4	-0.4
ZGAL_1345		Conserved hypothetical periplasmic protein	0.3	-2.7	3.3	0.5	-2.6	3.4	-1.5	-4.5	1.5
ZGAL_1346		Conserved hypothetical periplasmic protein	3.4	-1.1	4.9	4.7	0.2	6.1	2.7	-1.8	4.1
ZGAL_1347		Conserved hypothetical periplasmic protein	-0.2	-0.8	5.3	0.5	-0.1	5.9	-1.0	-1.6	4.5
ZGAL_1354	phyC	phyC 3-Phytase	-1.4	0.5	0.6	-1.0	0.9	1.0	-0.3	1.6	1.7
ZGAL_1356		TPR repeats protein	1.0	-0.9	-1.6	0.9	-1.0	-1.7	2.0	0.2	-0.5
ZGAL_1357		Putative protein	-0.1	0.0	0.1	0.7	0.8	0.9	1.8	1.9	2.0
ZGAL_1358	rpmA	rpmA Ribosomal protein L27	-0.2	-0.5	1.3	0.7	0.4	2.2	2.1	1.7	3.5
ZGAL_1359	rplU	rplU Ribosomal protein L21	-0.4	-0.7	1.8	0.4	0.1	2.6	0.8	0.5	3.0
ZGAL_1360		Conserved hypothetical membrane protein	2.7	1.0	-0.8	3.6	1.9	0.1	2.4	0.7	-1.1
ZGAL_1361		Metallopeptidase, family M16	-0.8	1.2	-0.2	-0.4	1.6	0.2	-1.0	0.9	-0.5
ZGAL_1362		Family M16 non-peptidase protein	-0.3	1.7	0.2	-0.7	1.3	-0.2	-1.1	0.9	-0.6
ZGAL_1364		Cytochrome c-containing protein	2.8	-1.6	-3.3	1.0	-3.3	-5.0	0.6	-3.7	-5.4
ZGAL_1365	irpA2	irpA2 Iron-regulated protein A	2.5	-1.7	-2.8	0.4	-3.9	-4.9	-0.8	-5.0	-6.1
ZGAL_1368		Conserved hypothetical periplasmic protein	-1.1	0.7	-0.1	0.3	2.1	1.2	-0.3	1.6	0.7
ZGAL_1369	gldD	gldD Gliding motility membrane lipoprotein	0.0	0.3	-1.0	0.5	0.8	-0.5	1.7	2.0	0.7
ZGAL_1370	gldE	gldE Gliding motility membrane protein	0.1	-0.4	-2.3	0.1	-0.4	-2.3	1.9	1.4	-0.6
ZGAL_1374	hupA	hupA DNA-binding protein HU	0.7	0.0	3.0	1.6	0.9	3.8	2.2	1.5	4.5
ZGAL_1375	rngA	rngA Ribonuclease G	0.0	0.8	0.5	0.2	1.0	0.7	1.0	1.8	1.5
ZGAL_1377		Conserved hypothetical periplasmic protein	-1.4	-0.5	1.0	-1.4	-0.5	0.9	-0.7	0.3	1.7
ZGAL_1380		Band 7 family protein	0.2	1.3	0.6	0.6	1.8	1.1	1.8	2.9	2.2
ZGAL_1381		Conserved hypothetical membrane protein	0.1	0.4	-1.5	0.1	0.4	-1.5	1.4	1.7	-0.2
ZGAL_1390		Putative membrane protein	0.3	2.2	0.2	2.0	3.9	1.8	3.9	5.8	3.7
ZGAL_1391		Putative protein	-0.5	0.6	-1.4	2.0	3.0	1.1	2.6	3.6	1.7
ZGAL_1392		Hypothetical membrane protein	-1.7	0.8	0.3	0.3	2.8	2.3	1.3	3.8	3.3
ZGAL_1393		Hypothetical lipoprotein	-1.0	1.1	0.0	1.2	3.3	2.2	2.6	4.6	3.6
ZGAL_1394		Putative membrane protein	-1.1	0.5	-0.7	0.9	2.5	1.3	2.1	3.7	2.5
ZGAL_1398		Conserved hypothetical protein	-0.4	0.2	-1.0	0.3	0.9	-0.3	2.4	2.9	1.7
ZGAL_1399		Hypothetical protein	-1.4	0.1	-0.2	0.4	1.8	1.6	1.7	3.1	2.9
ZGAL_1400		Hypothetical protein	-0.4	1.7	1.4	-0.7	1.4	1.0	1.0	3.1	2.8
ZGAL_1401		Conserved hypothetical periplasmic protein	-0.9	0.1	-1.3	-0.6	0.4	-0.9	0.2	1.3	-0.1
ZGAL_1402		Fibronectin type-III repeats protein	-0.6	0.3	-0.7	-0.2	0.6	-0.4	0.5	1.4	0.4
ZGAL_1403		Conserved hypothetical membrane protein	-0.6	0.3	-0.3	-0.2	0.7	0.0	0.7	1.6	0.9
ZGAL_1404	atpC1	atpC1 ATP synthase, F1 sector epsilon subunit	-2.5	-1.0	2.9	-2.5	-1.0	2.8	-0.9	0.6	4.5
ZGAL_1405	atpD1	atpD1 ATP synthase, F1 sector beta subunit	-1.2	-1.4	2.1	-1.3	-1.5	2.0	0.2	0.0	3.5
ZGAL_1406		Conserved hypothetical protein	2.0	1.4	2.7	2.2	1.6	2.9	2.2	1.6	2.8
ZGAL_1407		TonB-dependent Receptor	1.3	0.9	1.2	0.8	0.5	0.8	0.7	0.3	0.6
ZGAL_1412	panD	panD Aspartate 1-decarboxylase	1.2	-0.6	-0.4	1.8	0.0	0.2	1.5	-0.3	-0.1
ZGAL_1413		Conserved hypothetical membrane protein	1.2	-0.5	-0.4	2.1	0.5	0.5	1.6	0.0	0.0
ZGAL_1414		Esterase	-0.8	1.3	0.1	0.3	2.4	1.1	2.2	4.3	3.0
ZGAL_1421		Conserved hypothetical membrane protein	-0.7	1.9	-0.9	1.2	3.9	1.0	1.9	4.6	1.8
ZGAL_1425	nudF	nudF ADP-ribose pyrophosphatase	2.4	1.9	-3.0	2.5	2.0	-3.0	1.9	1.4	-3.5
ZGAL_1426		Ankyrin repeats protein	2.6	1.4	-4.5	1.2	0.0	-5.9	0.8	-0.4	-6.3
ZGAL_1427	katA1	katA1 Catalase	7.5	4.6	-2.2	6.7	3.8	-3.0	4.8	1.9	-4.9
ZGAL_143		Putative membrane lipoprotein	1.7	0.5	-0.6	0.9	-0.3	-1.3	1.1	-0.1	-1.1
ZGAL_1430		Two-component system - Response regulator, receiver domain	1.2	1.7	-0.6	1.1	1.6	-0.7	1.2	1.7	-0.5
ZGAL_1431		Putative membrane lipoprotein	2.4	0.2	-3.3	2.2	0.0	-3.5	2.2	0.0	-3.5
ZGAL_1432		TonB-dependent Receptor	2.3	1.0	-3.1	3.0	1.8	-2.3	2.4	1.2	-2.9
ZGAL_1433		Endonuclease/exonuclease/phosphatase family	-0.2	0.8	-1.2	0.5	1.5	-0.5	2.2	3.3	1.2
ZGAL_1434		Conserved hypothetical periplasmic protein	-1.4	2.0	0.7	-0.6	2.8	1.5	1.9	5.3	4.0
ZGAL_1439		Metallopeptidase, family M23	0.9	-0.6	-0.2	0.8	-0.7	-0.3	1.5	0.0	0.4
ZGAL_1444	uvrC	uvrC Excinuclease ABC, subunit C	0.8	0.1	-0.3	0.2	-0.5	-0.9	-0.7	-1.4	-1.8
ZGAL_1449	ileS	ileS Isoleucyl-tRNA synthetase	2.6	1.3	3.8	2.9	1.6	4.1	3.4	2.1	4.6
ZGAL_1450		Conserved hypothetical periplasmic protein	-2.1	-1.5	-0.7	-1.0	-0.4	0.4	1.1	1.7	2.4
ZGAL_1451		TonB-dependent Receptor	2.0	-0.7	-0.5	2.8	0.1	0.3	2.0	-0.7	-0.5
ZGAL_1456		Conserved hypothetical protein	-0.8	-0.7	1.5	-0.8	-0.7	1.5	-1.0	-0.9	1.3
ZGAL_1459		Conserved hypothetical protein	-1.4	-1.1	1.2	-1.7	-1.4	0.9	-2.0	-1.7	0.6
ZGAL_146		SusD-like lipoprotein	-1.0	0.7	-0.7	-1.2	0.4	-0.9	0.1	1.7	0.4
ZGAL_1463		Cytochrome c	-1.2	-0.6	2.0	-1.5	-0.9	1.7	-1.6	-1.0	1.6

ZGAL_1466		Conserved hypothetical lipoprotein	0.8	-2.2	-1.3	2.2	-0.9	0.1	2.5	-0.5	0.4
ZGAL_147		SusC-like TonB-dependent transporter	-2.3	1.1	-1.3	-2.2	1.1	-1.3	-1.5	1.9	-0.5
ZGAL_1474		Hypothetical membrane protein	-1.1	1.3	1.8	0.9	3.3	3.7	3.3	5.7	6.1
ZGAL_1475		Conserved hypothetical lipoprotein	0.2	-1.0	0.4	0.7	-0.4	1.0	1.0	-0.1	1.3
ZGAL_1476		SCP-like extracellular protein	1.8	2.9	1.2	1.4	2.5	0.8	1.6	2.8	1.1
ZGAL_1480		Aldehyde dehydrogenase	2.2	-0.9	-1.5	1.4	-1.6	-2.3	0.9	-2.2	-2.8
ZGAL_1481		Hypothetical protein	4.3	0.6	-0.4	6.1	2.3	1.3	3.6	-0.2	-1.2
ZGAL_1482		OmpA-like membrane protein	0.5	0.3	-1.5	1.4	1.2	-0.7	2.0	1.9	0.0
ZGAL_1483		Conserved hypothetical membrane protein	0.6	1.0	-0.4	2.2	2.6	1.2	2.8	3.2	1.7
ZGAL_1492		Conserved hypothetical protein	1.8	1.0	0.4	1.5	0.7	0.1	0.4	-0.4	-1.0
ZGAL_1493		NADP-dependent L-serine/L-allo-threonine dehydrogenase	1.9	0.3	0.0	1.3	-0.3	-0.7	-0.1	-1.7	-2.0
ZGAL_1495		MoxR-like ATPase	2.3	-0.1	-1.0	1.6	-0.8	-1.6	0.5	-1.9	-2.7
ZGAL_1496		vWA domain protein	1.1	0.2	-0.6	1.0	0.1	-0.7	-0.1	-1.0	-1.7
ZGAL_1497		Conserved hypothetical membrane protein	1.6	0.4	-0.2	1.0	-0.2	-0.7	0.3	-0.9	-1.4
ZGAL_1498	batA	batA Aerotolerance protein BatA	0.1	0.9	1.2	0.6	1.3	1.6	-0.7	0.0	0.4
ZGAL_15	icdA	icdA Isocitrate dehydrogenase NADP-dependent	-0.8	-0.2	0.4	-0.5	0.1	0.7	0.0	0.6	1.2
ZGAL_150		Conserved hypothetical membrane protein	2.0	1.3	-1.9	0.9	0.3	-2.9	1.0	0.4	-2.8
ZGAL_1502	batE	batE Aerotolerance protein BatE	0.4	0.4	1.3	0.6	0.6	1.4	0.2	0.2	1.0
ZGAL_1503		Conserved hypothetical membrane protein	-0.5	0.2	1.9	0.7	1.3	3.0	0.3	0.9	2.6
ZGAL_1504		Hypothetical membrane protein	1.8	-0.4	0.5	1.7	-0.5	0.4	1.1	-1.2	-0.3
ZGAL_1509		Conserved hypothetical protein	-1.4	0.1	1.1	-1.3	0.2	1.2	-0.6	0.9	1.9
ZGAL_151	trxB	trxB Thioredoxin reductase	0.6	0.5	-0.3	0.8	0.6	-0.2	2.1	1.9	1.2
ZGAL_1510		Conserved hypothetical protein	0.6	1.2	3.6	0.6	1.2	3.6	1.3	2.0	4.4
ZGAL_1511		Membrane fusion protein	1.5	0.6	1.8	0.4	-0.4	0.8	0.2	-0.6	0.5
ZGAL_1512		Multidrug efflux transporter	2.3	0.8	2.4	0.6	-0.9	0.7	0.0	-1.5	0.0
ZGAL_1513		Outer membrane efflux protein	2.2	0.9	2.1	0.6	-0.7	0.5	-1.0	-2.3	-1.1
ZGAL_152		Universal stress protein	-3.4	-0.2	-0.4	-2.4	0.7	0.5	-0.7	2.4	2.2
ZGAL_1521		ABC transporter, ATPase component	-0.4	0.2	1.3	-0.6	0.0	1.2	-0.9	-0.2	0.9
ZGAL_1523	asdA	asdA Aspartate-semialdehyde dehydrogenase	-2.6	-0.4	2.1	-2.6	-0.4	2.1	-3.2	-1.1	1.4
ZGAL_1538	ptsA	ptsA 6-Pyruvoyl tetrahydrobiopterin synthase	0.2	0.8	1.9	0.4	1.0	2.1	0.4	1.1	2.2
ZGAL_154	galK	galK Galactokinase	-1.7	-0.1	1.1	-2.1	-0.5	0.7	-1.5	0.1	1.3
ZGAL_1549		Two-component system - Sensor histidine kinase	0.9	0.7	0.3	0.8	0.6	0.2	0.2	-0.1	-0.5
ZGAL_1553		Nucleobase cation symporter	-1.2	-0.2	0.4	-0.2	0.8	1.4	0.6	1.6	2.2
ZGAL_1575		TRAP transporter, small permease subunit	-1.8	0.1	1.9	-1.3	0.6	2.4	-0.9	1.0	2.8
ZGAL_158		SusC-like TonB-dependent transporter	1.9	0.4	-1.7	2.7	1.2	-0.9	1.9	0.4	-1.7
ZGAL_1584		Putative protein	-1.7	0.4	0.2	0.6	2.7	2.5	-0.4	1.7	1.5
ZGAL_1590	acpP1	acpP1 Acyl carrier protein	0.3	0.7	1.8	0.7	1.1	2.3	1.8	2.1	3.3
ZGAL_1597		Putative protein	5.4	6.3	4.2	-0.9	0.1	-2.0	-0.5	0.5	-1.6
ZGAL_1598		Carboxymuconolactone decarboxylase family protein	4.1	3.6	2.7	0.7	0.2	-0.7	-0.1	-0.6	-1.4
ZGAL_1599		Conserved hypothetical periplasmic protein	5.7	4.0	3.2	1.8	0.1	-0.7	1.3	-0.4	-1.2
ZGAL_16		TonB-dependent Receptor	1.3	0.0	0.8	0.9	-0.5	0.3	0.1	-1.3	-0.5
ZGAL_160		Similar to ASPIC and UnbV protein containing FG-GAP repeats	1.4	0.3	-0.6	1.3	0.2	-0.7	1.0	-0.1	-1.0
ZGAL_1601		Putative small multi-drug export protein	1.2	-1.0	1.1	2.5	0.3	2.4	1.5	-0.7	1.3
ZGAL_1605		Hypothetical lipoprotein	-2.5	0.6	0.1	-1.4	1.7	1.2	0.6	3.6	3.1
ZGAL_1610	rpmF	rpmF Ribosomal protein L32	-0.1	-0.2	2.9	1.5	1.3	4.5	2.3	2.1	5.3
ZGAL_1611		Conserved hypothetical protein	1.1	-0.6	1.8	2.0	0.2	2.7	2.6	0.9	3.3
ZGAL_1614		Conserved hypothetical periplasmic protein	-1.5	0.7	0.2	-0.5	1.7	1.2	1.6	3.8	3.2
ZGAL_1615		Hypothetical lipoprotein	0.3	2.5	0.6	0.0	2.1	0.3	1.4	3.5	1.7
ZGAL_1619		Conserved hypothetical lipoprotein	1.3	0.2	-0.8	1.2	0.1	-0.8	1.8	0.7	-0.3
ZGAL_163	xylP	xylP Putative xylose-proton symporter	1.2	0.4	-0.6	1.6	0.9	-0.2	1.1	0.4	-0.7
ZGAL_164	xynA1	xynA1 Endo-beta-1,4-xylanase, family GH10	1.6	-0.2	-2.3	1.6	-0.2	-2.3	1.5	-0.4	-2.5
ZGAL_1640	sirC	sirC Precorrin-2 dehydrogenase	2.4	1.3	-0.2	1.7	0.6	-0.9	0.2	-0.9	-2.5
ZGAL_1641		Conserved hypothetical membrane protein	3.9	2.2	1.0	4.2	2.6	1.4	1.9	0.2	-1.0
ZGAL_1642		Flavoprotein, bacterial luciferase family	3.2	0.2	-0.7	1.8	-1.2	-2.1	1.1	-1.9	-2.7
ZGAL_1643		LacI-type transcriptional regulator	1.3	1.2	-0.9	2.0	1.9	-0.2	2.3	2.2	0.1
ZGAL_1644		Putative protein	-1.3	0.7	0.0	0.0	1.9	1.2	2.0	4.0	3.3
ZGAL_1645		Conserved hypothetical protein	-2.0	1.2	-0.1	-0.9	2.3	1.0	1.3	4.5	3.2
ZGAL_1646		Putative protein	-1.3	2.1	2.1	1.1	4.5	4.5	2.6	6.0	5.9
ZGAL_1647		Hypothetical periplasmic protein	-1.6	2.1	2.5	0.4	4.2	4.6	2.2	5.9	6.3
ZGAL_1650		ArsR-type transcriptional regulator	-1.1	0.3	2.4	-1.1	0.3	2.4	-1.2	0.1	2.2
ZGAL_1653		Hypothetical protein	-2.4	0.6	1.6	-1.8	1.3	2.3	-1.8	1.2	2.3
ZGAL_1654	hsdR2	HsdR2 Type I restriction enzyme ZgaDII, R subunit	-0.5	1.3	1.5	-1.0	0.8	0.9	-1.5	0.3	0.4
ZGAL_1660		Conserved hypothetical protein	-1.4	0.5	0.9	-0.8	1.1	1.5	-0.4	1.5	1.9
ZGAL_1668		Conserved hypothetical membrane protein	-1.3	1.7	1.0	-0.2	2.8	2.0	0.3	3.3	2.5
ZGAL_1669		TonB-dependent Receptor	-1.1	2.2	-0.8	-0.4	2.9	-0.1	-0.1	3.1	0.2
ZGAL_167		CAAX prenyl peptidase, family U48	-1.9	0.2	-1.7	-1.6	0.5	-1.4	-0.7	1.4	-0.6
ZGAL_1672		Conserved hypothetical protein	-2.1	1.1	0.7	-0.4	2.9	2.5	2.1	5.3	5.0
ZGAL_1673		Conserved hypothetical protein	-1.6	1.0	0.6	0.4	3.0	2.6	2.2	4.9	4.4
ZGAL_1675		Sodium/hydrogen exchanger	1.3	1.4	-0.4	2.6	2.7	0.9	2.1	2.2	0.4
ZGAL_1679		Aminopeptidase, family M1	0.4	-0.9	2.4	-0.6	-1.9	1.4	-1.4	-2.6	0.6
ZGAL_168		Conserved hypothetical protein	-2.9	1.7	1.6	-2.2	2.4	2.3	-1.3	3.3	3.2
ZGAL_1681		Carboxy-terminal processing peptidase, family S41	0.1	0.4	0.0	0.4	0.7	0.3	1.2	1.5	1.1

ZGAL_1682	fosB	fosB Metallothiol transferase FosB	-0.2	0.9	1.0	0.1	1.3	1.3	0.6	1.7	1.8
ZGAL_1688		Conserved hypothetical protein	0.1	1.6	0.9	0.3	1.8	1.1	1.0	2.6	1.9
ZGAL_1689		Hypothetical protein	-1.3	1.2	0.8	-0.5	1.9	1.5	0.1	2.5	2.2
ZGAL_1690		Conserved hypothetical protein	0.2	1.8	1.2	0.6	2.2	1.6	1.5	3.1	2.5
ZGAL_1691		Conserved hypothetical lipoprotein	-2.2	0.3	1.1	-0.9	1.6	2.4	-0.3	2.2	3.0
ZGAL_1695		Conserved hypothetical protein	2.1	0.1	-1.9	2.1	0.1	-1.9	1.6	-0.4	-2.4
ZGAL_17		Putative membrane lipoprotein	1.7	-0.8	-0.5	1.1	-1.4	-1.1	0.5	-1.9	-1.6
ZGAL_1703	folB	folB Dihydroneopterin aldolase	-1.4	0.5	2.2	-0.7	1.3	3.0	0.7	2.6	4.3
ZGAL_1704	sprF	sprF T9SS associated protein SprF	-1.1	2.8	1.4	0.4	4.3	2.9	2.2	6.1	4.7
ZGAL_1706		Conserved hypothetical protein	-0.7	2.5	1.3	0.7	3.9	2.7	2.0	5.2	3.9
ZGAL_1707		T9SS SprF family protein	-0.3	4.1	2.3	1.2	5.6	3.7	2.6	7.0	5.1
ZGAL_1708		Conserved hypothetical periplasmic protein	-1.0	3.7	2.7	0.3	5.0	4.0	1.5	6.2	5.2
ZGAL_1710		Conserved hypothetical membrane protein	3.2	2.3	0.8	1.1	0.1	-1.3	-0.4	-1.3	-2.8
ZGAL_1711		Conserved hypothetical membrane protein	2.6	2.2	0.7	1.4	1.0	-0.6	-0.3	-0.7	-2.2
ZGAL_1712		Conserved hypothetical protein	2.0	2.9	2.0	1.9	2.8	1.9	0.2	1.1	0.2
ZGAL_1713		Band 7 family protein	1.4	0.6	-1.0	0.8	0.0	-1.6	0.3	-0.5	-2.1
ZGAL_1717	mnmG	mnmG tRNA uridine 5-carboxymethylaminomethyl modification enzyme MnmG	-0.6	0.4	0.3	-0.5	0.4	0.3	0.3	1.2	1.1
ZGAL_1721		Outer membrane protein, OmpH family	-2.0	-0.2	0.9	-1.5	0.3	1.4	-1.3	0.6	1.7
ZGAL_1724	pgkA	pgkA Phosphoglycerate kinase	-1.0	-1.1	1.9	-1.6	-1.7	1.3	-2.0	-2.1	0.9
ZGAL_1727		T9SS-associated PG1058-like protein	-1.1	-1.2	-0.4	0.0	0.0	0.8	1.3	1.2	2.1
ZGAL_1728	tatA	tatA Sec-independent protein translocase TatA	-0.3	1.4	3.6	0.2	1.8	4.0	0.2	1.8	4.0
ZGAL_1730		Conserved hypothetical protein	0.2	0.3	2.1	-0.1	0.0	1.9	-0.8	-0.7	1.2
ZGAL_1736	rmlC	rmlC dTDP-4-dehydrorhamnose 3,5-epimerase	-0.6	1.4	0.0	-0.3	1.7	0.3	-0.5	1.4	0.0
ZGAL_1740	wbpB	wbpB UDP-N-acetyl-2-amino-2-deoxy-D-glucuronate oxidase	-1.6	0.4	1.2	-2.3	-0.2	0.5	-1.3	0.8	1.5
ZGAL_1742	wzxA	wzxA O-antigen translocase	-1.7	0.7	1.0	-0.9	1.6	1.8	0.8	3.3	3.5
ZGAL_1747	wbeiA	wbeiA O antigen biosynthesis protein WbeiA	-2.1	0.2	0.4	-1.0	1.3	1.5	-0.7	1.6	1.8
ZGAL_175		Conserved hypothetical membrane protein	1.8	0.3	-0.5	2.1	0.6	-0.3	2.4	1.0	0.1
ZGAL_1753		Conserved hypothetical membrane protein	-1.9	0.0	1.7	-1.3	0.6	2.3	-0.8	1.0	2.7
ZGAL_1757		TetR-type transcriptional regulator	0.1	2.4	-0.5	3.0	5.2	2.4	2.1	4.3	1.5
ZGAL_176		Conserved hypothetical periplasmic protein	2.2	-0.2	-0.4	3.2	0.9	0.7	2.6	0.3	0.1
ZGAL_1765		Ribonucleoside hydrolase	-1.4	0.1	-0.1	-0.7	0.8	0.6	0.2	1.8	1.5
ZGAL_1766		Patatin-like phospholipase	-0.4	0.7	0.3	0.1	1.2	0.8	0.3	1.4	0.9
ZGAL_177		Cytochrome c-containing protein	2.3	0.4	-0.9	2.9	1.0	-0.2	2.1	0.2	-1.1
ZGAL_1772		Putative protein	-0.6	1.6	2.1	-0.3	2.0	2.5	-0.3	2.0	2.5
ZGAL_1773	sprE	sprE Gliding motility membrane lipoprotein SprE	-0.6	1.2	1.5	0.2	1.9	2.3	1.5	3.2	3.6
ZGAL_1774		Conserved hypothetical protein	0.4	2.0	2.0	0.6	2.2	2.2	1.7	3.3	3.3
ZGAL_1775		Conserved hypothetical membrane protein	0.6	2.1	2.0	0.9	2.3	2.3	1.8	3.3	3.2
ZGAL_1776		Conserved hypothetical membrane protein	-1.9	0.2	0.1	-0.4	1.7	1.6	0.4	2.5	2.3
ZGAL_1777	atpB1	atpB1 ATP synthase, F0 sector A subunit	-1.5	-0.4	2.3	-0.2	0.9	3.7	0.7	1.7	4.5
ZGAL_1778	atpE1	atpE1 ATP synthase, F0 sector C subunit	-2.1	0.7	4.9	-1.5	1.4	5.6	-0.6	2.2	6.5
ZGAL_1779	atpF1	atpF1 ATP synthase, F0 sector B subunit	-1.3	-0.8	2.5	-2.0	-1.5	1.9	-0.1	0.4	3.8
ZGAL_178		conserved hypothetical periplasmic protein	1.9	0.0	-1.5	2.2	0.4	-1.1	1.5	-0.3	-1.8
ZGAL_1780	atpH	atpH ATP synthase, F1 sector delta subunit	-1.3	-0.4	2.4	-1.5	-0.6	2.2	-0.6	0.3	3.1
ZGAL_1782	atpG1	atpG1 ATP synthase, F1 sector gamma subunit	-2.3	-0.9	1.8	-2.5	-1.1	1.6	-3.0	-1.6	1.1
ZGAL_18		Putative membrane protein	2.2	0.5	0.2	1.9	0.3	-0.1	2.0	0.4	0.0
ZGAL_1806	gldH	gldH Gliding motility membrane lipoprotein	-0.6	0.3	-1.3	-0.6	0.4	-1.3	1.1	2.0	0.4
ZGAL_1807	pbp1A	pbp1A Penicillin-binding protein 1A, family GT51	-0.2	-1.0	-1.8	0.3	-0.5	-1.3	1.9	1.1	0.3
ZGAL_1810		Conserved hypothetical protein	-2.6	1.4	2.0	-0.5	3.4	4.1	0.9	4.8	5.5
ZGAL_1816		Hypothetical protein	1.9	-0.2	-1.3	1.5	-0.6	-1.6	0.6	-1.4	-2.5
ZGAL_1821	sdhC	sdhC Succinate dehydrogenase, cytochrome b558 subunit	-0.7	0.3	2.9	0.3	1.3	3.9	1.1	2.1	4.7
ZGAL_1822	sdhA	sdhA Succinate dehydrogenase, flavoprotein subunit	-1.3	0.1	2.8	-1.2	0.2	2.9	-0.3	1.0	3.7
ZGAL_1823	sdhB	sdhB Succinate dehydrogenase iron-sulfur subunit	-1.8	0.1	3.5	-1.3	0.6	4.0	-0.2	1.6	5.0
ZGAL_1825		Intracellular peptidase, family C56	3.3	2.3	2.3	2.0	1.1	1.0	0.7	-0.3	-0.4
ZGAL_1826		Conserved hypothetical protein	0.4	0.1	1.3	0.2	-0.1	1.0	0.0	-0.3	0.8
ZGAL_183		FAD-dependent GMC oxidoreductase, family AA3	1.1	1.3	0.3	2.0	2.2	1.2	1.9	2.2	1.2
ZGAL_1830	aqpZ	aqpZ Aquaporin Z	-0.9	0.3	0.1	0.8	2.0	1.8	1.6	2.7	2.5
ZGAL_1831	braB	braB Branched chain amino acid transport system II carrier protein	-0.7	0.4	-0.9	0.5	1.7	0.3	0.8	1.9	0.6
ZGAL_1833		Putative protein	-1.5	1.7	0.6	0.4	3.6	2.5	1.5	4.6	3.5
ZGAL_1834		Conserved hypothetical protein	-0.9	3.9	1.0	1.2	6.0	3.1	2.2	7.0	4.2
ZGAL_1835		Alpha/beta hydrolase-fold protein	1.2	1.4	-0.2	1.2	1.5	-0.2	1.3	1.5	-0.1
ZGAL_1837	sufA	sufA Protein SufA	2.4	1.2	-0.9	1.0	-0.2	-2.3	0.3	-0.9	-3.0
ZGAL_1838	sufB	sufB Protein SufB	2.3	0.6	-2.2	1.1	-0.6	-3.4	0.1	-1.6	-4.4
ZGAL_1846		Conserved hypothetical periplasmic protein	1.2	0.3	-1.4	2.0	1.0	-0.7	2.2	1.2	-0.5
ZGAL_1848	hfiX	hfiX GTP-binding protein HflX	1.5	0.6	-0.5	1.0	0.0	-1.1	-0.2	-1.1	-2.2
ZGAL_1851		Conserved hypothetical lipoprotein	-0.5	-0.2	-2.3	0.7	1.0	-1.2	2.5	2.9	0.7
ZGAL_1856		ATP-dependent helicase	-1.2	0.1	-0.8	-1.0	0.4	-0.6	0.3	1.6	0.7
ZGAL_1861	hemE	hemE Uroporphyrinogen decarboxylase	-0.5	0.0	2.2	-0.3	0.2	2.4	0.8	1.3	3.5
ZGAL_1862	hemCD	hemCD Porphobilinogen deaminase / Uroporphyrinogen-III synthase	-0.5	0.0	2.9	0.0	0.5	3.4	1.3	1.8	4.7
ZGAL_1863	hemA	hemA Glutamyl-tRNA-reductase	-0.2	-0.1	2.6	-0.4	-0.3	2.5	0.8	1.0	3.7
ZGAL_1869		Conserved hypothetical periplasmic protein	0.5	-0.1	-0.1	0.7	0.1	0.0	1.9	1.3	1.3
ZGAL_1871	hemH	hemH Ferrochelatase	2.2	1.9	-1.7	1.9	1.7	-2.0	0.7	0.4	-3.2

ZGAL_1876		Two-component system - Sensor histidine kinase	0.9	-0.5	-1.6	1.5	0.1	-1.1	0.9	-0.5	-1.7
ZGAL_1878		Putative exported protein	0.3	0.5	-0.1	1.1	1.3	0.7	2.4	2.6	2.0
ZGAL_1879		Conserved hypothetical protein	-0.5	-0.2	-0.7	0.1	0.4	-0.1	1.7	2.0	1.5
ZGAL_1888		Deoxycytidylate deaminase	-0.6	0.2	0.8	0.1	0.9	1.4	0.4	1.2	1.8
ZGAL_1889		Carboxy-terminal processing peptidase, family S41	1.1	-0.2	-0.8	1.6	0.3	-0.2	1.8	0.5	0.0
ZGAL_1895		Putative protein	0.5	-1.5	-2.1	3.2	1.2	0.6	2.2	0.2	-0.3
ZGAL_1896		Conserved hypothetical protein	0.6	-1.1	-2.0	2.6	0.9	0.0	2.3	0.5	-0.4
ZGAL_1898		Hypothetical periplasmic protein	3.4	-0.8	-1.4	3.9	-0.3	-0.9	1.8	-2.4	-3.0
ZGAL_19		Conserved hypothetical protein	1.0	-0.2	-0.4	0.6	-0.7	-0.8	1.1	-0.2	-0.4
ZGAL_1902		Hypothetical lipoprotein	0.8	-1.5	-2.1	2.7	0.4	-0.2	2.4	0.1	-0.5
ZGAL_1908		Hypothetical periplasmic protein	3.8	-1.9	-3.4	4.3	-1.4	-2.8	3.7	-2.0	-3.5
ZGAL_1909		Conserved hypothetical periplasmic protein	3.4	-0.6	-3.2	3.4	-0.6	-3.2	3.1	-0.9	-3.5
ZGAL_1910	rnrB1	rnrB1 Ribonucleoside-diphosphate reductase, small subunit	-0.7	0.8	2.2	-0.5	1.0	2.5	-0.5	1.1	2.5
ZGAL_1911	rnrA1	rnrA1 Ribonucleoside-diphosphate reductase, large subunit	-0.1	0.5	1.3	-0.6	-0.1	0.7	-1.1	-0.6	0.2
ZGAL_1921		Conserved hypothetical protein	-1.0	0.7	-0.6	-0.4	1.2	-0.1	-1.0	0.6	-0.7
ZGAL_1922		FAD-dependent GMC oxidoreductase, family AA3	0.9	0.4	-1.0	0.4	-0.1	-1.5	-0.4	-0.9	-2.3
ZGAL_1930		Conserved hypothetical lipoprotein	0.5	2.3	1.8	0.8	2.7	2.2	2.8	4.7	4.2
ZGAL_1931		Phosphate transporter family protein	-0.3	-0.1	0.1	0.2	0.5	0.7	0.6	0.8	1.1
ZGAL_1936	dxsA	dxsA 1-Deoxy-D-xylulose-5-phosphate synthase	2.8	-0.5	-1.3	3.0	-0.3	-1.1	1.4	-1.9	-2.7
ZGAL_1937	tadA	tadA tRNA-specific adenosine deaminase	-1.1	0.9	-0.2	-1.1	1.0	-0.1	-0.6	1.4	0.4
ZGAL_1938	cspA2	cspA2 Cold shock protein	2.1	2.9	4.0	2.2	3.0	4.1	2.5	3.3	4.4
ZGAL_1941	aspS	aspS Aspartyl-tRNA synthetase	-0.8	-0.2	1.7	-1.2	-0.6	1.3	-1.0	-0.4	1.5
ZGAL_1943		SusD-like lipoprotein	1.0	1.6	0.6	1.3	1.9	0.9	0.7	1.3	0.3
ZGAL_1949		RNA polymerase ECF-type sigma factor	2.2	1.1	1.5	1.5	0.4	0.8	1.2	0.1	0.5
ZGAL_1956		Two-component system - Sensor histidine kinase	-0.6	0.9	0.8	0.3	1.7	1.6	2.1	3.5	3.4
ZGAL_1957		Putative glycoside hydrolase, family GHnc	1.2	0.8	1.2	0.7	0.3	0.6	0.4	0.0	0.4
ZGAL_1959		Hypothetical membrane protein	-1.1	0.0	-0.4	-0.7	0.5	0.1	1.0	2.1	1.7
ZGAL_196		Glycoside hydrolase, family GH31	-0.9	0.4	1.2	-0.6	0.7	1.5	-0.4	0.9	1.7
ZGAL_1960		Conserved hypothetical protein	1.4	2.2	0.6	0.4	1.2	-0.4	0.7	1.4	-0.1
ZGAL_1962		Hypothetical protein	1.6	0.3	0.0	0.9	-0.4	-0.7	-0.1	-1.3	-1.7
ZGAL_1964	feoB	feoB Ferrous iron transport protein B	2.2	0.1	-1.3	0.8	-1.3	-2.6	0.3	-1.8	-3.1
ZGAL_1966		Conserved hypothetical membrane protein	1.8	-0.6	0.8	1.1	-1.3	0.0	0.4	-2.0	-0.7
ZGAL_1967	ecfE	ecfE Peptidase EcfE, family M50	-0.2	-0.3	2.1	0.3	0.1	2.6	0.8	0.6	3.1
ZGAL_197	fucA10	fucA10 Alpha-L-fucosidase, family GH29	-0.8	0.5	1.2	-0.9	0.4	1.1	-0.5	0.7	1.4
ZGAL_1975		Universal stress protein	-4.1	0.4	2.1	-2.6	2.0	3.7	-0.8	3.7	5.4
ZGAL_1976	pckA1	pckA1 Phosphoenolpyruvate carboxykinase [ATP]	-2.4	2.6	1.9	0.8	5.8	5.1	2.0	7.0	6.3
ZGAL_1977		Putative protein	-0.8	3.5	2.3	1.6	5.9	4.7	3.7	8.0	6.8
ZGAL_1978		Exopolysaccharide production protein	-2.1	1.1	-0.2	-0.1	3.0	1.8	-0.3	2.8	1.6
ZGAL_1983		Conserved hypothetical protein	-1.8	0.0	1.5	-1.8	0.0	1.4	-1.9	0.0	1.4
ZGAL_1987		Conserved hypothetical protein	-1.8	1.2	1.5	-1.1	1.8	2.2	-0.7	2.3	2.6
ZGAL_199		SusD-like lipoprotein	1.7	2.0	1.3	2.4	2.7	2.0	2.8	3.1	2.4
ZGAL_1990		Conserved hypothetical lipoprotein	0.7	1.6	-0.2	1.5	2.4	0.6	3.4	4.4	2.5
ZGAL_1991		Conserved hypothetical lipoprotein	2.2	-0.1	-1.1	2.6	0.3	-0.8	4.1	1.8	0.8
ZGAL_1992		Conserved hypothetical protein	-0.3	0.3	-0.1	0.2	0.9	0.4	0.2	0.9	0.4
ZGAL_1993		Glycosyltransferase, family GT2	-0.3	1.0	-0.1	0.3	1.5	0.4	0.5	1.7	0.6
ZGAL_1995		FAD-dependent amine oxidoreductase	-1.5	1.0	0.7	-0.1	2.4	2.1	-1.1	1.4	1.2
ZGAL_1996		NAD(P)-dependent sugar epimerase/dehydratase	-1.8	1.4	1.3	-0.3	2.9	2.8	-1.8	1.4	1.3
ZGAL_200		SusC-like TonB-dependent transporter	2.3	2.3	0.8	2.6	2.6	1.1	3.4	3.4	1.9
ZGAL_2003		Cytochrome c-containing protein	1.4	0.4	-1.2	1.6	0.6	-1.0	1.6	0.6	-1.0
ZGAL_2004		Conserved hypothetical periplasmic protein	2.1	1.3	0.6	2.6	1.8	1.1	2.7	1.9	1.2
ZGAL_2006		Endoribonuclease L-PSP	1.7	0.8	-0.1	1.9	0.9	0.0	1.1	0.1	-0.8
ZGAL_201		AraC-type transcriptional regulator	-0.6	0.4	-0.8	1.2	2.2	1.0	0.5	1.5	0.3
ZGAL_2010		Esterase	-0.9	1.4	0.4	0.5	2.8	1.8	2.2	4.5	3.5
ZGAL_2012		Putative protein	-2.3	2.0	3.8	-0.5	3.9	5.6	0.7	5.1	6.9
ZGAL_2013		Conserved hypothetical protein	1.1	0.6	0.6	0.6	0.0	0.0	0.4	-0.2	-0.2
ZGAL_2014	speA	speA Arginine decarboxylase	-0.1	0.4	1.5	-0.1	0.4	1.5	0.1	0.6	1.7
ZGAL_2015	speB	speB Agmatinase	0.9	0.5	3.3	0.3	-0.1	2.7	0.2	-0.1	2.6
ZGAL_2018		N-acetyltransferase / Carbon-Nitrogen hydrolase	1.0	0.3	-0.1	1.1	0.4	0.1	0.1	-0.6	-1.0
ZGAL_202		Conserved hypothetical protein	-0.3	0.5	-1.1	1.4	2.1	0.5	-0.1	0.7	-0.9
ZGAL_2021		SCP-like extracellular protein	-3.0	0.2	-1.3	3.6	6.7	5.2	3.3	6.4	5.0
ZGAL_2022		Conserved hypothetical periplasmic protein	1.1	4.3	3.0	2.9	6.2	4.8	5.2	8.4	7.0
ZGAL_2023		T9SS SprF family protein	2.4	3.8	2.9	4.3	5.8	4.8	5.7	7.2	6.2
ZGAL_2024		T9SS-associated PG1058-like protein	1.8	2.9	1.8	4.1	5.2	4.1	5.6	6.7	5.6
ZGAL_2025		NAD-dependent epimerase/dehydratase	-0.5	0.1	0.2	0.5	1.2	1.3	1.6	2.3	2.4
ZGAL_2028		Conserved hypothetical protein	-0.2	0.0	1.7	0.3	0.5	2.2	0.3	0.5	2.2
ZGAL_2029		Conserved hypothetical protein	0.0	0.7	1.4	1.9	2.7	3.3	3.1	3.8	4.5
ZGAL_2036		Conserved hypothetical protein	3.3	1.9	0.5	2.8	1.4	0.0	0.5	-0.9	-2.3
ZGAL_2041		Conserved hypothetical lipoprotein	3.0	-1.7	-2.6	4.1	-0.7	-1.6	3.9	-0.9	-1.8
ZGAL_2044		Conserved hypothetical periplasmic protein	-0.4	0.4	-0.6	-0.5	0.4	-0.7	0.8	1.7	0.7
ZGAL_2045		Hypothetical membrane protein	-0.7	1.6	-0.2	-0.7	1.5	-0.3	1.1	3.4	1.6
ZGAL_2046		Hypothetical protein	-1.4	1.4	-0.6	-0.4	2.4	0.3	1.4	4.2	2.2
ZGAL_2047		Hypothetical protein	0.0	1.4	-1.8	-0.3	1.1	-2.0	0.6	2.0	-1.1

ZGAL_205		Glycoside hydrolase, family GH117	2.9	2.1	2.2	3.8	3.0	3.1	1.4	0.6	0.7
ZGAL_2058		Conserved hypothetical periplasmic protein	1.5	0.1	1.0	1.2	-0.2	0.7	2.0	0.6	1.5
ZGAL_2059		Conserved hypotetical lipoprotein	0.1	-0.4	0.3	1.7	1.2	1.9	2.5	2.0	2.7
ZGAL_206		Sulfatase, family S1-17	5.2	1.6	1.6	5.4	1.8	1.8	2.6	-1.0	-1.0
ZGAL_2061	pgdA	pgdA Peptidoglycan N-acetylglucosamine deacetylase, family CE4	-1.2	1.1	0.7	0.4	2.8	2.4	1.9	4.2	3.8
ZGAL_2064	acpP2	acpP2 Acyl carrier protein	-0.8	0.3	1.1	0.0	1.1	1.9	0.7	1.8	2.6
ZGAL_2065		Conserved hypothetical protein	0.8	1.4	2.6	1.1	1.6	2.8	1.9	2.5	3.7
ZGAL_2069		ABC transporter, ATPase component	0.0	0.6	0.8	0.3	0.9	1.2	-0.1	0.6	0.8
ZGAL_207		Conserved hypothetical membrane protein	1.0	0.9	0.7	1.7	1.6	1.4	1.5	1.4	1.2
ZGAL_2073	fabZ2	fabZ2 (3R)-Hydroxymyristoyl-[acyl-carrier-protein] dehydratase	-0.1	0.3	1.4	-0.6	-0.2	0.9	0.4	0.9	1.9
ZGAL_2076		Acyltransferase	-0.1	0.0	-0.9	0.1	0.2	-0.7	1.3	1.4	0.5
ZGAL_2077	acpP3	acpP3 Acyl carrier protein	-1.3	1.1	1.0	-1.2	1.2	1.1	0.0	2.4	2.3
ZGAL_2078	fabB5	fabB5 3-oxoacyl-[acyl-carrier-protein] synthase	-0.5	0.5	0.2	-0.1	1.0	0.6	0.5	1.6	1.2
ZGAL_2080		KGW repeats protein	-0.3	0.4	1.3	-1.0	-0.3	0.6	-0.8	-0.1	0.9
ZGAL_2081	hutH	hutH Histidine ammonia-lyase	-0.7	0.4	1.4	-0.4	0.7	1.7	-0.2	0.9	1.9
ZGAL_2084		SusC-like TonB-dependent transporter	-1.0	1.0	-0.2	-0.8	1.3	0.0	-0.5	1.6	0.3
ZGAL_2086		Similar to ASPIC and UnbV protein containing FG-GAP repeats	-0.3	0.5	-0.1	-0.3	0.6	-0.1	0.2	1.0	0.4
ZGAL_2087		Similar to ASPIC and UnbV protein containing FG-GAP repeats	-1.2	0.6	-0.3	-1.1	0.8	-0.2	-0.6	1.3	0.3
ZGAL_209		Hypothetical lipoprotein, family CBM4	0.5	1.0	1.1	1.2	1.6	1.7	2.1	2.5	2.6
ZGAL_2093		Deacetylase, histone deacetylase family	2.3	0.1	-1.8	0.7	-1.6	-3.4	0.5	-1.7	-3.6
ZGAL_2097	metG	metG Methionyl-tRNA synthetase, class Ia	-1.2	-0.6	1.9	-1.6	-0.9	1.5	-1.0	-0.4	2.0
ZGAL_2099		Conserved hypothetical protein	0.4	2.9	2.8	1.2	3.7	3.5	2.7	5.2	5.1
ZGAL_210		Hypothetical lipoprotein	1.0	0.4	-0.2	1.2	0.5	0.0	1.5	0.9	0.3
ZGAL_2100		Conserved hypothetical protein	0.9	1.8	0.7	1.7	2.6	1.5	3.3	4.2	3.1
ZGAL_2106	mfdA	mfdA Transcription-repair coupling factor	0.7	1.7	2.8	0.9	1.9	3.0	0.6	1.7	2.8
ZGAL_2107	gorA	gorA Glutathione reductase	4.3	2.2	1.4	3.7	1.6	0.8	1.4	-0.7	-1.5
ZGAL_2108		Conserved hypothetical membrane protein	3.9	2.5	1.5	4.1	2.6	1.7	1.7	0.3	-0.7
ZGAL_2109		Metallo-phosphoesterase family	2.2	0.3	-1.1	2.1	0.2	-1.1	1.0	-1.0	-2.3
ZGAL_211		SusD-like lipoprotein	0.8	1.1	0.5	0.3	0.6	0.0	1.4	1.7	1.2
ZGAL_2111		Hypothetical lipoprotein	-1.0	0.2	-0.5	-1.0	0.2	-0.4	1.8	3.0	2.4
ZGAL_2112		Uncharacterized ATP-dependent helicase	2.2	2.4	2.5	2.2	2.3	2.5	1.1	1.2	1.3
ZGAL_2113	ligC	ligC DNA ligase	2.5	2.3	2.4	2.0	1.7	1.8	0.6	0.3	0.4
ZGAL_2114		Metallo-beta-lactamase superfamily protein	3.2	2.1	1.5	2.1	0.9	0.3	0.0	-1.1	-1.8
ZGAL_2115		Conserved hypothetical protein	-3.5	-0.4	3.1	-2.5	0.6	4.1	-1.6	1.5	5.0
ZGAL_2118		Conserved hypothetical protein	-2.9	1.7	2.6	-3.2	1.4	2.3	-4.5	0.1	1.0
ZGAL_2119	lysC	lysC Aspartate kinase III	-3.5	1.1	2.1	-2.9	1.7	2.8	-4.3	0.3	1.4
ZGAL_212		SusC-like TonB-dependent transporter	0.9	1.3	0.1	0.3	0.8	-0.4	1.2	1.7	0.5
ZGAL_2120		Phospholipid/glycerol Acyltransferase / hemolysin fusion	-1.2	0.9	0.4	-0.7	1.4	1.0	-1.3	0.8	0.3
ZGAL_2126		Divalent cation transporter	0.5	0.4	1.7	0.2	0.1	1.4	0.0	-0.1	1.3
ZGAL_213		Xyloglucan-binding SusD-like lipoprotein	1.4	1.4	0.5	1.3	1.2	0.4	1.7	1.6	0.7
ZGAL_2131		TPR repeats protein	2.2	0.6	0.9	1.7	0.0	0.4	1.0	-0.6	-0.3
ZGAL_2132		Putative protein	3.1	1.3	-1.1	4.4	2.5	0.2	2.3	0.4	-1.9
ZGAL_2134		Glyoxalase/Bleomycin resistance protein/Dioxygenase superfamily	-0.8	0.5	1.4	-0.2	1.0	1.9	-0.4	0.8	1.7
ZGAL_2137		Metalloendopeptidase, family M12	-0.2	0.9	-0.8	0.5	1.6	0.0	0.3	1.4	-0.2
ZGAL_214		SusC-like TonB-dependent transporter	0.0	0.6	0.0	0.8	1.4	0.7	0.7	1.3	0.7
ZGAL_2140	rplY	rplY Ribosomal protein L25	-0.5	-1.1	2.7	-1.2	-1.8	2.0	-0.2	-0.7	3.1
ZGAL_2141	prsA	prsA Ribose-phosphate pyrophosphokinase	-1.3	-0.5	1.5	-0.4	0.4	2.4	-0.3	0.5	2.5
ZGAL_2149		SusC-like TonB-dependent transporter	1.5	0.1	-1.7	1.3	-0.1	-1.8	0.9	-0.5	-2.2
ZGAL_2151		Conserved hypothetical membrane protein	2.5	-2.4	-2.0	1.4	-3.5	-3.2	1.5	-3.4	-3.0
ZGAL_2152		Hypothetical periplasmic protein	-2.2	0.2	2.6	-1.0	1.4	3.8	-0.1	2.3	4.7
ZGAL_2162	hypF	hypF Carbamoyltransferase HypF	-0.2	2.1	2.6	0.8	3.1	3.7	1.1	3.4	4.0
ZGAL_2164	hypA	hypA hydrogenase nickel incorporation protein HypA	1.9	1.4	1.8	1.3	0.8	1.2	0.5	0.0	0.5
ZGAL_2167		Hypothetical protein	2.0	1.4	2.8	1.5	0.9	2.3	1.0	0.4	1.9
ZGAL_2168	hyaD	hyaD Hydrogenase maturation protease, family A31	2.2	1.2	2.6	1.9	0.9	2.3	1.1	0.1	1.5
ZGAL_2169	hyaB	hyaB Ni-Fe hydrogenase precursor, large subunit	1.8	0.5	3.1	2.0	0.7	3.2	0.8	-0.5	2.1
ZGAL_2170	hyaA	hyaA Ni-Fe hydrogenase precursor, small subunit	0.9	0.0	2.6	1.1	0.2	2.9	-0.7	-1.6	1.1
ZGAL_2171		Conserved hypothetical protein	-3.6	0.8	2.9	-0.8	3.6	5.7	0.7	5.1	7.2
ZGAL_2172		Putative protein	-2.9	1.5	1.9	0.5	4.8	5.2	1.8	6.1	6.5
ZGAL_2176	rimM	rimM 16S rRNA processing protein RimM	0.0	-1.3	1.0	0.2	-1.1	1.2	0.9	-0.4	1.9
ZGAL_2177	rpsP	rpsP Ribosomal protein S16	-0.2	-1.4	3.1	0.8	-0.4	4.1	1.3	0.2	4.6
ZGAL_2178	dnaE1	dnaE1 DNA polymerase III, alpha subunit	-0.3	0.7	2.9	-0.4	0.6	2.8	-0.3	0.7	2.9
ZGAL_22	hisS	hisS Histidyl-tRNA synthetase	-1.1	-0.5	2.1	-0.8	-0.2	2.4	-0.7	-0.2	2.5
ZGAL_2221		Kinase, aminoglycoside phosphotransferase family	-0.8	-0.5	1.2	-0.4	0.0	1.6	-0.6	-0.2	1.4
ZGAL_2222		Nucleotidyl transferase	-0.9	-0.7	2.1	-1.4	-1.2	1.6	-1.3	-1.1	1.7
ZGAL_2226		Glycoside hydrolase, family GH63	1.4	-0.1	-1.1	1.7	0.3	-0.8	2.1	0.7	-0.4
ZGAL_223		ABC-2 type exporter, permease component	2.2	-0.7	-2.1	2.1	-0.8	-2.2	2.0	-0.8	-2.2
ZGAL_2232	hemN	hemN Oxygen-independent coproporphyrinogen III oxidase	-2.5	-0.5	2.7	-1.6	0.4	3.6	-0.2	1.7	5.0
ZGAL_2233		Universal stress protein	-2.4	1.6	2.1	-0.6	3.3	3.9	0.8	4.8	5.3
ZGAL_2235		Cytochrome c	-1.2	0.8	2.2	0.0	2.0	3.4	0.7	2.8	4.1
ZGAL_2236	nosZ	nosZ Nitrous oxide reductase	-1.3	2.9	3.2	0.7	4.9	5.2	1.4	5.7	5.9

ZGAL_2237		Conserved hypothetical membrane protein	-1.8	1.7	1.7	0.2	3.7	3.7	0.7	4.2	4.2
ZGAL_2238	nosL	nosL Copper-binding lipoprotein	-1.1	0.6	0.4	-0.2	1.5	1.3	0.5	2.2	2.1
ZGAL_2239		Flavin mononucleotide binding protein	-0.8	1.1	0.7	-0.4	1.5	1.1	0.9	2.7	2.4
ZGAL_2240	nosD	nosD Copper-binding periplasmic protein	-0.9	1.6	2.0	0.3	2.8	3.2	1.2	3.7	4.1
ZGAL_2241	nosF	nosF Copper ABC transporter , ATPase component	-0.5	0.7	0.1	0.1	1.4	0.7	1.2	2.5	1.8
ZGAL_2242	nosY	nosY Copper ABC importer, permease component	-0.8	0.7	0.4	0.5	2.1	1.8	1.3	2.8	2.5
ZGAL_2243		Conserved hypothetical membrane protein	-0.4	0.3	-0.4	0.3	1.0	0.3	1.5	2.2	1.6
ZGAL_2247		Rrf2-type transcriptional regulator	-1.0	1.2	-0.4	-1.1	1.1	-0.5	1.2	3.4	1.8
ZGAL_2248		Globin-like protein	-2.1	0.2	0.2	-0.9	1.4	1.5	0.7	3.0	3.0
ZGAL_2249	catB	catB 4-hydroxybutyrate coenzyme A transferase	-4.2	-0.2	0.8	-1.7	2.3	3.4	0.3	4.3	5.4
ZGAL_2250		Vanadium-dependent haloperoxidase	-0.8	0.6	-0.8	0.5	1.9	0.5	1.0	2.4	1.1
ZGAL_2251		Conserved hypothetical membrane protein	-0.8	3.0	2.4	0.3	4.1	3.4	1.3	5.1	4.4
ZGAL_2252	ccdA	ccdA Cytochrome C biogenesis protein	-2.6	4.2	3.9	0.1	6.9	6.6	0.7	7.5	7.2
ZGAL_2253	ccoH	ccoH FixH-like protein	-3.4	4.5	4.5	-1.3	6.5	6.5	-0.1	7.7	7.7
ZGAL_2254	ccoG	ccoG 4Fe-4S ferredoxin	-3.5	4.2	4.0	-0.6	7.1	7.0	-0.1	7.6	7.5
ZGAL_2255	ccoP	ccoP Cytochrome cbb3 oxidase, CcoP subunit	-3.5	3.2	3.2	-1.0	5.7	5.7	-0.1	6.6	6.6
ZGAL_2256	ccoQ	ccoQ Cytochrome cbb3 oxidase, CcoQ subunit	-3.4	2.6	3.7	-0.8	5.2	6.3	0.2	6.2	7.3
ZGAL_2257	ccoNO	ccoNO Cytochrome cbb3 oxidase, CcoN and CcoO subunits	-3.2	-0.3	2.8	-1.4	1.5	4.6	0.2	3.1	6.2
ZGAL_2258	ccoS	ccoS Cytochrome cbb3 oxidase maturation protein	-1.0	-0.3	4.2	-0.6	0.1	4.6	2.4	3.2	7.6
ZGAL_2259		Conserved hypothetical membrane protein	-1.1	1.0	1.4	0.2	2.2	2.6	1.6	3.7	4.0
ZGAL_2260	ccoI	ccoI Cation-transporting P-type ATPase	-1.0	0.2	1.3	0.0	1.2	2.3	1.7	2.8	4.0
ZGAL_2262		Universal stress protein	-2.0	-0.2	-0.4	-1.1	0.6	0.5	0.3	2.0	1.9
ZGAL_2263	ndhA2	ndhA2 FAD-dependent pyridine nucleotide-disulphide oxidoreductase, membrane	0.4	-0.3	0.8	1.0	0.3	1.4	0.5	-0.3	0.8
ZGAL_2266		NAD(P)H nitroreductase	2.1	-0.7	1.3	1.5	-1.4	0.6	0.5	-2.4	-0.4
ZGAL_2269		BlaI-type transcriptional repressor	4.0	-0.3	1.7	3.2	-1.0	0.9	2.4	-1.8	0.2
ZGAL_2270		BlaR1-type regulatory protein / TonB protein	2.9	0.2	1.3	1.6	-1.0	0.0	1.5	-1.2	-0.1
ZGAL_2271		O-linked N-acetylglucosaminyltransferase, family GT41	2.5	1.1	1.6	1.8	0.4	0.9	1.8	0.4	1.0
ZGAL_2283		conserved hypothetical protein	0.6	0.1	1.1	1.9	1.4	2.3	2.4	1.9	2.8
ZGAL_2284		Conserved hypothetical membrane protein	1.4	-0.2	-0.3	1.6	0.0	-0.2	2.4	0.8	0.6
ZGAL_2287	phnA	phnA PhnA protein	-3.0	0.4	2.1	-1.7	1.7	3.4	-0.8	2.6	4.3
ZGAL_2293		Anti-sigma factor	-2.5	-0.2	-0.3	-1.2	1.1	1.0	-0.7	1.7	1.5
ZGAL_2296		Conserved lipoprotein containing CBM22	2.4	-0.2	-1.5	1.5	-1.1	-2.4	1.3	-1.3	-2.6
ZGAL_2298		SusC-like TonB-dependent transporter	1.9	0.2	-0.8	2.0	0.3	-0.8	2.3	0.6	-0.4
ZGAL_23		Conserved hypothetical protein	-0.4	-1.3	2.0	-0.7	-1.5	1.8	0.0	-0.8	2.5
ZGAL_2300		Hypothetical protein	-0.4	0.7	-0.6	1.4	2.6	1.3	2.9	4.1	2.8
ZGAL_2302		Universal stress protein	-1.6	1.0	1.2	-1.8	0.8	1.0	0.3	2.9	3.0
ZGAL_2305		SusC-like TonB-dependent transporter	1.8	1.0	-0.7	1.7	0.9	-0.8	0.8	0.0	-1.7
ZGAL_2306		SusD-like lipoprotein	1.3	0.6	-0.4	1.7	0.9	-0.1	1.2	0.5	-0.6
ZGAL_2307		Conserved lipoprotein containing CBM22	1.6	0.7	0.0	1.5	0.6	-0.1	1.0	0.2	-0.5
ZGAL_2308		Putative glycoside hydrolase, family GHnc	1.0	0.5	-0.2	0.5	-0.1	-0.8	0.1	-0.5	-1.1
ZGAL_2310	bgaE	bgaE Beta-galactosidase, family GH2	-0.2	0.0	1.2	-0.8	-0.6	0.6	-1.0	-0.8	0.4
ZGAL_2311		Conserved hypothetical membrane protein	1.2	0.2	1.9	1.8	0.8	2.5	1.4	0.4	2.1
ZGAL_2312		TonB-dependent Receptor	0.9	-0.7	1.5	0.9	-0.7	1.5	-0.1	-1.7	0.5
ZGAL_2313		Conserved hypothetical lipoprotein	1.4	0.0	2.5	1.1	-0.4	2.2	-0.3	-1.8	0.8
ZGAL_2315		TonB-dependent Transducer	0.1	0.5	0.9	0.9	1.3	1.7	0.7	1.1	1.5
ZGAL_2326	sucA	sucA 2-oxoglutarate dehydrogenase E1 component	-1.1	-0.3	0.7	-1.0	-0.2	0.8	-0.6	0.3	1.3
ZGAL_2339	AsnS	AsnS Asparaginyl-tRNA synthetase	-1.0	-0.5	2.1	-1.4	-1.0	1.7	-0.8	-0.4	2.2
ZGAL_2340	acrB	acrB Acriflavin resistance protein	0.0	0.0	2.1	0.2	0.2	2.2	0.2	0.2	2.3
ZGAL_2344	tsfA	tsfA Elongation factor Ts (EF-Ts)	-3.2	-2.3	1.7	-3.0	-2.1	1.9	-2.5	-1.6	2.4
ZGAL_2345	rpsB	rpsB Ribosomal protein S2	-1.6	-1.4	1.6	-1.1	-1.0	2.0	-0.4	-0.2	2.8
ZGAL_2346	rpsI	rpsI Ribosomal protein S9	0.1	-1.2	1.0	-0.2	-1.6	0.7	0.9	-0.5	1.8
ZGAL_2347	rplM	rplM Ribosomal protein L13	0.2	-0.7	2.1	1.0	0.1	2.9	1.6	0.7	3.5
ZGAL_2348		Hypothetical membrane protein	-1.5	0.4	1.0	-1.1	0.8	1.3	1.1	3.1	3.6
ZGAL_2352		Metallophosphoesterase	3.0	-0.4	0.9	2.6	-0.8	0.5	1.8	-1.6	-0.3
ZGAL_2354		Conserved hypothetical membrane protein	0.6	0.0	1.3	0.4	-0.2	1.1	-0.1	-0.8	0.5
ZGAL_2361		Multiheme cytochrome c	-1.0	-1.0	1.8	-1.3	-1.3	1.5	-0.1	0.0	2.8
ZGAL_2362	hmoA	hmoA Molybdopterin oxidoreductase, iron-sulfur binding subunit	-1.4	-0.6	2.5	-2.3	-1.5	1.6	-1.7	-0.9	2.2
ZGAL_2363	hmoB	hmoB Molybdopterin oxidoreductase, membrane subunit	-1.9	-0.5	2.7	-1.9	-0.4	2.8	-2.3	-0.9	2.3
ZGAL_2364		Conserved hypothetical protein	-1.9	0.5	4.0	-1.8	0.6	4.0	-2.2	0.2	3.7
ZGAL_2365		Cytochrome C monohaem	-2.0	0.3	3.7	-2.0	0.3	3.6	-2.3	0.0	3.3
ZGAL_2366		Conserved membrane protein	-2.2	-0.6	2.5	-2.5	-0.9	2.1	-2.6	-1.0	2.1
ZGAL_2368	coxN	coxN Cytochrome c oxidase, subunit I	-2.5	0.3	2.0	-2.2	0.6	2.3	-2.1	0.6	2.4
ZGAL_2369		Conserved hypothetical protein	-1.1	0.3	0.2	-1.0	0.3	0.3	-0.2	1.1	1.1
ZGAL_2375	maeB	maeB NADP-dependent malate dehydrogenase / Phosphate acetyl/butaryl transferase	-0.8	-0.2	1.4	-1.2	-0.6	1.0	-1.0	-0.4	1.1
ZGAL_2376	ruvA	ruvA Holliday junction DNA helicase	0.0	1.8	2.8	0.3	2.1	3.2	1.8	3.6	4.6
ZGAL_2377	sprA	sprA T9SS outer membrane pore SprA	-0.8	1.6	1.7	0.3	2.7	2.8	1.8	4.1	4.2
ZGAL_2378	gcvH	gcvH Glycine-cleavage system H-protein	-1.0	-0.6	1.8	-1.3	-0.9	1.5	-0.6	-0.2	2.2
ZGAL_2382	coxC/ ctaE	coxC/ctaE Cytochrome C oxidase subunit III	0.5	0.1	1.7	0.6	0.2	1.8	1.6	1.2	2.8
ZGAL_2383		cyoCcyoC Cytochrome O ubiquinol oxidase, subunit III	-0.5	0.0	1.4	-0.3	0.2	1.6	0.1	0.6	2.0
ZGAL_2383	cyoC	cyoC Cytochrome O ubiquinol oxidase, subunit III	-0.5	0.0	1.4	-0.3	0.2	1.6	0.1	0.6	2.0

ZGAL_2384		Conserved hypothetical membrane protein	-2.9	0.0	1.9	-1.5	1.4	3.3	-0.4	2.5	4.4
ZGAL_2389		ABC exporter, permease component	1.0	-1.4	-0.2	1.8	-0.6	0.5	1.8	-0.6	0.5
ZGAL_2392		ABC exporter, ATPase component	1.1	-0.6	0.4	1.5	-0.2	0.8	1.3	-0.4	0.6
ZGAL_2393		ABC exporter, permease component	2.4	-0.1	-0.1	2.2	-0.3	-0.3	2.1	-0.5	-0.5
ZGAL_2394		ABC exporter, permease component	1.8	0.2	1.3	2.1	0.5	1.7	2.2	0.6	1.7
ZGAL_2395		Membrane fusion protein	1.4	0.9	1.8	1.2	0.7	1.6	1.3	0.8	1.7
ZGAL_2396		Outer membrane efflux protein	1.5	0.3	1.1	1.2	0.0	0.8	0.7	-0.5	0.3
ZGAL_2397		Family M22 non-peptidase protein	0.7	0.4	1.2	0.4	0.2	1.0	0.2	0.0	0.8
ZGAL_2398	yggB	yggB Mechanosensitive ion channel	2.6	0.0	1.8	2.0	-0.6	1.2	-0.1	-2.8	-0.9
ZGAL_2399		Conserved hypothetical protein	1.6	3.1	3.2	2.8	4.2	4.3	0.8	2.3	2.3
ZGAL_24		TonB-dependent Receptor	0.4	0.9	0.6	-0.1	0.5	0.2	-0.2	0.4	0.1
ZGAL_240		SusD-like lipoprotein	1.6	-0.6	-0.9	1.3	-0.9	-1.2	0.6	-1.5	-1.8
ZGAL_2401		T9SS SprF family protein	0.4	2.1	2.4	2.0	3.6	4.0	2.8	4.4	4.8
ZGAL_2404		Two-component system - Response regulator	-0.5	0.5	1.0	-0.4	0.5	1.1	0.0	0.9	1.5
ZGAL_2405	paaY	paaY Phenylacetic acid degradation o-acetyltransferase	-0.8	0.8	1.6	-0.8	0.7	1.5	-0.5	1.0	1.8
ZGAL_2414	sanA	sanA Protein involved in barrier function of the cell envelope	-0.1	0.9	-0.7	-0.2	0.7	-0.8	0.2	1.2	-0.4
ZGAL_2415		Hypothetical protein	0.2	3.2	-0.6	0.5	3.5	-0.3	2.0	5.0	1.2
ZGAL_2418	proA1	proA1 Glutamate-5-semialdehyde dehydrogenase (Gamma-glutamyl phosphate reductase)	-0.4	-0.9	2.2	-0.9	-1.4	1.8	-2.1	-2.6	0.6
ZGAL_2419	proB1	proB1 Glutamate 5-kinase (Gamma-glutamyl kinase)	-0.1	-0.7	1.9	-0.7	-1.3	1.3	-1.7	-2.3	0.4
ZGAL_2420	proC1	proC1 Pyrroline-5-carboxylate reductase	-0.9	-1.1	1.3	-0.9	-1.1	1.2	-2.5	-2.8	-0.4
ZGAL_2423		Hypothetical membrane protein	-1.2	0.1	0.6	-0.4	0.9	1.4	-0.3	1.0	1.5
ZGAL_2424		Hypothetical protein	-1.1	1.0	-0.1	-0.7	1.4	0.3	-0.4	1.7	0.6
ZGAL_2426		Hypothetical membrane protein	-2.0	0.1	0.1	-0.4	1.7	1.7	-0.1	2.0	2.0
ZGAL_243		Hypothetical protein	-1.4	2.0	-1.1	0.7	4.1	1.0	-0.7	2.7	-0.4
ZGAL_2432		Conserved hypothetical membrane protein	0.9	-0.7	-1.9	0.9	-0.7	-1.9	1.9	0.3	-0.9
ZGAL_2433		SusD-like lipoprotein	1.4	-0.4	-1.2	2.4	0.7	-0.1	3.7	1.9	1.1
ZGAL_2434		SusC-like TonB-dependent transporter	1.2	0.3	-0.7	2.3	1.4	0.4	3.0	2.1	1.1
ZGAL_2438	mutS1	mutS1 DNA mismatch repair protein MutS	-0.5	0.2	1.7	-1.0	-0.3	1.2	-1.1	-0.5	1.0
ZGAL_244	rnrA2	rnrA2 Ribonucleoside-diphosphate reductase, large subunit	-1.1	-0.6	3.6	-2.1	-1.6	2.6	-2.3	-1.9	2.3
ZGAL_2441	sppA	sppA Signal peptide peptidase A, family S49	-0.9	0.4	0.7	-0.9	0.4	0.7	-0.5	0.8	1.2
ZGAL_2442		OmpA-like periplasmic protein	-1.6	1.8	1.7	-1.1	2.3	2.2	1.0	4.4	4.3
ZGAL_2444		Conserved hypothetical periplasmic protein	-0.4	0.1	1.0	-0.1	0.4	1.4	0.9	1.4	2.3
ZGAL_2447		Conserved hypothetical protein	-0.5	1.4	-0.2	0.1	1.9	0.3	1.3	3.2	1.6
ZGAL_245	rnrB2	rnrB2 Ribonucleoside-diphosphate reductase, small subunit	-1.1	-0.4	3.3	-1.5	-0.8	2.9	-1.4	-0.6	3.1
ZGAL_245		rnrB2	-1.1	-0.4	3.3	-1.5	-0.8	2.9	-1.4	-0.6	3.1
ZGAL_2450	tigA	tigA Trigger factor	-1.5	-1.4	0.5	-1.4	-1.3	0.6	-0.4	-0.3	1.6
ZGAL_2456		T9SS-associated PG0189-like protein	0.4	0.4	0.9	1.7	1.7	2.1	3.0	3.0	3.5
ZGAL_2457	uppS	uppS Undecaprenyl pyrophosphate synthetase	0.7	1.3	2.2	1.7	2.3	3.1	1.4	2.0	2.9
ZGAL_2459		Outer membrane chaperone Skp (OmpH) family	0.7	-1.3	-1.7	1.7	-0.4	-0.7	1.9	-0.2	-0.6
ZGAL_2463		Hypothetical lipoprotein	-1.1	3.1	0.0	0.3	4.5	1.4	1.7	5.8	2.7
ZGAL_2465		Conserved hypothetical protein	0.0	0.9	1.5	0.1	1.0	1.5	0.1	0.9	1.5
ZGAL_2466	fabH3	fabH3 3-oxoacyl-[acyl-carrier-protein] synthase III	2.2	1.3	2.3	0.9	0.0	1.0	0.9	0.0	1.0
ZGAL_2477	hptA/ adkA	hptA/adkA Bifunctional protein Hypoxanthine-guanine phosphoribosyltransferase / Adenylate kinase	-1.3	-0.3	1.2	-1.1	-0.1	1.4	-1.0	0.1	1.5
ZGAL_2480		Hypothetical protein	-0.2	0.9	1.0	0.1	1.2	1.4	0.3	1.3	1.5
ZGAL_2481		Conserved hypothetical protein	-0.5	-0.7	0.0	-0.6	-0.9	-0.1	0.4	0.1	0.9
ZGAL_2482		Short-chain dehydrogenase/reductase	0.0	-0.1	1.6	-0.8	-0.8	0.9	-0.8	-0.8	0.8
ZGAL_2483		Conserved hypothetical protein	0.2	0.5	1.9	-0.4	-0.1	1.3	-0.8	-0.6	0.8
ZGAL_2485		T9SS SprF family protein	-0.3	0.8	0.0	0.3	1.5	0.7	0.8	2.0	1.1
ZGAL_2488	radC	radC DNA repair protein RadC	0.2	1.3	0.2	-0.6	0.4	-0.7	-0.9	0.1	-1.0
ZGAL_2491		Conserved hypothetical protein	1.5	0.6	0.0	0.9	0.0	-0.6	2.1	1.1	0.5
ZGAL_2492		Conserved hypothetical periplasmic protein	1.0	0.2	-0.2	1.5	0.7	0.3	3.0	2.2	1.8
ZGAL_2495		Rhomboid-like protease, family S54	-1.2	-0.5	0.8	-0.7	0.1	1.3	0.2	0.9	2.1
ZGAL_2497		Hypothetical lipoprotein	-0.6	1.9	1.9	-0.6	1.9	2.0	0.9	3.4	3.4
ZGAL_2498		SusD-like lipoprotein	0.4	1.5	0.9	0.5	1.5	0.9	1.7	2.7	2.1
ZGAL_2499		SusC-like TonB-dependent transporter	-1.7	0.8	0.3	-1.5	1.0	0.5	-0.5	2.0	1.5
ZGAL_25	rplI	rplI Ribosomal protein L9	-1.2	-1.6	0.8	-1.1	-1.6	0.9	0.1	-0.3	2.1
ZGAL_2501		Hypothetical membrane protein	-2.6	0.9	-0.1	-1.9	1.6	0.6	-2.1	1.3	0.4
ZGAL_2502		SusD-like lipoprotein	-2.7	0.6	0.0	-2.0	1.2	0.6	-2.0	1.3	0.7
ZGAL_2503		SusC-like TonB-dependent transporter	-1.3	1.2	-0.4	-1.1	1.3	-0.2	-0.9	1.6	0.0
ZGAL_2506	rpsL	rpsL Ribosomal protein S12	-0.1	-0.7	1.9	-0.2	-0.8	1.8	1.3	0.7	3.4
ZGAL_2507	rpsG	rpsG Ribosomal protein S7	-1.2	-1.8	0.4	-1.7	-2.3	-0.1	-0.1	-0.7	1.5
ZGAL_2508	fusA	fusA Translation elongation factor G	-0.3	-1.2	1.6	-1.1	-1.9	0.9	0.0	-0.8	2.0
ZGAL_2509	rpsJ	rpsJ Ribosomal protein S10	-1.2	-0.9	2.7	-1.1	-0.7	2.9	-0.6	-0.3	3.3
ZGAL_2510	rplC	rplC Ribosomal protein L3	-0.7	-1.7	1.6	-0.9	-2.0	1.3	-1.4	-2.4	0.9
ZGAL_2511	rplD	rplD Ribosomal protein L4	-2.2	-1.4	2.3	-1.9	-1.1	2.6	-1.7	-0.9	2.8
ZGAL_2512	rplW	rplW Ribosomal protein L23	-1.6	-1.1	1.3	-0.1	0.3	2.7	0.4	0.8	3.2
ZGAL_2514	rpsS	rpsS Ribosomal protein S19	-2.0	-1.4	1.4	-2.0	-1.3	1.4	-1.1	-0.4	2.4
ZGAL_2515	rplV	rplV Ribosomal protein L22	-2.1	-1.7	1.2	-2.5	-2.2	0.8	-1.5	-1.2	1.8
ZGAL_2518	rpmC	rpmC Ribosomal protein L29	-1.6	-1.6	1.9	-2.1	-2.1	1.4	-2.0	-2.0	1.5
ZGAL_2519	rpsQ	rpsQ Ribosomal protein S17	-1.6	-1.5	1.7	-2.6	-2.6	0.7	-2.6	-2.6	0.7

ZGAL_2520	rplN	rplN Ribosomal protein L14	-0.6	-1.5	1.8	-1.7	-2.6	0.7	-1.8	-2.7	0.6
ZGAL_2521	rplX	rplX Ribosomal protein L24	-1.8	-2.0	1.6	-2.5	-2.7	0.9	-2.7	-2.8	0.8
ZGAL_2522	rplE	rplE Ribosomal protein L5	-2.0	-1.7	2.0	-3.0	-2.7	1.0	-2.8	-2.4	1.3
ZGAL_2523	rpsN	rpsN Ribosomal protein S14	-2.7	-1.9	1.8	-2.5	-1.7	2.0	-1.9	-1.1	2.6
ZGAL_2524	rpsH	rpsH Ribosomal protein S8	-2.2	-1.2	2.3	-2.4	-1.4	2.2	-2.1	-1.1	2.5
ZGAL_2525	rplF	rplF Ribosomal protein L6	-1.6	-1.8	2.0	-1.9	-2.1	1.7	-1.9	-2.0	1.8
ZGAL_2526	rplR	rplR Ribosomal protein L18	-2.6	-1.5	2.6	-2.6	-1.6	2.5	-2.7	-1.6	2.5
ZGAL_2528	rpmD	rpmD Ribosomal protein L30	-2.7	-2.0	1.7	-3.4	-2.7	1.0	-3.2	-2.5	1.2
ZGAL_2529	rplO	rplO Ribosomal protein L15	-1.6	-0.8	2.2	-2.6	-1.8	1.2	-2.4	-1.7	1.3
ZGAL_2530	secY	secY Preprotein translocase, SecY subunit	-1.3	-1.4	1.8	-2.0	-2.0	1.1	-1.9	-2.0	1.2
ZGAL_2531	infA	infA Translation initiation factor IF-1	-1.4	-0.8	2.5	-1.3	-0.7	2.6	-1.2	-0.6	2.8
ZGAL_2532	rpsM	rpsM Ribosomal protein S13	-1.2	-0.1	3.7	-1.9	-0.8	3.0	-1.7	-0.5	3.2
ZGAL_2533	rpsK	rpsK Ribosomal protein S11	-1.2	-1.0	2.9	-2.4	-2.2	1.7	-2.2	-2.0	1.9
ZGAL_2534	rpsD	rpsD Ribosomal protein S4	-1.7	-0.7	3.0	-2.4	-1.4	2.3	-2.4	-1.5	2.2
ZGAL_2535	rpoA	rpoA DNA-dependent RNA polymerase, alpha subunit	-3.1	-1.5	2.7	-3.1	-1.6	2.7	-3.1	-1.6	2.7
ZGAL_2536	rplQ	rplQ Ribosomal protein L17	-2.4	-1.3	3.0	-3.3	-2.2	2.1	-3.3	-2.2	2.1
ZGAL_2537	carA	carA Carbamoyl-phosphate synthase small chain	-0.2	-0.4	1.9	-0.6	-0.8	1.5	-0.4	-0.7	1.6
ZGAL_2539	glgA	glgA Bacterial glycogen synthase, family GT5	-0.1	0.0	1.1	0.2	0.3	1.4	-0.4	-0.3	0.8
ZGAL_2541		DdaH family protein	-1.1	-0.3	0.9	-1.0	-0.2	1.0	-0.8	0.0	1.2
ZGAL_2545		Conserved membrane lipoprotein	-0.2	-3.9	-3.0	-0.3	-3.9	-3.0	2.1	-1.6	-0.7
ZGAL_2547		Two-component system - Sensor histidine kinase	2.4	-2.6	-1.4	1.5	-3.5	-2.3	2.8	-2.2	-1.0
ZGAL_2548		Two-component system - Response regulator	0.4	-5.4	-2.0	0.3	-5.5	-2.0	2.8	-3.0	0.4
ZGAL_2549		Hypothetical protein	0.3	-3.7	-1.3	0.6	-3.4	-1.0	3.2	-0.8	1.6
ZGAL_2550		Conserved membrane lipoprotein	1.4	-2.3	-0.9	3.3	-0.3	1.0	4.8	1.2	2.5
ZGAL_2551		Conserved hypotheical membrane protein	0.9	-1.4	-1.2	1.6	-0.7	-0.4	5.7	3.4	3.7
ZGAL_2552		Conserved membrane lipoprotein	0.3	-1.5	-0.2	0.2	-1.6	-0.3	5.7	3.9	5.1
ZGAL_2553		Hypothetical membrane protein	0.8	-0.9	-1.7	-0.2	-1.9	-2.7	4.7	2.9	2.2
ZGAL_2554		Conserved membrane lipoprotein	0.5	-0.8	-1.4	0.2	-1.1	-1.7	4.2	2.9	2.3
ZGAL_2555		Putative exported protein	1.3	-1.5	-1.4	1.8	-1.0	-0.9	8.2	5.4	5.5
ZGAL_2558		Putative protein	-1.0	2.3	1.6	0.6	3.9	3.2	1.7	5.0	4.3
ZGAL_2562	argS	argS Arginyl-tRNA synthetase	-1.6	-0.1	1.8	-1.6	-0.1	1.8	-0.9	0.6	2.6
ZGAL_2563		Conserved hypothetical protein	-1.0	0.5	1.3	-0.7	0.7	1.5	1.2	2.7	3.5
ZGAL_2564	thaA	thaA Threo-3-hydroxyaspartate ammonia-lyase (L-threo-3-hydroxyaspartate dehydratase)	-0.2	0.0	1.0	0.9	1.0	2.1	1.8	2.0	3.0
ZGAL_2569	ffh	ffh Signal recognition particle protein (SRP)	-0.4	-0.7	1.3	-0.8	-1.1	0.9	-0.7	-1.0	1.0
ZGAL_257		Cytochrome c-containing protein	2.8	-1.6	-2.2	2.3	-2.1	-2.7	2.1	-2.3	-2.9
ZGAL_2570	folD	folD Bifunctional methylenetetrahydrofolate dehydrogenase/cyclohydrolase	0.3	0.1	1.7	-0.6	-0.8	0.8	-0.6	-0.7	0.9
ZGAL_2571		Two-component system - Sensor histidine kinase	1.0	0.9	1.1	1.1	0.9	1.1	1.9	1.7	2.0
ZGAL_2575		Carbohydrate esterase, family CE1	0.1	0.8	1.4	-0.2	0.4	1.1	-1.1	-0.4	0.2
ZGAL_2579		Conserved hypothetical membrane protein	-0.1	0.5	1.2	0.1	0.7	1.4	-0.8	-0.2	0.6
ZGAL_2586		Conserved hypothetical protein	-1.1	0.3	1.6	-0.8	0.6	2.0	-0.7	0.7	2.1
ZGAL_2593		TetR-type transcriptional regulator	1.3	0.3	-0.7	0.9	0.0	-1.1	0.3	-0.7	-1.7
ZGAL_2599		Putative protein	-0.6	-0.1	-1.0	0.1	0.6	-0.3	2.2	2.7	1.8
ZGAL_26	rpsR	rpsR Ribosomal protein S18	-1.1	-1.0	1.2	-0.6	-0.5	1.7	0.2	0.4	2.6
ZGAL_2600	porA	porA Beta-porphyranase A, family GH16	-1.2	-1.2	-2.6	0.0	-0.1	-1.5	2.1	2.1	0.7
ZGAL_2603		Conserved hypothetical membrane protein	-2.8	0.4	3.0	-1.8	1.4	4.0	0.2	3.4	6.0
ZGAL_2604		Nuclease	-0.4	0.5	0.7	0.1	1.1	1.3	2.0	3.0	3.2
ZGAL_2605		Conserved hypothetical protein	3.7	2.6	2.4	3.3	2.3	2.0	0.9	-0.1	-0.4
ZGAL_2606		Conserved hypothetical protein	3.3	3.1	2.9	3.4	3.2	3.0	1.2	1.0	0.8
ZGAL_2607		Conserved hypothetical periplasmic protein	2.7	3.0	2.5	2.9	3.2	2.7	0.5	0.8	0.3
ZGAL_2608		Conserved hypothetical protein	4.0	2.7	2.2	2.6	1.3	0.8	0.3	-1.0	-1.5
ZGAL_2609		CsbD-like protein	3.4	4.7	5.9	2.8	4.0	5.2	0.8	2.1	3.3
ZGAL_2610		Conserved hypothetical protein	1.5	1.2	-0.1	0.9	0.6	-0.7	-0.1	-0.4	-1.7
ZGAL_2611		Conserved hypothetical protein	2.6	3.3	3.4	3.3	4.0	4.2	1.7	2.4	2.5
ZGAL_2612		Manganese/fer transporter	4.0	1.9	1.5	3.3	1.2	0.8	1.7	-0.4	-0.8
ZGAL_2613	pfp	pfp Diphosphate-fructose-6-phosphate 1-phosphotransferase	3.8	0.9	2.4	2.1	-0.9	0.7	0.9	-2.1	-0.5
ZGAL_2614	kdgK1	kdgK1 2-dehydro-3-deoxygluconokinase	4.0	1.5	3.6	3.4	0.8	3.0	2.8	0.2	2.4
ZGAL_2615		Acetoin(diacetyl) reductase	3.4	0.9	3.5	1.7	-0.9	1.7	1.4	-1.2	1.4
ZGAL_2616	exuT2	exuT2 Hexuronate transporter	3.6	0.8	2.0	2.7	-0.2	1.1	2.3	-0.5	0.7
ZGAL_2618	alyA2	alyA2 Alginate lyase, family PL7	4.7	1.7	2.9	3.5	0.5	1.7	3.1	0.1	1.3
ZGAL_2619		Conserved hypothetical membrane protein	5.5	1.3	2.4	4.0	-0.2	0.9	3.4	-0.8	0.3
ZGAL_2620		Alginate-specific SusD-like lipoprotein	4.7	0.6	1.4	3.3	-0.8	0.0	3.4	-0.7	0.1
ZGAL_2621		Alginate-specific SusC-like TonB-dependent transporter	4.8	1.1	1.8	4.7	1.0	1.6	5.0	1.3	2.0
ZGAL_2622		2-dehydro-3-deoxy-D-gluconate 6-dehydrogenase	3.4	0.6	1.8	2.4	-0.3	0.9	1.6	-1.2	0.0
ZGAL_2623	kdgF	kdgF Alginate degradation protein KdgF	7.1	1.8	3.0	5.1	-0.2	1.0	4.9	-0.4	0.7
ZGAL_2624	alyA3	alyA3 Alginate lyase, family PL17_2	6.7	0.3	1.0	6.3	-0.1	0.6	5.7	-0.6	0.1
ZGAL_2626		Xylose isomerase-like TIM barrel protein	3.9	-0.1	-0.8	3.3	-0.8	-1.4	3.0	-1.0	-1.6
ZGAL_2627		Conserved hypothetical protein	3.6	0.5	-0.3	3.2	0.1	-0.7	2.9	-0.1	-1.0
ZGAL_2628		Conserved hypothetical protein	3.8	0.5	-0.7	3.0	-0.3	-1.5	2.9	-0.4	-1.6
ZGAL_2629		Conserved hypothetical periplasmic protein	2.6	-0.7	-1.5	1.5	-1.8	-2.6	1.3	-2.0	-2.8
ZGAL_2634		Conserved hypothetical protein	5.1	-1.2	-1.6	5.8	-0.5	-0.9	3.3	-3.0	-3.4
ZGAL_2635		Hypothetical protein	2.1	-0.1	1.4	1.9	-0.3	1.2	1.5	-0.7	0.8
ZGAL_2637	gntK1	gntK1 Gluconokinase	3.1	-1.5	0.3	3.5	-1.0	0.8	3.6	-0.9	0.9

ZGAL_2638	iolC	iolC 5-dehydro-2-deoxygluconokinase	5.0	-0.2	0.2	5.1	-0.2	0.3	5.0	-0.3	0.1
ZGAL_2639		Possible dioxygenase	2.9	-0.4	-0.4	2.1	-1.2	-1.2	2.3	-0.9	-0.9
ZGAL_2642		conserved hypothetical membrane protein	-1.5	0.8	1.6	-0.3	2.0	2.8	-0.4	1.9	2.7
ZGAL_2643		Conserved hypothetical membrane protein	-2.0	0.4	1.6	-1.2	1.1	2.3	-1.2	1.2	2.4
ZGAL_2644		Conserved hypothetical membrane protein	-1.6	0.2	1.1	-0.6	1.2	2.2	-0.3	1.5	2.5
ZGAL_2645		Hypothetical membrane protein	-1.6	0.3	1.5	0.0	1.9	3.2	0.0	2.0	3.2
ZGAL_2646		Conserved hypothetical membrane protein	-1.9	-0.2	1.6	-0.3	1.4	3.2	-0.3	1.4	3.2
ZGAL_2647		Hypothetical protein	-2.3	0.3	1.6	-0.6	2.0	3.4	-0.7	1.8	3.2
ZGAL_2648		Conserved hypothetical protein	-0.6	0.3	1.3	-0.2	0.7	1.7	0.9	1.8	2.8
ZGAL_2649		Conserved hypothetical membrane protein	-0.7	-0.3	0.9	0.0	0.3	1.5	1.4	1.8	3.0
ZGAL_2650		TonB-like protein	-1.9	-0.3	1.2	-0.3	1.2	2.7	1.8	3.3	4.8
ZGAL_2651		Conserved hypothetical membrane protein	-1.2	0.7	2.3	-0.9	1.0	2.6	-0.8	1.1	2.7
ZGAL_2653		Putative protein	-0.9	0.0	0.0	0.0	0.9	0.9	0.9	1.8	1.8
ZGAL_2654		Conserved hypothetical protein	-1.7	0.7	2.0	-0.4	2.0	3.2	-0.3	2.1	3.4
ZGAL_2655		Conserved hypothetical protein	-1.7	0.8	2.3	0.1	2.6	4.1	-0.3	2.2	3.7
ZGAL_2656		Alpha/beta hydrolase-fold protein	-2.3	1.2	2.9	-1.2	2.3	3.9	-0.4	3.1	4.7
ZGAL_2657		Conserved hypothetical protein	-0.1	1.7	1.1	0.8	2.6	2.0	-0.1	1.6	1.0
ZGAL_2664		Beta-helix fold protein	-1.4	3.1	1.8	-1.6	2.9	1.6	-2.3	2.2	0.9
ZGAL_2665		Beta-helix fold protein containing CBM13	-1.0	3.6	2.4	-1.2	3.4	2.1	-2.1	2.5	1.3
ZGAL_267		SusC-like TonB-dependent transporter	1.9	-1.8	-1.4	1.8	-1.9	-1.5	1.9	-1.9	-1.5
ZGAL_2683		Conserved hypothetical membrane protein	-2.7	0.5	3.5	-0.6	2.6	5.6	1.3	4.5	7.5
ZGAL_2684		Hypothetical membrane protein	-2.7	1.5	0.0	-0.2	4.0	2.5	2.0	6.2	4.7
ZGAL_2685		Conserved hypothetical protein	-1.1	1.5	0.3	0.0	2.6	1.4	2.6	5.3	4.0
ZGAL_2686		Hypothetical membrane protein	0.1	0.6	-0.3	0.4	0.9	0.0	3.1	3.5	2.6
ZGAL_2689		Hypothetical membrane protein	-1.9	1.5	-2.2	0.2	3.6	0.0	2.3	5.7	2.1
ZGAL_269		One-component system sensor protein	0.9	0.2	-0.5	0.9	0.1	-0.5	0.5	-0.2	-0.9
ZGAL_2690		Conserved hypothetical periplasmic protein	-0.6	2.3	-0.5	0.6	3.5	0.7	2.9	5.8	3.0
ZGAL_2691		TonB-dependent Receptor	0.2	1.4	-0.2	1.3	2.5	0.9	3.5	4.7	3.1
ZGAL_2693		Conserved hypothetical protein	-1.5	1.1	2.4	0.2	2.8	4.1	1.1	3.7	5.0
ZGAL_2695		Hypothetical membrane protein	-0.4	0.0	1.3	1.1	1.5	2.8	1.0	1.4	2.7
ZGAL_2696	hsdS1	hsdS1 Type I restriction enzyme ZgaDI, S subunit	-2.3	1.1	1.8	-2.2	1.2	2.0	-2.4	0.9	1.7
ZGAL_27	rpsF	rpsF Ribosomal protein S6	-1.4	-0.8	1.7	-0.2	0.5	2.9	0.4	1.1	3.6
ZGAL_2702		Hypothetical protein	-1.4	1.1	0.5	-0.9	1.5	1.0	-0.5	1.9	1.4
ZGAL_2703		Ribbon-helix-helix fold protein	-2.1	-0.1	2.7	-1.1	0.9	3.8	-0.9	1.1	3.9
ZGAL_2705		Hypothetical membrane protein	-2.2	-0.5	0.4	-1.1	0.6	1.5	-0.7	1.0	1.9
ZGAL_2708	traP	traP Conjugative transposon proteinTraP	-1.4	-0.7	0.3	0.5	1.1	2.2	0.1	0.7	1.8
ZGAL_2709		Hypothetical protein	-1.1	0.4	2.4	-0.2	1.3	3.4	-0.5	1.0	3.0
ZGAL_271		SusC-like TonB-dependent transporter	0.5	1.1	0.2	0.7	1.2	0.4	-0.5	0.0	-0.8
ZGAL_2712		Hypothetical membrane protein	-1.5	1.0	1.7	-0.7	1.9	2.6	-0.7	1.8	2.5
ZGAL_2714		Saccharopine dehydrogenase (NADP(+), L-lysine-forming)	1.2	0.1	0.9	0.8	-0.3	0.5	0.7	-0.4	0.4
ZGAL_2716		Conserved hypothetical membrane protein	0.6	1.1	0.1	1.1	1.5	0.6	2.6	3.0	2.0
ZGAL_272		SusD-like lipoprotein	0.9	2.1	1.7	1.3	2.6	2.1	0.9	2.2	1.7
ZGAL_2725		Conserved hypothetical membrane protein	-2.8	0.9	-0.1	-0.3	3.4	2.4	1.5	5.2	4.2
ZGAL_2726		Conserved hypothetical membrane protein	1.7	-1.7	-0.1	2.2	-1.2	0.3	2.2	-1.2	0.4
ZGAL_2727	typA	typA GTP-binding protein TypA	-0.4	-1.2	0.8	-0.1	-0.9	1.0	0.7	-0.1	1.9
ZGAL_2728		Conserved hypothetical lipoprotein	2.9	0.0	-0.7	1.4	-1.5	-2.2	1.2	-1.6	-2.3
ZGAL_2734		TPR repeat-containing protein	0.4	-0.2	2.1	0.6	0.0	2.4	1.3	0.8	3.1
ZGAL_2735		Possible TonB-dependent Receptor	-0.2	-0.2	2.5	0.1	0.0	2.7	0.5	0.4	3.1
ZGAL_2736		Monohaem cytochrome C protein	0.2	1.3	0.6	1.1	2.3	1.6	-0.4	0.7	0.0
ZGAL_2740		Conserved hypothetical periplasmic protein	-2.0	0.6	0.3	-0.9	1.7	1.4	0.2	2.9	2.5
ZGAL_2741		Amidohydrolase	0.3	1.0	-0.1	1.0	1.6	0.6	1.6	2.2	1.2
ZGAL_2742		Conserved hypothetical periplasmic protein	1.4	-1.1	-0.2	0.0	-2.5	-1.5	-1.4	-3.9	-3.0
ZGAL_2747		Conserved hypothetical lipoprotein	0.3	4.5	4.0	2.5	6.6	6.1	3.9	8.1	7.6
ZGAL_2749	secD	secD Protein-export membrane protein secD	-1.1	-0.3	1.5	-0.9	-0.1	1.7	-0.2	0.7	2.5
ZGAL_2754	lgtA	lgtA Prolipoprotein diacylglyceryl transferase	0.1	-0.3	1.3	0.5	0.1	1.7	0.5	0.1	1.7
ZGAL_2756		Conserved hypothetical protein	5.6	1.4	1.4	5.7	1.5	1.5	4.3	0.1	0.1
ZGAL_2757		NAD dependent aldehyde dehydrogenase	5.9	1.0	0.9	5.3	0.3	0.3	4.0	-0.9	-1.0
ZGAL_2761		Conserved hypothetical periplasmic protein	-1.7	1.0	0.4	0.6	3.3	2.7	2.0	4.7	4.1
ZGAL_2762		Conserved hypothetical periplasmic protein	0.2	0.8	0.7	1.6	2.2	2.1	3.4	4.0	3.9
ZGAL_2763		Conserved hypothetical periplasmic protein	1.0	-1.3	-0.9	1.4	-0.9	-0.4	1.0	-1.3	-0.8
ZGAL_2764		Conserved hypothetical lipoprotein	3.2	-1.2	-1.2	3.2	-1.2	-1.3	2.0	-2.4	-2.4
ZGAL_2768	rpsT	rpsT Ribosomal protein S20	-1.6	0.2	3.7	0.1	2.0	5.5	0.9	2.7	6.2
ZGAL_2769		Conserved hypothetical membrane protein	0.1	1.0	-0.1	0.7	1.6	0.5	1.1	2.0	0.9
ZGAL_2771	rho	rho Transcription termination factor Rho	0.5	0.6	0.3	1.3	1.5	1.2	1.1	1.3	0.9
ZGAL_2772		Conserved hypothetical membrane protein	-0.6	1.3	2.3	0.2	2.1	3.1	0.2	2.1	3.1
ZGAL_2783		Conserved hypothetical membrane protein	1.9	-0.4	-0.9	1.8	-0.5	-1.0	0.7	-1.6	-2.1
ZGAL_2789	apt	apt Adenine phosphoribosyltransferase	2.3	-0.1	-0.7	1.7	-0.7	-1.3	1.2	-1.2	-1.8
ZGAL_2795		Rieske [2Fe-2S] iron-sulfur protein	-0.1	0.7	0.7	0.5	1.2	1.2	1.6	2.3	2.3
ZGAL_2796		Thioredoxin family protein	0.7	-1.0	-0.3	1.4	-0.3	0.3	1.9	0.3	0.9
ZGAL_2797	apbE2	apbE2 Thiamine biosynthesis protein apbE	0.0	-1.2	-0.4	1.1	-0.1	0.7	2.1	0.9	1.7
ZGAL_28		Two-component system - Response regulator	-1.1	0.6	-0.8	-0.3	1.4	-0.1	1.4	3.1	1.7
ZGAL_2801		Alpha/beta hydrolase-fold protein	1.7	0.8	1.8	1.9	1.0	2.0	1.4	0.6	1.6
ZGAL_2803		Conserved hypothetical lipoprotein	-0.5	0.0	-0.4	-0.1	0.4	0.0	1.2	1.7	1.3

ZGAL_2804	purU	purU Formyltetrahydrofolate deformylase	-0.8	0.7	0.0	0.1	1.6	0.9	0.5	1.9	1.3
ZGAL_2805		Conserved hypothetical protein	2.4	0.6	0.3	1.9	0.0	-0.3	2.5	0.6	0.3
ZGAL_2809		Conserved hypothetical lipoprotein	1.5	-1.8	-1.3	1.7	-1.6	-1.1	0.7	-2.6	-2.2
ZGAL_281		Conserved hypothetical lipoprotein	-1.4	-0.4	0.7	1.0	2.0	3.1	-0.1	0.9	2.1
ZGAL_2810		Family C56 non-peptidase protein	1.4	-1.2	-1.5	1.3	-1.2	-1.6	0.9	-1.6	-2.0
ZGAL_2816	crcB	crcB Protein CrcB	-1.0	0.1	0.7	1.1	2.2	2.7	2.1	3.2	3.7
ZGAL_2822		NAD(P)-dependent epimerase/dehydratase	3.0	0.2	-0.5	2.6	-0.3	-0.9	1.1	-1.8	-2.4
ZGAL_2823	grpE	grpE Co-chaperone HSP-70 protein	-2.2	-0.9	0.9	-1.0	0.3	2.1	0.5	1.8	3.5
ZGAL_2824	dnaJ	dnaJ Co-chaperone protein dnaJ	-1.0	-1.5	0.1	-0.8	-1.3	0.3	0.6	0.1	1.7
ZGAL_2830		Conserved hypothetical lipoprotein	-0.1	0.3	-1.3	2.0	2.4	0.8	1.5	1.9	0.3
ZGAL_2834	cspA3	cspA3 Cold shock protein CspA	-1.7	0.6	3.3	-0.2	2.1	4.8	0.4	2.6	5.4
ZGAL_2842	mdlA	mdlA Multidrug resistance-like, ATP-binding/permease	1.5	-0.3	0.9	1.4	-0.4	0.8	0.8	-1.0	0.2
ZGAL_2843	nusB	nusB N utilization substance protein B	-1.3	0.7	2.8	-0.7	1.2	3.4	0.4	2.3	4.5
ZGAL_2848	pepT	pepT Tripeptide aminopeptidase, family M20	-0.7	0.4	-0.1	-0.9	0.3	-0.2	0.1	1.3	0.8
ZGAL_2849		TonB-dependent Receptor	-0.9	2.6	-1.9	-0.5	2.9	-1.6	0.1	3.5	-1.0
ZGAL_285		Hypothetical membrane protein	-0.6	1.0	-0.1	0.0	1.5	0.5	1.3	2.8	1.8
ZGAL_2850		Conserved hypothetical periplasmic protein	-2.0	1.9	1.5	-0.1	3.9	3.4	1.8	5.7	5.3
ZGAL_2851	pyrD	pyrD Dihydroorotate dehydrogenase	-0.9	-0.2	1.5	0.0	0.7	2.4	0.4	1.1	2.8
ZGAL_2852		Conserved hypothetical periplasmic protein	-0.2	-0.1	0.5	0.1	0.2	0.8	0.5	0.6	1.2
ZGAL_2856		Conserved hypothetical lipoprotein	2.2	-0.9	-0.8	0.4	-2.7	-2.6	-0.8	-3.9	-3.8
ZGAL_286		Conserved hypothetical protein	-1.8	0.3	-1.6	-0.8	1.3	-0.6	0.2	2.3	0.4
ZGAL_2861	guaB	guaB Inosine-5'-monophosphate dehydrogenase	-0.2	-0.3	2.3	-0.6	-0.7	1.9	-0.2	-0.3	2.3
ZGAL_2864	lysA	lysA Diaminopimelate decarboxylase	-3.1	0.9	2.3	-3.0	1.0	2.4	-3.1	0.9	2.4
ZGAL_2867		Conserved hypothetical periplasmic protein	2.7	-0.1	0.0	2.6	-0.3	-0.2	0.7	-2.2	-2.1
ZGAL_2868	ald1	ald1 Alanine dehydrogenase	1.3	-0.9	-1.6	1.1	-1.0	-1.8	-0.2	-2.3	-3.1
ZGAL_287		Conserved hypothetical protein	-1.2	1.0	0.5	-0.2	2.0	1.5	-0.1	2.1	1.6
ZGAL_2872		TonB-dependent Receptor	1.9	-0.8	-1.6	0.8	-1.9	-2.7	1.4	-1.3	-2.1
ZGAL_2874		Conserved hypothetical protein	1.7	-2.5	-3.1	2.6	-1.6	-2.2	2.5	-1.7	-2.2
ZGAL_2876		Small heat shock protein	2.5	-1.3	2.4	3.6	-0.2	3.5	4.2	0.5	4.2
ZGAL_2880		ABC importer, permease component	1.8	-1.7	1.5	2.2	-1.4	1.8	2.4	-1.2	2.0
ZGAL_2881		ABC transporter, ATPase component	0.4	-3.0	0.1	1.0	-2.4	0.7	1.6	-1.8	1.3
ZGAL_2882		Conserved hypothetical protein	-0.4	0.6	-0.2	0.8	1.7	1.0	2.0	2.9	2.1
ZGAL_2888		Conserved hypothetical protein	-1.2	1.7	1.4	0.7	3.6	3.3	1.8	4.8	4.5
ZGAL_289		Hypothetical membrane protein	-1.9	0.2	-0.2	-0.5	1.5	1.1	-0.1	2.0	1.6
ZGAL_2891		Conserved hypothetical protein	-2.3	-0.3	2.1	-2.0	0.1	2.5	-1.1	1.0	3.4
ZGAL_2892	ctaA	ctaA Cytochrome aa3-controlling protein	-1.9	-0.4	0.6	-1.7	-0.2	0.8	-1.0	0.4	1.5
ZGAL_2893		T9SS-associated PG1058-like protein	0.6	1.1	0.7	1.2	1.7	1.3	2.0	2.6	2.1
ZGAL_2894		T9SS SprF family protein	0.4	0.4	-0.3	0.8	0.8	0.1	1.6	1.6	1.0
ZGAL_2895		Conserved hypothetical protein	0.1	2.7	2.4	1.7	4.3	4.0	2.7	5.3	5.0
ZGAL_2896		T9SS SprF family protein	0.3	0.9	1.4	0.9	1.5	2.0	0.5	1.1	1.6
ZGAL_2898	cca	cca Multifunctional CCA protein	0.0	-0.4	0.5	-0.1	-0.4	0.5	0.7	0.4	1.3
ZGAL_2902		Glycosyltransferase, family GT2	-0.6	1.1	1.2	-0.5	1.2	1.3	0.6	2.3	2.4
ZGAL_2903	waaE	waaE Lipopolysaccharide core biosynthesis glycosyltransferase, family GT2	-1.9	-0.9	-1.0	-0.7	0.2	0.2	0.9	1.8	1.8
ZGAL_2904	dapD	dapD 2,3,4,5-Tetrahydropyridine-2,6-dicarboxylate N-succinyltransferase	-2.6	-0.2	1.9	-2.6	-0.2	2.0	-2.2	0.2	2.4
ZGAL_2905	yqgF	yqgF Holliday junction resolvase	-1.2	-0.6	2.0	-0.8	-0.2	2.4	0.0	0.6	3.2
ZGAL_2906	defA	defA Formylmethionine deformylase	-0.4	-0.4	1.3	-0.4	-0.4	1.2	0.1	0.1	1.8
ZGAL_2907		Conserved hypothetical protein	-0.4	-0.1	3.2	1.3	1.6	4.8	2.0	2.3	5.6
ZGAL_2909		Two-component system - Sensor histidine kinase	1.1	-0.8	-1.5	6.7	4.8	4.1	2.3	0.3	-0.4
ZGAL_2910		Two-component system - Response regulator, receiver domain	0.1	0.1	0.6	3.7	3.7	4.1	1.0	1.0	1.4
ZGAL_2916		Hypothetical lipoprotein	-1.8	0.4	3.0	-0.3	1.9	4.5	-0.1	2.1	4.7
ZGAL_2920	gnlA	gnlA Gluconolactonase	-0.7	0.0	1.6	-0.5	0.2	1.8	-0.9	-0.2	1.4
ZGAL_2922	mazG	mazG Nucleoside triphosphate pyrophosphohydrolase MazG	-0.5	-0.6	1.6	-1.3	-1.4	0.9	-0.8	-0.9	1.3
ZGAL_2923	norM1	norM1 Multidrug resistance protein	-1.1	-0.7	0.9	-0.9	-0.5	1.1	-0.6	-0.2	1.4
ZGAL_2924		Conserved hypothetical protein	-0.8	0.2	1.1	-0.5	0.5	1.4	-0.1	1.0	1.8
ZGAL_2926		Glycosyltransferase, family GT83	-0.6	0.4	-0.4	0.1	1.1	0.3	0.7	1.7	0.9
ZGAL_293	crpA1	crpA1 Catabolite gene activator	1.1	0.9	-1.0	1.9	1.7	-0.1	3.0	2.8	0.9
ZGAL_2930	ohrB	ohrB Organic hydroperoxide resistance protein ohrB	3.5	0.1	1.9	2.9	-0.5	1.3	0.0	-3.5	-1.7
ZGAL_2931	mroA2	mroA2 Aldose 1-epimerase	1.4	-0.3	-0.2	0.8	-0.9	-0.9	0.1	-1.6	-1.6
ZGAL_2932	msrA3	msrA3 Peptide methionine sulfoxide reductase	2.6	-0.1	-1.4	1.6	-1.2	-2.4	0.9	-1.8	-3.0
ZGAL_2935		Putative protein	-1.2	-0.1	-1.7	2.0	3.1	1.5	1.3	2.5	0.9
ZGAL_2936		Conserved hypothetical periplasmic protein	-2.5	1.6	-1.9	1.9	6.0	2.5	0.8	4.9	1.4
ZGAL_2938		Two-component system - Sensor histidine kinase	0.1	1.1	-1.1	1.6	2.6	0.4	1.3	2.3	0.1
ZGAL_294		Conserved hypothetical membrane protein	-0.3	1.4	0.2	1.7	3.3	2.2	2.8	4.4	3.2
ZGAL_2940		Two-component system - Sensor histidine kinase	-0.5	1.1	-1.4	0.5	2.1	-0.4	0.7	2.3	-0.2
ZGAL_2941		Two-component system - Sensor histidine kinase	0.0	1.3	-1.3	2.5	3.7	1.2	1.2	2.4	-0.2
ZGAL_2944		Conserved hypothetical protein	-0.2	0.6	2.8	1.1	2.0	4.2	2.1	3.0	5.1
ZGAL_2948		ABC transporter, ATPase component	-0.5	-0.1	1.7	-0.7	-0.3	1.5	-0.7	-0.3	1.5
ZGAL_295		Heavy metal binding protein	-1.2	1.5	0.6	1.3	3.9	3.0	2.9	5.6	4.7
ZGAL_2950	pssA	pssA phosphatidylserine synthase	1.4	0.2	-0.5	0.5	-0.7	-1.4	0.0	-1.2	-1.9
ZGAL_2951	lptB	lptB Lipopolysaccharide-specific ABC transporter, ATPase component	1.7	-0.4	0.1	1.3	-0.8	-0.3	0.2	-1.9	-1.4

ZGAL_2956		Conserved hypothetical protein	1.9	1.1	-1.3	1.0	0.2	-2.3	0.4	-0.4	-2.9
ZGAL_296	glpE2	glpE2 Thiosulfate sulfurtransferase	-0.7	1.8	1.0	1.9	4.4	3.6	3.4	6.0	5.1
ZGAL_2960	rluF	rluF Ribosomal large subunit pseudouridine synthase F	-1.5	-0.1	0.6	-1.3	0.1	0.8	-0.5	1.0	1.6
ZGAL_2961		Conserved hypothetical protein	-0.5	0.4	-0.2	0.1	1.0	0.4	2.2	3.1	2.5
ZGAL_2962		Conserved hypothetical membrane protein	-0.1	1.0	-0.6	0.7	1.8	0.1	2.7	3.8	2.1
ZGAL_2968		MoxR-like ATPase	1.5	-0.3	-0.3	0.7	-1.0	-1.1	0.1	-1.6	-1.7
ZGAL_297		Beta-lactamase hydrolase-like protein	0.6	1.7	0.2	2.1	3.2	1.8	3.4	4.5	3.0
ZGAL_2971		Thiol-disulfide oxidoreductase	2.0	1.2	0.3	1.7	0.9	0.0	0.8	0.0	-1.0
ZGAL_2972	crtZ	crtZ Beta-carotene hydroxylase	2.3	2.5	1.8	2.6	2.8	2.2	1.2	1.4	0.8
ZGAL_2973	crtB	crtB Phytoene synthetase	2.3	2.1	1.1	1.2	1.0	0.1	1.0	0.8	-0.1
ZGAL_2974	crtI	crtI Phytoene dehydrogenase	2.4	1.9	1.4	1.8	1.3	0.8	1.0	0.4	0.0
ZGAL_2975		MerR-type transcriptional regulator	2.6	1.0	0.0	0.9	-0.7	-1.7	0.7	-0.9	-1.9
ZGAL_2978		Two-component system - Response regulator, receiver domain	3.6	5.7	-2.2	7.8	9.9	2.0	4.8	6.9	-1.0
ZGAL_2979		Heme NO Binding protein	-0.4	2.0	-1.8	2.6	5.0	1.1	0.4	2.8	-1.0
ZGAL_2980		Two-component system - Sensor histidine kinase	-0.6	1.6	-1.7	1.2	3.5	0.1	0.9	3.1	-0.2
ZGAL_2981		Conserved hypothetical protein	-0.1	1.4	-1.0	0.5	2.0	-0.4	1.8	3.2	0.8
ZGAL_2982		Two-component system - Sensor histidine kinase	-1.0	2.5	1.2	0.1	3.7	2.3	2.2	5.7	4.3
ZGAL_2983		Histidine-containing phosphotransfer protein	-1.4	2.4	0.7	0.6	4.3	2.7	1.9	5.7	4.0
ZGAL_2984		Two-component system - Response regulator	-0.1	0.8	-0.9	0.0	1.0	-0.7	1.4	2.4	0.7
ZGAL_2985		TPR repeats protein	-0.3	0.6	-1.0	1.5	2.4	0.9	2.5	3.4	1.9
ZGAL_2988		Conserved hypothetical membrane protein	0.9	0.7	-1.6	4.5	4.4	2.1	2.3	2.2	-0.2
ZGAL_2989		Conserved hypothetical membrane protein	1.6	4.5	1.9	4.8	7.7	5.1	6.5	9.4	6.8
ZGAL_2990		Glycosyltransferase, family GT4	2.1	2.3	2.4	4.8	4.9	5.1	6.3	6.4	6.6
ZGAL_2991		Dolichol-phosphate mannose synthase, family GT2	1.5	1.9	2.1	3.7	4.1	4.3	5.0	5.4	5.6
ZGAL_2992		TetR-type transcriptional regulator	4.4	3.5	1.0	1.8	0.9	-1.6	1.6	0.7	-1.8
ZGAL_2993		Carboxymuconolactone decarboxylase family protein	6.4	3.9	-0.1	0.8	-1.7	-5.8	0.9	-1.6	-5.7
ZGAL_2994		Hypothetical protein	6.9	6.3	2.6	2.2	1.6	-2.1	1.3	0.7	-3.0
ZGAL_2995		DSBA thioredoxin family protein	3.8	1.5	-0.3	0.0	-2.3	-4.2	0.4	-1.9	-3.8
ZGAL_2998		Universal stress protein	2.4	-0.6	-3.3	1.7	-1.3	-4.0	1.0	-2.1	-4.7
ZGAL_2999		Putative protein	2.5	0.4	-2.3	2.3	0.3	-2.5	1.3	-0.8	-3.5
ZGAL_3000		Conserved hypothetical protein	2.2	0.2	-2.3	2.5	0.6	-2.0	1.3	-0.6	-3.2
ZGAL_3006		Anti-sigma factor	-0.3	0.3	-1.0	1.0	1.6	0.3	1.0	1.6	0.3
ZGAL_3007		RNA polymerase ECF-type sigma factor	-0.4	0.7	1.3	0.3	1.4	2.0	-0.8	0.4	0.9
ZGAL_3008	kblA1	kblA1 Glycine C-acetyltransferase	1.7	-1.2	0.1	3.0	0.1	1.4	1.7	-1.2	0.1
ZGAL_3009		NAD-dependent epimerase/dehydratase	-0.2	-2.1	-0.2	2.4	0.5	2.3	0.4	-1.6	0.3
ZGAL_302		Globin-like protein	1.7	0.4	0.3	1.9	0.6	0.5	1.0	-0.3	-0.4
ZGAL_3021		Conserved hypothetical membrane protein	-0.7	-0.1	2.2	-0.3	0.2	2.6	0.3	0.9	3.2
ZGAL_3023	accA	accA Acetyl-coenzyme A carboxylase, carboxyl transferase subunit alpha	-0.9	-0.2	0.5	-0.6	0.0	0.8	-0.1	0.6	1.3
ZGAL_3031		AraC-type transcriptional regulator	2.1	-0.8	-1.8	0.6	-2.2	-3.3	0.8	-2.1	-3.1
ZGAL_3032		Hypothetical periplasmic protein	-1.7	1.2	0.5	-0.3	2.5	1.9	1.7	4.6	3.9
ZGAL_3033		Hypothetical periplasmic protein	0.0	-0.8	0.2	0.3	-0.6	0.5	2.0	1.2	2.2
ZGAL_3037	rpmI	rpmI Ribosomal protein L35	-1.1	0.1	0.7	-0.5	0.6	1.2	-0.4	0.7	1.3
ZGAL_3038	infC	infC Translation initiation factor IF-3	0.2	0.0	2.1	0.0	-0.1	1.9	0.4	0.2	2.3
ZGAL_3039	thrS	thrS Threonyl-tRNA synthetase	-1.1	-0.8	1.7	-0.6	-0.4	2.2	0.1	0.3	2.9
ZGAL_304	cysI	cysI Sulfite reductase [NADPH] hemoprotein beta-component	1.9	-0.5	4.0	2.5	0.0	4.6	1.2	-1.2	3.4
ZGAL_3047		Conserved azurin-containing protein	1.3	-0.5	-0.5	0.8	-1.1	-1.1	-0.4	-2.3	-2.3
ZGAL_305	cysJ	cysJ Sulfite reductase [NADPH] flavoprotein alpha-component	2.4	-0.9	5.4	2.1	-1.2	5.0	1.4	-1.9	4.3
ZGAL_3054		Putative membrane protein	-2.0	0.3	0.5	-0.4	1.9	2.1	0.2	2.5	2.7
ZGAL_3055		RNA polymerase ECF-type sigma factor	-2.3	0.9	3.0	-0.8	2.4	4.4	0.0	3.2	5.2
ZGAL_3057		Two-component system - Sensor histidine kinase	-1.1	0.6	1.3	-0.1	1.6	2.3	-0.1	1.6	2.3
ZGAL_3059		Two-component system - Response regulator	-1.4	0.8	0.1	-0.5	1.8	1.1	0.1	2.3	1.6
ZGAL_306		Peroxiredoxin	2.9	-1.9	3.4	2.9	-2.0	3.3	2.3	-2.5	2.8
ZGAL_3064		SusC-like TonB-dependent Transducer	-1.2	1.3	1.4	-0.4	2.0	2.2	0.2	2.7	2.8
ZGAL_3065		SusD-like lipoprotein	-1.8	0.6	1.4	-0.9	1.5	2.3	-0.5	1.9	2.7
ZGAL_3066		Chitin-binding lectin, family GH18	-1.2	0.9	1.4	-0.8	1.3	1.8	-0.3	1.7	2.3
ZGAL_3067		Hypothetical protein	-1.6	1.0	2.3	-0.8	1.9	3.1	-0.5	2.2	3.4
ZGAL_3074		Hypothetical protein	-1.6	0.5	1.2	-0.5	1.6	2.4	-0.7	1.4	2.2
ZGAL_3084		Hypothetical protein	-0.2	0.3	3.4	0.1	0.5	3.6	-0.6	-0.2	2.9
ZGAL_3085		Hypothetical protein	-0.4	1.0	1.6	0.3	1.7	2.3	0.4	1.8	2.4
ZGAL_3086		FMN / Fe-S cluster binding protein	-0.5	2.4	2.8	-0.7	2.1	2.5	-1.6	1.3	1.6
ZGAL_3093	traK	traK Conjugative transposon protein TraK	-1.3	0.3	1.5	1.0	2.5	3.8	2.6	4.1	5.3
ZGAL_3095		Hypothetical membrane protein	-1.7	-0.8	0.9	-0.8	0.1	1.8	-0.2	0.7	2.4
ZGAL_3096		Hypothetical membrane protein	-0.7	1.6	3.1	0.4	2.6	4.1	-0.3	2.0	3.5
ZGAL_3099		Metallopeptidase, family M23	-1.3	-0.4	1.1	-0.6	0.2	1.8	-0.2	0.7	2.2
ZGAL_3103	traN	traN Conjugative transposon protein TraN	-0.5	0.7	1.3	0.3	1.6	2.1	0.6	1.8	2.4
ZGAL_3112		Anti-sigma factor	-0.9	0.9	1.3	-0.2	1.6	2.0	0.5	2.3	2.7
ZGAL_3129		Conserved hypothetical periplasmic protein	0.0	0.0	1.8	-0.3	-0.3	1.5	-0.3	-0.3	1.5
ZGAL_3132	rocD	rocD Ornithine aminotransferase	0.7	-0.1	1.7	0.1	-0.7	1.2	0.0	-0.8	1.1
ZGAL_3133		Conserved hypothetical membrane protein	0.2	1.0	1.5	-0.1	0.7	1.2	-0.5	0.4	0.9
ZGAL_3137		Conserved hypothetical lipoprotein	1.5	-0.5	-0.4	0.7	-1.3	-1.1	0.3	-1.7	-1.6
ZGAL_3138	iscS	iscS Cysteine desulfurase	-1.2	0.3	2.1	-1.1	0.4	2.1	-1.2	0.3	2.0

ZGAL_3141		Metallopeptidase, family M23	-0.5	-0.1	1.2	-0.9	-0.5	0.7	-0.3	0.1	1.3
ZGAL_3142		Conserved hypothetical protein	-1.2	-0.1	1.4	-0.5	0.6	2.2	0.5	1.6	3.2
ZGAL_3143		Conserved hypothetical protein	-1.2	0.3	1.2	-0.7	0.8	1.7	-0.1	1.5	2.3
ZGAL_3150	dagA3	dagA3 3,6-anhydro-D-galactosidase, family GH127	1.7	0.3	-0.8	1.1	-0.3	-1.4	1.4	-0.1	-1.2
ZGAL_3154	dauC	dauC 2-Dehydro-3-deoxygalactonokinase	-0.5	0.2	0.8	0.1	0.8	1.3	-0.8	-0.2	0.4
ZGAL_316		Alpha-glucosidase, family GH97	1.8	-0.1	-1.2	0.7	-1.1	-2.3	0.5	-1.3	-2.4
ZGAL_3161		Carbohydrate kinase	1.6	0.9	0.5	1.9	1.2	0.8	1.8	1.2	0.8
ZGAL_3162		Conserved hypothetical oxydoreductase	1.9	0.9	0.0	1.0	0.1	-0.8	0.5	-0.5	-1.3
ZGAL_3164		Cytochrome c-containing lipoprotein	2.3	1.5	0.8	1.7	1.0	0.3	1.0	0.3	-0.4
ZGAL_3165		Conserved hypothetical membrane protein	1.8	1.6	1.4	0.9	0.7	0.5	1.3	1.1	0.9
ZGAL_3166		Conserved hypothetical protein	3.3	2.3	1.9	3.1	2.1	1.8	2.5	1.5	1.1
ZGAL_3167		Conserved hypothetical protein	2.7	1.6	1.6	0.7	-0.4	-0.4	1.2	0.1	0.1
ZGAL_3170		Xylose isomerase-like TIM barrel protein	2.9	1.4	1.7	1.5	0.0	0.4	1.2	-0.3	0.1
ZGAL_3171		NAD(P)-dependent oxidoreductase	2.3	0.9	0.5	1.7	0.4	0.0	1.2	-0.1	-0.6
ZGAL_3172	fclA	fclA GDP-L-fucose synthetase	-1.1	-0.6	1.8	-1.6	-1.1	1.3	-1.3	-0.7	1.7
ZGAL_3173	gmdA	gmdA GDP-mannose 4,6-dehydratase	-1.5	-1.1	1.0	-1.5	-1.2	0.9	-0.9	-0.6	1.5
ZGAL_3177		FAD-dependent GMC oxidoreductase, family AA3	0.5	0.3	0.9	1.4	1.2	1.8	0.6	0.4	1.0
ZGAL_3178		Conserved hypothetical membrane protein	0.3	0.5	1.6	0.6	0.9	1.9	-0.2	0.1	1.2
ZGAL_3179		Xylose isomerase-like TIM barrel protein	0.1	0.1	1.5	-0.2	-0.2	1.3	-1.0	-1.0	0.4
ZGAL_3183	dssA	dssA Sheath polysaccharide lyase, family PL9_4	-0.7	0.2	-0.3	0.2	1.1	0.6	2.1	2.9	2.5
ZGAL_3187		Integron-related Integrase	0.7	1.4	-0.9	1.1	1.7	-0.6	1.4	2.1	-0.2
ZGAL_3188		Conserved hypothetical lipoprotein	-0.4	0.5	3.0	-0.1	0.8	3.3	0.5	1.4	4.0
ZGAL_3189		TonB-dependent Receptor	0.0	0.5	2.3	0.4	0.8	2.6	0.5	0.9	2.7
ZGAL_3190		Fur-type transcriptional regulator	-0.9	1.0	3.1	-0.5	1.4	3.6	-0.8	1.1	3.2
ZGAL_3191		Conserved hypothetical membrane protein	-0.4	-0.4	1.8	-0.6	-0.6	1.5	-0.5	-0.5	1.7
ZGAL_3193		Hypothetical protein	-1.0	0.9	1.5	-0.5	1.5	2.1	-0.6	1.3	1.9
ZGAL_3194		Transposase, family 20	1.3	-0.8	-1.8	1.2	-1.0	-1.9	0.7	-1.5	-2.4
ZGAL_3196		Hypothetical protein	-1.6	0.6	1.2	-1.2	1.1	1.7	-1.1	1.2	1.8
ZGAL_3200		Conserved hypothetical protein	-0.1	0.8	0.1	0.8	1.6	0.9	1.0	1.8	1.1
ZGAL_3202		Short-chain dehydrogenase/reductase	-0.2	1.0	0.1	1.1	2.3	1.4	1.7	2.9	1.9
ZGAL_3203		Hypothetical protein	0.9	1.9	2.6	1.7	2.7	3.5	1.2	2.2	3.0
ZGAL_3208		Oxidoreductase complex, membrane subunit	-2.7	2.0	1.0	-1.1	3.6	2.6	-0.1	4.6	3.7
ZGAL_3209		Oxidoreductase complex, iron-sulfur subunit	-2.3	2.9	2.0	-1.2	4.0	3.1	0.2	5.5	4.5
ZGAL_3210		Diheme cytochrome c	-3.0	2.8	1.8	-1.4	4.4	3.4	0.7	6.5	5.5
ZGAL_3211	napB	napB Diheme cytochrome c NapB	-2.4	1.9	0.5	-1.0	3.4	2.0	1.1	5.5	4.1
ZGAL_3212	napA	napA Periplasmic nitrate reductase, catalytic subunit	-3.2	0.1	0.1	-1.9	1.4	1.4	-0.3	3.0	3.0
ZGAL_3213		Conserved hypothetical protein	-2.9	0.4	1.5	-3.0	0.3	1.5	0.1	3.4	4.5
ZGAL_3214	moeA1	moeA1 Molybdopterin biosynthesis protein	-2.9	-0.3	0.3	-0.8	1.8	2.5	0.4	3.0	3.7
ZGAL_3215	modE	modE LysR-type transcriptional regulator	-2.5	1.0	1.4	0.2	3.8	4.2	1.5	5.1	5.5
ZGAL_3216	moaE2	moaE2 Molybdopterin synthase, large subunit	-2.2	1.1	0.8	0.3	3.5	3.3	2.2	5.4	5.2
ZGAL_3217		Conserved hypothetical periplasmic protein	-2.1	1.1	1.2	-0.5	2.8	2.9	0.8	4.1	4.2
ZGAL_3220		LuxR-type transcriptional regulator	-1.1	1.3	1.5	-0.1	2.3	2.5	0.6	3.0	3.2
ZGAL_3229		Conserved hypothetical membrane protein	-1.5	0.4	1.0	0.3	2.2	2.8	0.9	2.9	3.4
ZGAL_3230		Crp/Fnr-type transcriptional regulator	-1.6	0.8	2.3	-0.4	2.0	3.5	0.5	2.9	4.4
ZGAL_3232		Conserved hypothetical protein	0.0	0.3	-0.3	-0.3	0.0	-0.6	1.1	1.3	0.7
ZGAL_3248		Conserved hypothetical protein	-2.6	-0.3	-0.3	-1.2	1.1	1.1	0.3	2.6	2.6
ZGAL_3249		Conserved hypothetical protein	-1.5	0.5	1.2	-0.1	1.9	2.7	0.9	2.9	3.6
ZGAL_3250	nadR	nadR Nicotinamide-nucleotide adenylyltransferase / Ribosylnicotinamide kinase	-1.4	-0.8	-0.2	-0.6	0.0	0.5	1.1	1.7	2.2
ZGAL_3251	pnuC2	pnuC2 Nicotinamide mononucleotide transporter	-0.3	0.3	0.9	0.9	1.5	2.1	1.6	2.2	2.8
ZGAL_3252		TonB-dependent Receptor	-0.7	0.0	0.0	0.1	0.9	0.9	1.9	2.7	2.7
ZGAL_3253		Conserved hypothetical protein	-0.9	0.6	0.7	-0.6	0.9	0.9	0.5	2.0	2.1
ZGAL_3257		Conserved hypothetical protein	1.0	-4.1	-0.5	0.9	-4.3	-0.7	2.9	-2.3	1.3
ZGAL_3258		Sulfatase, family S1-29	1.1	-3.3	-0.6	1.5	-2.9	-0.2	3.2	-1.2	1.5
ZGAL_326		FAD dependent oxidoreductase	1.3	0.0	0.2	1.1	-0.2	0.0	0.0	-1.3	-1.1
ZGAL_3262		Conserved hypothetical protein	-0.3	0.8	0.7	0.1	1.1	1.1	2.5	3.5	3.5
ZGAL_3265		Conserved hypothetical protein	-2.3	1.7	1.1	0.0	4.0	3.3	1.4	5.4	4.8
ZGAL_3269		Carbohydrate esterase, family CE1	-1.3	-0.1	0.4	0.0	1.2	1.6	1.1	2.3	2.8
ZGAL_327		Short-chain dehydrogenase/reductase	0.8	0.9	1.7	1.5	1.6	2.4	0.8	0.9	1.7
ZGAL_3270		Crp/Fnr-type transcriptional regulator	-1.3	1.2	2.4	0.3	2.8	4.1	0.3	2.8	4.1
ZGAL_3275		Hypothetical membrane protein	-2.0	0.3	1.4	-0.3	2.0	3.1	-0.1	2.2	3.3
ZGAL_3276		Conserved hypothetical membrane protein	-1.9	0.4	2.2	-0.7	1.6	3.4	-0.8	1.6	3.3
ZGAL_328		Conserved hypothetical protein	2.0	-0.1	-0.8	1.4	-0.7	-1.4	0.2	-1.9	-2.6
ZGAL_3285		Conserved hypothetical protein	-0.4	1.5	2.8	1.4	3.4	4.7	2.5	4.5	5.8
ZGAL_3286		Conserved hypothetical protein	-0.8	1.6	2.5	0.7	3.1	3.9	1.5	3.9	4.8
ZGAL_3287		Conserved hypothetical membrane protein	-0.9	1.4	2.5	0.3	2.6	3.7	0.3	2.6	3.8
ZGAL_3288		Conserved hypothetical protein	-2.1	0.4	0.9	-1.1	1.4	1.8	-0.7	1.7	2.2
ZGAL_3289		Hypothetical protein	-0.8	1.9	3.8	-0.2	2.6	4.5	0.5	3.2	5.2
ZGAL_3290		Conserved hypothetical membrane protein	-1.9	0.8	3.2	-0.2	2.5	4.9	-0.1	2.7	5.1
ZGAL_3291	ereA	ereA Erythromycin esterase	-1.4	1.8	1.7	-0.4	2.7	2.6	0.1	3.3	3.2
ZGAL_3292		Conserved hypothetical membrane protein	-1.2	0.4	0.8	0.0	1.5	2.0	0.1	1.7	2.1
ZGAL_3293		Hypothetical protein	-2.2	1.2	1.1	-1.6	1.8	1.6	1.1	4.5	4.4
ZGAL_3294		Conserved hypothetical protein	-0.9	2.2	2.4	0.8	4.0	4.1	2.3	5.5	5.6
ZGAL_3295		Hypothetical membrane protein	-1.4	2.3	2.7	1.0	4.8	5.1	2.8	6.6	6.9

ZGAL_3296		Hypothetical periplasmic protein	-1.2	0.5	0.6	-0.4	1.3	1.4	1.3	3.1	3.2
ZGAL_3298		Two-component system - Response regulator	-1.8	0.6	0.8	0.2	2.6	2.8	1.9	4.3	4.5
ZGAL_3299		Conserved hypothetical protein	-0.6	-0.2	1.2	0.3	0.7	2.2	2.2	2.6	4.0
ZGAL_3304		TonB-dependent Receptor	-0.6	1.6	1.2	1.0	3.2	2.7	2.3	4.4	4.0
ZGAL_3305		Conserved hypothetical protein	-1.0	1.6	-0.2	0.5	3.1	1.3	1.6	4.3	2.5
ZGAL_3306		Putative protein	-1.4	2.9	0.1	0.4	4.7	1.9	1.6	5.9	3.1
ZGAL_3309		Conserved hypothetical protein	0.1	0.1	-1.2	0.2	0.2	-1.1	1.4	1.5	0.2
ZGAL_331		RNA polymerase ECF-type sigma factor	2.3	0.0	-0.8	1.5	-0.8	-1.6	1.2	-1.1	-1.9
ZGAL_3313		Hypothetical protein	-0.7	-0.7	-0.8	-0.2	-0.3	-0.4	2.0	2.0	1.9
ZGAL_3314		Hypothetical membrane protein	0.7	0.1	-0.7	1.0	0.4	-0.4	3.1	2.5	1.7
ZGAL_3315		Putative membrane protein	-0.6	0.5	0.1	0.3	1.3	0.9	2.1	3.1	2.7
ZGAL_3317		Crp/Fnr-type transcriptional regulator	-1.9	0.7	1.0	-1.5	1.1	1.4	-0.4	2.2	2.5
ZGAL_3326	doxDA	doxDA Thiosulphate:quinone oxidoreductase	-0.6	-0.7	2.2	-0.2	-0.3	2.6	0.2	0.1	3.0
ZGAL_3327		Hypothetical membrane protein	-0.4	0.5	3.4	1.0	2.0	4.8	0.7	1.7	4.5
ZGAL_3332		Conserved hypothetical membrane protein	-0.9	0.9	1.3	0.1	2.0	2.3	0.1	1.9	2.2
ZGAL_3339		SusC-like TonB-dependent transporter	0.8	-0.6	-1.3	1.2	-0.2	-0.9	1.8	0.4	-0.3
ZGAL_334		Putative glycoside hydrolase, family GHnc	2.4	-1.4	-0.7	2.3	-1.4	-0.7	1.4	-2.3	-1.7
ZGAL_3348	nagB1	nagB1 Glucosamine-6-phosphate deaminase	1.5	-0.5	-0.2	2.0	0.0	0.3	1.2	-0.8	-0.5
ZGAL_3349		Glycoside hydrolase, family GH20	2.1	-1.5	-1.2	1.8	-1.8	-1.5	1.0	-2.6	-2.3
ZGAL_3352	nahA3	nahA3 Beta-N-acetylhexosaminidase, family GH20	0.0	-0.1	1.6	0.3	0.2	1.9	0.2	0.1	1.8
ZGAL_3353		Serine peptidase, family S12	-0.6	-3.3	-1.1	0.6	-2.1	0.1	2.1	-0.6	1.6
ZGAL_3354		Conserved hypothetical lipoprotein	2.1	-0.1	-0.2	1.3	-0.9	-1.0	0.2	-1.9	-2.0
ZGAL_3355	pfpI	pfpI Intracellular peptidase, family C56	1.7	-0.7	0.4	0.2	-2.2	-1.0	-0.5	-2.9	-1.7
ZGAL_3356		SusC-like TonB-dependent transporter	-1.3	1.9	-1.6	-1.2	2.0	-1.5	-0.7	2.5	-0.9
ZGAL_3360		Conserved hypothetical protein	-1.0	0.5	0.0	0.3	1.7	1.2	2.0	3.4	3.0
ZGAL_3366		Sulfate transporter	2.8	-1.2	1.1	2.1	-1.8	0.5	-0.1	-4.1	-1.8
ZGAL_3367	canA3	canA3 Carbonate dehydratase	2.3	-0.5	1.2	1.9	-1.0	0.8	-1.2	-4.1	-2.3
ZGAL_3369		Putative protein	-1.1	2.0	3.0	-1.3	1.8	2.8	-1.2	1.8	2.9
ZGAL_3371		Hypothetical membrane protein	-1.5	1.8	1.5	0.0	3.3	3.0	2.6	5.8	5.5
ZGAL_3372		Hypothetical membrane protein	-1.3	1.7	1.4	-0.2	2.8	2.5	2.3	5.2	5.0
ZGAL_3373		Hypothetical protein	-2.6	2.6	1.3	-0.1	5.1	3.8	2.2	7.5	6.2
ZGAL_3381		Conserved hypothetical protein	-0.9	0.7	1.2	0.1	1.7	2.1	0.2	1.7	2.2
ZGAL_3382		Conserved hypothetical protein	-0.3	0.9	1.4	0.6	1.8	2.3	0.6	1.8	2.2
ZGAL_3386		Conserved hypothetical protein	-0.9	0.7	1.2	0.1	1.7	2.1	0.2	1.7	2.2
ZGAL_3387		Rhs family protein	0.1	1.8	1.6	0.4	2.2	2.0	1.2	2.9	2.7
ZGAL_3388		Conserved hypothetical protein	1.2	1.9	1.8	2.1	2.8	2.6	2.9	3.6	3.4
ZGAL_3389		Vgr family protein	0.8	1.9	1.2	1.8	2.9	2.2	2.3	3.4	2.8
ZGAL_3391		Hypothetical membrane protein	-1.0	1.1	0.8	0.1	2.2	1.9	1.2	3.3	3.0
ZGAL_3392		Putative protein	-0.3	3.3	2.2	0.9	4.5	3.4	2.4	6.0	4.9
ZGAL_3393		Hypothetical membrane protein	1.6	-0.1	-0.9	2.3	0.5	-0.2	3.9	2.1	1.3
ZGAL_3394		Hypothetical periplasmic protein	1.7	0.4	-0.3	0.1	-1.2	-1.9	2.4	1.1	0.4
ZGAL_3395		Conserved hypothetical protein	-2.0	1.7	1.2	0.4	4.1	3.6	1.7	5.4	4.9
ZGAL_34	serA1/ serB	serA1/serB D-3-phosphoglycerate dehydrogenase / Phosphoserine phosphatase	-3.0	-0.6	1.9	-2.7	-0.4	2.2	-1.5	0.8	3.4
ZGAL_3400		Hypothetical protein	-0.9	0.9	0.8	0.4	2.3	2.1	1.3	3.2	3.1
ZGAL_3403		Conserved hypothetical protein	-1.0	1.1	2.0	-0.6	1.5	2.4	-0.6	1.5	2.4
ZGAL_3409		AraC-type transcriptional regulator	-1.3	0.7	1.5	-0.6	1.5	2.2	-0.5	1.5	2.3
ZGAL_3410		Conserved hypothetical lipoprotein	1.1	2.2	3.4	2.4	3.5	4.8	3.8	4.9	6.1
ZGAL_3411		Putative protein	0.5	1.2	1.0	2.4	3.0	2.9	2.9	3.6	3.4
ZGAL_3412		Kelch repeats protein	0.0	0.9	0.9	0.7	1.6	1.6	1.6	2.5	2.5
ZGAL_3416		Conserved hypothetical protein	-1.6	0.8	1.7	-1.0	1.5	2.4	-1.3	1.2	2.1
ZGAL_3420		Conserved hypothetical protein	-0.8	1.1	2.3	0.2	2.1	3.3	0.2	2.1	3.3
ZGAL_3421		Conserved hypothetical protein	-1.2	1.0	2.0	-0.4	1.9	2.9	-0.4	1.8	2.9
ZGAL_3424		Conserved hypothetical protein	0.0	0.6	1.1	1.5	2.1	2.6	1.1	1.7	2.2
ZGAL_3425		Conserved hypothetical protein	-1.7	0.5	1.3	0.0	2.1	3.0	-0.7	1.5	2.4
ZGAL_3436		Conserved hypothetical membrane protein	2.8	0.6	-0.7	3.0	0.8	-0.5	2.0	-0.2	-1.5
ZGAL_3437		TonB-dependent Receptor	-2.6	1.0	0.9	-0.5	3.1	3.0	0.4	3.9	3.9
ZGAL_3438		Conserved hypothetical protein	-2.0	-0.3	0.8	-3.4	-1.7	-0.6	-0.7	1.0	2.1
ZGAL_3439		One-component system sensor protein	-0.3	-0.2	0.9	-0.2	-0.1	1.0	-0.6	-0.5	0.5
ZGAL_3441		SusC-like TonB-dependent transporter	3.6	2.1	1.8	3.5	1.9	1.6	4.3	2.8	2.5
ZGAL_3445	uglA1	uglA1 Unsaturated glucuronyl hydrolase, family GH88	4.2	3.4	2.8	4.3	3.5	2.9	6.0	5.2	4.6
ZGAL_3446		Carbohydrate esterase, family CE10	2.1	1.3	1.0	1.5	0.7	0.4	2.9	2.1	1.8
ZGAL_3448	mdsA3	mdsA3 Mucin-desulfating sulfatase, family S1-11	2.7	2.5	1.9	1.6	1.3	0.8	1.9	1.7	1.1
ZGAL_3449		Conserved hypothetical periplasmic protein	2.4	2.1	1.9	0.9	0.6	0.4	1.1	0.9	0.7
ZGAL_3450		Alpha-L-fucosidase, family GH141	2.6	2.0	1.5	0.8	0.2	-0.4	1.1	0.5	0.0
ZGAL_3451	alfA5	alfA5 Alpha-L-fucosidase, family GH29 / Acetylesterase	2.5	1.6	1.4	0.6	-0.2	-0.5	0.8	-0.1	-0.3
ZGAL_3452		Polysaccharide lyase, family PLnc	4.4	3.4	2.5	3.9	3.0	2.1	5.0	4.1	3.1
ZGAL_3453		Possible pyridine nucleotide-disulphide oxidoreductase	3.9	3.0	1.9	1.5	0.6	-0.5	3.5	2.6	1.5
ZGAL_3454		Acetylesterase, lipase-GDSL family	3.5	2.5	2.1	1.7	0.7	0.4	1.5	0.5	0.2
ZGAL_3455		Sulfatase, family S1-17	3.3	2.1	1.3	2.3	1.1	0.3	2.3	1.1	0.3
ZGAL_3457		Conserved hypothetical protein	1.9	1.5	1.4	1.1	0.7	0.6	0.3	-0.2	-0.3
ZGAL_3459	kduI3	kduI3 4-deoxy-L-threo-5-hexosulose-uronate ketol-isomerase	1.6	1.6	2.9	-0.5	-0.5	0.8	-0.8	-0.8	0.5
ZGAL_3460	kduD2	kduD2 2-keto-3-deoxygluconate oxidoreductase	1.4	1.1	2.4	-0.7	-0.9	0.3	-1.6	-1.9	-0.6

ZGAL_3464	alfA4	alfA4 Alpha-L-fucosidase, family GH29	4.1	1.7	1.3	3.7	1.2	0.9	2.5	0.0	-0.3
ZGAL_3465		Sulfatase, family S1-15	2.8	1.6	1.2	2.0	0.8	0.4	0.9	-0.3	-0.7
ZGAL_3467		SusC-like TonB-dependent transporter	3.8	2.6	1.8	2.5	1.3	0.5	1.5	0.2	-0.6
ZGAL_3468		SusD-like lipoprotein	4.2	3.3	2.5	3.1	2.2	1.4	2.1	1.2	0.4
ZGAL_3469		Sulfatase, family S1-17	3.8	2.4	1.7	2.6	1.3	0.6	1.9	0.6	-0.1
ZGAL_347	bglX2	bglX2 Beta-glucosidase, family GH3	1.2	-0.3	-0.5	1.5	0.0	-0.2	1.9	0.3	0.2
ZGAL_3470		Putative glycoside hydrolase, family GHnc	3.4	2.2	1.4	2.5	1.3	0.5	2.6	1.3	0.6
ZGAL_3471		L-fuconate dehydratase	2.9	1.2	0.9	2.0	0.3	0.0	1.9	0.1	-0.1
ZGAL_3473		Fumarylacetoacetate hydrolase family protein	1.2	0.3	-0.3	0.6	-0.3	-0.9	0.1	-0.8	-1.4
ZGAL_3474		Short-chain dehydrogenase/reductase	1.0	0.9	0.2	0.1	-0.1	-0.8	0.2	0.1	-0.6
ZGAL_3475	fucP1	fucP1 L-fucose-proton symporter	1.6	0.5	0.1	1.3	0.2	-0.2	0.5	-0.6	-1.0
ZGAL_3476	lldD2	lldD2 L-lactate dehydrogenase [cytochrome]	-0.5	0.7	-0.1	-0.4	0.7	-0.1	1.2	2.4	1.6
ZGAL_3477		Conserved hypothetical lipoprotein	-2.8	-0.6	-0.4	-2.2	0.0	0.2	0.5	2.7	2.8
ZGAL_3478		Conserved hypothetical protein	0.2	3.0	2.4	1.3	4.1	3.5	3.9	6.7	6.1
ZGAL_3479		Metallo-beta-lactamase superfamily protein	-1.0	2.5	1.9	0.9	4.5	3.9	2.8	6.3	5.7
ZGAL_3480		Conserved hypothetical protein	-0.5	2.6	2.5	1.0	4.1	4.0	3.1	6.2	6.1
ZGAL_3481		Small-conductance mechanosensitive channel	-1.3	2.3	1.8	1.3	4.9	4.4	2.5	6.1	5.6
ZGAL_3483		Universal stress protein	-1.3	2.1	1.6	1.4	4.8	4.3	2.5	5.8	5.4
ZGAL_3484		Universal stress protein	-1.2	0.6	2.1	-1.3	0.6	2.1	-0.3	1.6	3.1
ZGAL_3485	trxA	trxA Thioredoxin	-1.9	0.4	1.8	0.1	2.4	3.8	0.6	2.9	4.3
ZGAL_3486		Conserved hypothetical protein	-2.3	0.8	1.1	0.0	3.1	3.4	1.0	4.1	4.4
ZGAL_3487	uppA	uppA Uracil phosphoribosyltransferase	-0.9	0.4	0.0	0.4	1.7	1.4	1.5	2.8	2.5
ZGAL_3488	pmr1	pmr1 Calcium-transporting P-type ATPase	-0.2	1.1	0.0	0.7	2.0	0.8	1.4	2.8	1.6
ZGAL_3489		Membrane fusion protein	-2.1	-0.2	1.0	-0.8	1.1	2.3	0.2	2.1	3.2
ZGAL_3490	lolC	lolC Lipoprotein-specific ABC transporter, permease component	-2.7	0.8	0.7	-0.2	3.3	3.2	1.1	4.7	4.5
ZGAL_3491	lolD1	lolD1 Lipoprotein-specific ABC transporter, ATPase component	-2.1	1.3	1.2	0.4	3.8	3.7	2.4	5.8	5.7
ZGAL_3491		lolD1	-2.1	1.3	1.2	0.4	3.8	3.7	2.4	5.8	5.7
ZGAL_3492		Conserved hypothetical protein	0.2	2.3	2.0	1.7	3.7	3.5	3.6	5.6	5.4
ZGAL_3493		Conserved hypothetical protein	-0.9	1.1	0.8	1.2	3.2	2.9	2.9	4.9	4.6
ZGAL_3494		Conserved hypothetical protein	0.0	-0.5	-0.7	1.5	1.0	0.8	2.4	1.9	1.7
ZGAL_3511		SusC-like TonB-dependent transporter	1.2	0.8	-0.1	2.0	1.5	0.7	0.9	0.5	-0.4
ZGAL_3512		SusD-like lipoprotein	3.1	0.7	-0.5	3.4	1.0	-0.2	2.5	0.0	-1.2
ZGAL_3513		Sulfatase, family S1-20	2.5	0.9	0.6	3.1	1.5	1.2	2.0	0.4	0.1
ZGAL_3515		Sulfatase, family S1-20	1.4	0.8	0.1	1.8	1.2	0.6	1.2	0.7	0.0
ZGAL_3516		Endo-1,4-beta-xylanase, family GH30_4	1.9	0.5	0.4	1.2	-0.2	-0.3	1.2	-0.2	-0.3
ZGAL_3518		Sulfatase, family S1-17	1.5	-0.3	-1.4	1.2	-0.6	-1.7	1.5	-0.3	-1.4
ZGAL_3528		RNA polymerase ECF-type sigma factor	2.1	0.3	-2.2	1.7	-0.2	-2.6	1.7	-0.1	-2.6
ZGAL_3535	afcA5	afcA5 Alpha-L-fucosidase, family GH95	1.7	-0.1	-0.9	0.7	-1.0	-1.9	0.4	-1.4	-2.2
ZGAL_3542		SusC-like TonB-dependent transporter	1.5	-0.2	-1.0	1.8	0.1	-0.7	1.2	-0.5	-1.3
ZGAL_3545		AraC-type transcriptional regulator	1.6	-0.8	-0.7	1.2	-1.2	-1.1	0.0	-2.5	-2.4
ZGAL_3551		Conserved hypothetical periplasmic protein	3.7	3.0	4.1	3.2	2.4	3.6	0.7	-0.1	1.1
ZGAL_3552		Two-component system - Response regulator, receiver domain	2.8	2.3	1.2	1.6	1.0	0.0	0.2	-0.3	-1.4
ZGAL_3555		Putative protein	0.5	1.4	0.7	0.1	0.9	0.3	0.0	0.9	0.3
ZGAL_3557		Hypothetical membrane protein	3.9	3.0	2.7	2.4	1.6	1.2	1.4	0.6	0.2
ZGAL_3558		Conserved hypothetical protein	3.8	3.3	2.9	3.0	2.5	2.0	1.4	0.9	0.5
ZGAL_3559	katA2	katA2 Catalase	3.7	2.2	1.5	3.1	1.6	0.9	0.6	-0.8	-1.6
ZGAL_3560		Hypothetical protein	2.7	2.4	2.1	2.7	2.4	2.0	0.2	-0.1	-0.4
ZGAL_3562		Conserved hypothetical protein	3.6	2.2	1.4	2.3	0.9	0.1	0.2	-1.2	-2.0
ZGAL_3563		Conserved hypothetical membrane protein	3.3	2.3	1.1	3.0	2.0	0.8	0.9	-0.1	-1.3
ZGAL_3564		Putative protein	2.2	3.0	3.0	2.1	2.9	2.9	0.3	1.0	1.0
ZGAL_3565		Conserved hypothetical protein	4.1	3.5	2.3	2.5	1.9	0.8	0.8	0.2	-1.0
ZGAL_3566	pldA	pldA Phospholipase A1	2.1	2.2	0.4	2.1	2.2	0.4	0.5	0.5	-1.2
ZGAL_357		SusC-like TonB-dependent Transducer	1.7	0.1	-1.7	1.5	-0.1	-1.9	1.4	-0.1	-2.0
ZGAL_3573	agaB	agaB Beta-agarase B, family GH16	1.4	0.2	-0.4	1.2	0.0	-0.7	0.6	-0.5	-1.2
ZGAL_3583		Two-component system - Response regulator, receiver domain	-0.9	2.2	0.9	-0.3	2.8	1.5	2.0	5.0	3.8
ZGAL_3584		Two-component system - Sensor histidine kinase	-1.1	1.3	-0.6	-0.4	2.0	0.1	0.8	3.1	1.3
ZGAL_3589		GreA-like transcription elongation factor	1.5	0.4	-0.7	1.3	0.2	-0.9	1.4	0.3	-0.8
ZGAL_3590		Conserved hypothetical periplasmic protein	2.3	0.9	0.1	1.8	0.4	-0.4	2.2	0.8	0.0
ZGAL_3591	gdhB	gdhB Glutamate dehydrogenase (NAD(P)(+))	2.0	0.8	-0.5	1.9	0.8	-0.6	1.7	0.6	-0.8
ZGAL_3592	rnkA	rnkA Regulator of nucleoside diphosphate kinase	3.4	0.7	-0.8	2.3	-0.4	-1.9	2.8	0.0	-1.5
ZGAL_360		Conserved hypothetical protein	2.4	0.0	-1.7	2.0	-0.4	-2.0	1.8	-0.6	-2.2
ZGAL_3611		Conserved hypothetical periplasmic protein	3.3	-0.1	-1.6	2.8	-0.7	-2.2	1.6	-1.9	-3.4
ZGAL_3612		Possible FAD dependent oxidoreductase	1.7	0.4	-1.4	1.3	0.0	-1.8	1.1	-0.2	-2.0
ZGAL_362		AraC-type transcriptional regulators	1.7	-0.6	-1.9	0.9	-1.3	-2.6	0.4	-1.9	-3.2
ZGAL_363		Ligand-binding sensor protein	-0.1	0.7	0.5	-0.1	0.7	0.5	0.6	1.4	1.2
ZGAL_3637		SusC-like TonB-dependent transporter	1.1	-0.6	-1.9	1.1	-0.6	-1.9	1.8	0.2	-1.1
ZGAL_3638		SusD-like lipoprotein	2.1	0.1	-0.7	1.4	-0.7	-1.4	1.6	-0.5	-1.3
ZGAL_3641	mroA3	mroA3 Aldose 1-epimerase	1.1	0.8	0.9	1.5	1.2	1.3	1.1	0.8	0.9
ZGAL_3647		Hypothetical protein	-2.0	2.3	1.2	0.1	4.4	3.2	1.0	5.3	4.2
ZGAL_3648		T9SS SprF family protein	-1.4	3.1	2.0	0.1	4.5	3.5	1.5	5.9	4.9
ZGAL_3649		T9SS-associated PG1058-like protein	-2.0	2.4	1.9	-0.1	4.2	3.8	1.0	5.3	4.9

ZGAL_3650		Conserved hypothetical protein	1.2	3.0	0.2	2.5	4.2	1.4	2.0	3.8	1.0
ZGAL_3651		T9SS SprF family protein	1.2	3.7	1.9	2.2	4.7	2.9	2.4	4.8	3.0
ZGAL_3652		T9SS-associated PG1058-like protein	1.2	3.3	1.8	2.7	4.8	3.3	2.3	4.4	2.9
ZGAL_3653	thiS	thiS Sulfur transfer protein ThiS	0.5	1.1	1.6	0.4	1.0	1.5	1.3	1.8	2.3
ZGAL_3660		Conserved hypothetical membrane protein	-0.6	0.1	1.9	0.9	1.6	3.4	2.0	2.6	4.4
ZGAL_3664		TPR repeats protein	1.9	0.1	-1.6	2.2	0.5	-1.3	1.2	-0.6	-2.3
ZGAL_3665		Two-component system - Sensor histidine kinase	2.6	-0.9	-2.1	1.8	-1.7	-2.9	1.3	-2.1	-3.3
ZGAL_3666		Two-component system - Response regulator	1.8	-0.3	-1.6	1.6	-0.5	-1.8	1.6	-0.5	-1.8
ZGAL_3670		Conserved hypothetical membrane protein	-1.1	-0.4	1.2	-0.3	0.4	2.0	-0.5	0.2	1.8
ZGAL_3672	argD2	argD2 Acetylornithine aminotransferase	1.5	-0.4	-1.6	0.5	-1.3	-2.5	0.2	-1.7	-2.9
ZGAL_3673		Conserved hypothetical periplasmic protein	1.6	-0.2	0.4	1.1	-0.6	-0.1	0.8	-1.0	-0.5
ZGAL_3674	purA	purA Adenylosuccinate synthase	-0.1	0.5	1.8	-0.5	0.1	1.5	0.6	1.1	2.5
ZGAL_3675	furA1	furA1 Ferric uptake regulation protein	-1.9	0.9	2.7	-1.3	1.5	3.2	-0.9	1.9	3.6
ZGAL_3680	moaE1	moaE1 Molybdopterin synthase, large subunit	1.9	-0.1	0.1	1.3	-0.7	-0.5	0.0	-2.0	-1.8
ZGAL_3681	moaA	moaA Molybdenum cofactor biosynthesis protein A	1.7	-0.2	-0.5	0.6	-1.3	-1.6	-0.6	-2.5	-2.8
ZGAL_3682	moaC	moaC Molybdenum cofactor biosynthesis protein C	1.7	0.1	0.0	0.9	-0.7	-0.7	-0.6	-2.2	-2.2
ZGAL_3683	mobA	mobA Molybdopterin-guanine dinucleotide biosynthesis protein A	2.3	-0.2	0.2	1.2	-1.2	-0.8	-0.2	-2.6	-2.3
ZGAL_3684	moeB	moeB Molybdopterin synthase activating protein	1.8	-0.3	-0.1	0.9	-1.2	-1.0	-0.4	-2.6	-2.4
ZGAL_3685		Permease	2.1	-0.1	0.4	1.6	-0.5	-0.1	0.4	-1.7	-1.2
ZGAL_369	susA	susA Alpha-amylase SusA, family GH13_7	-3.4	-0.2	1.0	-3.4	-0.3	1.0	-3.1	0.0	1.3
ZGAL_3691	mutL	mutL DNA mismatch repair protein MutL	1.3	-0.2	-0.3	1.4	-0.1	-0.1	1.2	-0.3	-0.4
ZGAL_3692		Conserved hypothetical membrane protein	1.2	0.5	0.5	1.2	0.5	0.6	1.7	0.9	1.0
ZGAL_3693	ribH	ribH Riboflavin synthase beta chain	0.1	-0.3	1.0	0.6	0.3	1.6	1.4	1.1	2.4
ZGAL_3694		TPR repeats protein	-0.4	-0.7	0.8	0.2	-0.1	1.3	0.9	0.6	2.0
ZGAL_3698	ndkA	ndkA Nucleoside diphosphate kinase	-0.8	-0.8	1.5	0.1	0.0	2.4	0.6	0.6	2.9
ZGAL_3700		Phosphoesterase	0.7	0.5	1.3	1.2	1.0	1.8	1.4	1.2	2.0
ZGAL_3702	ppiA	ppiA peptidyl-prolyl cis-trans isomerase	-0.2	-0.1	1.2	-0.5	-0.4	0.8	-0.6	-0.4	0.8
ZGAL_3703	bglC	bglC Endo-beta-1,4-glucanase, family GH5_2	1.0	-1.0	-2.4	2.0	0.1	-1.4	3.8	1.8	0.4
ZGAL_3704		DUF805 family protein	-2.0	-0.3	-0.6	0.2	1.9	1.6	2.2	3.9	3.5
ZGAL_3706		Conserved hypothetical membrane protein	1.4	-0.5	0.4	1.7	-0.2	0.7	1.0	-0.8	0.1
ZGAL_3710		Conserved hypothetical periplasmic protein	1.5	-0.1	0.2	1.1	-0.4	-0.2	1.9	0.3	0.6
ZGAL_3711	parB	parB Chromosome-partitioning protein parB	0.6	0.3	0.2	1.3	0.9	0.8	1.4	1.1	1.0
ZGAL_3712	parA	parA Chromosome partitioning protein ParA	1.3	-0.1	-0.1	1.4	0.1	0.1	1.6	0.2	0.3
ZGAL_3714	udk	udk Uridine kinase	-0.2	-0.2	0.7	-0.1	0.0	0.9	0.3	0.3	1.3
ZGAL_3727		Conserved hypothetical protein	-0.4	3.4	2.0	1.5	5.4	3.9	2.8	6.7	5.2
ZGAL_3728		Carbohydrate esterase, family CE1	1.3	0.4	0.0	1.1	0.2	-0.3	0.8	-0.1	-0.6
ZGAL_3729		Conserved hypothetical protein	1.8	0.5	-0.2	1.4	0.1	-0.7	1.2	-0.1	-0.8
ZGAL_3735	pfkA	pfkA 6-Phosphofructokinase, isoenzyme 1	-0.4	-0.2	1.9	-0.4	-0.3	1.8	-0.2	0.0	2.1
ZGAL_3736	gapA	gapA Glyceraldehyde 3-phosphate dehydrogenase	-2.7	-0.9	2.5	-3.3	-1.5	1.9	-2.8	-1.0	2.4
ZGAL_3739		Conserved hypothetical periplasmic protein	2.1	0.0	0.0	1.3	-0.8	-0.8	1.3	-0.8	-0.9
ZGAL_374		Conserved hypothetical protein	-0.7	1.2	0.2	0.2	2.1	1.1	0.6	2.5	1.5
ZGAL_3740	amiA	amiA N-acetylmuramoyl-L-alanine amidase	-0.4	0.3	0.7	0.0	0.6	1.0	0.3	1.0	1.3
ZGAL_3745		Beta-N-acetylhexosaminidase, family GH3 / Serine peptidase, family S12	-0.9	0.2	1.0	-0.7	0.5	1.2	0.0	1.1	1.9
ZGAL_3746		Glycosyltransferase, family GT4	2.1	0.5	-2.4	0.6	-1.0	-3.9	0.5	-1.2	-4.1
ZGAL_3747		Conserved hypothetical protein	2.1	1.0	-2.0	0.8	-0.2	-3.2	0.5	-0.5	-3.5
ZGAL_3748		OmpA-like periplasmic protein	1.4	0.4	-1.9	2.3	1.4	-1.0	0.8	-0.1	-2.5
ZGAL_3749		Conserved hypothetical protein	2.7	-1.2	-2.9	2.6	-1.3	-3.0	3.0	-0.9	-2.7
ZGAL_375	traO	traO Conjugative transposon protein TraO	0.6	1.4	0.0	0.9	1.7	0.4	1.6	2.4	1.1
ZGAL_3752	algI1	algI1 Poly(beta-D-mannuronate) O-acetylase	-0.7	0.0	-0.4	-0.7	-0.1	-0.5	1.5	2.1	1.7
ZGAL_3753		Conserved hypothetical protein	-0.1	0.0	-0.9	-0.1	-0.1	-0.9	1.5	1.6	0.8
ZGAL_3756		ATP-grasp protein	-1.3	0.1	0.5	-0.6	0.8	1.2	-0.2	1.2	1.6
ZGAL_3757		Beta-(1,4)-galactosyltransferase, Family GT2	-1.4	1.1	1.4	-0.5	2.0	2.3	-1.7	0.8	1.2
ZGAL_3759	capM	capM Capsular polysaccharide biosynthesis glycosyltransferase, family GT4	0.1	0.9	1.3	0.8	1.5	1.9	2.3	3.1	3.5
ZGAL_376		Conserved hypothetical lipoprotein	-1.3	1.7	0.0	-0.2	2.9	1.2	0.6	3.7	2.0
ZGAL_3760		Glycosyltransferase, family GT4	-1.4	0.7	0.8	-0.8	1.2	1.4	0.9	2.9	3.1
ZGAL_3761	asnB2	asnB2 Asparagine synthase B	-1.1	0.9	1.1	0.4	2.4	2.6	1.8	3.8	4.0
ZGAL_3762		Glycosyltransferase, family GT4	-0.2	0.9	1.1	0.1	1.3	1.4	1.1	2.3	2.4
ZGAL_3763	asnB3	asnB3 Asparagine synthase B	-0.7	1.1	0.5	0.2	1.9	1.3	1.4	3.1	2.6
ZGAL_3764		Conserved hypothetical protein	-1.4	0.7	1.4	-0.9	1.2	1.9	-0.3	1.8	2.5
ZGAL_3766		Glycosyltransferase, family GT4	-0.8	0.6	0.9	0.5	1.9	2.2	0.6	1.9	2.2
ZGAL_3768		Conserved hypothetical membrane protein	-0.3	0.3	0.2	0.5	1.2	1.0	1.0	1.6	1.5
ZGAL_3769		Glycosyltransferase, family GT2	0.2	0.6	-0.1	0.6	1.0	0.3	2.2	2.6	1.9
ZGAL_377		Hypothetical protein	-1.5	0.7	0.1	-0.8	1.3	0.7	0.1	2.3	1.7
ZGAL_3770	pelA1	pelA1 Pectate lyase, family PL1	1.4	0.9	1.1	1.9	1.3	1.6	3.7	3.1	3.3
ZGAL_3772	wbpP	wbpP UDP-N-acetylglucosamine 4-epimerase	-1.2	0.4	0.9	-0.8	0.8	1.3	-0.9	0.7	1.3
ZGAL_3773		Conserved hypothetical membrane protein	-1.1	0.6	1.0	0.1	1.8	2.2	0.3	2.1	2.4
ZGAL_3774	pelA2	pelA2 Pectate lyase, family PL1	-0.2	-0.9	0.4	-0.2	-0.8	0.4	1.4	0.8	2.0
ZGAL_3775		beta-glucuronidase, family GH154	-0.1	0.7	1.2	0.3	1.1	1.5	0.1	0.9	1.4
ZGAL_3776		Hypothetical membrane protein	-1.4	-0.2	0.3	0.2	1.4	1.9	0.2	1.4	1.9
ZGAL_3777	algI2	algI2 Poly(beta-D-mannuronate) O-acetylase	-0.8	0.4	0.9	-0.2	1.0	1.5	0.0	1.2	1.7
ZGAL_378		Hypothetical protein	-1.1	0.8	0.0	-0.5	1.4	0.7	0.4	2.2	1.5
ZGAL_3782		PLP-dependent aminotransferase	0.3	0.8	-0.2	2.1	2.5	1.6	1.4	1.8	0.8

ZGAL_3783	capD	capD Polysaccharide biosynthesis protein CapD	-0.5	0.6	-0.1	0.4	1.5	0.8	0.9	2.0	1.3
ZGAL_3784		Polysaccharide export protein	-0.6	-0.1	1.2	-0.3	0.2	1.5	0.0	0.5	1.8
ZGAL_3785	ptkA	ptkA Tyrosine-protein kinase	-1.2	0.1	1.7	-1.1	0.2	1.8	-1.2	0.1	1.7
ZGAL_3786		Hypothetical protein containing CBM6	-1.0	0.6	0.8	0.0	1.6	1.8	-0.9	0.7	0.9
ZGAL_3787	capC	capC Tyrosine-protein phosphatase	-1.1	1.1	2.3	-0.5	1.8	3.0	0.8	3.1	4.3
ZGAL_379		Putative protein	-1.6	0.6	0.1	-0.4	1.8	1.2	-0.1	2.1	1.5
ZGAL_3791		Conserved hypothetical protein	1.9	0.7	-3.1	0.7	-0.4	-4.3	2.1	1.0	-2.9
ZGAL_3793	apbE3	apbE3 Thiamine biosynthesis protein apbE	0.5	0.7	0.0	1.2	1.4	0.7	2.1	2.2	1.6
ZGAL_3795		Major facilitator family transporter	1.4	0.5	-0.5	0.4	-0.5	-1.5	0.3	-0.6	-1.6
ZGAL_3796		Conserved hypothetical protein	2.3	0.0	-1.1	1.4	-0.9	-2.0	0.6	-1.6	-2.7
ZGAL_3797		Conserved hypothetical protein	2.1	1.0	-0.8	1.5	0.4	-1.4	0.6	-0.5	-2.3
ZGAL_380		Hypothetical protein	-0.9	1.5	1.0	-0.4	1.9	1.4	0.2	2.5	2.0
ZGAL_3800		Conserved hypothetical periplasmic protein	2.5	1.1	-0.8	1.1	-0.3	-2.2	0.5	-0.9	-2.8
ZGAL_3801		Conserved hypothetical membrane protein	2.5	0.9	-0.1	0.5	-1.1	-2.1	0.1	-1.6	-2.6
ZGAL_3809		Conserved hypothetical protein	1.5	0.0	-1.3	0.7	-0.8	-2.1	0.7	-0.9	-2.1
ZGAL_3815		Conserved hypothetical protein	2.0	0.4	-0.7	0.7	-0.9	-2.0	0.6	-1.0	-2.1
ZGAL_3816		Endo-beta-1,2-glucanase, family GH144	1.5	0.5	-0.3	1.9	0.9	0.2	1.1	0.2	-0.6
ZGAL_3820		Conserved hypothetical periplasmic protein	2.3	0.2	-2.9	1.4	-0.6	-3.8	1.9	-0.1	-3.2
ZGAL_3824		Conserved hypothetical membrane protein	1.7	1.0	0.1	1.1	0.4	-0.5	1.5	0.9	-0.1
ZGAL_3827		Conserved hypothetical membrane protein	1.4	-0.3	-1.6	2.0	0.3	-1.0	0.7	-1.0	-2.3
ZGAL_3828		Conserved hypothetical lipoprotein	1.8	-1.7	-3.0	2.6	-0.9	-2.2	4.0	0.5	-0.8
ZGAL_3829	dnaN	dnaN DNA polymerase III, beta chain	-0.7	-0.6	1.6	-0.8	-0.7	1.5	-1.0	-1.0	1.2
ZGAL_3833	phoH	phoH Protein PhoH	0.0	0.1	1.0	0.3	0.4	1.4	0.7	0.8	1.8
ZGAL_3835	dnaQ	dnaQ DNA polymerase III, epsilon subunit	-0.8	0.3	1.0	-0.1	1.0	1.8	0.2	1.3	2.0
ZGAL_3839		Small heat shock protein	0.1	3.5	4.4	1.8	5.3	6.2	4.5	7.9	8.8
ZGAL_3841		Conserved hypothetical protein	-0.4	-0.1	0.0	0.4	0.8	0.8	2.0	2.3	2.4
ZGAL_3842	clsA2	clsA2 Cardiolipin synthetase	0.0	0.0	-0.7	0.9	0.9	0.3	1.8	1.8	1.2
ZGAL_3843		Patatin-like phospholipase	-1.5	1.5	1.0	0.5	3.4	2.9	1.9	4.8	4.4
ZGAL_3844		Two-component system - Sensor histidine kinase	-1.6	1.2	1.2	0.4	3.1	3.1	1.4	4.2	4.2
ZGAL_3845		Cyclic nucleotide-binding dependent two-component system - Response regulator	0.1	0.7	-0.5	0.9	1.5	0.3	1.2	1.8	0.6
ZGAL_3846		Conserved hypothetical protein	0.1	1.2	0.0	0.7	1.8	0.5	1.8	2.9	1.7
ZGAL_3847		Conserved hypothetical membrane protein	-0.3	1.7	0.7	1.8	3.9	2.9	3.0	5.0	4.0
ZGAL_3848		Conserved hypothetical membrane protein	0.5	4.0	4.4	2.1	5.6	6.0	4.1	7.6	8.0
ZGAL_3849		Hypothetical protein	0.9	2.2	2.1	1.8	3.1	2.9	3.4	4.7	4.5
ZGAL_3850		Conserved hypothetical protein	0.4	2.4	2.1	1.4	3.4	3.1	2.7	4.7	4.4
ZGAL_3851		Conserved hypothetical protein	-1.8	3.9	3.8	1.6	7.3	7.2	3.6	9.2	9.2
ZGAL_3852		ABC-2 type exporter, permease component	-0.2	2.0	1.0	2.6	4.8	3.8	3.5	5.7	4.7
ZGAL_3853		ABC-2 type exporter, permease component	0.3	2.1	1.8	2.8	4.6	4.3	4.6	6.4	6.1
ZGAL_3854		Membrane fusion protein	0.5	3.1	3.0	2.3	4.9	4.8	4.6	7.2	7.1
ZGAL_3855		Outer membrane efflux protein	0.5	2.6	3.0	2.0	4.1	4.5	3.9	6.0	6.5
ZGAL_3856		Multi-pass membrane transporter	-0.6	1.5	-0.2	0.9	3.0	1.3	3.0	5.0	3.4
ZGAL_3857	ubiB	ubiB Possible ubiquinone biosynthesis protein UbiB	-1.4	1.5	1.6	0.2	3.1	3.2	1.9	4.9	5.0
ZGAL_3858		Conserved hypothetical protein	-3.2	1.2	3.5	-1.9	2.4	4.7	0.3	4.7	6.9
ZGAL_3859	rcaA	rcaA Respiratory chain complexes assembly ATP-dependent metalloprotease	-1.2	2.1	2.4	1.1	4.4	4.7	2.2	5.6	5.9
ZGAL_3860		Carboxymuconolactone decarboxylase family protein	-1.4	1.6	3.1	0.2	3.2	4.7	1.7	4.7	6.2
ZGAL_3861		Conserved hypothetical protein	0.8	3.3	3.7	2.6	5.1	5.5	3.8	6.3	6.7
ZGAL_3862		Universal stress protein	0.8	3.3	2.6	2.1	4.6	3.9	3.8	6.3	5.6
ZGAL_3863		Conserved hypothetical protein	1.2	3.2	2.3	3.5	5.5	4.6	5.0	7.1	6.1
ZGAL_3864	glkA	glkA Glucokinase (Glucose kinase)	0.0	1.8	1.8	2.8	4.7	4.7	3.6	5.4	5.4
ZGAL_3865	fbaB	fbaB Fructose-bisphosphate aldolase, class 1	1.2	1.9	1.2	3.2	3.9	3.2	4.3	5.1	4.4
ZGAL_3866	pfkB	pfkB 6-Phosphofructokinase, isozyme 2	1.2	2.3	1.0	3.3	4.5	3.1	4.3	5.4	4.1
ZGAL_3867	gpmA	gpmA 2,3-bisphosphoglycerate-dependent phosphoglycerate mutase	1.6	2.0	1.2	3.2	3.6	2.8	4.4	4.8	4.0
ZGAL_3868	ldhA	ldhA D-lactate dehydrogenase	-0.1	1.9	1.9	2.5	4.5	4.5	3.3	5.4	5.4
ZGAL_3869	ppsA	ppsA Pyruvate, water dikinase (Phosphoenolpyruvate synthase)	1.1	2.2	1.7	2.3	3.4	2.9	4.1	5.2	4.8
ZGAL_387		Transposase (pseudogene), Mutator family	0.8	0.4	-0.9	1.8	1.3	0.0	1.1	0.6	-0.7
ZGAL_3871	atpD2	atpD2 ATP synthase, F1 sector beta subunit	1.6	2.4	3.2	3.3	4.1	4.9	5.0	5.8	6.6
ZGAL_3871		atpD2	1.6	2.4	3.2	3.3	4.1	4.9	5.0	5.8	6.6
ZGAL_3872	atpC2	atpC2 ATP synthase, F1 sector epsilon subunit	1.4	2.8	4.1	3.1	4.5	5.8	5.5	6.9	8.2
ZGAL_3873	atpI	atpI ATP synthase gene 1	2.8	2.8	3.1	2.8	2.8	3.1	5.5	5.5	5.8
ZGAL_3874		Conserved hypothetical membrane protein	0.5	3.7	4.6	3.1	6.3	7.2	5.8	9.0	9.9
ZGAL_3875	atpB2	atpB2 ATP synthase, F0 sector A subunit	-0.2	1.9	1.8	2.8	4.9	4.8	4.5	6.6	6.5
ZGAL_3876	atpE2	atpE2 ATP synthase, F0 sector C subunit	0.3	1.6	1.5	2.1	3.4	3.3	3.9	5.1	5.0
ZGAL_3877	atpF2	atpF2 ATP synthase, F0 sector B subunit	0.1	2.1	1.3	2.2	4.2	3.4	4.2	6.2	5.3
ZGAL_3878	atpA2	atpA2 ATP synthase, F1 sector alpha subunit	-0.5	1.9	1.8	2.6	4.9	4.9	3.9	6.3	6.3
ZGAL_3879	atpG2	atpG2 ATP synthase, F1 sector gamma subunit	0.0	0.8	-0.4	2.1	2.8	1.6	3.5	4.3	3.1
ZGAL_388		Hypothetical lipoprotein	0.0	1.0	-0.5	0.7	1.7	0.2	0.6	1.6	0.1
ZGAL_3880		Conserved hypothetical protein	0.0	0.4	-0.1	-0.1	0.4	-0.2	2.0	2.4	1.9
ZGAL_3881		ABC importer, periplasmic component	1.9	2.3	0.9	3.6	4.0	2.6	5.7	6.2	4.8
ZGAL_3882		ABC importer, ATPase component	1.9	2.4	1.5	4.5	5.0	4.2	5.6	6.2	5.3
ZGAL_3883		ABC importer, permease component	1.2	3.0	1.9	4.1	5.9	4.8	5.3	7.1	6.0
ZGAL_3885		Voltage-gated chloride channel	-0.7	1.2	1.2	1.7	3.6	3.5	3.4	5.3	5.2

ZGAL_3886	cgaA	cgaA Glucan 1,4-alpha-glucosidase, family GH15	-0.1	1.5	1.2	2.2	3.8	3.5	3.7	5.3	5.1
ZGAL_3898		Conserved hypothetical protein	3.3	-0.5	-3.4	3.2	-0.6	-3.5	1.1	-2.8	-5.7
ZGAL_390		Putative protein	0.2	2.0	3.0	1.3	3.0	4.0	1.2	2.9	3.9
ZGAL_3901		Two-component system hybrid - Sensor histidine kinase/Chemotaxis proteins	-0.3	1.1	-0.4	-0.5	0.8	-0.7	-0.4	0.9	-0.6
ZGAL_391		Hypothetical protein	-1.4	1.1	2.0	-0.4	2.2	3.1	0.3	2.9	3.8
ZGAL_3912		Hypothetical lipoprotein	2.3	0.4	-1.0	1.4	-0.5	-1.9	1.4	-0.5	-1.9
ZGAL_3917		Hypothetical membrane protein	1.0	-2.0	-3.5	2.0	-1.0	-2.6	2.2	-0.7	-2.3
ZGAL_3919		Conserved hypothetical protein	-1.4	-0.6	-0.3	-0.3	0.6	0.8	1.4	2.2	2.4
ZGAL_392		Putative protein	0.3	1.4	2.0	1.3	2.4	2.9	2.3	3.4	3.9
ZGAL_3920		Hypothetical membrane protein	-1.4	-0.7	0.1	-0.4	0.4	1.2	1.1	1.8	2.6
ZGAL_3929		Conserved hypothetical protein	-0.5	-0.8	-1.8	-0.2	-0.5	-1.5	1.4	1.1	0.1
ZGAL_393		Conserved hypothetical membrane protein	-1.4	1.4	2.3	-0.4	2.4	3.4	0.7	3.5	4.4
ZGAL_3936	afcA7	afcA7 Alpha-L-fucosidase, family GH95	1.8	-0.1	-0.6	1.2	-0.7	-1.2	0.6	-1.3	-1.8
ZGAL_3937		beta-L-arabinofuranosidase, family GH127	1.9	-0.3	-0.6	1.2	-0.9	-1.2	0.3	-1.8	-2.2
ZGAL_3939		Serine endopeptidase, family S54	-0.7	0.6	0.5	0.2	1.5	1.4	2.5	3.8	3.6
ZGAL_394		Hypothetical protein	-0.9	1.4	2.9	-0.5	1.8	3.3	0.8	3.2	4.7
ZGAL_3940		AraC-type transcriptional regulator	-0.9	0.3	1.4	-2.4	-1.2	-0.1	-2.2	-1.0	0.1
ZGAL_3941	hxlB	hxlB 3-Hexulose-6-phosphate isomerase	-3.2	-0.2	2.4	-6.9	-4.0	-1.3	-6.2	-3.2	-0.5
ZGAL_3942	hxlA	hxlA 3-Hexulose-6-phosphate synthase	-5.0	-1.5	2.8	-8.9	-5.4	-1.0	-7.6	-4.1	0.3
ZGAL_3947		Endonuclease/exonuclease/phosphatase family	1.1	1.1	0.7	1.2	1.2	0.8	2.9	2.9	2.5
ZGAL_395		Conserved hypothetical protein	-0.8	1.9	3.5	-1.0	1.8	3.4	0.3	3.0	4.6
ZGAL_3951	xynA2	xynA2 Endo-beta-1,4-xylanase, family GH10	1.9	0.1	-0.9	0.9	-0.8	-1.8	0.9	-0.9	-1.8
ZGAL_3952	xynB	xynB Endo-beta-1,4-xylanase, family GH10	2.6	-0.7	-1.0	2.8	-0.5	-0.7	2.1	-1.2	-1.4
ZGAL_3954		Conserved hypothetical periplasmic protein	2.5	0.8	-1.2	1.9	0.1	-1.8	2.0	0.3	-1.7
ZGAL_3956		DNA/RNA non-specific endonuclease	0.0	2.1	-0.4	0.9	3.0	0.5	1.4	3.5	1.0
ZGAL_396		Conserved hypothetical protein	-0.4	0.3	0.9	-0.4	0.2	0.8	0.4	1.1	1.6
ZGAL_3961	hupB	hupB DNA-binding protein HU, beta chain	-2.7	0.5	4.8	-2.1	1.1	5.4	-2.6	0.6	4.9
ZGAL_3965		YbeD-like Protein	-0.7	0.6	2.1	0.0	1.3	2.8	0.1	1.4	2.9
ZGAL_3966		Conserved hypothetical protein	-0.1	0.8	2.1	0.2	1.0	2.4	0.6	1.5	2.8
ZGAL_3967	murA	murA UDP-N-acetylglucosamine 1-carboxyvinyltransferase	-0.5	-0.1	2.0	-0.1	0.3	2.4	0.8	1.2	3.3
ZGAL_3968		Conserved hypothetical protein	-0.7	-0.2	1.8	-0.4	0.1	2.1	0.7	1.2	3.2
ZGAL_397		Conserved hypothetical protein	-1.1	0.3	0.3	-0.8	0.7	0.7	0.5	2.0	1.9
ZGAL_3970		conserved hypothetical lipoprotein	-0.6	2.7	1.7	1.1	4.3	3.3	2.3	5.6	4.6
ZGAL_3971	phrA	phrA Deoxyribodipyrimidine photo-lyase	2.5	1.8	1.2	1.9	1.1	0.6	2.6	1.9	1.4
ZGAL_3972		Short-chain dehydrogenase/reductase	2.2	1.4	0.3	2.0	1.2	0.0	1.2	0.4	-0.8
ZGAL_3973		Conserved hypothetical protein	2.6	0.7	-0.9	1.5	-0.4	-2.0	1.2	-0.7	-2.3
ZGAL_3974		Conserved hypothetical periplasmic protein	1.4	0.2	-1.1	0.8	-0.4	-1.7	0.4	-0.9	-2.1
ZGAL_3975		Conserved hypothetical periplasmic protein	-0.6	-0.6	1.5	-1.5	-1.5	0.6	-1.7	-1.7	0.4
ZGAL_3978		Carbohydrate esterase, family CE14	1.1	0.4	0.4	1.0	0.3	0.2	0.6	-0.1	-0.2
ZGAL_398		Conserved hypothetical protein	-1.2	4.1	4.9	0.8	6.1	6.9	1.9	7.2	7.9
ZGAL_3980		Conserved hypothetical membrane protein	1.7	-0.2	-0.8	0.2	-1.7	-2.3	-0.7	-2.6	-3.3
ZGAL_3984	nrfI	nrfI Protein NrfI	-0.1	0.0	2.4	0.0	0.0	2.4	0.2	0.2	2.6
ZGAL_3987		SusC-like TonB-dependent Transducer	1.2	0.0	-2.7	1.9	0.6	-2.1	2.1	0.8	-1.9
ZGAL_399		PKD repeats protein	-1.5	0.3	0.7	-0.5	1.3	1.7	0.9	2.7	3.1
ZGAL_4		Conserved hypothetical periplasmic protein	0.8	-0.6	1.4	1.8	0.4	2.4	1.8	0.4	2.4
ZGAL_40	csdA	csdA RNA helicase CsdA	-0.7	-0.8	1.6	-0.9	-1.0	1.4	-0.2	-0.3	2.1
ZGAL_400		Peptidase, family C40	-2.2	1.2	1.6	-0.3	3.1	3.5	1.1	4.4	4.8
ZGAL_4000	norM2	norM2 Multidrug resistance protein	0.4	-0.6	0.7	1.2	0.2	1.6	1.3	0.3	1.7
ZGAL_4003		Two-component system - Sensor histidine kinase	0.5	0.6	-0.1	1.1	1.2	0.4	2.4	2.6	1.8
ZGAL_4007		Metallopeptidase, family M28	-1.5	-0.6	1.3	-1.7	-0.9	1.1	-1.6	-0.7	1.2
ZGAL_401		Conserved hypothetical protein	-0.3	0.6	0.4	-0.3	0.6	0.4	1.3	2.2	2.0
ZGAL_4012		Proline racemase	0.0	0.3	2.1	-0.2	0.2	2.0	-0.9	-0.5	1.3
ZGAL_4014	cydA	cydA Cytochrome d ubiquinol oxidase subunit I	-0.1	-0.8	1.3	-0.1	-0.8	1.3	0.2	-0.5	1.6
ZGAL_4017		GCN5-related N-acetyltransferase	1.3	0.2	-0.2	0.5	-0.5	-0.9	0.4	-0.6	-1.0
ZGAL_402		Conserved hypothetical membrane protein	-0.4	0.9	0.8	0.1	1.4	1.3	2.1	3.4	3.2
ZGAL_4022		Conserved hypothetical protein	-1.2	0.6	1.5	-0.4	1.4	2.3	-0.1	1.6	2.6
ZGAL_4024		Conserved hypothetical protein	-1.2	0.6	0.6	-1.0	0.9	0.9	-0.2	1.6	1.6
ZGAL_4025	menA	menA 1,4-dihydroxy-2-naphthoate octaprenyltransferase	0.3	0.6	0.0	1.0	1.2	0.6	1.0	1.3	0.7
ZGAL_4026		two-component system - Response regulator	-1.5	1.5	-0.2	-1.0	2.0	0.2	-0.8	2.2	0.5
ZGAL_4027		Two-component system - Sensor histidine kinase	-0.5	1.3	0.8	-0.3	1.5	1.0	0.2	2.0	1.5
ZGAL_403		Conserved hypothetical protein	-1.2	0.2	0.5	-1.4	0.1	0.4	0.6	2.0	2.3
ZGAL_4038		Conserved hypothetical membrane protein	0.5	-1.3	-1.0	1.1	-0.7	-0.4	2.3	0.5	0.8
ZGAL_404		Conserved hypothetical membrane protein	-2.2	-0.1	1.3	-2.3	-0.2	1.2	-0.6	1.5	2.8
ZGAL_4040		Conserved hypothetical protein	-1.0	1.0	4.5	0.0	1.9	5.5	0.6	2.5	6.0
ZGAL_4041		TonB-dependent Receptor	0.1	-2.3	-0.1	0.2	-2.2	0.0	1.4	-1.1	1.1
ZGAL_4042		Conserved hypothetical membrane protein	1.8	-2.0	-0.9	1.5	-2.3	-1.2	1.6	-2.2	-1.1
ZGAL_4044	prfB	prfB Peptide chain release factor 2	-0.2	-0.1	0.8	-0.7	-0.6	0.3	0.2	0.3	1.3
ZGAL_4045		Transglutaminase-like protein	1.6	1.1	0.7	2.1	1.6	1.2	2.6	2.1	1.6
ZGAL_4046		Conserved hypothetical protein	1.8	0.4	-1.3	1.5	0.0	-1.6	1.2	-0.3	-1.9
ZGAL_405	clpB2	clpB2 Chaperone ClpB	-1.3	0.6	1.3	-1.3	0.5	1.2	-0.4	1.4	2.1
ZGAL_4050		OmpA-like periplasmic protein	-2.0	-1.2	-2.5	-0.1	0.8	-0.6	1.8	2.6	1.3
ZGAL_4052		Conserved hypothetical protein	-0.9	0.4	1.8	-1.3	0.0	1.5	-1.0	0.3	1.7

ZGAL_4054	cysK1	cysK1 Cysteine synthase A	0.7	0.8	0.8	1.0	1.0	1.1	1.1	1.1	1.2
ZGAL_4055	kblA3	kblA3 Glycine C-acetyltransferase	-0.5	-0.5	1.1	-0.7	-0.6	0.9	0.1	0.2	1.8
ZGAL_4056		Conserved hypothetical protein	-0.5	0.4	1.1	0.1	0.9	1.6	1.3	2.2	2.8
ZGAL_4057		Conserved hypothetical membrane protein	0.0	2.1	1.6	1.8	3.9	3.5	3.3	5.4	4.9
ZGAL_4058		Conserved hypothetical protein	2.2	-0.1	0.4	1.9	-0.4	0.0	1.3	-1.0	-0.5
ZGAL_406		Conserved hypothetical protein	-2.3	0.8	1.3	-1.6	1.5	2.0	-0.4	2.7	3.2
ZGAL_4068	uvrA1	uvrA1 Excinuclease ABC, subunit A	0.3	0.5	1.0	-0.3	-0.2	0.4	-0.4	-0.2	0.3
ZGAL_407		Conserved hypothetical protein	-1.4	1.3	1.0	-1.0	1.6	1.4	-0.1	2.6	2.3
ZGAL_4071		RNA polymerase ECF-type sigma factor	-3.7	3.8	4.6	-1.7	5.9	6.6	1.1	8.7	9.4
ZGAL_4072	nth	nth Endonuclease III	-0.5	0.7	0.8	0.8	1.9	2.1	2.5	3.6	3.8
ZGAL_4074		Conserved hypothetical protein	-0.8	0.2	1.3	-0.8	0.1	1.2	-0.1	0.8	2.0
ZGAL_4075		Metallo-beta-lactamase superfamily protein	1.7	0.8	0.7	1.9	1.0	0.9	2.0	1.0	1.0
ZGAL_4076		Conserved hypothetical periplasmic protein	0.7	0.3	0.5	0.4	0.0	0.2	1.3	0.9	1.2
ZGAL_4079		Conserved hypothetical membrane protein	-2.2	0.4	0.0	-1.2	1.3	1.0	-1.0	1.6	1.2
ZGAL_408		Vgr family protein	-0.3	3.2	2.1	1.5	5.0	3.8	2.2	5.7	4.5
ZGAL_4082		Glycosyltransferase, family GT2	2.2	-0.1	-0.5	2.1	-0.1	-0.5	1.9	-0.4	-0.8
ZGAL_4084		Putative protein	-0.5	-0.8	1.3	0.8	0.5	2.6	2.2	1.8	3.9
ZGAL_409		Hypothetical protein	-0.4	4.3	4.1	1.3	5.9	5.7	2.5	7.1	6.9
ZGAL_4090		Conserved hypothetical protein	-0.6	0.8	3.0	-0.5	0.9	3.1	0.9	2.3	4.6
ZGAL_4091	czcA	czcA Cation efflux transporter	-2.4	0.0	1.2	-1.9	0.6	1.8	-0.1	2.4	3.6
ZGAL_4092	czcB	czcB cation efflux system protein	-2.4	0.3	-0.4	-2.3	0.4	-0.3	-0.6	2.2	1.5
ZGAL_4093		Conserved hypothetical protein	-1.8	1.7	1.4	-1.1	2.4	2.2	-0.2	3.4	3.1
ZGAL_4096		TonB-dependent Receptor	1.4	-0.8	0.1	0.0	-2.2	-1.2	-0.9	-3.1	-2.2
ZGAL_4098		Conserved hypothetical protein	0.1	0.7	3.0	1.2	1.8	4.2	1.8	2.4	4.8
ZGAL_4099		Thiol-disulfide oxidoreductase	-0.6	-0.3	0.5	-0.6	-0.3	0.5	0.3	0.7	1.5
ZGAL_41		Conserved hypothetical periplasmic protein	2.2	-0.1	0.0	1.4	-0.9	-0.8	1.1	-1.2	-1.2
ZGAL_410		Conserved hypothetical protein	1.4	4.3	3.9	1.8	4.7	4.3	3.0	5.9	5.5
ZGAL_4100		Conserved membrane protein	-1.0	0.7	1.2	-0.6	1.1	1.7	0.3	2.0	2.6
ZGAL_4103	lolD2	lolD2 Lipoprotein-specific ABC transporter, ATPase component	0.1	0.7	1.1	0.6	1.1	1.6	1.0	1.6	2.0
ZGAL_4107	suoX	suoX Sulfite oxidase	1.7	-1.4	-1.5	2.2	-0.9	-1.0	1.4	-1.7	-1.8
ZGAL_4108		Conserved hypothetical protein	1.5	-1.3	-1.4	1.3	-1.5	-1.5	1.2	-1.6	-1.7
ZGAL_411		Hypothetical protein	0.0	1.9	2.3	0.8	2.7	3.2	2.1	4.0	4.5
ZGAL_4110		TonB-dependent Receptor	1.1	0.2	1.8	1.4	0.5	2.2	1.3	0.4	2.0
ZGAL_4115	serA2	serA2 D-3-phosphoglycerate dehydrogenase	-2.5	-0.8	2.2	-1.9	-0.3	2.8	-1.3	0.3	3.4
ZGAL_4116	serC	serC Phosphoserine aminotransferase (Phosphoserine transaminase)	-1.2	-0.8	1.7	-1.6	-1.1	1.3	-1.0	-0.5	1.9
ZGAL_4118	fdx	fdx Ferredoxin	-0.5	0.2	1.4	-0.2	0.4	1.6	0.4	1.0	2.3
ZGAL_4119		TonB-dependent Transducer	-2.6	0.8	0.3	-2.3	1.0	0.6	-1.1	2.2	1.7
ZGAL_412		Conserved hypothetical protein	-1.3	1.5	3.5	-0.4	2.3	4.3	0.8	3.5	5.5
ZGAL_4120		anti-sigma factor	-0.4	1.0	0.3	0.4	1.7	1.0	0.7	2.1	1.3
ZGAL_4121		RNA polymerase ECF-type sigma factor	-3.0	-0.4	0.2	-0.9	1.6	2.3	-1.2	1.3	2.0
ZGAL_4122	engD	engD GTP-dependent nucleic acid-binding protein EngD	-0.8	-0.7	1.5	-0.2	-0.2	2.0	0.6	0.7	2.9
ZGAL_4125		Conserved hypothetical protein	1.1	0.6	-1.2	0.8	0.3	-1.5	0.3	-0.2	-2.1
ZGAL_4128		Conserved hypothetical protein	1.3	-0.8	-0.3	0.4	-1.7	-1.2	0.0	-2.1	-1.6
ZGAL_4129		Kelch repeats protein	-2.2	0.4	-0.7	0.7	3.3	2.2	0.6	3.2	2.2
ZGAL_413		Conserved hypothetical protein	-1.6	0.6	1.4	-0.1	2.0	2.9	0.6	2.8	3.7
ZGAL_4130	alyA4	alyA4 Alginate lyase, family PL6_1	4.5	0.3	1.3	4.5	0.2	1.2	5.0	0.8	1.8
ZGAL_4131	alyA5	alyA5 Exo-alginate lyase, family PL7_5	5.5	1.2	2.2	3.7	-0.6	0.4	4.5	0.2	1.1
ZGAL_4132	alyA6	alyA6 Alginate lyase, family PL6_1	5.2	0.8	1.6	4.9	0.4	1.2	4.5	0.1	0.8
ZGAL_4133		Two-component system - Sensor histidine kinase	4.1	1.0	-2.4	3.3	0.2	-3.2	3.1	-0.1	-3.4
ZGAL_4134		Two-component system - Response regulator	3.5	1.1	-2.3	2.4	0.0	-3.4	1.9	-0.5	-3.9
ZGAL_4136		Conserved hypothetical membrane protein	-0.4	0.5	-0.6	1.1	2.0	1.0	2.9	3.8	2.7
ZGAL_4139	corA	corA Magnesium transport protein CorA	1.1	0.0	-1.5	0.4	-0.7	-2.2	-0.1	-1.1	-2.7
ZGAL_4140		Serine peptidase, family S9	1.2	0.3	1.0	1.1	0.1	0.8	0.5	-0.5	0.2
ZGAL_4143		Conserved hypothetical protein	0.6	0.6	1.8	0.6	0.5	1.7	-0.1	-0.1	1.1
ZGAL_4145	gabD	gabD Succinate-semialdehyde dehydrogenase	1.0	-1.1	0.0	0.6	-1.4	-0.3	-0.5	-2.6	-1.5
ZGAL_4151		Histidine-containing phosphotransfer protein	-2.5	2.8	2.1	-0.4	4.9	4.2	1.6	6.9	6.2
ZGAL_4152		Response regulator receiver	-0.3	2.9	2.2	1.2	4.4	3.8	3.1	6.3	5.7
ZGAL_4153		Conserved hypothetical membrane protein	0.1	0.3	-0.4	1.1	1.4	0.6	2.9	3.2	2.4
ZGAL_4154		Glycosyltransferase, family GT2	0.0	0.7	-0.2	1.4	2.1	1.2	2.6	3.3	2.4
ZGAL_4155		Hypothetical membrane protein	-0.4	-0.6	-1.2	1.1	0.8	0.2	2.4	2.1	1.5
ZGAL_4156		Conserved hypothetical periplasmic protein	-1.0	-0.7	-2.0	0.9	1.3	0.0	2.4	2.7	1.4
ZGAL_4157		Conserved hypothetical protein	-3.0	1.6	0.6	-1.2	3.4	2.4	0.9	5.5	4.6
ZGAL_4158	rpoD2	rpoD2 RNA polymerase sigma factor rpoD	1.6	-0.4	-1.4	1.1	-0.9	-1.9	0.4	-1.7	-2.6
ZGAL_4161		ATP-dependent helicase	-1.4	0.1	0.3	-1.2	0.3	0.5	-0.7	0.9	1.1
ZGAL_4163		Two-component system - Response regulator, receiver domain	-0.9	1.2	1.2	-0.5	1.6	1.7	1.2	3.3	3.4
ZGAL_4164		Two-component system - Sensor histidine kinase	-0.7	1.9	1.0	0.2	2.8	1.9	1.7	4.3	3.4
ZGAL_4165		Two-component system - Response regulator, receiver domain	1.7	2.5	0.5	2.3	3.1	1.1	2.0	2.8	0.8
ZGAL_4166		Two-component system - Sensor histidine kinase	0.9	1.7	-0.8	1.4	2.1	-0.3	1.5	2.2	-0.2
ZGAL_4172		Metallopeptidase, family M14	1.0	0.3	-0.3	1.8	1.1	0.5	0.9	0.3	-0.3
ZGAL_4173		Putative membrane protein	0.8	1.1	0.4	2.9	3.1	2.4	1.6	1.9	1.2
ZGAL_4174		OmpA-like lipoprotein	-1.6	-2.5	0.1	-0.8	-1.7	0.8	1.0	0.1	2.6

ZGAL_4175		von Willebrand factor type A protein	0.9	-0.8	1.3	0.3	-1.3	0.8	1.3	-0.3	1.7
ZGAL_4177	iorB	iorB Isoquinoline 1-oxidoreductase beta subunit	1.4	0.7	0.6	1.0	0.3	0.2	-0.1	-0.8	-0.9
ZGAL_4178		XdhC family protein	0.7	1.6	1.5	0.9	1.8	1.7	-0.1	0.8	0.7
ZGAL_4179		PucB-like protein	0.3	1.1	1.1	0.7	1.5	1.5	0.2	1.1	1.1
ZGAL_4180		Amidohydrolase	0.2	1.0	1.3	0.8	1.5	1.8	0.4	1.2	1.4
ZGAL_4181		Metallopeptidase, family M4	1.3	0.4	-0.8	0.3	-0.5	-1.7	0.0	-0.9	-2.1
ZGAL_4183	dhlB	dhlB (S)-2-haloacid dehalogenase	1.6	-0.2	0.4	1.8	0.0	0.6	2.2	0.3	1.0
ZGAL_4184		Putative protein	2.3	1.2	3.0	2.8	1.7	3.5	2.3	1.1	3.0
ZGAL_4187		Conserved hypothetical protein	-1.1	1.3	1.4	-0.2	2.2	2.3	1.9	4.4	4.5
ZGAL_4189		Conserved hypothetical periplasmic protein	0.4	-0.9	0.3	1.2	-0.1	1.1	0.8	-0.5	0.7
ZGAL_419		Conserved hypothetical protein	-1.4	0.1	1.4	-0.3	1.2	2.4	0.0	1.5	2.7
ZGAL_4191		NAD dependent epimerase/dehydratase family protein	3.4	2.6	2.4	3.0	2.2	2.1	0.9	0.1	0.0
ZGAL_4194		Putative protein	-0.7	1.1	0.9	-0.2	1.6	1.4	0.3	2.1	1.9
ZGAL_4195		Conserved hypothetical protein	-0.6	1.5	1.2	0.5	2.6	2.3	2.0	4.1	3.8
ZGAL_4196		GCN5-related N-acetyltransferase	-1.0	1.0	0.8	0.3	2.3	2.1	1.7	3.7	3.5
ZGAL_4203	agaA	agaA Beta-agarase A, family GH16	1.4	1.1	-0.8	1.7	1.4	-0.5	2.8	2.4	0.6
ZGAL_4204		MORN repeat protein	0.3	0.6	-0.1	1.0	1.3	0.5	2.9	3.1	2.4
ZGAL_4205		Putative protein	-0.4	0.3	-1.2	0.1	0.8	-0.7	2.1	2.8	1.3
ZGAL_4209		Conserved hypothetical protein	-2.0	0.4	0.3	-0.9	1.5	1.4	0.5	2.9	2.8
ZGAL_421		Conserved hypothetical protein	-0.9	0.2	0.0	-0.1	1.0	0.8	1.1	2.1	2.0
ZGAL_4210		Hypothetical lipoprotein	-1.5	0.4	0.5	-0.5	1.4	1.5	1.0	2.9	3.0
ZGAL_4214		Conserved hypothetical protein	-0.6	2.4	0.9	-0.2	2.7	1.2	2.2	5.2	3.7
ZGAL_4215		Hypothetical protein	-0.8	0.1	-0.8	-0.9	0.0	-0.9	0.9	1.8	0.9
ZGAL_4216		Hypothetical lipoprotein	-0.7	0.8	0.2	0.0	1.6	1.0	2.0	3.6	2.9
ZGAL_4224		MarR-type transcriptional regulator	4.6	2.2	2.3	5.0	2.6	2.7	4.3	1.9	2.0
ZGAL_4225		Conserved hypothetical membrane protein	3.4	2.0	1.5	4.3	2.9	2.4	3.7	2.4	1.8
ZGAL_4226		Crp/Fnr-type transcriptional regulator	0.2	0.8	-0.3	0.9	1.6	0.5	0.8	1.4	0.3
ZGAL_4228		Intracellular peptidase, family C56	2.4	1.1	-0.7	2.5	1.2	-0.6	1.6	0.3	-1.5
ZGAL_4229		Iron-containing alcohol dehydrogenase family	2.2	0.4	-0.9	2.1	0.3	-1.0	1.2	-0.6	-1.9
ZGAL_4230		Probable NADP-dependent oxidoreductase	2.3	0.4	-1.3	2.7	0.8	-0.8	1.7	-0.1	-1.8
ZGAL_4231		NAD(P)H-flavin oxidoreductase	1.9	0.5	-1.0	2.4	0.9	-0.6	1.5	0.0	-1.5
ZGAL_4232		TetR-type transcriptional regulator	2.2	-0.7	-2.1	1.8	-1.1	-2.4	1.3	-1.6	-3.0
ZGAL_4235	ddc	ddc L-2,4-diaminobutyrate decarboxylase	1.7	-1.3	-0.2	2.5	-0.5	0.6	1.3	-1.8	-0.7
ZGAL_4241		AraC-type transcriptional regulator	1.7	0.0	-1.6	1.8	0.1	-1.5	2.6	0.9	-0.7
ZGAL_4248	alkB2	alkB2 Alpha-ketoglutarate-dependent dioxygenase	-1.3	-0.8	0.8	-0.2	0.2	1.8	-0.3	0.2	1.8
ZGAL_4252		Conserved hypothetical protein	1.9	-1.4	-0.2	1.2	-2.1	-0.9	1.3	-2.0	-0.8
ZGAL_4253		ATP-dependent helicase	-1.7	-0.1	1.9	-0.8	0.8	2.9	0.1	1.7	3.7
ZGAL_4259		Conserved hypothetical protein	-4.2	-1.2	-2.0	-3.3	-0.3	-1.0	-1.3	1.7	0.9
ZGAL_4261	rbsA	rbsA Ribose ABC importer, ATPase component	-2.9	0.0	0.6	-3.2	-0.3	0.4	-1.5	1.3	2.0
ZGAL_4267	agaC	agaC Beta-agarase AgaC, family GH16	-0.7	1.4	0.4	0.6	2.7	1.7	2.7	4.8	3.7
ZGAL_4268		Parallel beta-helix fold protein	-1.0	1.6	1.3	1.2	3.8	3.5	2.8	5.3	5.0
ZGAL_4269		Acid phosphatase/vanadium-dependent haloperoxidase family protein	1.4	0.2	-1.8	1.1	-0.1	-2.1	0.4	-0.8	-2.8
ZGAL_4272		Conserved hypothetical protein	1.4	0.0	-1.4	1.6	0.2	-1.2	5.2	3.8	2.4
ZGAL_4273		Hypothetical periplasmic protein	2.0	1.1	-1.8	1.4	0.5	-2.4	0.9	0.0	-2.9
ZGAL_4274		Outer membrane efflux protein	1.3	-0.8	-0.6	0.0	-2.1	-2.0	3.4	1.3	1.5
ZGAL_4275	macA	macA Macrolide-specific membrane fusion protein	0.7	-1.3	-1.7	0.3	-1.6	-2.0	4.2	2.3	1.9
ZGAL_4276	macC	macC Macrolide-specific ABC exporter, ATPase component	1.5	-0.5	-1.2	1.6	-0.4	-1.1	3.5	1.5	0.8
ZGAL_4277	macB	macB Macrolide-specific ABC exporter, permease component	1.3	0.3	-0.1	1.0	0.0	-0.4	2.1	1.1	0.7
ZGAL_4279		ABC-1 type exporter - Permease/ATP-binding protein	-1.3	0.6	0.9	-0.1	1.7	2.0	0.1	1.9	2.3
ZGAL_4284		Possible co-chaperone	-1.4	-0.5	2.1	0.7	1.6	4.3	1.2	2.1	4.8
ZGAL_4287	cspA5	cspA5 Cold shock protein	-0.5	1.5	5.4	1.6	3.7	7.5	1.2	3.3	7.1
ZGAL_4288		Hypothetical lipoprotein	-0.1	1.8	3.9	2.7	4.6	6.7	2.1	4.0	6.1
ZGAL_4289		Conserved hypothetical membrane protein	2.7	-4.6	-0.8	2.6	-4.7	-0.9	4.0	-3.3	0.5
ZGAL_4291		DEAD/DEAH RNA helicase	-1.0	-0.5	1.1	-1.4	-0.9	0.7	-0.9	-0.4	1.2
ZGAL_4293		Hypothetical periplasmic protein	-1.2	-1.1	1.5	-0.5	-0.5	2.2	0.2	0.3	2.9
ZGAL_4294		Hypothetical protein	-0.2	-0.1	2.3	0.1	0.3	2.6	0.9	1.0	3.4
ZGAL_4295		Two-component system - Sensor histidine kinase	-1.2	0.7	0.7	0.3	2.2	2.2	1.5	3.4	3.4
ZGAL_4297		Hypothetical membrane protein	2.1	-0.6	-2.1	2.5	-0.2	-1.7	1.4	-1.3	-2.8
ZGAL_4299		DUF6 family protein	-2.5	-0.4	1.0	-1.4	0.7	2.1	-1.1	0.9	2.4
ZGAL_4301		Conserved hypothetical protein	-1.0	0.9	1.0	-0.1	1.8	2.0	0.2	2.2	2.3
ZGAL_4302		Conserved hypothetical protein	-0.2	1.8	2.8	-0.3	1.8	2.8	0.3	2.4	3.4
ZGAL_4306		Hypothetical periplasmic protein	1.7	-0.6	-2.6	2.6	0.3	-1.7	1.7	-0.6	-2.6
ZGAL_4307		Conserved hypothetical lipoprotein	1.4	-0.2	-3.5	2.3	0.7	-2.7	1.1	-0.4	-3.8
ZGAL_4309		Putative protein	2.7	1.1	0.0	2.1	0.5	-0.6	1.0	-0.6	-1.7
ZGAL_4310		Conserved hypothetical periplasmic protein	-0.3	1.3	0.5	0.5	2.1	1.4	2.4	4.0	3.2
ZGAL_4317		Hypothetical membrane protein	-0.7	1.1	0.4	-1.1	0.6	0.0	0.1	1.9	1.2
ZGAL_4318		Conserved hypothetical protein	-2.2	-0.9	2.8	-1.8	-0.5	3.1	-0.7	0.6	4.3
ZGAL_4319		Conserved hypothetical periplasmic protein	-0.1	0.7	1.2	-0.4	0.3	0.8	0.7	1.5	2.0
ZGAL_4321		Na+/H+ antiporter	0.6	-0.5	-0.5	1.6	0.6	0.6	1.4	0.4	0.4
ZGAL_4324		Conserved hypothetical periplasmic protein	-1.4	1.9	2.3	-0.2	3.1	3.5	1.8	5.1	5.5
ZGAL_4325		Hypothetical lipoprotein	-1.4	-0.1	-1.4	-0.7	0.6	-0.7	1.3	2.6	1.3
ZGAL_4326		Endo-beta-1,4-glucuronan lyase, family PL31	-2.4	4.2	1.7	-0.2	6.4	3.9	0.7	7.3	4.8

ZGAL_4327	alyA7	alyA7 Alginate lyase, family PL14_3	-1.9	1.7	0.0	-2.0	1.6	-0.2	-0.6	3.0	1.2
ZGAL_4332		hypothetical protein	0.1	0.8	1.6	-0.5	0.2	1.0	-0.1	0.6	1.3
ZGAL_4333		Hypothetical protein	1.4	-1.6	-2.6	2.8	-0.2	-1.3	2.8	-0.2	-1.3
ZGAL_4340		Conserved hypothetical periplasmic protein	2.9	0.6	-0.7	1.9	-0.4	-1.7	2.8	0.5	-0.8
ZGAL_4341	ybhR	ybhR ABC-2 type exporter, permease component	2.9	0.7	-0.9	3.3	1.1	-0.5	3.6	1.4	-0.2
ZGAL_4348		Conserved hypothetical protein	-0.2	2.1	1.5	1.1	3.3	2.7	3.0	5.3	4.7
ZGAL_4349		Hypothetical periplasmic protein	0.7	2.9	1.8	1.6	3.8	2.7	3.3	5.5	4.3
ZGAL_4350		Conserved hypothetical protein	0.8	0.4	-0.5	2.1	1.7	0.7	3.5	3.1	2.1
ZGAL_4353		Glycosyltransferase, family GT4	-1.8	0.1	-0.5	-0.7	1.2	0.6	0.2	2.1	1.6
ZGAL_4354		Hypothetical protein	-2.4	0.4	-0.3	-1.7	1.1	0.4	0.3	3.1	2.3
ZGAL_4355		Hypothetical membrane protein	-1.1	1.3	0.5	-0.7	1.7	0.9	2.1	4.5	3.6
ZGAL_4356		Glycosyltransferase, family GT4	-2.3	0.3	-1.1	-1.0	1.7	0.3	1.0	3.7	2.3
ZGAL_4357		LemA family protein	-3.9	0.4	-1.1	-1.8	2.5	1.0	0.1	4.4	3.0
ZGAL_4358		Conserved hypothetical protein	-0.2	1.3	2.1	-0.2	1.3	2.1	0.2	1.8	2.6
ZGAL_4363	sqrA	sqrA Sulfide:quinone oxidoreductase	1.7	0.0	-2.0	1.8	0.1	-1.9	0.8	-0.9	-2.9
ZGAL_4364		Hypothetical protein	3.4	-0.7	-1.9	4.5	0.4	-0.8	3.6	-0.6	-1.7
ZGAL_437		Conserved hypothetical protein	-0.7	-0.1	0.3	1.1	1.7	2.1	2.3	2.9	3.3
ZGAL_4379		Conserved hypothetical periplasmic protein	1.9	1.1	-3.3	2.3	1.5	-2.9	0.7	-0.1	-4.5
ZGAL_438		Conserved hypothetical protein	-0.1	0.5	0.1	0.7	1.2	0.8	1.3	1.8	1.4
ZGAL_4385	fabZ3	fabZ3 (3R)-Hydroxymyristoyl-[acyl-carrier-protein] dehydratase	1.9	1.8	1.2	1.8	1.6	1.1	0.4	0.2	-0.3
ZGAL_4386		Short-chain dehydrogenase/reductase	2.5	1.3	0.4	1.8	0.7	-0.2	0.8	-0.4	-1.3
ZGAL_4387		Type III polyketide synthase	1.8	1.3	0.3	1.9	1.4	0.4	0.3	-0.3	-1.3
ZGAL_4388		Methyltransferase family protein	1.2	0.4	-0.8	1.4	0.6	-0.7	0.1	-0.7	-1.9
ZGAL_4391		Conserved hypothetical lipoprotein	1.4	-1.7	-0.3	1.2	-1.9	-0.5	2.4	-0.7	0.7
ZGAL_4392	bkdA1	bkdA1 2-Oxoisovalerate dehydrogenase, E1 component	0.2	0.3	1.5	0.3	0.4	1.7	0.0	0.1	1.4
ZGAL_4396	udpA	udpA Uridine phosphorylase	1.3	0.7	0.1	1.4	0.9	0.3	1.4	0.8	0.2
ZGAL_4399	ungA	ungA Uracil-DNA glycosylase	2.4	-1.3	-1.6	1.9	-1.7	-2.0	0.1	-3.5	-3.9
ZGAL_4406		FAD-dependent oxidoreductase	-1.0	-0.6	1.3	-1.4	-1.0	0.9	-1.2	-0.8	1.2
ZGAL_4407		Conserved hypothetical periplasmic protein	-1.0	0.2	-0.6	-0.4	0.8	0.1	0.9	2.0	1.3
ZGAL_4409		Conserved hypothetical lipoprotein	-0.9	1.4	0.6	1.6	3.8	3.0	2.8	5.0	4.3
ZGAL_4417		Conserved hypothetical protein	-3.0	1.1	2.1	-0.4	3.8	4.8	1.3	5.4	6.5
ZGAL_4418		Hypothetical periplasmic protein	-1.4	0.6	1.0	0.2	2.3	2.7	2.0	4.1	4.5
ZGAL_4419		Metallo-beta-lactamase superfamily protein	0.4	0.6	0.6	1.1	1.3	1.3	1.7	1.9	1.9
ZGAL_4421		Hypothetical periplasmic protein	-1.6	1.4	2.2	-1.4	1.7	2.4	-0.3	2.7	3.5
ZGAL_4422		Conserved hypothetical protein	-1.4	1.7	2.8	-0.5	2.7	3.8	0.4	3.6	4.7
ZGAL_4423		Conserved hypothetical protein	-1.8	1.3	2.0	-0.4	2.7	3.4	0.4	3.5	4.1
ZGAL_4431		Hypothetical membrane protein	-1.5	1.4	2.3	-0.5	2.3	3.2	-0.2	2.6	3.5
ZGAL_4432		Conserved hypothetical protein	-1.8	1.3	2.0	-0.4	2.7	3.4	0.4	3.5	4.1
ZGAL_4436		AsnC/Lrp-type transcriptional regulator	-0.9	0.3	0.6	-0.6	0.6	1.0	0.7	1.8	2.2
ZGAL_4437		Conserved hypothetical protein	-1.0	1.4	0.7	0.0	2.4	1.7	2.3	4.7	4.0
ZGAL_4438		Conserved hypothetical protein	-2.4	1.3	1.1	-0.2	3.5	3.3	1.6	5.3	5.2
ZGAL_4439		Conserved hypothetical protein	1.3	0.1	-0.7	1.6	0.4	-0.4	0.9	-0.3	-1.2
ZGAL_4443		Long chain dehydrogenase/reductase	-2.1	0.3	0.2	-0.6	1.8	1.8	1.5	3.9	3.8
ZGAL_4444	aldB	aldB Alpha-acetolactate decarboxylase	-2.2	1.0	0.5	0.8	4.1	3.6	2.9	6.1	5.6
ZGAL_4445		Permease	-2.0	0.0	-0.6	0.4	2.3	1.8	2.4	4.4	3.8
ZGAL_4446		OsmC-like protein	-1.9	0.4	-0.2	-0.9	1.4	0.9	0.7	2.9	2.4
ZGAL_4447		Thioredoxin-like protein	-3.4	0.7	0.2	-1.5	2.7	2.2	0.1	4.3	3.8
ZGAL_445		Hypothetical protein	-1.2	0.4	1.1	-0.6	0.9	1.6	-0.9	0.7	1.3
ZGAL_4450		Sodium-dependent transporter	-1.4	-0.3	0.8	-0.6	0.6	1.7	0.0	1.1	2.2
ZGAL_4453		YceI family protein	-5.6	-1.4	1.0	-4.6	-0.4	2.0	-2.6	1.7	4.0
ZGAL_4454		Conserved hypothetical periplasmic protein	-6.6	0.7	1.4	-4.2	3.0	3.8	-2.3	4.9	5.7
ZGAL_4455		YceI family protein	-4.2	0.8	0.1	-2.3	2.7	1.9	-0.6	4.3	3.6
ZGAL_4457		Hypothetical periplasmic protein	-1.8	0.1	-0.4	-1.0	0.9	0.5	-0.2	1.7	1.2
ZGAL_4459		Conserved hypothetical lipoprotein	1.8	-0.2	0.0	0.6	-1.5	-1.2	0.3	-1.8	-1.5
ZGAL_4460		Alpha/beta hydrolase-fold protein	2.0	-0.9	0.6	1.8	-1.0	0.5	1.9	-0.9	0.6
ZGAL_4461		Serine peptidase, family S12	1.7	-0.2	0.1	1.9	0.0	0.4	2.6	0.7	1.1
ZGAL_447		Conserved hypothetical membrane protein	-0.1	0.6	-0.3	-0.2	0.6	-0.4	1.9	2.6	1.7
ZGAL_4470		Fatty acid hydroxylase family protein	0.5	-0.1	0.0	1.0	0.4	0.5	1.7	1.1	1.2
ZGAL_4471		3-oxoacyl-[acyl-carrier-protein] synthase III	-0.3	0.0	-0.2	-0.6	-0.3	-0.5	0.8	1.1	0.9
ZGAL_448		LemA family protein	-0.2	-0.1	-1.0	0.1	0.1	-0.8	1.8	1.9	1.0
ZGAL_4490		Conserved hypothetical protein	1.8	0.1	-0.7	0.4	-1.3	-2.1	-0.4	-2.1	-2.9
ZGAL_450		Conserved hypothetical membrane protein	0.3	0.1	-2.1	1.0	0.8	-1.4	2.3	2.1	-0.1
ZGAL_4500		Putative membrane lipoprotein	-5.7	-2.8	0.1	-6.0	-3.1	-0.2	-4.4	-1.5	1.5
ZGAL_4501		TonB-dependent Receptor	-5.3	-4.1	-0.6	-4.6	-3.3	0.2	-2.2	-1.0	2.5
ZGAL_4508	hisIE	hisIE Histidine biosynthesis bifunctional protein HisIE	-1.1	-0.1	1.3	-1.8	-0.8	0.5	-2.1	-1.1	0.2
ZGAL_4509	hisF	hisF Imidazole glycerol phosphate synthase subunit HisF	0.9	0.2	1.6	-0.8	-1.5	-0.1	-1.8	-2.4	-1.1
ZGAL_451		Hypothetical lipoprotein	-2.4	2.2	-0.7	1.7	6.3	3.3	4.1	8.7	5.8
ZGAL_4510	hisA	hisA 1-(5-phosphoribosyl)-5-[(5-phosphoribosylamino)methylideneamino] imidazole-4-carboxamide isomerase	0.1	0.2	1.7	-1.6	-1.5	0.0	-2.5	-2.4	-0.9
ZGAL_4511		Bacterial 23S rRNA protein	-0.9	-0.2	1.9	-1.6	-0.8	1.2	-2.5	-1.8	0.3
ZGAL_4512	hisH	hisH Imidazole glycerol phosphate synthase subunit HisH	-0.7	0.1	2.7	-1.6	-0.7	1.8	-2.6	-1.7	0.9
ZGAL_4513	hisB	hisB Histidine biosynthesis bifunctional protein HisB	-0.9	-0.6	2.1	-1.7	-1.4	1.3	-2.7	-2.4	0.2

ZGAL_4516		GCN5-related N-acetyltransferase	-0.7	-1.3	1.6	-1.3	-1.9	1.0	-1.6	-2.2	0.6
ZGAL_4517	hisG	hisG ATP phosphoribosyltransferase	0.0	-1.1	1.3	-0.8	-1.9	0.5	-0.9	-2.0	0.4
ZGAL_452		Conserved hypothetical periplasmic protein	-0.3	2.4	-1.4	1.2	3.9	0.1	2.4	5.1	1.4
ZGAL_4522	sucD	sucD Succinyl-CoA ligase [ADP-forming] subunit alpha	0.1	-0.4	1.4	0.0	-0.5	1.3	-0.1	-0.6	1.2
ZGAL_4524	efp	efp Elongation factor P	-1.1	0.5	2.0	-1.3	0.3	1.7	-0.8	0.9	2.3
ZGAL_4525	lpxA	lpxA Acyl-[acyl-carrier-protein]--UDP-N-acetylglucosamine O-acyltransferase	-0.1	1.2	2.5	-0.3	1.1	2.4	0.5	1.8	3.1
ZGAL_4527	lpxD2	lpxD2 UDP-3-O-[3-hydroxymyristoyl] glucosamine N-acyltransferase	-0.2	0.4	1.0	-0.2	0.3	1.0	0.6	1.2	1.8
ZGAL_4531		Putative membrane lipoprotein	-0.3	1.3	1.4	0.2	1.8	1.9	2.3	3.9	4.0
ZGAL_4532		Conserved hypothetical membrane protein	-0.1	1.6	-0.2	1.5	3.2	1.4	2.8	4.5	2.8
ZGAL_4534		Conserved hypothetical membrane protein	-0.7	0.3	0.7	0.2	1.1	1.6	0.9	1.8	2.3
ZGAL_4544		Fatty acid hydroxylase family protein	2.6	1.9	-0.2	3.4	2.7	0.5	1.7	1.0	-1.2
ZGAL_4545	parC	parC DNA topoisomerase IV, subunit A	-0.1	1.4	0.7	-0.5	1.0	0.2	-0.4	1.1	0.4
ZGAL_4548		FMN / Fe-S cluster binding protein	-0.4	0.4	1.6	0.3	1.1	2.3	0.6	1.4	2.6
ZGAL_4550		Conserved hypothetical membrane protein	-1.5	0.6	0.5	-0.5	1.6	1.6	1.4	3.5	3.4
ZGAL_4551		Phospholipase, Patatin family	0.0	-0.4	0.1	0.4	0.0	0.4	1.6	1.2	1.6
ZGAL_4557	leuD	leuD 3-Isopropylmalate dehydratase, small subunit	-0.1	0.6	2.6	-0.8	-0.2	1.9	-0.1	0.6	2.6
ZGAL_4558	cimA	cimA Possible (R)-citramalate synthase	-0.4	0.3	2.2	-0.7	0.0	1.9	-0.1	0.6	2.5
ZGAL_4559	LeuB1	LeuB1 3-Isopropylmalate dehydrogenase	-2.0	0.4	1.9	-2.5	-0.2	1.4	-2.2	0.1	1.7
ZGAL_4562		AraC-type transcriptional regulator	2.1	0.2	-1.5	2.5	0.5	-1.1	1.6	-0.3	-2.0
ZGAL_4563		AraC-type transcriptional regulator	1.9	1.0	-1.4	3.1	2.3	-0.2	2.0	1.1	-1.3
ZGAL_4565	gapN	gapN glyceraldehyde 3-phosphate dehydrogenase, NADP-dependent	-1.1	1.0	-0.8	-1.1	1.0	-0.8	-0.8	1.3	-0.4
ZGAL_4566	ilvA	ilvA threonine ammonia-lyase (or Threonine dehydratase)	-1.6	1.3	3.0	-1.7	1.2	2.9	-1.9	1.1	2.8
ZGAL_4567	ilvC	ilvC Ketol-acid reductoisomerase	-1.4	0.0	2.9	-2.0	-0.6	2.3	-1.9	-0.5	2.4
ZGAL_4568	ilvH	ilvH Acetolactate synthase small subunit	-1.5	1.2	3.6	-1.2	1.5	3.9	-0.5	2.2	4.6
ZGAL_4569		S-adenosylmethionine-dependent O-methyltransferase	-0.5	1.0	4.0	-0.7	0.8	3.8	-0.1	1.4	4.4
ZGAL_4570	ilvB	ilvB Acetolactate synthase, large subunit	-0.9	0.6	3.8	-1.2	0.3	3.5	-0.4	1.1	4.3
ZGAL_4571	ilvD	ilvD Dihydroxy-acid dehydratase	0.9	1.1	3.4	-0.1	0.1	2.4	0.7	0.9	3.2
ZGAL_4575		Conserved hypothetical protein	-0.6	4.6	2.6	1.3	6.4	4.5	3.9	9.0	7.1
ZGAL_4576		Conserved hypothetical membrane protein	-0.4	1.8	0.5	1.5	3.8	2.5	3.0	5.2	3.9
ZGAL_4582		Conserved hypothetical protein	-1.0	1.5	2.0	-0.7	1.9	2.4	0.1	2.6	3.1
ZGAL_4583		PIN-like protein	-1.7	1.0	1.3	-0.3	2.4	2.7	0.3	3.0	3.3
ZGAL_4599	comM	comM Competence protein comM	1.0	1.0	-0.8	1.4	1.4	-0.3	1.4	1.4	-0.3
ZGAL_460		RNA polymerase ECF-type sigma factor	0.1	1.7	0.0	0.7	2.3	0.6	-0.2	1.4	-0.3
ZGAL_4600	quiP	quiP Acyl-homoserine lactone acylase, family S45	1.2	0.5	-0.2	1.5	0.8	0.1	1.2	0.5	-0.2
ZGAL_4601	dsbD	dsbD Thiol:disulfide interchange protein	1.7	-0.6	-0.5	0.8	-1.5	-1.4	0.9	-1.4	-1.3
ZGAL_4604		Putative protein	2.8	2.2	1.8	3.8	3.1	2.8	5.1	4.5	4.1
ZGAL_4606		Conserved hypothetical membrane protein	0.9	0.4	-0.6	2.2	1.8	0.7	3.5	3.1	2.1
ZGAL_461		PKD repeats containing lipoprotein	-0.7	-0.2	-0.2	0.0	0.5	0.5	1.2	1.7	1.7
ZGAL_4610	trxA	trxA Thioredoxin	1.9	1.0	-2.1	0.8	0.0	-3.1	0.4	-0.4	-3.6
ZGAL_4615	ftsK	ftsK DNA translocase FtsK	-0.2	-1.0	0.3	0.8	0.0	1.3	1.1	0.3	1.6
ZGAL_4616		Conserved hypothetical periplasmic protein	1.2	-1.4	-0.4	2.3	-0.3	0.7	1.7	-1.0	0.0
ZGAL_4617		Conserved hypothetical membrane protein	1.6	-0.4	-0.9	1.9	-0.1	-0.6	1.4	-0.6	-1.1
ZGAL_4618	ribAB	ribAB Riboflavin biosynthesis protein RibAB	1.7	-0.5	-0.5	1.0	-1.2	-1.2	1.5	-0.7	-0.7
ZGAL_4622		SusD-like lipoprotein	2.0	0.6	-0.1	1.1	-0.4	-1.1	0.7	-0.7	-1.4
ZGAL_4624		Conserved hypothetical periplasmic protein	0.5	-0.3	1.4	-0.1	-0.9	0.8	-0.5	-1.3	0.4
ZGAL_4633		Two-component system - Response regulator	-1.9	3.8	2.9	-0.7	4.9	4.0	1.5	7.2	6.3
ZGAL_4634		T9SS SprF family protein	0.9	5.2	3.7	1.5	5.8	4.3	3.6	7.9	6.4
ZGAL_4635		T9SS-associated PG1058-like protein	1.3	5.9	4.6	1.0	5.6	4.3	3.3	7.9	6.6
ZGAL_4637	gapB	gapB Glyceraldehyde 3-phosphate dehydrogenase	4.1	1.0	-1.1	2.8	-0.3	-2.5	0.4	-2.7	-4.8
ZGAL_4638	mroA5	mroA5 Aldose 1-epimerase	1.0	0.4	-1.3	1.2	0.6	-1.1	0.6	0.1	-1.6
ZGAL_464	yqfF	yqfF Conserved hypothetical protein	-1.0	0.6	0.5	-0.8	0.8	0.7	-0.7	0.9	0.8
ZGAL_4648		Putative membrane protein	1.0	1.6	1.7	2.0	2.6	2.7	2.3	2.8	3.0
ZGAL_465	thlA	thlA Acetyl-CoA acetyltransferase	-0.8	-0.1	1.1	-0.6	0.1	1.3	-0.4	0.3	1.5
ZGAL_4652		Putative protein	-2.0	0.8	1.3	-1.8	1.0	1.5	-1.3	1.5	2.0
ZGAL_4654	dgoT	dgoT D-galactonate transporter	-1.8	0.0	0.7	-0.9	0.9	1.6	-0.9	0.9	1.6
ZGAL_4661	kduD1	kduD1 2-deoxy-D-gluconate-3-dehydrogenase	2.1	0.4	-2.5	0.7	-0.9	-3.9	0.1	-1.6	-4.5
ZGAL_4673		Carbohydrate esterase, family CE1	2.3	1.5	0.3	2.2	1.5	0.3	1.3	0.5	-0.6
ZGAL_4674	adhI	adhI Alcohol dehydrogenase class 3 / S-(hydroxymethyl)glutathione dehydrogenase	0.7	1.2	0.5	0.4	0.8	0.1	-0.2	0.3	-0.4
ZGAL_4676	fdxA3	fdxA3 2Fe-2S ferredoxin	3.5	1.9	0.5	1.8	0.2	-1.2	-0.1	-1.7	-3.1
ZGAL_4677		6-O-methyl-D-galactose demethylase	2.5	1.0	0.4	1.9	0.4	-0.2	0.5	-0.9	-1.5
ZGAL_468	gyrA	gyrA DNA gyrase, subunit A	-0.7	-0.5	2.2	-0.7	-0.4	2.2	-0.5	-0.2	2.4
ZGAL_4682	uxaB	uxaB Altronate oxidoreductase	-1.9	0.3	1.3	-2.1	0.1	1.1	-2.3	-0.1	0.9
ZGAL_4690		Conserved cytochrome c-containing protein	1.6	-0.3	-1.8	0.9	-0.9	-2.5	0.7	-1.1	-2.7
ZGAL_4699		SusC-like TonB-dependent transporter	0.7	0.1	-1.5	0.3	-0.3	-1.9	1.4	0.9	-0.8
ZGAL_47		Small-conductance mechanosensitive channel	2.7	0.5	-0.9	3.0	0.7	-0.6	3.0	0.8	-0.6
ZGAL_470		Conserved hypothetical protein	-0.1	2.7	-0.4	2.2	5.0	1.9	0.8	3.6	0.5
ZGAL_4705		Conserved hypothetical membrane protein	-0.6	-0.1	-0.9	0.9	1.5	0.7	0.8	1.4	0.6
ZGAL_4706		Conserved hypothetical protein	1.1	0.7	0.3	0.6	0.1	-0.2	1.2	0.8	0.4
ZGAL_4707		Conserved hypothetical membrane protein	-0.8	0.7	1.2	0.4	2.0	2.4	1.7	3.2	3.6
ZGAL_4708	dnaK	dnaK Molecular chaperone DnaK	-0.3	-1.7	2.0	-0.4	-1.9	1.8	0.5	-1.0	2.7

ZGAL_4711	sugE	sugE Quaternary ammonium compound-resistance protein SugE	-1.1	0.2	0.5	-0.2	1.1	1.4	0.4	1.7	2.0
ZGAL_4716		Conserved hypothetical periplasmic protein	1.5	0.6	-1.4	1.6	0.7	-1.4	1.1	0.2	-1.8
ZGAL_4719		Conserved hypothetical lipoprotein	1.4	-1.3	-1.1	1.3	-1.3	-1.2	0.7	-2.0	-1.9
ZGAL_472	thrA	thrA Aspartate kinase I / Homoserine dehydrogenase I	-1.4	-1.2	1.5	-2.2	-2.0	0.7	-2.2	-1.9	0.7
ZGAL_4722		Conserved hypothetical protein	-0.7	0.6	0.3	-0.3	1.0	0.7	-0.3	1.0	0.6
ZGAL_4723	leuA	leuA 2-Isopropylmalate synthase	1.4	1.5	2.1	0.3	0.4	1.0	1.0	1.2	1.7
ZGAL_4727		Fasciclin family protein	-0.1	0.3	-0.2	0.2	0.6	0.1	1.1	1.5	1.1
ZGAL_4728		Conserved hypothetical membrane protein	1.6	1.3	0.5	2.2	2.0	1.2	1.7	1.4	0.6
ZGAL_4729		Conserved hypothetical lipoprotein	-0.4	1.5	1.0	0.6	2.5	2.0	2.2	4.2	3.6
ZGAL_473	thrB	thrB Homoserine kinase	-1.0	-0.1	2.3	-1.1	-0.2	2.2	-2.0	-1.1	1.4
ZGAL_4730		ABC transporter, ATPase component	-0.6	-0.6	1.4	-0.8	-0.8	1.2	0.1	0.1	2.1
ZGAL_4731		Conserved hypothetical lipoprotein	2.2	0.6	-0.3	2.0	0.4	-0.6	2.1	0.5	-0.5
ZGAL_4732	talA2	talA2 Transaldolase	-1.9	-0.4	2.5	-1.7	-0.2	2.7	-1.4	0.1	3.0
ZGAL_4733		Short-chain dehydrogenase/reductase	-1.0	-0.7	0.5	0.3	0.6	1.8	0.4	0.7	1.9
ZGAL_4738		Two-component system - Response regulator	0.3	1.1	2.0	1.0	1.8	2.7	2.3	3.1	3.9
ZGAL_4739		Two-component system - Sensor histidine kinase	2.2	0.5	0.6	1.5	-0.2	-0.1	1.3	-0.4	-0.3
ZGAL_474	thrC1	thrC1 Threonine synthase	-0.7	0.8	2.1	-1.3	0.2	1.5	-2.1	-0.6	0.7
ZGAL_4740		Two-component system - Response regulator	3.0	-1.0	-1.1	1.4	-2.6	-2.7	0.8	-3.2	-3.3
ZGAL_4741		Hypothetical protein	-0.2	0.8	1.4	0.1	1.1	1.7	1.3	2.3	2.9
ZGAL_4745	clpB1	clpB1 Chaperone ClpB	0.1	-1.4	0.7	0.4	-1.2	0.9	1.3	-0.2	1.9
ZGAL_4747		Conserved hypothetical periplasmic protein	0.7	0.9	2.1	0.5	0.7	1.9	0.3	0.5	1.8
ZGAL_4748		Conserved hypothetical protein	-0.8	1.5	0.3	0.3	2.6	1.4	1.4	3.7	2.5
ZGAL_4749	smpB	smpB SsrA-binding protein	-0.9	0.1	-0.2	-1.2	-0.2	-0.5	0.0	1.0	0.6
ZGAL_4753		Alpha/beta barrel fold protein	0.2	0.3	1.7	-0.7	-0.6	0.8	-0.7	-0.6	0.9
ZGAL_476	gcvT	gcvT Aminomethyltransferase (Glycine-cleavage system T-protein)	-0.6	0.1	1.2	-1.0	-0.3	0.8	-1.1	-0.3	0.7
ZGAL_4762		Glycosyltransferase, family GT2	-2.1	-0.2	0.7	-1.8	0.0	0.9	-1.7	0.2	1.1
ZGAL_4765		Conserved hypothetical periplasmic protein	0.5	0.7	0.5	0.9	1.2	1.0	2.9	3.2	3.0
ZGAL_4768		Conserved hypothetical lipoprotein	0.9	-0.2	0.1	1.4	0.2	0.5	0.8	-0.3	0.0
ZGAL_4771		5'nucleotidase, substrate binding subunit	0.0	0.3	1.2	-0.5	-0.2	0.7	-0.3	-0.1	0.8
ZGAL_48		Conserved hypothetical lipoprotein	1.9	-3.8	-2.6	1.0	-4.6	-3.4	1.8	-3.8	-2.6
ZGAL_489	dnaX	dnaX DNA polymerase III, gamma/tau chain	-1.2	0.1	2.3	-0.7	0.5	2.8	-0.5	0.8	3.0
ZGAL_49		Conserved hypothetical protein	0.8	-3.7	-2.6	1.4	-3.1	-2.0	1.9	-2.5	-1.4
ZGAL_493	aroB1	aroB1 3-Dehydroquinate synthase	-0.4	-0.3	0.9	-0.2	-0.2	1.0	0.2	0.3	1.4
ZGAL_50		Conserved hypothetical protein	0.7	-3.9	-2.4	0.9	-3.7	-2.2	1.7	-2.9	-1.4
ZGAL_506	rpsA	rpsA Ribosomal protein S1	-1.8	-1.6	1.0	-0.6	-0.5	2.2	0.4	0.6	3.2
ZGAL_507	ygaU	ygaU Protein YgaU, family CBM50	-0.4	0.8	0.4	-0.2	1.0	0.6	1.1	2.3	1.8
ZGAL_509	lonA	lonA Endopeptidase La, family S16	-1.1	-1.4	2.0	-0.8	-1.1	2.3	0.5	0.3	3.7
ZGAL_511		RNA polymerase ECF-type sigma factor	1.8	-4.3	-1.0	2.6	-3.5	-0.3	2.3	-3.8	-0.6
ZGAL_512		Conserved hypothetical membrane protein	2.0	-3.6	-4.1	1.4	-4.3	-4.8	1.8	-3.8	-4.3
ZGAL_513		Conserved hypothetical protein	2.2	-3.6	-3.6	1.9	-3.8	-3.9	2.7	-3.1	-3.1
ZGAL_515		Major facilitator family transporter	-0.2	-0.2	-0.5	0.3	0.4	0.0	1.7	1.8	1.4
ZGAL_517		Alpha-glucosidase, family GH31	-0.7	0.2	0.8	-0.5	0.4	1.0	-0.5	0.4	1.0
ZGAL_521	msrB1	msrB1 Peptide methionine sulfoxide reductase msrB	2.7	-0.1	-2.4	1.0	-1.8	-4.2	-0.2	-3.0	-5.3
ZGAL_522		Conserved hypothetical protein	1.9	0.3	-2.2	1.2	-0.4	-2.9	0.2	-1.5	-3.9
ZGAL_523	bfmBC	bfmBC Dihydrolipoyl dehydrogenase, E3 component of branched-chain alpha-keto acid dehydrogenase complex	-1.3	-0.5	1.4	-1.1	-0.3	1.5	-0.1	0.6	2.5
ZGAL_524		Conserved hypothetical membrane protein	-1.4	0.0	0.8	0.1	1.5	2.3	2.2	3.6	4.5
ZGAL_525		Conserved hypothetical periplasmic protein	-0.8	1.4	1.0	0.8	3.0	2.6	3.0	5.1	4.8
ZGAL_53		Carboxy-terminal processing peptidase, family S41	0.6	-1.6	0.0	1.3	-0.8	0.8	1.8	-0.4	1.2
ZGAL_531	ndhA1	ndhA1 NADH dehydrogenase	-0.2	0.2	0.3	0.1	0.5	0.6	0.6	1.1	1.2
ZGAL_536		NUDIX hydrolase	2.2	0.4	0.6	1.8	0.0	0.2	0.4	-1.5	-1.2
ZGAL_538		RDD family membrane protein	-0.2	0.4	0.0	-0.2	0.4	0.0	1.0	1.6	1.2
ZGAL_54		Carboxy-terminal processing peptidase, family S41	1.1	0.3	1.1	1.2	0.4	1.2	2.5	1.7	2.4
ZGAL_540		Conserved hypothetical membrane protein	-1.9	0.8	0.2	-0.8	1.9	1.4	0.4	3.0	2.5
ZGAL_541		Conserved hypothetical membrane protein	-0.7	-0.2	-0.5	0.0	0.5	0.2	1.6	2.2	1.8
ZGAL_542		Conserved hypothetical membrane protein	-0.8	-0.9	-1.3	-0.2	-0.3	-0.7	1.5	1.4	1.0
ZGAL_544		vWA domain protein	0.5	0.7	-1.7	0.6	0.8	-1.7	1.2	1.4	-1.0
ZGAL_546		Hypothetical protein	0.1	1.9	3.2	0.5	2.3	3.6	0.0	1.8	3.1
ZGAL_549		Conserved hypothetical protein	1.9	0.0	-0.3	1.3	-0.6	-0.9	0.0	-1.9	-2.2
ZGAL_553		Fasciclin repeats protein	3.3	1.0	-0.7	1.9	-0.4	-2.1	1.4	-0.9	-2.7
ZGAL_554	oxaA	oxaA Inner membrane protein oxaA	-1.7	-1.1	0.9	-1.8	-1.2	0.9	-0.6	0.1	2.1
ZGAL_556		Conserved hypothetical protein	-1.5	0.7	1.2	-0.9	1.3	1.9	-1.6	0.6	1.2
ZGAL_57	fkpA	fkpA FKBP-type peptidyl-prolyl cis-trans isomerase	-0.8	-0.1	1.7	-0.8	-0.1	1.6	-0.8	-0.1	1.7
ZGAL_576		Metallo-beta-lactamase superfamily protein	1.1	-1.8	-2.3	1.6	-1.4	-1.9	1.9	-1.1	-1.6
ZGAL_577		Conserved hypothetical membrane protein	1.7	-1.3	-1.4	1.7	-1.2	-1.3	2.3	-0.7	-0.8
ZGAL_581		Conserved hypothetical protein	3.5	-1.4	-3.8	1.9	-3.1	-5.5	0.4	-4.6	-6.9
ZGAL_582	arsC	arsC Protein arsC	2.8	-2.0	-3.8	0.8	-4.0	-5.8	0.4	-4.4	-6.3
ZGAL_583	arsB	arsB Arsenite resistance protein	1.7	-1.7	-2.4	0.4	-3.0	-3.7	-0.1	-3.6	-4.3
ZGAL_590		MiaB-like tRNA modifying protein	0.0	-0.5	0.5	-0.6	-1.1	-0.1	0.7	0.2	1.2
ZGAL_591		Serine peptidase, family S12	1.1	-2.8	-0.8	1.4	-2.5	-0.5	2.1	-1.8	0.2
ZGAL_593		Conserved hypothetical protein	-2.2	-1.1	2.4	-0.6	0.5	4.0	1.0	2.1	5.6
ZGAL_594	rpmG	rpmG Ribosomal protein L33	-1.1	-0.2	3.6	0.6	1.4	5.3	2.1	3.0	6.8
ZGAL_595	rpmB	rpmB Ribosomal protein L28	-1.0	0.3	4.3	0.6	1.9	5.8	1.7	3.0	7.0

ZGAL_607	htpG	htpG Chaperone protein htpG	-2.2	-1.9	2.5	-1.5	-1.2	3.2	0.0	0.3	4.7
ZGAL_614		Conserved hypothetical membrane protein	-2.3	0.4	-0.3	-2.2	0.5	-0.3	-0.5	2.2	1.4
ZGAL_615		Conserved hypothetical periplasmic protein	-6.8	0.6	3.8	-4.5	3.0	6.1	-0.9	6.5	9.7
ZGAL_617	alkB1	alkB1 Alpha-ketoglutarate-dependent dioxygenase	0.5	0.1	-0.8	1.1	0.7	-0.2	1.6	1.2	0.3
ZGAL_619	pbp1B	pbp1B Penicillin-binding protein 1B, family GT51	3.0	0.0	1.4	2.2	-0.8	0.6	1.5	-1.5	-0.1
ZGAL_620		Hydrolase HAD superfamily	2.1	0.6	2.3	1.1	-0.4	1.4	0.3	-1.2	0.6
ZGAL_622		Conserved hypothetical protein	-0.8	1.6	2.2	-0.2	2.2	2.8	-0.2	2.2	2.8
ZGAL_626		Conserved hypothetical lipoprotein	-0.9	-0.8	0.5	-1.0	-0.8	0.5	-0.2	0.0	1.3
ZGAL_627		Conserved hypothetical protein	-0.6	0.2	3.0	0.2	0.9	3.8	0.9	1.6	4.5
ZGAL_631		Thrombospondin type 3 repeats protein	-0.6	1.8	0.4	0.8	3.2	1.8	1.6	4.0	2.7
ZGAL_632		T9SS SprF family protein	0.2	3.0	2.7	1.6	4.5	4.2	2.8	5.6	5.4
ZGAL_633		Thrombospondin type 3 repeats protein	-0.4	2.8	2.2	0.7	3.9	3.3	2.0	5.1	4.5
ZGAL_634		Conserved hypothetical protein	-1.4	2.4	1.3	0.1	4.0	2.8	1.0	4.9	3.7
ZGAL_636		Conserved beta helix fold protein	-0.8	1.4	0.4	0.3	2.5	1.5	1.7	3.9	2.9
ZGAL_638		T9SS-associated PG1058-like protein	-0.8	1.0	1.8	-1.3	0.4	1.3	-1.9	-0.1	0.7
ZGAL_642		Conserved hypothetical protein	-0.1	0.8	1.9	-0.1	0.9	1.9	-0.6	0.4	1.4
ZGAL_643	rpoC	rpoC DNA-dependent RNA polymerase, beta-prime subunit	-0.9	-0.7	2.4	-2.2	-1.9	1.1	-2.8	-2.6	0.5
ZGAL_644	rpoB	rpoB DNA-dependent RNA polymerase, beta subunit	-1.2	-1.1	1.5	-1.9	-1.8	0.8	-1.8	-1.7	0.9
ZGAL_645	rplL	rplL Ribosomal protein L7/L12	-2.9	-0.8	1.7	-2.3	-0.2	2.3	-2.7	-0.6	1.9
ZGAL_656	rpoX	rpoX Sigma-54 modulation protein	-0.3	2.0	3.0	0.1	2.3	3.4	0.4	2.6	3.7
ZGAL_657	xerC	xerC Tyrosine recombinase XerC	-0.1	0.0	-0.4	-0.7	-0.5	-0.9	0.6	0.7	0.4
ZGAL_660		Sodium / alanine symporter	0.9	0.3	0.8	1.0	0.4	0.9	0.5	-0.1	0.4
ZGAL_664	glpE1	glpE1 Thiosulfate sulfurtransferase	-2.0	0.1	0.3	-1.3	0.7	1.0	-0.5	1.5	1.7
ZGAL_670	trpC	trpC Indole-3-glycerol phosphate synthase	-0.9	-0.9	1.5	-1.6	-1.6	0.8	-2.4	-2.4	0.0
ZGAL_672	trpB1	trpB1 Tryptophan synthase beta subunit	-0.9	0.2	1.8	-0.5	0.5	2.2	-1.3	-0.3	1.4
ZGAL_675		Conserved hypothetical protein	-0.2	0.7	0.3	0.4	1.3	0.9	1.2	2.1	1.7
ZGAL_677		Conserved hypothetical protein	-0.1	1.0	0.0	0.4	1.5	0.5	-0.5	0.6	-0.4
ZGAL_684	coaD	coaD Phosphopantetheine adenylyltransferase	1.0	0.5	-0.5	0.2	-0.3	-1.3	-0.1	-0.6	-1.6
ZGAL_685		Two-component system - Sensor histidine kinase	0.1	0.9	-2.0	0.4	1.2	-1.8	0.9	1.8	-1.2
ZGAL_686		Two-component system - Response regulator, receiver domain	0.5	2.2	-0.9	1.2	3.0	-0.2	2.1	3.9	0.8
ZGAL_689	pyrE	pyrE Orotate phosphoribosyltransferase	-0.9	-0.2	1.4	-0.9	-0.3	1.4	-0.3	0.3	2.0
ZGAL_69		Two-component system hybrid - Sensor histidine kinase/Response regulator, receiver domain	0.6	0.6	0.1	0.8	0.7	0.3	1.8	1.7	1.3
ZGAL_692		Iojap family protein	-0.5	0.9	3.9	0.2	1.7	4.6	1.5	3.0	6.0
ZGAL_693	ftsH	ftsH Cell division protein FtsH	-0.6	-0.5	1.1	0.1	0.1	1.7	1.0	1.0	2.6
ZGAL_694		Conserved hypothetical protein	-0.4	0.7	1.6	0.5	1.7	2.6	1.7	2.9	3.8
ZGAL_695	cdsA	cdsA Phosphatidate cytidylyltransferase	-0.4	0.4	0.6	0.2	1.0	1.2	0.8	1.6	1.8
ZGAL_697		Acyl-CoA binding protein	1.1	0.7	0.1	0.6	0.2	-0.4	0.8	0.4	-0.2
ZGAL_698		Creatinase family protein	1.3	0.1	-0.9	1.1	-0.1	-1.1	0.5	-0.7	-1.6
ZGAL_699		Fatty acid hydroxylase family protein	2.3	-0.5	-1.8	2.2	-0.5	-1.8	1.2	-1.5	-2.9
ZGAL_70		Conserved hypothetical protein	1.0	0.7	1.2	-0.5	-0.8	-0.3	2.2	1.9	2.4
ZGAL_700		Conserved hypothetical periplasmic protein	2.3	-0.4	-1.7	1.5	-1.2	-2.5	0.4	-2.3	-3.6
ZGAL_703		Conserved hypothetical protein	0.0	-0.3	1.4	1.3	1.1	2.7	2.2	1.9	3.6
ZGAL_704		Conserved PDZ-containing protein	2.4	-0.1	-1.8	1.4	-1.2	-2.8	0.8	-1.7	-3.4
ZGAL_706	murB	murB UDP-N-acetylenolpyruvoylglucosamine reductase	-0.1	0.3	1.0	1.2	1.6	2.4	2.1	2.5	3.2
ZGAL_707		RNA polymerase ECF-type sigma factor	1.2	-0.6	-2.0	1.4	-0.4	-1.9	2.0	0.2	-1.3
ZGAL_708		Conserved hypothetical membrane protein	1.8	-0.7	-2.9	1.6	-0.9	-3.1	2.4	0.0	-2.2
ZGAL_71	alkK	alkK Medium-chain-fatty-acid-CoA ligase	1.1	1.0	-0.5	0.8	0.7	-0.8	0.0	-0.1	-1.6
ZGAL_710		RNA polymerase ECF-type sigma factor	1.4	-0.7	-0.8	0.8	-1.4	-1.5	0.9	-1.2	-1.3
ZGAL_713		Two-component system hybrid - Sensor histidine kinase/Response regulator, receiver domain	-0.1	0.4	0.0	0.3	0.8	0.4	1.9	2.4	2.0
ZGAL_716		Conserved hypothetical protein	-1.4	-0.4	1.3	0.2	1.2	3.0	0.6	1.6	3.4
ZGAL_721		Flavastacin, family M12	-0.7	0.4	-0.9	0.4	1.5	0.2	3.1	4.2	2.9
ZGAL_726	tatA	tatA Sec-independent protein translocase	-1.5	0.5	1.6	-1.3	0.7	1.9	-1.1	0.9	2.0
ZGAL_727		Aminopeptidase, family M1	1.9	0.0	0.2	1.0	-0.9	-0.7	0.3	-1.7	-1.4
ZGAL_729		Conserved hypothetical periplasmic protein	2.0	-0.5	-0.5	1.5	-1.0	-1.0	-0.1	-2.6	-2.6
ZGAL_73		Conserved hypothetical periplasmic protein	-0.8	0.0	0.9	0.2	1.0	2.0	0.3	1.1	2.0
ZGAL_730		Conserved hypothetical periplasmic protein	2.2	-0.4	0.3	1.7	-1.0	-0.2	0.6	-2.0	-1.3
ZGAL_731		Conserved hypothetical periplasmic protein	1.5	-0.3	0.1	1.2	-0.5	-0.1	0.1	-1.7	-1.3
ZGAL_735		Metallopeptidase, family M15	0.3	-1.1	-0.3	1.2	-0.2	0.6	1.7	0.3	1.1
ZGAL_736		Metallopeptidase, family M48	0.7	-1.3	-1.8	1.3	-0.7	-1.1	1.7	-0.4	-0.8
ZGAL_737		Ankyrin repeats protein	2.1	-1.7	-1.4	2.8	-1.1	-0.7	1.9	-1.9	-1.6
ZGAL_74		Conserved hypothetical membrane protein	-0.6	0.6	1.2	-0.1	1.1	1.8	0.3	1.6	2.2
ZGAL_742		Conserved hypothetical protein	-1.9	0.5	3.0	-1.5	1.0	3.5	-1.9	0.5	3.0
ZGAL_743	nqrF	nqrF Na(+)-translocating NADH-quinone reductase subunit F	-1.2	-0.5	3.6	-1.3	-0.6	3.5	-1.8	-1.1	3.0
ZGAL_744	nqrE	nqrE Na(+)-translocating NADH-quinone reductase subunit E	-1.0	-0.6	3.6	-0.8	-0.4	3.7	-1.3	-0.9	3.2
ZGAL_745	nqrD	nqrD Na(+)-translocating NADH-quinone reductase subunit D	-1.0	-1.0	3.1	-1.6	-1.6	2.6	-1.8	-1.8	2.4
ZGAL_746	nqrC	nqrC Na(+)-translocating NADH-quinone reductase subunit C	-0.6	-0.2	3.8	-1.1	-0.8	3.2	-0.7	-0.3	3.7
ZGAL_747	nqrB	nqrB Na(+)-translocating NADH-quinone reductase subunit B	-0.4	-0.8	2.4	-1.0	-1.5	1.8	-0.1	-0.6	2.7

ZGAL_748	nqrA	nqrA Na(+)-translocating NADH-quinone reductase subunit A	0.6	-0.1	2.5	0.5	-0.2	2.4	1.7	1.0	3.6
ZGAL_749		T9SS plug protein	-0.6	0.2	0.6	0.0	0.8	1.2	0.0	0.8	1.2
ZGAL_75	clsA1	clsA1 Cardiolipin synthetase	1.8	2.0	1.2	1.8	2.1	1.3	0.7	1.0	0.1
ZGAL_750		Conserved hypothetical membrane protein	-0.4	0.9	-0.3	1.6	3.0	1.7	1.4	2.7	1.5
ZGAL_751	apaG	apaG Protein ApaG	1.2	0.0	0.9	1.4	0.1	1.1	0.8	-0.5	0.4
ZGAL_757		Conserved hypothetical protein	0.9	2.7	-3.8	1.9	3.7	-2.8	2.0	3.8	-2.7
ZGAL_758	trkH	trkH Trk system potassium uptake protein trkH	0.1	0.5	-0.1	0.6	1.0	0.4	1.2	1.6	1.0
ZGAL_759	trkA	trkA Trk system potassium uptake protein trkA	-0.2	0.0	-0.1	0.6	0.8	0.7	1.1	1.3	1.2
ZGAL_761	sprT	sprT T9SS associated SprT protein	0.3	0.5	0.9	1.1	1.3	1.7	2.1	2.3	2.7
ZGAL_767	rpsO	rpsO Ribosomal protein S15	-0.7	0.5	3.5	0.9	2.1	5.2	1.2	2.3	5.4
ZGAL_769	rpoD1	rpoD1 RNA polymerase sigma factor rpoD	2.3	-1.5	-2.3	1.2	-2.6	-3.4	1.5	-2.3	-3.1
ZGAL_772	add	add Adenosine deaminase	2.4	-0.1	-0.1	1.8	-0.6	-0.6	0.8	-1.7	-1.7
ZGAL_778		Conserved hypothetical membrane protein	-0.5	0.5	1.2	0.0	1.0	1.6	-0.5	0.6	1.2
ZGAL_779		TonB-dependent Receptor	0.1	1.0	0.9	-0.1	0.8	0.8	-0.7	0.2	0.2
ZGAL_781		Conserved hypothetical membrane protein	1.7	0.8	1.1	1.3	0.4	0.7	0.8	-0.1	0.2
ZGAL_783		Conserved hypothetical membrane protein	1.4	0.1	-0.9	2.8	1.5	0.5	1.0	-0.3	-1.3
ZGAL_786	dusA	dusA tRNA-dihydrouridine synthase A	0.5	0.3	-0.4	0.9	0.7	-0.1	2.1	2.0	1.2
ZGAL_787		hypothetical membrane protein	0.3	2.2	1.7	2.7	4.7	4.2	5.1	7.1	6.6
ZGAL_789	yqeY	yqeY Conserved hypothetical protein	0.2	0.4	2.8	0.4	0.6	3.0	0.7	0.9	3.3
ZGAL_79		MiaB-like tRNA modifying protein	-0.4	0.0	0.9	-0.5	-0.2	0.7	0.0	0.4	1.2
ZGAL_790	ftsZ	ftsZ Cell division protein FtsZ	-0.9	-0.2	1.5	-1.7	-1.1	0.7	-2.2	-1.5	0.2
ZGAL_791	ftsA	ftsA Cell division protein FtsA	-0.8	0.2	2.1	-1.4	-0.4	1.5	-1.5	-0.6	1.4
ZGAL_792	ftsQ	ftsQ Possible cell division protein ftsQ	-0.4	0.3	1.6	-0.9	-0.2	1.1	-0.4	0.2	1.6
ZGAL_794	murG	murG Undecaprenyldiphospho-muramoylpentapeptide beta-N- acetylglucosaminyltransferase, family GT28	0.8	0.4	1.7	0.0	-0.4	1.0	-0.8	-1.2	0.2
ZGAL_796	murD	murD UDP-N-acetylmuramoylalanine-D-glutamate ligase	-0.7	0.3	2.3	-1.5	-0.4	1.5	-1.6	-0.5	1.4
ZGAL_797	mraY	mraY Phospho-N-acetylmuramoyl-pentapeptide-transferase	-0.9	0.1	1.5	-1.1	-0.1	1.3	-1.2	-0.2	1.2
ZGAL_798	murE	murE UDP-N-acetylmuramoylalanyl-D-glutamate-2,6-diaminopimelate ligase	-2.6	-0.4	1.6	-2.9	-0.7	1.3	-2.6	-0.3	1.6
ZGAL_8	degP	degP Peptidase Do, family S1	3.2	-0.9	-1.2	1.9	-2.2	-2.4	1.2	-2.9	-3.1
ZGAL_80		Conserved hypothetical protein	-0.6	-0.7	0.6	-0.4	-0.6	0.8	0.6	0.4	1.8
ZGAL_808	gldC	gldC Gliding motility protein	-1.6	-0.2	1.3	-1.8	-0.5	1.1	-1.1	0.3	1.8
ZGAL_81	rpmE	rpmE Ribosomal protein L31	-1.2	-0.6	3.7	1.1	1.8	6.0	2.0	2.7	6.9
ZGAL_818	queA	queA S-adenosylmethionine:tRNA ribosyltransferase-isomerase	-1.3	-1.2	0.6	-1.0	-0.9	0.9	-0.1	0.0	1.8
ZGAL_819	aroA	aroA 3-Phosphoshikimate 1-carboxyvinyltransferase	-1.5	-0.3	1.9	-1.3	-0.1	2.1	-1.3	-0.1	2.0
ZGAL_822		Conserved hypothetical periplasmic protein	-1.3	0.4	-0.2	0.3	2.0	1.4	-0.2	1.5	0.9
ZGAL_824	engC	engC GTPase engC	-0.4	0.5	0.8	-0.1	0.9	1.1	0.1	1.1	1.3
ZGAL_826	aroGH	aroGH 3-Deoxy-7-phosphoheptulonate synthase / Chorismate mutase	-1.8	-2.0	1.6	-3.0	-3.3	0.4	-2.6	-2.9	0.8
ZGAL_827	tyrA	tyrA Prephenate dehydrogenase	-0.5	-1.6	2.0	-1.6	-2.7	0.9	-1.1	-2.2	1.4
ZGAL_828	dapL	dapL LL-diaminopimelate aminotransferase	-0.5	-1.2	1.8	-0.7	-1.3	1.6	-0.8	-1.4	1.5
ZGAL_83		Conserved hypothetical membrane protein	-1.0	-0.4	0.3	-0.2	0.5	1.1	0.5	1.2	1.9
ZGAL_831		hypothetical protein	4.0	2.2	2.3	3.8	2.0	2.1	1.2	-0.6	-0.5
ZGAL_834		Conserved hypothetical protein	-1.3	0.0	1.4	-0.2	1.0	2.5	0.7	2.0	3.4
ZGAL_838		Hypothetical protein	-0.7	1.7	2.9	-0.1	2.2	3.5	-0.2	2.2	3.4
ZGAL_839	yumC1	yumC1 Ferredoxin-NADP reductase	-0.3	0.2	2.4	-0.4	0.1	2.3	-0.7	-0.3	2.0
ZGAL_84	arnC1	arnC1 Undecaprenyl-phosphate 4-deoxy-4-formamido-L-arabinose transferase, family GT2	-1.0	-0.1	0.8	-0.6	0.3	1.2	-0.3	0.6	1.5
ZGAL_85	pgcA	pgcA Phosphoglucomutase	-1.1	-0.4	0.5	-1.3	-0.5	0.4	-0.5	0.2	1.1
ZGAL_856	metK	metK Methionine adenosyltransferase (S-adenosylmethionine synthetase)	-0.6	-0.4	0.7	0.2	0.4	1.5	0.6	0.8	1.9
ZGAL_857		TonB-dependent Receptor	1.2	-4.3	-1.7	0.7	-4.7	-2.2	2.3	-3.2	-0.7
ZGAL_858		Conserved hypothetical periplasmic protein	1.1	-4.8	-1.4	0.7	-5.2	-1.8	2.7	-3.2	0.2
ZGAL_86	msbA	msbA Lipid A export ATP-binding/permease protein	-2.4	0.3	1.2	-1.6	1.0	1.9	-1.4	1.2	2.1
ZGAL_863	ppa	ppa Inorganic pyrophosphatase	-2.6	-0.5	2.5	-1.8	0.3	3.3	-0.4	1.7	4.8
ZGAL_864		Conserved hypothetical membrane protein	-0.7	-0.7	0.2	-0.1	-0.1	0.8	0.5	0.5	1.3
ZGAL_865	pdhB	pdhB Pyruvate dehydrogenase, E1 component subunit beta of pyruvate dehydrogenase complex	-0.9	-0.9	1.6	-0.9	-0.8	1.7	-0.4	-0.4	2.1
ZGAL_869	nupC	nupC Nucleoside permease NupC	-1.0	-0.2	0.0	-0.2	0.5	0.8	0.2	1.0	1.2
ZGAL_870	thyA	thyA Thymidylate synthase	0.1	0.0	1.7	-0.7	-0.8	0.9	0.1	0.0	1.6
ZGAL_871		Conserved hypothetical protein	3.0	1.8	1.4	1.6	0.4	0.0	0.3	-0.9	-1.3
ZGAL_872		Conserved hypothetical protein	2.7	0.8	-0.9	1.4	-0.5	-2.2	0.8	-1.2	-2.8
ZGAL_873		Conserved hypothetical protein	2.3	1.0	-1.2	0.6	-0.7	-2.9	1.1	-0.2	-2.4
ZGAL_874		Carbohydrate binding module, family CBM48	-0.2	0.6	0.6	0.8	1.6	1.6	1.5	2.3	2.2
ZGAL_878	murI	murI Glutamate racemase	-0.3	0.1	1.3	-0.5	-0.1	1.2	-0.7	-0.3	0.9
ZGAL_879	cda1	cda1 Calcium-dependent ATPase	-1.8	-0.7	0.9	-2.3	-1.1	0.4	-1.6	-0.5	1.1
ZGAL_880		ABC transporter, permease component	-1.0	0.2	0.9	-0.6	0.5	1.2	-0.7	0.5	1.2
ZGAL_881		ABC transporter, ATPase component	0.0	0.3	1.4	0.2	0.5	1.6	0.0	0.4	1.5
ZGAL_882		Conserved hypothetical membrane protein	0.9	1.3	1.0	1.0	1.4	1.0	1.1	1.5	1.2
ZGAL_888	pdhA	pdhA Pyruvate dehydrogenase, E1 component subunit alpha of pyruvate dehydrogenase complex	-1.1	-0.4	1.0	-1.7	-0.9	0.5	-1.1	-0.4	1.1
ZGAL_889	cdd	cdd Cytidine deaminase	-0.4	-0.1	0.0	0.1	0.5	0.5	0.9	1.3	1.3
ZGAL_89		Conserved hypothetical protein	1.3	-3.2	-2.0	0.6	-4.0	-2.7	2.0	-2.6	-1.4
ZGAL_890		T9SS-associated protein PorV	0.0	1.2	1.1	1.0	2.2	2.2	2.2	3.5	3.4

ZGAL_891	gldJ	gldJ Gliding motility membrane lipoprotein	-0.2	0.8	0.9	-0.1	0.9	1.0	1.6	2.7	2.7
ZGAL_893		MscS family protein	0.8	-1.4	-3.1	0.9	-1.3	-3.0	1.8	-0.3	-2.0
ZGAL_894		Putative protein	1.9	-0.9	-3.5	1.1	-1.7	-4.3	1.9	-0.8	-3.5
ZGAL_895		Hypothetical protein	1.1	-0.8	-3.3	1.4	-0.4	-2.9	2.3	0.4	-2.0
ZGAL_900		Endonuclease	-0.3	0.3	0.5	1.5	2.1	2.3	2.6	3.2	3.4
ZGAL_902	folC	folC Folylpolyglutamate synthase / Dihydrofolate synthase	0.1	0.5	1.0	0.5	0.9	1.4	1.8	2.2	2.7
ZGAL_903	tolA	tolA Protein TolA	0.5	0.8	1.8	0.1	0.4	1.4	1.5	1.8	2.8
ZGAL_904	tolR	tolR Protein TolR	0.1	1.1	2.0	0.4	1.4	2.4	1.6	2.6	3.5
ZGAL_905	tolQ	tolQ Protein TolQ	-0.1	0.5	1.5	0.2	0.8	1.8	0.3	0.9	1.9
ZGAL_91	rsmB	rsmB Ribosomal RNA small subunit methyltransferase B	0.2	-0.8	1.6	0.6	-0.4	2.0	1.0	0.1	2.5
ZGAL_910	gltB	gltB Glutamate synthase [NADPH] small chain	-1.1	1.4	2.3	-1.3	1.1	2.1	-1.9	0.6	1.5
ZGAL_913		Sulfatase, family S1-23	1.5	0.9	-0.3	1.3	0.7	-0.5	0.6	0.0	-1.2
ZGAL_914		SusD-like lipoprotein	1.3	0.6	-0.2	1.1	0.4	-0.4	0.7	0.0	-0.8
ZGAL_915		SusC-like TonB-dependent Transducer	0.7	0.9	-0.8	0.9	1.1	-0.6	0.5	0.8	-0.9
ZGAL_918		Conserved hypothetical membrane protein	1.7	0.5	0.0	1.7	0.5	0.1	1.0	-0.2	-0.6
ZGAL_919		D-tagatose 3-epimerase	1.8	0.6	-0.3	1.7	0.5	-0.4	1.0	-0.2	-1.1
ZGAL_92	purL	purL Phosphoribosylformylglycinamidine synthase	-1.2	0.3	2.9	-1.0	0.6	3.2	-0.1	1.5	4.0
ZGAL_920		AraC-type transcriptional regulator	1.9	-0.6	-1.7	1.3	-1.1	-2.3	0.9	-1.5	-2.7
ZGAL_921		Conserved cytochrome c-containing protein	2.1	0.4	-0.8	1.4	-0.2	-1.5	0.6	-1.0	-2.3
ZGAL_922		SusC-like TonB-dependent transporter	2.7	0.5	-0.5	1.9	-0.3	-1.3	1.7	-0.5	-1.5
ZGAL_923		SusD-like lipoprotein	3.0	0.7	1.0	1.1	-1.1	-0.9	1.6	-0.6	-0.4
ZGAL_93		Conserved hypothetical periplasmic protein	-0.2	1.2	0.5	2.5	3.9	3.1	4.6	6.0	5.2
ZGAL_930		Conserved hypothetical periplasmic protein	0.4	0.2	1.8	0.3	0.1	1.7	0.2	0.0	1.6
ZGAL_934		Serine peptidase, family S8	2.5	0.0	-0.6	3.0	0.6	0.0	1.4	-1.1	-1.7
ZGAL_940		Conserved hypothetical protein	3.3	-1.0	-2.6	3.1	-1.1	-2.8	2.9	-1.4	-3.0
ZGAL_946		Conserved hypothetical protein	0.8	-1.4	-3.6	1.1	-1.0	-3.3	2.1	0.0	-2.2
ZGAL_947		Conserved hypothetical protein	2.7	-2.0	-2.7	4.0	-0.7	-1.4	3.6	-1.0	-1.7
ZGAL_949		Conserved hypothetical protein	1.1	-2.1	-0.9	3.4	0.2	1.4	3.1	-0.1	1.1
ZGAL_952		Conserved hypothetical protein	-0.2	-1.7	-1.2	1.0	-0.5	0.0	2.4	1.0	1.5
ZGAL_953	lysS	lysS Lysyl-tRNA synthetase	-0.3	-0.7	1.8	-0.5	-0.9	1.5	0.0	-0.4	2.1
ZGAL_954		Conserved cytochrome c-containing protein	2.0	0.2	-1.1	1.8	0.0	-1.3	0.9	-0.9	-2.2
ZGAL_955		Conserved hypothetical protein	2.0	0.9	0.5	2.1	1.0	0.6	1.1	0.0	-0.3
ZGAL_957		Conserved hypothetical membrane protein	1.9	-0.9	-2.8	1.3	-1.4	-3.3	1.2	-1.6	-3.5
ZGAL_958	sdcS	sdcS Sodium-dependent dicarboxylate transporter sdcS	0.6	-0.2	-2.0	1.3	0.5	-1.3	2.0	1.1	-0.7
ZGAL_959		Conserved hypothetical periplasmic protein	-2.4	1.9	2.2	0.5	4.8	5.2	3.7	8.0	8.4
ZGAL_961		Conserved hypothetical periplasmic protein	3.0	-4.2	-1.0	2.2	-5.0	-1.8	3.4	-3.7	-0.6
ZGAL_963	hemL	hemL Glutamate-1-semialdehyde 2,1-aminomutase	-0.5	0.3	1.5	-0.4	0.4	1.5	-0.4	0.4	1.6
ZGAL_965	dcyD	dcyD D-cysteine desulfhydrase	-0.5	0.8	0.4	-0.3	1.1	0.7	0.9	2.2	1.8
ZGAL_966		Conserved hypothetical protein	-2.0	2.1	2.7	0.8	4.9	5.5	2.1	6.2	6.8
ZGAL_968		Conserved hypothetical periplasmic protein	2.1	-0.4	0.2	2.4	-0.1	0.6	1.6	-0.9	-0.3
ZGAL_97		23S ribosomal protein	0.6	0.2	2.1	1.1	0.6	2.5	1.9	1.4	3.3
ZGAL_972		Conserved hypothetical protein	1.2	0.3	-0.8	0.6	-0.3	-1.4	-0.2	-1.1	-2.3
ZGAL_977	alaS	alaS Alanyl-tRNA synthetase	-0.8	0.0	1.5	-1.1	-0.3	1.2	-1.1	-0.4	1.2
ZGAL_98	fadA	fadA 3-Ketoacyl-CoA thiolase	2.9	0.0	1.5	2.3	-0.5	1.0	2.8	-0.1	1.5
ZGAL_980		LemA family protein	2.7	0.5	-0.7	3.0	0.8	-0.5	2.8	0.6	-0.6
ZGAL_982		Conserved hypothetical membrane protein	1.8	0.0	-1.1	1.8	0.0	-1.1	2.3	0.5	-0.6
ZGAL_984		TonB-dependent Receptor	1.7	-0.2	-1.1	1.5	-0.4	-1.3	0.6	-1.3	-2.2
ZGAL_99	fadE	fadE Acyl-CoA dehydrogenase	2.6	0.3	2.0	2.1	-0.2	1.5	2.3	0.1	1.8
ZGAL_992		Hypothetical protein	-0.1	0.0	0.1	0.6	0.8	0.8	3.6	3.8	3.8
ZGAL_995		Anti-sigma factor	-1.8	0.1	-0.7	-0.4	1.5	0.6	0.1	1.9	1.1
ZGAL_997		SusD-like lipoprotein	-0.3	0.0	-0.6	-0.4	-0.1	-0.7	1.8	2.1	1.4
ZGAL_999		Sulfatase, family S1-23	-1.1	0.2	0.6	-0.8	0.5	0.9	-0.4	0.9	1.3
ZGALAM_0075	rpmH	rpmH 50S ribosomal protein L34	0.6	0.5	4.3	3.1	3.0	6.8	3.5	3.4	7.3
ZGALAM_0112		conserved protein of unknown function	-2.2	0.4	1.3	-0.7	1.8	2.7	-0.1	2.4	3.3
ZGALAM_0664		protein of unknown function	-2.4	0.1	1.2	-1.4	1.1	2.2	-0.5	1.9	3.1
ZGALAM_0667	rpsU	rpsU 30S ribosomal protein S21	0.3	0.8	3.9	2.0	2.6	5.7	2.4	2.9	6.0
ZGALAM_0748		conserved protein of unknown function	0.4	1.3	0.4	1.7	2.6	1.8	2.3	3.2	2.4
ZGALAM_0815		protein of unknown function	-1.7	0.9	1.9	-0.5	2.1	3.1	-0.5	2.1	3.2
ZGALAM_0886		protein of unknown function	-1.3	0.9	-0.5	-0.9	1.4	-0.1	0.2	2.4	1.0
ZGALAM_0908		protein of unknown function	1.7	0.0	-2.0	2.9	1.3	-0.7	3.1	1.4	-0.6
ZGALAM_0909		exported protein of unknown function	3.2	2.9	1.3	5.5	5.1	3.6	5.5	5.1	3.6
ZGALAM_0971		exported protein of unknown function	-2.0	3.4	4.2	0.2	5.6	6.4	1.9	7.4	8.1
ZGALAM_1098		protein of unknown function	4.1	2.1	-0.9	3.2	1.2	-1.8	1.0	-1.0	-3.9
ZGALAM_2086		conserved protein of unknown function	1.3	1.0	0.1	-0.5	-0.8	-1.6	-2.0	-2.3	-3.2
ZGALAM_2223		protein of unknown function	-1.1	1.1	0.7	0.1	2.2	1.9	1.4	3.6	3.2
ZGALAM_2285		transposase (fragment)	-1.0	1.4	0.7	0.5	2.9	2.2	2.5	4.9	4.2
ZGALAM_2286		protein of unknown function	-0.8	2.7	0.8	-0.2	3.3	1.4	2.5	6.0	4.1
ZGALAM_2603		protein of unknown function	1.2	0.4	3.3	3.3	2.5	5.4	4.0	3.2	6.2
ZGALAM_2793		conserved exported protein of unknown function	-0.6	0.5	2.0	1.4	2.5	4.0	2.2	3.3	4.8
ZGALAM_2794		conserved exported protein of unknown function	-1.5	0.8	2.6	0.4	2.7	4.5	0.6	3.0	4.8
ZGALAM_2911		conserved exported protein of unknown function	-1.3	1.5	-1.6	1.8	4.5	1.4	0.9	3.7	0.6
ZGALAM_3022		protein of unknown function	-1.0	0.6	1.6	0.1	1.7	2.7	0.7	2.2	3.3
ZGALAM_3035		protein of unknown function	-2.3	0.1	2.2	-0.7	1.7	3.8	-0.2	2.2	4.3
ZGALAM_3051		protein of unknown function	-2.9	-0.9	1.5	-0.6	1.4	3.8	-1.1	0.9	3.3
ZGALAM_3367		exported protein of unknown function	0.2	0.8	-0.8	0.6	1.2	-0.3	1.8	2.4	0.8
ZGALAM_3626		protein of unknown function	-1.3	1.6	2.6	-1.0	1.9	3.0	0.1	3.0	4.1
ZGALAM_3666		protein of unknown function	0.8	0.2	1.4	1.7	1.1	2.3	2.0	1.4	2.6

ZGALAM_3727	protein of unknown function	3.6	-0.4	-1.3	3.7	-0.4	-1.3	4.1	0.0	-0.9
ZGALAM_3970	protein of unknown function	-1.8	0.4	1.2	-1.1	1.1	1.9	-0.9	1.4	2.1
ZGALAM_4041	conserved exported protein of unknown function	2.4	-3.0	-2.8	2.7	-2.7	-2.5	2.0	-3.4	-3.2
ZGALAM_4044	conserved protein of unknown function	-0.9	0.8	2.7	-0.3	1.5	3.4	-0.5	1.2	3.1
ZGALAM_4047	conserved protein of unknown function	-1.9	1.9	3.9	-0.2	3.6	5.7	1.7	5.5	7.6
ZGALAM_4132	conserved protein of unknown function	-3.1	3.6	4.2	-0.1	6.5	7.2	1.5	8.1	8.8
ZGALAM_4331	protein of unknown function	-2.1	-0.2	-1.0	-0.6	1.3	0.4	0.3	2.2	1.4
ZGALAM_4358	protein of unknown function	1.3	1.0	-2.3	1.9	1.6	-1.6	2.2	1.9	-1.4
ZGALAM_4614	protein of unknown function	0.3	4.0	3.4	0.0	3.7	3.1	3.2	6.9	6.3
ZGALAM_4720	conserved exported protein of unknown function	1.7	5.5	7.6	3.3	7.0	9.2	4.3	8.0	10.2

Table V.S4: Genes upregulated with at least one macroalgae when compared both with the polysaccharides and maltose (Bonferroni-adjusted p-value < 0.05 and log2FC > 2). MA: Macroalgae. "L" means they are induced with *Laminaria*, "F" with *Fucus* and "A" with *Ascophyllum*. Genes likely involved antioxidant activity were highlighted in grey, genes involved in T9SS in orange and GHs or PLs in purple. Gene homologs were searched in the genome of the other *Zobellia* spp. used in this study. Green = homolog found; Yellow = homolog not found. Zgal: *Z. galactanivorans* Dsij^{T}; Zamu*: Z. amurskyensis* KMM 3526^{T}; Zlam: *Z. laminariae* KMM 3676^{T}; Zrus: *Z. russellii* KMM 3677^{T}; ZrosF08: *Z. roscoffensis* Asnod1-F08^{T}; ZrosB02: *Z. roscoffensis* Asnod2-B02-B; ZnedB07: *Z. nedashkovskayae* Asnod2-B07-B^{T}; ZnedE08: *Z. nedashkovskayae* Asnod3-E08-A.

GeneID	Gene name	Gene function	MA	Zgal	Zamu	Zlam	Zrus	Zros F08	Zros B02	Zned B07	Zned E08
ZGAL_81	rpmE	Ribosomal protein L31	A								
ZGAL_93		Conserved hypothetical periplasmic protein; CTD belonging to TIGRFAM family TIGR04183	F A								
ZGAL_114	sodC	Superoxide dismutase [Cu-Zn]	L								
ZGAL_115		Bacterial surface antigen	F								
ZGAL_199		SusD-like lipoprotein	A								
ZGAL_205		Glycoside hydrolase, family GH117	L F								
ZGAL_209		Hypothetical lipoprotein, family CBM4	A								
ZGAL_294		Conserved hypothetical membrane protein	A								
ZGAL_295		Heavy metal binding protein	A								
ZGAL_296	glpE2	Thiosulfate sulfurtransferase	A								
ZGAL_297		Beta-lactamase hydrolase-like protein	A								
ZGAL_392		Putative protein	A								
ZGAL_402		Conserved hypothetical membrane protein	A								
ZGAL_408		Vgr family protein	A								
ZGAL_410		Conserved hypothetical protein	A								
ZGAL_437		Conserved hypothetical protein	A								
ZGAL_451		Hypothetical lipoprotein	A								
ZGAL_524		Conserved hypothetical membrane protein	A								
ZGAL_525		Conserved hypothetical periplasmic protein	A								
ZGAL_632		T9SS SprF family protein	A								
ZGAL_706	murB	UDP-N-acetylenolpyruvoylglucosamine reductase	A								
ZGAL_721		Flavastacin, family M12	A								
ZGAL_761	sprT	T9SS associated SprT protein	A								
ZGAL_787		hypothetical membrane protein	A								
ZGAL_831		hypothetical protein	L								
ZGAL_890		T9SS-associated protein PorV	A								
ZGAL_900		Endonuclease	A								
ZGAL_959		Conserved hypothetical periplasmic protein	A								
ZGAL_966		Conserved hypothetical protein	A								
ZGAL_992		Hypothetical protein	A								
ZGAL_1071		Ribonuclease BN family protein	L F								
ZGAL_1072		Short-chain dehydrogenase/reductase	L								
ZGAL_1073		Conserved hypothetical protein	L								
ZGAL_1074		Conserved hypothetical membrane protein	L F								
ZGAL_1077		Citrate transporter family protein	F								
ZGAL_1078		Small-conductance mechanosensitive channel	L F								
ZGAL_1080		Putative membrane protein	L F								
ZGAL_1082	topA2	DNA topoisomerase 1B	L								
ZGAL_1083		Conserved hypothetical protein	L								
ZGAL_1085		Putative membrane protein	L F								
ZGAL_1086		Conserved hypothetical protein	F								

ZGAL_1089		Two-component system - Sensor histidine kinase	L	
ZGAL_1099		Alpha/beta hydrolase-fold protein	L F	
ZGAL_1101		Peroxiredoxin	L	
ZGAL_1102	gdhA	Glucose 1-dehydrogenase	L	
ZGAL_1103		Short-chain dehydrogenase/reductase SDR	L F	
ZGAL_1104		Hypothetical protein	L	
ZGAL_1105		Conserved hypothetical protein	L F	
ZGAL_1124		Conserved hypothetical periplasmic protein; CTD belonging to TIGRFAM family TIGR04183	F A	
ZGAL_1144		Receptor-like protein kinase	A	
ZGAL_1182	alyA1	Endo-guluronate lyase AlyA1, family PL7_3	A	
ZGAL_1302		Conserved hypothetical protein	A	
ZGAL_1390		Putative membrane protein	A	
ZGAL_1393		Hypothetical lipoprotein	A	
ZGAL_1394		Putative membrane protein	A	
ZGAL_1414		Esterase	A	
ZGAL_1474		Hypothetical membrane protein	A	
ZGAL_1597		Putative protein	L	
ZGAL_1598		Carboxymuconolactone decarboxylase family protein	L	
ZGAL_1599		Conserved hypothetical periplasmic protein	L	
ZGAL_1610	rpmF	Ribosomal protein L32	A	
ZGAL_1646		Putative protein	A	
ZGAL_1673		Conserved hypothetical protein	A	
ZGAL_1704	sprF	T9SS associated protein SprF	A	
ZGAL_1707		T9SS SprF family protein	A	
ZGAL_1712		Conserved hypothetical protein	L	
ZGAL_1757		TetR-type transcriptional regulator	F	
ZGAL_1825		Intracellular peptidase, family C56	L	
ZGAL_1834		Conserved hypothetical protein	A	
ZGAL_1878		Putative exported protein	A	
ZGAL_1930		Conserved hypothetical lipoprotein	A	
ZGAL_1956		Two-component system - Sensor histidine kinase	A	
ZGAL_1977		Putative protein	A	
ZGAL_1990		Conserved hypothetical lipoprotein	A	
ZGAL_2010		Esterase	A	
ZGAL_2021		SCP-like extracellular protein	F A	
ZGAL_2022		Conserved hypothetical periplasmic protein; CTD belonging to TIGRFAM family TIGR04131	F A	
ZGAL_2023		T9SS SprF family protein	L F A	
ZGAL_2024		T9SS-associated PG1058-like protein	F A	
ZGAL_2029		Conserved hypothetical protein	A	
ZGAL_2059		Conserved hypotetical lipoprotein	A	
ZGAL_2099		Conserved hypothetical protein	A	
ZGAL_2100		Conserved hypothetical protein	A	
ZGAL_2112		Uncharacterized ATP-dependent helicase	L F	
ZGAL_2113	ligC	DNA ligase	L	
ZGAL_2300		Hypothetical protein	A	
ZGAL_2399		Conserved hypothetical protein	F	
ZGAL_2401		T9SS SprF family protein	A	
ZGAL_2456		T9SS-associated PG0189-like protein	A	
ZGAL_2551		Conserved hypotheical membrane protein	A	
ZGAL_2552		Conserved membrane lipoprotein	A	
ZGAL_2553		Hypothetical membrane protein	A	
ZGAL_2554		Conserved membrane lipoprotein	A	
ZGAL_2555		Putative exported protein	A	
ZGAL_2605		Conserved hypothetical protein	L F	

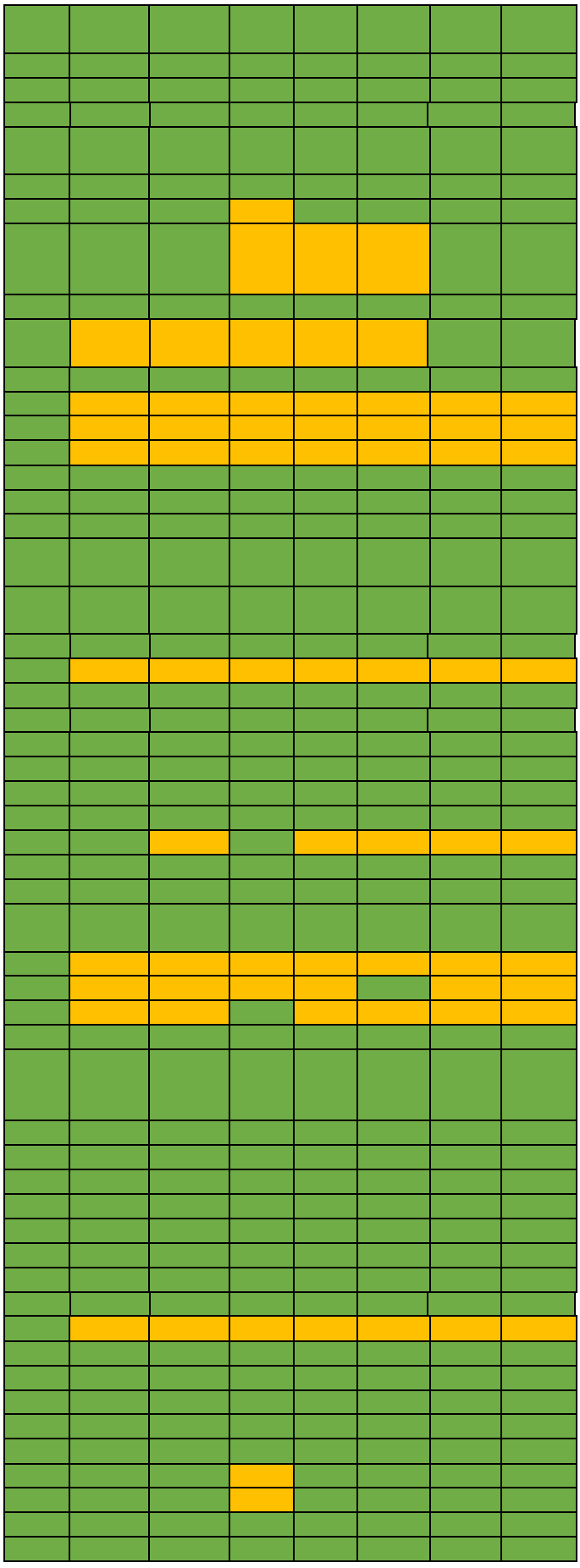

ZGAL_2606		Conserved hypothetical protein	L F	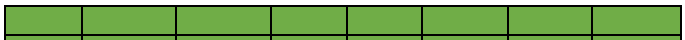
ZGAL_2607		Conserved hypothetical periplasmic protein	L F	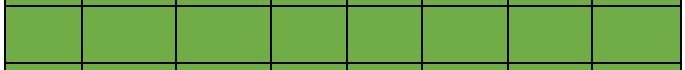
ZGAL_2608		Conserved hypothetical protein	L	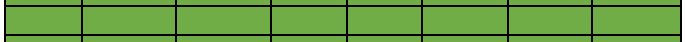
ZGAL_2609		CsbD-like protein	L F	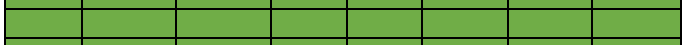
ZGAL_2611		Conserved hypothetical protein	L F	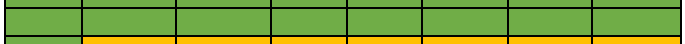
ZGAL_2684		Hypothetical membrane protein	A	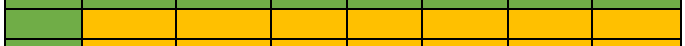
ZGAL_2685		Conserved hypothetical protein	A	
ZGAL_2686		Hypothetical membrane protein	A	
ZGAL_2690		Conserved hypothetical periplasmic protein	A	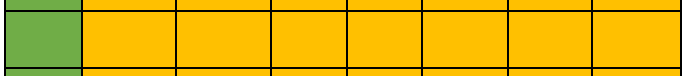
ZGAL_2691		TonB-dependent Receptor	A	
ZGAL_2716		Conserved hypothetical membrane protein	A	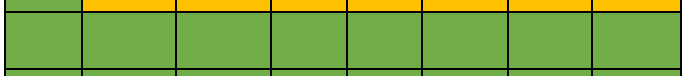
ZGAL_2747		Conserved hypothetical lipoprotein	F A	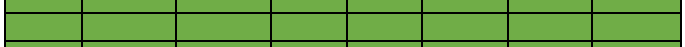
ZGAL_2761		Conserved hypothetical periplasmic protein; CTD belonging to TIGRFAM family TIGR04131	A	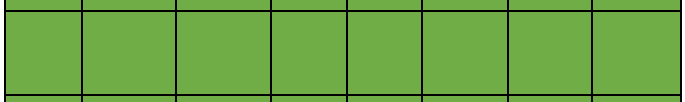
ZGAL_2762		Conserved hypothetical periplasmic protein; CTD belonging to TIGRFAM family TIGR04131	A	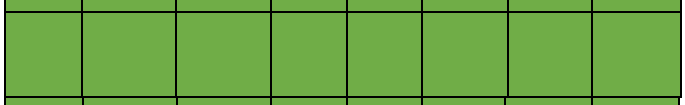
ZGAL_2816	crcB	Protein CrcB	A	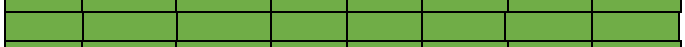
ZGAL_2893		T9SS-associated PG1058-like protein	A	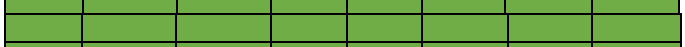
ZGAL_2895		Conserved hypothetical protein	A	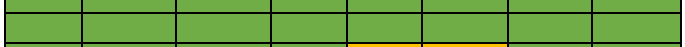
ZGAL_2909		Two-component system - Sensor histidine kinase	F	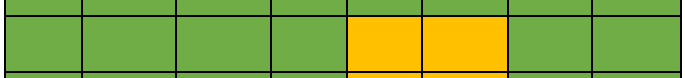
ZGAL_2910		Two-component system - Response regulator, receiver domain	F	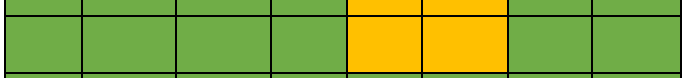
ZGAL_2944		Conserved hypothetical protein	A	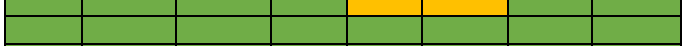
ZGAL_2961		Conserved hypothetical protein	A	
ZGAL_2962		Conserved hypothetical membrane protein	A	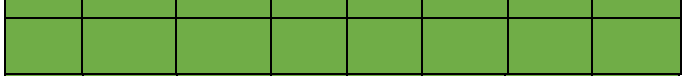
ZGAL_2972	crtZ	Beta-carotene hydroxylase	F	
ZGAL_2982		Two-component system - Sensor histidine kinase	A	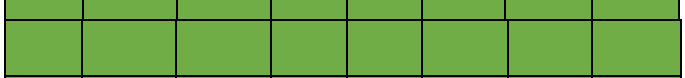
ZGAL_2988		Conserved hypothetical membrane protein	F	
ZGAL_2989		Conserved hypothetical membrane protein	F A	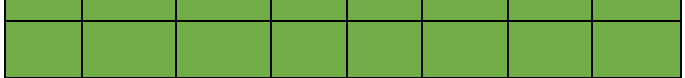
ZGAL_2990		Glycosyltransferase, family GT4	L F A	
ZGAL_2991		Dolichol-phosphate mannose synthase, family GT2	F A	
ZGAL_2994		Hypothetical protein	L	
ZGAL_3093	traK	Conjugative transposon protein TraK	A	
ZGAL_3183	dssA	Sheath polysaccharide lyase, family PL9_4	A	
ZGAL_3216	moaE2	Molybdopterin synthase, large subunit	A	
ZGAL_3262		Conserved hypothetical protein	A	
ZGAL_3285		Conserved hypothetical protein	A	
ZGAL_3294		Conserved hypothetical protein	A	
ZGAL_3295		Hypothetical membrane protein	A	
ZGAL_3299		Conserved hypothetical protein	A	
ZGAL_3315		Putative membrane protein	A	
ZGAL_3371		Hypothetical membrane protein	A	
ZGAL_3372		Hypothetical membrane protein	A	
ZGAL_3373		Hypothetical protein	A	
ZGAL_3388		Conserved hypothetical protein	F A	
ZGAL_3389		Vgr family protein	A	
ZGAL_3410		Conserved hypothetical lipoprotein	A	
ZGAL_3411		Putative protein	F A	
ZGAL_3445	uglA1	Unsaturated glucuronyl hydrolase, family GH88	A	
ZGAL_3478		Conserved hypothetical protein	A	
ZGAL_3479		Metallo-beta-lactamase superfamily protein	A	

ZGAL_3480		Conserved hypothetical protein	A
ZGAL_3481		Small-conductance mechanosensitive channel	A
ZGAL_3483		Universal stress protein	A
ZGAL_3491	lolD1	Lipoprotein-specific ABC transporter, ATPase component	A
ZGAL_3492		Conserved hypothetical protein	A
ZGAL_3493		Conserved hypothetical protein	A
ZGAL_3551		Conserved hypothetical periplasmic protein	L F
ZGAL_3557		Hypothetical membrane protein	L
ZGAL_3558		Conserved hypothetical protein	L
ZGAL_3560		Hypothetical protein	L F
ZGAL_3565		Conserved hypothetical protein	L
ZGAL_3651		T9SS SprF family protein	F A
ZGAL_3652		T9SS-associated PG1058-like protein	F A
ZGAL_3704		DUF805 family protein	A
ZGAL_3727		Conserved hypothetical protein; CTD belonging to TIGRFAM family TIGR04131	A
ZGAL_3759	capM	Capsular polysaccharide biosynthesis glycosyltransferase, family GT4	A
ZGAL_3770	pelA1	Pectate lyase, family PL1	A
ZGAL_3839		Small heat shock protein	A
ZGAL_3847		Conserved hypothetical membrane protein	A
ZGAL_3848		Conserved hypothetical membrane protein	A
ZGAL_3849		Hypothetical protein	A
ZGAL_3850		Conserved hypothetical protein	A
ZGAL_3851		Conserved hypothetical protein	A
ZGAL_3852		ABC-2 type exporter, permease component	F A
ZGAL_3853		ABC-2 type exporter, permease component	F A
ZGAL_3854		Membrane fusion protein	A
ZGAL_3855		Outer membrane efflux protein	A
ZGAL_3856		Multi-pass membrane transporter	A
ZGAL_3861		Conserved hypothetical protein	A
ZGAL_3862		Universal stress protein	A
ZGAL_3863		Conserved hypothetical protein	F A
ZGAL_3864	glkA	Glucokinase (Glucose kinase)	F A
ZGAL_3865	fbaB	Fructose-bisphosphate aldolase, class 1	F A
ZGAL_3866	pfkB	6-Phosphofructokinase, isozyme 2	F A
ZGAL_3867	gpmA	2,3-bisphosphoglycerate-dependent phosphoglycerate mutase	F A
ZGAL_3868	ldhA	D-lactate dehydrogenase	A
ZGAL_3869	ppsA	Pyruvate, water dikinase (Phosphoenolpyruvate synthase)	F A
ZGAL_3871	atpD2	ATP synthase, F1 sector beta subunit	F A
ZGAL_3872	atpC2	ATP synthase, F1 sector epsilon subunit	A
ZGAL_3873	atpI	ATP synthase gene 1	A
ZGAL_3874		Conserved hypothetical membrane protein	A
ZGAL_3875	atpB2	ATP synthase, F0 sector A subunit	A A
ZGAL_3876	atpE2	ATP synthase, F0 sector C subunit	A
ZGAL_3877	atpF2	ATP synthase, F0 sector B subunit	A
ZGAL_3878	atpA2	ATP synthase, F1 sector alpha subunit	F A
ZGAL_3879	atpG2	ATP synthase, F1 sector gamma subunit	A
ZGAL_3881		ABC importer, periplasmic component	F A
ZGAL_3882		ABC importer, ATPase component	F A
ZGAL_3883		ABC importer, permease component	F A
ZGAL_3885		Voltage-gated chloride channel	A
ZGAL_3886	cgaA		A

ZGAL_3939		Serine endopeptidase, family S54	A	
ZGAL_3947		Endonuclease/exonuclease/phosphatase family	A	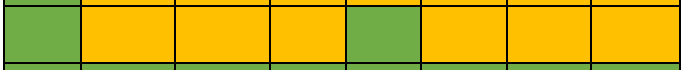
ZGAL_3970		conserved hypothetical lipoprotein	A	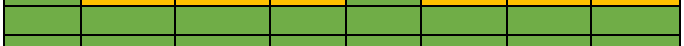
ZGAL_4057		Conserved hypothetical membrane protein	A	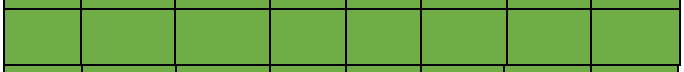
ZGAL_4072	nth	Endonuclease III	A	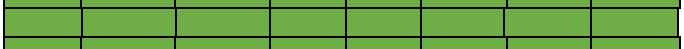
ZGAL_4136		Conserved hypothetical membrane protein	A	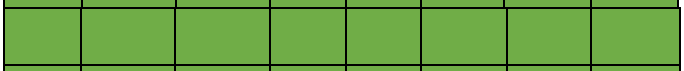
ZGAL_4152		Response regulator receiver	A	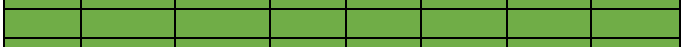
ZGAL_4153		Conserved hypothetical membrane protein	A	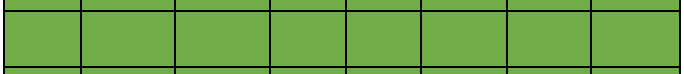
ZGAL_4154		Glycosyltransferase, family GT2	A	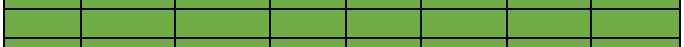
ZGAL_4173		Putative membrane protein	F	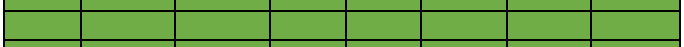
ZGAL_4191		NAD dependent epimerase/dehydratase family protein	L F	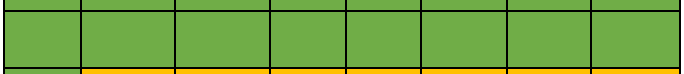
ZGAL_4204		MORN repeat protein	A	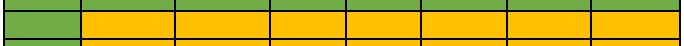
ZGAL_4216		Hypothetical lipoprotein	A	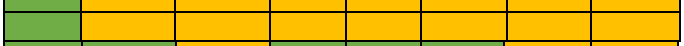
ZGAL_4267	agaC	Beta-agarase AgaC, family GH16	A	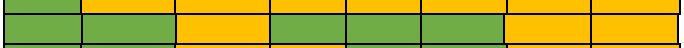
ZGAL_4268		Parallel beta-helix fold protein	A	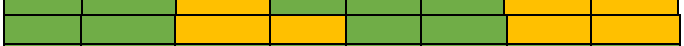
ZGAL_4272		Conserved hypothetical protein	A	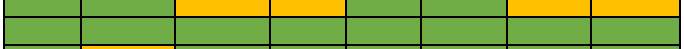
ZGAL_4288		Hypothetical lipoprotein	F	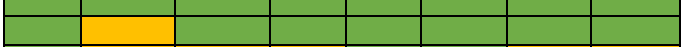
ZGAL_4310		Conserved hypothetical periplasmic protein; CTD belonging to TIGRFAM family TIGR04183	A	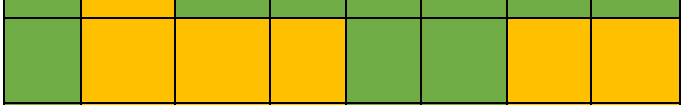
ZGAL_4348		Conserved hypothetical protein	A	
ZGAL_4349		Hypothetical periplasmic protein	A	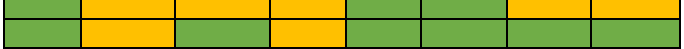
ZGAL_4350		Conserved hypothetical protein	A	
ZGAL_4355		Hypothetical membrane protein	A	
ZGAL_4409		Conserved hypothetical lipoprotein	A	
ZGAL_4437		Conserved hypothetical protein	A	
ZGAL_4444	aldB	Alpha-acetolactate decarboxylase	A	
ZGAL_4532		Conserved hypothetical membrane protein	A	
ZGAL_4575		Conserved hypothetical protein	A	
ZGAL_4576		Conserved hypothetical membrane protein	A	
ZGAL_4604		Putative protein	A	
ZGAL_4606		Conserved hypothetical membrane protein	A	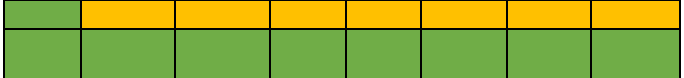
ZGAL_4634		T9SS SprF family protein	A	
ZGAL_4635		T9SS-associated PG1058-like protein	A	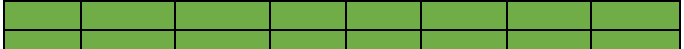
ZGAL_4729		Conserved hypothetical lipoprotein	A	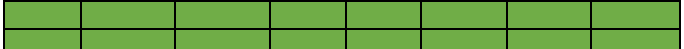
ZGAL_4738		Two-component system - Response regulator	A	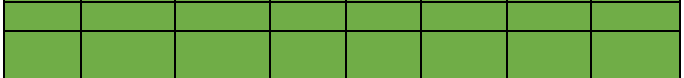
ZGAL_4765		Conserved hypothetical periplasmic protein	A	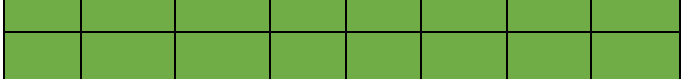
ZGALAM_0075	rpmH	50S ribosomal protein L34	F A	
ZGALAM_0667	rpsU	30S ribosomal protein S21	A	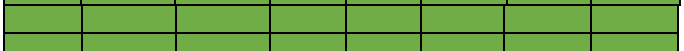
ZGALAM_0748		conserved protein of unknown function	A	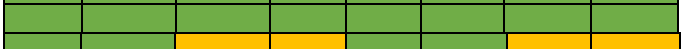
ZGALAM_0909		exported protein of unknown function	F A	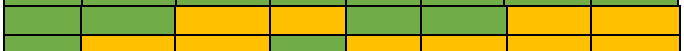
ZGALAM_2285		transposase (fragment)	A	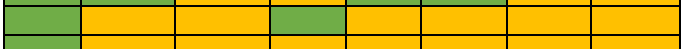
ZGALAM_2286		protein of unknown function	A	
ZGALAM_2603		protein of unknown function	A	
ZGALAM_2793		conserved exported protein of unknown function	A	
ZGALAM_4614		protein of unknown function	A	
ZGALAM_4720		conserved exported protein of unknown function	F A	

Table V.S5: Spearman correlation between the number of GHs, PLs, CEs or Sulfatases with the generation time. *Z. nedashkovskayae* Asnod3-E08-A was removed from the analysis as the measured OD was not reliable given the aggregates formation.

	rho	p-value
GH	-0.90	0.006
PL	0.45	0.305
CE	-0.20	0.667
Sulfatases	-0.52	0.229
Total	-0.64	0.139

Table V.S6: Genes upregulated with *Laminaria* when compared to maltose (Bonferroni-adjusted p-value < 0.05 and log2FC > 2). Gene homologs were searched in the genome of the other *Zobellia* spp. used in this study. Green = homolog found; Yellow = homolg not found. Zgal: *Z. galactanivorans* Dsij^{T}; Zamu: *Z. amurskyensis* KMM 3526^{T}; Zlam: *Z. laminariae* KMM 3676^{T}; Zrus*: Z. russellii* KMM 3677^{T}; ZrosF08: *Z. roscoffensis* Asnod1-F08^{T}; ZrosB02: *Z. roscoffensis* Asnod2-B02-B; ZnedB07*: Z. nedashkovskayae* Asnod2-B07-B^{T}; ZnedE08: *Z. nedashkovskayae* Asnod3-E08-A.

GeneID	Gene name	Gene function	Zgal	Zamu	Zlam	Zrus	Zros F08	Zros B02	Zned B07	Z.ed E08
ZGAL_8	degP	degP Peptidase Do, family S1								
ZGAL_18		Putative membrane protein								
ZGAL_41		Conserved hypothetical periplasmic protein								
ZGAL_47		Small-conductance mechanosensitive channel								
ZGAL_98	fadA	fadA 3-Ketoacyl-CoA thiolase								
ZGAL_99	fadE	fadE Acyl-CoA dehydrogenase								
ZGAL_112		Serine peptidase, family S9								
ZGAL_114	sodC	sodC Superoxide dismutase [Cu-Zn]								
ZGAL_115		Bacterial surface antigen								
ZGAL_176		Conserved hypothetical periplasmic protein								
ZGAL_177		Cytochrome c-containing protein								
ZGAL_200		SusC-like TonB-dependent transporter								
ZGAL_205		Glycoside hydrolase, family GH117								
ZGAL_206		Sulfatase, family S1-17								
ZGAL_223		ABC-2 type exporter, permease component								
ZGAL_257		Cytochrome c-containing protein								
ZGAL_305	cysJ	cysJ Sulfite reductase [NADPH] flavoprotein alpha-component								
ZGAL_306		Peroxiredoxin								
ZGAL_331		RNA polymerase ECF-type sigma factor								
ZGAL_334		Putative glycoside hydrolase, family GHnc								
ZGAL_360		Conserved hypothetical protein								
ZGAL_512		Conserved hypothetical membrane protein								
ZGAL_513		Conserved hypothetical protein								
ZGAL_521	msrB1	msrB1 Peptide methionine sulfoxide reductase msrB								
ZGAL_536		NUDIX hydrolase								
ZGAL_553		Fasciclin repeats protein								
ZGAL_581		Conserved hypothetical protein								
ZGAL_582	arsC	arsC Protein arsC								
ZGAL_619	pbp1B	pbp1B Penicillin-binding protein 1B, family GT51								
ZGAL_620		Hydrolase HAD superfamily								
ZGAL_699		Fatty acid hydroxylase family protein								
ZGAL_700		Conserved hypothetical periplasmic protein								
ZGAL_704		Conserved PDZ-containing protein								
ZGAL_729		Conserved hypothetical periplasmic protein								
ZGAL_730		Conserved hypothetical periplasmic protein								
ZGAL_737		Ankyrin repeats protein								
ZGAL_769	rpoD1	rpoD1 RNA polymerase sigma factor rpoD								
ZGAL_772	add	add Adenosine deaminase								
ZGAL_831		hypothetical protein								
ZGAL_871		Conserved hypothetical protein								
ZGAL_872		Conserved hypothetical protein								
ZGAL_873		Conserved hypothetical protein								
ZGAL_921		Conserved cytochrome c-containing protein								
ZGAL_922		SusC-like TonB-dependent transporter								
ZGAL_923		SusD-like lipoprotein								

ZGAL_934		Serine peptidase, family S8
ZGAL_940		Conserved hypothetical protein
ZGAL_947		Conserved hypothetical protein
ZGAL_954		Conserved cytochrome c-containing protein
ZGAL_968		Conserved hypothetical periplasmic protein
ZGAL_980		LemA family protein
ZGAL_1071		Ribonuclease BN family protein
ZGAL_1072		Short-chain dehydrogenase/reductase
ZGAL_1073		Conserved hypothetical protein
ZGAL_1074		Conserved hypothetical membrane protein
ZGAL_1075		Possible Sigma-54 modulation protein
ZGAL_1076		Putative protein
ZGAL_1077		Citrate transporter family protein
ZGAL_1078		Small-conductance mechanosensitive channel
ZGAL_1079		Conserved hypothetical membrane protein
ZGAL_1080		Putative membrane protein
ZGAL_1082	topA2	topA2 DNA topoisomerase 1B
ZGAL_1083		Conserved hypothetical protein
ZGAL_1084		Conserved hypothetical protein
ZGAL_1085		Putative membrane protein
ZGAL_1089		Two-component system - Sensor histidine kinase
ZGAL_1091		AraC-type transcriptional regulator
ZGAL_1092		Conserved hypothetical protein
ZGAL_1094	dpsA2	dpsA2 DNA protection during starvation protein
ZGAL_1099		Alpha/beta hydrolase-fold protein
ZGAL_1100		Putative protein
ZGAL_1101		Peroxiredoxin
ZGAL_1102	gdhA	gdhA Glucose 1-dehydrogenase
ZGAL_1103		Short-chain dehydrogenase/reductase SDR
ZGAL_1104		Hypothetical protein
ZGAL_1105		Conserved hypothetical protein
ZGAL_1132		Conserved hypothetical protein
ZGAL_1133		Conserved cytochrome c -containing protein
ZGAL_1178	msrB2	msrB2 Peptide methionine sulfoxide reductase msrB
ZGAL_1179	msrA1	msrA1 Peptide methionine sulfoxide reductase msrA
ZGAL_1180		Conserved hypothetical membrane protein
ZGAL_1181	msrA2	msrA2 Peptide methionine sulfoxide reductase msrA
ZGAL_1182	alyA1	alyA1 Endo-guluronate lyase AlyA1, family PL7_3
ZGAL_1205		Conserved hypothetical lipoprotein
ZGAL_1208		AraC-type transcriptional regulator
ZGAL_1213		Conserved hypothetical membrane protein
ZGAL_1219		Conserved hypothetical periplasmic protein
ZGAL_1220		FAD-dependent pyridine nucleotide-disulfide oxidoreductase
ZGAL_1222		Conserved hypothetical protein
ZGAL_1223	rhaB	rhaB Alpha-L-rhamnosidase, family GH78
ZGAL_1282		Conserved hypothetical periplasmic protein
ZGAL_1312		Conserved hypothetical membrane protein
ZGAL_1313	lys9	lys9 Saccharopine dehydrogenase (NADP(+), L-glutamate-forming) (Saccharopine reductase)
ZGAL_1346		Conserved hypothetical periplasmic protein
ZGAL_1360		Conserved hypothetical membrane protein
ZGAL_1364		Cytochrome c-containing protein
ZGAL_1365	irpA2	irpA2 Iron-regulated protein A

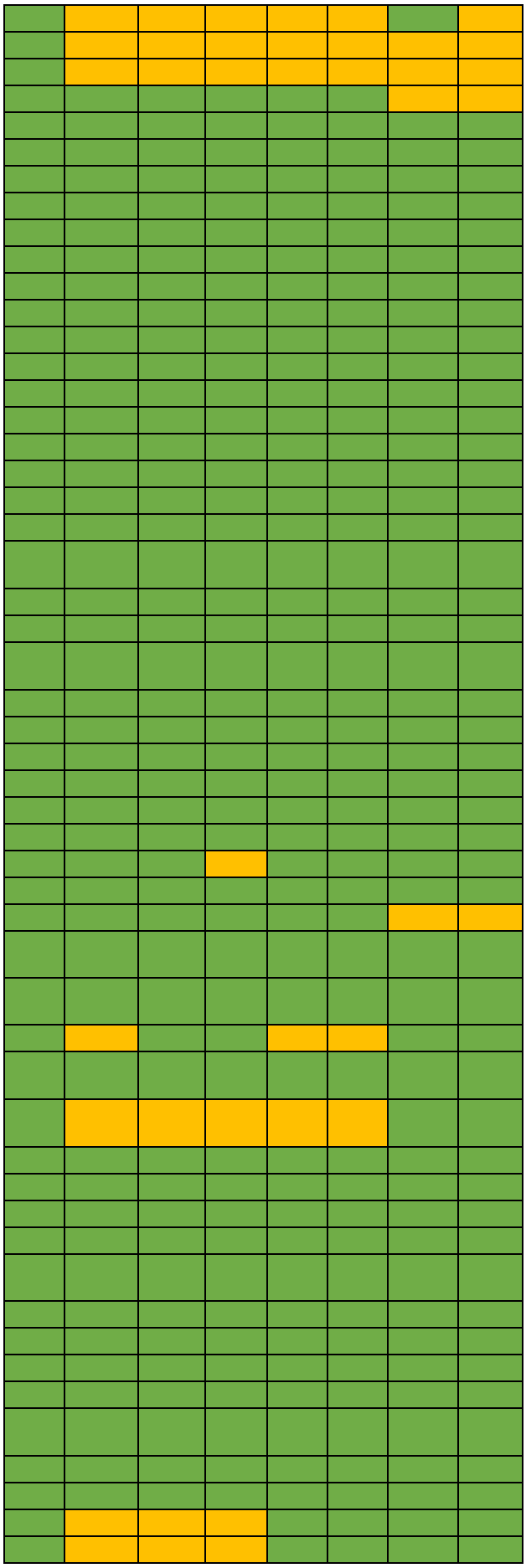

ZGAL_1425	nudF	nudF ADP-ribose pyrophosphatase
ZGAL_1426		Ankyrin repeats protein
ZGAL_1427	katA1	katA1 Catalase
ZGAL_1431		Putative membrane lipoprotein
ZGAL_1432		TonB-dependent Receptor
ZGAL_1480		Aldehyde dehydrogenase
ZGAL_1481		Hypothetical protein
ZGAL_1495		MoxR-like ATPase
ZGAL_1512		Multidrug efflux transporter
ZGAL_1513		Outer membrane efflux protein
ZGAL_1597		Putative protein
ZGAL_1598		Carboxymuconolactone decarboxylase family protein
ZGAL_1599		Conserved hypothetical periplasmic protein
ZGAL_1640	sirC	sirC Precorrin-2 dehydrogenase
ZGAL_1641		Conserved hypothetical membrane protein
ZGAL_1642		Flavoprotein, bacterial luciferase family
ZGAL_1695		Conserved hypothetical protein
ZGAL_1710		Conserved hypothetical membrane protein
ZGAL_1711		Conserved hypothetical membrane protein
ZGAL_1712		Conserved hypothetical protein
ZGAL_1825		Intracellular peptidase, family C56
ZGAL_1837	sufA	sufA Protein SufA
ZGAL_1838	sufB	sufB Protein SufB
ZGAL_1871	hemH	hemH Ferrochelatase
ZGAL_1898		Hypothetical periplasmic protein
ZGAL_1908		Hypothetical periplasmic protein
ZGAL_1909		Conserved hypothetical periplasmic protein
ZGAL_1936	dxsA	dxsA 1-Deoxy-D-xylulose-5-phosphate synthase
ZGAL_1949		RNA polymerase ECF-type sigma factor
ZGAL_1964	feoB	feoB Ferrous iron transport protein B
ZGAL_1991		Conserved hypothetical lipoprotein
ZGAL_2004		Conserved hypothetical periplasmic protein
ZGAL_2023		T9SS SprF family protein
ZGAL_2036		Conserved hypothetical protein
ZGAL_2041		Conserved hypothetical lipoprotein
ZGAL_2093		Deacetylase, histone deacetylase family
ZGAL_2107	gorA	gorA Glutathione reductase
ZGAL_2108		Conserved hypothetical membrane protein
ZGAL_2109		Metallo-phosphoesterase family
ZGAL_2112		Uncharacterized ATP-dependent helicase
ZGAL_2113	ligC	ligC DNA ligase
ZGAL_2114		Metallo-beta-lactamase superfamily protein
ZGAL_2131		TPR repeats protein
ZGAL_2132		Putative protein
ZGAL_2151		Conserved hypothetical membrane protein
ZGAL_2168	hyaD	hyaD Hydrogenase maturation protease, family A31
ZGAL_2266		NAD(P)H nitroreductase
ZGAL_2269		BlaI-type transcriptional repressor
ZGAL_2270		BlaR1-type regulatory protein / TonB protein
ZGAL_2271		O-linked N-acetylglucosaminyltransferase, family GT41
ZGAL_2296		Conserved lipoprotein containing CBM22
ZGAL_2352		Metallophosphoesterase
ZGAL_2393		ABC exporter, permease component
ZGAL_2398	yggB	yggB Mechanosensitive ion channel

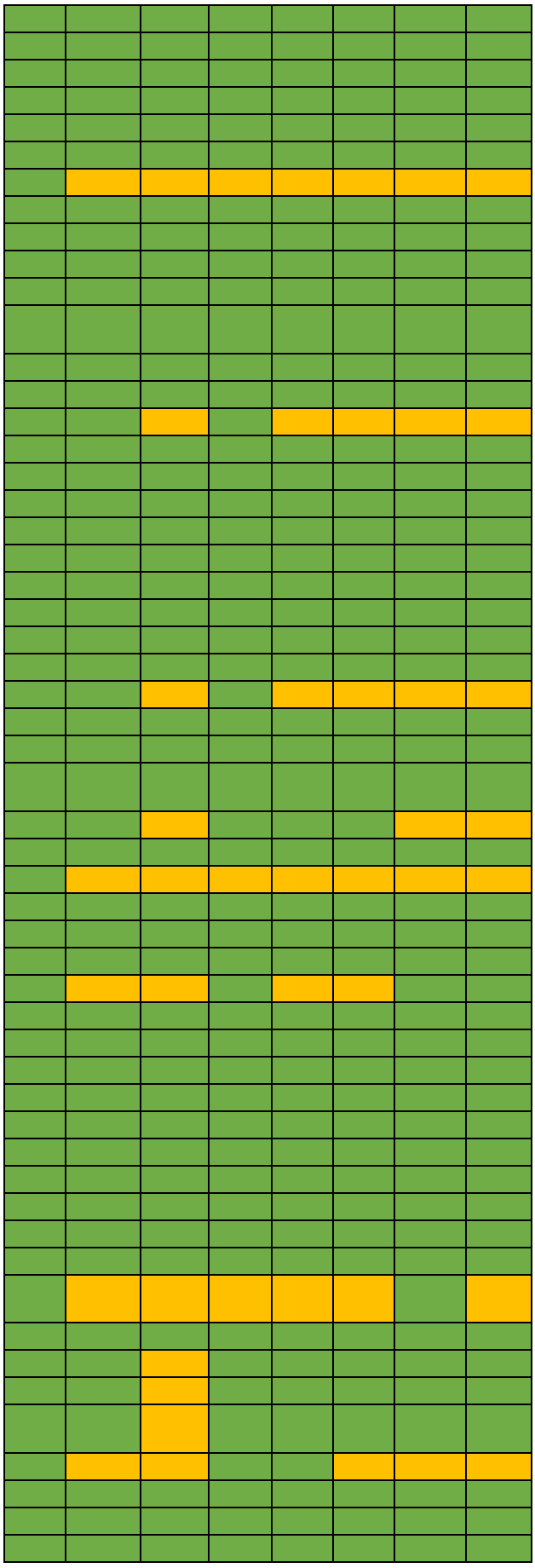

ZGAL_2466	fabH3	fabH3 3-oxoacyl-[acyl-carrier-protein] synthase III
ZGAL_2605		Conserved hypothetical protein
ZGAL_2606		Conserved hypothetical protein
ZGAL_2607		Conserved hypothetical periplasmic protein
ZGAL_2608		Conserved hypothetical protein
ZGAL_2609		CsbD-like protein
ZGAL_2611		Conserved hypothetical protein
ZGAL_2612		Manganese/fer transporter
ZGAL_2613	pfp	pfp Diphosphate-fructose-6-phosphate 1-phosphotransferase
ZGAL_2614	kdgK1	kdgK1 2-dehydro-3-deoxygluconokinase
ZGAL_2615		Acetoin(diacetyl) reductase
ZGAL_2616	exuT2	exuT2 Hexuronate transporter
ZGAL_2618	alyA2	alyA2 Alginate lyase, family PL7
ZGAL_2619		Conserved hypothetical membrane protein
ZGAL_2620		Alginate-specific SusD-like lipoprotein
ZGAL_2621		Alginate-specific SusC-like TonB-dependent transporter
ZGAL_2622		2-dehydro-3-deoxy-D-gluconate 6-dehydrogenase
ZGAL_2623	kdgF	kdgF Alginate degradation protein KdgF
ZGAL_2624	alyA3	alyA3 Alginate lyase, family PL17_2
ZGAL_2626		Xylose isomerase-like TIM barrel protein
ZGAL_2627		Conserved hypothetical protein
ZGAL_2628		Conserved hypothetical protein
ZGAL_2629		Conserved hypothetical periplasmic protein
ZGAL_2634		Conserved hypothetical protein
ZGAL_2635		Hypothetical protein
ZGAL_2637	gntK1	gntK1 Gluconokinase
ZGAL_2638	iolC	iolC 5-dehydro-2-deoxygluconokinase
ZGAL_2639		Possible dioxygenase
ZGAL_2728		Conserved hypothetical lipoprotein
ZGAL_2756		Conserved hypothetical protein
ZGAL_2757		NAD dependent aldehyde dehydrogenase
ZGAL_2764		Conserved hypothetical lipoprotein
ZGAL_2789	apt	apt Adenine phosphoribosyltransferase
ZGAL_2805		Conserved hypothetical protein
ZGAL_2822		NAD(P)-dependent epimerase/dehydratase
ZGAL_2856		Conserved hypothetical lipoprotein
ZGAL_2867		Conserved hypothetical periplasmic protein
ZGAL_2876		Small heat shock protein
ZGAL_2930	ohrB	ohrB Organic hydroperoxide resistance protein ohrB
ZGAL_2932	msrA3	msrA3 Peptide methionine sulfoxide reductase
ZGAL_2971		Thiol-disulfide oxidoreductase
ZGAL_2972	crtZ	crtZ Beta-carotene hydroxylase
ZGAL_2973	crtB	crtB Phytoene synthetase
ZGAL_2974	crtI	crtI Phytoene dehydrogenase
ZGAL_2975		MerR-type transcriptional regulator
ZGAL_2978		Two-component system - Response regulator, receiver domain
ZGAL_2990		Glycosyltransferase, family GT4
ZGAL_2992		TetR-type transcriptional regulator
ZGAL_2993		Carboxymuconolactone decarboxylase family protein
ZGAL_2994		Hypothetical protein
ZGAL_2995		DSBA thioredoxin family protein
ZGAL_2998		Universal stress protein

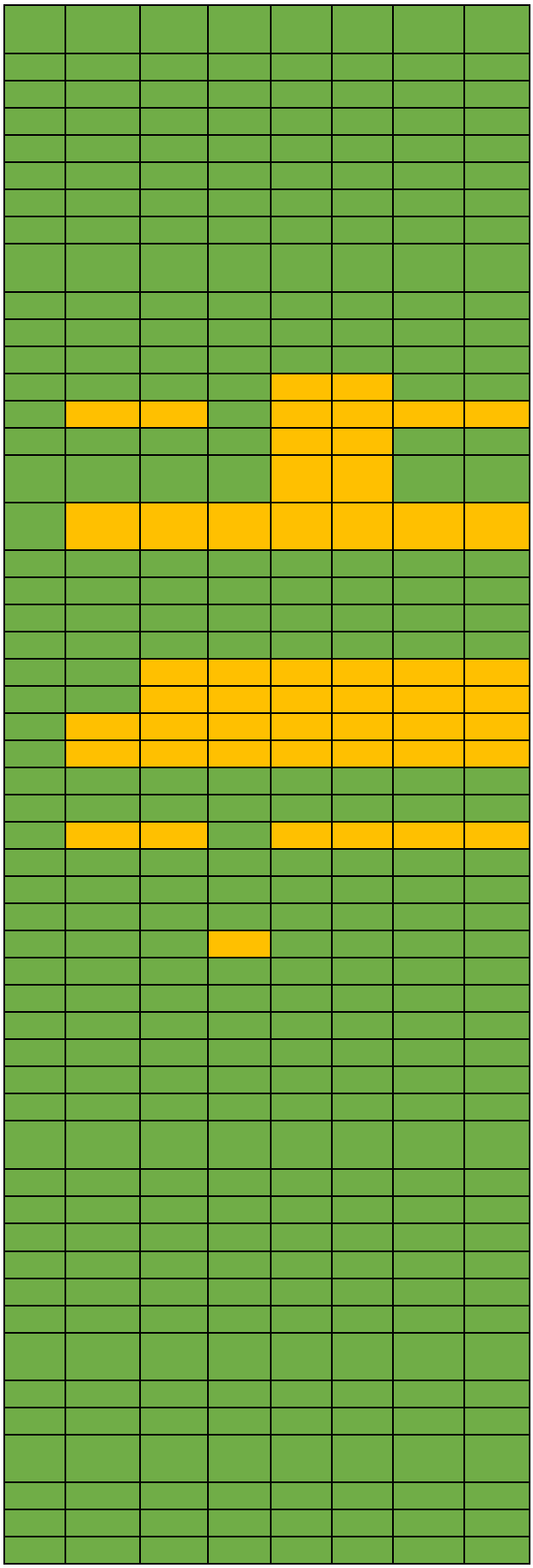

ZGAL_2999		Putative protein
ZGAL_3000		Conserved hypothetical protein
ZGAL_3031		AraC-type transcriptional regulator
ZGAL_3164		Cytochrome c-containing lipoprotein
ZGAL_3166		Conserved hypothetical protein
ZGAL_3167		Conserved hypothetical protein
ZGAL_3170		Xylose isomerase-like TIM barrel protein
ZGAL_3171		NAD(P)-dependent oxidoreductase
ZGAL_3349		Glycoside hydrolase, family GH20
ZGAL_3354		Conserved hypothetical lipoprotein
ZGAL_3366		Sulfate transporter
ZGAL_3367	canA3	canA3 Carbonate dehydratase
ZGAL_3436		Conserved hypothetical membrane protein
ZGAL_3441		SusC-like TonB-dependent transporter
ZGAL_3448	mdsA3	mdsA3 Mucin-desulfating sulfatase, family S1-11
ZGAL_3449		Conserved hypothetical periplasmic protein
ZGAL_3450		Alpha-L-fucosidase, family GH141
ZGAL_3451	alfA5	alfA5 Alpha-L-fucosidase, family GH29 / Acetylesterase
ZGAL_3453		Possible pyridine nucleotide-disulphide oxidoreductase
ZGAL_3454		Acetylesterase, lipase-GDSL family
ZGAL_3455		Sulfatase, family S1-17
ZGAL_3464	alfA4	alfA4 Alpha-L-fucosidase, family GH29
ZGAL_3465		Sulfatase, family S1-15
ZGAL_3467		SusC-like TonB-dependent transporter
ZGAL_3468		SusD-like lipoprotein
ZGAL_3469		Sulfatase, family S1-17
ZGAL_3470		Putative glycoside hydrolase, family GHnc
ZGAL_3471		L-fuconate dehydratase
ZGAL_3512		SusD-like lipoprotein
ZGAL_3513		Sulfatase, family S1-20
ZGAL_3528		RNA polymerase ECF-type sigma factor
ZGAL_3551		Conserved hypothetical periplasmic protein
ZGAL_3552		Two-component system - Response regulator, receiver domain
ZGAL_3557		Hypothetical membrane protein
ZGAL_3558		Conserved hypothetical protein
ZGAL_3559	katA2	katA2 Catalase
ZGAL_3560		Hypothetical protein
ZGAL_3562		Conserved hypothetical protein
ZGAL_3563		Conserved hypothetical membrane protein
ZGAL_3565		Conserved hypothetical protein
ZGAL_3566	pldA	pldA Phospholipase A1
ZGAL_3590		Conserved hypothetical periplasmic protein
ZGAL_3592	rnkA	rnkA Regulator of nucleoside diphosphate kinase
ZGAL_3611		Conserved hypothetical periplasmic protein
ZGAL_3638		SusD-like lipoprotein
ZGAL_3665		Two-component system - Sensor histidine kinase
ZGAL_3683	mobA	mobA Molybdopterin-guanine dinucleotide biosynthesis protein A
ZGAL_3685		Permease
ZGAL_3739		Conserved hypothetical periplasmic protein
ZGAL_3746		Glycosyltransferase, family GT4
ZGAL_3747		Conserved hypothetical protein
ZGAL_3749		Conserved hypothetical protein

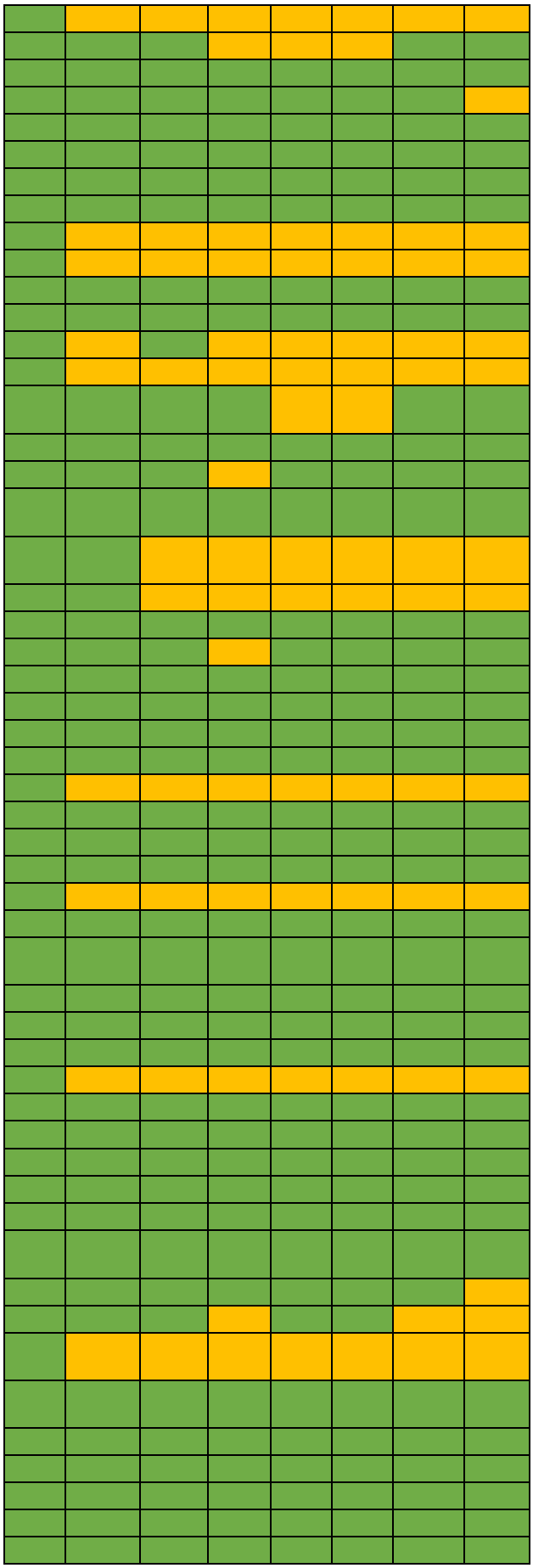

ZGAL_3796		Conserved hypothetical protein
ZGAL_3797		Conserved hypothetical protein
ZGAL_3800		Conserved hypothetical periplasmic protein
ZGAL_3801		Conserved hypothetical membrane protein
ZGAL_3820		Conserved hypothetical periplasmic protein
ZGAL_3898		Conserved hypothetical protein
ZGAL_3912		Hypothetical lipoprotein
ZGAL_3952	xynB	xynB Endo-beta-1,4-xylanase, family GH10
ZGAL_3954		Conserved hypothetical periplasmic protein
ZGAL_3971	phrA	phrA Deoxyribodipyrimidine photo-lyase
ZGAL_3972		Short-chain dehydrogenase/reductase
ZGAL_3973		Conserved hypothetical protein
ZGAL_4058		Conserved hypothetical protein
ZGAL_4082		Glycosyltransferase, family GT2
ZGAL_4130	alyA4	alyA4 Alginate lyase, family PL6_1
ZGAL_4131	alyA5	alyA5 Exo-alginate lyase, family PL7_5
ZGAL_4132	alyA6	alyA6 Alginate lyase, family PL6_1
ZGAL_4133		Two-component system - Sensor histidine kinase
ZGAL_4134		Two-component system - Response regulator
ZGAL_4184		Putative protein
ZGAL_4191		NAD dependent epimerase/dehydratase family protein
ZGAL_4224		MarR-type transcriptional regulator
ZGAL_4225		Conserved hypothetical membrane protein
ZGAL_4228		Intracellular peptidase, family C56
ZGAL_4229		Iron-containing alcohol dehydrogenase family
ZGAL_4230		Probable NADP-dependent oxidoreductase
ZGAL_4232		TetR-type transcriptional regulator
ZGAL_4273		Hypothetical periplasmic protein
ZGAL_4297		Hypothetical membrane protein
ZGAL_4309		Putative protein
ZGAL_4340		Conserved hypothetical periplasmic protein
ZGAL_4341	ybhR	ybhR ABC-2 type exporter, permease component
ZGAL_4364		Hypothetical protein
ZGAL_4386		Short-chain dehydrogenase/reductase
ZGAL_4399	ungA	ungA Uracil-DNA glycosylase
ZGAL_4544		Fatty acid hydroxylase family protein
ZGAL_4562		AraC-type transcriptional regulator
ZGAL_4622		SusD-like lipoprotein
ZGAL_4637	gapB	gapB Glyceraldehyde 3-phosphate dehydrogenase
ZGAL_4661	kduD1	kduD1 2-deoxy-D-gluconate-3-dehydrogenase
ZGAL_4673		Carbohydrate esterase, family CE1
ZGAL_4676	fdxA3	fdxA3 2Fe-2S ferredoxin
ZGAL_4677		6-O-methyl-D-galactose demethylase
ZGAL_4731		Conserved hypothetical lipoprotein
ZGAL_4739		Two-component system - Sensor histidine kinase
ZGAL_4740		Two-component system - Response regulator
ZGALAM_0909		exported protein of unknown function
ZGALAM_1098		protein of unknown function
ZGALAM_3727		protein of unknown function
ZGALAM_4041		conserved exported protein of unknown function

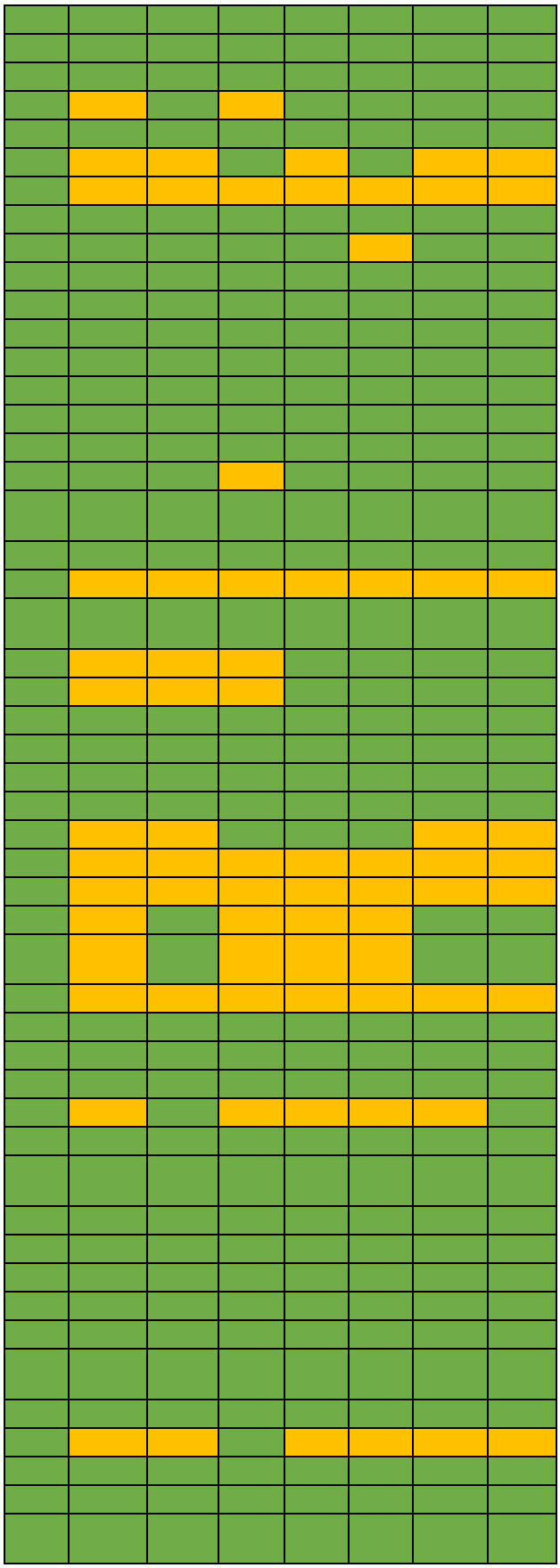

Part 2:
Degradation of fresh red macroalgae

I. Introduction

Z. galactanivorans Dsij^T was isolated from the red macroalgae *Delessaria sanguinea* (Potin *et al.*, 1991). It is able to grow with brown (alginate, FCSP, laminarin) and red (agar, carrageenans and porphyran) algal polysaccharides (Barbeyron, Thomas, *et al.*, 2016) and the utilization system of some of these polysaccharides were deciphered (Hehemann *et al.*, 2012; Thomas *et al.*, 2012; Ficko-Blean *et al.*, 2017). In Part 1 we demonstrated that besides its ability to grow with purified brown algal polysaccharides, *Z. galactanivorans* Dsij^T was also efficient to use and degrade fresh brown algal tissues, hence highlighting its role as a pioneer bacterium in brown algae utilization. Here we aimed to assess if this pioneer behavior can be extended to red macroalgae.

II. Methods

Macroalgae treatment, pre-cultures and microcosm set up were carried out as described in Part 1. Different red macroalgae (*Chondrus crispus* Stackhouse 1797, *Mastocarpus stellatus* (Stackhouse) Guiry 1984, *Palmaria palmata* (Linnaeus) F.Weber & D.Mohr 1805, *Gracilaria* sp. Greville, 1830, and *Grateloupia turuturu* Y.Yamada 1941) collected on the seashore in front of the Station Biologique de Roscoff or at the Bloscon site (Roscoff) were tested for growth. Growth was assessed in Marine Minimum Medium (MMM) with macroalgae pieces as the sole carbon source. Some experiments were conducted by adding 4 $g.l^{-1}$ maltose in the algae-containing microcosms.

Growth with crushed red algae was also tested. Collected algae were rinsed with 0.2 µm filtered seawater, dried at 50 °C overnight in oven and crushed in a blender, resulting in a mix of algal powder and small tissue pieces (1-20 mm^2). A part of this mixture was added in the microcosms as is (40 mg) while another part was autoclaved (121 °C for 15 min) in 1X saline solution before being added (approximatively equal to 40 mg). Microcosms were inoculated at an initial optical density (OD_{600}) of 0.05 or 0.1 and growth was monitored by OD_{600} measurements.

NB: the ratio wet weight / dry weight was assessed for the different algae after the night at 50 °C. I used it to add approximately the same amount of carbon between the microcosms containing fresh and dried algae.

III. Results and Discussion

Z. galactanivorans Dsij^T was unable to grow on fresh algae pieces from *Chondrus crispus*, *Mastocarpus stellatus*, *Gracilaria* sp. and *Palmaria palmata* (growth on *Grateloupia turuturu* was not tested at that time) collected between March and June 2019 when inoculated at an initial optical density OD_{600} equal to 0.05 or 0.1 (data not shown).

This absence of growth with red algal tissues contrasted with what was observed with brown algae (cf. Part I of this Chapter). Several hypotheses were raised to explain this discrepancy. Brown and red macroalgae might secrete different secondary metabolites or display different defense mechanisms when facing bacterial attack. For example, both red and brown macroalgae release bromine and iodine compounds as defense compounds but red algae have a stronger propensity for bromocarbons production while brown algae are potent producers of iodocarbons (Leedham *et al.*, 2013). *Z. galactanivorans* Dsij^T contains 3 known vanadium haloperoxidases strictly specific for iodide oxidation (Fournier *et al.*, 2014) and is able to accumulate high amount of iodine (Barbeyron, Thomas, *et al.*, 2016), but no bromoperoxidases were reported to date. An haloacid dehalogenase that dehalogenates bromo- and iodoacetic acids (Grigorian *et al.*, 2021) was however recently characterized. It is possible that some molecules produced by red algae might inhibit the growth of *Z. galactanivorans*. To test this hypothesis, we supplemented the microcosms containing red algae (either *Chondrus crispus*, *Palmaria palmata* or *Grateloupia turuturu*) with maltose, a carbon source that *Z. galactanivorans* is able to use for its growth. As shown in **Figure V.7A**, *Z. galactanivorans* was able to grow in the presence of red algae when maltose was added (OD_{600} > 1), meaning that growth is not inhibited by red algal metabolites. Compared with *G. turuturu* and *P. palmata*, a delay is observed with *C. crispus* due to the formation of big bacterial cells aggregates in the early stage of the growth which biased the OD measurements. The *G. turuturu* tissues were completely degraded as shown in **Figure V.7B**, while it was not the case for *P. palmata* and *C. crispus.* Therefore, besides the utilization of maltose, *Z. galactanivorans* was able to degrade and probably to use the tissues of this algal species as carbon source. This observation is consistent with the higher maximal optical density obtained with *G. turuturu* (1.4 against 1.2 for the other two species).

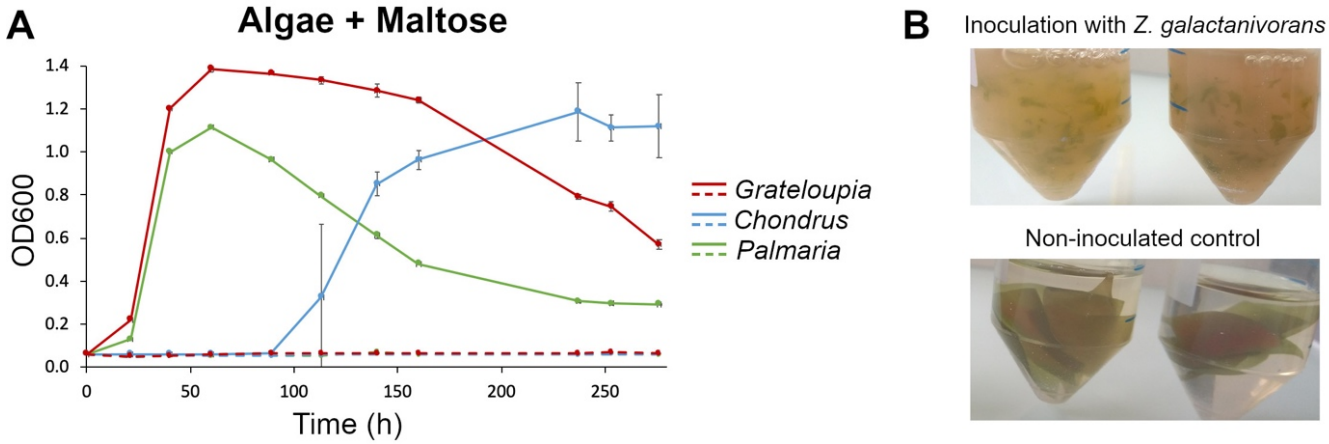

Figure V.7: Evaluation of the impact of red macroalgae released compounds on *Z. galactanivorans* Dsij^T growth. (A) Bacterial growth when *Z. galactanivorans* was inoculated (solid lines) with three different red algae in minimum medium supplemented with maltose. The dotted lines represent the non-inoculated controls. Values are mean of independent duplicates ± standard error. (B) Photographs of microcosms containing Grateloupia pieces + maltose in the presence or absence of *Z. galactanivorans.*

Another reason explaining the absence of growth with several red algae tissues could lie in their thallus composition. It was reported that several species exhibit a complex multilayer cuticle at their surface as detailed for *C. crispus* (Hanic and Craigie, 1969; Craigie *et al.*, 1992). Red algae cuticle composition differs from the ECM and was reported to mainly include proteins with carbohydrates (pectic structures, chitin, mannan, sulfated polysaccharides) (Craigie *et al.*, 1992). Moreover, it was suggested that bromophenols potentially condense in the cuticle of red algae (Pedersen *et al.*, 1979; Craigie *et al.*, 1992). To my knowledge, such cuticle was not reported for the brown algae tested in Part 1. *Zobellia galactanivorans* Dsij^T might not be equipped to degrade this cuticle, hindering the access to ECM polysaccharides. This hypothesis was tested by cultivating *Z. galactanivorans* either in the presence of fresh macroalgae pieces or with dried crushed algae that had previously been autoclaved or not. By crushing the algae, I aimed to increase the availability of the polysaccharides. Moreover, their accessibility was likely even higher after autoclaving as high temperatures favor their extraction (this was confirmed by the gelling mixture obtained after autoclaving). With autoclaved crushed algae, *Z. galactanivorans* was able to grow with the three algae species, *C. crispus*, *P. palmata* and *G. turuturu* (OD_{600} ≈ 0.2-0.3) while no growth was observed in the non-inoculated controls (**Figure V.8**).

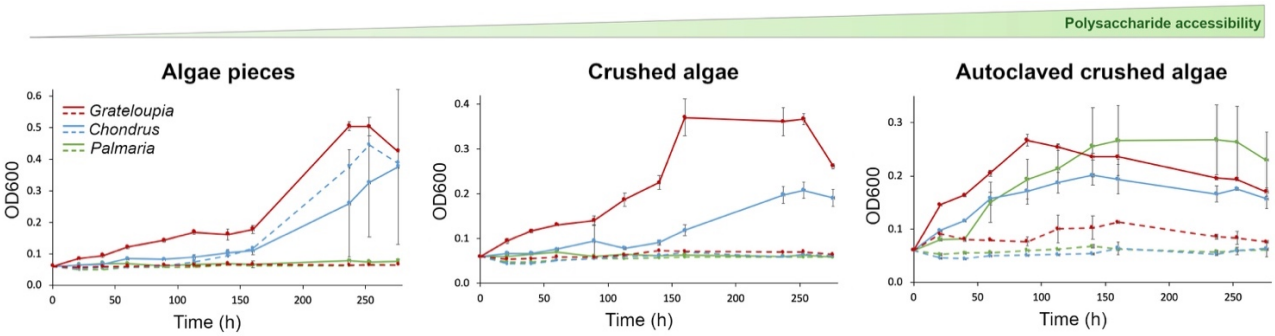

Figure V.8: Bacterial growth when *Z. galactanivorans* Dsij^T was inoculated with either whole algae pieces (left), crushed algae (middle) or autoclaved crush algae (right). The dotted lines represent the non-inoculated controls. Values are mean of independent duplicates ± standard error.

With non-autoclaved crushed algae and fresh algae pieces, distinct behaviors were observed depending on the algal species. *Z. galactanivorans* was unable to grow with *P. palmata* in both conditions. Given its ability to use *P. palmata* compounds when the alga was crushed and autoclaved, it would suggest that *Z. galactanivorans* is able to feed on the substrates offered by *P. palmata*, substrates which would be inaccessible in intact thallus.

For *C. crispus*, a growth was detected with crushed algae (OD_{600} ≈ 0.2) but with an important lag phase (120 h) compared with autoclaved crushed algae. In the latter condition, the polysaccharide extraction by heating likely allowed their immediate uptake. Bacterial growth was also detected with fresh *C. crispus* pieces with or without *Z. galactanivorans* inoculation meaning the growth was likely due to epiphytic communities resistant to the antibiotics. Hence, similar to *P. palmata*, *Z. galactanivorans* growth is favored by a higher accessibility of the polysaccharides.

By contrast, *Z. galactanivorans* grew with *G. turuturu* either with crushed algae ($OD_{600} \approx 0.35$) or fresh algae pieces ($OD_{600} \approx 0.5$) while no growth was detected in the non-inoculated controls. It is worth noting that final OD was higher with fresh algae. Crushed algae underwent high temperatures (50 °C overnight and 121 °C for 15 min when autoclaved) that might have destroyed compounds potentially used by *Z. galactanivorans* such as vitamins or proteins for example. The bacterial growth on fresh algae could also be partly due to opportunist epiphytic communities that would grow only in the presence of *Z. galactanivorans* by benefiting from the released degradation products due to the action of *Z. galactanivorans*. Such interaction phenomenon would not occur on autoclaved crushed algae as the tissues were sterilized, it would explain the lower final OD reached with those tissues. Also, it seems that we can distinguish two growth phases with non-autoclaved algae: a first phase that exhibit a low growth rate (until 90 h for crushed algae and 160 h for fresh algae) followed by second phase with a higher growth rate. Consistent with the theory of pioneer/opportunist interactions, the first phase could be due to the growth of *Z. galactanivorans* that might favor the later growth of opportunist epiphytic bacteria (it should be noted that these potential opportunists cannot use maltose according to **Figure V.7A**). The two distinct phases can also result in the successive utilization of different compounds by *Z. galactanivorans* (a preliminary degradation of specific compounds that would allow the access to other substrates).

Overall, *Z. galactanivorans* is able to use fresh pieces of *G. turuturu* thallus but not *C. crispus* or *P. palmata*. *C. crispus* is a carrageenophyte algae (Kopp and Perez, 1961), *P. palmata* thallus contains mix-linked xylans (Morgan *et al.*, 1980; Lahaye *et al.*, 1993) and *G. turuturu* is composed of hybrid agar-carrageenans (kappa/iota) polymers (Denis *et al.*, 2009; Cardoso *et al.*, 2019). According to the literature, *G. turuturu* would not possess a proteic cuticle unlike the other two, but its surface is rather covered by a thick mucilage coat (10–12 µm thick), such as kelp (Craigie *et al.*, 1992; Deniaud *et al.*, 2003; Cecere *et al.*, 2011). Hence these experiments would confirm our hypothesis claiming that polysaccharides might be hardly accessible within the thallus of some red macroalgae, potentially due their proteic cuticle. By contrast, the carrageenan mucilage coat of *G. turuturu* might represent an external carbon source easily accessible that might favor rapid cell multiplication and biofilm formation and hence facilitate the attack and degradation of the ECM. Integrative study could then be carried out during the growth of *G. turuturu* to decipher and compare the degradation mechanisms involved in red algae degradation to the results obtained with brown algae (Part 1).

Chapter VI:

Preliminary characterization of a PUL involved in FCSP degradation

Résumé du chapitre

Dans le chapitre précédent, l'analyse du transcriptome complet de *Z. galactanivorans* Dsij^T au cours de la dégradation d'algues fraîches a révélé l'induction de plusieurs PUL non caractérisés par rapport à la condition contrôle. C'est le cas de la région génomique comprise entre les gènes *zgal_3440* et *zgal_3455* qui code notamment des fucosidases et des sulfatases et qui est ainsi prédite pour cibler des FCSP. En particulier, le gène *zgal_3452*, codant une polysaccharide lyase qui n'appartient à aucune famille de PL actuellement répertoriée (PLnc), est fortement induit en présence de macroalgues et pourrait représenter un déterminant génétique clé dans la dégradation de macroalgues fraîches.

Au cours de ce chapitre l'enzyme ZGAL_3452 a été surexprimée de manière recombinante et purifiée afin de rechercher son substrat préférentiel. Une activité enzymatique a été mise en évidence en présence de pectine de pomme et de FCSP provenant de l'algue *Cladosiphon okamuranus* (qui a la particularité de contenir un pourcentage significatif d'acide galacturonique). Au vu de la difficulté à détecter des produits de dégradation à l'aide de diverses méthodes analytiques et suite à des analyses bio-informatiques, nous avons émis l'hypothèse que cette lyase serait plus efficace sur des oligosaccharides libérés suite à la dégradation préalable du polymère par d'autres enzymes. Un PUL putatif contenant ZGAL_3452 a ainsi été identifié et 12 enzymes d'intérêt ont été surexprimées et purifiées en petit volume afin de tester leur activité sur un large panel de FCSP. Ces expériences ont permis de révéler l'action successive d'une PL40 (ZGAL_3449) et d'une GH88 (ZGAL_3445) sur des FCSP de *Laminaria digitata*. La PL40 initierait la dépolymérisation du polysaccharide et libèrerait notamment un di- ou trisaccharide, tandis que la GH88 (ZGAL_3445) agirait de manière exolytique sur les oligosaccharides insaturés issue de l'action de la PL40 et libèrerait un monosaccharide insaturé. L'activité de la PLnc a pu être mise en évidence en présence de ZGAL_3449 et 3445 mais ce résultat n'a pas toujours été confirmé et requiert des analyses plus poussées. Nos diverses analyses bio-informatiques et biochimiques nous portent à croire que ce PUL ciblerait des structures particulières de FCSP, riches en acide uroniques et se rapprochant certainement de certaines structures de pectine comme les rhamnogalacturonan-II.

C'est la première fois chez *Z. galactanivorans* Dsij^T qu'une activité fucanolytique est expérimentalement démontrée, en ce sens, ce chapitre constitue un premier travail préliminaire dans la caractérisation d'un PUL ciblant des FCSP chez cet organisme modèle.

J'ai effectué l'ensemble des expérimentations et analyses de ce chapitre, à l'exception des clonages et transformations réalisés par Robert Larocque, des manipulations sur la colonne HPSEC effectuées par Diane Jouanneau et des analyses de spectrométrie de masse réalisées par la plateforme BIBS.

I. Introduction

Fucose-Containing Sulfated Polysaccharides (FCSPs) are complex brown algal ECM polysaccharides and are still poorly characterized. They encompass polysaccharides with backbone structures exclusively based on fucopyranosyl residues (fucans) and those based on a variety of other glycosyl residues (fucoidans). Previous analytical studies revealed that, in addition to their high content in fucose, FCSPs they also contain small amounts of various other monosaccharides such as glucose, galactose, xylose, mannose, rhamnose and/or uronic acids and various substituents like sulfate or acetyl groups (Jiao *et al.*, 2011; Ale and Meyer, 2013; Deniaud-Bouët *et al.*, 2017). Also, these structural data reported important variations depending on species, season, location, tissue aging, etc. Based on this structural diversity and complexity, it is considered that there is no basic FCSPs structure and that the structure and composition of FCSPs cannot be predicted with certainty for any algal individual (Ale and Meyer, 2013). It should also be kept in mind that FCSPs composition might differ depending on the extraction method used and any comparison between different studies should be done carefully (Sichert *et al.*, 2021).

Consequently, the enzymatic machinery involved in the catabolism of FCSPs is still poorly understood. Only a few studies focusing on the isolation and characterization of FCSP-modifying enzymes from marine bacteria and molluscs have been performed. Enzymes specifically involved in FCSPs degradation are called fucoidanases and are reviewed in (Kusaykin *et al.*, 2015). They include exo-fucoidanases (also found as α-L-fucosidases), which cleave fucose molecules from the nonreducing end of FCSPs, and endo-fucoidanases which cleave the glycoside bonds within the FCSPs chain. Three exo-fucoidanases from *Vibrio* sp. N-5 (Furukawa *et al.*, 1992) and several bacterial endo-fucoidanases from "*Fucobacter marina*" SA-0082^{T} (Sakai, Kimura, and Kato, 2003), [*Alteromonas*] sp. SN-1009 (Sakai *et al.*, 2004; Zhu *et al.*, 2021), *Mariniflexile fucanivorans* SW5^{T} (Colin *et al.*, 2006), *Formosa algae* F89^{T} (Silchenko *et al.*, 2014, 2017; Silchenko, Rasin, Kusaykin, *et al.*, 2018), *Psychromonas* sp. (Vickers *et al.*, 2018), *Wenyingzhuangia fucanilytica* CZ1127^{T} (Shen *et al.*, 2020; Zueva *et al.*, 2020) and *Formosa haliotis* LMG 28520^{T} (Vuillemin *et al.*, 2020) have been characterized and display different substrate specificity. Most of the identified fucoidanases are glycoside hydrolases (GHs), however, a FCSP lyase cleaving FCSPs from the brown alga *Kjellmaniella crassifolia* was discovered by (Sakai, Kimura, Kojima, *et al.*, 2003). Until recently, all the characterized GHs were endo-α-1,4-L-fucanase and belonged to the CAZy family GH107 (CAZy database, http://www.cazy.org, Lombard *et al.*, 2014), but the family GH168 was created after Shen *et al.*, 2020 who reported the endo-α-1,3-L-fucanase FunA from *Wenyingzhuangia fucanilytica* CZ1127^{T}. In addition, sulfatases and deacetylases from marine bacteria, which remove substituents but are not responsible for decreasing the molecular weight of FCSPs, were isolated. Two sulfatases which belong to the families S1_17 and S1_25 (SulfAtlas database, http://abims.sb-roscoff.fr/sulfatlas/, Barbeyron *et al.*, 2016) and catalyze the cleavage of sulfate groups on fucose in FCSPs were functionally characterized by Silchenko, Rasin, Zueva, *et al.*,

2018, as well as a fucoidan deacetylase (family CE7) removing the acetyl group in FCSPs from *Cladosiphon okamuranus* (Nagao *et al.*, 2017). These studies also demonstrated that multiple enzymes, including CAZymes and sulfatases, are successively involved in FCSPs degradation (Nagao *et al.*, 2017; Silchenko, Rasin, Zueva, *et al.*, 2018; Sichert *et al.*, 2020).

The activity of FCSP-hydrolyzing enzymes is not easily evidenced as the quantitative and high-throughput reducing sugars assays method appears to be ineffective with FCSPs (Colin *et al.*, 2006), as well as the colorimetric method tested by (Nelson, 1944). To date, even if it only allows qualitative analyses, the most effective way to screen for FCSPs hydrolysis is to analyze the degradation products by electrophoresis in polyacrylamide gel. The oligosaccharides can be either labeled with a fluorophore (FACE) or detected with alcian blue and silver nitrate (C-PAGE, only for charged sugars).

The analysis of the *Z. galactanivorans* Dsij^T transcriptome during fresh macroalgae degradation (Chapter V) revealed that several genes were highly expressed compared to maltose but also to purified algal polysaccharides (**Figure VI.1**). In particular, the genomic region between *zgal_3440* and *zgal_3455* was strongly triggered. It corresponds to the putative PUL34 and the beginning of PUL35 annotated in Barbeyron, Thomas, *et al.*, 2016, two PULs predicted to target FCSPs as they contain many fucosidases and sulfatases. This cluster of genes might then contain promising enzymatic tools to degrade FCSPs in fresh algae. The genes *zgal_3441* (SusC-like TBDR), *zgal_3445* (unsaturated glucuronyl hydrolase GH88) and *zgal_3452* (PL) were especially overexpressed in the presence of *Laminaria digitata*, *Fucus serratus* and *Ascophyllum nodosum*.

The gene *zgal_3452* encodes a polysaccharide lyase that does not belong to any known CAZy family (PLnc). To date, no fucoidanase, and more generally no FCSPs-modifying enzyme, was identified and characterized in *Z. galactanivorans* Dsij^T. As this PL is a promising candidate as a FCSPs-degrading enzyme, the recombinant enzyme was expressed and purified to unravel its potential role in FCSPs degradation. More globally we also tried to delimitate the PUL containing this enzyme and we investigated FCSPs processing by the 12 enzymes of the identified putative PUL.

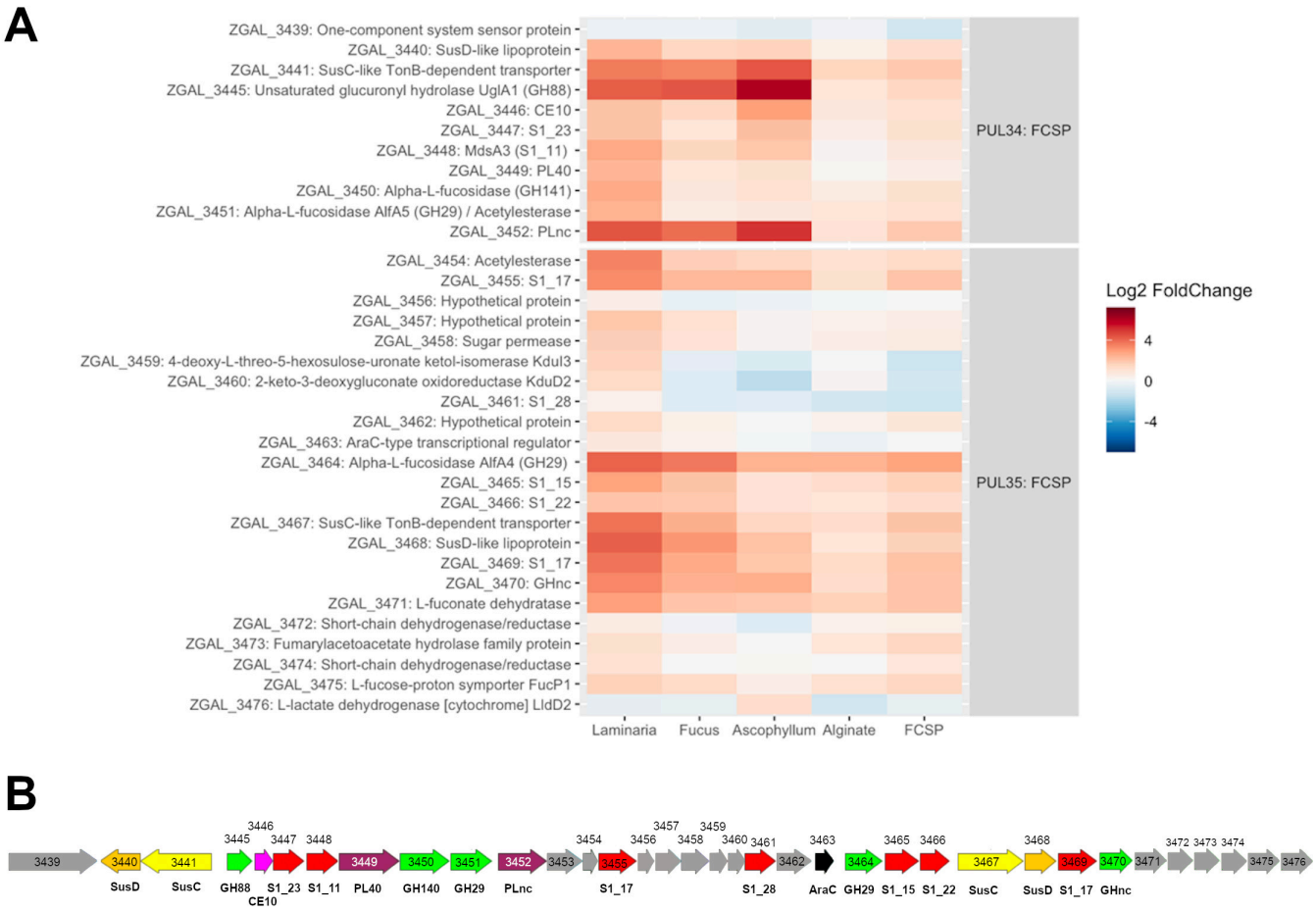

Figure VI.1: Induction by fresh macroalgae of a gene cluster dedicated to FCSP utilization in *Z. galactanivorans* Dsij^T. (A) The heatmap represents the log2FC (complex carbon source vs. maltose) of individual genes contained in the PULs 34 and 35 predicted to degrade FCSPs. Modified from Figure V.3B. (B) Cartography of the genomic region represented in the heatmap. Genes are colored depending on their putative function. Green: GH; Burgundy: PL; Pink: CE; Red: Sulfatases; Yellow: SusC-like TBDT; Orange: SusD-like; Black: AraC transcriptional regulator; Grey: Others. CAZy and Sulfatase family are indicated as well as the SusCD-like proteins and the AraC transcriptional regulator.

II. Methods

1. Bioinformatic analyses

Z. galactanivorans Dsij^T transcripts obtained during the growth on *L. digitata* and maltose (see Chapter V) were mapped on the reference genome of the strain using Bowtie2 (Langmead and Salzberg, 2012) with the Galaxy platform (https://galaxy.sb-roscoff.fr). Transcripts visualization and quantification was done using the Integrative Genomic Viewer (IGV) software (v2.8.0). Base pair coverage was quantified between the genes *zgal_3439* and *zgal_3469*.

To identify putative promoters, the consensus sequence "TTG/TAnnTTTG" (-7 and -33 motifs with a spacer of 17-23 bp) conserved in *Flavobacterium* spp. strains (Chen *et al.*, 2007) was searched using the MiscroScope platform (https://mage.genoscope.cns.fr). Putative rho–independent transcription

terminators were identified with the ARNold server (http://rssf.i2bc.paris-saclay.fr/toolbox/arnold/) following the rules described in Georg *et al.*, 2009: the terminator must contain (1) at least 4 G-T or G-C pairs; (2) at most 2 nt spacer between stem and T-tail; (3) at least 3 'T' in the proximal part; (4) at most 1 'G' in the proximal part; (5) a 'T' in position 2 or 3 in the proximal part; (6) at most 3 purines or 3 cytosines in the distal part; (7) at least 4 'T''s in the tail; (8) no multiloop and at most 1 bulged nucleotide and (9) free energy of the stem-loop at most -8.0 kcal/mol. The proximal part corresponds to the first 5 bases of the tail and 4 following the distal part.

The localization of the proteins contained in the PUL of interest were predicted using SignalP (Nielsen *et al.*, 1997), TMHMM (Krogh *et al.*, 2001), LipoP (Juncker *et al.*, 2003) and PSORT-B (Gardy *et al.*, 2003).

2. Expression of the recombinant proteins

The cloning of the coding region of the 13 different target modules (without signal peptide when present) into the expression vector pFO4 (fusion His-tag) and plasmid transformation in *Escherichia coli* BL21 (DE3) expression strain was previously done by the Marine Glycobiology group (**Table VI.1**), following the protocol described in Groisillier *et al.*, 2010.

Table VI.1: Characteristics of the cloned genes used in this study. Except for *zgal_3445* that was cloned by Thomas *et al.*, 2012, cloning and plasmid transformations were performed beforehand by Robert Larocque. *zgal_3451* encodes two different modules that were expressed separately, an acetylesterase at the C-terminal domain (CTD) and a fucosidase at the N-terminal domain (NTD). Molecular weights and extinction coefficients were retrieved from the bioinformatics resource portal ExPASy (ProtParam tool).

Gene ID	Plasmid ID	Functional annotation	Molecular weight (kDa)	Molar extinction coefficient ($M^{-1}cm^{-1}$)
zgal_3445	-	Unsaturated glucuronyl hydrolase UglA1 (GH88)	45.4	79550
zgal_3446	pZG305	Carbohydrate esterase (CE10)	29.7	21890
zgal_3447	pZG37	Sulfatase (S1_23)	52.5	65110
zgal_3448	pZG38	Sulfatase (S1_11)	56.3	109460
zgal_3449	pZG306	Unknown function	103.8	142560
zgal_3450	pZG139	α-L-fucosidase (GH141)	86.7	133855
zgal_3451 CTD	pZG309	Acetylesterase (CE3/CE12?)	22.9	29910
zgal_3451 NTD	pZG308	α-L-fucosidase Alf5 (GH29)	48.6	108080
zgal_3452	pZG140	PLnc	85.0	148880
zgal_3453	pZG310	Possible pyridine nucleotide-disulphide oxidoreductase	60.1	87335
zgal_3454	pZG311	Acetylesterase (CE3/CE12?)	24.4	18910
zgal_3455	pZG39	Sulfatase (S1_17)	65.9	121950
zgal_3461	pZG40	Sulfatase (S1_28)	53.6	61685

Glycerol stocks of the recombinant strains were swabbed on LB-agar petri dishes supplemented with ampicillin (100 µg.ml^{-1}) and resistant colonies precultured in 5 ml of LB-Ampicillin medium at 37 °C overnight. Expression of the recombinant proteins was performed in the autoinducible ZYP-5052 medium (Studier, 2005) containing ampicillin (100 µg.ml^{-1}) for 72 h under agitation at 20 °C. After centrifugation, cell pellets were stored at -20 °C until purification. All proteins were expressed in small volume by inoculating 5 ml of ZYP medium with, 5 µl of the preculture. The recombinant protein ZGAL_3452 was also expressed in 1 l of ZYP medium (inoculum 1/200) for large-scale purification. The 1 l ZYP culture was divided in 4 x 250 ml volumes and centrifuged at 18 000 rpm for 20 min. Cell pellets were stored at -20 °C until further purification.

3. Enzyme purification

a. Small-scale purification of recombinant enzymes from the PUL

Cell pellets were resuspended on ice in lysis buffer (20 mM Tris-HCl pH 8, 500 mM NaCl, 1mM EDTA, 0.1 % Triton) supplemented with DNAse (10 U.µl^{-1}). Cell sonication was performed (6 x 10 sec with at least 1 min on ice between each repetition on an Ultrasonic Processor GE50 [setting 25, amplitude 55]) and lysis checked under the microscope. After centrifugation (14 000 rpm, 30 min, 4 °C), recombinant soluble proteins contained in the supernatant were purified on His SpinTrap mini-columns (GE Healthcare) following the manufacturer instructions. Briefly, proteins were loaded and washed on the column with a binding buffer (20 mM Tris-HCl pH 8, 500 mM NaCl, 10 mM imidazole) and eluted in 200 µl of an elution buffer (20 mM Tris-HCl pH 8, 500 mM NaCl, 1 M imidazole). Total, soluble and eluted fractions were analyzed by SDS-PAGE on 12 % (w/v) polyacrylamide gels, followed by staining with Coomassie blue. Imidazole was removed by ultrafiltration with a 10 kDa cut-off in 20 mM Tris-HCl pH 8, 500 mM NaCl. The concentration of each enzyme was assessed by measuring the absorbance at 280 nm with a Nanodrop and the enzymes were stored at 4 °C.

b. Large-scale purification of the recombinant enzyme ZGAL_3452

Three cell pellets (corresponding to 750 ml of culture) were each resuspended in 10 ml of lysis buffer (20 mM Tris-HCl pH 7.5, 500 mM NaCl, 20 mM imidazole, 5 U.µl^{-1}DNAse) containing 1 tablet of cOmplete™, EDTA-free Protease Inhibitor Cocktail (Merck) and pooled. Mechanical lysis was achieved by sonication (Branson Digital Sonifier SFX 250) at 40 % of the maximal power (5 x 5 sec with 1 min on ice between each repetition, this was done 4 times until cell lysis was evidenced under the microscope). The lysate was centrifuged (18 000 rpm, 60 min, 4 °C) and the supernatant filtered with 0.2 µm syringe filters before being loaded on a 5 ml HisTrap HP column charged with nickel (GE Healthcare). Proteins were eluted using a linear gradient of imidazole (20 mM – 1 M) in 100 ml at 5 ml.min^{-1}. Fractions showing the presence of the recombinant protein at the expected molecular weight by SDS-PAGE were pooled. Proteins were concentrated by ultrafiltration (4200 rpm) on 10 kDa PES

membranes (PALL) and purified on a size-exclusion chromatography column Superdex200, HiLoad 16/60 (GE Healthcare) at 1 ml.min^{-1} flow rate (25 mM Tris-HCl pH7.5, 200 mM NaCl). After SDS-PAGE analysis, the eluted fractions containing the protein of interest were pooled, concentrated as described above and the enzyme concentration was measured using Nanodrop. Dynamic light scattering measurements were done on 30 µl of purified and concentrated protein solutions with a ZetaSizer Nano instrument (Malvern).

4. Enzymatic activity assays

a. Substrates tested

The different commercial purified polysaccharides (commercially available) and home-made ECM extracts (alcohol-insoluble residues, AIRs) used for enzyme characterization are listed below in **Table VI.2**. They were solubilized in 50 mM Tris-HCl pH 8 at a final concentration of 2 g.l^{-1} unless stated otherwise. FCSPs were ultrafiltrated on 10 kDa Amicon Ultra cellulose membrane (Merck - Millipore) to remove small oligosaccharides initially present in the commercial products.

Table VI.2: Overview of the different substrates used in this study. AIRs and FCSPs from *Pelvetia canaliculata* were previously extracted by Kévin Hardouin and Jasna Nikolic respectively. FCSPs extracted from other brown algae were ordered from the same supplier as in Sichert et al., 2021, who analyzed monosaccharides content after ion-exchange purification (to remove contaminants from cross-linked compounds).

Type	Organism	Supplier	Main type of uronic acids
Alginate	mainly *Laminaria digitata*	Danisco	Mannuronic (ManA) & Guluronic (GulA)
AIR	*Pelvetia canaliculata*	Home-made	unknown
FCSP	*Chorda filum*	Elicityl	unknown
FCSP	*Cladosiphon okamuranus*	Carbosynth	Glucuronic (GlcA) & Galacturonic (GalA) (Sichert *et al.*, 2021)
FCSP	*Durvillaea potatorum*	Carbosynth	Glucuronic (Sichert *et al.*, 2021)
FCSP	*Ecklonia maxima*	Carbosynth	Glucuronic (Sichert *et al.*, 2021)
FCSP	*Fucus serratus*	Carbosynth	Glucuronic (Sichert *et al.*, 2021)
FCSP	*Fucus vesiculosus*	Carbosynth	Glucuronic (Sichert *et al.*, 2021)
FCSP	*Laminaria digitata*	Carbosynth	unknown
FCSP	*Laminaria japonica*	Carbosynth	unknown
FCSP	*Lessonia nigrescens*	Carbosynth	unknown
FCSP	*Macrocystis pyrifera*	Carbosynth	Glucuronic (Sichert *et al.*, 2021)
FCSP	*Pelvetia canaliculata*	Home-made	unknown
FCSP	*Undaria pinnatifida*	Elicityl	Glucuronic (Sichert *et al.*, 2021)
Heparin	Porcine intestinal mucosa	Sigma	Iduronic (IdoA) & Glucuronic
Pectin	Apple	Sigma	Galacturonic
Pectin	Citrus	Sigma	Galacturonic
Ulvan	*Ulva armoricana*	Elicityl	Iduronic & Glucuronic

b. Unsaturated uronic acid assays

Polysaccharide lyases cleave uronic acid-containing polysaccharides via a β-elimination mechanism, resulting in unsaturated oligomeric products having a double bond in the non-reducing end residue, which absorbs in UV. The lyase activity was then followed in real-time by measuring the increase in absorbance at 235 nm (Spark Tecan) every 30 sec during 20 min (unless stated otherwise). Each measurement was done in 200 µl, either in duplicate or in triplicate.

c. C-PAGE analysis

Carbohydrate-PolyAcrylamide Gel Electrophoresis (C-PAGE) was performed to qualitatively analyze polysaccharide degradation (Zablackis and Perez, 1990). This technique separates oligo-saccharides according to their size and charge. Five microliters of the enzymatic reaction were added to 15 µl of 10 % sucrose with 0.01% phenol red and 5 µl of this mix were loaded on a 0.75 mm thick polyacrylamide gel composed of a 6 % stacking gel and a 30 % running gel in 50 mM Tris pH 8.7, 1 mM EDTA. Migration was achieved in 50 mM Tris-HCl, 1 mM EDTA (pH 8.7) for 1 h at 200 V and coloration in 5 $mg.ml^{-1}$ of alcian blue for 10 min. After 2 h discoloration in milliQ-water, the gel was soaked in 0.4 % silver nitrate (10 min) and rinsed 3 times with milliQ-water. Oligosaccharides were revealed using a solution of 70 $mg.ml^{-1}$ sodium carbonate with 1.6 $mg.ml^{-1}$ formaldehyde. The reaction was stopped by the addition of 17.5 M acetic acid.

d. FACE analysis

Fluorophore-Assisted Carbohydrate Electrophoresis (FACE) is another electrophoresis technique to investigate the products of hydrolysis (Jackson, 1996). Degradation products (approximatively 50 µg of material) were dried in a speed-vacuum centrifuge and dissolved in 2 µl of 0.1 M AMAC (2-aminoacridonein) in acetic acid:DMSO (3:17; v/v) and 2 µl of 1 M $NaBH_3CN$ in DMSO for at least 4 h at 37 °C. The AMAC-labeled saccharides were dried under vacuum for 1 h, resuspended in 20 µl of 25 % glycerol and 5 µl were loaded on polyacrylamide gel (6 % stacking gel in 1.5 M Tris/Glycine pH 8.8 and 30 % running gel in 0.5 M Tris/Glycine pH 6.8). Migration was performed at 4 °C in 25 mM Tris-HCl pH 8.5, 192 mM glycine for 2 h at 200 V. Oligosaccharides were visualized under UV with a transilluminator. FACE is a more sensitive approach than C-PAGE and allows the detection of mono- and di-saccharides, while the resistant polysaccharide fraction is not visible as AMAC binds to the reducing ends of the oligosaccharides.

e. TLC

Thin Layer Chromatography (TLC) is a suitable method to detect small oligosaccharides. Two microliters of reaction mixture were spotted on silica gel-60 TLC aluminum plates (Merck). Migration was performed in acetic acid/ethyl acetate/water (25:31:22; v/v/v) for 50 min. The oligosaccharides

were visualized by immersing plates in 0.2 % napthoresorcinol/10 % sulfuric acid (1:2; v/v) in ethanol, followed by heating on a hot-plate for 10 min.

f. HPSEC

High Pressure Size Exclusion Chromatography (HPSEC) was also conducted to detect oligosaccharides. Filtered samples (100 µl, 0.22 µm) were injected on analytical Superdex 200 Increase and Superdex 30 Increase (Cytiva) columns connected in series. The elution was conducted in 0.1 M $LiNO_3$ using an isocratic Thermo Ultimate 3000 pump working at a flow rate of 0.5 $mg.ml^{-1}$. The chromatography experiments were monitored using a Wyatt Optilab Rex refractive index detector. Chromeleon software (Thermo) was used for data acquisition.

g. Mass spectrometry

Incubations performed in 50 mM ammonium bicarbonate pH 7 were sent for MALDI-MS and ESI-MS analyses at the BIBS platform (INRAE, UR 1268) to try to characterize the nature of the degradation products.

III. Results & Discussion

1. Purification of the polysaccharide lyase ZGAL_3452

The predicted product of the *zgal_3452* gene is a protein of 768 amino acids, with a theoretical molecular mass of 85 kDa. It is annotated as polysaccharide lyase which does not belong to any known CAZy family. The recombinant protein ZGAL_3452 was successfully expressed by *E. coli* BL21 (DE3) in ZYP medium and purified by nickel affinity chromatography followed by size-exclusion chromatography. The chromatogram obtained after the size-exclusion step is shown in **Figure VI.2A**. Three peaks were detected and their apparent molecular mass, calculated using the calibration of the column, was approximately of 944, 398 and 115 kDa. SDS-PAGE analysis indicated that under denaturing conditions, only one protein was detected in the fractions corresponding to the last two peaks (**Figure VI.2B**). Its apparent molecular mass was around 80-90 kDa, in line with the expected theoretical mass of 85 kDa. Therefore, the second and third peaks might contain ZGAL_3452 under its tetrameric and dimeric form, respectively. The fractions 31 to 38, corresponding to the second peak, were pooled together (form A, tetramer) as well as the fractions 39 to 47 corresponding to the third peak (form B, dimer). The first peak (fractions 25 to 30) does not contain the protein of interest and might be the result of protein aggregates. Dynamic light scattering measurements were only performed for the form B as a precipitate formed for the form A which might not be stable. The size distribution analysis indicates that the form B is monodisperse in solution, as one peak representing 99.9 % of the sample mass is observed

(**Figure VI.2C**). The estimated molecular weight was 240 ± 39 kDa, which also suggests that the form B corresponds to the dimeric form of ZGAL_3452.

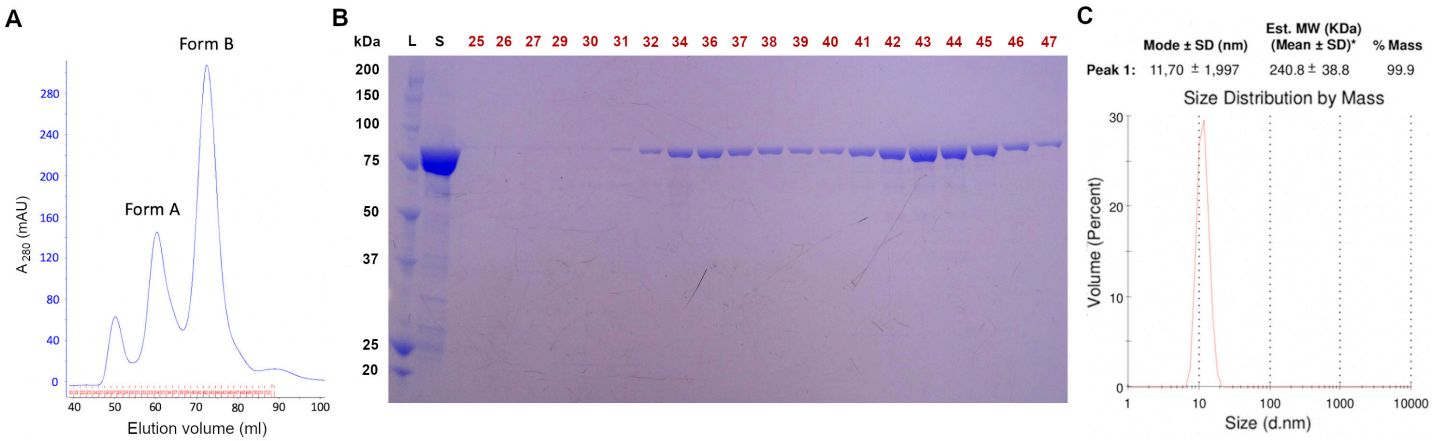

Figure VI.2: Purification of the recombinant protein ZGAL_3452. (A) Elution profile from the size-exclusion chromatography. (B) SDS-PAGE analysis of the different eluted fractions (red numbers). L: molecular-weight size ladder. S: total soluble protein after the affinity purification. (C) Dynamic light scattering analysis of the dimeric form.

2. Screening for a natural substrate cleaved by ZGAL_3452

In order to assess the ability of the polysaccharide lyase ZGAL_3452 to cleave uronic acid-containing polysaccharides, its activity was first tested with 6 substrates containing diverse type of uronic acids (**Table VI.2**). Reactions were conducted with 17.5 µg of form A or 7.5 µg of form B added to 0.4 mg of substrate with 2 mM $CaCl_2$ and monitored by measuring the increase in absorbance at 235 nm (A235) over time (**Figure VI.3A**). AIRs are total extracts of the algal ECM and were used as a substrate as they include a mixture of the different carbohydrates produced by the algae. AIRs from the algae *Pelvetia canaliculata* were chosen due to the high FCSP content in this species (Ale and Meyer, 2013). No increase in A_{235} was detected in any condition after 20 min of monitoring (data not shown). Consequently, one measure per day was conducted during 4 days. **Figure VI.3A** displays the activity measured after 3 days of incubation. The highest activity (170.7 U per mg of enzyme) was detected after 3 days for the form B incubated with apple pectin. For all substrates, the measured activity was 2-10 fold higher with form B than form A. All reaction mixtures were analyzed on C-PAGE. Low-molecular weight (LMW) oligosaccharides were only visible on the gel when form B was incubated with pectin, with a decrease of the high-molecular weight (HMW) size fraction. (**Figure VI.3B**). No oligosaccharides were detected in the negative control lanes, when the enzyme was either denatured by heat (lane 2) or replaced by buffer (lane 3).

A

	Heparin	Pectin	Ulvan	Alginate	FCSP	AIR
Form A	0	17.7	3.2	2.3	32.7	10.1
Form B	7.6	170.7	54.5	29.8	60.6	58.0

B

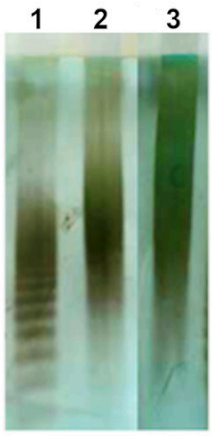

Figure VI.3: ZGAL_3452 activity on uronic acids-containing polysaccharides. (A) Activity ($\Delta A_{235}.mg^{-1}$ of enzyme) after 3 days of incubation measured with unsaturated uronic acid assays. Reaction were carried out in 50 mM Tris-HCl pH 7.5 at 22 °C. For each condition, the value at the initial time was subtracted from the value after 3 days. The value obtained with the denatured enzyme was then subtracted from the value obtained with active enzyme. (B) C-PAGE analysis of the pectin degradation product resulting from the action of the dimeric form B. 1: Active enzyme. 2: Boiled enzyme. 3: No enzyme.

Pectin consists essentially of α-(1-4)-linked D-galacturonic acid residues. The activity of ZGAL_3452 was evidence on pectin with two different methods, by measuring the increase of unsaturated ends and by C-PAGE. However, the action of the PL was not immediate as degradation was visible after 3 days of incubation. The experimental conditions, such as pH, temperature or NaCl concentration might not have been optimal for this enzyme. It is also likely that apple pectin is not the natural substrate of ZGAL_3452, explaining the limited and slow activity. ZGAL_3452 might therefore cleave galacturonic acid (GalA) bound in more complex substrates with other residues which would improve the recognition of the cleavage site. Since *zgal_3452* is located near several genes encoding fucosidases and sulfatases, we hypothesized it was part of a gene cluster involved in FCSP degradation. Following this idea, we searched in the literature for FCSP extracts containing galacturonic acid residues. Sichert *et al.*, 2021 analyzed the composition of FCSPs from seven different brown algal species after ion-exchange purification and only detected GalA in FCSPs from *Cladosiphon okamuranus* (less than 10 % of the purified fraction). In another study, Nishide *et al.*, 1990 reported that FCSPs from different *Sargassum* species contained significant amount of GalA, up to 28 % in *Sargassum fusiformis* (formerly *Hizikia fusiformis*). With a different method, Hu *et al.*, 2014 also detected GalA in *S. fusiformis* FCSPs (6.5 %).

We further tested the activity of the dimer ZGAL_3452 (form B) on eleven FCSPs from different algal species, including *C. okamuranus*. We were unable to get FCSPs from *S. fusiformis*. The increase in A_{235} was monitored for 20 min and the highest activity was detected with *C. okamuranus* FCSPs (increase of 2.6 absorbance units per min and per mg of enzyme, while the increase is below 0.7 with the other algal species) (**Figure VI.4**). *C. okamuranus* FCSPs are mainly made of α-1,3-Fucose repeating units with additional α-1,2-GlcA (Sichert *et al.*, 2021) and were the only FCSPs known to

contain significant amount of GalA among the eleven tested. Hence, these results support the hypothesis that ZGAL_3452 would cleave GalA residues within FCSPs.

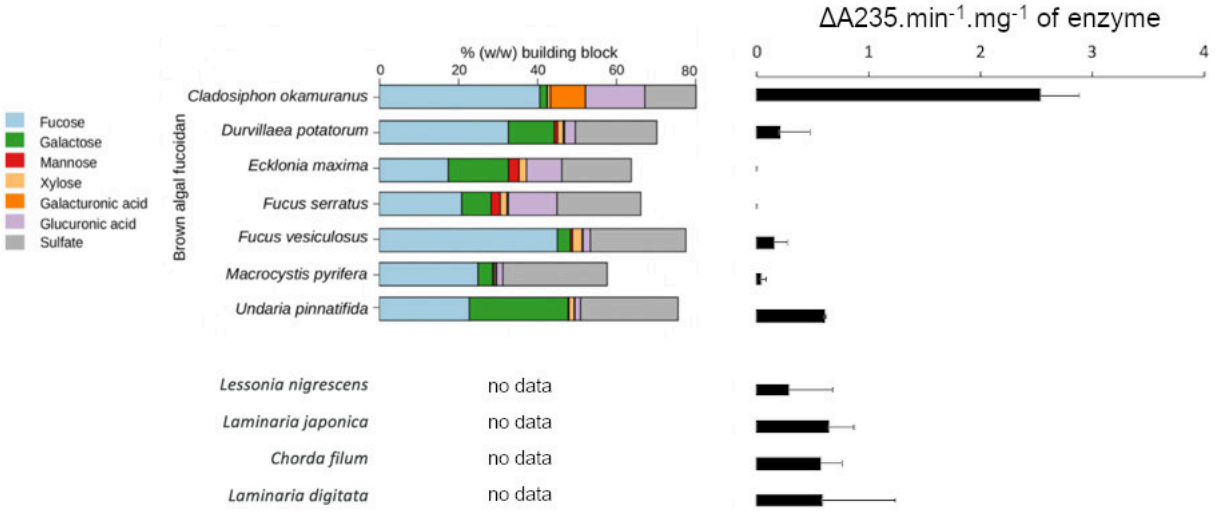

Figure VI.4: ZGAL_3452 activity on FCSPs from diverse macroalgae. 5 µl of dimeric enzyme at 1.8 mg.ml^{-1} was incubated with 195 µl of 0.2 % FCSPs in 50 mM Tris-HCl pH 7.5. Reactions were carried out with 2 mM $CaCl_2$ at 22 °C. The monosaccharides and sulfate content in the FCSPs analyzed in Sichert et al., 2021 is shown.

In order to improve the detection of the enzymatic activity, the optimal parameters were assessed. The effect of the tested enzymatic parameters was similar for both forms (**Figure VI.5**). ZGAL_3452 activity was assayed in Tris-HCl buffer between pH 7 and 9 and in MOPS buffer between pH 6 and 7.5. In both buffers, the maximum activity was obtained at pH 7, a value similar to optimum obtained for already characterized marine bacterial fucoidanases (Kusaykin *et al.*, 2015). The activity of ZGAL_3452 was also assayed at different temperatures ranging between 20 and 42 °C. The activity peaks at 25-30 °C and decreases after 30 °C. It was shown that the addition of NaCl in the reaction mix inhibits the activity of the lyase. Finally, the effect of divalent cations on the activity was investigated. The assays indicate that the addition of $CaCl_2$ or $MgCl_2$ enhanced the activity of the tetrameric form A (175 and 157 % of the activity without cation) but had no impact on the activity of the dimeric form B. The addition of $ZnCl_2$ inhibited the activity of both forms (only 30 % of activity remained).

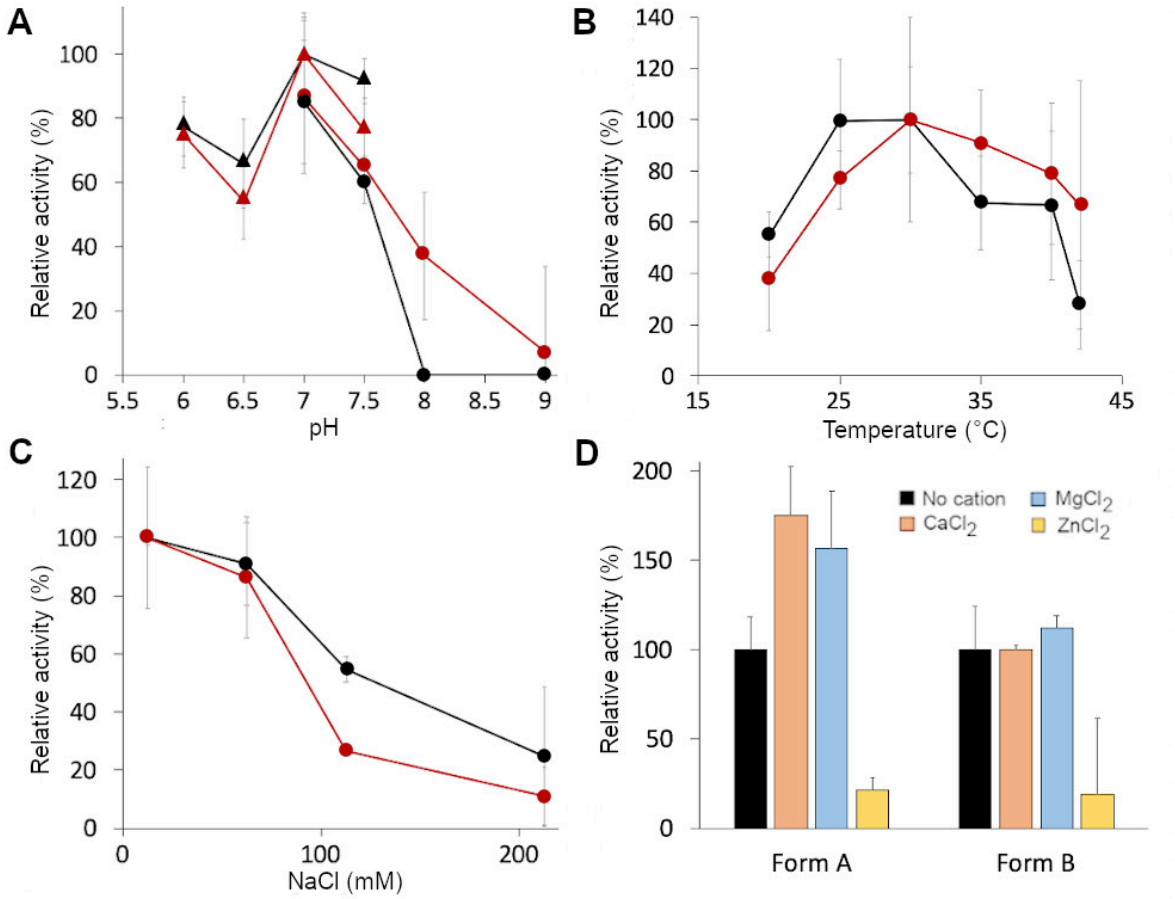

Figure VI.5: Effects of various buffer and pH values, incubation temperatures, NaCl concentrations and divalent cation addition on the activity of ZGAL_3452 under its dimeric (black) or tetrameric (red) form. (A) pH effect. Experiments were undertaken at 22 °C with no NaCl nor cation addition either in 50 mM Tris-HCl (round) or 50 mM MOPS (triangle) buffer. The activity in MOPS pH 7 buffer was considered as a reference for the maximum activity. (B) Temperature effect. Reactions were carried out in 50 mM Tris-HCl pH 7.5, no NaCl nor cation was added. The activity at 30 °C was set at 100 %. (C) Effect of NaCl concentration. Reactions were carried out in 50 mM Tris-HCl pH 7.5 at 22 °C, no cation was added. The activity at 12.5 mM (NaCl present only the enzyme buffer) was set at 100 %. (D) Effect of divalent cation addition. Reactions were carried out in 50 mM Tris-HCl pH 7.5 at 22 °C with either $CaCl_2$, $MgCl_2$ or $ZnCl_2$ addition (2 mM). The condition without cation was set at 100 %. All reactions were done in triplicate, 5 µl of enzyme at 1.8 $mg.ml^{-1}$ was incubated with 195 µl of 0.1 % FCSPs from *C. okamuranus*. For NaCl variations, 175 µl of substrate was used and 20 µl of NaCl at different concentrations.

Using the determined optimal conditions, A_{235} was followed for 2 h after the addition of ZGAL_3452. **Figure VI.6** shows that after an initial rise in absorbance during the first 20 min, A235 decreased to reach its initial value after 1 h. This profile is typical of exo-lyases as the released unsaturated monosaccharides are non-enzymatically and spontaneously converted to α-keto acids that does not absorb in UV (Preiss and Ashwell, 1963). The decrease in absorbance is not linear as a second peak is observed after a small decrease. This might be due to an equilibrium between the release of unsaturated monosaccharides and its spontaneous transformation in α-keto acids.

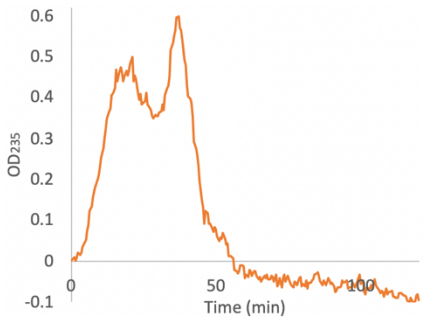

Figure VI.6: Two hours kinetic degradation of *C. okamuranus* FCSPs. A_{235} was measured at 25 °C in 50 mM Tris-HCl pH 7. Reactions were conducted with 5 µl of dimeric enzyme at 1.8 $mg.ml^{-1}$ added to 195 µl of 0.1 % FCSPs from *C. okamuranus*. The curve is duplicate mean.

As its incubation with *C. okamuranus* FCSP led to an increase in A_{235}, suggesting the release of oligosaccharides with an unsaturated uronic acid residue at the nonreducing-end, these experiments confirmed that ZGAL_3452 is a lyase and that is would act exolytically on the galacturonic acid residues present in FCSPs.

To characterize the degradation products, reactions were later analyzed by C-PAGE, FACE and TLC but no LMW oligosaccharides were observed in the presence of ZGAL_3452 (**Figure VI.7**).

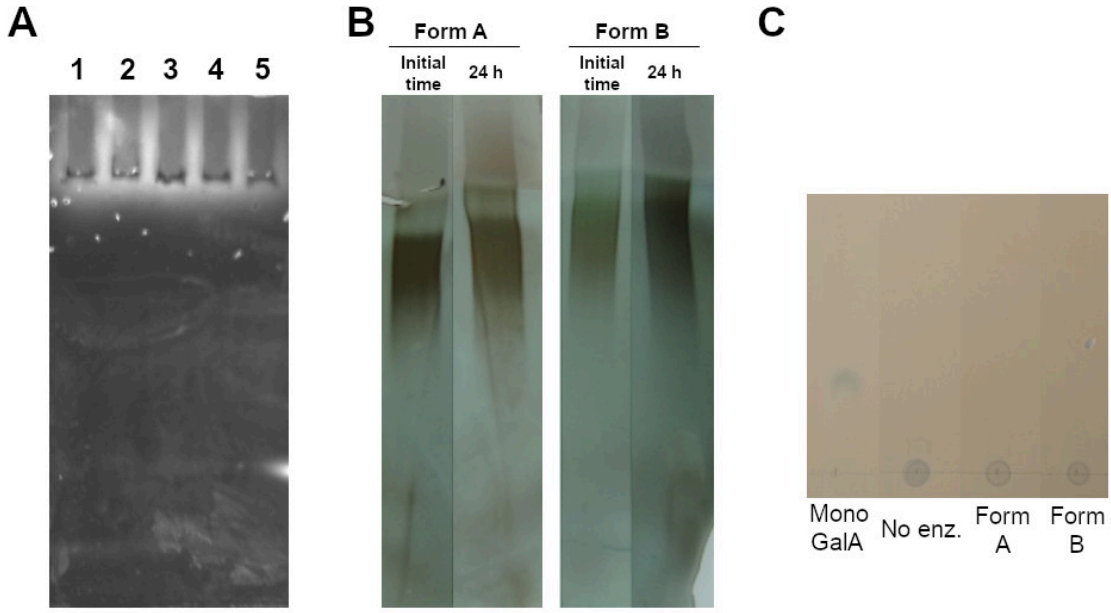

Figure VI.7: Activity of ZGAL_3452 on *C. okamuranus* FCSPs analyzed by FACE (A), C-PAGE (B) and TLC (C). Reactions were carried out overnight at 25 °C with 5 µl of enzyme at 1.8 $mg.ml^{-1}$ added to 195 µl of 0.2 % FCSPs in 50 mM Tris-HCl pH7.5. (A) 1: No enzyme; 2: Boiled form A; 3: Active form A; 4: Boiled form B; 5: Active form B. (C) 0.1 % galacturonic acid monosaccharide (Mono GalA) was analyzed on TLC as a size reference.

MALDI-MS analyses were also carried out but did not report any effect of the enzyme (data not shown). As GalA represents only a minor fraction of the FCSPs from *C. okamuranus* used in the assays, it is likely that the motifs recognized by the enzyme are scarce within the substrate and hence the released degradation products would not be concentrated enough to be detected.

FCSPs are complex substrates with various ramifications and substituents (mainly sulfate and acetyl groups). ZGAL_3452 might not be highly active on the intact polysaccharides but rather on substrates that have already undergone some enzymatic modifications. To test this hypothesis, several strategies were implemented to modify *C. okamuranus* FCSPs prior to incubation with ZGAL_3452. They were incubated with three recombinant fucoidanases from *Mariniflexile fucanivorans* SW5^T expressed and purified in the laboratory (Nikolic, unpublished results) and active on FCSPs from *P. canaliculata*. However, no degradation products were detected on C-PAGE and FACE with *C. okamuranus* FCSPs. The latter were also cleaved by acid hydrolysis and incubated with ZGAL_3452 but the pattern observed in C-PAGE and FACE was identical with or without the PL (data not shown).

The gene *zgal_3452* is located in the same locus with several sulfatases and fucosidases and then predicted to belong to a PUL specialized in FCSP degradation. Within a PUL, the genes are usually co-regulated and the encoded enzymes are specialized to depolymerize a particular type of polysaccharides (Ficko-Blean *et al.*, 2017; Ndeh *et al.*, 2017; Reisky *et al.*, 2019; McKee *et al.*, 2021). A pre-degradation of the FCSPs by other enzymes of the PUL, such as fucoidanases or sulfatases, might be necessary before the action of ZGAL_3452 as it might enhance the accessibility of the recognition site. Hence, to better understand the potential biological role of ZGAL_3452, we bioinformatically analyzed the genomic region around the gene *zgal_3452* to delimitate a putative PUL and to hypothesize on a degradation pathway. The enzymes of interest were purified and the activity of various enzyme cocktails was tested on several FCSPs to find a natural substrate targeted by the PUL. The implemented strategy is described in the following parts.

3. Bioinformatic analysis of the putative PUL containing *zgal_3452*

The genomic region between the genes *zgal_3439* and *zgal_3470* (corresponding approximately to PUL34 and 35 in Chapter V) was overexpressed when *Z. galactanivorans* was grown in presence of *Laminaria digitata* as carbon source compared to maltose. The number of transcripts mapping on the forward strand was quantified for each base pair of the region of interest for these two conditions (**Figure VI.8**). As PULs are clusters of co-regulated genes, the genome coverage is a reliable tool to hypothesize on the limits of this putative PUL.

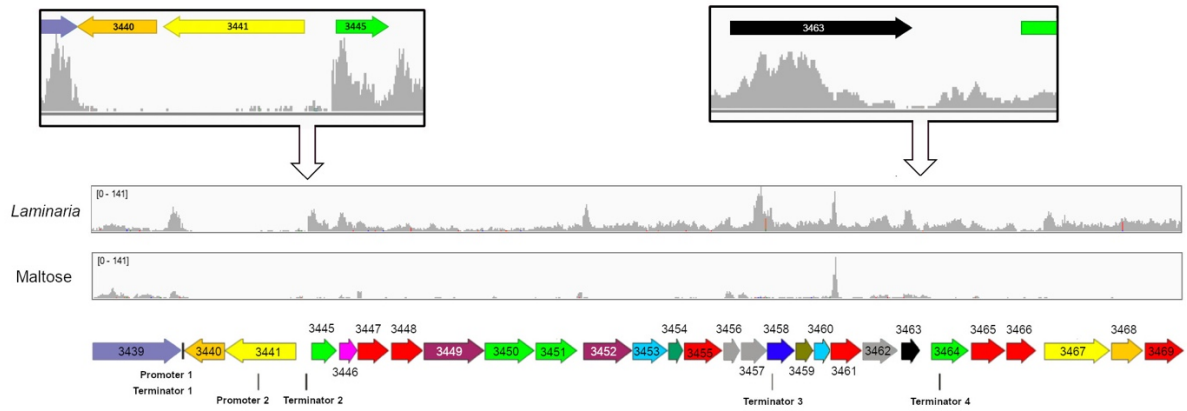

Figure VI.8: Base pair coverage by the transcripts of the genomic region of interest (*zgal_3439 - zgal_3469*) when *Z. galactanivorans* was grown on *Laminaria digitata* tissues or maltose. Genes are colored depending on their putative function. Green: GH; Burgundy: PL; Pink: CE; Red: Sulfatases; Dark Green: Acetylesterase; Yellow: SusC-like TBDT; Orange: SusD-like; Black: AraC transcriptional regulator; Brown: Isomerase; Light blue: Oxidoreductases; Dark blue: Permease; Violet: Sensor protein; Grey: Unknown function.

A sharp increase in transcript coverage was observed just upstream the gene *zgal_3445* when cells were grown with *L. digitata* tissues. Less obvious, a decrease in transcript abundance was observed between *zgal_3463* and *zgal_3464*. An increase in transcript coverage was also detected just upstream the pair susC-/susD-like (*zgal_3467*/*3468*) suggesting that it could be the beginning of another PUL. This analysis indicates that *zgal_3452* might be located in a PUL delimitated by [*zgal_3445 – zgal_3463*] or [*zgal_3445 – zgal_3466*].

Consensus promoter sequences and rho-independent terminators were searched in this genomic region to identify patterns that control the gene expression and to refine this analysis. Two sequences matching the consensus promoter and 4 putative terminators were found (**Table VI.3**). Promoter 1 was found on the reverse strand and would be likely related to another cluster. Promoter 2 was detected on the forward strand upstream *zgal_3445*, while terminators were identified between *zgal_3439* and *zgal_3440* (Terminator 1), upstream *zgal_3445* (Terminator 2), between *zgal_3457* and *zgal_3458* (Terminator 3) and between *zgal_3463* and *zgal_3464* (Terminator 4). These data therefore support the presumption that the genes *zgal_3445* and *zgal_3463* are the limits of the PUL.

Table VI.3: Sequence of the different putative promoters and rho-independent terminators. For promoters, the nucleotides corresponding to the consensus sequence are in bold.

Name	Sequence
Promoter 1	3’ **CAAAACTA**CAAAACAATTTTTCTACC**CAA** 5’
Promoter 2	5’ **TTG**CTTCGTGACTGAAAGTACTTA**TAGCTTTG** 3’
Terminator 1	5’ GGAAAGAAAAATCCTTCC 3’
Terminator 2	5’ GCAGCTGTACGGAAAGTACAGCTGC 3’
Terminator 3	5’ TACCCTTTTATGGATAGGGGTA 3’
Terminator 4	3’ TCGTGGTAACCAGCAAACACCACGA 5’

The putative subcellular localization of the enzymes of this delimited PUL is represented in **Figure VI.9**. ZGAL_3452 contains an uncleaved signal peptide and thus is predicted to be anchored in the cytoplasmic membrane, suggesting its inability to access and recognize complex HMW polysaccharides. Its action could then rely on the pre-degradation of the FCSPs by other enzymes such as GHs, esterases or sulfatases localized at the cell surface or secreted in the medium (Silchenko, Rasin, Zueva, *et al.*, 2018). Indeed, by contrast, the other CAZymes of the PUL, as well as 3 out of the 4 sulfatases and the oxidoreductase, possess a cleaved signal peptide and are then predicted as extracellular or periplasmic enzymes. ZGAL_3449 was recently assigned by the CAZy database as polysaccharide lyase from the family PL40. To date, the only described member in this family is an endo ulvan lyase from *Formosa agariphila* KMM 3901^T initiating ulvan depolymerization outside of the bacterial cell by cleaving between sulfated rhamnose and iduronic or glucuronic acid (P10_PLnc in Reisky *et al.*, 2019). ZGAL_3449 sequence only shares 24 % identity (e-value 2.10^{-36}) with this enzyme (blastp). ZGAL_3445 belongs to the family GH88 and is an unsaturated glucuronyl hydrolase (named UglA1). These enzymes are involved in the catabolism of unsaturated oligosaccharides produced by polysaccharide lyases (Itoh *et al.*, 2006). ZGAL_3450 and the N-terminal domain (NTD) of ZGAL_3451 are α-L-fucosidases predicted to belong to the family GH141 and GH29 respectively. Two enzymes were characterized in the GH141 family. The first one is an α-L-fucosidase from *Bacteroides thetaiotaomicron* VPI-5482 involved in the release of fucose that is substituted at O-3 with 2-O-methyl-α-d-xylose, it cleaves an α-1,4 linkage between a fucose and a rhamnose residue in rhamnogalacturonan-II (Ndeh *et al.*, 2017). The second one is an endoxylanase from *Clostridium thermocellum* (Heinze *et al.*, 2017). ZGAL_3450 is weakly related to both enzymes with 23 % (e-value 8.10^{-12}) and 22 % (e-value 1.10^{-10}) sequence identity respectively. The family GH29 contains 44 characterized enzymes all encompassing an exolytic α-L-fucosidase activity with a broad substrate specificity, including hydrolysis of fucose that is linked α-1–3/4/6 to N-acetylglucosamine (Lombard *et al.*, 2014). Three carbohydrate esterases are encountered in this putative PUL. ZGAL_3446 belongs to the family CE10, however this family has been removed from CAZy since most of its members appeared to be esterases active against non-carbohydrate substrates. The C-terminal domain (CTD) of ZGAL_3451 and ZGAL_3454 belong to the lipase-GDSL family which includes families CE3/CE12. CE3 consists of acetyl xylan esterase while CE12 members include pectin acetylesterases, rhamnogalacturonan acetylesterase and acetyl xylan esterase. Regarding the sulfatases, ZGAL_3447 and ZGAL_3461 belong to the subfamilies S1_23 and S1_28 respectively, which do not have any known activity according to the SulfAtlas database (Barbeyron, Brillet-Guéguen, *et al.*, 2016). ZGAL_3448 was classified in the S1_11 subfamily whose members exhibit N-acetylglucosamine-6-sulfatase and disulfoglucosamine-6-sulfatase activity, meaning they hydrolyze sulfate groups at the C6 position. They are then unlikely to act on fucose but rather desulfate other residues within FCSPs. ZGAL_3455 is predicted to be anchored in the cytoplasmic membrane and to belong to the subfamily S1_17 whose members are exo-fucose-2-sulfatases and endo-3,6-anhydro-D-galactose-2-sulfatases acting on fucose-oligosaccharides or α-

carrageenans respectively and then believed to specifically hydrolyze sulfate groups in C2. ZGAL_3459 and ZGAL_3460 are a 4-deoxy-L-threo-5-hexosulose-uronate ketol-isomerase (KduI3) and a 2-keto-3-deoxygluconate oxidoreductase (KduD2) respectively. They were predicted to be localized in the cytoplasm and to be involved in pectin-derived monosaccharides processing in pectinolytic microorganisms (Condemine *et al.*, 1986; Condemine and Robert-Baudouy, 1991). Their role in unsaturated galacturonate and glucuronate processing under osmotic stress conditions in *E. coli* was evidenced by Rothe *et al.*, 2013. A KduI is also involved in ulvan degradation by *F. agariphila* KMM 3901^T (Reisky *et al.*, 2019).

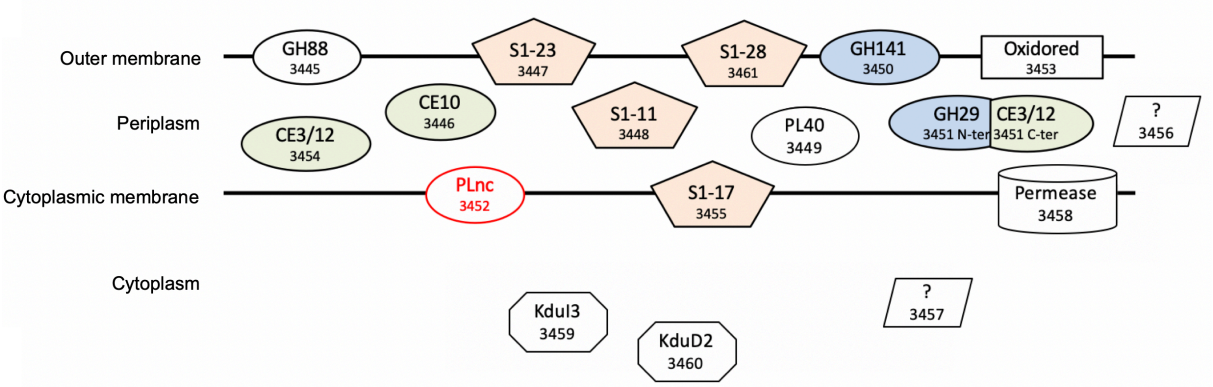

Figure VI.9: Schematic representation of the putative location of the enzymes composing the delimited PUL. CAZymes are represented by ovals, sulfatases by pentagons, permeases by cylinders, oxidoreductases by rectangles, enzymes for downstream processing of monomers by octagons and enzymes with unknown function by parallelograms. Sulfatases are colored in orange, fucosidases in blue and carbohydrates esterases in green. For CAZymes and sulfatases, the family number is indicated.

Given these bioinformatic predictions and our previous experiments on ZGAL_3452, the substrate targeted by this PUL might be FCSPs containing structures similar to pectin.

It is interesting to note that homologs of the endo-1,3-fucanase (GH168) from *Wenyingzhuangia fucanilytica* CZ1127 (Shen *et al.*, 2020) were found in 5 *Zobellia* species, *Z. laminariae* KMM 3676, the two *Z. roscoffensis* strains and the two *Z. nedashkovskayae* strains (between 48 and 52% sequence identity) and that those GH168 homologs are just adjacent to the homologs of the gene *zgal_3449*. Although it was not found in *Z. galactanivorans* Dsij^T, this observation would strengthen the hypothesis that the PUL is directed toward the degradation of FCSPs.

All the proteins displayed in **Figure VI.9** were further expressed heterologously in *E. coli* except for ZGAL_3459 and 3460, which are believed to act as downstream processing enzymes, ZGAL_3458, which is a sugar permease and then not involved in carbohydrate modification, as well as ZGAL_3456 and 3457, whose function is unknown, as no plasmid construction was performed for the corresponding genes. The N- and C-terminal domain of ZGAL_3451 were expressed separately. Sulfatases from the

family S1 require a post-traductional modification that might not occur when produced as recombinant enzymes. Therefore, the activity of the four recombinant sulfatases was previously tested in the laboratory by Tristan Barbeyron on the synthetic substrate 4-methylumbelliferyl sulfate which is fluorescent when cleaved by sulfatases. Only ZGAL_3461 appeared to be active on this substrate, which does not prevent however enzymatic activity on natural substrates.

4. Purification of the different enzymes encoded by the putative PUL

Twelve enzymes acting on carbohydrates encoded by genes within the putative PUL delimited above (*zgal_3445* - *zgal_3463*) were expressed in *E. coli* BL21(DE3) and purified on His SpinTrap columns (**Table VI.1**). Their expression was analyzed by SDS-PAGE (**Figure VI.10**).

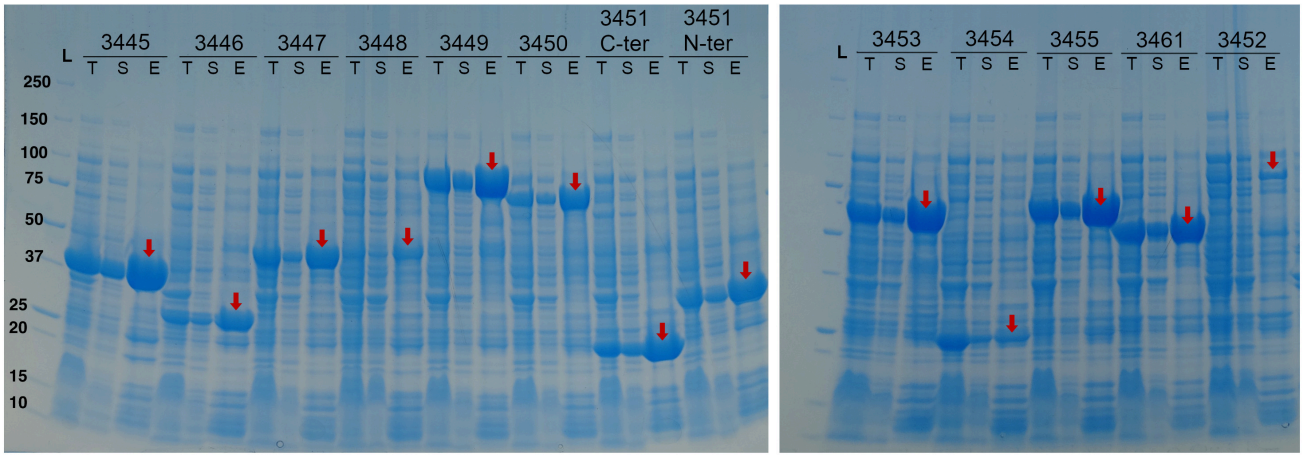

Figure VI.10: SDS-PAGE analyses of recombinant protein expression in *E. coli* BL21(DE3). Three fractions were analyzed for each enzyme: total (T), soluble (S) and eluted on His SpinTrap column (E). Proteins were expressed in ZYP5052 medium for 72h à 20 °C. Red arrows indicate the protein band at the expected size. L: molecular-weight size ladder.

A band at the expected molecular-weight was observed for each recombinant protein in the eluted fraction meaning that the proteins were successfully expressed. Except for the recombinant strains containing the genes *zgal_3448*, *zgal_3454* and *zgal_3452*, the expression levels were high. Other proteins are still present in the fractions eluted after purification but should not interfere in the following preliminary activity assays as it is unlikely that *E. coli* proteins act on specific algal polysaccharides. As no size exclusion chromatography was performed here, the dimeric and tetrameric forms of ZGAL_3452 were not separated for the activity assays.

5. Screening of the substrate targeted by the PUL

All 12 partially purified enzymes were pooled (0.1 $mg.ml^{-1}$ of each enzyme) and the protein cocktail was incubated overnight with 0.2 % FCSPSs from different macroalgae (listed in **Table VI.2**) and with apple and citrus pectin. The reaction products were analyzed by FACE and C-PAGE. No significant difference with the substrate alone was observed following the addition of enzymes for the different

substrates, except for *L. digitata* FCSPs. For the latter, two bands (**Figure VI.11A**, band 1 and 2 in lane 1) are visible on FACE gel after incubation with the cocktail, while these are absent from the substrate alone (lane 2) or with boiled inactivated enzymes (lane 3). However, this degradation profile is not detected on C-PAGE (**Figure VI.11B**) where all the lanes display the same pattern (a discoloration occurred on lane 1 due to a technical issue).

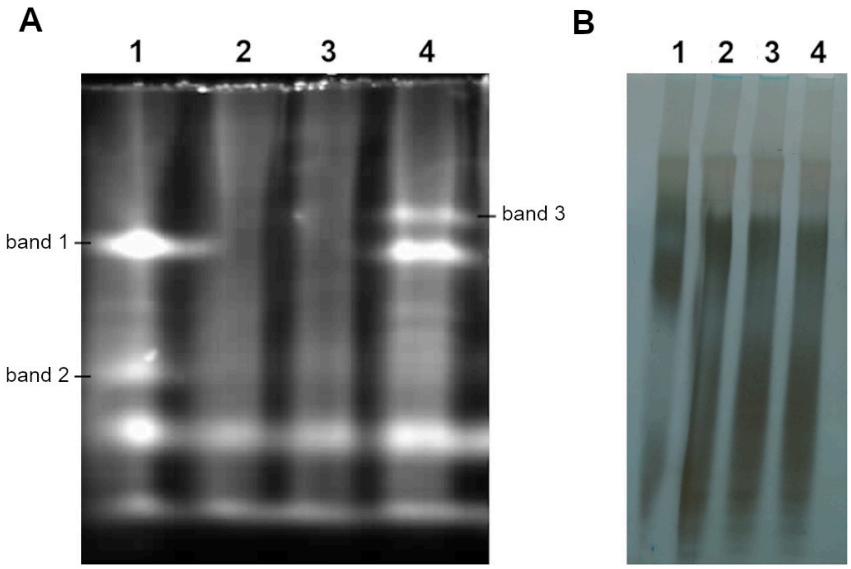

Figure VI.11: Analysis by FACE (A) and C-PAGE (B) of the *L. digitata* FCSP degradation by the enzyme cocktail. 1: enzyme cocktail. 2: no enzyme. 3: boiled enzyme cocktail. 4: enzyme cocktail without ZGAL_3452. Reactions were conducted by adding 20 µl of enzyme cocktail to 180 µl of 0.2 % FCSPs from *L. digitata* in 50 mM Tris-HCl pH 7.5 with 2 mM $CaCl_2$ and 1X metal mix (50 µM $FeCl_3$, 20 µM $CaCl_2$, 10 µM each of $MnCl_2$ and $ZnSO_4$, and 2 µM each of $CoCl_2$, $CuCl_2$, $NiCl_2$, Na_2MoO_4, Na_2SeO_3, and H_3BO_3 in ~60 µM HCl). The final concentration of each enzyme in the reaction was 0.01 $mg.ml^{-1}$. Reactions were incubated overnight at 37 °C. On the FACE gel the bands below band 2 are not a specificity of this substrate as they were also observed for other substrates.

An enzyme mix that does not contain ZGAL_3452 was incubated with *L. digitata* FCSPs to investigate a potential role of the PLnc in its degradation (lane 4). In the absence of ZGAL_3452, the intense band 1 is still visible while another, less intense band, is present above it (band 3). Following these observations, it seems that some enzymes in the cocktail can hydrolyze the FCSPs from *L. digitata* and that the degradation products (corresponding to band 3) are recognized by ZGAL_3452 which cleaves them to produce lower molecular weight (LMW) oligosaccharides (band 2). It is worth noting that despite initially present small oligosaccharides were removed from FCSPs products, it did not prevent for the presence of smears in the background of the gel.

HPSEC analyses were also performed on these reaction mixtures (**Figure VI.12**), showing slight differences between the conditions. The peak 1 corresponds to HMW fraction of the polysaccharides and its area displayed a 32 % decrease in the presence of the enzyme cocktail (with or without ZGAL_3452), compared to the negative controls (no enzyme or boiled enzymes). This decrease of the HMW fraction coincided with the formation of peak 2 corresponding to compounds with lower

molecular weight. However, the intensity of this second peak is too low compared to the measured decreased of peak 1 and likely do not represent all the degradation products. Some products could be eluted at the same time as the buffer compounds and would therefore be undetectable. We could also note that the intensity of peak 2 is higher when ZGAL_3452 was added to the cocktail, suggesting a slight activity of this enzyme on the substrate or on degradation from other enzymes in the cocktail.

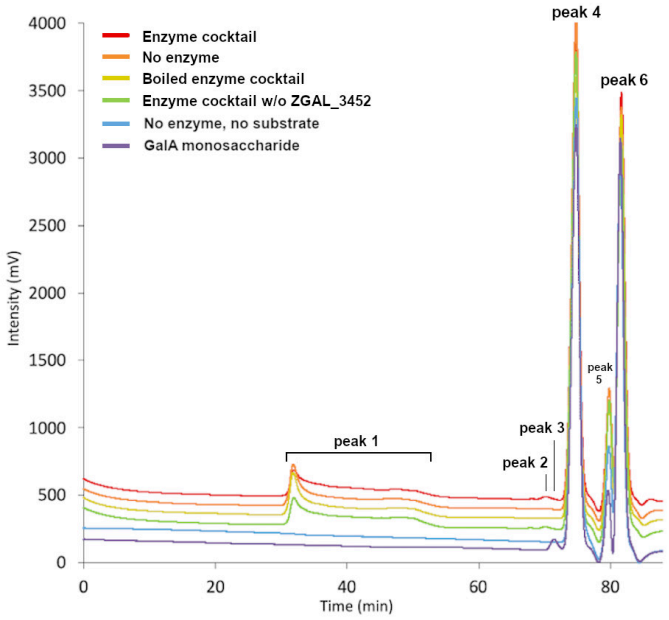

Peak area (mV*min)

	peak 1 32 min	peak 2 70 min	peak 3 71.5 min	peak 4 75 min	peak 5 80 min	peak 6 82 min
Enzyme cocktail	387	32	0	5163	857	3945
No enzyme	568	0	0	5355	1066	4006
Boiled enzyme cocktail	566	0	0	4792	946	3953
Enzyme cocktail w/o ZGAL_3452	392	17	0	5188	1134	3868
No enzyme, no substrate	0	0	0	4801	883	3619
GalA monosaccharide	0	0	93	4470	520	3738

Figure VI.12: HPSEC analysis of the *L. digitata* FCSP degradation by the enzyme cocktail. Reactions were conducted by adding 20 µl of enzyme cocktail to 180 µl of 0.2 % FCSPs from *L. digitata* in 50 mM Tris-HCl pH 7.5 with 2 mM $CaCl_2$ and 1X metal mix. The final concentration of each enzyme in the reaction was 0.01 $mg.ml^{-1}$. Reactions were incubated overnight at 37 °C. 0.013 % galacturonic acid monosaccharide in the same buffer as the samples was also analyzed as a size reference.

Also, peaks 4, 5 and 6 were eluted after 75 min, and correspond to Tris compounds and salts as they are also visible when no substrate or enzymes were added. No information regarding the exact composition or size distribution is available for the FCSPs from *L. digitata*. Therefore, 0.013 % GalA monosaccharide was added in the same buffer as the samples (without substrate or enzymes) and was analyzed to roughly estimate the size of the degradation products. GalA monosaccharide was eluted after 71.5 min (peak 3) suggesting that peak 2 likely corresponds to disaccharide. However, the elution time also depends of the 3D conformation of the eluted compounds (type of monosaccharides, substituents, linkages, etc.) and no size standards are available for *L. digitata* FCSPs as its composition remains unknown. Another small peak seems to be formed after 85 min only in the presence of ZGAL_3452 in the cocktail but it might be an artefact as it is eluted after the salts.

The enzymatic reactions were followed by unsaturated uronic acid assays to demonstrate the effect of the PL after a first hydrolysis by the other enzymes of the putative PUL (**Figure VI.13**). With no enzyme, A_{235} stayed stable around 0.4, corresponding to the substrate intrinsic absorbance. After the addition of the mixture containing all the enzymes except ZGAL_3452, A_{235} remained around 0.5, the

0.1 difference with the condition without enzyme might result from the absorbance in UV of some enzymes. When only ZGAL_3452 was added, A_{235} slightly increased around 0.5, suggesting that ZGAL_3452 alone has a very limited capacity to cleave *L. digitata* FCSPs. On the other hand, with all the enzymes of the PUL, including ZGAL_3452, an absorbance of 0.7 was measured initially, followed by an increase to 0.85 and a decrease. As discussed above, this decrease could be the result of an exo-lyase activity. Given the 0.2 absorbance gap observed at the first measure between the cocktail with ZGAL_3452 or without it, the action of the different enzymes cleaving the polysaccharide might start immediately after their addition to the substrate (there are approximatively 10 sec between enzyme addition and the first measure). Hence, those results support the hypothesis that ZGAL_3452 would act on the degradation products released by other enzymes of the PUL.

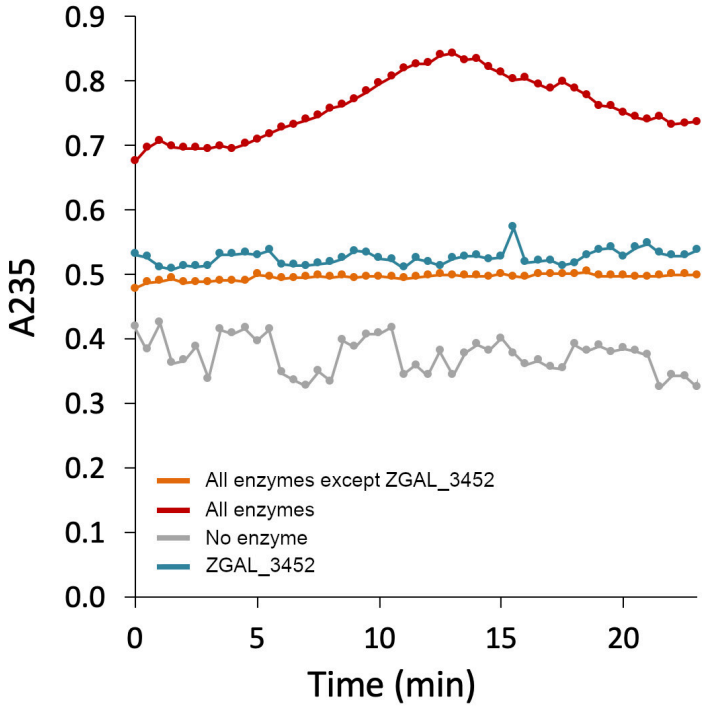

Figure VI.13: Activity of the enzyme cocktail monitored by unsaturated uronic acid assays. Reactions were conducted at 25 °C by adding 20 µl of enzyme cocktail to 180 µl of 0.2 % FCSPs from *L. digitata* in 50 mM Tris-HCl pH 7.5 with 2 mM $CaCl_2$ and 1X metal mix. The final concentration of each enzyme in the reaction was 0.01 $mg.ml^{-1}$. Reactions were done in simplicate.

It should be noted that although ZGAL_3449 is predicted to be a polysaccharide lyase (PL40), no increase in absorbance due to the release of unsaturated uronic acids was detected in its presence (orange curve). Either this enzyme is not involved in the hydrolysis of these FCSPs, or other enzymes in the cocktail rapidly converted the released degradation products in other compounds that do not absorb in UV.

To further investigate which enzymes within the cocktail have the ability to cleave *L. digitata* FCSPs, each putative GH or PL was incubated individually with the substrate (**Figure VI.14**). This includes two fucosidases of family GH141 and GH29 (ZGAL_3450 and ZGAL_3451 NTD, respectively), the

GH88 unsaturated glucuronyl hydrolase UglA1 (ZGAL_3445) and the PL40 (ZGAL_3449). An intense band was observed with ZGAL_3449 and likely corresponds to the band 1 in **Figure VI.11A**. Additional bands of higher migration velocity can be identified but with much lower intensity. The observation of only one intense band and not a degradation scale might result from the important incubation time (overnight) leading to the accumulation of one product. Kinetics assays should be carried out in the future to test this hypothesis. Alternatively, ZGAL_3449 might have a very specific activity as it might recognize a specific sequence of monosaccharides and cleave a specific linkage. Its annotation as a polysaccharide lyase was confirmed by the increase in A_{235} detected following the addition of the enzyme (**Figure VI.15**) demonstrating the release of unsaturated uronic acids from *L. digitata* FCSPs. No sign of hydrolysis was identified for the other GHs/PLs. ZGAL_3450 and ZGAL_3451 NTD are fucosidases and probably process LMW oligosaccharides released by fucoidanases (Silchenko, Rasin, Zueva, *et al.*, 2018). The profile obtained with ZGAL_3449 alone or with ZGAL_3449 + ZGAL_3452 is similar (**Figure VI.14**), suggesting that the latter could not cleave the degradation products released after the action of ZGAL_3449. Moreover, the addition of the sulfatases (ZGAL_3447, 3448, 3455 and 3461) or the esterases (ZGAL_3446, 3451 CTD, 3454) of the PUL did not enhance any enzymatic activity, suggesting that they might be active on downstream products, as observed for the degradation of ulvan by *F. agariphila* KMM 3901^T (Reisky *et al.*, 2019).

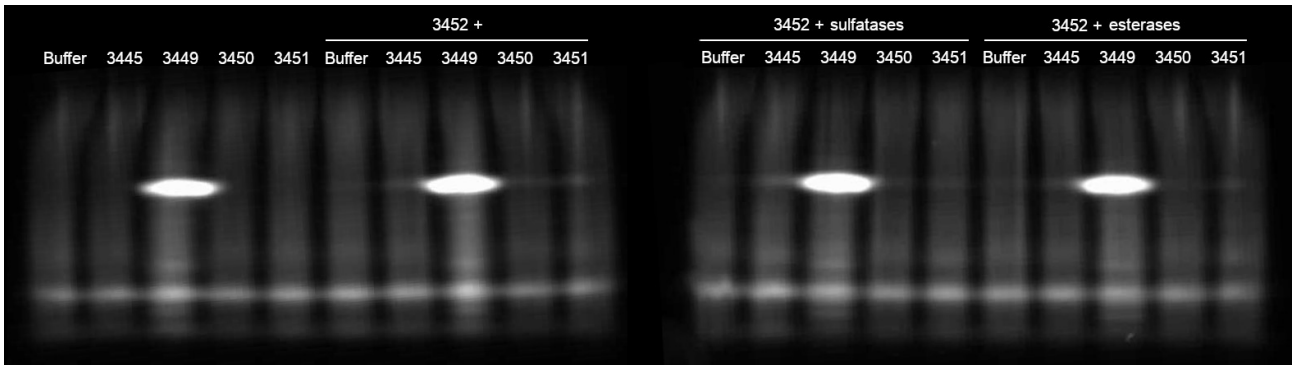

Figure VI.14: FACE analysis of the degradation of *L. digitata* FCSPs by each known or putative GH/PL of the PUL. Reactions were conducted overnight at 37 °C in 50 mM Tris-HCl pH 7.5 with 2 mM $CaCl_2$ and 1X metal mix by mixing 4 µg of the corresponding GH/PL with 364 µg of *L. digitata* FCSPs. The effect of ZGAL_3452 was tested by adding 4 µg of the enzyme. Sulfatases and esterases effect was tested by adding a cocktail containing all the sulfatases or all the esterases of the PUL (2 µg final of each enzyme in the reaction mixture).

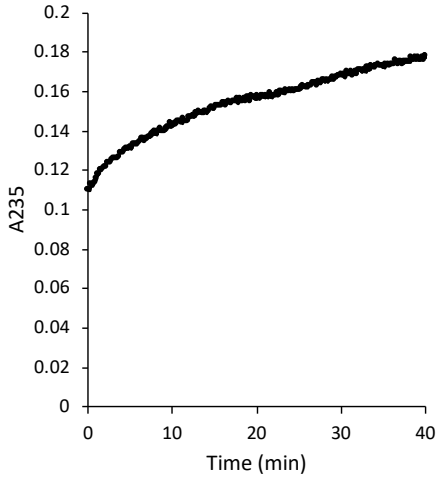

Figure 15: Activity of ZGAL_3449 assayed by measuring the increase in released unsaturated uronic acids. Reactions were conducted at room temperature in 50 mM Tris-HCl pH 7.5 with 2 mM CaCl2 and 1X metal mix by mixing 5 µg of enzyme with 940 µg of *L. digitata* FCSPs. The absorbance was monitored using a spectrophotometer and the blank was done with a mixture without enzyme. It should be noted that the enzyme was 4.5 months old (stored at 4 °C) when this kinetic was conducted. Hence, activity is likely underestimated compared to the fresh enzyme.

The different putative GHs were combined with ZGAL_3449 in the presence or not of ZGAL_3452 (**Figure VI.16**). The FACE gels show that ZGAL_3445 is active when combined with ZGAL_3449 as a second band is observed (likely corresponding to band 3 in **Figure VI.11A**). The GH88 unsaturated glucuronyl hydrolase ZGAL_3445 is predicted to cleave unsaturated oligosaccharides produced by polysaccharide lyases and to release a saccharide and an unsaturated uronic acid monosaccharide, the latter being non-enzymatically converted immediately to α-keto acid (not absorbing in UV). Hence, this result supports the conclusion that ZGAL_3449 would be a PL and explains the absence of an increase in A_{235} (**Figure VI.13**) when FCSPs are incubated with the enzyme cocktail without ZGAL_3452 (ZGAL_3449 degradation products were immediately used by ZGAL_3445 whose released products were immediately and spontaneously converted in compounds not absorbing in UV). The consecutive action of a GH88 cleaving a PL40 degradation products was observed by Reisky *et al.*, 2019 for ulvan assimilation by *F. agariphila* KMM 3901^T. The enzyme cocktail as well as ZGAL_3449 alone were incubated with ulvan but no degradation product was visible on FACE gel (data not shown), suggesting that the family PL40 is polyspecific.

If ZGAL_3445 uses the products released by ZGAL_3449, we would have expected the apparition of a band with a lower molecular weight than the one produced following the action of ZGAL_3449, corresponding to the cleavage of the unsaturated residue at the non-reducing end. Yet, the additional band observed with ZGAL_3445 has a lower migration velocity than the intense band released by ZGAL_3449. On FACE gels, oligosaccharides migrate according to their size but also to their charge. As FCSPs are negatively charged polysaccharides, sugars were labelled with AMAC, which does not confer any charge at the pH used (unlike ANTS, the other fluorophore commonly used for FACE

analysis). Hence, here the migration is more impacted by the native charge of the oligosaccharides and this might explain why the band due to the action of ZGAL_3445 has a lower velocity.

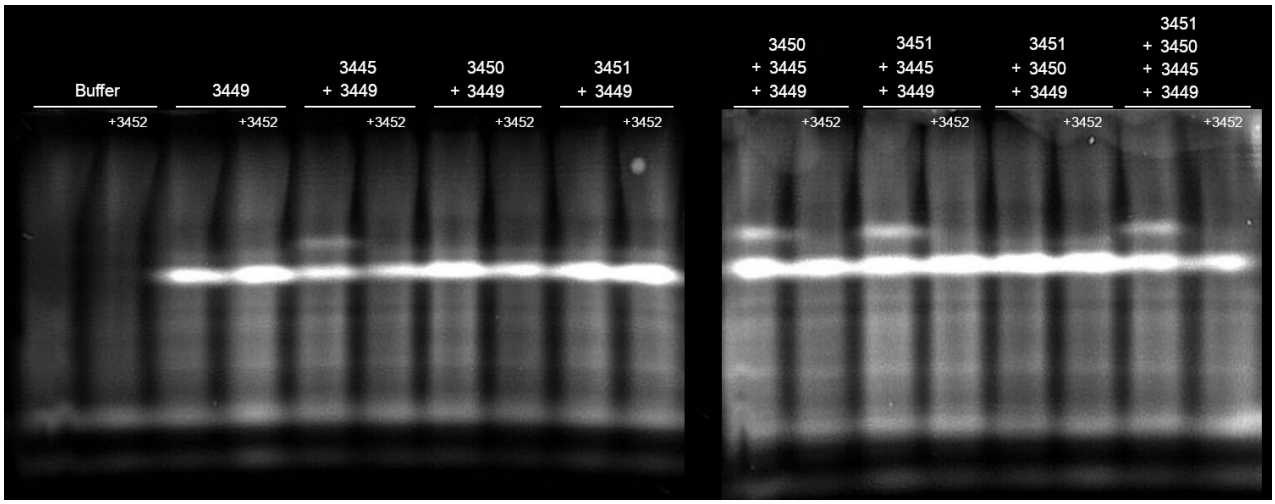

Figure VI.16: FACE analysis of the *L. digitata* FCSP degradation by combined enzymes. Reactions were conducted overnight at 37 °C in 50 mM Tris-HCl pH 7.5 with 2 mM $CaCl_2$ and 1X metal mix by mixing 4 µg of the corresponding enzyme with 364 µg of *L. digitata* FCSPs. 2 µg of each sulfatases and esterases were added.

In the presence of ZGAL_3452, the band obtained following the action of ZGAL_3445 is not visible. This would indicate that the oligosaccharides produced after the hydrolysis by ZGAL_3445 were cleaved by ZGAL_3452. Nevertheless, no additional band which would correspond to the action of ZGAL_3452 is detected. Several hypotheses could explain this result: (i) the products of the degradation are not labelled by AMAC or are uncharged and would not migrate into the gel (ii) the released products could represent only a minor amount of the sample and would be undetectable, or (iii) ZGAL_3452 is not active on the products released by ZGAL_3445 but rather inhibits its activity. This last hypothesis could be easily tested by adding ZGAL_3452 a few hours after the addition of ZGAL_3449 and ZGAL_3445 instead of adding the three enzymes simultaneously.

These reaction mixtures were also analyzed by HPSEC (**Figure VI.17**). The presence of ZGAL_3449 systematically led to a decrease of the HMW fraction (peak 1) together with an increase of a LMW product (peak 2). With ZGAL_3445 alone a very small decrease of peak 1 was observed (7 % compared to 45 % with ZGAL_3449 alone). This decrease might be an artefact but it might also suggest that ZGAL_3445 cleaves traces of unsaturated oligosaccharides contained in the substrate. However, when ZGAL_3449 and ZGAL_3445 were added simultaneously, the area of peak 1 decreased by 57 %, which is higher than the 45 % decrease observed with ZGAL_3449 alone. This higher decrease of the HMW fraction could result of the independent actions of ZGAL_3449 and ZGAL_3445. As peak 2 does not decrease when ZGAL_3449 and 3445 were added (it even increased), it seems that ZGAL_3445 does not cleave the putative disaccharide released by the action of ZGAL_3449. However, it is possible that the difference in the elution time between a mono- and a disaccharide would not be detected.

When the three enzymes were combined, the area of peak 1 was higher than with only ZGAL_3449 + ZGAL_3445. It seems then that ZGAL_3452 would inhibit the action of ZGAL_3445.

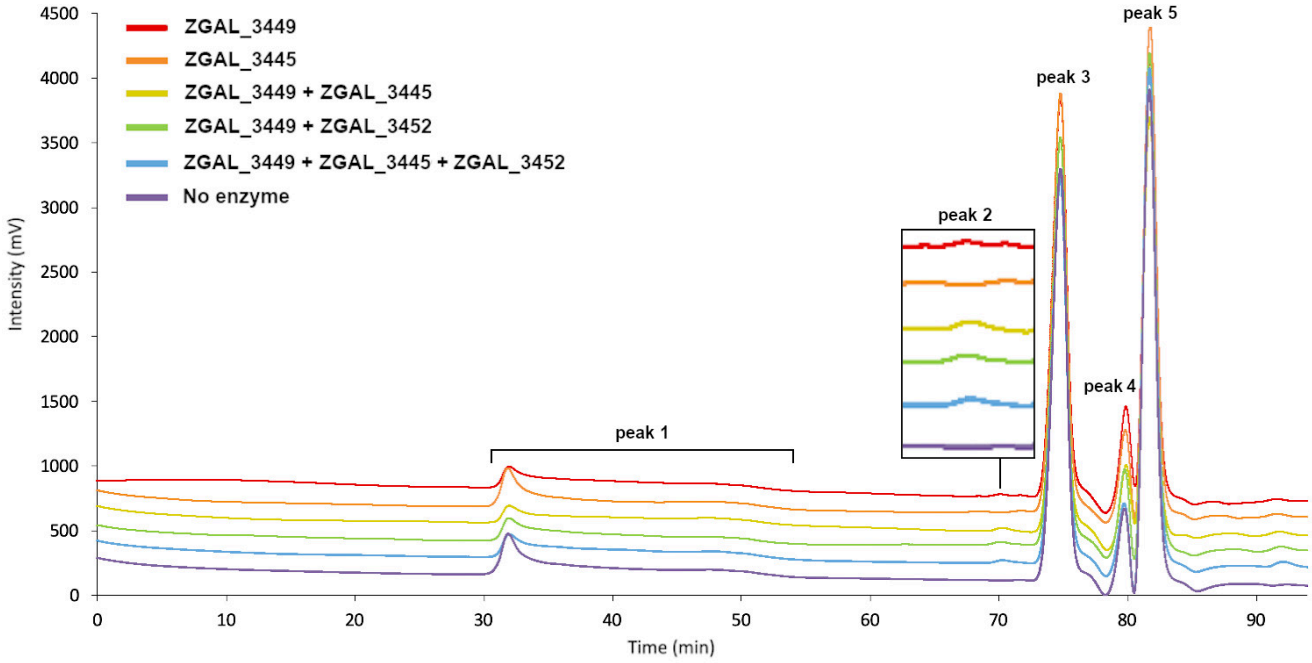

Peak area (mV*min)

	peak 1 32 min	peak 2 70 min	peak 3 75 min	peak 4 80 min	peak 5 82 min
ZGAL_3449	320	17	4462	858	4317
ZGAL_3445	539	0	4594	698	4564
ZGAL_3449 + ZGAL_3445	250	36	4095	662	4076
ZGAL_3449 + ZGAL_3452	357	20	4563	650	4629
ZGAL_3449 + ZGAL_3445 + ZGAL_3452	348	24	4667	751	5031
No enzyme	579	0	4593	660	4710

Figure VI.17: HPSEC analysis of the *L. digitata* FCSP degradation by combined enzymes. Reactions were conducted as described in Figure VI.16.

IV. Conclusion

Our different experimentations indicated that the polysaccharide lyase ZGAL_3452 would be active on FCSPs containing galacturonic acid residues, such as *C. okamuranus* FCSPs. The biochemical characterization of the enzyme was then performed with this substrate. However, the activity detected by absorbance measurements was not confirmed when using other analytical technics, suggesting that this substrate does not contain the motifs preferentially recognized by the enzyme.

As polysaccharides are commonly degraded following the sequential action of different enzymes, the putative PUL containing ZGAL_3452 was analyzed bioinformatically to investigate the mode of action of a fucanolytic system and not just of a single enzyme.

The ability of the PUL to degrade *L. digitata* FCSPs is consistent with its overexpression when *Z. galactanivorans* was grown on fresh tissues from this alga. As discussed in Chapter V, the importance to characterize this PUL then also lies in its putative key role in fresh algal biomass degradation. No degradation profile was observed with the other FCSPs tested, even the ones extracted from other kelps, suggesting a narrow substrate specificity. This observation is not surprising given the important FCSPs diversity observed between algal species. In this chapter, through bioinformatic analyses and diverse analytical methods and for the first time in *Z. galactanivorans* Dsij^T, we experimentally identified several enzymes active on FCSPs. It then constitutes a preliminary work toward the characterization of a first fucoidanolytic PUL in the genus *Zobellia* and paves the way for deeper investigations.

We raised here the potential catalytic cascade of different CAZymes involved in the degradation of FCSPs from *L. digitata*, particularly focusing on a PL40 (ZGAL_3449), a GH88 (UglA1, ZGAL_3445) and a PLnc (ZGAL_3452). The PL40 would initiate the FCSP depolymerization and the produced unsaturated oligosaccharides (putatively a disaccharide) would be further processed by UglA1. The role of the PLnc remains unclear. This PUL seems to have functional similarities with the ulvan PUL characterized in *F. agariphila* KMM 3901^T. Ulvan is mainly composed of rhamnose, xylose and GluA. Together with the fact that an activity was detected for ZGAL_3452 on pectin (mainly composed of rhamnose and GalA, the main component of pectin structures) and FCSPs from *C. okamuranus* (containing GalA and GluA among various other monosaccharides), we could hypothesize that the PUL *zgal_3445* - *zgal_3463* putatively targets FCSPs containing significant amounts of rhamnose and GalA/GluA residues. FCSPs is a term gathering a large variety of diverse substrates as it goes from homopolymers of sulfated L-fucose to sulfated polysaccharides containing at least one fucose residue in a branch (Deniaud-Bouët *et al.*, 2017). The targeted substrate could be a pectin-like polysaccharide containing sparse fucose residues, likely similar to rhamnogalacturonan-II (RGII) a complex branched pectic polysaccharide containing fucose residues (Pellerin *et al.*, 1996). Pectin structures are present in some freshwater green algae (e.g. Domozych *et al.*, 2012; Herburger *et al.*, 2019), but was believed to be absent from brown and red algae. However, pectin-like structures were reported in recent study. Using specific cell wall-directed monoclonal antibodies, Koch *et al.*, 2019 showed that the rhamnogalacturonan-I (RGI, one of the major components of pectins) probe targeted carbohydrate structures in *L. digitata* exudates, while Raimundo *et al.*, 2016 reported that RGI/arabinogalactan probe bound to epitopes in *Fucus vesiculosus* thallus and suggest they might in fact target galactans structure, likely associated with FCSPs. Moreover, Lee *et al.*, 2020 detected high amounts of galacturonic acids (5-63 %) in polysaccharides extracted from brown, red and green algae. Hence, these studies support the notion that pectin-like compounds are present in marine algae. The presence of such structures in purified algal extracts might differ depending on the method used as Raimundo *et al.*, 2016 only detected pectin-like structures in compounds extracted with water and mostly with $CaCl_2$. They are then likely to be co-extracted with alginate and would not be abundant in FCSP extracts.

Further experimentations are needed to clarify and deepen the obtained results. The different bands observed on FACE gels could be purified and analyzed in NMR or mass spectrometry to characterize the structure of the degradation products. Also, all incubations presented here were performed overnight. A kinetic analysis of the released degradation should be carried out as different degradation profiles could be observed and could help to decipher the mode of action of the enzymes. Moreover, crystallographic analyses would help unravel their function by resolving the enzyme structure. ZGAL_3452 production was carried out for crystallogenesis analyses but the purified enzyme precipitated during the concentration step. Finally, the optimal activity of the PUL may be directed against a substrate that was not yet tested. Hence, consequentially to what I previously mentioned, the activity screening should be performed with a much larger set of substrates to find the natural substrate, including total algal extracts or pectin-like structures.

In *Z. galactanivorans*, different PULs predicted to target FCSPs could work together with the PUL described here to degrade specific FCSPs, especially the adjacent PUL35. The α-L-fucosidase (GH29, ZGAL_3464) contained in this PUL was previously biochemically characterized using the artificial compound pNP-fucose as a substrate in the PhD thesis of Maria Matard-Mann, 2017. Yet, its natural substrate is still unknown. Attempts to decipher the function of the GHnc ZGAL_3470 were also conducted in the same thesis but no fucanolytic activity was evidenced on the different AIRs and synthetic substrates tested. Also, enzymes encoded by isolated genes in *Z. galactanivorans* Dsij^{T} genome could assist PUL-encoded enzymes to degrade the substrate. Finally, *Z. galactanivorans* might lack key hydrolytic enzymes to completely assimilate some FCSP structures and hence rely on the action of other bacterial communities highly specialized in FCSP degradation to produce them. *Z. galactanivorans* is efficient to use a broad range of algal polysaccharides (alginate, FCSPs, laminarin, agar, carrageenans) while other taxa such as '*Lentimonas'* spp. (*Verrucomicrobia*) are highly specialized in the assimilation of FCSPs as they possess an incredibly large set of fucanolytic tools but lack the ability to use other algal carbohydrates like alginate (Sichert *et al.*, 2020). Hence, mutual cooperative interactions could occur in the bacterial consortia between taxa displaying different metabolic strategies.

Overall, the experimental identification and characterization of PULs targeting such complex and diverse polysaccharides such as FCSPs is a difficult and time-consuming task regarding the lack of data in FCSPs structural composition. The characterization of fucanolytic enzymes already appeared to be of great interest to fill the gap in FCSP structural characterization.

Chapter VII:

Deciphering cooperative bacterial interactions during macroalgal degradation

Résumé du chapitre

Les bactéries marines hétérotrophes sont les principaux dégradeurs de la biomasse algale. Toutes ne sont cependant pas équitablement équipées pour l'utilisation de substrats complexes. En fonction des outils enzymatiques dont elles disposent, les communautés bactériennes mettraient en place différentes stratégies écologiques pour leur croissance. Les bactéries possédant un vaste arsenal enzymatique serait capable d'initier la dégradation de matière organique complexe, telle que des tissus de macroalgues, en produisant des enzymes extracellulaires. Ces bactéries pionnières libèreraient alors dans le milieu des produits de dégradation (produits d'hydrolyses ou métabolites secondaires) assimilables par d'autres taxons moins bien équipés. Ces derniers bénéficieraient ainsi de l'action des bactéries pionnières pour croitre sans participer à la production d'enzymes, on les qualifie donc d'opportunistes.

Il a été montré au cours des précédents chapitres que le genre *Zobellia*, et en particulier la souche *Z. galactanivorans* Dsij^T avait la capacité d'utiliser les tissus d'algues frais pour sa croissance. La sécrétion d'enzymes extracellulaires conduisant à cette dégradation et l'accumulation d'oligo-alginate mesurée dans d'autres études suggèrent que cette souche, par la libération de nombreux produits de dégradation dans le milieu, pourrait supporter la croissance d'autres populations de la communauté bactérienne. Une étude préliminaire a d'ailleurs montré que la dégradation de macroalgues par *Z. galactanivorans* pouvait favoriser la croissance de certains taxons, incapable de croître en son absence, tels que des membres du genre *Tenacibaculum*.

Ce chapitre se concentre donc sur l'identification, suivi de la caractérisation, des mécanismes d'interactions coopératives entre la bactérie pionnière *Z. galactanivorans* Dsij^T et des bactéries opportunistes. Les souches du genre *Tenacibaculum* disponibles au laboratoire ont été testées comme potentiels partenaires opportunistes. Les sondes FISH développées au cours de cette thèse ont été utilisées afin de dissocier la croissance des deux genres.

En particulier, j'ai montré que lorsque *T. aestuarii* et *T. halocynthiae* n'étaient pas en mesure d'utiliser les tissues d'algues comme seule source de carbone, la présence de *Z. galactanivorans* leur permettait de croître.

Les différentes expériences menées n'ont pas encore permis de caractériser les mécanismes d'interactions mais suggèrent des variations saisonnières de ces interactions coopératives au sein des communautés. D'autres pistes sont discutées afin de poursuivre ces recherches, notamment les méthodes de sélection d'autres potentiels candidats opportunistes.

I. Introduction

Marine heterotrophic microbial communities are thought to be the main contributors of algal biomass recycling (Mann, 1982). However, not all the consumers of soluble algal compounds are equally equipped to feed on complex algal substrates (Enke *et al.*, 2019). Based on their genomic potential for polysaccharide hydrolysis, bacterial communities are believed to display different ecological growth strategies. Bacteria able to initiate the breakdown of complex solid-phase organic matter by secreting extracellular hydrolytic enzymes are reported as pioneers of the degradation (or primary consumers). The released degradation products constitute new substrate niches for other less efficient community members, considered as opportunistic bacteria (or secondary consumers) which do not effectively contribute to the degradation process (Hehemann *et al.*, 2016; Jiménez *et al.*, 2017; Arnosti *et al.*, 2020; Pollak *et al.*, 2021; Pontrelli *et al.*, 2021). Different types of cooperative interactions were described (Cavaliere *et al.*, 2017; Reintjes *et al.*, 2019, see **Figure I.8** in Chapter I). They could be mediated by public goods production, such as hydrolytic enzymes, whose beneficial actions are shared with the local communities. Public goods might be exploited by specific communities, reported as exploiters, unable to cleave complex biomass but efficient in the uptake and use of the low molecular weight resulting products (Pollak *et al.*, 2021). In addition, the pioneer bacterial cells likely directly excrete secondary metabolites (amino acids, organic acids, vitamins, co-factors, etc.) as by-products or waste products that could be directly consumed by scavenger bacterial communities, resulting in metabolic cross-feeding. For example, Enke *et al.*, 2019 characterized such cross-feeding interactions with alginate as the carbon source. Unravelling the mechanisms that drive pioneer/opportunist cooperative interactions during the degradation of fresh macroalgal biomass is essential to better understand the processes governing algae recycling in coastal ecosystem.

Previous analyses showed that *Zobellia galactanivorans* secreted alginolytic enzymes and that alginate oligosaccharides accumulated in the medium when it was grown on alginate or *Laminaria digitata* tissues (Zhu *et al.*, 2017; Dudek *et al.*, 2020; Chapter V). It would suggest that Z. *galactanivorans* likely acts as a sharing pioneer during algal degradation and not as a selfish one (characterized by extracellular enzymes tethered to the external membrane and not secreted in the medium to limit product diffusion). Besides, Zhu *et al.*, 2017 revealed that the degradation of fresh macroalgae by *Z. galactanivorans* Dsij^T could favor the growth of opportunistic taxa and especially of *Tenacibaculum* representatives, unable to grow in the absence of *Z. galactanivorans*. *Tenacibaculum* spp. might then represent potential opportunistic bacteria, exploiting the hydrolysis products or scavenging the by-products released by *Z. galactanivorans* during the degradation.

The flavobacterial genus *Tenacibaculum* comprises 32 validly described species that display an important genetic diversity. Some of them are well known fish pathogens (Avendaño-Herrera *et al.*, 2006). *Tenacibaculum* spp. are regularly reported on macroalgae, especially on green and red ones

(Hollants *et al.*, 2013),. Although their role in macroalgae degradation remains unclear, one recent study found a Polysaccharide Utilization Loci (PUL) homologous to the *Z. galactanivorans* Dsij^T carrageenan PUL in *Tenacibaculum jejuense* CNURIC013^T genome (Ficko-Blean *et al.*, 2017). Moreover, members of the genus *Tenacibaculum* were identified as active incorporators of carbon from alginate within a natural seawater community (Thomas *et al.*, 2021) and PULs encoding alginate lyases were reported in *Tenacibaculum* metagenome-assembled genomes (Bunse *et al.*, 2021). A high CAZyme variability among the species is observed as their number varies between 34 and 102 for the 8 *Tenacibaculum* genomes available in the CAZy database (which is still largely below the 221 CAZymes found in *Z. galactanivorans* Dsij^T) (Lombard *et al.*, 2014). These observations highlight that the genus *Tenacibaculum* was not reported for having strong abilities to degrade complex algal polysaccharides but is probably involved in the process of macroalgal recycling. This reinforces the initial hypothesis claiming that *Tenacibaculum* spp. might represent good opportunistic candidates. Finally, *Tenacibaculum* spp. might be poorly equipped to cope with algal toxic compounds such as halogen compounds, as it is one of the two genera within the *Flavobacteriaceae* family to not encode Type II haloacid dehalogenase (Grigorian *et al.*, 2021). In the same study, the growth of two *Tenacibaculum* species tested (*T. discolor* LL0411.1.1^T and *T. gallaicum* A37.1^T) was inhibited by iodo and bromoacetic acid, while *Z. galactanivorans* Dsij^T was more tolerant. *Tenacibaculum* spp. might possess other unknown enzymes to cope with algal defenses but they could also rely on the detoxification action of other taxa.

It should be mentioned that a previous project, supported by the team (ANR Blue Enzymes coordinated by the Dr. Gurvan Michel) and aiming to assess catabolic profiles of *Tenacibaculum* spp. on diverse sugars, revealed that none of the *Tenacibaculum* spp. were able to grow in marine minimum medium (MMM) supplemented with glucose or starch (for *T. xiamenense* et *T. litopenaei* only, growth was observed after 6 days on glucose and starch respectively). Further physiologic and genomic experiments conducted in MMM with. *T. jejuense* showed that the strain did not grow with various simple sugars or polysaccharides (as alginate) as the sole carbon source probably because it was not able to synthesize some amino acids with NH_4Cl as sole nitrogen source. In particular the addition of proline supported the growth on glucose (Dr. Tristan Barbeyron, personal communication).

In this chapter, we tested if cooperative interactions occurred between the pioneer strain *Z. galactanivorans* Dsij^T and putative opportunist strains belonging to the genus *Tenacibaculum*. A collection of 21 *Tenacibaculum* strains were screened for their growth in minimum medium containing fresh pieces of the kelp *Laminaria digitata*, either in monocultures or in co-cultures with *Z. galactanivorans* Dsij^T. The growth of each bacterial partner was monitored using specific CARD-FISH probes to identify successful pioneer/opportunist interactions. Further characterization of the interaction mechanisms was attempted with the selected *Z. galactanivorans*/*Tenacibaculum* sp. tandem.

II. Methods

1. Algae treatment

Healthy mature *Laminaria digitata* were collected at the Bloscon site (48°43'29.982'' N, 03°58'8.27'' W) in Roscoff (Brittany, France). The meristem part of the tissues was cut into small pieces (squares of side 1.5-2 cm) with a sterile scalpel. The resident epibiotic microbiome was cleaned by immersion in 0.1 % Triton in milli-Q water for 10 min followed by 1 % iodine povidone in milli-Q water for 5 min. Algae pieces were rinsed in sterilized autoclaved seawater for 2 hours.

2. Growth experiment

Precultures were grown from glycerol stock in Zobell 2216 medium (ZoBell, 1941) at ambient temperature for 3 days. Cell pellets were washed twice in 1X saline solution before being inoculated in the microcosms at OD_{600} 0.05 in minimum marine medium (referred to as MMM, described in (Thomas, Barbeyron, *et al.*, 2011) and complemented with 100 $\mu g.ml^{-1}$ kanamycin, 100 $\mu g.ml^{-1}$ streptomycin, 50 $\mu g.ml^{-1}$ neomycin and 14 $\mu g.ml^{-1}$ colistin to which *Z. galactanivorans* $Dsij^T$ and *Tenacibaculum* spp. are resistant). The treated *Laminaria digitata* pieces were added as the sole carbon source. Cultures were conducted in 50 ml Falcon tubes or in 250 ml Erlenmeyer at 20 °C under agitation. *Tenacibaculum* spp. were grown either in monoculture or in co-culture with *Z. galactanivorans* $Dsij^T$.

To further characterize the interactions, the spent supernatant from a 3 days-old *Z. galactanivorans* culture with macroalgae in MMM was collected, centrifuged twice (4200 rpm, 10 min) and filtered three times with 0.2 µm syringe filters. *Tenacibaculum* spp. were grown on the resulting filtrate supplemented with NH_4Cl in the presence or not of algal pieces.

For each experiment, bacterial growth was monitored by OD measurements and CARD-FISH analysis. Culture medium (between 200 and 800 µl) was sampled at different time points, centrifuged (11 000 rpm, 10 min) and cell pellets were resuspended in 2 % PFA in PBS overnight at 4 °C. Fixed cells were washed twice in PBS and stored in PBS:EtOH (1:1, v/v) at -20 °C before CARD-FISH analysis.

3. CARD-FISH probes design

Sequential CARD-FISH allows the detection of two distinct taxonomic groups in a single sample. It was used to monitor the respective growth of *Z. galactanivorans* and *Tenacibaculum* spp. during the co-culture experiments. The *Zobellia*-specific probe ZOB137 for CARD-FISH experiments was designed in Brunet *et al.,* 2021, accepted, [Chapter IV]) using the ARB software, as well as three helper oligonucleotides enhancing the probe signal. In the same way, a *Tenacibaculum*-specific probe (TEN281) was designed to target all the known strains of the genus except for *T. maritimum* as its

sequence is too divergent from the other *Tenacibaculum* species. This probe was tested successfully in the laboratory on pure cultures from 4 different *Tenacibaculum* strains (*T. crassostreae* JO-1^T, *T. lutimaris* TF-26^T, *T. skagerrakense* D30^T and *T. soleae* LL04 12.1.7^T) and no signal was detected with the strain *Imperialibacter roseus*^{T} P4^T that has only one mismatch within the 16S rRNA sequence targeted by the probe. The optimal formamide concentration for the hybridization was 35 % (see method in Brunet *et al.,* 2021, accepted, in Chapter IV Part 1).

Probes labeled with the horseradish peroxidase (HRP) were ordered from Biomers and helper oligonucleotides from Eurogentech (**Table VII.1**). All probes and helper oligonucleotides were resuspended in nuclease-free water and diluted to a working stock concentration of 8.4 pmol.µl^{-1}.

Table VII.1: Characteristic of the probes and helper oligonucleotides designed in this chapter.

Type	Name	Targeted group	Sequence (5' to 3')	Group coverage (%)	Number of outgroup hits
Probe	ZOB137-HRP	*Zobellia* spp.	GGCTATCCCACAGTAGGG	100	2
Probe	TEN281-HRP	*Tenacibaculum* spp. except *T. maritimum*	CTCAGACCCCCTACCTAT	90	63
Helper	H116	-	GGYAGATYGTATACGCSTTGC	-	-
Helper	H155	-	GTMTTAATCCAAATTTCTCTG	-	-
Helper	H176	-	CACATGGTACCATTTTACGGC	-	-

4. Sequential CARD-FISH

Fixed cells were harvested onto a 0.2 µm polycarbonate membrane (Cytiva) with a vacuum pump. Filter portions were embedded in 0.1 % LE agarose and dried on parafilm for 20 min at 37 °C. Cells were further permeabilized with lysozyme (10 mg.ml^{-1}, 15 min, 37 °C) and filters were washed twice in 50 ml of milli-Q water. Endogenous peroxidases were inactivated by short incubation in 0.1 M HCl followed by 10 min in 3 % H_2O_2 and washing steps (5 min in 50 ml of 1X PBS and shortly in 50 ml of milli-Q water). Filter portions were air-dried on Whatman paper before the first hybridization step with the *Zobellia*-specific probe. They were dipped and covered with the hybridization mix (0.9 M NaCl, 20 mM Tris-HCl pH8, 35 % formamide, 1 % blocking reagent, 10 % dextran sulfate, 0.02 % SDS, 28 nM of ZOB137-HRP probe and each helper) on parafilm in a humid chamber and incubated for 2.5 h at 46 °C. Samples were washed 15 min in a preheated washing buffer (70 mM NaCl, 1 M Tris-HCl pH8, 5 mM EDTA pH8, 0.01 % SDS) at 48 °C and 15 min in 1X PBS before being covered with a detection solution (1X PBS, 2 M NaCl, 0.1 % blocking reagent, 10 % dextran sulfate, 0.0015 % H_2O_2 and 1 µg.ml^{-1} of $Alexa_{546}$-labeled tyramides) for the first amplification step (45 min, 46 °C). HRP were inactivated by dipping the filters in 3 % H_20_2 for 10 min followed by washes in 1X PBS, milli-Q water and 96 % EtOH and kept overnight at -20 °C. The second hybridization and amplification steps were performed in the same fashion, with the TEN281-HRP probe and the fluorochrome $Alexa_{488}$. Filters were washed 10 min

in 1X PBS in the dark, twice briefly in 50 ml of milli-Q water and dehydrated in 50 ml of 96 % EtOH for 1 min. DAPI (1 µg.mg^{-1}) counter-staining was performed and slides were mounted once samples were completely dried with Citifluor:Vectashield (3:1). Cells were visualized with a Leica DMi8 epifluorescent microscope equipped with an oil objective 63X and a Leica DFC3000 G camera (Wetzlar, Germany). *Zobellia* and *Tenacibaculum* cells were automatically counted after background subtraction using the ImageJ software (Schneider *et al.*, 2012).

III. Results & Discussion

1. *Tenacibaculum aestuarii* benefits from the presence of *Z. galactanivorans* to grow with algal tissues

As a first screening, four phylogenetically distant *Tenacibaculum* species were grown on *L. digitata* tissues in monocultures or in co-cultures with *Z. galactanivorans* Dsij^{T}. In the absence of *Z. galactanivorans*, the different *Tenacibaculum* strains did not grow with the algae as the sole carbon source, except for *T. litoreum* CL-TF13^{T} (OD = 0.34) which was not further analyzed (**Figure VII.1A**) to identify cooperative interactions. The co-culture OD curves were similar to the one obtained with *Z. galactanivorans* alone. It can be noticed that the co-culture with *T. aestuarii* reached a higher cell density than the *Z. galactanivorans* monoculture (approximate gap of 0.5 unit). *Zobellia* and *Tenacibaculum* specific growth in the co-cultures were assessed by sequential CARD-FISH on the free-living bacteria. Micrographs revealed an important increase of the *T. aestuarii* SMK-4^{T} cell density after 43 h and 115 h compared with initial time (**Figure VII.1B**). This growth was less pronounced for *T. crassostreae* JO-1^{T}, while *T. skagerrakense* D30^{T} did not grow at all. Thus, this experiment indicated that algal degradation by *Z. galactanivorans* Dsij^{T} boosted *T. aestuarii* SMK-4^{T} growth.

These potential cooperative interactions were checked for *T. aestuarii* in a similar independent experiment (**Figure VII.2**). As already observed in the first experiment, the cell density within the co-cultures was higher than in the *Z. galactanivorans* monoculture. CARD-FISH analysis followed by cell counts confirmed the exponential growth of *T. aestuarii* during algal degradation in the presence of *Z. galactanivorans* but not in the monoculture. The number of *T. aestuarii* cells per µl of culture reached 2.8x10^{7} after 91 h. These experiments support the hypothesis proposed in Chapter V claiming that *Z. galactanivorans* cells would act as sharing pioneers by supporting the growth of other taxa. At this point it is unknown whether the opportunist cells benefit from the released hydrolytic products or secondary metabolites. Such cooperative interactions were already reported during the degradation of alginate and chitin (Enke *et al.*, 2019; Pontrelli *et al.*, 2021) but to my knowledge never with fresh macroalgae.

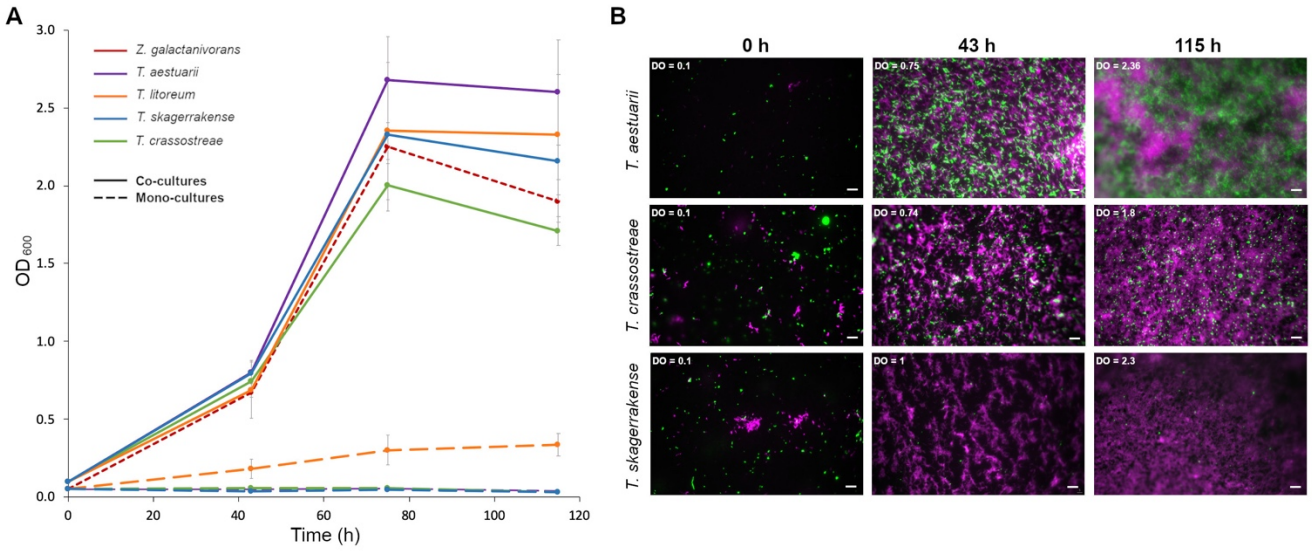

Figure VII.1: Screening for opportunistic interactions. (A) Growth curves of the different mono- and co-cultures at 20 °C in MMM with *L. digitata* as sole carbon source. Values are replicate mean ± s.d. (n = 2). (B) One replicate of the *T. aestuarii* SMK-4^T, *T. crassostreae* JO-1^T and *T. skagerrakense* D30^T co-cultures were analyzed over time by sequential CARD-FISH. Micrographs are overlays of the *Zobellia* (magenta) and *Tenacibaculum* (green) signals. Scale = 10 µm.

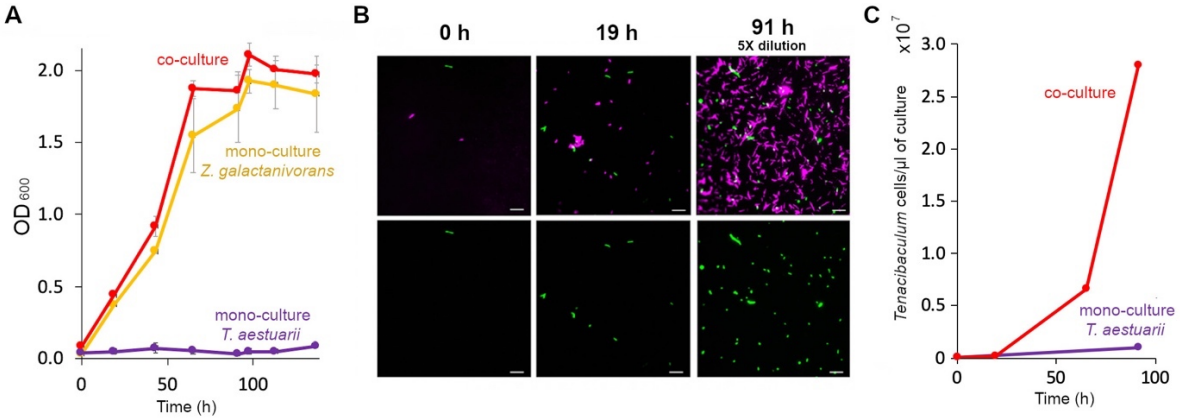

Figure VII.2: Cooperative interactions between *Z. galactanivorans* Dsij^T and *T. aestuarii* SMK-4^T. (A) Co-culture and monoculture growth with *L. digitata* as sole carbon source in MMM. Values are replicate mean ± s.d. (n = 2). (B) Micrographs obtained after sequential CARD-FISH. At 91 h cell were diluted 5X. Scale = 10 µm. Top row: overlay of the signals specific to *Zobellia* (magenta) and *Tenacibaculum* (green). Bottom row: same field with only the *Tenacibaculum* signal. (C) *Tenacibaculum* cell concentration during the degradation. Cells from 5 different microscopic fields were counted.

Co-cultures of *T. aestuarii* were also investigated with two deletion mutant strains available for *Z. galactanivorans* Dsij^T, namely Δ*alyA1* and Δ*ausR*, lacking the genes encoding the alginate lyase AlyA1 and the transcriptional regulator of the alginolytic system AusR, respectively (Zhu *et al.*, 2017; Dudek *et al.*, 2020). Compared to the *Z. galactanivorans* wild type (WT) strain, Δ*ausR* has a longer lag phase while *ΔalyA1* has a lower growth rate and displayed a lower final cell density. Such results were already observed and discussed in Zhu *et al.*, 2017 and Dudek *et al.*, 2020 during the degradation of alginate (and macroalgae tissues for *ΔalyA1*). It indicates that these mutants are less efficient to rapidly degrade macroalgae and shed light on the key role of the deleted genes in the utilization of fresh algal biomass.

For each *Z. galactanivorans* strains, the co-culture growth was slightly higher compared to the respective monoculture (**Figure VII.3A**).

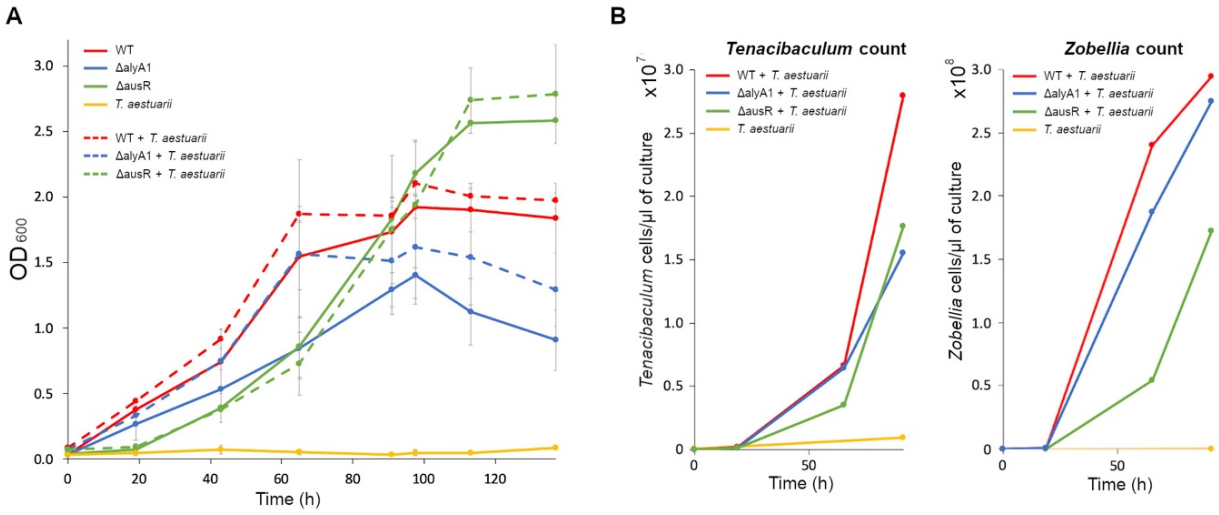

Figure VII.3: Effect of deletion of selected genes in *Z. galactanivorans* Dsij^T on the interactions with *T. aestuarii* SMK-4^T. (A) Bacterial growth. Values are replicate mean ± s.d. (n = 2). (B) *Tenacibaculum* and *Zobellia* cell concentration during the degradation of *L. digitata* tissues. Cells from 5 different microscopic fields were counted after sequential CARD-FISH.

The *Tenacibaculum* cell count indicated that with *Z. galactanivorans* WT strain, the final density of *Tenacibaculum* was almost twice higher than when grown with the mutants. This observation suggests that the growth of *T. aestuarii* is tightly dependent on the growth of *Z. galactanivorans* (**Figure VII.3B**). Δ*alyA1* and Δ*ausR* have lower growth rate, as such, they released fewer degradation products for *T. aestuarii* consumption, whose growth was consequently impacted. *T. aestuarii* exhibits a growth even despite the absence of the protein AlyA1, which is the main secreted alginate lyase secreted by *Z. galactanivorans* (its deletion led to an important decrease of released of uronic acid on alginate and algae, Zhu *et al.*, 2017). It could suggest that *T. aestuarii* can grow with low amount of oligo-alginate and/or potentially use products derived from other carbon sources or secondary metabolites. On the other hand, this *T. aestuarii* growth observed with Δ*alyA1* is twice lower compared with WT which lets us think that *T. aestuarii* growth might be tightly coupled with the release of oligo-alginates and that it can use them for its growth. A limited release of oligo-alginates also induced a lower growth of *Z. galactanivorans* that might then release fewer secondary metabolites usable by *T. aestuarii.* Many hypotheses are possible regarding the carbon source that might favor the growth of *T. aestuarii* and the latter likely benefits from various types of degradation products. It should also be noticed that *Zobellia* was not outcompeted by *Tenacibaculum* as its density was 10 times higher. The *T. aestuarii* increase seems delayed compared to *Z. galactanivorans* (**Figure VII.3B**). *T. aestuarii* growth possibly starts after a sufficient accumulation of degradation products or secondary metabolites, suggesting that the ratio might equilibrate later during the degradation. For example, with Δ*ausR* co-culture, the *Zobellia* density was only 3 times higher than *Tenacibaculum* after 137 h (data not shown). Such succession pattern was illustrated by Datta *et al.*, 2016 and Pontrelli *et al.*, 2021 during chitin degradation.

2. Attempts to characterize *Z. galactanivorans*/*T. aestuarii* cooperative interactions

Further experiments to characterize the interactions were carried out with the pair *Z. galactanivorans*/*T. aestuarii* using different strategies. First, *T. aestuarii* was grown with the soluble products released by *Z. galactanivorans* during the degradation of *L. digitata*, without the addition of fresh algal pieces (**Figure VII.4**, top row). No growth was detected (data not shown), meaning that the strain was unable to use the low molecular weight sugars or the metabolic by-products exposed by *Z. galactanivorans.* No alginate lyases or alginate downstream processing enzymes were predicted in *T. aestuarii* genome, suggesting it is probably unable to use alginate oligosaccharides produced by *Z. galactanivorans*. It is also possible that metabolites from *Z. galactanivorans* are not stable and need to be freshly released to be assimilated by *Tenacibaculum*. Physical contact between *T. aestuarii* and *Z. galactanivorans* and/or the algae might also be needed. The two bacterial partners might form aggregates to avoid product diffusion and allow *T. aestuarii* to efficiently uptake the products released by *Z. galactanivorans* (Ebrahimi *et al.*, 2019). Another possibility lies in the fact that the interactions might not rely on chemical interactions but rather on biological or physical mechanisms (Worrich *et al.*, 2019). For example, via cell aggregation, *Zobellia* might act as a physical barrier, protecting *T. aestuarii* from the toxic compounds released by algae under stress.

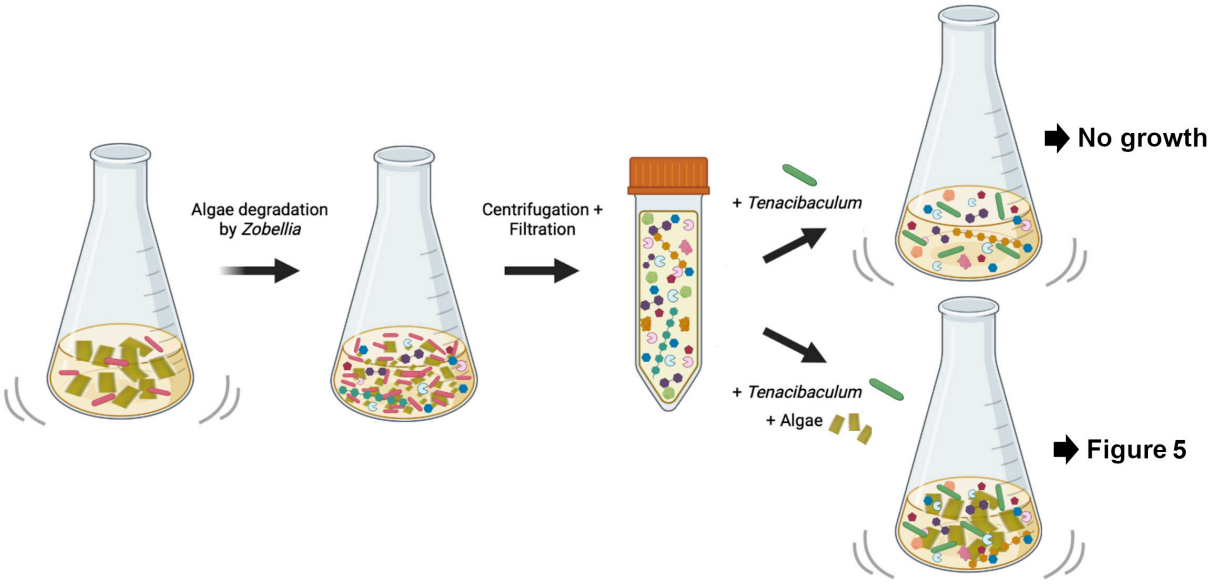

Figure VII.4: Schema of the experiments carried out to assess the impact of the products released by *Z. galactanivorans* Dsij^T on *T. aestuarii* SMK-4^T growth. *Z. galactanivorans* (depicted as pink cells) was grown with *L. digitata* and the culture supernatant containing the soluble products (i.e. secreted enzymes, degradation products and secondary metabolites) was filtered with a 0.2 µm cut-off to remove bacterial cells. *T. aestuarii* (depicted as green cells) was grown on the filtrate with or without the addition of fresh algae. Different cut-off could be applied to separate the degradation products. Illustration prepared using the BioRender app (https://app.biorender.com/).

The same experiment was implemented with the addition of new fresh algal tissues in the filtered spent medium (**Figure VII.4**, bottom row). The aim was to test whether *T. aestuarii* exploits the enzymes

secreted by *Z. galactanivorans* (public goods) to use fresh algal compounds. First, I observed a bacterial growth in the non-inoculated controls (**Figure VII.5A**, black solid line), while it was not the case with algae in fresh MMM (black dotted line). The newly added algae were fully degraded after 3 days, indicating that the enzymes released by *Z. galactanivorans* were still active and effectively broke down the algae. CARD-FISH analysis with DAPI counterstaining confirmed the presence of bacteria and revealed the cells did not belong to the genera *Zobellia* or *Tenacibaculum* (**Figure VII.5B**). Therefore, products released by *Z. galactanivorans* could favor the growth of natural epiphytic bacterial communities resistant to the antibiotics used, highlighting once again its probable role of sharing pioneer within the communities. Bacterial growth reached higher densities in the microcosms where *T. aestuarii* was inoculated in the spent medium with fresh algae (**Figure VII.5A**, red solid line), and CARD-FISH confirmed that cells belonged to *Tenacibaculum* (**Figure VII.5B**). However, this result cannot be directly interpreted as cross-feeding of *T. aestuarii* on *Z. galactanivorans* products when considering another control performed in parallel. Indeed, during this experiment *T. aestuarii* was also able to grow in fresh minimum medium with *L. digitata* as the sole carbon source (**Figure VII.5A**, red dotted line). This ability of *T. aestuarii* to grow alone on algal tissues is in contradiction to what I previously observed (**Figure VII.2** and **VII.3**) and was further confirmed in additional experiments (data not shown). This experiment was performed with algae harvested in January 2021 (and the same observation was made in March 2021) while the previous screening was done in June-July 2020. It is likely that the algal chemical composition and the algal microbiota vary with the seasons and/or the environmental parameters, which might impact *T. aestuarii* growth. Schiener *et al.*, 2015 studied the seasonal variations of *L. digitata* thallus chemical composition. However, the same study also assessed that the highest polyphenol levels were found in summer. Such compounds were already reported to exhibit an antimicrobial activity (Nagayama *et al.*, 2002). Protein content in algae, which were reported to be highest in the first quarter of the year, might also partially control the growth of the *Tenacibaculum* spp. Hence the algal compounds used by *T. aestuarii* might be less abundant or less accessible during the summer months. By breaking down the extracellular algal matrix, *Z. galactanivorans* might enhance their accessibility or expose other low molecular weight carbon sources, favoring *T. aestuarii* growth. Overall, our results suggest that cooperative interactions within the bacterial communities might be seasonally dependent.

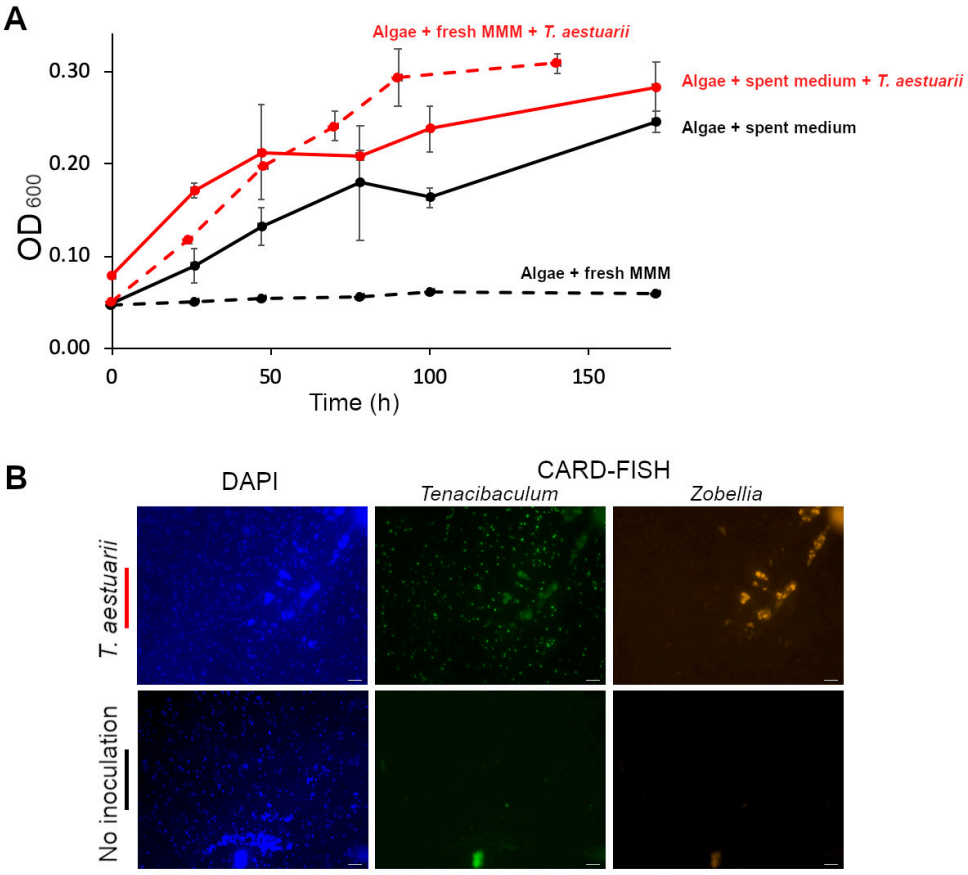

Figure VII.5: *T. aestuarii* SMK-4^T growth with *L. digitata* in medium containing degradation products released by *Z. galactanivorans* Dsij^T. (A) Bacterial growth in microcosms supplemented with fresh *L. digitata* in fresh MMM (dotted line) or in the supernatant collected after *L. digitata* degradation by *Z. galactanivorans* (solid line) (schema in Figure VII.4, bottom row). Values are replicate mean ± s.d. (n = 2). (B) Micrographs obtained after CARD-FISH analysis on culture medium containing the spent supernatant (t = 171 h). Left: DAPI counterstaining. Middle: CARD-FISH *Tenacibaculum* specific signal. Right: CARD-FISH *Zobellia* specific signal. Scale = 10 µm.

3. Screening for other opportunistic partners within the genus *Tenacibaculum*

Interestingly, we found out that *T. aestuarii* SMK-4^T was able to use fresh macroalgae in the absence of *Z. galactanivorans*. We decided to determine if this ability was shared or not within the genus to further select potential opportunistic partners that would require the presence of *Z. galactanivorans* to grow.

The 21 *Tenacibaculum* strains available in the laboratory were grown with intact *L. digitata* collected in March 2021 as the sole carbon source (**Figure VII.6A**). Ten strains displayed a significant growth on algal tissues (final OD between 0.2 and 0.5, red curves). No sign of tissue degradation was visible for any strain suggesting that they do not use the main structural component of brown the algal extracellular matrix (alginate and FCSPs) for their growth but rather algal exudates or algal metabolites. This would explain the limited growth compared with *Z. galactanivorans* that has a final cell density around 1.5-2 (see for example **Figure VII.1A**). They might instead feed on algal exudates (algae cut might have favored exudation) or various algal metabolites. The growth of 4 other *Tenacibaculum* strains remains

unclear (orange curves) as very slow increases were detected at one time point or replicate curves did not follow the same trend, while seven strains did not grow at all on the algae (green curves). For two strains, the growth on macroalgae varied according to the season as *T. aestuarii* SMK-4^T and *T. crassostreae* JO-1^T grew on algal tissues collected in March but not in June. While with two other strains, the presence or absence of growth was similar regardless of the harvesting period (*T. litoreum* CL-TF13^T and *T. skagerrakense* D30^T). Hence for some strains, the growth on macroalgae might be driven by seasonal parameters.

Different physiological behaviors were observed within the *Tenacibaculum* genus. The capacity to use algal compounds seems to be conserved between strains of the same clade (**Figure VII.6B**). Comparative genomic analysis would help unravel the mechanisms enabling the assimilation of algal compounds.

As mentioned in the introduction, none of the *Tenacibaculum* spp. were able to grow in MMM supplemented with glucose or starch, potentially because of amino acid autotrophies. However, in this study I evidenced the growth, in presence of *L. digitata* as carbon source, of at least 14 *Tenacibaculum* strains out of the 21 tested, either in monoculture or in co-culture with *Z. galactanivorans*. It would suppose that algal tissue (or their treatment-resistant microbiota) would provide amino acids necessary for their growth of *Tenacibaculum* strains as well as vitamins or co-factors.

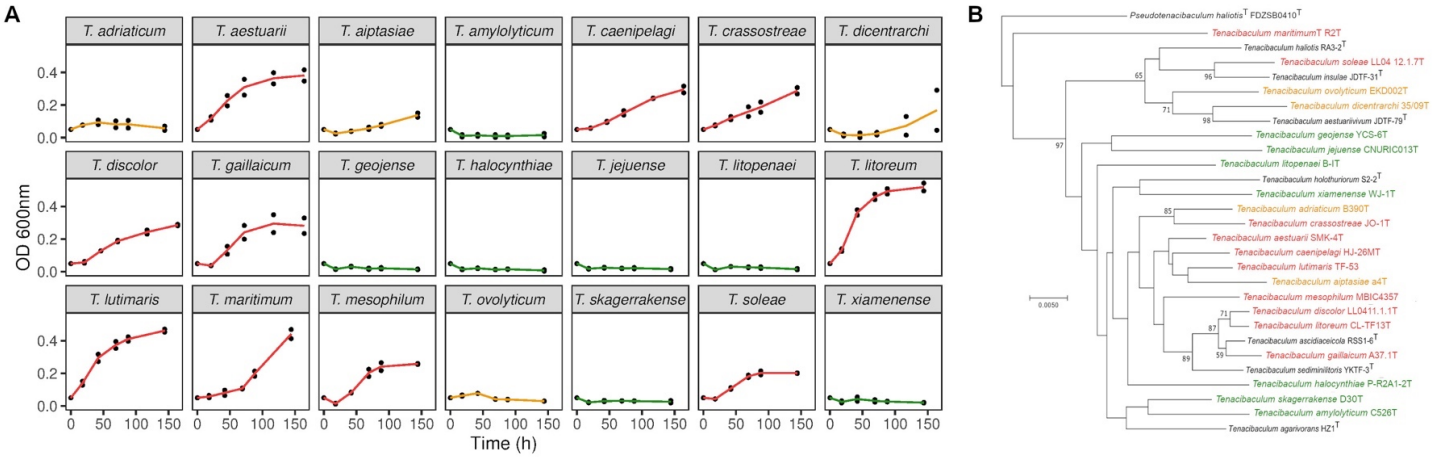

Figure VII.6: Fresh algal utilization by *Tenacibaculum* spp. (A) Growth of the 21 *Tenacibaculum* strains on *L. digitata* tissues. Lines are means of independent replicates (n = 2) and were colored according to the growth behavior of the strain. Red: final OD between 0.2 and 0.5; Orange: unclear behavior (slow increase, replicate variability); Green: no growth. (B) Phylogenetic tree of the 16S rRNA gene from described species belonging to the genus *Tenacibaculum*. Done by the Drs. Tristan Barbeyron and Gurvan Michel and modified to color the strain names according to their ability to grow on fresh tissues as in panel A.

The seven strains unable to grow alone with fresh algae as carbon source were cultivated in mono and co-culture with *Z. galactanivorans* to screen for opportunistic interactions (**Figure VII.7**). No growth was detected in monocultures, confirming the previous observations. CARD-FISH analyses performed on the medium after 4 days of culture revealed that *T. halocynthiae* P-R2A1-2^T grew in the co-culture,

$5.4x10^5$ cells per µl were counted at 92 h. However, this amount is 50 times lower than what was obtained for *T. aestuarii* SMK-4^T suggesting only limited cooperative interactions. This result still needs to be confirmed in another independent experiment.

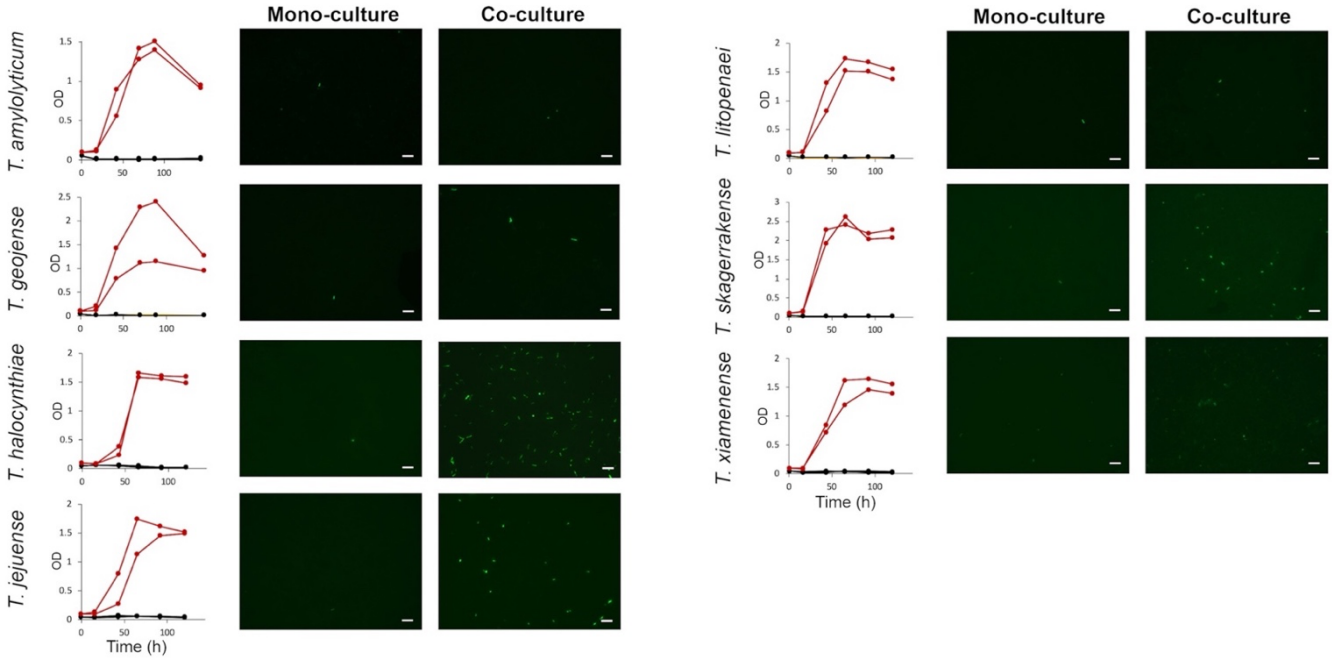

Figure VII.7: Screening for opportunistic interactions between *Z. galactanivorans* Dsij^T and selected *Tenacibaculum* strains. Bacterial density of the mono- (black) and co-cultures (red) are shown on the left (conducted in duplicates). Micrographs show CARD-FISH signal specific to *Tenacibaculum*. Scale = 10 µm

I did not have the time to perform further experiments to characterize the interactions with this newly identified opportunistic strain. To avoid potential issues with the stability of the released degradation products, co-culture systems as shown in **Figure VII.8** are available in the laboratory and would be useful to follow distinctly the growth of each partner in real-time. Filters with different cut-off can be used to distinguish among the degradation products and help to formulate hypotheses on the type(s) of interactions occurring.

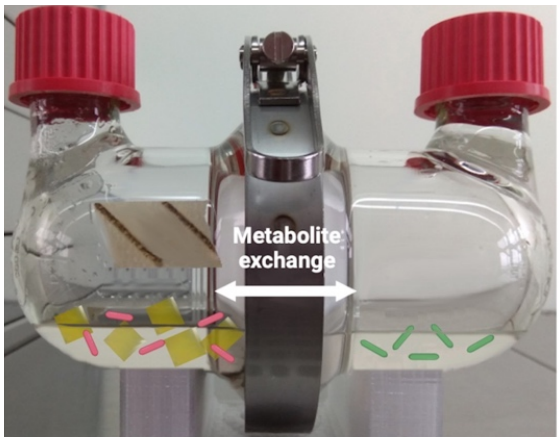

Figure VII.8: Co-culture system designed to physically separate the two partners while allowing the metabolic exchanges. This specific vessel is sold by Witeg (ref 0861050, Germany). Photo was modified with BioRender.

IV. Conclusion

In this chapter, it was shown that if *T. aestuarii* SMK-4^T and *T. halocynthiae* P-R2A1-2^T were not able to use fresh algal tissues in monoculture, the presence of *Z. galactanivorans* Dsij^T allowed them to grow. It confirmed the existence of cooperative interactions between these two genera as reported by Zhu *et al.*, 2017. Initially, we aimed to characterize these interactions by incubating the opportunistic partner with the degradation products released by *Z. galactanivorans*, filtered at different cut-offs in order to distinguish between enzymes and secondary metabolites. This would allow to test which type of products benefits the opportunists. We assessed that *T. aestuarii* was not able to grow on spent medium from algal degradation by *Z. galactanivorans*, the degradation products being potentially unstable, not concentrated enough (too diffuse in the medium), or maybe because the interactions are based on physical mechanisms. The seasonal variability of macroalgae thallus made any further characterization difficult as *T. aestuarii* later showed the ability to assimilate fresh algal tissues in the absence of *Z. galactanivorans*. This result emphasizes that within the communities the metabolic interaction might vary depending of different parameters and in particular according to season. Such phenomenon was reported in Zhao *et al.*, 2016 and Lin *et al.*, 2019 which demonstrated important variations in co-occurrence networks between seasons for freshwater bacterial communities. Interaction characterization was not performed with *T. halocynthiae* due to time issues, but the limited growth detected in the presence of *Z. galactanivorans* would suggest that it might not be the most relevant partner to further characterize these interactions.

Other potential opportunistic bacterial partners may need to be considered to characterize cooperative interactions during algal degradation and several criteria might be essential to consider. Bioinformatic analyses would be useful to assess the genomic capacities of a strain to degrade algal polysaccharides and interact with macroalgae (presence of genes putatively involved in the response to algal defense, biofilm formation, etc.). This would help to identify putative candidates involved in algae recycling and their role in this process. Such approach was implemented by Pollak *et al.*, 2021 during the degradation of chitin: they developed a genomic-based model to predict pioneers, exploiters and scavengers within natural communities by detecting genes evolutionarily and/or physically (colocalized in the genome) linked to chitinases. They concluded that chitin public good exploiters are active in natural chitin degrading microbial communities. Hence an alternative could be to select opportunistic partners frequently found in macroalgae-dominated habitats. Looking for partners living in the same ecological niches as *Zobellia* members, whose widespread distribution on macroalgae was assessed in Chapter IV (Part 2), is also more ecologically relevant as established interactions are more likely to occur between them rather than with microorganisms living in different environments. *Tenacibaculum* spp. were already reported on macroalgae but members of the genus were mainly isolated from marine animals or sediment (see references in **Table II.2**). In this chapter we showed that natural algae-attached bacteria,

resistant to the antibiotics used and cultivable in the laboratory, could potentially exploit public goods or scavenge by-products released during the algal degradation by *Z. galactanivorans* Dsij^T. Communities enriched on macroalgae in decomposition might also represent a relevant source of potential natural candidates as degradation metabolic processes might be highly active in those environments. In Chapter IV, we sampled the microbiota of diverse healthy and decaying macroalgae through the year. In the near future, metabarcoding analysis on the DNA and RNA extracted from these samples might bring more information regarding the composition of this community and co-occurrence networks could be performed on these data to identify potential interactions between *Zobellia* and other taxa. CARD-FISH allows specific single cells detection within the biofilm and could also help to select opportunist taxa. As interactions might be favored by a close spatial localization to limit the diffusion of the released metabolites, the identification of physically associated taxa with *Zobellia* might be relevant.

When possible, comparative genomics with such taxa tightly associated with macroalgae could be performed to screen for strains that share important genomic similarities with *Z. galactanivorans* Dsij^T without encoding key genetic determinants for fresh algal degradation as they might be relevant candidates as exploiters.

The ecological strategies observed within natural communities from macroalgae-dominated habitats would help to identify a broad range of potential opportunistic candidates. The construction of specific synthetic communities encompassing these relevant taxa could be a more efficient approach to evidence and characterize interactions taking place during algae assimilation.

Chapter VIII:

General Discussion

Par Nolwen Le Duff

The objectives of my PhD project were to decipher the ecological and metabolic strategies of specialist bacteria during the degradation of fresh macroalgae. The bacterial catabolic mechanisms governing the utilization of various algal polysaccharides have been unveiled the last 20 years. By contrast, to my knowledge, there is no extensive study reporting information on the mechanisms controlling the utilization of fresh algal tissues as they appear in the environment. I tried to fill this gap by addressing the metabolic and ecological strategies that drive macroalgae utilization at different scales, from the study of the bacterial community composition during an *in situ* degradation process to the preliminary characterization of a specific PUL induced by macroalgae (**Figure VIII.1**). Diverse complementary approaches were implemented, including microbiology, transcriptomics, biochemistry, genomics and bioinformatic analysis. The flavobacterial species *Zobellia galactanivorans* Dsij^T was used as a study case to unravel the strategies of bacteria able to initiate the breakdown of macroalgae.

I. What did we learn?

I first studied the degradation of macroalgae from a global ecological point of view by assessing the impact of the accumulation and degradation of kelps on the bacterial communities (Chapter III). Through a collaborative study with ecologists we revealed the dynamic succession of the bacterial epiphytic communities during a 6-month *in situ* experiment simulating kelp detritus accumulation. The accumulation led to variations in abundance, taxonomic composition and structure of the epiphytic bacterial communities and to a lesser extent of the underlying sediment communities. A biphasic succession of the epiphytic communities was identified. The initial resident microbiota was first rapidly outcompeted by specific taxa known as algal-polysaccharide degraders such as *Bacteroidia* members. The tissues were later colonized by other taxa acting as secondary colonizers. Those distinct phases of succession would suggest different ecological strategies within the bacterial communities with early degraders that would initiate the degradation and expose new substrate niches for other less specialized populations that would dominate the microbiota during the late stage of the degradation.

After this overview in the behavior of the whole bacterial communities during macroalgae degradation, I focused on specialist algal-polysaccharides degraders and on the genus *Zobellia* in particular. Its high abilities to degrade algal polysaccharides are well-known and polysaccharide utilization systems of *Z. galactanivorans* Dsij^T have been largely studied during the last 20 years. However, the distribution of the genus *Zobellia* in the environment was never assessed. In Chapter IV, I optimized and validated qPCR and CARD-FISH protocols for the specific detection of the genus *Zobellia* in macroalgae-dominated habitats. CARD-FISH probes were used to study the behavior of *Z. galactanivorans* Dsij^T during the degradation *in vitro* experiments, as shown in Chapter V. These new tools will also be powerful approaches to assess the ecological strategies of *Zobellia* spp. in the wild and bring out their interactions with their host or with the other bacterial community members. As a first example of application, qPCR was applied in this thesis to determine the seasonal variations in the prevalence and

abundance of *Zobellia* spp. at the surface of distinct macroalgae. *Zobellia* spp. were detected on the five species of macroalgae I sampled, suggesting that the genus is part of the resident algal microbiota and establishes stable interactions with algae. The relative and absolute abundance of the genus *Zobellia* varied depending on the seasons as it peaked in February-March and October-November (0.3-0.5 %) and was at its lowest in July-August (0-0.002 %). We evidenced that *Zobellia* spp. abundance might be driven by temperature fluctuations and suggested that algal thallus composition might also explain its abundance variations. This study also revealed an important enrichment of *Zobellia* spp. on stranded decaying algae (up to 8 %), a very interesting result that highlights the important role of the genus during the algal degradation process.

In Chapter V, I unveiled the ability of the *Zobellia* spp. to initiate the degradation of fresh macroalgae. All were able to grow with algal tissues as the sole carbon source but only *Z. galactanivorans* Dsij^T caused important tissue damages. The others strains might likely lack some key genetic determinants for a drastic degradation of the ECM. Consequently, I narrowed the study window on the strain *Z. galactanivorans* Dsij^T to decipher the specific metabolic mechanisms involved in the utilization of fresh macroalgae. It was able to initiate the utilization of three brown macroalgal species, *Laminaria digitata*, *Fucus serratus* and *Ascophyllum nodosum,* and to completely decompose the thallus of *L. digitata.* Its capacity to perform the initial attack of the ECM by secreting extracellular enzymes, even when it is not in contact with the algal tissues, revealed its role as a sharing pioneer taxon. Its transcriptomic profile shifted toward the induction of several PULs dedicated to the utilization of brown algal ECM polysaccharides (alginate and FCSPs). Interestingly, a subset of genes was specifically induced in cells grown on intact algae compared to soluble polysaccharides. It notably includes genes involved in protection against oxidative burst, type IX secretion system proteins and novel uncharacterized PULs. *Z. galactanivorans* Dsij^T growth was also tested with red algae tissues. Its capacity to use fresh red macroalgae as the sole carbon source seemed dependent of the thallus composition and we suggested that the presence of a proteic cuticle at the surface of several red macroalgal species might hinder the accessibility of the polysaccharides.

One of the uncharacterized PULs induced during fresh brown macroalgae degradation and predicted to be involved in FCSP assimilation, was further studied in Chapter VI. I initiated its bioinformatic and biochemical characterization. I experimentally showed an activity of different enzymes (a PL40, a GH88 and a PLnc) on FCSPs for the first time for *Z. galactanivorans* Dsij^T and proposed a potential catalytic cascade of these different CAZymes. I conclude that the substrate targeted by this PUL would be FCSPs rich in uronic acids, with a structure likely similar to rhamnogalacturonan-II.

As discussed in Chapter III, the bacterial communities exhibit different functional groups likely implementing different strategies to use algal compounds. In the Chapter V, I demonstrated the sharing pioneer behavior of *Z. galactanivorans* Dsij^T during fresh macroalgae degradation, suggesting that the

degradation products could further support the growth of other taxa. Chapter VII was thereby devoted to identify cooperative interactions during macroalgae degradation, between the pioneer strain *Z. galactanivorans* Dsij^{T} and *Tenacibaculum* spp. that were predicted as potential opportunistic bacteria. Using the newly designed CARD-FISH *Tenacibaculum*- and *Zobellia*-specific probes (Chapter IV), I successfully demonstrated that the degradation of fresh macroalgae by *Z. galactanivorans* Dsij^{T} favored the growth of *T. aestuarii* SMK-4^{T} and *T. halocynthiae* P-R2A1-2^{T} while these two strains did not grow in its absence. Several approaches were intended to characterize the mechanisms that would govern such interactions, but the results of the experiments implemented did not allow us to determine specific types of interactions.

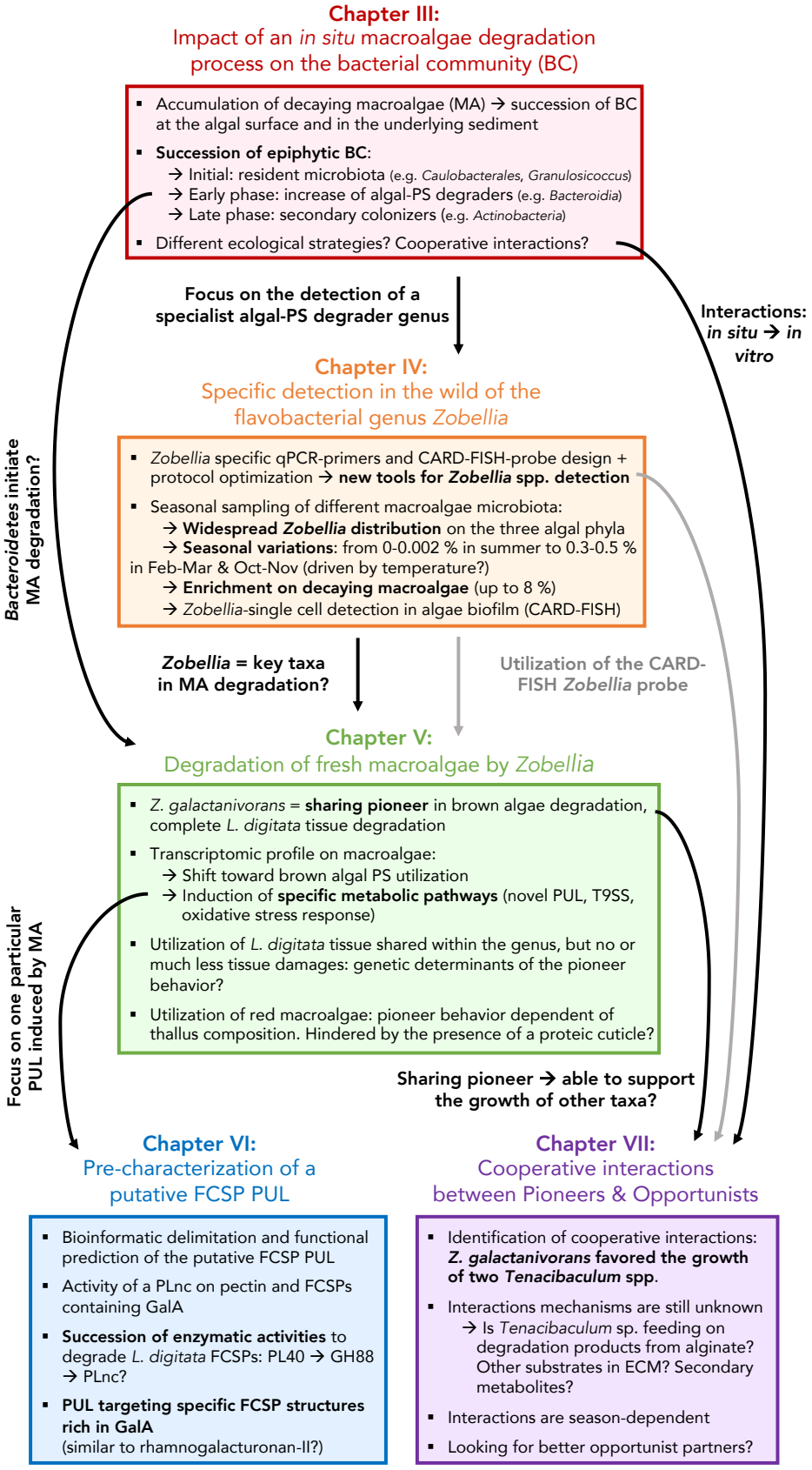

Figure VIII.1: Schematic depicting the main conclusions of my thesis and the different connections between the chapters. BC: bacterial communities; MA: macroalgae; PS: polysaccharides; FCSP: fucose-containing sulfated polysaccharides; PL: polysaccharide lyase; GH: glycoside hydrolase; PUL: polysaccharide utilization loci; T9SS: type-IX secretion system; GalA: galacturonic acid.

II. Focus points

1. Importance to consider whole algal tissues to study bacterial degradation

In comparison to purified polysaccharide degradation, the utilization of fresh macroalgae tissues is more time-consuming as it requires collecting algae in the wild (the experiments are then depending on the tide cycles and coefficients). Algae need to be treated beforehand to limit contaminations within the microcosms. Moreover, algae are living organisms whose composition and microbiota is changing according to many biological and physico-chemical parameters. The reproducibility of the experiments might then become difficult (Chapter V and VII are good examples) and interpretations are more complex as many variables need to be considered. The use of cultured algae could limit this variability as algae are grown in controlled conditions. However, algae cultivation is a complicated and long-time process, protocols are only available for a limited number of algal species and cultures would not be fully axenic. The ECM composition would also likely differs from the wild specimens (thicker and probably more complex thallus in the wild) and the responses might not be representative to what happen in the field.

Considering whole algal thallus and not just extracted purified polysaccharides is crucial to improve our comprehension of macroalgae recycling. I showed here that some metabolic regulations occurring during the utilization of fresh macroalgae differed from the responses detected with single purified polysaccharides. This approach allowed me to shed light on the function of uncharacterized PULs involved in macroalgae degradation, whose induction was undetectable using the purified polysaccharides (a screening with a large set of substrates might have helped to reveal their importance but that would have been less efficient). Some substrates might represent only minor fractions of the algal thallus and might then be hard to extract. Moreover, polysaccharide extraction protocols likely modify the way they appear in nature by modifying their composition and structure. It might be particularly true with FCSPs that are strongly heterogeneous. The utilization of mixture of carbon sources encountered in the algal tissues could also be monitored at different time points to assess potential substrate prioritization order. Besides unraveling specific carbohydrate utilization systems, the growth on fresh macroalgae also brings out other essential functions to feed on algal tissues such as oxidative stress response and the specific secretion system T9SS.

Also, the use of macroalgae could help to distinguish more precisely the different behaviors taking place in microbial communities and assess different functional group based on their catabolic abilities. We already know that some taxa are able to breakdown intact algal ECM, such as *Z. galactanivorans* Dsij^{T}. By contrast, some taxa can use purified algal polysaccharides but cannot initiate the attack of the ECM, such as *Alteromonas macleodii* toward *Ecklonia* sp. (Koch *et al.*, 2020) and other non-specialist taxa can only feed on the released degradation products.

As their tissues were completely disintegrated in the presence of *Z. galactanivorans* Dsij^T, *Laminaria digitata* as a brown alga and *Grateloupia turuturu* as a red alga emerged as the best algal species to go deeper in the characterization of the mechanisms governing macroalgae recycling.

2. Relevance to use *Z. galactanivorans* Dsij^T as a model of pioneer bacteria

The different results obtained in this thesis strengthen the relevance of *Z. galactanivorans* Dsij^T as study case to unravel the mechanisms controlling macroalgae degradation. The strain was already well-known as a model to study purified algal polysaccharide degradation and allowed the discovery of several metabolic pathways. Here, by assessing its role of sharing pioneer in macroalgae degradation, we showed that it is also a relevant model to start to decipher the mechanisms controlling the initial attack of fresh macroalgae tissues. Moreover, the *Zobellia* genus is widespread on macroalgae and its proportion at the surface of decaying algae is largely increased compared to healthy ones. These results support the assumption that thanks to its potent catabolic abilities, the genus actively participates in the decaying process of macroalgae in the wild, strengthening its ecological importance. *Z. galactanivorans* Dsij^T was also reported to allow the growth of non-specialist taxa with fresh tissues. Hence, besides being a relevant strain for unraveling new catabolic mechanisms, we suggested it would also be a valuable candidate to study bacterial-macroalgae interactions as well as cooperative interactions within the bacterial communities, using the newly developed molecular tools for its specific detection.

III. Perspectives

1. The exploration of the *Z. galactanivorans* CAZome still has a long life ahead

The degradation systems for the utilization of the main algal polysaccharides of brown and red algae were already characterized for *Z. galactanivorans* Dsij^T, except for FCSPs whose degradation mechanisms are particularly difficult to identify given its structural complexity. In order to pursue the discovery of novel CAZymes and novel enzymatic activities, the implementation of integrative studies on fresh macroalgae are crucial. The transcriptomic analysis carried out in this project revealed which predicted PULs were of particular interest, allowed their better delimitation, identify good candidates for further biochemical characterization and informed on the nature of the natural targeted substrate. This approach greatly facilitated the preliminary characterization of a PUL involved in FCSPs degradation. We now have an idea of the type of structures targeted by the PUL and demonstrated the activity of several enzymes. Further works need to be performed following this study to characterize the first complete assimilation pathway of FCSP structures in *Z. galactanivorans* Dsij^T. They should focus on the characterization of the released oligosaccharides and include enzymatic assays on a larger set of

substrates, especially FCSPs with pectin-like structures. The Marine Glycobiology group is strongly interested in FCSPs degradation by other marine heterotrophic bacteria under the BreakingAlg project coordinated by Gurvan Michel. The future outcomes could help in the deeper characterization of the *Z. galactanivorans* PUL studied in this thesis. For example, purified FCSPs oligosaccharides resulting from enzymatic degradation could potentially be used as new substrates and comparative genomic analyses could improve functional predictions.

Using transcriptomic analyses and comparative genomics among the *Zobellia* spp. I shed light on several genes that might confer to *Z. galactanivorans* Dsij^T its unique ability to initiate the attack of the algal ECM. Among the described strains I tested, only *Z. galactanivorans* Dsij^T completely degrades the *Laminaria* tissues. However, another *Zobellia* strain recently isolated by the group but not yet described (F. Thomas, personal communication) was also tested and caused important tissue damages. The sequencing and annotation of its genome and its integration in the comparative genomic analyses would help to better target relevant candidate genes for the breakdown of intact biomass. The construction of *Z. galactanivorans* Dsij^T deletion mutants for these candidate genes should be performed in the future. Testing the abilities of the mutant strains to use fresh algal biomass and to favor the growth of other taxa will help to investigate the biological role of the knocked-out genes in the pioneer behavior of the strain. A deletion protocol for *Z. galactanivorans* Dsij^T was developed and already applied to assess the crucial role of the alginolytic enzyme AlyA1 in the degradation of intact macroalgae (Zhu *et al.*, 2017).

In this thesis I mostly focused on the degradation of brown macroalgae. To better understand macroalgae recycling in coastal ecosystems, future studies should also seek to unravel strategies to breakdown red macroalgae. I already reported growth differences between the utilization of red and brown algae. Indeed, *Z. galactanivorans* Dsij^T was successfully grown with the three brown algae tested but with only one red macroalgae over the five tested. I suggested that the cuticle of some red algae might hinder its abilities to initiate the attack of the ECM. A screening for its growth on a larger set of red and brown macroalgae would allow a better characterization of its pioneer behavior and would also help to find more red algae species that *Z. galactanivorans* Dsij^T can use for its growth. It would be interesting to assess the transcriptomic profile of *Z. galactanivorans* Dsij^T during the degradation of such species and compare the regulation of genes involved in carbohydrate degradation (as it was done for purified polysaccharides by Thomas *et al.*, 2017), but also in stress response, biofilm formation and secretion systems. An analysis of gene expression at different time points during the degradation should also be carried out to describe more precisely the different steps of the degradation process. Such detailed study would help to identify substrate prioritization and to gain insights into the ECM composition. The induction of some specific PULs or more generally of gene clusters might suggest the presence of still poorly characterized compounds (because they are poorly abundant and/or difficult to extract). Carbohydrates-binding proteins contained in such PULs, as SusD proteins or CBMs, could be used as probes to detect those poorly characterized polysaccharides within algal ECM (Salmeán *et al.*, 2018).

2. The detection of *Zobellia* in the wild: promising perspectives

In this project, I successfully developed two complementary molecular tools for the specific detection of *Zobellia* in the wild. To complement the seasonal monitoring on macroalgae presented in Chapter IV, I performed 16S rRNA gene metabarcoding on all the DNA samples. Sequence analysis will help to link the variations in abundance of the genus *Zobellia* with the succession of other taxa. Besides this seasonal study, the prevalence and abundance of the genus *Zobellia* was also assessed in different seawater fractions (inferior or superior to 3 µm) at the Estacade SOMLIT station (Roscoff coast) over 8 years within the ALGAVOR project (F. Thomas, personal communication). An extensive utilization of the qPCR specific primers on healthy, diseased or decaying macroalgae from different geographical locations and through several years, as well as its detection in seawater and in marine sediment would greatly improve our knowledge on the functional role of this genus. Moreover, these *Zobellia*-specific primers will greatly facilitate the isolation of new *Zobellia* strains as they will reveal relevant ecological niches to sample and can be used to screen the isolates and hence sequence only the *Zobellia* strains.

The utilization of the CARD-FISH *Zobellia*-specific probe is really precious for laboratory experiments. I used it here as a way to check for bacterial contaminations, to assess tissue colonization during the degradation and to identify cooperative interactions with other taxa. Its efficiency on wild samples is more difficult as *Zobellia* cells represent less than 0.5 % of the community on healthy algae. The signal of the few cells is also masked by the strong algal autofluorescence. The protocol needs to be improved (for example by testing resin inclusion techniques) to assess precisely the spatial localization of the genus within the biofilm. Coupled with probes targeting other taxa it would help unveil the localization of single *Zobellia* cells within the spatial organization of bacterial communities and hence identify potential bacterial interactions. In particular, a method allowing the simultaneous detection of numerous taxa was developed (Valm *et al.*, 2012) and successfully applied on kelp tissue (Ramirez-Puebla *et al.*, 2020).

3. Macroalgae degradation at the community scale

This thesis shed light on the succession of the bacterial communities during degradation in order to underline the importance of specific taxa during this process and identify different functional strategies. Specific bacterial interactions were identified between *Z. galactanivorans* Dsij^T and *Tenacibaculum* spp. but their characterization was difficult. Most members of the *Tenacibaculum* genus were not isolated from macroalgae, unlike *Zobellia* strains. Hence the selection of specific putative opportunist partners within algae microbiota might be more ecologically relevant as established interactions are more likely to occur between taxa sharing the same ecological niches in natural environment. I showed in Chapter VII that natural epiphytic communities could grow with macroalgae degraded by the secretome of *Z. galactanivorans*. Such strains exhibiting an opportunist behavior could be isolated to build specific

synthetic communities. The use of those communities could greatly improve the attempts to decipher the mechanisms governing the interactions.

Moreover, a recent approach developed by Thomas *et al.*, 2020 coupled the labeling of cultured brown algal biomass with ^{13}C with HISH-SIMS and DNA-SIP to detect cell-specific alginate uptake and identify alginate incorporators (Thomas *et al.*, 2021). ^{13}C-labelled macroalgae tissues are of great interest to trace the fate of algal biomass during the degradation and would allow the identification of taxa specifically involved in the uptake of fresh macroalgae. Isotopic tracing would thereby be a powerful tool to unravel and characterize bacterial interactions. It would be a way to monitor the incorporation of fresh algal tissues in the cells through time either when focusing on interactions between two selected partners, but also within natural bacterial communities to decipher the different ecological strategies taking place in these complex assemblages.

4. A valuable strain for biotechnological applications?

This thesis might also pave the way for future biotechnology applications based on the valorization of cultured or stranded algae. Given its potent capacities to entirely breakdown fresh macroalgal biomass, such as *L. digitata* or *G. turuturu* tissues, *Z. galactanivorans* would constitute a valuable microorganism to implement biological alternatives (less energetic) to the actual physico-chemical pre-treatments applied in the macroalgae refinery process. Hence, the utilization of its secretome, and in particular of key enzymes identified as essential for an efficient tissue degradation, could be developed in industrial protocols seeking to optimize the initial macroalgae hydrolysis using natural methods. This non-GMO and non-pathogenic strain able to process algal biomass could then be of particular interest in industries that are subject to many safety standards (e.g. cosmetics, pharmacy, etc.).

Overall, this thesis represents the first attempts to decipher the strategies of pioneer bacteria during the breakdown of fresh macroalgae. Our results advance the understanding of the mechanisms governing macroalgae recycling by marine heterotrophic bacteria and open many doors for promising future studies.

Annexes

Annexe 1: Thomas, F., Dittami, S.M., Brunet, M., Le Duff, N., Tanguy, G., Leblanc, C., and Gobet, A. (2020) Evaluation of a new primer combination to minimize plastid contamination in 16S rDNA metabarcoding analyses of alga-associated bacterial communities. *Environ Microbiol Rep* **12**: 30-37

In this paper, I did the DNA extractions from the microbiota of *L. hyperborea* samples.

environmental microbiology reports

Environmental Microbiology Reports (2020) **12**(1), 30–37 doi:10.1111/1758-2229.12806

EMIR - Brief report

Evaluation of a new primer combination to minimize plastid contamination in 16S rDNA metabarcoding analyses of alga-associated bacterial communities

François Thomas,[1*] Simon M. Dittami,[1] Maéva Brunet,[1] Nolwen Le Duff,[1] Gwenn Tanguy,[2] Catherine Leblanc[1] and Angélique Gobet[1,3*]

[1]*Station Biologique de Roscoff (SBR), Sorbonne Université, CNRS, Integrative Biology of Marine Models (LBI2M), 29680, Roscoff, France.*

[2]*Station Biologique de Roscoff, CNRS, Sorbonne Université, FR2424, Genomer, 29680, Roscoff, France.*

[3]*MARBEC, Ifremer, IRD, Université de Montpellier, CNRS, 34203, Sète, France.*

Summary

Plant- and alga-associated bacterial communities are generally described via 16S rDNA metabarcoding using universal primers. As plastid genomes encode 16S rDNA related to cyanobacteria, these data sets frequently contain >90% plastidial sequences, and the bacterial diversity may be under-sampled. To overcome this limitation we evaluated *in silico* the taxonomic coverage for four primer combinations targeting the 16S rDNA V3-V4 region. They included a forward primer universal to *Bacteria* (S-D-Bact-0341-b-S-17) and four reverse primers designed to avoid plastid DNA amplification. The best primer combination (NOCHL) was compared to the universal primer set in the wet lab using a synthetic community and samples from three macroalgal species. The proportion of plastid sequences was reduced by 99%–100% with the NOCHL primers compared to the universal primers, irrespective of algal hosts, sample collection and extraction protocols. Additionally, the NOCHL primers yielded a higher richness while maintaining the community structure. As *Planctomycetes*, *Verrucomicrobia* and *Cyanobacteria* were underrepresented (70%–90%) compared to universal primers, combining the NOCHL set with taxon-specific primers may be useful for a complete description of the alga-associated bacterial diversity. The NOCHL primers represent an innovation to study algal holobionts without amplifying host plastid sequences and may further be applied to other photosynthetic hosts.

*For correspondence. E-mail fthomas@sb-roscoff.fr; Tel.: +33256452148; Fax +33298292324. **E-mail angelique.gobet@ifremer.fr; Tel. +33499573250; Fax +33499573294.

Introduction

Numerous studies on algae-associated bacteria have highlighted their importance for the health and physiology of the algal holobiont as well as for biomass degradation (Barott *et al*., 2011; Egan *et al*., 2013, 2014; Singh and Reddy, 2016). Bacteria can be abundant on macroalgal surfaces, ranging from 10^6 to 10^7 cells cm^{-2}, and encompass a large phylogenetic diversity (van der Loos *et al*., 2019). These communities are distinct from bacterial assemblages found in the surrounding seawater or on inert surfaces (Burke *et al*., 2011; Stratil *et al*., 2014; Lemay *et al*., 2018). The composition of algae-associated bacterial communities has been shown to be host-specific and to vary depending on algal tissue, seasons, sampling sites and physiological status of the algae (Staufenberger *et al*., 2008; Lachnit *et al*., 2011; Miranda *et al*., 2013; Stratil *et al*., 2013; Zozaya-Valdes *et al*., 2015; Aires *et al*., 2016; Paix *et al*., 2019). A common approach to characterize these algae-associated communities is metabarcoding, whereby a selected variable region of the 16S rDNA is sequenced using a primer set universal to *Bacteria* [e.g., forward: S-D-Bact-0341-b-S-17/reverse: S-D-Bact-0785-a-A-21 (Klindworth *et al*., 2013)] Due to the classical sampling strategies for macroalgae-associated microbiomes [e.g., algal surface scraping or tissue grinding (Bengtsson *et al*., 2012; Aires *et al*., 2016)], one major issue is that bacterial DNA samples are often contaminated with algal DNA. Primers with a large taxonomic coverage for *Bacteria* will tend to also amplify 16S rDNA sequences from plastids. This is because plastid genomes, deriving from endosymbiosis events, still encode 16S rDNA closely related to their cyanobacterial ancestors. Data sets obtained from brown algal field samples using common universal primers may

contain over 90% of sequences affiliated to plastid DNA (Leblanc, personal data). This high proportion of plastidial sequences decreases the sequencing depth for bacterial epibionts and reduces the power of diversity analyses. One strategy to allow a large coverage of *Bacteria* while minimizing 16S gene amplification from plastids is to design a primer in a region that differs between plastid sequences and those of *Bacteria*. Chelius and Triplett have identified such a region between the positions 783 and 799 of the 16S rDNA (following the *E. coli* numbering system) and they designed the 799F primer that includes four mismatches with chloroplasts to amplify *Bacteria* while avoiding chloroplast amplification from maize roots (Chelius and Triplett, 2001). The resulting primer was then used in combination with primer 1193R (amplification product 394 bp) in several studies on bacterial communities associated with plants (Sagaram *et al*., 2009; Bodenhausen *et al*., 2013) or macroalgae (Vieira *et al*., 2016; Aires *et al*., 2018; Serebryakova *et al*., 2018). However, this primer set still yielded up to 38% of sequences affiliated to chloroplasts (Sagaram *et al*., 2009). Several sets of primers including the 799F primer with or without modifications were subsequently designed and tested to minimize plastid contamination on samples from plants and algae (Hanshew *et al*., 2013; Miranda *et al*., 2013; Aires *et al*., 2016). These primer sets target the V5–V8 or V5–V9 regions, yielding products of about 590 or 750 bp respectively. Although suitable for the 454 pyrosequencing technology used in the latter studies, this fragment length is not compatible with the current Illumina v3 sequencing chemistry, which produces paired-end reads of 2 × 300 bp. Allowing for a recommended overlap of at least 50 bp, the total product length for this technology should not exceed 500 bp. Our objective was to evaluate primer combinations matching these criteria while minimizing plastid contamination in 16S rDNA metabarcoding analyses by: (i) comparing the efficiency of a primer set universal to *Bacteria* and that of four primer combinations avoiding plastid amplification *in silico*, (ii) comparing the efficiency of the best primer combination from the *in silico* results with that of the universal primer set in the wet lab.

Results and discussion

In silico *evaluation of primer combinations to minimize the amplification of plastid sequences*

We evaluated several sets of primers to amplify a 450 bp fragment spanning the V3 and V4 regions of the 16S rDNA while minimizing the amplification of plastid sequences (Table S1). These primer sets were designed by combining the universal forward primer S-D-Bact-0341-b-S-17 (Klindworth *et al*., 2013) with reverse primers corresponding to the reverse complement of four V5–V8 forward primers previously used in 454 pyrosequencing to minimize chloroplast contamination (Hanshew *et al*., 2013). The four new primer combinations (*E. coli* position 341–785) covers most of the region amplified by the original V34 set (*E. coli* position 341–799), ensuring the comparability of data. The performance of these different primer combinations was tested by running an *in silico* PCR on the SILVA database ssu-132 with the RefNR sequence collection, using the online tool SILVA TestPrime 1.0 (Klindworth *et al*., 2013). The universal V34 combination with the original reverse primer S-D-Bact-0785-a-A-21 had an *in silico* predicted coverage for plastids (Table 1) ranging from 57.3% to 88.3% with zero or two allowed mismatches respectively. By contrast, three of the four new combinations (NOCHL, NOCHL3 and NOCHL6 but not NOCHL7, Table S1) showed consistently low predicted coverage for plastids, even with two allowed mismatches (2.7%, 1.1% and 1.1% respectively). The overall coverage of these three primer combinations for all bacterial sequences remained high (79% with no mismatch, 85%–90% with two mismatches). However, the NOCHL3 and NOCHL6 primer sets were predicted to perform poorly on a number of phyla, including *Planctomycetes* (12% coverage with two mismatches) and *Verrucomicrobia* (17% coverage), which are known to be part of alga-associated microbial communities (Bengtsson and Øvreås, 2010; Lage and Bondoso, 2014; Vollmers *et al*., 2017). For all taxa, the NOCHL combination had equal or better coverage than the NOCHL3 and NOCHL6 combinations, notably for *Planctomycetes* (82.3%) and *Verrucomicrobia* (48.7%). The NOCHL combination was, therefore, considered the most promising candidate to minimize plastid contamination while maintaining the overall bacterial diversity and chosen to prepare Illumina-sequencing libraries.

Comparison of primer performances in the wet lab

Performances of the NOCHL and V34 primer combinations were compared *in vitro* using different types of samples. As a positive control for the metabarcoding experiment, we constructed a mock community based on the genomic DNA of pure bacterial isolates. Genomic DNA was extracted from a total of 32 sequenced bacterial strains (Table S2) and mixed in known proportions to assemble the mock community. Furthermore, the microbiota associated with three brown algal species was sampled according to different approaches. The filamentous brown alga *Ectocarpus subulatus* samples were collected 5 km North of the Hopkins River Falls (Australia) and whole tissues were ground before DNA extraction. Blade samples of *Laminaria hyperborea* sporophytes were collected at the coast off Roscoff (Brittany, France) and soaked in a lysis buffer for DNA extraction. The blades of *L. digitata* sporophytes from Roscoff were

Table 1. *In silico* predicted coverage of selected bacterial taxa, relative to the sequences available in the Silva SSU r132 database for different primer combinations using TestPrime 1.0.

	0 mismatch					2 mismatches				
	V34	NOCHL	NOCHL3	NOCHL6	NOCHL7	V34	NOCHL	NOCHL3	NOCHL6	NOCHL7
Acidobacteria	92.0	43.1	43.2	43.1	43.3	95.7	95.0	45.3	45.1	96.2
Actinobacteria	82.4	82.5	82.7	82.6	82.7	86.6	96.3	96.5	96.1	86.9
Aquificae	89.3	89.6	90.2	89.9	90.5	95.0	95.5	95.8	95.5	96.1
Bacteroidetes	89.8	88.8	89.3	89.0	89.4	95.4	95.8	95.2	94.8	95.9
Chlamydiae	82.8	65.9	65.9	65.9	66.4	96.7	96.9	79.7	79.7	96.7
Chloroflexi	39.0	19.3	20.8	20.7	21.1	88.7	48.6	30.3	30.3	88.6
Cyanobacteria	76.2	0.6	0.6	0.6	0.6	92.4	1.9	0.9	0.9	88.6
Chloroplasts	57.3	0.7	0.7	0.7	0.7	88.3	2.7	1.1	1.1	81.3
Deinococcus-Thermus	92.9	92.6	92.6	92.6	93.0	96.7	96.9	96.3	96.2	96.7
Epsilonbacteraeota	93.9	85.1	85.9	85.5	85.8	96.8	96.6	88.6	88.2	97.3
Firmicutes	88.2	84.0	84.9	84.7	85.0	94.2	92.8	90.5	90.1	94.7
Fusobacteria	87.1	86.1	87.0	86.7	87.2	94.9	94.0	93.9	93.6	95.3
Gemmatimonadetes	89.6	89.2	89.8	89.4	89.8	93.6	94.7	95.5	94.4	94.9
Planctomycetes	73.5	10.6	10.6	10.5	10.7	85.1	82.3	12.0	11.9	85.8
Proteobacteria	90.0	89.0	89.4	89.2	89.4	95.7	94.3	93.6	93.1	96.2
Spirochaetes	75.7	70.5	70.7	70.3	70.7	88.2	94.6	85.6	85.1	88.4
Verrucomicrobia	87.3	16.2	16.3	16.3	16.5	93.0	48.7	17.2	17.1	92.5
All Bacteria	86.6	79.1	79.6	79.3	79.6	93.6	90.1	85.3	84.9	93.9

A length of 3 bases of 0-mismatch zone at 3′ end of primers was chosen for tests with two allowed mismatches in the sequence.

swabbed for DNA extraction. All samplings were performed in triplicate. Details on sampling and DNA extraction protocols are available in Supporting Information. Amplicon and library preparation were carried out following the standard Illumina protocol (Illumina web page, 2018), including several negative controls, as detailed in Supporting Information. Both the NOCHL and V34 primer pairs successfully amplified about 450-bp fragment covering a similar region (V3–V4) of the bacterial 16S rDNA. Sequencing libraries were prepared in parallel for each sample (nine algal samples, one mock community and six negative controls) using each primer pair. Sequencing was carried out using one run of an Illumina Miseq yielding a total of 5,549,008 read pairs. Sequences were deposited at the ENA under project accession number PRJEB33453. After quality checks and removal of exogenous contaminations, low-quality sequences, and blanks (see Supporting Information), 2,784,253 assembled reads remained for data analysis. Sequences were clustered, assigned to operational taxonomic units (OTUs) at 97% identity, taxonomically classified with RDP classifier (Wang *et al*., 2007) on the Silva SSU database release 132 (Quast *et al*., 2013) and filtered to remove rare OTUs (see details in Supporting Information). The final data set comprised 3009 OTUs.

First, we compared metabarcoding results from the primer combinations V34 and NOCHL on the mock community. The sequencing error rate calculated as in Kozich *et al*. (2013) from the mock community data sets was 0.54% for both the V34 and NOCHL libraries. A total of 65 OTUs were detected in the rarefied mock community data sets. The expected relative proportion p_i of 16S rDNAs from strain *i* was calculated as follows:

$$p_i = \frac{\frac{q}{M_i} \times c_i}{\sum_{i=1}^{32} \frac{q_i}{M_i} \times c_i}$$

where q_i is the mass of DNA from strain *i* added in the MOCK community, M_i is the molecular weight of the complete genome for strain *i* and c_i is the number of 16S rDNA gene copies in the genome of strain *i*. At the genus level, poor correlations (Pearson coefficient < 0.4) were obtained between the expected 16S rDNA proportions in the mock community and the relative abundance of taxa found in V34 or NOCHL libraries (Table 2). From the 26 genera represented in the mock community, 18 and 20 were detected in the V34 and NOCHL data sets respectively. Both primer combinations did not detect the six genera *Nonlabens*, *Agrococcus*, *Arthrobacter*, *Dokdonia*, *Roseovarius* and *Imperialibacter*. Sequences from these genera might either not be amplified by the primer sets, or more likely be merged to closely related sequences during OTU clustering. In addition, *Roseobacter* and *Hoeflea* were missed by the V34 primer combination, whereas their relative abundance was close to the expected value in the NOCHL data set. With both primer pairs, about 30% of sequences could not be classified down to the genus level, leading to discrepancies between expected and measured proportions. A striking example is *Vibrio*: its expected abundance of 24.63% was largely underestimated at about 8% with both primer pairs, whereas 11% of sequences were assigned to unclassified

Table 2. Genus-level comparison of theoretical relative abundance in the mock community with the measured abundance in libraries sequenced with V34 or NOCHL primers.

	Relative abundance of sequences in the mock community (%)		
Genus	Theory	Primers V34	Primers NOCHL
Vibrio	24.63	8.28	8.78
Formosa	9.72	3.04	2.53
Maribacter	9.42	5.41	5.24
Zobellia	7.24	5.07	3.04
Alteromonas	5.29	1.01	1.35
Nonlabens	5.02	0.00	0.00
Psychrobacter	2.59	6.08	4.05
Microbacterium	2.79	0.51	0.34
Agrococcus	2.74	0.00	0.00
Sphingomonas	2.51	1.52	2.20
Arthrobacter	2.42	0.00	0.00
Dokdonia	2.35	0.00	0.00
Paracoccus	2.31	2.87	4.22
Polaribacter	2.15	8.78	9.12
Roseovarius	1.94	0.00	0.00
Cobetia	1.94	5.24	6.25
Winogradskyella	1.91	1.35	2.03
Roseobacter	1.90	0.00	1.35
Cellulophaga	1.77	3.38	2.53
Mariniflexile	1.74	1.86	1.01
Pseudoalteromonas	1.71	11.82	11.99
Hoeflea	1.57	0.00	1.86
Bosea	1.30	0.68	0.84
Imperialibacter	1.23	0.00	0.00
Rhodopirellula	1.15	1.69	0.51
Dinoroseobacter	0.68	0.51	0.17
unclass. *Acidimicrobiales*	–	0.34	0.00
unclass. *Vibrionaceae*	–	11.49	10.81
unclass. *Sphingobacteriales*	–	5.24	6.93
unclass. *Micrococcaceae*	–	3.89	3.04
unclass. *Flavobacteriaceae*	–	5.41	4.05
unclass. *Rhodobacteraceae*	–	1.52	3.21
Krokinobacter	–	1.86	2.03
unclass. *Gammaproteobacteria*	–	0.34	0.34
unclass. *Actinobacteria*	–	0.34	0.00
unclass. *Proteobacteria*	–	0.17	0.00
unclass. *Alteromonadaceae*	–	0.00	0.17
unclass *Hyphomonadaceae*	–	0.34	0.00
Correlation coefficient Theory vs. Observed for genera present in the mock community		0.39	0.38

Unclass., unclassified.

Vibrionaceae. On the contrary, both primer combinations largely overestimated the proportion of *Pseudoalteromonas*, possibly due to the proximity with sequences from *Alteromonas* (Gauthier *et al*., 1995). Although the NOCHL combination had a suboptimal predicted coverage for *Planctomycetes* (Table 1), it still detected the planctomycetal genus *Rhodopirellula* in the mock community, underestimating it by 56%. On the other hand, the V34 combination overestimated *Rhodopirellula* by 47%. As expected, correlations between theoretical and measured proportions were much better (Pearson coefficient > 0.9) at the family level for both primer combinations (Table S3). All 13 families represented in the mock community were detected using the NOCHL combination, whereas the V34 combination missed the *Phyllobacteriaceae* family. Altogether, the performance of the NOCHL combination was found to be comparable to the V34 set on the mock community in terms of sensitivity and accuracy.

We further compared the efficiency of the primer combinations V34 and NOCHL in field samples, characterizing the bacterial community associated with *Ectocarpus subulatus* (ECTO), *Laminaria digitata* (LDIG) and *Laminaria hyperborea* (LHYP). The relative abundance of sequences affiliated to plastids ranged from 0.6% to 66% in the V34 data set (Fig. 1). The highest relative abundances of plastid sequences were found when algal tissues were ground (ECTO) or soaked in lysis buffer (LHYP) before DNA extraction, compared to the swab-based technique (LDIG). It was drastically reduced by 99%–100% with the NOCHL combination in all three types of alga-associated samples analysed (Fig. 1), with relative abundance of plastid 16S rDNA sequences ranging from 0% to 0.3%. This confirms that the new primer combination succeeds at minimizing plastid contamination, irrespective of the algal host, sample collection and DNA extraction protocol. The NOCHL combination was more efficient at reducing plastid contamination compared to a previous Illumina metabarcoding analysis of *Ectocarpus*-associated bacterial communities. In that former study, a modified set of 341F and 806R primers still yielded 32% of plastid sequences despite a central mismatch to avoid plastid DNA amplification (Dittami *et al*., 2016).

Alpha-diversity analyses tended to show higher values of OTU richness (observed OTUs) and diversity (Shannon and Simpson indices) with the NOCHL combination compared to V34 before removal of plastid

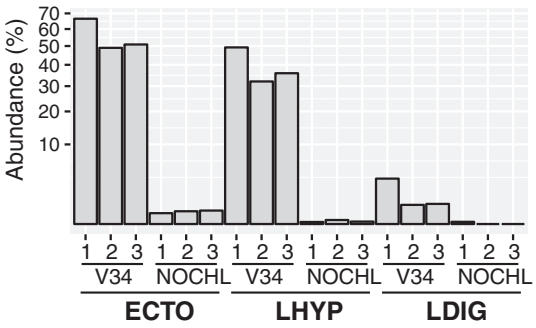

Fig. 1. Relative abundance of sequences affiliated to plastid OTUs using the V34 or NOCHL primer sets. Bacterial communities were analysed in triplicate samples from different algal hosts: ECTO, *Ectocarpus subulatus*; LHYP, *Laminaria hyperborea*; LDIG, *Laminaria digitata*.

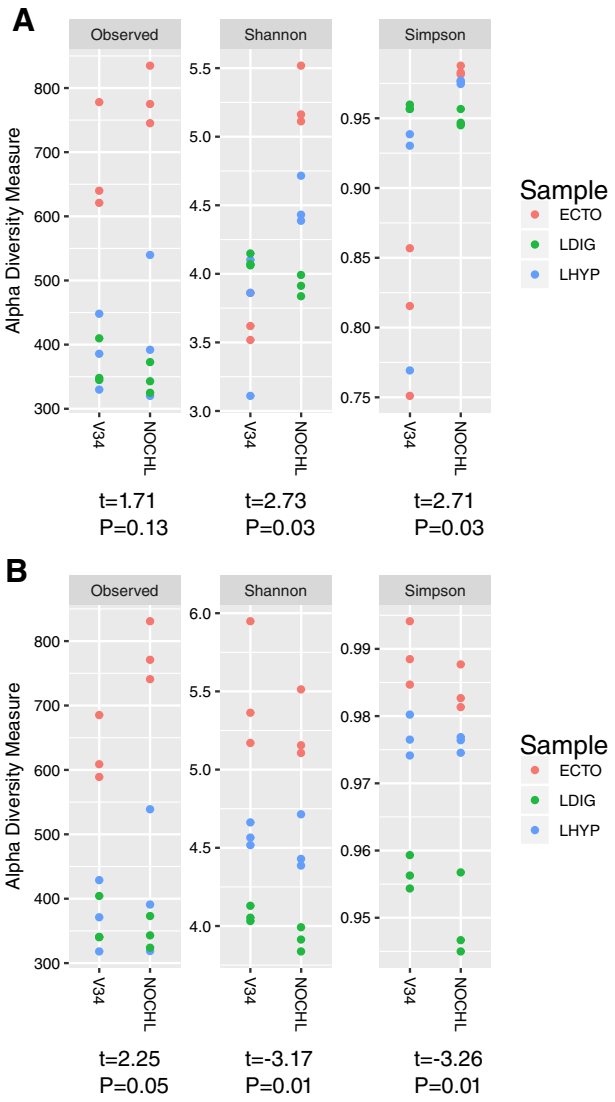

Fig. 2. Richness and diversity estimates before (A) and after (B) removal of OTUs affiliated to plastids. Data were subsampled at 8358 sequences per sample prior to analysis. Observed, observed OTU richness; Shannon, Shannon index; Simpson, Simpson index; ECTO, *Ectocarpus subulatus*; LDIG, *Laminaria digitata*; LHYP, *Laminaria hyperborea*. Results of paired Student's *t*-test testing the effect of the set of primers on each measured estimate are reported below each panel (df = 8).

sequences (Fig. 2A). This overall effect was found significant for Shannon and Simpson diversity indices and was more pronounced for samples from *E. subulatus* and *L. hyperborea*, After removal of plastid sequences (Fig. 2B), the NOCHL primer combination yielded significantly higher richness than V34 (Student's *t*-test, $P = 0.05$) with an overall increase of 10%. Again, this effect was more pronounced for ECTO and LHYP samples. Indeed, ECTO and LHYP samples, where plastid contamination was the highest (Fig. 1), showed the strongest effect of plastidial sequence removal on sequencing depth (Fig. S1). This exemplifies the issue faced with universal primers, where a large amount of plastid-affiliated sequences can decrease the sequencing depth for target bacterial sequences and reduce the evenness. After removal of plastid sequences, lower Shannon and Simpson diversity indices were detected with the NOCHL combination compared with V34 (−3.2% and −0.5% lower values for Shannon and Simpson respectively). This was mostly due to an increase in these indices for V34 data sets after removal of plastid sequences, while they stayed stable for the NOCHL data sets. Although not the main focus of this work, we noticed that bacterial communities retrieved from *Ectocarpus* were more diverse than those from the two *Laminaria* species. This might be due to the nature of the samples as well as the extraction protocol where entire algal specimens were ground for *Ectocarpus* (i.e., including the endomicrobiota), while for *Laminaria* the extraction protocols only targeted surface-attached bacteria. Joint hierarchical clustering of OTU-level data sets for both primer pairs after removal of plastid sequences showed that samples grouped according to algal host rather than primer pair (Fig. 3A).

The relative abundance of phyla was generally similar between paired sets of samples (Fig. 3B). Notable exceptions were the *Planctomycetes*, *Verrucomicrobia* and *Cyanobacteria* that had lower relative abundance in the NOCHL libraries compared to V34 (Table S4). We further searched for differential OTUs between pairs of samples sequenced with the V34 or NOCHL combination. This analysis was performed with the edgeR package (Robinson *et al*., 2009) on the non-transformed data set after removal of plastid sequences and accounted for the paired design of the study, i.e. the same samples were sequenced with the two primer combinations. The significance threshold was set at $\alpha = 5\%$ after Benjamini–Hochberg correction for multiple testing. Out of the 2852 OTUs remaining after discarding plastids, the edgeR analysis detected 39 differential OTUs (i.e., 1.4%) between primer combinations (Table S5). All differential OTUs were more abundant in the V34-amplified data set compared to NOCHL. The majority of them belonged to *Verrucomicrobiae* and *Planctomycetacia* (Fig. 4), partly reflecting the lower predicted coverage of NOCHL for these taxa. The apparent lower abundance of *Planctomycetacia* OTUs using the NOCHL primer set could also be in part due to their overestimation with the V34 combination, as shown in the mock community analysis (Table 2). The highest fold-change was found for OTU00082 belonging to *Cyanobacteria*. The lower abundance of *Cyanobacteria* was inevitable since plastids and extant cyanobacteria share a common ancestor and therefore

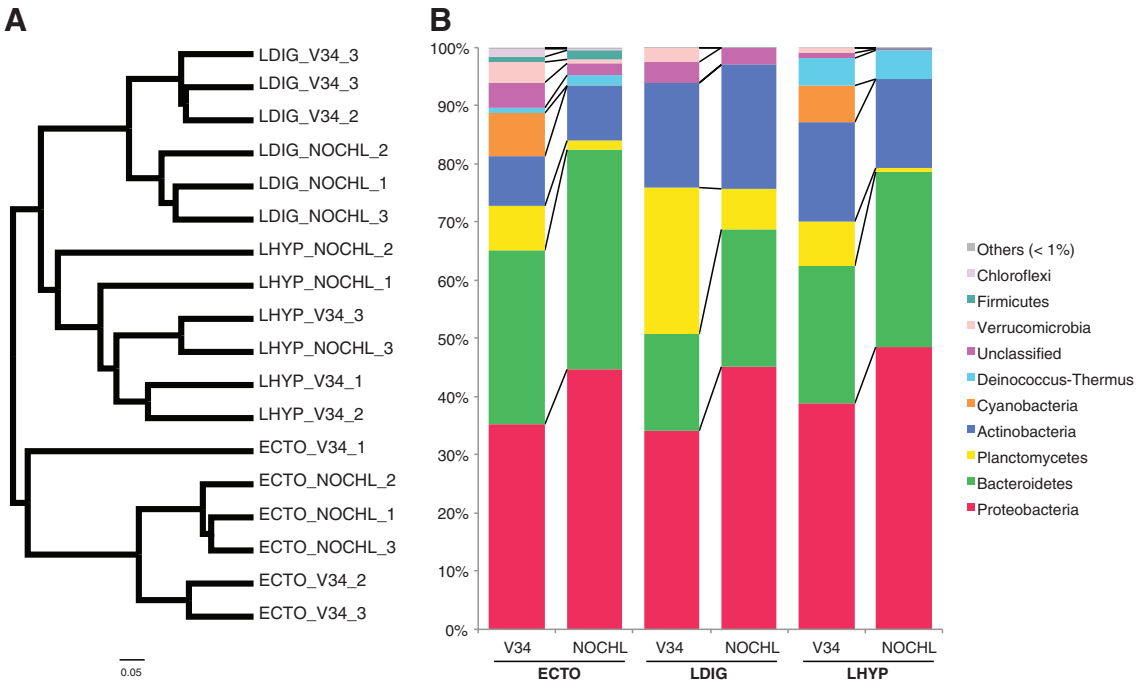

Fig. 3. Effect of the primer pair on the detected bacterial community composition, after removal of OTUs affiliated to plastids.
A. Hierarchical clustering calculated on Hellinger-transformed data based on Morisita–Horn distance using the complete linkage algorithm.
B. Taxonomic composition based on the phylum level.

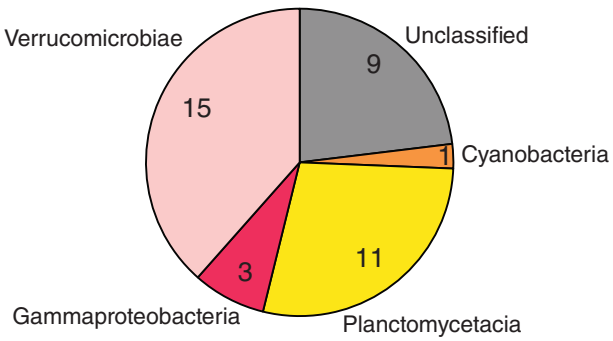

Fig. 4. Taxonomic affiliation of the 39 differential OTUs detected with edgeR, depending on the primer pair. All of these OTUs received higher coverage with the V34 primers.

have homologous 16S rDNA sequences (Giovannoni *et al*., 1988; Delwiche, 1999).

Conclusions

Considering that plastid sequences can represent more than 90% of all sequences in one sample when using universal primer sets, the bacterial diversity in a sample may be underrepresented. The new primer set NOCHL is efficient to avoid amplifying plastid sequences from an algal host while identifying a significantly higher bacterial richness than with the universal primers V34, given identical sequencing efforts. This validates that fewer plastid sequences in the samples lead to larger access to bacterial sequences thus recovering more of the bacterial diversity. However, as some bacterial groups may be underrepresented, this primer set may be combined with taxon-specific primers (e.g., for *Planctomycetes*) for more complete coverage of *Bacteria*. Still, the data obtained with the NOCHL and universal V34 primer sets are comparable since the targeted regions are the same and patterns of the community structure are similar. Although validated here on macroalgal samples, this primer set may be useful to characterize bacterial communities from other environments where plastid contamination can be an issue such as terrestrial plants, microalgae, or gut microbiota of herbivores.

Acknowledgements

We warmly thank Gaëlle Correc and Sylvie Rousvoal for help with sampling as well as Florian de Bettignies and Dominique Davoult for providing samples. We thank Frédérique Le Roux and Christian Jeanthon for providing bacterial strains. This work has benefited from the facilities of the Genomer platform and from the computational resources of the ABiMS bioinformatics platform (FR 2424, CNRS-Sorbonne Université, Roscoff), which are part of the Biogenouest core facility network. This work has benefited from the support of the French Government via the National Research Agency investment expenditure program IDEALG (ANR-10-BTBR-04). F.T., S.M.D., and C.L. acknowledge

support by the Centre National de la Recherche Scientifique (CNRS). A.G. acknowledges support by the Institut Français de Recherche pour l'Exploitation de la Mer (IFREMER).

References

Aires, T., Muyzer, G., Serrão, E.A., and Engelen, A.H. (2018) Unravelling seaweeds bacteriomes. In *Protocols for Macroalgae Research*. Charrier, B., Wichard, T., and Reddy, C. R.K. (eds). Boca Raton: CRC Press, pp. 95–113.

Aires, T., Serrão, E.A., and Engelen, A.H. (2016) Host and environmental specificity in bacterial communities associated to two highly invasive marine species (genus *Asparagopsis*). *Front Microbiol* **7**: 1–14.

Barott, K.L., Rodriguez-Brito, B., Janouškovec, J., Marhaver, K.L., Smith, J.E., Keeling, P., and Rohwer, F.L. (2011) Microbial diversity associated with four functional groups of benthic reef algae and the reef-building coral *Montastraea annularis*. *Environ Microbiol* **13**: 1192–1204.

Bengtsson, M.M., and Øvreås, L. (2010) *Planctomycetes* dominate biofilms on surfaces of the kelp *Laminaria hyperborea*. *BMC Microbiol* **10**: 261.

Bengtsson, M.M., Sjøtun, K., Lanzén, A., and Øvreås, L. (2012) Bacterial diversity in relation to secondary production and succession on surfaces of the kelp *Laminaria hyperborea*. *ISME J* **6**: 2188–2198.

Bodenhausen, N., Horton, M.W., and Bergelson, J. (2013) Bacterial communities associated with the leaves and the roots of *Arabidopsis thaliana*. *PLoS One* **8**: e56329.

Burke, C., Thomas, T., Lewis, M., Steinberg, P., and Kjelleberg, S. (2011) Composition, uniqueness and variability of the epiphytic bacterial community of the green alga *Ulva australis*. *ISME J* **5**: 590–600.

Chelius, M.K., and Triplett, E.W. (2001) The diversity of archaea and bacteria in association with the roots of *Zea mays* L. *Microb Ecol* **41**: 252–263.

Delwiche, C.F. (1999) Tracing the thread of plastid diversity through the tapestry of life. *Am Nat* **154**: S164–S177.

Dittami, S.M., Duboscq-Bidot, L., Perennou, M., Gobet, A., Corre, E., Boyen, C., and Tonon, T. (2016) Host-microbe interactions as a driver of acclimation to salinity gradients in brown algal cultures. *ISME J* **10**: 51–63.

Egan, S., Fernandes, N.D., Kumar, V., Gardiner, M., and Thomas, T. (2014) Bacterial pathogens, virulence mechanism and host defence in marine macroalgae. *Environ Microbiol* **16**: 925–938.

Egan, S., Harder, T., Burke, C., Steinberg, P., Kjelleberg, S., and Thomas, T. (2013) The seaweed holobiont: understanding seaweed-bacteria interactions. *FEMS Microbiol Rev* **37**: 462–476.

Gauthier, G., Gauthier, M., and Christen, R. (1995) Phylogenetic analysis of the genera *Alteromonas*, *Shewanella*, and *Moritella* using genes coding for small-subunit rRNA sequences and division of the genus *Alteromonas* into two genera, *Alteromonas* (emended) and *Pseudoalteromonas* gen. nov., and proposal of twelve new species combinations. *Int J Syst Bacteriol* **45**: 755–761.

Giovannoni, S.J., Turner, S., Olsen, G.J., Barns, S., Lane, D. J., and Pace, N.R. (1988) Evolutionary relationships among cyanobacteria and green chloroplasts. *J Bacteriol* **170**: 3584–3592.

Hanshew, A.S., Mason, C.J., Raffa, K.F., and Currie, C.R. (2013) Minimization of chloroplast contamination in 16S rRNA gene pyrosequencing of insect herbivore bacterial communities. *J Microbiol Methods* **95**: 149–155.

Illumina Web Page (2018) 16S Metagenomic Sequencing Library Preparation.

Klindworth, A., Pruesse, E., Schweer, T., Peplies, J., Quast, C., Horn, M., and Glöckner, F.O. (2013) Evaluation of general 16S ribosomal RNA gene PCR primers for classical and next-generation sequencing-based diversity studies. *Nucleic Acids Res* **41**: 1–11.

Kozich, J.J., Westcott, S.L., Baxter, N.T., Highlander, S.K., and Schloss, P.D. (2013) Development of a dual-index sequencing strategy and curation pipeline for analyzing amplicon sequence data on the MiSeq Illumina sequencing platform. *Appl Environ Microbiol* **79**: 5112–5120.

Lachnit, T., Meske, D., Wahl, M., Harder, T., and Schmitz, R. (2011) Epibacterial community patterns on marine macroalgae are host-specific but temporally variable. *Environ Microbiol* **13**: 655–665.

Lage, O.M., and Bondoso, J. (2014) *Planctomycetes* and macroalgae, a striking association. *Front Microbiol* **5**: 1–9.

Lemay, M., Martone, P., Keeling, P., Burt, J., Krumhansl, K., Sanders, R., and Parfrey, L. (2018) Sympatric kelp species share a large portion of their surface bacterial communities. *Environ Microbiol* **20**: 658–670.

Miranda, L.N., Hutchison, K., Grossman, A.R., and Brawley, S.H. (2013) Diversity and abundance of the bacterial community of the red macroalga *Porphyra umbilicalis*: did bacterial farmers produce macroalgae? *PLoS One* **8**: e58269.

Paix, B., Othmani, A., Debroas, D., Culioli, G., and Briand, J. F. (2019) Temporal covariation of epibacterial community and surface metabolome in the Mediterranean seaweed holobiont *Taonia atomaria*. *Environ Microbiol* **21**: 3346–3363. https://doi.org/10.1111/1462-2920.14617.

Quast, C., Pruesse, E., Yilmaz, P., Gerken, J., Schweer, T., Yarza, P., *et al*. (2013) The SILVA ribosomal RNA gene database project: improved data processing and web-based tools. *Nucleic Acids Res* **41**: D590–D596.

Robinson, M.D., McCarthy, D.J., and Smyth, G.K. (2009) edgeR: a bioconductor package for differential expression analysis of digital gene expression data. *Bioinformatics* **26**: 139–140.

Sagaram, U.S., Deangelis, K.M., Trivedi, P., Andersen, G.L., Lu, S.E., and Wang, N. (2009) Bacterial diversity analysis of huanglongbing pathogen-infected citrus, using phyloChip arrays and 16S rRNA gene clone library sequencing. *Appl Environ Microbiol* **75**: 1566–1574.

Serebryakova, A., Aires, T., Viard, F., Serrão, E.A., and Engelen, A.H. (2018) Summer shifts of bacterial communities associated with the invasive brown seaweed *Sargassum muticum* are location and tissue dependent. *PLoS One* **13**: 1–18.

Singh, R.P., and Reddy, C.R.K. (2016) Unraveling the functions of the macroalgal microbiome. *Front Microbiol* **6**: 1–8.

Staufenberger, T., Thiel, V., Wiese, J., and Imhoff, J.F. (2008) Phylogenetic analysis of bacteria associated with *Laminaria saccharina*. *FEMS Microbiol Ecol* **64**: 65–77.

Stratil, S.B., Neulinger, S.C., Knecht, H., Friedrichs, A.K., and Wahl, M. (2013) Temperature-driven shifts in the epibiotic bacterial community composition of the brown macroalga *Fucus vesiculosus*. *Microbiology* **2**: 338–349.

Stratil, S.B., Neulinger, S.C., Knecht, H., Friedrichs, A.K., and Wahl, M. (2014) Salinity affects compositional traits of epibacterial communities on the brown macroalga *Fucus vesiculosus*. *FEMS Microbiol Ecol* **88**: 272–279.

van der Loos, L.M., Eriksson, B.K., and Falcão Salles, J. (2019) The macroalgal holobiont in a changing sea. *Trends Microbiol* **27**: 635–650.

Vieira, C., Engelen, A.H., Guentas, L., Aires, T., Houlbreque, F., Gaubert, J., *et al*. (2016) Species specificity of bacteria associated to the brown seaweeds *Lobophora* (Dictyotales, Phaeophyceae) and their potential for induction of rapid coral bleaching in *Acropora muricata*. *Front Microbiol* **7**: 1–13.

Vollmers, J., Frentrup, M., Rast, P., Jogler, C., and Kaster, A.K. (2017) Untangling genomes of novel Planctomycetal and Verrucomicrobial species from Monterey bay kelp forest metagenomes by refined binning. *Front Microbiol* **8**: 472.

Wang, Q., Garrity, G.M., Tiedje, J.M., and Cole, J.R. (2007) Naive Bayesian classifier for rapid assignment of rRNA sequences into the new bacterial taxonomy. *Appl Environ Microbiol* **73**: 5261–5267.

Zozaya-Valdes, E., Egan, S., and Thomas, T. (2015) A comprehensive analysis of the microbial communities of healthy and diseased marine macroalgae and the detection of known and potential bacterial pathogens. *Front Microbiol* **6**: 1–9.

Supporting Information

Additional Supporting Information may be found in the online version of this article at the publisher's web-site:

Appendix S1: Supplementary Methods

Supplementary Table 1: The five primer combinations tested in TestPrime 1.0. The S-D-Bact primers were selected from (Klindworth *et al*., 2012) while the 799F_ primers were inspired from (Hanshew, Mason, Raffa, & Currie, 2013).

Supplementary Table 2: Strains and genomic DNA quantities used for the mock community. Genomic DNA was extracted from a total of 32 sequenced bacterial strains following standard procedures and quantified on a Qubit 3.0 fluorometer using a Qubit ds-DNA BR kit.

Supplementary Table 3: Comparison between the theoretical and the observed relative abundance of families in the mock community in libraries sequenced with V34 or NOCHL primers. Unclass., unclassified.

Supplementary Table 4: Relative abundance of phyla (%, mean of individual triplicate samples) in datasets after removal of OTUs affiliated to plastids. These values were used to plot Figure 3B.

Supplementary Table 5: Differential OTUs between datasets obtained with the primer pairs V34 and NOCHL, detected with edgeR.

Supplementary Figure 1: Rarefaction analysis of datasets obtained with V34 and NOCHL primer sets before (A) and after (B) removal of plastid-related sequences.

References

Abdullah, M.I. and Fredriksen, S. (2004) Production, respiration and exudation of dissolved organic matter by the kelp *Laminaria hyperborea* along the west coast of Norway. *J Mar Biol Assoc United Kingdom* **84**: 887–894.

Ale, M.T. and Meyer, A.S. (2013) Fucoidans from brown seaweeds: An update on structures, extraction techniques and use of enzymes as tools for structural elucidation. *RSC Adv* **3**: 8131–8141.

Allouch, J., Helbert, W., Henrissat, B., and Czjzek, M. (2004) Parallel substrate binding sites in a β-agarase suggest a novel mode of action on double-helical agarose. *Structure* **12**: 623–632.

Allouch, J., Jam, M., Helbert, W., Barbeyron, T., Kloareg, B., Henrissat, B., and Czjzek, M. (2003) The Three-dimensional Structures of Two β-Agarases. *J Biol Chem* **278**: 47171–47180.

Alonso-Sáez, L., Díaz-Pérez, L., and Morán, X.A.G. (2015) The hidden seasonality of the rare biosphere in coastal marine bacterioplankton. *Environ Microbiol* **17**: 3766–3780.

Alonso, C., Warnecke, F., Amann, R., and Pernthaler, J. (2007) High local and global diversity of Flavobacteria in marine plankton. *Environ Microbiol* **9**: 1253–1266.

Amann, R. and Fuchs, B.M. (2008) Single-cell identification in microbial communities by improved fluorescence *in situ* hybridization techniques. *Nat Rev Microbiol* **6**: 339–348.

Amann, R.I., Binder, B.J., Olson, R.J., Chisholm, S.W., Devereux, R., and Stahl, D.A. (1990) Combination of 16S rRNA-targeted oligonucleotide probes with flow cytometry for analyzing mixed microbial populations. *Appl Environ Microbiol* **56**: 1919–1925.

Amsler, C.D. and Fairhead, V.A. (2005) Defensive and Sensory Chemical Ecology of Brown Algae. *Adv Bot Res* **43**: 1–91.

Anderson, K.L. and Salyers, A.A. (1989) Biochemical evidence that starch breakdown by *Bacteroides thetaiotaomicron* involves outer membrane starch-binding sites and periplasmic starch-degrading enzymes. *J Bacteriol* **171**: 3192–3198.

Ar Gall, E., Küpper, F.C., and Kloareg, B. (2004) A survey of iodine content in *Laminaria digitata*. *Bot Mar* **47**: 30–37.

Arnosti, C. (2011) Microbial extracellular enzymes and the marine carbon cycle. *Ann Rev Mar Sci* **3**: 401–425.

Arnosti, C., Wietz, M., Brinkhoff, T., Hehemann, J.-H., Probant, D., Zeugner, L., and Amann, R. (2020) The biogeochemistry of marine polysaccharides: sources, inventories, and bacterial drivers of the carbohydrate cycle. *Ann Rev Mar Sci* **13**: 9.1-9.28.

Avendaño-Herrera, R., Toranzo, A.E., and Magariños, B. (2006) *Tenacibaculosis* infection in marine fish caused by *Tenacibaculum maritimum*: A review. *Dis Aquat Organ* **71**: 255–266.

Azam, F., Fenchel, T., Field, J., Gray, J., Meyer-Reil, L., and Thingstad, F. (1983) The Ecological Role of Water-Column Microbes in the Sea. *Mar Ecol Prog Ser* **10**: 257–263.

Azam, F. and Malfatti, F. (2007) Microbial structuring of marine ecosystems. *Nat Rev Microbiol* **5**: 782–791.

Bacchetti De Gregoris, T., Aldred, N., Clare, A., and Burgess, J.G. (2011) Improvement of phylum- and

class-specific primers for real-time PCR quantification of bacterial taxa. *J Microbiol Methods* **86**: 351–356.

Bader, G.D. and Hogue, C.W.V. (2003) An automated method for finding molecular complexes in large protein interaction networks. *BMC Bioinformatics* **4**: 1–27.

Ballestriero, F., Thomas, T., Burke, C., Egan, S., and Kjelleberg, S. (2010) Identification of compounds with bioactivity against the nematode *Caenorhabditis elegans* by a screen based on the functional genomics of the marine bacterium *Pseudoalteromonas tunicata* D2. *Appl Environ Microbiol* **76**: 5710–5717.

Barberi, O.N., Byron, C.J., Burkholder, K.M., St. Gelais, A.T., and Williams, A.K. (2020) Assessment of bacterial pathogens on edible macroalgae in coastal waters. *J Appl Phycol* **32**: 683–696.

Barbeyron, T., Brillet-Guéguen, L., Carré, W., Carrière, C., Caron, C., Czjzek, M., et al. (2016) Matching the diversity of sulfated biomolecules: Creation of a classification database for sulfatases reflecting their substrate specificity. *PLoS One* **11**: 1–33.

Barbeyron, T., Carpentier, F., L'Haridon, S., Schüler, M., Michel, G., and Amann, R. (2008) Description of Maribacter forsetii sp. nov., a marine *Flavobacteriaceae* isolated from North Sea water, and emended description of the genus *Maribacter*. *Int J Syst Evol Microbiol* **58**: 790–797.

Barbeyron, T., Gerard, A., Potin, P., Henrissat, B., and Kloareg, B. (1998) The kappa-carrageenase of the marine bacterium Cytophaga drobachiensis. Structural and phylogenetic relationships within family-16 glycoside hydrolases. *Mol Biol Evol* **15**: 528–537.

Barbeyron, T., L'Haridon, S., Corre, E., Kloareg, B., and Potin, P. (2001) *Zobellia galactanovorans* gen. nov., sp. nov., a marine species of *Flavobacteriaceae* isolated from a red alga, and classification of [*Cytophaga*] *uliginosa* (ZoBell and Upham 1944) Reichenbach 1989 as *Zobellia uliginosa* gen. nov., comb. nov. *Int J Syst Evol Microbiol* **51**: 985–997.

Barbeyron, T., Michel, G., Potin, P., Henrissat, B., and Kloareg, B. (2000) ι-Carrageenases constitute a novel family of glycoside hydrolases, unrelated to that of κ-carrageenases. *J Biol Chem* **275**: 35499–35505.

Barbeyron, T., Thiébaud, M., Le Duff, N., Martin, M., Corre, E., Tanguy, G., et al. (2021) *Zobellia roscoffensis* sp. nov. and *Zobellia nedashkovskayae* sp. nov., two flavobacteria from the epiphytic microbiota of the brown alga *Ascophyllum nodosum*, and emended description of the genus *Zobellia*. *Int J Syst Evol Microbiol* **71**:.

Barbeyron, T., Thomas, F., Barbe, V., Teeling, H., Schenowitz, C., Dossat, C., et al. (2016) Habitat and taxon as driving forces of carbohydrate catabolism in marine heterotrophic bacteria: Example of the model algae-associated bacterium *Zobellia galactanivorans* DsijT. *Environ Microbiol* **18**: 4610–4627.

Bauer, M., Kube, M., Teeling, H., Richter, M., Lombardot, T., Allers, E., et al. (2006) Whole genome analysis of the marine *Bacteroidetes* "*Gramella forsetii*" reveals adaptations to degradation of polymeric organic matter. *Environ Microbiol* **8**: 2201–2213.

Bengtsson, M.M., Sjøtun, K., and øvreås, L. (2010) Seasonal dynamics of bacterial biofilms on the kelp *Laminaria hyperborea*. *Aquat Microb Ecol* **60**: 71–83.

Benner, R. and Amon, R.M.W. (2015) The size-reactivity continuum of major bioelements in the Ocean. *Ann Rev Mar Sci* **7**: 185–205.

de Bettignies, F., Dauby, P., Thomas, F., Gobet, A., Delage, L., Bohner, O., et al. (2020) Degradation dynamics and processes associated with the accumulation of *Laminaria hyperborea* (Phaeophyceae) kelp fragments: an in situ experimental approach. *J Phycol* **56**: 1481–1492.

Bjursell, M.K., Martens, E.C., and Gordon, J.I. (2006) Functional genomic and metabolic studies of the adaptations of a prominent adult human gut symbiont, *Bacteroides thetaiotaomicron*, to the suckling period. *J Biol Chem* **281**: 36269–36279.

Blumenkrantz, N. and Asboe-Hansen, G. (1973) New method for quantitative determination of uronic acids. *Anal Biochem* **54**: 484–489.

Bolger, A.M., Lohse, M., and Usadel, B. (2014) Trimmomatic: A flexible trimmer for Illumina sequence data. *Bioinformatics* **30**: 2114–2120.

Bringloe, T.T., Starko, S., Wade, R.M., Vieira, C., Kawai, H., De Clerck, O., et al. (2020) Phylogeny and Evolution of the Brown Algae. *CRC Crit Rev Plant Sci* **39**: 281–321.

Brouwer, H., Coutinho, P.M., Henrissat, B., and de Vries, R.P. (2014) Carbohydrate-related enzymes of important Phytophthora plant pathogens. *Fungal Genet Biol* **72**: 192–200.

Bruhn, A., Janicek, T., Manns, D., Nielsen, M.M., Balsby, T.J.S., Meyer, A.S., et al. (2017) Crude fucoidan content in two North Atlantic kelp species, *Saccharina latissima* and *Laminaria digitata*—seasonal variation and impact of environmental factors. *J Appl Phycol* **29**: 3121–3137.

Brunet, M., de Bettignies, F., Le Duff, N., Tanguy, G., Davoult, D., Leblanc, C., et al. (2021) Accumulation of detached kelp biomass in a subtidal temperate coastal ecosystem induces succession of epiphytic and sediment bacterial communities. *Environ Microbiol* **23**: 1638–1655.

Bunse, C., Koch, H., Breider, S., Simon, M., and Wietz, M. (2021) Sweet spheres: succession and CAZyme expression of marine bacterial communities colonizing a mix of alginate and pectin particles. *Environ Microbiol* **23**: 3130–3148.

Burke, C., Steinberg, P., Rusch, D., Kjelleberg, S., and Thomas, T. (2011) Bacterial community assembly based on functional genes rather than species. *Proc Natl Acad Sci U S A* **108**: 14288–14293.

Cardoso, I., Cotas, J., Rodrigues, A., Ferreira, D., Osoria, N., and Pereira, L. (2019) Extraction and Analysis of Compounds with Antibacterial Potential from the Red Alga *Grateloupia turuturu*. *J Mar Sci Eng* **7**: 220.

Carpenter, L.J. and Liss, P.S. (2000) On temperate sources of bromoform and other reactive organic bromine gases. *J Geophys Res Atmos* **105**: 20539–20547.

Case, R., Longford, S., Campbell, A., Low, A., Tujula, N.A., Steinberg, P.D., and Kjelleberg, S. (2010) Temperature induced bacterial virulence and bleaching disease in a chemically defended marine macroalga. *Environ Microbiol* **13**: 529–537.

Cavaliere, M., Feng, S., Soyer, O., and Jiménez, J. (2017) Cooperation in microbial communities and their biotechnological applications. *Environ Microbiol* **19**: 2949–2963.

Cecere, E., Moro, I., Wolf, M., Petrocelli, A., Verlaque, M., and Sfriso, A. (2011) The introduced seaweed *Grateloupia turuturu* (Rhodophyta, Halymeniales) in two Mediterranean transitional water systems. *Bo* **54**: 23–33.

Chen, S., Bagdasarian, M., Kaufman, M.G., and Walker, E.D. (2007) Characterization of strong promoters from an environmental *Flavobactenum hibernum* strain by using a green fluorescent protein-based reporter system. *Appl Environ Microbiol* **73**: 1089–1100.

Chen, X., Hu, Y., Yang, B., Gong, X., Zhang, N., Niu, L., et al. (2015) Structure of lpg0406, a carboxymuconolactone decarboxylase family protein possibly involved in antioxidative response from *Legionella pneumophila*. *Protein Sci* **24**: 2070–2075.

Chernysheva, N., Bystritskaya, E., Likhatskaya, G., Nedashkovskaya, O., and Isaeva, M. (2021) Genome-wide analysis of PL7 alginate lyases in the genus *Zobellia*. *Molecules* **26**: 2387.

Chernysheva, N., Bystritskaya, E., Stenkova, A., and Golovkin, I. (2019) Comparative genomics and CAZyme genome repertoires of marine *Zobellia amurskyensis* KMM 3526T and *Zobellia laminariae* KMM 3676T. *Mar Drugs*. **17**: 661.

Chevolot, L., Mulloy, B., Ratiskol, J., Foucault, A., and Colliec-Jouault, S. (2001) A disaccharide repeat unit is the major structure in fucoidan from two species of brown algae. *Carbohydr Res* **330**: 529–535.

Choi, D.H., Kim, Y.G., Hwang, C.Y., Yi, H., Chun, J., and Cho, B.C. (2006) *Tenacibaculum litoreum* sp. nov., isolated from tidal flat sediment. *Int J Syst Evol Microbiol* **56**: 635–640.

Christiansen, L., Pathiraja, D., Bech, P.K., Schultz-johansen, M., Hennessy, R., Teze, D., et al. (2020) A Multifunctional Polysaccharide Utilization Gene Cluster in *Colwellia echini* Encodes Enzymes for the Complete Degradation of κ-Carrageenan, ι-Carrageenan, and Hybrid β/κ -Carrageenan. *mSphere* **5**: 1–16.

Cocquempot, L., Delacourt, C., Paillet, J., Riou, P., Aucan, J., Castelle, B., et al. (2019) Coastal ocean and nearshore observation: A French case study. *Front Mar Sci* **6**:324.

Coelho, S.M. and Cock, J.M. (2020) Brown Algal Model Organisms. *Annu Rev Genet* **54**: 71–92.

Cole, J.J. (1982) Interactions between bacteria and algae in aquatic ecosystems. *Annu Rev Ecol Syst* **13**: 291–314.

Colin, C., Leblanc, C., Michel, G., Wagner, E., Leize-Wagner, E., Van Dorsselaer, A., and Potin, P. (2005) Vanadium-dependent iodoperoxidases in *Laminaria digitata*, a novel biochemical function diverging from brown algal bromoperoxidases. *J Biol Inorg Chem* **10**: 156–166.

Colin, S., Deniaud, E., Jam, M., Descamps, V., Chevolot, Y., Kervarec, N., et al. (2006) Cloning and biochemical characterization of the fucanase FcnA: Definition of a novel glycoside hydrolase family specific for sulfated fucans. *Glycobiology* **16**: 1021–1032.

Condemine, G., Hugouvieux-Cotte-Pattat, N., and Robert-Baudouy, J. (1986) Isolation of *Erwinia chrysanthemi* kduD mutants altered in pectin degradation. *J Bacteriol* **165**: 937–941.

Condemine, G. and Robert-Baudouy, J. (1991) Analysis of an *Erwinia chrysanthemi* gene cluster involved in pectin degradation. *Mol Microbiol* **5**: 2191–2202.

Correc, G., Hehemann, J.-H., Czjzek, M., and Helbert, W. (2011) Structural analysis of the degradation products of porphyran digested by *Zobellia galactanivorans* β-porphyranase A. *Carbohydr Polym* **83**: 277–283.

Cosse, A., Leblanc, C., and Potin, P. (2007) Dynamic Defense of Marine Macroalgae Against Pathogens: From Early Activated to Gene-Regulated Responses. *Adv Bot Res* **46**: 221–266.

Cosse, A., Potin, P., and Leblanc, C. (2009) Patterns of gene expression induced by oligoguluronates reveal conserved and environment-specific molecular defense responses in the brown alga *Laminaria digitata*. *New Phytol* **182**: 239–250.

Craigie, J.S., Correa, J., and Gordon, M. (1992) Cutickes from *Chondrus crispus* (Rhodophyta). *J Phycol* **28**: 777–786.

Cumashi, A., Ushakova, N.A., Preobrazhenskaya, M.E., D'Incecco, A., Piccoli, A., Totani, L., et al. (2007) A comparative study of the anti-inflammatory, anticoagulant, antiangiogenic, and antiadhesive activities of nine different fucoidans from brown seaweeds. *Glycobiology* **17**: 541–

552.

Cuskin, F., Lowe, E.C., Temple, M.J., Zhu, Y., Cameron, E.A., Pudlo, N.A., et al. (2015) Corrigendum: Human gut Bacteroidetes can utilize yeast mannan through a selfish mechanism. *Nature* **520**: 388.

Daims, H., Brühl, A., Amann, R., Schleifer, K.H., and Wagner, M. (1999) The domain-specific probe EUB338 is insufficient for the detection of all bacteria: Development and evaluation of a more comprehensive probe set. *Syst Appl Microbiol* **22**: 434–444.

Datta, M.S., Sliwerska, E., Gore, J., Polz, M.F., and Cordero, O.X. (2016) Microbial interactions lead to rapid micro-scale successions on model marine particles. *Nat Commun* **7**:.

Deniaud-Bouët, E., Hardouin, K., Potin, P., Kloareg, B., and Hervé, C. (2017) A review about brown algal cell walls and fucose-containing sulfated polysaccharides: Cell wall context, biomedical properties and key research challenges. *Carbohydr Polym* **175**: 395–408.

Deniaud-Bouët, E., Kervarec, N., Michel, G., Tonon, T., Kloareg, B., and Hervé, C. (2014) Chemical and enzymatic fractionation of cell walls from Fucales: Insights into the structure of the extracellular matrix of brown algae. *Ann Bot* **114**: 1203–1216.

Deniaud, E., Fleurence, J., and Lahaye, M. (2003) Preparation and chemical characterization of cell wall fractions enriched in structural proteins from *Palmaria palmata* (Rhodophyta). *Bot Mar* **46**: 366–377.

Denis, C., Morancais, M., Gaudin, P., and Fleurence, J. (2009) Effect of enzymatic digestion on thallus degradation and extraction of hydrosoluble compounds from *Grateloupia turuturu*. *Bot Mar* **52**: 262–267.

Dogs, M., Wemheuer, B., Wolter, L., Bergen, N., Daniel, R., Simon, M., and Brinkhoff, T. (2017) Rhodobacteraceae on the marine brown alga *Fucus spiralis* are abundant and show physiological adaptation to an epiphytic lifestyle. *Syst Appl Microbiol* **40**: 370–382.

Domozych, D.S., Ciancia, M., Fangel, J.U., Mikkelsen, M.D., Ulvskov, P., and Willats, W.G.T. (2012) The cell walls of green algae: A journey through evolution and diversity. *Front Plant Sci* **3**:82.

Douglas, G.M., Maffei, V.J., Zaneveld, J., Yurgel, S.N., Brown, J.R., Taylor, C.M., et al. (2020) PICRUSt2: An improved and extensible approach for metagenome inference. *bioRxiv* 672295.

Duarte, C., Middelburg, J.J., and Caraco, N. (2005) Major role of marine vegetation on the oceanic carbon cycle. *Biogeosciences* **2**: 1–8.

Duarte, C.M. (2017) Reviews and syntheses: Hidden forests, the role of vegetated coastal habitats in the ocean carbon budget. *Biogeosciences* **14**: 301–310.

Duarte, C.M. and Cebrian, J. (1996) The Fate of Marine Autotrophic Consumption. *Limnol Oceanogr* **41**: 1758–1766.

Duchesne, L.C. and Larson, D.W. (1989) Cellulose and the Evolution of Plant Life. *Bioscience* **39**: 238–241.

Ducklow, H.W. (1983) Production and fate of bacteria in the ocean. *Bioscience* **33**: 494–501.

Ducklow, H.W., Kirchman, D.L., Quinby, H.L., Carlson, C.A., and Dam, H.G. (1993) Stocks and dynamics of bacterioplankton carbon during the spring bloom in the eastern North Atlantic Ocean. *Deep Res Part II* **40**: 245–263.

Dudek, M., Dieudonné, A., Jouanneau, D., Rochat, T., Michel, G., Sarels, B., and Thomas, F. (2020) Regulation of alginate catabolism involves a GntR family repressor in the marine flavobacterium

Zobellia galactanivorans DsijT. *Nucleic Acids Res* **48**: 7786–7800.

Duggins, D.O. and Eckman, J.E. (1997) Is kelp detritus a good food for suspension feeders? Effects of kelp species, age and secondary metabolites. *Mar Biol* **128**: 489–495.

Duggins, D.O., Simenstad, C., and Estes, J.A. (1989) Magnification of Secondary Production by Kelp Detritus in Coastal Marine Ecosystems. *Science (80-)* **245**: 170–173.

Ebrahimi, A., Schwartzman, J., and Cordero, O.X. (2019) Cooperation and spatial self-organization determine rate and efficiency of particulate organic matter degradation in marine bacteria. *PNAS* **116**: 23309–23316.

Eckroat, T.J., Greguske, C., and Hunnicutt, D.W. (2021) The Type 9 Secretion System is required for *Flavobacterium johnsoniae* biofilm formation. *Front Microbiol* **12**: 660887.

Edwards, U., Rogall, T., Blöcker, H., Emde, M., and Böttger, E.C. (1989) Isolation and direct complete nucleotide determination of entire genes. Characterization of a gene coding for 16S ribosomal RNA. *Nucleic Acids Res* **17**: 7843–7853.

Egan, S., Fernandes, N.D., Kumar, V., Gardiner, M., and Thomas, T. (2014) Bacterial pathogens, virulence mechanism and host defence in marine macroalgae. *Environ Microbiol* **16**: 925–938.

Egan, S., Harder, T., Burke, C., Steinberg, P., Kjelleberg, S., and Thomas, T. (2013) The seaweed holobiont: Understanding seaweed-bacteria interactions. *FEMS Microbiol Rev* **37**: 462–476.

Egan, S., Thomas, T., and Kjelleberg, S. (2008) Unlocking the diversity and biotechnological potential of marine surface associated microbial communities. *Curr Opin Microbiol* **11**: 219–225.

Enke, T.N., Datta, M.S., Schwartzman, J., Cermak, N., Schmitz, D., Barrere, J., et al. (2019) Modular assembly of polysaccharide-degrading marine microbial communities. *Curr Biol* **29**: 1528-1535.e6.

Escudié, F., Auer, L., Bernard, M., Mariadassou, M., Cauquil, L., Vidal, K., et al. (2018) FROGS: Find, Rapidly, OTUs with Galaxy Solution. *Bioinformatics* **34**: 1287–1294.

Ewels, P., Magnusson, M., Lundin, S., and Käller, M. (2016) MultiQC: Summarize analysis results for multiple tools and samples in a single report. *Bioinformatics* **32**: 3047–3048.

Falkowski, P.G., Barber, R.T., and Smetacek, V. (1998) Biogeochemical controls and feedbacks on ocean primary production. *Science* **281**: 200–206.

Falkowski, P.G., Scholes, R., Boyle, E., Canadell, J., Canfield, D., Elser, J., et al. (2000) The global carbon cycle: a test of our knowledge of earth as a system. *Science* **290**: 291–296.

Ferguson, A.D., Hofmann, E., Coulton, J.W., Diederichs, K., and Welte, W. (1998) Siderophore-mediated iron transport: Crystal structure of FhuA with bound lipopolysaccharide. *Science* **282**: 2215–2220.

Fernandes, A.D., Reid, J.N.S., Macklaim, J.M., McMurrough, T.A., Edgell, D.R., and Gloor, G.B. (2014) Unifying the analysis of high-throughput sequencing datasets: Characterizing RNA-seq, 16S rRNA gene sequencing and selective growth experiments by compositional data analysis. *Microbiome* **2**:.

Fernandes, N., Case, R.J., Longford, S.R., Seyedsayamdost, M.R., Steinberg, P.D., Kjelleberg, S., and Thomas, T. (2011) Genomes and virulence factors of novel bacterial pathogens causing bleaching disease in the marine red alga *Delisea pulchra*. *PLoS One* **6**(12): e27387.

Fernández-Gómez, B., Richter, M., Schüler, M., Pinhassi, J., Acinas, S.G., González, J.M., and Pedrós-

Alió, C. (2013) Ecology of marine bacteroidetes: A comparative genomics approach. *ISME J* **7**: 1026–1037.

Ficko-Blean, E., Duffieux, D., Rebuffet, É., Larocque, R., Groisillier, A., Michel, G., and Czjzek, M. (2015) Biochemical and structural investigation of two paralogous glycoside hydrolases from *Zobellia galactanivorans:* Novel insights into the evolution, dimerization plasticity and catalytic mechanism of the GH117 family. *Acta Crystallogr Sect D Biol Crystallogr* **71**: 209–223.

Ficko-Blean, E., Préchoux, A., Thomas, F., Rochat, T., Larocque, R., Zhu, Y., et al. (2017) Carrageenan catabolism is encoded by a complex regulon in marine heterotrophic bacteria. *Nat Commun* **8**: 1685.

Field, C., Behrenfeld, M., Raderson, J., and Falkowski, P.G. (1998) Primary production of the biosphere: integrating terrestrial and oceanic components. *Science* **281**: 237–270.

Filisetti-Cozzi, T. and Carpita, N. (1991) Measurement of uronic acids without interference from neutral sugars. *Anal Biochem* **197**: 15162.

Filote, C., Santos, S.C.R., Popa, V.I., Botelho, C.M.S., and Volf, I. (2021) Biorefinery of marine macroalgae into high-tech bioproducts: a review, Springer International Publishing.

Fletcher, H.R., Biller, P., Ross, A.B., and Adams, J.M.M. (2017) The seasonal variation of fucoidan within three species of brown macroalgae. *Algal Res* **22**: 79–86.

Fleurence, J. (1999) The enzymatic degradation of algal cell walls: A useful approach for improving protein accessibility? *J Appl Phycol* **11**: 313–314.

Flewelling, A.J., Ellsworth, K.T., Sanford, J., Forward, E., Johnson, J.A., and Gray, C.A. (2013) Macroalgal endophytes from the atlantic coast of canada: A potential source of antibiotic natural products? *Microorganisms* **1**: 175–187.

Florez, J.Z., Camus, C., Hengst, M.B., and Buschmann, A.H. (2017) A functional perspective analysis of macroalgae and epiphytic bacterial community interaction. *Front Microbiol* **8**: 2561.

Florez, J.Z., Camus, C., Hengst, M.B., Marchant, F., and Buschmann, A.H. (2019) Structure of the epiphytic bacterial communities of *Macrocystis pyrifera* in localities with contrasting nitrogen concentrations and temperature. *Algal Res* **44**: 101706.

Fournier, J.B., Rebuffet, E., Delage, L., Grijol, R., Meslet-Cladière, L., Rzonca, J., et al. (2014) The vanadium iodoperoxidase from the marine *Flavobacteriaceae* species *Zobellia galactanivorans* reveals novel molecular and evolutionary features of halide specificity in the vanadium haloperoxidase enzyme family. *Appl Environ Microbiol* **80**: 7561–7573.

Frette, L., Jørgensen, N.O.G., Irming, H., and Kroer, N. (2004) *Tenacibaculum skagerrakense* sp. nov., a marine bacterium isolated from the pelagic zone in Skagerrak, Denmark. *Int J Syst Evol Microbiol* **54**: 519–524.

Fries, N. (1979) Physiological Characteristics of *Mycosphaerella ascophylli*, a Fungal Endophyte of the Marine Brown Alga *Ascophyllum nodosum*. *Physiol Plant* **45**: 117–121.

Furukawa, S., Fujikawa, T., Koga, D., and Ide, A. (1992) Production of fucoidan-degrading enzymes, fucoidanase, and fucoidan sulfatase by *Vibrio* sp. N-5. *Bull Japanese Soc Sci Fish* **58**: 1499–1503.

Gachon, C., Sime-Ngando, T., Strittmatter, M., Chambouvet, A., and Kim, G. (2010) Algal diseases: spotlight on a black box. *Trends Plant Sci* **15**: 633_640.

Galland-Irmouli, A.V., Fleurence, J., Lamghari, R., Luçon, M., Rouxel, C., Barbaroux, O., et al. (1999) Nutritional value of proteins from edible seaweed *Palmaria palmata* (Dulse). *J Nutr Biochem* **10**:

353–359.

Garbary, D.J., Brown, N.E., MacDonell, H.J., and Toxopeux, J. (2017) *Ascophyllum* and its symbionts — A complex symbiotic community on North Atlantic shores. In *Algal and Cyanobacteria Symbioses*. pp. 547–572.

Gardy, J.L., Spencer, C., Wang, K., Ester, M., Tusnády, G.E., Simon, I., et al. (2003) PSORT-B: Improving protein subcellular localization prediction for Gram-negative bacteria. *Nucleic Acids Res* **31**: 3613–3617.

Georg, J., Vob, B., Scholz, I., Mitschke, J., Wilde, A., and Hess, W.R. (2009) Evidence for a major role of antisense RNAs in cyanobacterial gene regulation. *Mol Syst Biol* **5**: 305.

Gilbert, J.A., Field, D., Swift, P., Newbold, L., Oliver, A., Smyth, T., et al. (2009) The seasonal structure of microbial communities in the Western English Channel. *Environ Microbiol* **12**: 3132–3139.

Gilbert, J.A., Steele, J.A., Caporaso, J.G., Steinbrück, L., Reeder, J., Temperton, B., et al. (2012) Defining seasonal marine microbial community dynamics. *ISME J* **6**: 298–308.

Gobet, A., Mest, L., Perennou, M., Dittami, S.M., Caralp, C., Coulombet, C., et al. (2018) Seasonal and algal diet-driven patterns of the digestive microbiota of the European abalone *Haliotis tuberculata*, a generalist marine herbivore. *Microbiome* **6**: 60.

Graham, L. and Wilcox, L. (2000) The origin of alternation of generation in land plant: a focus on matrotrophy and hexose transport. *Philos Trans R Soc B Biol Sci* **355**: 757–767.

Gralka, M., Szabo, R., Stocker, R., and Cordero, O.X. (2020) Trophic interactions and the drivers of microbial community assembly. *Curr Biol* **30**: R1176–R1188.

Granado, I. and Caballero, P. (2001) Feeding rates of *Littorina striata* and *Osilinus atratus* in relation to nutritional quality and chemical defenses of seaweeds. *Mar Biol* **138**: 1213–1224.

Grigorian, E., Groisillier, A., Thomas, F., Leblanc, C., and Delage, L. (2021) Functional characterization of a L-2-haloacid dehalogenase from *Zobellia galactanivorans* DsijT suggests a role in haloacetic acid catabolism and a wide distribution in marine environments. *Front Microbiol* **12**: 725997.

Groisillier, A., Hervé, C., Jeudy, A., Rebuffet, E., Pluchon, P.F., Chevolot, Y., et al. (2010) MARINE-EXPRESS: Taking advantage of high throughput cloning and expression strategies for the post-genomic analysis of marine organisms. *Microb Cell Fact* **9**: 1–11.

Groisillier, A., Labourel, A., Michel, G., and Tonon, T. (2015) The mannitol utilization system of the marine bacterium *Zobellia galactanivorans*. *Appl Environ Microbiol* **81**: 1799–1812.

Groisillier, A., Shao, Z., Michel, G., Goulitquer, S., Bonin, P., Krahulec, S., et al. (2014) Mannitol metabolism in brown algae involves a new phosphatase family. *J Exp Bot* **65**: 559–570.

Grondin, J.M., Tamura, K., Déjean, G., Abbott, D.W., and Brumer, H. (2017) Polysaccharide utilization loci: Fueling microbial communities. *J Bacteriol* **199**: 1–15.

Gu, X., Fu, L., Pan, A., Gui, Y., Zhang, Q., and Li, J. (2021) Multifunctional alkalophilic α-amylase with diverse raw seaweed degrading activities. *AMB Express* **11**: 139.

Guiry, M.D. (2012) How many species of algae are there? *J Phycol* **48**: 1057–1063.

Han, B., Zhang, S., Wang, P., and Wang, C. (2018) Effects of water flow on submerged macrophyte-biofilm systems in constructed wetlands. *Sci Rep* **8**: 1–12.

Handa, N., Terada, T., Doi-katayama, Y., HIrota, H., Tame, J., Park, A., et al. (2005) Crystal structure of a novel polyisoprenoid-binding protein from *Thermus thermophilus* HB8. *Protein Sci* **14**: 1004–

1010.

Hanic, L.A. and Craigie, J.S. (1969) Studies on the algal cuticle. *J Phycol* **5**: 89–102.

Hansell, D.A., Carlson, C.A., Repeta, D.J., and Schlitzer, R. (2009) Dissolved organic matter in the ocean a controversy stim ulates new insights. *Oceanography* **22**: 202–211.

Hara, S., Terauchi, K., and Koike, I. (1991) Abundance of viruses in marine waters: Assessment by epifluorescence and transmission electron microscopy. *Appl Environ Microbiol* **57**: 2731–2734.

Harms, H., Poehlein, A., Thürmer, A., and König, G.M. (2017) Draft Genome Sequence of *Zobellia* sp. Strain OII3, Isolated from the Coastal Zone of the Baltic Sea. *Genome Annoucements* **5**: 5–6.

Haug, A., Larsen, B., and Smidsrød, O. (1974) Uronic acid sequence in alginate from different sources. *Carbohydr Res* **32**: 217–225.

Hehemann, J.H., Arevalo, P., Datta, M.S., Yu, X., Corzett, C.H., Henschel, A., et al. (2016) Adaptive radiation by waves of gene transfer leads to fine-scale resource partitioning in marine microbes. *Nat Commun* **7**: 12860.

Hehemann, J.H., Correc, G., Barbeyron, T., Helbert, W., Czjzek, M., and Michel, G. (2010) Transfer of carbohydrate-active enzymes from marine bacteria to Japanese gut microbiota. *Nature* **464**: 908–912.

Hehemann, J.H., Correc, G., Thomas, F., Bernard, T., Barbeyron, T., Jam, M., et al. (2012) Biochemical and structural characterization of the complex agarolytic enzyme system from the marine bacterium *Zobellia galactanivorans*. *J Biol Chem* **287**: 30571–30584.

Heindl, H., Wiese, J., and Imhoff, J.F. (2008) *Tenacibaculum adriaticum* sp. nov., from a bryozoan in the Adriatic Sea. *Int J Syst Evol Microbiol* **58**: 542–547.

Heinze, S., Mechelke, M., Kornberger, P., Liebl, W., Schwarz, W.H., and Zverlov, V. V. (2017) Identification of endoxylanase XynE from *Clostridium thermocellum* as the first xylanase of glycoside hydrolase family GH141. *Sci Rep* **7**: 11178.

Hentati, F., Tounsi, L., Djomdi, D., Pierre, G., Delattre, C., Ursu, A.V., et al. (2020) Bioactive polysaccharides from seaweeds. *Molecules* **25**: 3152.

Herburger, K., Xin, A., and Holzinger, A. (2019) Homogalacturonan accumulation in cell walls of the green alga *Zygnema* sp. (charophyta) increases desiccation resistance. *Front Plant Sci* **10**: 540.

Hettle, A.G., Hobbs, J.K., Pluvinage, B., Vickers, C., Abe, K.T., Salama-Alber, O., et al. (2019) Insights into the κ/ι-carrageenan metabolism pathway of some marine *Pseudoalteromonas* species. *Commun Biol* **2**: 474.

Hierholtzer, A., Chatellard, L., Kierans, M., Akunna, J.C., and Collier, P.J. (2013) The impact and mode of action of phenolic compounds extracted from brown seaweed on mixed anaerobic microbial cultures. *J Appl Microbiol* **114**: 964–973.

Holdt, S.L. and Kraan, S. (2011) Bioactive compounds in seaweed: Functional food applications and legislation. *J Appl Phycol* **23**: 543–597.

Hollants, J., Leliaert, F., De Clerck, O., and Willems, A. (2013) What we can learn from sushi: A review on seaweed-bacterial associations. *FEMS Microbiol Ecol* **83**: 1–16.

Holmström, C., Egan, S., Franks, A., McCloy, S., and Kjelleberg, S. (2002) Antifouling activities expressed by marine surface associated *Pseudoalteromonas* species. *FEMS Microbiol Ecol* **41**: 47–58.

Hu, P., Xue, R., Li, Z., Chen, M., Sun, Z., Jiang, J., and Huang, C. (2014) Structural investigation and immunological activity of a heteropolysaccharide from *Sargassum fusiforme*. *Carbohydr Res* **390**: 28–32.

Ihua, M.W., FitzGerald, J.A., Guiheneuf, F., Jackson, S.A., Claesson, M.J., Stengel, D.B., and Dobson, A.D.W. (2020) Diversity of bacteria populations associated with different thallus regions of the brown alga *Laminaria digitata*. *PLoS One* **15**:.

Itoh, T., Hashimoto, W., Mikami, B., and Murata, K. (2006) Crystal structure of unsaturated glucuronyl hydrolase complexed with substrate: Molecular insights into its catalytic reaction mechanism. *J Biol Chem* **281**: 29807–29816.

Ivanova, E.P., Bakunina, I.Y., Sawabe, T., Hayashi, K., Alexeeva, Y. V., Zhukova, N. V., et al. (2002) Two species of culturable bacteria associated with degradation of brown algae *Fucus evanescens*. *Microb Ecol* **43**: 242–249.

Jackson, P. (1996) The Analysis of Fluorophore-Labeled Carbohydrates by Polyacrylamide Gel Electrophoresis. *Appl Biochem Biotechnol - Part B Mol Biotechnol* **5**: 101–123.

Jam, M., Flament, D., Allouch, J., Potin, P., Thion, L., Kloareg, B., et al. (2005) The endo-β-agarases AgaA and AgaB from the marine bacterium *Zobellia galactanivorans*: Two paralogue enzymes with different molecular organizations and catalytic behaviours. *Biochem J* **385**: 703–713.

Jensen, P. and Fenical, W. (1995) The Relative Abundance and Seawater Requirements of Gram-Positive Bacteria in Near-Shore Tropical Marine Samples. *Microb Ecol* **29**: 249–257.

Jiao, G., Yu, G., Zhang, J., and Ewart, H.S. (2011) Chemical structures and bioactivities of sulfated polysaccharides from marine algae. *Mar Drugs* **9**: 196–233.

Jiménez, D.J., Dini-Andreote, F., DeAngelis, K.M., Singer, S.W., Salles, J.F., and van Elsas, J.D. (2017) Ecological Insights into the Dynamics of Plant Biomass-Degrading Microbial Consortia. *Trends Microbiol* **25**: 788–796.

Jones, C.G., Lawton, J.H., Shachak, M., and Organisms, M. (1994) Organisms as Ecosystem Engineers Author (s): Clive G . Jones , John H . Lawton and Moshe Shachak Published by : Wiley on behalf of Nordic Society Oikos. *Oikos* **69**: 373–386.

Jönsson, M., Allahgholi, L., Sardari, R.R.R., Hreggviosson, G.O., and Karlsson, E.N. (2020) Extraction and modification of macroalgal polysaccharides for current and next-generation applications. *Molecules* **25**: 930.

Jouanneau, D., Klau, L.J., Larocque, R., Jaffrennou, A., Duval, G., Le Duff, N., et al. (2021) Structure–function analysis of a new PL17 oligoalginate lyase from the marine bacterium *Zobellia galactanivorans* DsijT . *Glycobiology* **31**(10):1364-1377.

Juncker, A.S., Willenbrock, H., von Heijne, G., Brunak, S., Nielsen, H., and Krogh, A. (2003) Prediction of lipoprotein signal peptides in Gram-negative bacteria. *Protein Sci* **12**: 1652–1662.

Jung, K.A., Lim, S.R., Kim, Y., and Park, J.M. (2013) Potentials of macroalgae as feedstocks for biorefinery. *Bioresour Technol* **135**: 182–190.

Jung, S.Y., Oh, T.K., and Yoon, J.H. (2006) *Tenacibaculum aestuarii* sp. nov., isolated from a tidal flat sediment in Korea. *Int J Syst Evol Microbiol* **56**: 1577–1581.

Kabisch, A., Otto, A., König, S., Becher, D., Albrecht, D., Schüler, M., et al. (2014) Functional characterization of polysaccharide utilization loci in the marine *Bacteroidetes* "*Gramella forsetii*" KT0803. *ISME J* **8**: 1492–1502.

Kane, M.D., Poulsen, L.K., and Stahl, D.A. (1993) Monitoring the enrichment and isolation of sulfate-reducing bacteria by using oligonucleotide hybridization probes designed from environmentally derived 16S rRNA sequences. *Appl Environ Microbiol* **59**: 682–686.

Kang, S.J., Lee, S.Y., Lee, M.H., Oh, T.K., and Yoon, J.H. (2011) *Tenacibaculum geojense* sp. nov., isolated from seawater. *Int J Syst Evol Microbiol* **62**: 18–22.

Kaoutari, A. El, Armougom, F., Gordon, J.I., Raoult, D., and Henrissat, B. (2013) The abundance and variety of carbohydrate-active enzymes in the human gut microbiota. *Nat Rev Microbiol* **11**: 497–504.

Keeling, P.J. (2010) The endosymbiotic origin, diversification and fate of plastids. *Philos Trans R Soc B Biol Sci* **365**: 729–748.

Khan, S.T., Fukunaga, Y., Nakagawa, Y., and Harayama, S. (2007) Emended descriptions of the genus *Lewinella* and of *Lewinella cohaerens*, *Lewinella nigricans* and *Lewinella persica*, and description of *Lewinella lutea* sp. nov. and *Lewinella marina* sp. nov. *Int J Syst Evol Microbiol* **57**: 2946–2951.

Kidby, D.K. and Davidson, D.J. (1973) Ferricyanide estimation of sugars in the nanomole range. *Anal Biochem* **55**: 321–325.

Kim, J.-H., Lee, G., Shin, Y., and Kim, J. (1992) A study on the relationships between the epiphytic microbes and the blight of *Porphyra* species from the coastal waters of the yellow sea, Korea. *Bull Korean Fish Soc* **25**: 307–313.

Kim, Y.O., Park, S., Nam, B.H., Jung, Y.T., Kim, D.G., Jee, Y.J., and Yoon, J.H. (2013) *Tenacibaculum halocynthiae* sp. nov., a member of the family *Flavobacteriaceae* isolated from sea squirt *Halocynthia roretzi*. *Antonie van Leeuwenhoek, Int J Gen Mol Microbiol* **103**: 1321–1327.

Kirchman, D.L. (2008) Microbial Ecology of the Oceans.

Kirchman, D.L. (2002) The ecology of *Cytophaga-Flavobacteria* in aquatic environments. *FEMS Microbiol Ecol* **39**: 91–100.

Kjeldgaard, N.O. and Kurland, C.G. (1963) The distribution of soluble and ribosomal RNA as a function of growth rate. *J Mol Biol* **6**: 341–348.

Klindworth, A., Pruesse, E., Schweer, T., Peplies, J., Quast, C., Horn, M., and Glöckner, F.O. (2013) Evaluation of general 16S ribosomal RNA gene PCR primers for classical and next-generation sequencing-based diversity studies. *Nucleic Acids Res* **41**: e1.

Kloareg, B., Badis, Y., Cock, J.M., and Michel, G. (2021) Role and evolution of the extracellular matrix in the acquisition of complex multicellularity in eukaryotes: A macroalgal perspective. *Genes* **12**: 1059.

Kloareg, B. and Quatrano, R.S. (1988) Structure of the cell walls of marine algae and ecophysiological functions of the matrix polysaccharides. *Ocean Mar Biol Annu Rev* **26**: 259–315.

Koch, H., Dürwald, A., Schweder, T., Noriega-Ortega, B., Vidal-Melgosa, S., Hehemann, J.H., et al. (2019) Biphasic cellular adaptations and ecological implications of *Alteromonas macleodii* degrading a mixture of algal polysaccharides. *ISME J* **13**: 92–103.

Koch, H., Freese, H.M., Hahnke, R.L., Simon, M., and Wietz, M. (2019) Adaptations of *Alteromonas* sp. 76-1 to polysaccharide degradation: A CAZyme plasmid for ulvan degradation and two alginolytic systems. *Front Microbiol* **10**: 504.

Koch, H., Germscheid, N., Freese, H.M., Noriega-Ortega, B., Lücking, D., Berger, M., et al. (2020)

Genomic, metabolic and phenotypic variability shapes ecological differentiation and intraspecies interactions of *Alteromonas macleodii*. *Sci Rep* **10**: 809.

Kopp, J. and Perez, R. (1961) Contribution à l'étude de l'algue rouge *Chondrus crispus* stack. Relation entre la croissance, la potentialité sexuelle, la quantité et la composition des carraghénanes. *Rev des Trav l'Institut des Pêches Marit* **42**: 291–324.

Kopplin, G., Rokstad, A.M., Mélida, H., Bulone, V., Skjåk-Bræk, G., and Aachmann, F.L. (2018) Structural Characterization of Fucoidan from *Laminaria hyperborea*: Assessment of Coagulation and Inflammatory Properties and Their Structure-Function Relationship. *ACS Appl Bio Mater* **1**: 1880–1892.

Kornprobst, J. (2005) Substances naturelles d'origine marine. Chimiodiversité-Pharmacodiversité-Biotechnologie. 1. Généralités-Microorganismes-Algues.

Koropatkin, N.M., Cameron, E.A., and Martens, E.C. (2012) How glycan metabolism shapes the human gut microbiota. *Nat Rev Microbiol* **10**: 323–335.

Krassowski, M. (2020) krassowski/complex-upset.

Krause-Jensen, D. and Duarte, C. (2016) Substantial role of macroalgae in marine carbon sequestration. *Nat Geosci* **9**: 737–742.

Krogh, A., Larsson, B., Von Heijne, G., and Sonnhammer, E.L.L. (2001) Predicting transmembrane protein topology with a hidden Markov model: Application to complete genomes. *J Mol Biol* **305**: 567–580.

Kumar, V., Zozaya-Valdes, E., Kjelleberg, S., Thomas, T., and Egan, S. (2016) Multiple opportunistic pathogens can cause a bleaching disease in the red seaweed *Delisea pulchra*. *Environ Microbiol* **18**: 3962–3975.

Küpper, F.C., Carpenter, L.J., McFiggans, G.B., Palmer, C.J., Waite, T.J., Boneberg, E.M., et al. (2008) Iodide accumulation provides kelp with an inorganic antioxidant impacting atmospheric chemistry. *Proc Natl Acad Sci U S A* **105**: 6954–6958.

Küpper, F.C., Kloareg, B., Guern, J., and Potin, P. (2001) Oligoguluronates elicit an oxidative burst in the brown algal kelp *Laminaria digitata*. *Plant Physiol* **125**: 278–291.

Küpper, F.C., Müller, D.G., Peters, A.F., Kloareg, B., and Potin, P. (2002) Oligoalginate recognition and oxidative burst play a key role in natural and induced resistance of sporophytes of Laminariales. *Ann Oper Res* **28**: 2057–2081.

Küpper, F.C., Schweigert, N., Ar Gall, E., Legendre, J.M., Vilter, H., and Kloareg, B. (1998) Iodine uptake in Laminariales involves extracellular, haloperoxidase-mediated oxidation of iodide. *Planta* **207**: 163–171.

Kusaykin, M.I., Silchenko, A.S., Zakharenko, A.M., and Zvyagintseva, T.N. (2015) Fucoidanases. *Glycobiology* **26**: 3–12.

Labourel, A., Jam, M., Jeudy, A., Hehemann, J.H., Czjzek, M., and Michel, G. (2014) The β-glucanase ZgLamA from *Zobellia galactanivorans* evolved a bent active site adapted for efficient degradation of algal laminarin. *J Biol Chem* **289**: 2027–2042.

Labourel, A., Jam, M., Legentil, L., Sylla, B., Hehemann, J.H., Ferrières, V., et al. (2015) Structural and biochemical characterization of the laminarinase ZgLamCGH16 from *Zobellia galactanivorans* suggests preferred recognition of branched laminarin. *Acta Crystallogr* **D71**: 173–184.

Lachnit, T., Blümel, M., Imhoff, J.F., and Wahl, M. (2009) Specific epibacterial communities on

macroalgae: Phylogeny matters more than habitat. *Aquat Biol* **5**: 181–186.

Lachnit, T., Meske, D., Wahl, M., Harder, T., and Schmitz, R. (2011) Epibacterial community patterns on marine macroalgae are host-specific but temporally variable. *Environ Microbiol* **13**: 655–665.

Lage, O.M. and Graça, A.P. (2016) Biofilms: An Extra Coat on Macroalgae. *Algae - Org Imminent Biotechnol*.

Lahaye, M., Michel, C., and Barry, J.-L. (1993) Chemical, physicochemical and in-vitro fermentation characteristics of dietary fibres from *Palmaria palmata* (L.) Kuntze. *Food Chem* **47**: 29–36.

Lahaye, M. and Robic, A. (2007) Structure and function properties of Ulvan, a polysaccharide from green seaweeds. *Biomacromolecules* **8**: 1765–1774.

Lami, R., Grimaud, R., Sanchez-Brosseau, S., Six, C., Thomas, F., West, N.J., et al. (2021) Marine bacterial models for experimental biology. In *Handbook of Marine Model Organisms in Experimental Biology*. Boutet, A. and Schierwater, B. (eds).

Langmead, B. and Salzberg, S.L. (2012) Fast gapped-read alignment with Bowtie 2. *Nat Methods* **9**: 357–359.

Lankiewicz, T.S., Cottrell, M.T., and Kirchman, D.L. (2016) Growth rates and rRNA content of four marine bacteria in pure cultures and in the Delaware estuary. *ISME J* **10**: 823–832.

Lasica, A.M., Ksiazek, M., Madej, M., and Potempa, J. (2017) The Type IX Secretion System (T9SS): Highlights and Recent Insights into Its Structure and Function. *Front Cell Infect Microbiol* **7**: 215.

Leblanc, C., Colin, C., Cosse, A., Delage, L., La Barre, S., Morin, P., et al. (2006) Iodine transfers in the coastal marine environment: the key role of brown algae and of their vanadium-dependent haloperoxidases. *Biochimie* **88**: 1773–1785.

Lee, K.A., Choi, W.Y., Park, G.H., Jeong, Y., Park, A., Lee, Y., and Kang, D.H. (2020) Study on marine pectin extraction and its antioxidant activities from 14 marine algae under different extraction solvents. *J Korean Soc Food Sci Nutr* **49**: 677–685.

Lee, Y.S., Baik, K.S., Park, S.Y., Kim, E.M., Lee, D.H., Kahng, H.Y., et al. (2009) *Tenacibaculum crassostreae* sp. nov., isolated from the Pacific oyster, *Crassostrea gigas*. *Int J Syst Evol Microbiol* **59**: 1609–1614.

Leedham, E., Hughes, C., Keng, F., Phang, S., Malin, G., and Sturges, W. (2013) Emission of atmospherically significant halocarbons by naturally occurring and farmed tropical macroalgae. *Biogeosciences Discuss* **10**: 483–528.

Lemay, M., Martone, P., Keeling, P., Burt, J., Krumhansl, K., Sanders, R., and Parfrey, L. (2018) Sympatric kelp species share a large portion of their surface bacterial communities. *Environ Microbiol* **20**: 658–670.

Lex, A., Gehlenborg, N., and Strobelt, H. (2014) UpSet: Visualization of intersecting sets. *IEEE Trans Vis Comput Graph* **20**: 1983–1992.

Li, Y., Wei, J., Yang, C., Lai, Q., Chen, Z., Li, D., et al. (2013) *Tenacibaculum xiamenense* sp. nov., an algicidal bacterium isolated from coastal seawater. *Int J Syst Evol Microbiol* **63**: 3481–3486.

Lin, Y., Zhao, D., Zeng, J., Cao, X., and Jiao, C. (2019) Network analysis reveals seasonal patterns of bacterial community networks in Lake Taihu under aquaculture conditions. *Water* **11**: 1868.

Lombard, V., Golaconda Ramulu, H., Drula, E., Coutinho, P.M., and Henrissat, B. (2014) The carbohydrate-active enzymes database (CAZy) in 2013. *Nucleic Acids Res* **42**: 490–495.

Longhurst, A., Sathyendranath, S., Platt, T., and Caverhill, C. (1995) An estimate of global primary production in the ocean from satellite radiometer data. *J Plankton Res* **17**: 1245–1271.

van der Loos, L.M., Eriksson, B.K., and Falcão Salles, J. (2019) The Macroalgal Holobiont in a Changing Sea. *Trends Microbiol* **27**: 635–650.

Lopes, G., Sousa, C., Silva, L.R., Pinto, E., Andrade, P.B., Bernardo, J., et al. (2012) Can phlorotannins purified extracts constitute a novel pharmacological alternative for microbial infections with associated inflammatory conditions? *PLoS One* **7**: e31145.

Lorbeer, A., Lahnstein, J., Fincher, G., Su, P., and Zhang, W. (2014) Kinetics of conventional and microwave-assisted fucoidan extractions from the brown alga, *Ecklonia radiata*. *J Appl Phycol* **27**: 2079–2087.

Louca, S., Parfrey, L.W., and Doebeli, M. (2016) Decoupling function and taxonomy in the global ocean microbiome. *Science* **353**: 1272–1277.

Love, M.I., Huber, W., and Anders, S. (2014) Moderated estimation of fold change and dispersion for RNA-seq data with DESeq2. *Genome Biol* **15**: 1–21.

Ludwig, W., Strunk, O., Westram, R., Richter, L., Meier, H., Yadhukumar, A., et al. (2004) ARB: A software environment for sequence data. *Nucleic Acids Res* **32**: 1363–1371.

Mabeau, S. and Kloareg, B. (1987) Isolation and analysis of the cell walls of brown algae: *Fucus spiralis*, *F. ceranoides*, *F. vesiculosus*, *F. serratus*, *Bifurcaria bifurcata* and *Laminaria digitata*. *J Exp Bot* **38**: 1573–1580.

Mabeau, S., Kloareg, B., and Joseleau, J.-P. (1990) Fractionation and analysis of fucans from brown algae. *Phytochemistry* **29**: 2441–2445.

Mahé, F., Rognes, T., Quince, C., de Vargas, C., and Dunthorn, M. (2014) Swarm: robust and fast clustering method for amplicon-based studies. *PeerJ* **2**: e593.

Mahé, F., Rognes, T., Quince, C., de Vargas, C., and Dunthorn, M. (2015) Swarmv2: Highly-scalable and high-resolution amplicon clustering. *PeerJ* **2015**: e1420.

Mann, K. (1982) Ecology of coastal waters - A systems approach, Berkeley: University of California Press.

Mann, K. (1973) Seaweeds: Their Productivity and Strategy for Growth. *Science* **182**: 1154–1157.

Martens, E.C., Koropatkin, N.M., Smith, T.J., and Gordon, J.I. (2009) Complex glycan catabolism by the human gut microbiota: The bacteroidetes sus-like paradigm. *J Biol Chem* **284**: 24673–24677.

Martin, M., Barbeyron, T., Martin, R., Portetelle, D., Michel, G., and Vandenbol, M. (2015) The cultivable surface microbiota of the brown alga *Ascophyllum nodosum* is enriched in macroalgal-polysaccharide-degrading bacteria. *Front Microbiol* **6**: 1487.

Martin, M., Portetelle, D., Michel, G., and Vandenbol, M. (2014) Microorganisms living on macroalgae: Diversity, interactions, and biotechnological applications. *Appl Microbiol Biotechnol* **98**: 2917–2935.

Masella, A.P., Bartram, A.K., Truszkowski, J.M., Brown, D.G., and Neufeld, J.D. (2012) PANDAseq: paired-end assembler for Illumina sequences. *BMC Bioinformatics* **13**: 31.

Matard-Mann, M. (2017) Recherche et caractérisation de nouvelles enzymes de bactéries marines actives sur les polysaccharides algaux.

Matuso, Y., Imagawa, H., Nishizawa, M., and Shizuri, Y. (2005) Isolation of an Algal Morphogenesis

Inducer from a Marine Bacterium. *Science* **307**: 1598.

McKee, L.S., La Rosa, S.L., Westereng, B., Eijsink, V.G., Pope, P.B., and Larsbrink, J. (2021) Polysaccharide degradation by the *Bacteroidetes*: mechanisms and nomenclature. *Environ Microbiol Rep* **13**: 559–581.

Mcmurdie, P.J. and Holmes, S. (2013) phyloseq : An R package for reproducible interactive analysis and graphics of microbiome census data. *PLoS One* **8**: 1–11.

Michel, G., Tonon, T., Scornet, D., Cock, J.M., and Kloareg, B. (2010) Central and storage carbon metabolism of the brown alga *Ectocarpus siliculosus*: Insights into the origin and evolution of storage carbohydrates in Eukaryotes. *New Phytol* **188**: 67–81.

Mišurcová, L. (2011) Chemical Composition of Seaweeds. *Handb Mar Macroalgae Biotechnol Appl Phycol* 171–192.

MŁodzinska, E. (2009) Survey of plant pigments: Molecular and environmental determinants of plant colors. *Acta Biol Cracoviensia Ser Bot* **51**: 7–16.

Morgan, K.C., Wright, J.L.C., and Simpson, F.J. (1980) Review of Chemical Constituents of the Red Alga *Palmaria palmata* (Dulse). *Econ Bot* **34**: 27–50.

Murtagh, F. and Legendre, P. (2014) Ward's hierarchical clustering method: clustering criterion and agglomerative algorithm. *J Classif* **31**: 274–295.

Nagao, T., Kumabe, A., Komatsu, F., Yagi, H., Suzuki, H., and Ohshiro, T. (2017) Gene identification and characterization of fucoidan deacetylase for potential application to fucoidan degradation and diversification. *J Biosci Bioeng* **124**: 277–282.

Nagaoka, M., Shibata, H., Kimura-Takagi, I., Hashimoto, S., Kimura, K., Makino, T., et al. (1999) Structural study of fucoidan from *Cladosiphon okamuranus* TOKIDA. *Glycoconj J* **16**: 19–26.

Nagata, T. (2000) Production mechanisms of dissolved organic matter. In *Microbial Ecology of the Oceans*. pp. 121–152.

Nagayama, K., Iwamura, Y., Shibata, T., Hirayama, I., and Nakamura, T. (2002) Bactericidal activity of phlorotannins from the brown alga *Ecklonia kurome*. *J Antimicrob Chemother* **50**: 889–893.

Naretto, A., Fanuel, M., Ropartz, D., Rogniaux, H., Larocque, R., Czjzek, M., et al. (2019) The agar-specific hydrolase ZgAgaC from the marine bacterium *Zobellia galactanivorans* defines a new GH16 protein subfamily. *J Biol Chem* **294**: 6923–6939.

Nasrolahi, A., Stratil, S.B., Jacob, K.J., and Wahl, M. (2012) A protective coat of microorganisms on macroalgae: Inhibitory effects of bacterial biofilms and epibiotic microbial assemblages on barnacle attachment. *FEMS Microbiol Ecol* **81**: 583–595.

Navarro-Garcia, F., Ruiz-Perez, F., Cataldi, Á., and Larzábal, M. (2019) Type VI secretion system in pathogenic *Escherichia coli*: Structure, role in virulence, and acquisition. *Front Microbiol* **10**: 1965.

Nazemi, F., Karimi, K., Denayer, J.F.M., and Shafiei, M. (2021) Techno-economic aspects of different process approaches based on brown macroalgae feedstock: A step toward commercialization of seaweed-based biorefineries. *Algal Res* **58**: 102366.

Ndeh, D., Rogowski, A., Cartmell, A., Luis, A.S., Baslé, A., Gray, J., et al. (2017) Complex pectin metabolism by gut bacteria reveals novel catalytic functions. *Nature* **544**: 65–70.

Nedashkovskaya, O.I., Suzuki, M., Vancanneyt, M., Cleenwerck, I., Lysenko, A.M., Mikhailov, V. V.,

and Swings, J. (2004) *Zobellia amurskyensis* sp. nov., *Zobellia laminariae* sp. nov. and *Zobellia russellii* sp. nov., novel marine bacteria of the family *Flavobacteriaceae*. *Int J Syst Evol Microbiol* **54**: 1643–1648.

Nedwell, D.B. and Rutter, M. (1994) Influence of temperature on growth rate and competition between two psychrotolerant antarctic bacteria: Low temperature diminishes affinity for substrate uptake. *Appl Environ Microbiol* **60**: 1984–1992.

Nelson, N. (1944) A photometric adaptation of Somogyi method for determination of glicose. *J Biol Chem* **03**: 375–380.

Neumann, A.M., Balmonte, J.P., Berger, M., Giebel, H.A., Arnosti, C., Voget, S., et al. (2015) Different utilization of alginate and other algal polysaccharides by marine *Alteromonas macleodii* ecotypes. *Environ Microbiol* **17**: 3857–3868.

Newell, R., Field, J., and Griffiths, C. (1982) Energy Balance and Significance of Microorganisms in a Kelp Bed Community. *Mar Ecol Prog Ser* **8**: 103–113.

Nielsen, H., Engelbrecht, J., Brunak, S., and von Heijne, G. (1997) A Neural Network Method for Identification of Prokaryotic and Eukaryotic Signal Peptides and Prediction of their Cleavage Sites. *Int J Neural Syst* **8**: 581–599.

Niklas, K.J. (2004) The Cell Walls that Bind the Tree of Life. *Bioscience* **54**: 831.

Nishide, E., Anzai, H., Uchida, N., and Nisizawa, K. (1990) Sugar constituents of fucose-containing polysaccharides from various Japanese brown algae. *Hydrobiologia* **204**–**205**: 573–576.

Nitschke, U., Walsh, P., McDaid, J., and Stengel, D.B. (2018) Variability in iodine in temperate seaweeds and iodine accumulation kinetics of *Fucus vesiculosus* and *Laminaria digitata* (Phaeophyceae, Ochrophyta). *J Phycol* **54**: 114–125.

Norderhaug, K.M., Fredriksen, S., and Nygaard, K. (2003) Trophic importance of *Laminaria hyperborea* to kelp forest consumers and the importance of bacterial degradation to food quality. *Mar Ecol Prog Ser* **255**: 135–144.

Nürnberger, T., Brunner, F., Kemmerling, B., and Piater, L. (2004) Innate immunity in plants and animals: Striking similarities and obvious differences. *Immunol Rev* **198**: 249–266.

O'Sullivan, L., Murphy, B., McLoughlin, P., Duggan, P., Lawlor, P.G., Hughes, H., and Gardiner, G.E. (2010) Prebiotics from marine macroalgae for human and animal health applications. *Mar Drugs* **8**: 2038–2064.

Oh, Y.S., Kahng, H.Y., Lee, D.H., and Lee, S.B. (2012) *Tenacibaculum jejuense* sp. nov., isolated from coastal seawater. *Int J Syst Evol Microbiol* **62**: 414–419.

Oksanen, J., Blanchet, F.G., Kindt, R., Legendre, P., Minchin, P.R., O'Hara, R.B., et al. (2013) vegan: Community Ecology Package.

Padilla, D.K. (1985) Structural resistance of algae to herbivores - A biomechanical approach. *Mar Biol* **90**: 103–109.

Paix, B., Othmani, A., Debroas, D., Culioli, G., and Briand, J.F. (2019) Temporal covariation of epibacterial community and surface metabolome in the Mediterranean seaweed holobiont *Taonia atomaria*. *Environ Microbiol* **21**: 3346–3363.

Paix, B., Potin, P., Schires, G., Le Poupon, C., Misson, B., Leblanc, C., et al. (2021) Synergistic effects of temperature and light affect the relationship between *Taonia atomaria* and its epibacterial community: a controlled conditions study . *Environ Microbiol* **23**:6777-6797.

Palmer, J.D., Soltis, D.E., and Chase, M.W. (2004) The plant tree of life: An overview and some points of view. *Am J Bot* **91**: 1437–1445.

Park, S. and Yoon, J.H. (2013) *Tenacibaculum caenipelagi* sp. nov., a member of the family *Flavobacteriaceae* isolated from tidal flat sediment. *Antonie van Leeuwenhoek, Int J Gen Mol Microbiol* **104**: 225–231.

Parys, S., Kehraus, S., Pete, R., Küpper, F.C., Glombitza, K.W., and König, G.M. (2009) Seasonal variation of polyphenolics in *Ascophyllum nodosum* (Phaeophyceae). *Eur J Phycol* **44**: 331–338.

Patro, R., Duggal, G., Love, M.I., Irizarry, R.A., and Kingsford, C. (2017) Salmon provides fast and bias-aware quantification of transcript expression. *Nat Methods* **14**: 417–419.

Paul, N.A., De Nys, R., and Steinberg, P.D. (2006) Chemical defence against bacteria in the red alga *Asparagopsis armata*: Linking structure with function. *Mar Ecol Prog Ser* **306**: 87–101.

Paul, V., Cruz-Rivera, E., and Thacker, R. (2001) Chemical mediation of macroalgal-herbivore interactions: ecological and evolutionary perspectives. In *Marine chemical ecology. CRC Marine Science Series*. McClintock, J.B. et al. (ed)., pp. 227–265.

Pavia, H., Cervin, G., Lindgren, A., and Åberg, P. (1997) Effects of UV-B radiation and simulated herbivory on phlorotannins in the brown alga *Ascophyllum nodosum*. *Mar Ecol Prog Ser* **157**: 139–146.

Pedersen, M., Saenger, P., Rowan, K.S., and Hofsten, A. V. (1979) Bromine, Bromophenols and Floridorubin in the Red Alga *Lenormandia prolifera*. *Physiol Plant* **46**: 121–126.

Pellerin, P., Doco, T., Vidal, S., Williams, P., Brillouet, J.M., and O'Neill, M.A. (1996) Structural characterization of red wine rhamnogalacturonan II. *Carbohydr Res* **290**: 183–197.

Perez, R. (1969) Étude Biometrique d'Une Population De *Laminaria digitata* Lamouroux De L'Etage Infralittoral Profond. *Rev des Trav l'Institut des Pêches Marit* **33**: 117–135.

Pernthaler, A., Pernthaler, J., and Amann, R. (2002) Fluorescence *in situ* hybridization and catalyzed reporter deposition for the identification of marine bacteria. *Appl Environ Microbiol* **68**: 3094–3101.

Piñeiro-Vidal, M., Carballas, C.G., Gómez-Barreiro, O., Riaza, A., and Santos, Y. (2008) *Tenacibaculum soleae* sp. nov., isolated from diseased sole (*Solea senegalensis* Kaup). *Int J Syst Evol Microbiol* **58**: 881–885.

Piñeiro-Vidal, M., Gijón, D., Zarza, C., and Santos, Y. (2012) *Tenacibaculum dicentrarchi* sp. nov., a marine bacterium of the family *Flavobacteriaceae* isolated from European sea bass. *Int J Syst Evol Microbiol* **62**: 425–429.

Piñeiro-Vidal, M., Riaza, A., and Santos, Y. (2008) *Tenacibaculum discolor* sp. nov. and *Tenacibaculum gallaicum* sp. nov., isolated from sole (*Solea senegalensis*) and turbot (*Psetta maxima*) culture systems. *Int J Syst Evol Microbiol* **58**: 21–25.

Pluvinage, B., Grondin, J.M., Amundsen, C., Klassen, L., Moote, P.E., Xiao, Y., et al. (2018) Molecular basis of an agarose metabolic pathway acquired by a human intestinal symbiont. *Nat Commun* **9**: 1043.

Pollak, S., Gralka, M., Sato, Y., Schwartzman, J., Lu, L., and Cordero, O.X. (2021) Public good exploitation in natural bacterioplankton communities. *Sci Adv* **7**: eabi4717.

Pomeroy, L.R. (1974) The ocean's food web, a changing paradigm. *Bioscience* **24**: 499–504.

Ponce, N.M.A. and Stortz, C.A. (2020) A comprehensive and comparative analysis of the fucoidan compositional data across the Phaeophyceae. *Front Plant Sci* **11**: 556312.

Pontrelli, S., Szabo, R., Pollak, S., Schwartzman, J., Ledezma, D., Cordero, O.X., and Sauer, U. (2021) Hierarchical control of microbial community assembly. *bioRxiv*.

Popper, Z.A., Michel, G., Hervé, C., Domozych, D.S., Willats, W.G.T., Tuohy, M.G., et al. (2011) Evolution and diversity of plant cell walls: From algae to flowering plants. *Annu Rev Plant Biol* **62**: 567–590.

Potin, P., Sanseau, A., Le Gall, Y., Rochas, C., and Kloareg, B. (1991) Purification and characterization of a new k-carrageenase from a marine *Cytophaga*-like bacterium. *Eur J Biochem* **201**: 241–247.

Preiss, J. and Ashwell, G. (1962) Alginic acid metabolism in bacteria. II. The enzymatic reduction of 4-deoxy-L-erythro-5-hexoseulose uronic acid to 2-keto-3-deoxy-D-gluconic acid. *J Biol Chem* **237**: 317–321.

Preiss, J. and Ashwell, G. (1963) Polygalacturonic acid metabolism in bacteria. I. Enzymatic formation of 4-deoxy-L-threo-5-hexoseulose uronic acid. *J Biol Chem* **238**: 1571–1583.

Provasoli L. (1958) Effect of Plant Hormones on *Ulva*. *Biol Bull* **114**: 375–384.

R Core Team (2018) R: A language and environment for statistical computing.

Raimundo, S.C., Avci, U., Hopper, C., Pattathil, S., Hahn, M.G., and Popper, Z.A. (2016) Immunolocalization of cell wall carbohydrate epitopes in seaweeds: presence of land plant epitopes in *Fucus vesiculosus* L. (Phaeophyceae). *Planta* **243**: 337–354.

Raimundo, S.C., Pattathil, S., Eberhard, S., Hahn, M.G., and Popper, Z.A. (2017) β-1,3-Glucans are components of brown seaweed (Phaeophyceae) cell walls. *Protoplasma* **254**: 997–1016.

Ramirez-Puebla, S.T., Weigel, B.L., Jack, L., Schlundt, C., Pfister, C.A., and Welch, Mark, J.L. (2020) Spatial organization of the kelp microbiome at micron scales. *bioRxiv*.

Rebuffet, E., Barbeyron, T., Jeudy, A., Jam, M., Czjzek, M., and Michel, G. (2010) Identification of catalytic residues and mechanistic analysis of family GH82 ℓ-carrageenases. *Biochemistry* **49**: 7590–7599.

Rebuffet, E., Groisillier, A., Thompson, A., Jeudy, A., Barbeyron, T., Czjzek, M., and Michel, G. (2011) Discovery and structural characterization of a novel glycosidase family of marine origin. *Environ Microbiol* **13**: 1253–1270.

Reichenbach, H. (1989) Genus I. Cytophaga Winogradsky 1929. In *Bergey's Manual of Systematic Bacteriology, vol. 3*. Staley, J.T., Bryant, M.P., Pfenning, N., and Holt, J.G. (eds)., pp. 2015–2050.

Reintjes, G., Arnosti, C., Fuchs, B., and Amann, R. (2019) Selfish, sharing and scavenging bacteria in the Atlantic Ocean: a biogeographical study of bacterial substrate utilisation. *ISME J* **13**: 1119–1132.

Reintjes, G., Arnosti, C., Fuchs, B.M., and Amann, R. (2017) An alternative polysaccharide uptake mechanism of marine bacteria. *ISME J* **11**: 1640–1650.

Reisky, L., Préchoux, A., Zühlke, M.K., Bäumgen, M., Robb, C.S., Gerlach, N., et al. (2019) A marine bacterial enzymatic cascade degrades the algal polysaccharide ulvan. *Nat Chem Biol* **15**: 803–812.

Rognes, T., Flouri, T., Nichols, B., Quince, C., and Mahé, F. (2016) VSEARCH: A versatile open source tool for metagenomics. *PeerJ* **4**: e2584.

Rothe, M., Alpert, C., Loh, G., and Blaut, M. (2013) Novel Insights into *E. coli*'s Hexuronate

Metabolism: KduI Facilitates the Conversion of Galacturonate and Glucuronate under Osmotic Stress Conditions. *PLoS One* **8**:.

Sakai, T., Kawai, T., and Kato, I. (2004) Isolation and characterization of a fucoidan-degrading marine bacterial strain and its fucoidanase. *Mar Biotechnol* **6**: 335–346.

Sakai, T., Kimura, H., and Kato, I. (2003) Purification of sulfated fucoglucuronomannan lyase from bacterial strain of *Fucobacter marina* and study of appropriate conditions for its enzyme digestion. *Mar Biotechnol* **5**: 380–387.

Sakai, T., Kimura, H., Kojima, K., Shimanaka, K., Ikai, K., and Kato, I. (2003) Marine bacterial sulfated fucoglucuronomannan (SFGM) lyase digests brown algal SFGM into trisaccharides. *Mar Biotechnol* **5**: 70–78.

Salaün, S., la Barre, S., Santos-Goncalvez, M. Dos, Potin, P., Haras, D., and Bazire, A. (2012) Influence of Exudates of the Kelp *Laminaria digitata* on Biofilm Formation of Associated and Exogenous Bacterial Epiphytes. *Microb Ecol* **64**: 359–369.

Salmeán, A.A., Duffieux, D., Harholt, J., Qin, F., Michel, G., Czjzek, M., et al. (2017) Insoluble (1 → 3), (1 → 4)-β-Dglucan is a component of cell walls in brown algae (Phaeophyceae) and is masked by alginates in tissues. *Sci Rep* **7**: 2880.

Salmeán, A.A., Guillouzo, A., Duffieux, D., Jam, M., Matard-Mann, M., Larocque, R., et al. (2018) Double blind microarray-based polysaccharide profiling enables parallel identification of uncharacterized polysaccharides and carbohydrate-binding proteins with unknown specificities. *Sci Rep* **8**: 2500.

Sato, K., Naito, M., Yukitake, H., Hirakawa, H., Shoji, M., McBride, M.J., et al. (2010) A protein secretion system linked to bacteroidete gliding motility and pathogenesis. *PNAS* **107**: 276–281.

Schaechter, M., MaalOe, O., and Kjeldgaard, N.O. (1958) Dependency on Medium and Temperature of Cell Size and Chemical Composition during Balanced Growth of Salmonella typhimurium. *J Gen Microbiol* **19**: 592–606.

Schiel, D.R. and Foster, M.S. (2006) The population biology of large brown seaweeds: Ecological consequences of multiphase life histories in dynamic coastal environments. *Annu Rev Ecol Evol Syst* **37**: 343–372.

Schiener, P., Black, K.D., Stanley, M.S., and Green, D.H. (2015) The seasonal variation in the chemical composition of the kelp species *Laminaria digitata*, *Laminaria hyperborea*, *Saccharina latissima* and *Alaria esculenta*. *J Appl Phycol* **27**: 363–373.

Schneider, C.A., Rasband, W.S., and Eliceiri, K.W. (2012) NIH Image to ImageJ: 25 years of image analysis. *Nat Methods* **9**: 671–675.

Schoenwaelder, M. and Wiencke, C. (2000) Phenolic compounds in the embryo development of several northern hemisphere fucoids. *Plant Biol* 24–33.

Seiderer, L. and Newell, R. (1985) Relative significance of phytoplankton, bacteria and plant detritus as carbon and nitrogen resources for the kelp bed filter-feeder *Choromytilus mendionalis*. *Mar Ecol Prog Ser* **22**: 127–139.

Serebryakova, A., Aires, T., Viard, F., Serrão, E.A., and Engelen, A.H. (2018) Summer shifts of bacterial communities associated with the invasive brown seaweed *Sargassum muticum* are location and tissue dependent. *PLoS One* **13**: e0206734.

Sfriso, A.A., Gallo, M., and Baldi, F. (2017) Seasonal variation and yield of sulfated polysaccharides in seaweeds from the Venice Lagoon. *Bot Mar* **60**: 339–349.

Shannon, E. and Abu-Ghannam, N. (2016) Antibacterial derivatives of marine algae: An overview of pharmacological mechanisms and applications. *Mar Drugs* **14**: 81.

Shannon, P., Markiel, A., Ozier, O., Baliga, N.S., Wang, J.T., Ramage, D., et al. (2003) Cytoscape: A software Environment for integrated models of biomolecular interaction networks. *Genome Res* **13**: 2498–2504.

Shen, J., Chang, Y., Zhang, Y., Mei, X., and Xue, C. (2020) Discovery and Characterization of an Endo-1,3-Fucanase From Marine Bacterium *Wenyingzhuangia fucanilytica*: A Novel Glycoside Hydrolase Family. *Front Microbiol* **11**: 1674.

Sheu, S.Y., Lin, K.Y., Chou, J.H., Chang, P.S., Arun, A.B., Young, C.C., and Chen, W.M. (2007) *Tenacibaculum litopenaei* sp. nov., isolated from a shrimp mariculture pond. *Int J Syst Evol Microbiol* **57**: 1148–1153.

Shipman, J.A., Berleman, J.E., and Salyers, A.A. (2000) Characterization of four outer membrane proteins involved in binding starch to the cell surface of *Bacteroides thetaiotaomicron*. *J Bacteriol* **182**: 5365–5372.

Sichert, A., Corzett, C.H., Schechter, M., Unfried, F., Markert, S., Becher, D., et al. (2020) *Verrucomicrobia* use hundreds of enzymes to digest the algal polysaccharide fucoidan. *Nat Microbiol* **5**: 1026–1039.

Sichert, A., Le Gall, S., Klau, L.J., Laillet, B., Rogniaux, H., Aachmann, F.L., and Hehemann, J.H. (2021) Ion-exchange purification and structural characterization of five sulfated fucoidans from brown algae. *Glycobiology* **31**: 352–357.

Silchenko, A.S., Kusaykin, M.I., Zakharenko, A.M., Menshova, R. V., Khanh, H.H.N., Dmitrenok, P.S., et al. (2014) Endo-1,4-fucoidanase from Vietnamese marine mollusk *Lambis* sp. which producing sulphated fucooligosaccharides. *J Mol Catal B Enzym* **102**: 154–160.

Silchenko, A.S., Rasin, A.B., Kusaykin, M.I., Malyarenko, O.S., Shevchenko, N.M., Zueva, A.O., et al. (2018) Modification of native fucoidan from *Fucus evanescens* by recombinant fucoidanase from marine bacteria *Formosa algae*. *Carbohydr Polym* **193**: 189–195.

Silchenko, A.S., Rasin, A.B., Zueva, A.O., Kusaykin, M.I., Zvyagintseva, T.N., Kalinovsky, A.I., et al. (2018) Fucoidan Sulfatases from Marine Bacterium *Wenyingzhuangia fucanilytica* CZ1127T. *Biomolecules* **8**: 98.

Silchenko, A.S., Ustyuzhanina, N.E., Kusaykin, M.I., Krylov, V.B., Shashkov, A.S., Dmitrenok, A.S., et al. (2017) Expression and biochemical characterization and substrate specificity of the fucoidanase from *Formosa algae*. *Glycobiology* **27**: 254–263.

Singh, R.P., Mantri, V.A., Reddy, C.R.K., and Jha, B. (2011) Isolation of seaweed-associated bacteria and their morphogenesis-inducing capability in axenic cultures of the green alga *Ulva fasciata*. *Aquat Biol* **12**: 13–21.

Skerratt, J.H., Bowman, J.P., Hallegraeff, G., James, S., and Nichols, P.D. (2002) Algicidal bacteria associated with blooms of a toxic dinoflagellate in a temperate Australian estuary. *Mar Ecol Prog Ser* **244**: 1–15.

Skriptsova, A., Khomenko, V., and Vladimir Isakov, I. (2004) Seasonal changes in growth rate, morphology and alginate content in *Undaria pinnatifida* at the northern limit in the Sea of Japan (Russia). *J Appl Phycol* **16**: 17–21.

Skriptsova, A. V., Shevchenko, N.M., Tarbeeva, D. V., and Zvyagintseva, T.N. (2012) Comparative Study of Polysaccharides from Reproductive and Sterile Tissues of Five Brown Seaweeds. *Mar Biotechnol* **14**: 304–311.

Sørensen, I., Domozych, D., and Willats, W.G.T. (2010) How have plant cell walls evolved? *Plant Physiol* **153**: 366–372.

Staufenberger, T., Thiele, S., Wiese, J., and Imhoff, J.F. (2008) Phylogenetic analysis of bacteria associated with *Laminaria saccharina*. *Microb Ecol* **64**: 65–77.

Steneck, R.S., Graham, M.H., Bourque, B.J., Corbett, D., Erlandson, J.M., Estes, J.A., and Tegner, M.J. (2002) Kelp forest ecosystems: Biodiversity, stability, resilience and future. *Environ Conserv* **29**: 436–459.

Studier, F.W. (2005) Protein production by auto-induction in high density shaking cultures. *Protein Expr Purif* **41**: 207–234.

Suttle, C.A. (2007) Marine viruses - Major players in the global ecosystem. *Nat Rev Microbiol* **5**: 801–812.

Suzuki, M., Nakagawa, Y., Harayama, S., and Yamamoto, S. (2001) Phylogenetic analysis and taxonomic study of marine *Cytophaga*-like bacteria: Proposal for *Tenacibaculum* gen. nov. with *Tenacibaculum maritimum* comb. nov. and *Tenacibaculum ovolyticum* comb. nov., and description of *Tenacibaculum mesophilum* sp. nov. and *Tenacibaculum amylolyticum* sp. nov. *Int J Syst Evol Microbiol* **51**: 1639–1652.

Takeda, M., Iohara, K., Shinmaru, S., Suzuki, I., and Koizumi, J. (2000) Purification and properties of an enzyme capable of degrading the sheath of *Sphaerotilus natans*. *Appl Environ Microbiol* **66**: 4998–5004.

Takemura, A.F., Chien, D.M., and Polz, M.F. (2014) Associations and dynamics of vibrionaceae in the environment, from the genus to the population level. *Front Microbiol* **5**: 38.

Tancula, E., Feldhaus, M.J., Bedzyk, L.A., and Salyers, A.A. (1992) Location and characterization of genes involved in binding of starch to the surface of *Bacteroides thetaiotaomicron*. *J Bacteriol* **174**: 5609–5616.

Tang, K., Lin, Y., Han, Y., and Jiao, N. (2017) Characterization of potential polysaccharide utilization systems in the marine Bacteroidetes *Gramella flava* JLT2011 using a multi-omics approach. *Front Microbiol* **8**: 220.

Taylor, R.B., Sotka, E., and Hay, M.E. (2002) Tissue-specific induction of herbivore resistance: Seaweed response to amphipod grazing. *Oecologia* **132**: 68–76.

Teeling, H., Fuchs, B.M., Becher, D., Klockow, C., Gardebrecht, A., Bennke, C.M., et al. (2012) Substrate-controlled succession of marine bacterioplankton populations induced by a phytoplankton bloom. *Science (80-)* **336**: 608–611.

Terrapon, N., Lombard, V., Drula, É., Lapébie, P., Al-Masaudi, S., Gilbert, H.J., and Henrissat, B. (2018) PULDB: The expanded database of Polysaccharide Utilization Loci. *Nucleic Acids Res* **46**: D677–D683.

Thomas, F. (2011) Identification et caractérisation du système alginolytique de la bactérie marine *Zobellia galactanivorans*.

Thomas, F., Barbeyron, T., and Michel, G. (2011) Evaluation of reference genes for real-time quantitative PCR in the marine flavobacterium *Zobellia galactanivorans*. *J Microbiol Methods* **84**: 61–6.

Thomas, F., Barbeyron, T., Tonon, T., Génicot, S., Czjzek, M., and Michel, G. (2012) Characterization of the first alginolytic operons in a marine bacterium: from their emergence in marine *Flavobacteriia* to their independent transfers to marine *Proteobacteria* and human gut *Bacteroides*.

Environ Microbiol **14**: 2379–94.

Thomas, F., Bordron, P., Eveillard, D., and Michel, G. (2017) Gene expression analysis of *Zobellia galactanivorans* during the degradation of algal polysaccharides reveals both substrate-specific and shared transcriptome-wide responses. *Front Microbiol* **8**: 1808.

Thomas, F., Dittami, S.M., Brunet, M., Le Duff, N., Tanguy, G., Leblanc, C., and Gobet, A. (2020) Evaluation of a new primer combination to minimize plastid contamination in 16S rDNA metabarcoding analyses of alga-associated bacterial communities. *Environ Microbiol Rep* **12**: 30–37.

Thomas, F., Duff, N. Le, Leroux, C., Dartevelle, L., Thomas, F., Duff, N. Le, et al. (2020) Isotopic labelling of cultured macroalgae and isolation of 13 C-labelled cell wall polysaccharides for trophic investigations To cite this version : HAL Id : hal-03035113.

Thomas, F., Le Duff, N., Wu, T. Di, Cébron, A., Uroz, S., Riera, P., et al. (2021) Isotopic tracing reveals single-cell assimilation of a macroalgal polysaccharide by a few marine *Flavobacteria* and *Gammaproteobacteria*. *ISME J* **15**: 3062–3075.

Thomas, F., Hehemann, J.H., Rebuffet, E., Czjzek, M., and Michel, G. (2011) Environmental and gut *Bacteroidetes*: The food connection. *Front Microbiol* **2**: 93.

Thomas, F., Lundqvist, L.C.E., Jam, M., Jeudy, A., Barbeyron, T., Sandström, C., et al. (2013) Comparative characterization of two marine alginate lyases from *Zobellia galactanivorans* reveals distinct modes of action and exquisite adaptation to their natural substrate. *J Biol Chem* **288**: 23021–23037.

Toth, G.B. and Pavia, H. (2000) Water-borne cues induce chemical defense in a marine alga (*Ascophyllum nodosum*). *Proc Natl Acad Sci U S A* **97**: 14418–14420.

Traving, S.J., Thygesen, U.H., Riemann, L., and Stedmon, C.A. (2015) A model of extracellular enzymes in free-living microbes: Which strategy pays off? *Appl Environ Microbiol* **81**: 7385–7393.

Tsai, H.L., Tai, C.J., Huang, C.W., Chang, F.R., and Wang, J.Y. (2017) Efficacy of low-molecular-weight fucoidan as a supplemental therapy in metastatic colorectal cancer patients: A double-blind randomized controlled trial. *Mar Drugs* **15**: 122.

Tujula, N.A., Holmström, C., Mußmann, M., Amann, R., Kjelleberg, S., and Crocetti, G.R. (2006) A CARD-FISH protocol for the identification and enumeration of epiphytic bacteria on marine algae. *J Microbiol Methods* **65**: 604–607.

Ulitzur, S. (1974) *Vibrio parahaemolyticus* and *Vibrio alginolyticus*: Short generation-time marine bacteria. *Microb Ecol* **1**: 127–135.

Valm, A.M., Mark Welch, J.L., and Borisy, G.G. (2012) CLASI-FISH: Principles of combinatorial labeling and spectral imaging. *Syst Appl Microbiol* **35**: 496–502.

Verhaeghe, E.F., Fraysse, A., Guerquin-Kern, J.L., Wu, T. Di, Devès, G., Mioskowski, C., et al. (2008) Microchemical imaging of iodine distribution in the brown alga *Laminaria digitata* suggests a new mechanism for its accumulation. *J Biol Inorg Chem* **13**: 257–269.

Vickers, C., Liu, F., Abe, K., Salama-Alber, O., Jenkins, M., Springate, C.M.K., et al. (2018) Endo-fucoidan hydrolases from glycoside hydrolase family 107 (GH107) display structural and mechanistic similarities to α-L-fucosidases from GH29. *J Biol Chem* **293**: 18296–18308.

Vuillemin, M., Silchenko, A.S., Cao, H.T.T., Kokoulin, M.S., Trang, V.T.D., Holck, J., et al. (2020) Functional Characterization of a New GH107 Endo-α-(1,4)-Fucoidanase from the Marine

Bacterium *Formosa haliotis*. *Mar Drugs* **18**: 562.

Wallner, G., Amann, R., and Beisker, W. (1993) Optimizing fluorescent *in situ* hybridization with rRNA-targeted oligonucleotide probes for flow cytometric identification of microorganisms. *Cytometry* **14**: 136–143.

Wang, H., Li, J., Zheng, T., Hill, R.T., and Hu, X. (2013) *Imperialibacter roseus* gen. nov., sp. nov., a novel bacterium of the family *Flammeovirgaceae* isolated from Permian groundwater. *Int J Syst Evol Microbiol* **63**: 4136–4140.

Wang, J.T., Chou, Y.J., Chou, J.H., Chen, C.A., and Chen, W.M. (2008) *Tenacibaculum aiptasiae* sp. nov., isolated from a sea anemone *Aiptasia pulchella*. *Int J Syst Evol Microbiol* **58**: 761–766.

Wang, Q., Garrity, G.M., Tiedje, J.M., and Cole, J.R. (2007) Naive Bayesian classifier for rapid assignment of rRNA sequences into the new bacterial taxonomy. *Appl Environ Microbiol* **73**: 5261–7.

Weber, A., Kögl, S.A., and Jung, K. (2006) Time-dependent proteome alterations under osmotic stress during aerobic and anaerobic growth in *Escherichia coli*. *J Bacteriol* **188**: 7165–7175.

Weigel, B.L. and Pfister, C.A. (2019) Successional dynamics and seascape-level patterns of microbial communities on the canopy-forming kelps *Nereocystis luetkeana* and *Macrocystis pyrifera*. *Front Microbiol* **10**: 346.

Weinberger, F. and Friedlander, M. (2000) Endogenous and exogenous elicitors of a hypersensitive response in *Gracilaria conferta* (Rhodophyta). *J Appl Phycol* **12**: 139–145.

West, S.A., Griffin, A.S., Gardner, A., and Diggle, S.P. (2006) Social evolution theory for microorganisms. *Nat Rev Microbiol* **4**: 597–607.

Whitman, W., Coleman, D., and Wiebe, W. (1998) Prokaryotes: The unseen majority. *Proc Natl Acad Sci U S A* **95**: 6578–6583.

Wickham, H. (2009) ggplot2, Springer-Verlag New York.

Wickham, H. (2016) Use R! ggplot2: Elegant graphics for data analysis. Second Edition.

Wietz, M., Wemheuer, B., Simon, H., Giebel, H.A., Seibt, M.A., Daniel, R., et al. (2015) Bacterial community dynamics during polysaccharide degradation at contrasting sites in the Southern and Atlantic Oceans. *Environ Microbiol* **17**: 3822–3831.

Wilhelm, S.W. and Suttle, C.A. (1999) Viruses and nutrient cycles in the sea. *Bioscience* **49**: 781–788.

Worrich, A., Musat, N., and Harms, H. (2019) Associational effects in the microbial neighborhood. *ISME J* **13**: 2143–2149.

Xia, L.C., Steele, J.A., Cram, J.A., Cardon, Z.G., Simmons, S.L., Vallino, J.J., et al. (2011) Extended local similarity analysis (eLSA) of microbial community and other time series data with replicates. *BMC Syst Biol* **5**: S15.

Yang, S.H., Oh, J.H., Seo, H.S., Lee, J.H., and Kwon, K.K. (2018) *Marinirhabdus citrea* sp. nov., a marine bacterium isolated from a seaweed. *Int J Syst Evol Microbiol* **68**: 547–551.

Yoon, J.H., Kang, S.J., and Oh, T.K. (2005) *Tenacibaculum lutimaris* sp. nov., isolated from a tidal flat in the Yellow Sea, Korea. *Int J Syst Evol Microbiol* **55**: 793–798.

Zablackis, E. and Perez, J. (1990) A partially pyruvated carrageenan from hawaiian *Grateloupia filicina* (Cryptonemiales, Rhodophyta). *Bot Mar* **33**: 273–276.

Zayed, A. and Ulber, R. (2020) Fucoidans: Downstream processes and recent applications. *Mar Drugs* **18**: 170.

Zeng, Y., Himmel, M.E., and Ding, S.Y. (2017) Visualizing chemical functionality in plant cell walls Mike Himmel. *Biotechnol Biofuels* **10**: 263.

Zhao, D., Shen, F., Zeng, J., Huang, R., Yu, Z., and Wu, Q.L. (2016) Network analysis reveals seasonal variation of co-occurrence correlations between *Cyanobacteria* and other bacterioplankton. *Sci Total Environ* **573**: 817–825.

Zhao, X., Guo, F., Hu, J., Zhang, L., Xue, C., Zhang, Z., and Li, B. (2016) Antithrombotic activity of oral administered low molecular weight fucoidan from *Laminaria Japonica*. *Thromb Res* **144**: 46–52.

Zhou, G., Sun, Y.P., Xin, H., Zhang, Y., Li, Z., and Xu, Z. (2004) *In vivo* antitumor and immunomodulation activities of different molecular weight lambda-carrageenans from *Chondrus ocellatus*. *Pharmacol Res* **50**: 47–53.

Zhu, C., Liu, Z., Ren, L., Jiao, S., Zhang, X., Wang, Q., et al. (2021) Overexpression and biochemical characterization of a truncated endo-α (1 → 3)-fucoidanase from alteromonas sp. SN-1009. *Food Chem* **353**: 129460.

Zhu, Y., Chen, P., Bao, Y., Men, Y., Zeng, Y., Yang, J., et al. (2016) Complete genome sequence and transcriptomic analysis of a novel marine strain *Bacillus weihaiensis* reveals the mechanism of brown algae degradation. *Sci Rep* **6**: 38248.

Zhu, Y., Thomas, F., Larocque, R., Li, N., Duffieux, D., Cladière, L., et al. (2017) Genetic analyses unravel the crucial role of a horizontally acquired alginate lyase for brown algal biomass degradation by *Zobellia galactanivorans*. *Environ Microbiol* **19**: 2164–2181.

Zilber-Rosenberg, I. and Rosenberg, E. (2008) Role of microorganisms in the evolution of animals and plants: The hologenome theory of evolution. *FEMS Microbiol Rev* **32**: 723–735.

ZoBell, C. (1941) Studies on marine bacteria. I. The cultural requirements of heterotrophic aerobes. *J Mar Res* **4**:75

ZoBell, C. and Upham, H. (1944) A list of marine bacteria including descriptions of sixty new species, Berkeley ; Los Angeles : University of California Press, 1944. (ed).

Zubia, M., Payri, C., and Deslandes, E. (2008) Alginate, mannitol, phenolic compounds and biological activities of two range-extending brown algae, *Sargassum mangarevense* and *Turbinaria ornata* (Phaeophyta: Fucales), from Tahiti (French Polynesia). *J Appl Phycol* **20**: 1033–1043.

Zueva, A.O., Silchenko, A.S., Rasin, A.B., Kusaykin, M.I., Usoltseva, R. V., Kalinovsky, A.I., et al. (2020) Expression and biochemical characterization of two recombinant fucoidanases from the marine bacterium *Wenyingzhuangia fucanilytica* CZ1127T. *Int J Biol Macromol* **164**: 3025–3037.

Abstract

Macroalgae constitute a large reservoir of organic matter worldwide. It is long known that heterotrophic bacteria are key players in algal biomass recycling. To date, numerous works focused on the degradation and assimilation of purified algal polysaccharides, leading to discovery of new enzymes and complete catabolic pathways. However, this strategy does not reflect the structural complexity of the algal extracellular matrix. In this thesis I implemented diverse approaches to decipher the ecological and metabolic strategies of bacteria specialized in the utilization of fresh macroalgae. I evidenced a succession of the epiphytic microbiota during *in situ* macroalgae decomposition, shedding light on the utilization of distinct substrate niches by successive bacterial communities. Protocols of qPCR and CARD-FISH were optimized for the specific detection of the known algal-polysaccharides degrader genus *Zobellia.* Their application revealed a widespread season-dependent distribution of the genus at the surface of macroalgae. Its particularly high abundance and activity on decaying algae emphasized its key role in the algal degradation processes. I demonstrated that *Zobellia galactanivorans* Dsij^T has the capacity to use fresh brown algae as a sole carbon source, highlighting a specific pioneer degrader behaviour. The analysis of its transcriptome revealed the induction of a subset of genes, including novel uncharacterized polysaccharide utilization loci (PULs), specifically induced with intact algae compared to purified polysaccharides. The preliminary characterization of one of these PULs demonstrated its role in the degradation of fucose-containing sulfated polysaccharides from *Laminaria digitata* and led to the discovery of novel enzymatic activities in *Z. galactanivorans*. Through co-culture experiments I showed that *Z. galactanivorans* supported the growth of *Tenacibaculum* strains with macroalgae, bringing out cooperative interactions between pioneer and opportunist bacteria. By studying macroalgae degradation mechanisms at different scales, this thesis contributes to unveil the strategies of heterotrophic marine bacteria in the fate of macroalgal biomass.

Résumé

Les macroalgues représentent un immense stock de matière organique à travers le monde. Les bactéries hétérotrophes sont largement reconnues comme des acteurs clés du recyclage de cette biomasse algale. De nombreuses études se sont attachées à caractériser de nouvelles enzymes et voies cataboliques complètes pour la dégradation des polysaccharides algaux purifiés. Cependant, ces mécanismes ne reflètent vraisemblablement pas la complexité des réponses mises en œuvre pour la dégradation d'algues entières. Au cours de ma thèse, j'ai ainsi étudié les stratégies écologiques et métaboliques de bactéries spécialisées dans l'utilisation des macroalgues fraîches. J'ai d'abord mis en évidence une succession du microbiote épiphyte au cours de la décomposition de macroalgues *in situ*, mettant en lumière l'utilisation de différents types de substrats par des communautés successives. Des protocoles de qPCR et CARD-FISH ont été optimisés pour la détection spécifique du genre *Zobellia.* Ce dernier a été détecté sur des macroalgues brunes, rouges et vertes et son abondance fluctue au cours de l'année. Son abondance et son activité particulièrement élevées dans le microbiote d'algues en décomposition soulignent son rôle clé dans les processus de dégradation des algues. J'ai démontré en particulier que la souche *Zobellia galactanivorans* Dsij^T avait la capacité d'utiliser les algues brunes comme seule source de carbone, mettant ainsi en évidence son comportement pionnier dans l'attaque des tissus algaux. L'analyse de son transcriptome a révélé un ensemble de gènes, dont certains au sein de nouveaux loci dédiés à l'utilisation de polysaccharide (PUL) non caractérisés, spécifiquement induits en présence d'algues fraîches par rapport aux polysaccharides purifiés. La caractérisation préliminaire de l'un de ces PUL a établi son rôle dans la dégradation de polysaccharides sulfatés contenant des résidus fucoses provenant de *Laminaria digitata,* et a conduit à la découverte de nouvelles activités enzymatiques chez *Z. galactanivorans*. Au cours d'expériences de co-cultures j'ai montré que des souches du genre *Tenacibaculum* n'étaient capables de croître à partir de macroalgues qu'en présence de *Z. galactanivorans*, révélant de probables interactions coopératives. En étudiant les mécanismes de dégradation des macroalgues à différentes échelles, cette thèse contribue à dévoiler les stratégies des bactéries marines hétérotrophes dans le devenir de la biomasse algale.